EVALUATION OF THE POTENTIAL OF NANO SELENIUM IN AMELIORATION OF TOXICITY IMPARTED BY CANCER CHEMOTHERAPEUTIC DRUGS SUCH AS CYCLOPHOSPHAMIDE AND CISPLATIN USING MOUSE MODEL

Thesis submitted by

Arin Bhattacharjee

Doctor of Philosophy (Pharmacy)

Department of Pharmaceutical Technology,
Faculty Council of Engineering & Technology
Jadavpur University
Kolkata, India

2018

JADAVPUR UNIVERSITY

KOLKATA – 700 032, INDIA

INDEX NO. 240/16/Ph.

1. Title of the thesis:

Evaluation of The Potential of Nano Selenium In Amelioration of Toxicity Imparted By Cancer Chemotherapeutic Drugs Such as Cyclophosphamide and Cisplatin Using Mouse Model

2. Name, Designation & Institution of the Supervisors:

- Dr. Sudin Bhattacharya
  Senior Scientific Officer (Senior Assistant Director Grade)
  Head, Department of Cancer Chemoprevention,
  Chittaranjan National Cancer Institute.
  37, S. P. Mukherjee Road, Kolkata – 700 026, India.

- Prof. (Dr.) Jaydip Biswas
  Director, Chittaranjan National Cancer Institute.
  Chittaranjan National Cancer Institute.
  37, S. P. Mukherjee Road, Kolkata – 700 026, India.

- Prof. (Dr.) Tuhinadri Sen,
  Professor, Division of Pharmacology,
  Department of Pharmaceutical Technology,
  Jadavpur University.
  188, Raja S. C. Mallick Road, Kolkata – 700 032, India.

3. List of Publication:

1. **Bhattacharjee A,** Basu A, Ghosh P, Biswas J, Bhattacharya S. Protective effect of Selenium nanoparticle against cyclophosphamide induced hepatotoxicity and genotoxicity in Swiss albino mice. ***Journal of Biomaterial Application*****.** 2014: 29(2):303-317. DOI: 10.1177/0885328214523323.

- **Bhattacharjee A,** Basu A, Biswas J, Bhattacharya S. Nano-Se attenuates cyclophosphamide-induced pulmonary injury through modulation of oxidative stress and DNA damage in Swiss albino mice. ***Molecular and Cellular Biochemistry***. 2015; 405(1-2):243-56. DOI: 10.1007/s11010-015-2415-1.

2. **Bhattacharjee A,** Basu A, Biswas J, Sen T, Bhattacharya S. Chemoprotective and chemosensitizing properties of selenium nanoparticle (Nano-Se) during adjuvant therapy with cyclophosphamide in tumor-bearing mice. ***Molecular and Cellular Biochemistry.*** 2017; 424(1-2):13-33. DOI: 10.1007/s11010-016-2839-2.

3. **Bhattacharjee A,** Basu A, Sen T, Biswas J, Bhattacharya S. Nano-Se as a novel candidate in the management of oxidative stress related disorders and cancer. ***Nucleus.*** 2017: 60: 137**.** DOI: doi.org/10.1007/s13237-016-0183-2.

4. List of Patents: Nil.

5. List of Presentations in National/International

International:

- **Bhattacharjee A**, Biswas J, Bhattacharya S. "Evaluation of the potential of nanoselenium in amelioration of toxicity imparted by cancer chemotherapeutic drugs such as cyclophosphamide using mouse model". Poster presentation in the **30st Annual convention of the Indian Association for Cancer Research (IACR) and International symposium on 'Signaling Network and Cancer'** from 6th–9th February, 2011 at Indian Institute of Chemical Biology (IICB-CSIR), Kolkata, West Bengal, India.

- **Bhattacharjee A**, Singha Roy S, , Ghosh P, Biswas J, Bhattacharya S. "Evaluation of the potential of nanoselenium in amelioration of toxicity imparted by cancer chemotherapeutic drugs such as cisplatin using mouse model". Poster presentation in the **31st Annual convention of the Indian Association for Cancer Research (IACR) and International symposium on 'Cancer genomics and its Impact in the Clinics'** from 26th–29th January, 2012 at Advanced Centre for Treatment, Research and Education in Cancer (ACTREC), Tata Memorial Centre, Kharghar, Navi Mumbai, India.

CERTIFICATE FROM THE SUPERVISORS

This is to certify that the thesis entitled "Evaluation of The Potential of Nano- Se in Amelioration of Toxicity Imparted By Cancer Chemotherapeutic Drugs Such as Cyclophosphamide and Cisplatin Using Mouse Model" submitted by Shri Arin Bhattacharjee, who got his name registered on 25.07.2011 for the award of Ph. D. (Pharmacy) degree of Jadavpur University is absolutely based upon his own work under the supervision of Dr. Sudin Bhattacharya, Prof. (Dr.) Jaydip Biswas and Prof. (Dr.) Tuhinadri Sen that neither his thesis nor any part of the thesis has been submitted for any degree/diploma or any other academic award anywhere before.

1._____1

Dr. Sudin Bhattacharya
(Signature of the Supervisor and date with Office seal)

2._____i

Prof. (Dr.) Jaydep Biswas
(Signature of the Supervisor and date with Office seal)

3._____

Prof. (Dr.) Tuhinadri Sen
(Signature of the Supervisor and date with Office seal)

Dedicated to

My Family & My son Hridaan

ACKNOWLEDGEMENTS

This thesis becomes a reality with the kind support and help of many individuals. I would like to extend my sincere thanks and gratitude to all of them without whom this would have been a mere dream.

Foremost, I want to offer this endeavor to our God Almighty for the wisdom he bestowed upon me, strength, peace of mind and good health in order to finish this research.

I am highly indebted to my supervisor **Dr. Sudin Bhattacharya**, Senior Scientific Officer (Senior Assistant Director Grade) and Head, Department of Cancer Chemoprevention, Chittaranjan National Cancer Institute, Kolkata without whose guidance, patience and support this wouldn't have been possible. He was the one who gave me the strength to dream and paved the way of turning my dream into reality. Like a toddler who learns to explore the world, he taught me every aspect of my research, being by my side like a father figure. He held my hands when I fell, pushed me to move ahead and embraced every failures on my way, scolded me when I felt lost of track. He was the one who embraced both my failures and achievement with élan.

I would like to express my humble regards to my Co-Supervisor **Prof. (Dr.) Jaydip Biswas**, who also happens to be the Director, Chittaranjan National Cancer Institute (CNCI), Kolkata, for giving me immense help and support during my research as well as bestowing me with the Institutional infrastructure. He has been like a pillar of strength to me. I cannot thank him enough for giving me his precious time even in his busy schedule.

I would like to express my deep sense of gratitude to Late **Prof. (Dr.) Tuhinadri Sen,** Division of Pharmacology, Department of Pharmaceutical Technology, Jadavpur University, Kolkata. I am heartbroken as I cannot share this moment with him in person but he will always remain in my heart. His sudden demise has left shattered yet I am sure he is witnessing it from where ever he is. His support by my side has always been my fuel to carry on. I miss him a lot. May his soul rest in peace in heaven.

A special thanks to **Prof. (Dr.) Amalesh Samanta**, Division of Microbiology, Department of Pharmaceutical Technology, Jadavpur University, Kolkata as not only professionally but also personally he was always there for me as my philosopher and guide in true sense of the term.

I express my sincere gratitude to Officer – in – Charge (Research wing) **Dr. Chinmay Kumar Panda** for not only ensuring unfettered access to the institutional facilities but also showering his wit and affection on me. The past and present Academic Coordinator, **Dr. Sandip Majumder** and **Dr. Sutapa Mukherjee** for their effortless support towards the smooth running of fellowship and their guidance during Ph.D. registration and coursework examination. I am also thankful to **Dr. Avijit Rakshit**, Head, Animal Care and Maintenance Department and all other staffs of the said department for proving me animals and working environment for my study. I am also grateful to the staffs of **Central Research Instrumentation facility** (CRIF) for providing smooth and uninterrupted access to instrumental facility.

I would like to express my gratitude to words my co-workers for helping me during my research tenure, especially to **Dr. Abhishek Basu** for his professional as well as personal help at times.

I would like to address my gratitude to few peoples of Jadavpur University also who helped throughtout the proceeding of my Ph.D. degree: **Prof. (Dr.) Pulak Kumar Mukherjee**, Head, and Department of Pharmaceutical Technology, **Prof. (Dr.) Chiranjib Bhattacharjee**, Dean, FET **Dr. Bholanath Karmakar**, Principal Secretary, FET and the other official staffs of the Faculty of Engineering and Technology (FET).

Everything will go haywire if not for grounding forces, called family. I bestow my love, gratitude and greatest thanks to my family members who were always there for me. They supported me without anything in return.

Finally, a humble gratitude to **Indian Council of Medical Research (ICMR), Govt. of India** for providing me Senior Research Fellowship without which this journey would not been started and run soomthly.

Lastly, my thanks and appreciation goes to each and every person who have willingly help me out with their abilities to achieve this dream.

Arin Bhattacharjee

CONTENTS

Page No.

Introduction

Introduction

Cancer is a group of diseases characterized by uncontrolled growth and invasion and sometimes metastasis and also second leading cause of death worldwide next to cardiovascular diseases in both developed and developing countries and is therefore, of worldwide concern **(American Cancer Society, 2014)**. According to WHO, cancer accounted for 7.9 million deaths (around 13% of all deaths) in 2007, with 38% in developed countries and 62% in developing countries. By 2030, nearly 21.4 million new cancer cases and more than 13.2 million deaths are projected to occur in the world **(Globocan, 2008)**.

At the beginning of this century, comprehensive treatment for malignant neoplasm had progressed considerably with advances in molecular targeted therapy, immunotherapy and gene therapy. However, chemotherapy is still the primary treatment.

Cyclophosphamide (CP) is one of the universally acclaimed antineoplastic drugs for its therapeutic efficacy against a variety of hematological and solid malignancies, and autoimmune disorders like rheumatoid arthritis, systemic lupus erythematosus, and multiple sclerosis **(Ghosh et al., 2015)**. It has no activity against cancer cells *in vitro* until it undergoes metabolic activation catalyzed by liver cytochrome P450 **(Zhang et al., 2006)** to yield three major cytotoxic metabolites: 4-hydroxy-CP, phosphoramide mustard, and acrolein. These metabolites can alkylate nucleophilic sites in DNA, RNA, and protein such as –SH, –COOH, $–NH_2$ and –OH **(Zhang et al., 2008)**, which cause bone marrow toxicity, pulmonary toxicity, bladder toxicity, gonadal toxicity, and mutagenic effects **(Nafees et al., 2015)**. Acrolein which is a toxic metabolite responsible for production of reactive oxygen species (ROS) and enhancement of lipid peroxidation (LPO). The acute toxicities of cyclophosphamide are associated primarily with its genotoxicity **(Selvakumar et al., 2006)**. Moreover, cyclophosphamide can bind to DNA and induces DNA damage in the form of strand breaks, DNA–DNA cross-links, interstrand and intrastrand, as well as DNA-protein cross-links **(Basu et al., 2015)**. Cyclophosphamide induced nucleic acid damage may lead to DNA mutations that result in cytotoxicity, carcinogenicity and teratogenicity **(Saba et al., 2013).**

Another very important and frequently used anti-neoplastic agent is cisplatin that was discovered in 1970 as an inhibitor of growth in *Eschericia coli* **(Rosenberg et al., 1969)**.

Cisplatin is widely used for the treatment of various types of solid tumors, ovarian cancer, non-small-cell lung carcinoma (NSCLC), head and neck cancer (HNC) including testicular and uterine cervical carcinomas **(Dasari et al., 2014)**. Many of the biological properties and effects of cispaltin have been well-documented with numerous reports indicating that the cellular DNA is the primary target of its anticancer activity **(Attia et al., 2012)**. The mechanism of cytotoxicity of cisplatin is known to be due to the formation of cross-linking with nucleic acids and proteins. The cytotoxicity of cisplatin is correlated closely with platinum DNA interstrand bifunctional N-7 adducts at d(GpG) and d(ApG) **(Dasari et al., 2014)**. However, full therapeutic efficacy of this drug is limited by the development of various side effects in the host, including nephrotoxicity and genotoxicity. The major target site of cisplatin toxicity is the kidney: 20% of patients receiving high-dose cisplatin develop severe renal dysfunction **(Ahmed et al., 2014)**. Cisplatin-induced nephrotoxicity occurs through direct tubular toxicity, inflammation, vascular factors and oxidative stress **(Sung et al., 2008)**. Oxidative stress is caused by various free oxygen radicals in kidney, including the superoxide anion, the hydrogen peroxide and the hydroxyl radical. Reactive oxygen species (ROS) also important in enhancing inflammation through the activation of nuclear factor-kB (NF-κB). Oxidative stress and inflammation have been suggested to be the major mechanisms in the pathogenesis of cisplatin-induced nephrotoxicity **(Rahman et al., 2006)**. It was also reported that cisplatin caused a dose and time dependent increase of the number of cells with DNA damage **(Basu et al., 2015)**. This genotoxic effect may lead to the initiation of unrelated tumors years after the chemotherapy cessation. Besides that, it has been demonstrated that cisplatin has a potential for genetic events in the non tumor cells of both humans and animals **(Attia et al, 2012)**.

Although the broad-spectrum clinical applications of chemotherapeutic drugs for tumor treatment, as a double-edged sword, inducing severe toxic side effects, such as myelosuppression, severe damage to digestive tract, liver, kidneys and other vital organs, restrict their therapeutic efficacy, even directly or indirectly lead to death by reducing body's natural anti-tumor immunity **(Lheureux et al., 2011)**. Pharmacologically speaking, to overcome the side effects of chemotherapy, a variety of drugs, such as elevated white blood cell drug, painkillers, antiemetic and so on are employed for clinic

use to improve patients' quality of life. However, with increased administration of adjuvant drugs which can not fundamentally change cachexia of cancer patients, some new side effects will come into being. Cancer survivors receive a wide range of advice from many sources about foods they should eat, foods they should avoid, how they should exercise, and what types of supplements or herbal remedies they should take. Unfortunately, this advice is often conflicting **(Doyle et al., 2006)**. So, patients are often given complementary therapy, which is believed to improve the quality of life, improve immune system function, prolong the life, or relieve the symptoms **(Richardson et al., 2000)**. The potential role of antioxidant supplements in cancer therapy has been investigated for a number of years through research in cell lines, in animals, and in patient populations. Several studies suggest that supplementation with antioxidants can influence the response to chemotherapy as well as the development of adverse side effects that results from treatment with antineoplastic agents. A growing body of evidence suggests that a combination of treatment of chemotherapy and chemopreventive agents with anticarcinogenic activity may enhance the efficacy of chemotherapeutics and/or reduce the systemic toxicity induced by chemotherapy **(Saeidnia and Abdollahi, 2013)**. Moreover, cancer patients often have low-antioxidant levels before initiating treatment **(Ladas et al., 2004)**, therefore, administration of antioxidant exacerbates oxidative stress in cancer patients and allowing patients to tolerate chemotherapy for the full course of treatment and possibly at higher doses **(Conklin, 2004)**. As a result, patients may have better tumor response rates and increased chances of survival.

Selenium is an essential and unique trace element that plays a crucial role in health and disease. Selenium exerts many cellular physiological functions mediated by it's incorporation into selenoproteins, mainly in the form of selenocysteine (SeCys), the 21st amino acid. Functionally there are at least two different enzyme families of selenoproteins: Glutathione peroxidases (GP*x*) and thioredoxin reductases (TrxR). Being a cofactor of these antioxidant enzymes selenium takes part in scavenging free radicals, thus protecting cells, membranes and cell organelles from lipid peroxidation, enzymes and nucleic acids from the harmful effects of ROS **(Fernandes and Gandin, 2014)**. Epidemiological and animal studies indicated that many human diseases could be prevented by increasing dietary selenium mainly due to the antioxidative or cancer

chemopreventive properties of selenium compounds **(Klein, 2004)**. The major chemical forms of selenium are organic, as selenomethionine (SeMet), SeCys, and metylselenocysteine (MeSeCys), and inorganic as selenite **(Letavayová, et al., 2006)**. The antioxidant and pro-oxidant effects of selenium as well as its bioavailability and toxicity depend on its chemical form **(El-Bayoumy and Sinha, 2004; Kong et al., 2011)**. A number of experiments have revealed that some molecular selenium compound both organic compounds such as selenomethionine (SeMet), metylselenocysteine (MeSeCys) and inorganic compounds like selenite and selenite possess chemopreventive effects **(Sugie et al., 2000)** and also have anticancer activity at high dosage **(Zeng et al., 2013)**. The US National Academy of Sciences recommends that selenium intake should not exceed 400µg per day and the recommended daily intake is 55µg for adults. However recently some authors published that long-term selenium administration may worsen glucose homeostasis **(Zhou et al., 2013)**. In diabetic patients' 200µg daily dose for 3 months resulted in hyperglycemia despite the normal selenium plasma concentrations (72µg/L) **(Faghihi et al., 2013)**.

Therefore, the development of new species of selenium with higher anticarcinogenic and chemoprotective efficacy but better tolerance continues to be a priority among the researchers. In this regards, cancer nanotechnology (a multidisciplinary scientific field merging chemistry, biology, bioengineering and medicine) has raised extraordinary high expectation in oncotherapy in the last two decades. Nanoparticles of both metallic and non-metallic origin are under research and development for applications in various nanomedicine fields. Selenium nanoparticles (Nano-Se) have recently garnered a great deal of attention as potential cancer therapeutic payloads, due to their excellent biological activities and low toxicity **(Zhang et al., 2008)**. Many studies showed that Nano-Se exhibited promising *in vitro* and *in vivo* antioxidant activities through the activation of selenoenzymes **(Huang et al., 2003)**.

The present study was undertaken to evaluate the chemoprotective efficacy of selenium nanoparticles (Nano-Se) against the toxic side effects of cyclophosphamide and cisplatin in normal and Ehrlich ascites carcinoma (EAC) bearing mice model. This investigation is carried out to provide information how the selenium nanoparticles (Nano-Se) reduced the toxic side effects imparted by the cancer chemotherapeutic drugs on non-specific rather

than tumor-specific targets. As per our knowledge, there might not be any reports of chemoprotective effect of Nano-Se against chemotherapeutic drug induced systemic toxicities. Nontoxic dose of selenium nanoparticles (Nano-Se) was also standardized in normal mice. The whole experimental work is divided into following chapters:

Chapter I: Synthesis, characterization, dose selection and comparative toxicological study of Nano-Se with inorganic and organic selenium in mice.

Chapter II: Protection of cyclophosphamide induced cellular toxicity by Nano-Se in mice.

Chapter III: Chemoprotective and chemoenhacing properties of Nano-Se against cyclophosphamide induced toxicities without compromising its antitumour properties in Ehrlich ascites carcinoma bearing mice

Chapter IV: Prevention of cisplatin induced toxicity at cellular and organ level by nano-Se in mice.

Chapter V: Chemoprotective and chemoenhancing properties of Nano-Se against cisplatin induce cellular toxicities in Ehrlich ascites carcinoma bearing mice.

Previously, cancer chemopreventive and antitumor activity of selenium compounds was reported. But no investigation is performed till date to study the role of Nano-Se as an adjuvant therapy along with chemotherapy in the management of cancer. This thesis report has evaluated for the first time the chemoprotective and chemoenhancing effect of Nano-Se as monotherapy as well as combination therapy in normal and tumor bearing mice. The outcome of this research will help to proceed towards the goal of finding a suitable agent for patients with cancer, receiving chemotherapy to improve the response rate and quality of life.

Review of Literature

Cancer

Cancer is a disease of misguided cells which have high potential of excess proliferation without apparent relation to the physiological demand of the process. It is world's second killer after cardiovascular disease and it ever was killed 7.6 million people in 2010, out of them three quarters were from in low and middle income countries. That number is expected to increase to 9.0 million up to 2015 and rise further to 11.5 million in 2030 **(WHO, 2014)**. Cancer is caused by mutations in somatic cells even though inherited genetic mutations may predispose some individuals to certain types of cancer (**Lodish et al., 2000)**. Cancer cells can be defined and separated from normal cells by collectively possessing a number of capabilities. These comprise evading cell death, self sufficiency in growth signals and insensitivity to anti-growth signals, angiogenesis and tissue invasion. The capabilities are considered to be sequentially acquired over time through clonal selection causing a progressive transformation to malignancy. Early events are suggested to be self sufficiency in growth signals and insensitivity to anti-growth signals while late events are tissue invasion and limitless replicative potential **(Hanahan and Weinberg, 2000)**.

Cancer chemoprevention

Cancer chemoprevention was defined as the administration of agents to prevent induction, to inhibit, or to delay the progression of cancer **(Sporn et al., 1979)** or as the inhibition or reversal of carcinogenesis at a premalignant stage **(Kellof et al., 2000)**. It makes use of suitable pharmacological agents **(Kelloff and Hwak, 2004)** or of dietary agents, under the form either of macronutrients, micronutrients, or non-nutritive phytochemicals **(Ferguson et al., 2004)**.

For a rational implementation of chemoprevention strategies it is essential not only to assess safety and efficacy of candidate chemopreventive agents in preclinical models and in humans but also to understand their mechanisms of action.

Classification of mechanisms of chemopreventive agents

In 1988, De Flora and Ramel **(Flora and Ramel, 1998)** proposed a detailed classification of inhibitors of mutagenesis and carcinogenesis. This scheme takes into account the three

general levels of prevention in connection with the possible mechanisms of cancer chemopreventive agents. In particular, primary prevention, having the goal of preventing the occurrence of the malignant disease, includes inhibition of mutation and cancer initiation, either in the extracellular environment or inside cells, followed by inhibition of tumor promotion. Secondary prevention exploits a variety of mechanisms aimed at inhibiting progression of a timely diagnosed benign tumor towards malignancy. Tertiary prevention has the goal of preventing local relapses of the disease and of inhibiting invasion and metastasis. Although tertiary prevention falls outside the definition of cancer chemoprevention in strict sense, it is illustrated in **Fig. 1** because a number of mechanisms coincide with those exploitable in primary prevention and secondary prevention settings. A further target of chemoprevention is prevention of second primary tumors, either synchronous or metachronous. This kind of intervention, which is often pursued in chemoprevention trials, may be viewed in the framework of primary prevention in that it is addressed to individuals who are apparently "healthy" with regard to the tumor that may become apparent at a later stage. Alternatively, it can be viewed in the framework of secondary prevention since the possible second tumor, albeit clinically silent, is at an advanced stage when the intervention is made **(Flora, et al., 2001).**

PRIMARY PREVENTION

1. Inhibition of mutation and cancer initiation in the extracellular environment or in nontarget cells

- 1.1. Inhibition of uptake of mutagens/carcinogens
  - 1.1.1. Inhibition of penetration
  - 1.1.2. Removal from the organism
- 1.2. Inhibition of the endogenous formation of mutagens and carcinogens
  - 1.2.1. Inhibition of the nitrosation reaction
  - 1.2.2. Modification of the intestinal microbial flora
- 1.3. Complexation, dilution and/or deactivation of mutagens/carcinogens outside cells
  - 1.3.1. By physical or mechanical means
  - 1.3.2. By chemical reaction
  - 1.3.3. By enzyme–catalyzed reaction
- 1.4. Favoring absorption of protective agents
- 1.5. Stimulation of trapping and detoxification in nontarget cells

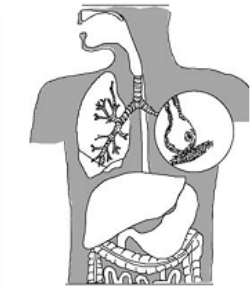

2. Inhibition of mutation and cancer initiation in target cells

- 2.1. Modification of transmembrane transport
  - 2.1.1. Inhibition of cellular uptake
  - 2.1.2. Stimulation of extrusion outside cells
- 2.2. Modification of metabolism
  - 2.2.1. Inhibition of activation of promutagens/ procarcinogens by Phase I enzymes
  - 2.2.2. Induction of Phase I detoxification and Phase II conjugation pathways, or acceleration of decomposition of reactive metabolites
  - 2.2.3. Stimulation of activation, coordinated with detoxification and blocking of reactive metabolites

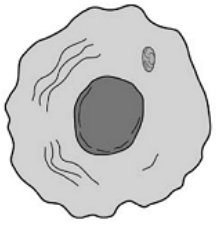

- 2.3. Blocking or competition
  - 2.3.1. Trapping of electrophiles by either chemical reaction or enzyme–catalyzed conjugation
  - 2.3.2. Antioxidant activity and scavenging of reactive oxygen species
  - 2.3.3. Protection of DNA nucleophilic sites
- 2.4. Inhibition of cell replication
- 2.5. Maintenance of DNA structure and modulation of DNA metabolism and repair
  - 2.5.1. Increase of fidelity of DNA replication and repair
  - 2.5.2. Stimulation of repair and/or reversion of DNA damage
  - 2.5.3. Inhibition of error-prone repair pathways
  - 2.5.4. Correction of hypomethylation
  - 2.5.5. Inhibition of histone deacetylation
  - 2.5.6. Blocking of telomerases or inhibition of their activity
- 2.6. Control of gene expression
  - 2.6.1. Targeted inactivation of oncogenes
  - 2.6.2. Inhibition of oncogene expression
  - 2.6.3. Inhibition of oncogene sequences or activity
    - 2.6.3.1. Inhibition of translation targeted to oncogene mRNA
    - 2.6.3.2. Inhibition of transcription of specific DNA sequences
    - 2.6.3.3. Blocking of target genes
    - 2.6.2.4. Farnesyltransferase inhibition
  - 2.6.4. Neutralization or post–translational modification of oncogene products
  - 2.6.5. Replacement of deleted tumor suppressor genes
  - 2.6.6. Mimicking the DNA binding of tumor suppressor genes by antiidiotypic antibodies
  - 2.6.7. Killing of cells lacking tumor suppressor genes

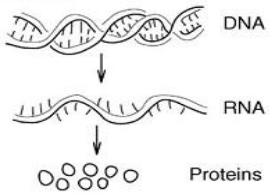

3. Inhibition of tumor promotion

- 3.1. Inhibition of genotoxic effects (see 1 and 2)
- 3.2. Antioxidant activity and scavenging of free radicals
- 3.3. Antiinflammatory activity
  - 3.3.1. Cyclooxygenase inhibition
  - 3.3.2. Lipooxygenase inhibition
  - 3.3.3. Inhibition of inducible nitric oxide synthase
  - 3.3.4. Leukotriene receptor antagonism
- 3.4. Inhibition of proteases
- 3.5. Inhibition of cell proliferation
  - 3.5.1. Inhibition of ornithine decarboxylase
  - 3.5.2. Promoting proteasomal degradation of cyclins
  - 3.5.3. Interference with multiple signaling pathways
- 3.6. Induction of cell differentiation
- 3.7. Modulation of cell apoptosis
- 3.8. Signal transduction modulation
- 3.9. Protection of intercellular communications

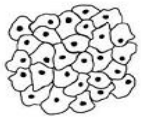

SECONDARY PREVENTION

4. *Inhibition of tumor progression*
   - 4.1. Inhibition of genotoxic effects (see 1 and 2)
   - 4.2. Antioxidant activity and scavenging of free radicals
   - 4.3. Inhibition of proteases
   - 4.4. Signal transduction modulation
   - 4.5. Effects on the hormonal status
     - 4.5.1. Selective estrogen receptor modulation
     - 4.5.2. Aromatase inhibition
     - 4.5.3. Selective blocking of prostaglandin E_2 receptors
     - 4.5.4. Decrease in ovarian hormones by dietary isoflavones
     - 4.5.5. Inhibiting the pituitary secretion of luteinizing hormone
     - 4.5.6. Preventing conversion of testosterone into dehydrotestosterone by 5α–reductase
     - 4.5.7. Selective androgen receptor antagonism
   - 4.6. Effects on the immune system
   - 4.7 Inhibition of angiogenesis
   - 4.8 Antineoplastic activity by either mechanical, physical, chemical, or biological means

TERTIARY PREVENTION

5. *Inhibition of invasion and metastasis*
   - 5.1. Antioxidant activity and scavenging of free radicals
   - 5.2. Signal transduction modulation
   - 5.3. Inhibition of cell proliferation (see 3.4)
   - 5.4. Modulation of cell apoptosis
   - 5.5. Induction of cell differentiation
   - 5.6. Inhibition of angiogenesis
   - 5.7. Effect on cell-adhesion molecules
   - 5.8. Inhibition of proteases involved in basement membrane degradation and modulation of the interaction with the extracellular matrix
   - 5.9. Activation of antimetastasis genes

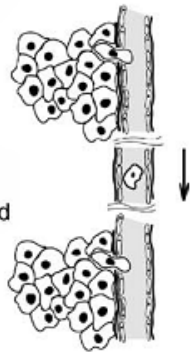

Figure 1: Mechanisms of inhibitors of mutagenesis and carcinogenesis

Chemotherapy in cancer

In the early 1900s, the famous German chemist Paul Ehrlich set about developing drugs to treat infectious diseases. He was the one who coined the term ‘‘chemotherapy’’ and defined it as the use of chemicals to treat disease. He was also the first person to document the effectiveness of animal models to screen a series of chemicals for their potential activity against diseases, an accomplishment that had major ramifications for cancer drug development. In 1908, his use of the rabbit model for syphilis led to the development of arsenicals to treat this disease. Ehrlich was also interested in drugs to treat cancer, including aniline dyes and the first primitive alkylating agents, but apparently was not optimistic about the chance for success. The laboratory where this work was done had a sign over the door that read, ‘‘Give up all hope oh ye who enter’’ **(DeVita and Chu, 2008).**

Chemotherapy is one of three pillars of cancer treatment along with surgical treatment and radiation therapy. Chemotherapy treatment can be used for the following intents: curing, prolonging survival, or palliation. Chemotherapy uses drugs (organic drugs or metal-containing) to destroy cancer cells often in a non-specific way. The drugs differ in their mechanism and side effects. When combined with other modes of treatment chemotherapy can (a) reduce the bulk of tumor lump before surgery or radiation (neo-adjuvant), (b) kill the remaining cancer cells after surgery or radiation (adjuvant) and (c) destroy recurrent and metastatic cancer cells. These drugs can be administered using several methods namely injection, intra-arterial (IA), intra-peritoneal (IP), intravenous (IV), topically and orally (**Strebhardt and Ullrich, 2008; Hajdu, 2005**).

There are several chemotherapeutic agents which can be classified as alkylating agents, proliferation inhibitors, enzyme inhibitors, DNA intercalators and antimetabolites, DNA-synthesis inhibitors and membrane permeability modifiers. Some very common drugs which are widely used in medical practice according to National Institute of Health (NIH-USA) are doxorubicin, epirubicin, bleomycin, fluorouracil, vincristine, vinblastine, etoposide, teniposide, chlorambucil, melphalan, busulfan, carmustine (BCNU), lomustine (CCNU), streptozotocin, thiotepa, dacarbazine (DTIC), methotrexate, cytarabine, azaribine, mercaptopurine, thioguanine, actinomycin D, plicamycin, mitomycin-C, asparaginase, procarbazine, hydroxyurea, topotecan, irinotecan, gemcitabine,

temozolamide, capecitabine, tezacitabine, mechlorethamine, cyclophosphamide, mitoxantrone, and tegafur **(NIH)**.

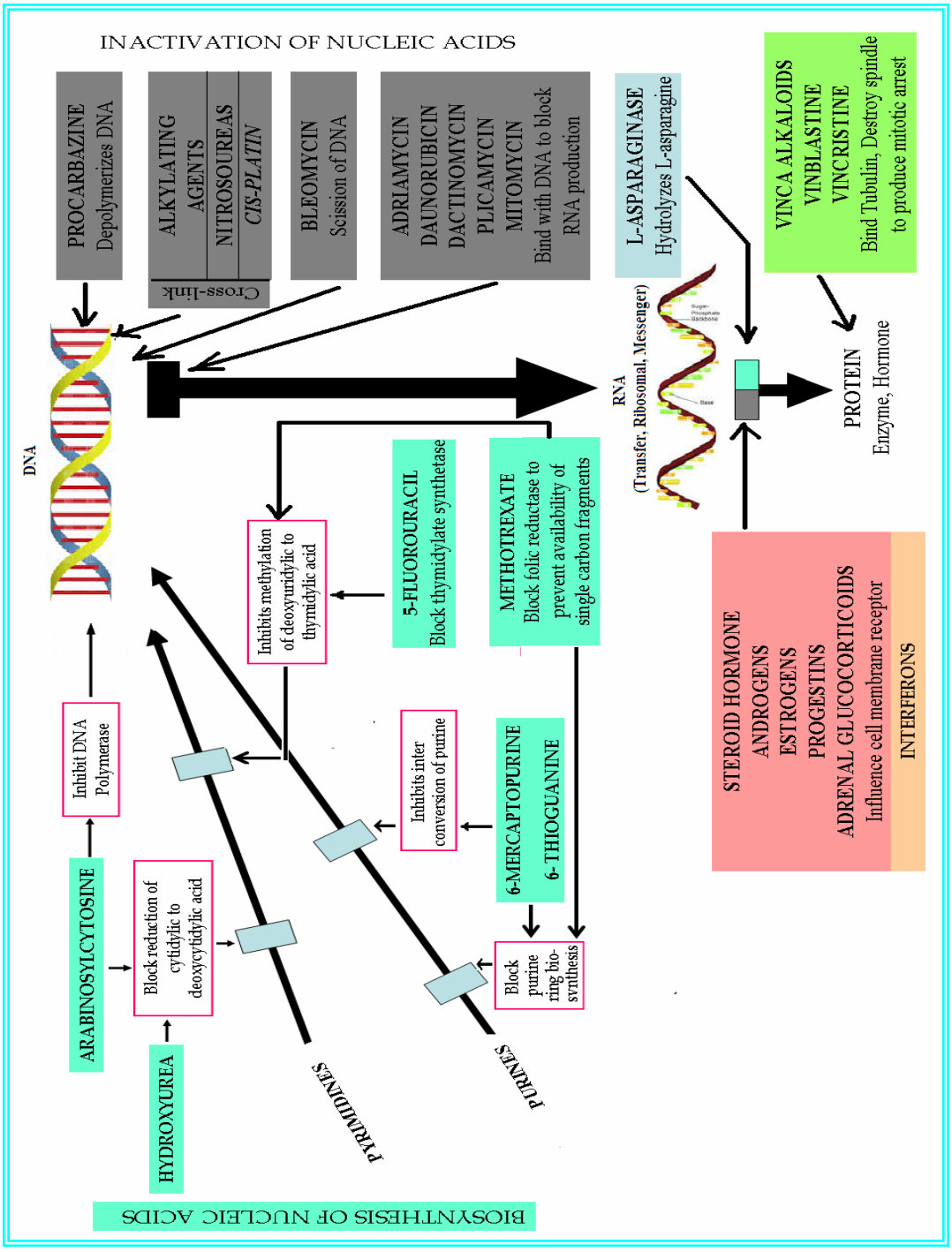

Figure 2: Different types of chemotherapeutic drugs and their site of mechanism action

Although chemotherapy kills cancer cells, it can damage normal cells and cause significant side effects. The side effects vary depending on the particular chemotherapy drug, dosage, route of administration and patient characteristics. Some chemotherapy side effects can be severe enough to require hospitalization. The side effects may include:

- Immunosupression and myelosupresion **(Lissoni et al., 1997):**
  - Low white blood cell counts which increases the risk of infection
  - Low red blood cell counts (anemia) which can require transfusion
  - Low platelet counts which can lead to bleeding
- Damage and irritation to cells lining to the digestive tract which can produce **(Lissoni et al., 1997)**:
  - Nausea and vomiting
  - Diarrhea
- Neurological side effects **(Tannock et al., 2004):**
  - Numbness and tingling or shooting pains, most often in the fingers and toes.
  - Tiredness, confusion and depression
- Secondary neoplasm **(Hijiya et al., 2007)**
- Infertility **(Brydøy et al., 2007)**
- Nephrotoxicity **(Amudha et al., 2007)**
- Teratogenicity **(Arnon et al., 2001),** etc.

Cyclophosphamide

The oxazaphosphorine cyclophosphamide (2-[bis-(2-chloroethyl)amino]-tetrahydro-2H-1,3,2-oxazaphosphorine-2-oxide, Cytoxan, the most frequently used nitrogen mustard for antineoplastic chemotherapy and an essential component of many effective drug combinations.

Cyclophosphamide was synthesized in 1958 and it soon became apparent that these drugs are activated in the liver (by cytochrome P450) and not by the tumor. CP used as a single agent, but more frequently, in combination with other anticancer agents in management of a wide spectrum of solid tumors and hematological malignancies. The combined use of CP with other anticancer drugs in the chemotherapy is intended to obtain synergistic or additive anticancer effect resulting from complementary mechanisms of action (**Hermans et al., 2003**).

Mechanism of action of CP

Like other alkylating agents, the alkylating nitrogen mustards of CP work through the covalent bonding of highly reactive alkyl groups with nucleophilic groups of nucleic acids. Covalent binding to cellular proteins is also possible. Following metabolic activation, bifunctional alkylating nitrogen mustards of CP are generated, which are capable of reacting with the Nitrogen-7 (N^7) atom of purine bases in DNA, especially when they are flanked by adjacent guanines **(Fig. 3) (Kohn et al., 1987)**.

At alkaline or neutral pH, the nitrogen mustard is converted to chemically reactive carbonium ion through imonium ion. Carbonium ion reacts with the N^7 of the guanine residue in DNA to form a covalent linkage. The second arm in phosphoramide mustard can react with a second guanine moiety in an opposite DNA strand or in the same strand to form crosslinks **(Springer et al., 1998)**. The O^6 atom of guanine may also be a target for oxazaphosphorines **(Friedman et al., 1999)**.

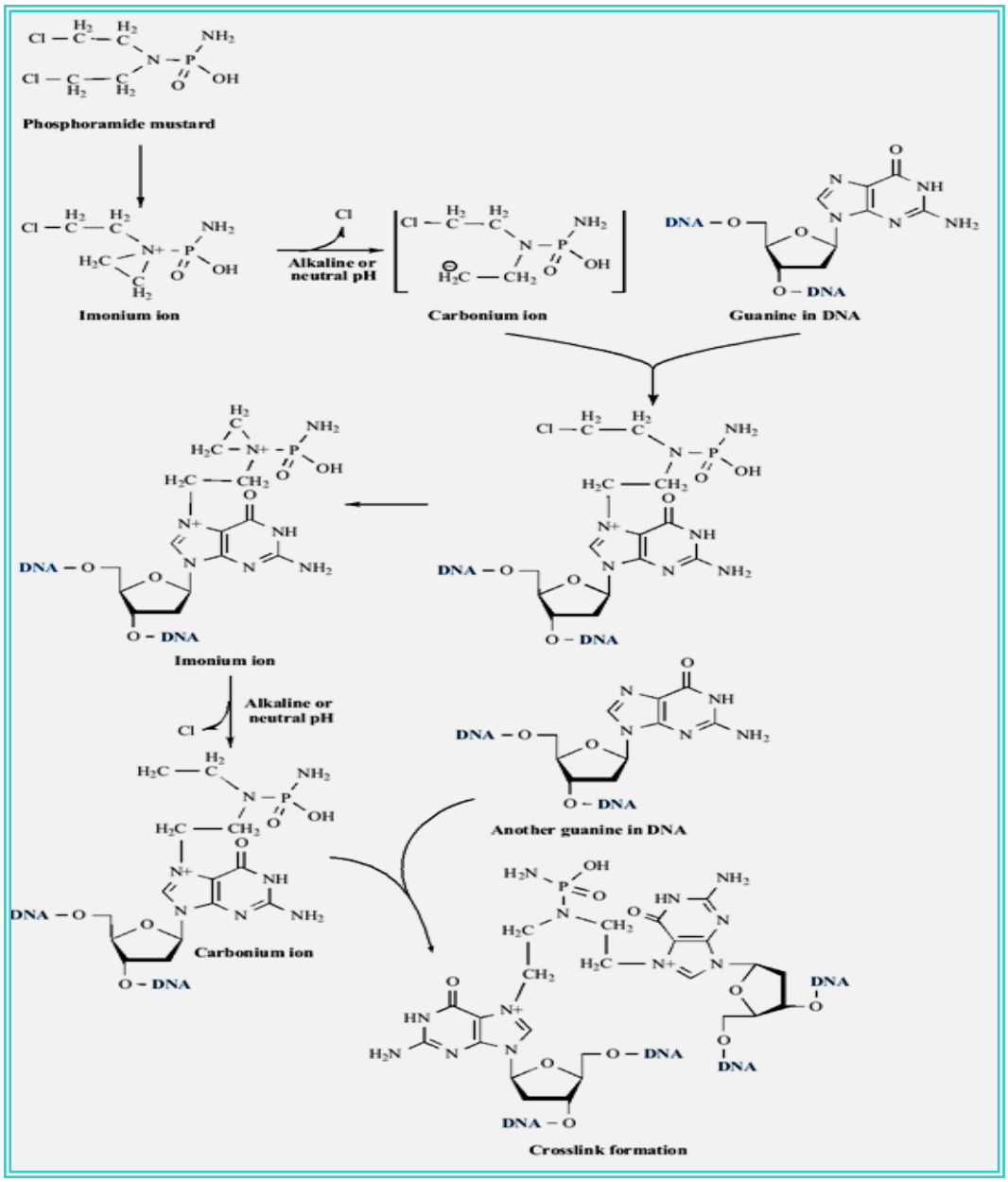

Figure 3: Mechanism action of Cyclophosphamide

CP, as with all other alkylating agents, destroy tumor cells through apoptosis (programmed cell death) initiated by DNA damage, modulation of cell cycle and other anti proliferative effects (**Bhatia et al., 1995**). It is generally accepted that the main mechanism that results in cell death is inhibition of DNA replication, as the interlinked strands do not allow separation of the two strands (**Schwartz and Waxman, 2001**).

Apoptosis is characterized by a cascade like activation of intracellular cysteine-proteases (i.e. caspases). Distinct caspase cascades are involved in receptor mediated or chemical induced apoptosis (**Sun et al., 1999**). Drug induced apoptosis is always mediated by the mitochondrial pathway leading to activation of the initiator caspase-9, which in turn activates the effectors caspases-3 and caspase-7 (**Bruce et al., 1966**).

In addition to the final alkylating metabolites, chloroacetaldehyde (CAA) and acrolein are also related to the cytotoxicity of CP. CAA induces depletion of intracellular sulthydryl agents including reduced glutathione (GSH), resulting in cytotoxicity **(Bruggemann et al., 1997)**. Therefore, stimulation of cellular GSH synthesis may protect against cytotoxicity of CP. Acrolein is able to induce single strand DNA break that is possibly associated to the cytotoxicity of CP **(Crook et al., 1986)**.

Metabolism of CP

The metabolic pathways of CP in humans are shown in **Fig**. **4**. As a prodrug, CP is converted to active alkylating mustard by the liver in the body **(Sladek, 1988)**. The initial activation of CP is 4-hydroxylation at C^4 of oxazophosphorine ring to form 4-OH-CP **(Colvin et al, 1976)**. Multiple cytochrome P450 (CYP) enzymes including CYP2B6, CYP2C9 and CYP3A4 in the liver are responsible for CP 4-hydroxylation **(Chen et al., 2004; Huang et al., 2000)**. CYP2B6 is the major contributor (a mean of ~45% of total metabolism) for the activation of CP, compared with 25% and 12% for CYP3A4 and CYP2C9, respectively **(Chen et al., 2004)**. Other CYPs including CYP2A6, CYP2C8 and CYP2C19 also make a minor contribution to CP 4-hydroxylation **(Chang et al., 1993)**. By contrast, the inactivation pathway of CP involves minor (~10%) side chain oxidation (N-dechloroethylation) primarily by CYP3A4/3A5 and, to a minor extent, by CYP2B6 to generate 3-dechloroethylifosfamide and the neurotoxic and nephrotoxic byproduct CAA **(Ren et al., 1997)**.

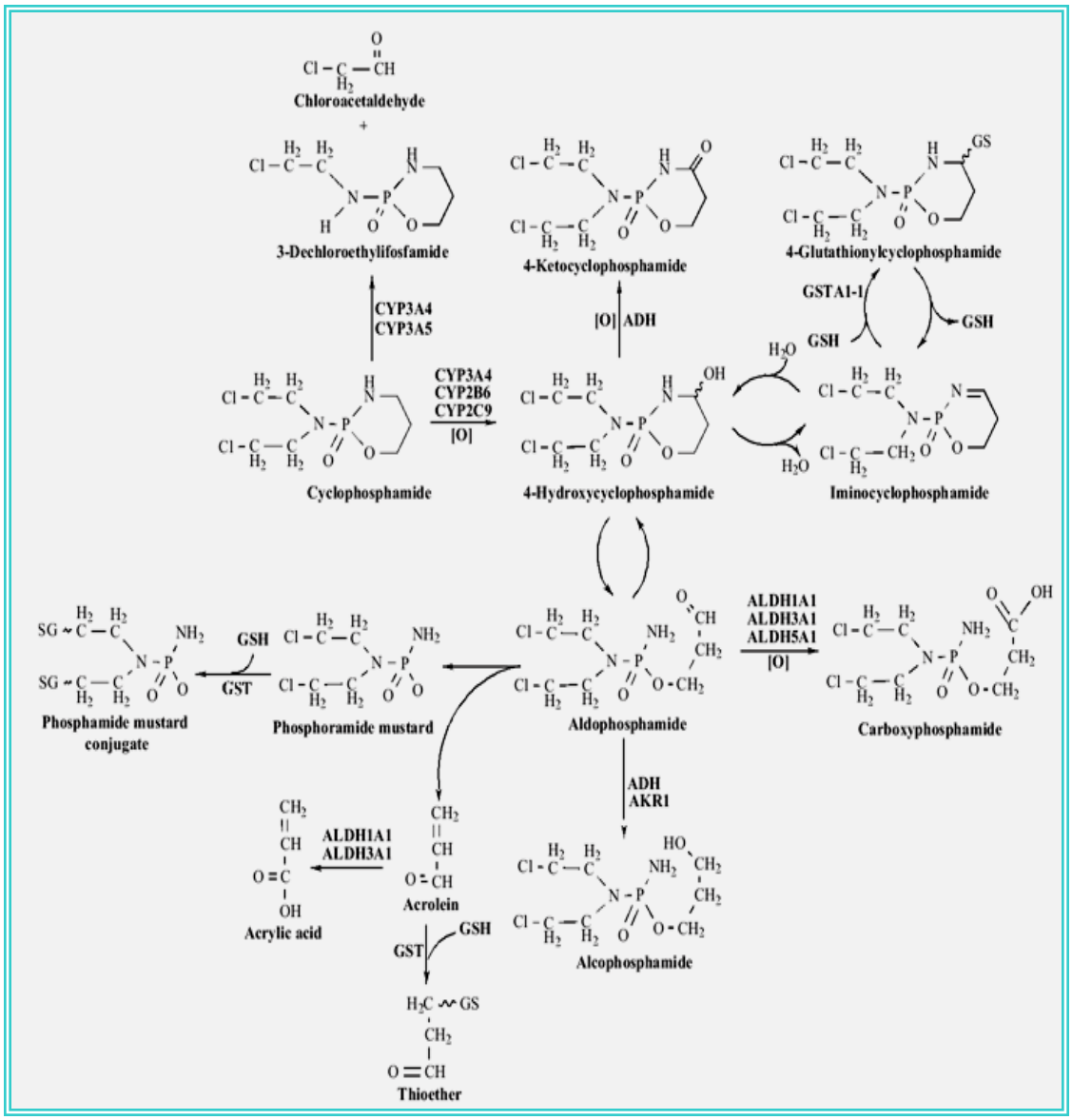

Figure 4: Metabolism of Cyclophosphamide

4-OH-CP is a major circulating metabolite of CP that enters tumor cells and decomposes through its tautomer aldophosphamide (an aldehyde intermediate) by spontaneous 3-elimination to form ultimate cytotoxic phosphoramide mustard (N,N-bis-2-(2-chloroethyl) phosphorodiamidic acid) and an equimolar amount of the byproduct acrolein (a highly electrophilic α,β-unsaturated aldehyde) **(Colvin, 1999)**. Alternatively, aldophosphamide can be oxidized by alcohol dehydrogenase (ADH) and aldo-keto reductase (AKR1) to generate alcophosphamide. Alternatively, 4-OH-CP is detoxified to O-carboxyethylcyclophosphoramide mustard (CPM, namely, carboxyphosphamide) by

cytosolic ALDH1A1, and to a much lesser extent, by ALDH3A1 and ALDH5A1 **(Moreb et al., 2005; Yule et al., 2004)**. Furthermore, 4-OH-CP is oxidized by ADH to non-toxic 4-keto-cyclophosphamide (4-keto-CP) **(Boddy et al., 1992)**, but to a much lesser extent compared with CEPM formation. Moreover, 4-OH-CP undergoes reversible dehydration to form iminocyclophosphamide that is further conjugated with intracellular reduced glutathione (GSH) by glutathione-S-transferase (GST) A1, A2, Ml, and P1, giving rise to non-toxic 4-glutathionylcyclophosphamide (GSCY) **(Dirven et al., 1994)**.

The resultant phosphoramide mustard is a bifunctional alkylator of DNA and the ultimate cytotoxic metabolite of CP **(Struck et al., 1975)**. The alkylation involves generation of the intermediate phosphoramide aziridinium ion through an intramolecular nucleophilic attack (cyclization reaction) of the nitrogen on the 3-carbon of a chloroethyl chain **(Ludeman, 1999)**. Cellular thiols (e.g., GSH) and other nucleophiles react rapidly with phosphoramide aziridinium ions, resulting in thioether products **(Gamcsik et al., 1999)**. CEPM is one of the major chemically stable metabolites of CP, which are easily detected in patient plasma and urine However, acrolein is a highly reactive aldehyde that covalently binds to cellular macromolecules and subsequently disrupts the function and causes organ toxicity **(Brock et al., 1979)**. It is detoxified by conjugation with GSH via GSTs in hepatocytes **(Gurtoo et al., 1981)** and this may cause intracellular GSH depletion and injuries of the hepatocytes **(DeLeve, 1996)**. Reaction of GSH with acrolein is via nucleophilic addition at the β-carbon atom, generating stable thioether compounds **(Ramu et al., 1996).**

Antitumor activity of CP

CP is the most widely used alkylating agent in the treatment for hematological malignancies and a variety of solid tumors, including leukemia **(Rao et al., 2005)**, breast cancer **(Goncalves et al., 2005)**, lung cancer **(Hobdy et al., 2004)**, lymphomas **(Escalon et al., 2005)**, prostate cancer **(Nicolini et al., 2004)**, ovarian cancer **(Morgan et al., 2001)**, and multiple myeloma **(Dimopoulos et al., 2004)**. Although its role in the treatment for ovarian cancer and small-cell lung cancer is declining, CP continues to be used in treatment of breast cancer as a critical component of the CMF, CEF (CP, epirubicin, and 5 -fluorouracil), MVC (mitoxantrone, vinblastine, and CP) and TAC

(docetaxel, doxorubicin and CPA) regimen **(O'Regan et al., 2005)**. Higher doses of CP are used in the treatment prior to bone marrow transplantation for aplastic anemia, leukemia and other malignancies **(Szumilas et al., 2005)**.

Toxicity of CP

In cancer patients, CP is primarily activated by CYP3A4, CYP2C9 and CYP2B6 in the liver, followed by erythrocyte mediated transport of the activated metabolites to the tumor tissue via blood circulation. However, these activated metabolites also gain entry into normal tissues, where they may induce host toxicity. For CP, the usual dose limited toxicity is myelosuppression. At higher doses used prior to marrow transplantation, the dose limited toxicity is cardiac toxicity **(Peters et al., 1989)**. Besides cardiac toxicity, hemorrhagic cystitis, water retention and hyponatremia are found in patients receiving high dose CP.

Acrolein is the causal agent to hemorrhagic cystitis. Using mesna (sodium-2-mercaptoethanesulfonate) can reduce the incidence of hemorrhagic cystitis **(Brock and Pohl, 1986)**. A direct effect of CP on the renal tubules leads to excess water retention.

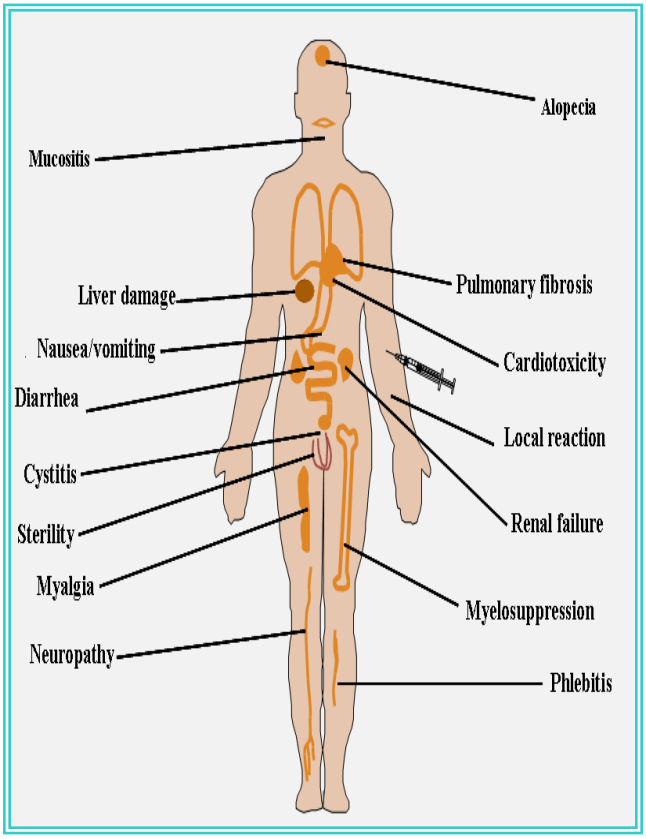

Figure 5: Organ specific toxicity of Cyclophophamide

This can be managed by hydration with isotonic fluids. In women receiving CP, methotrexate and fluorouracil for treatment of breast cancer, the severe toxicity thromboembolic events have been reported **(Pritchard et al., 1997)**. Elevation of serum level of amino transferases in patients treated with CP has also been reported. This CP induced liver injury results from metabolites of CP, especially acrolein and is mainly dose dependent **(Honjo et al., 1988)**. Metabolites of CP have been demonstrated to be

teratogens and carcinogens in animals. Malformations have been associated to first trimester exposure to CP (**Zemlickis et al., 1993)**. Several studies suggested CP as a single chemotherapeutic agent induced leukemia in human The mechanisms are unknown, but this may be associated with the cytogenetic toxicity of CP. Patients with breast cancer and inheritance of a combined gene deletion of GSTM1 and GSTT1 might bear an increased risk to develop a secondary CP induced hematological neoplasia **(Haas et al., 2002)**.

Cisplatin

The great impact in the treatment of cancer of the platinum coordination complex cisplatin, [cis-diamminedichloro platinum (II)] or CDDP is a paradigm within the use of metals in medicine. Cisplatin is the queen of chemotherapy among over 700 FDA-approved drugs with applications in more than 50% of human cancers, including the lucrative non-small cell lung cancer (**Boulikas, 2007**).

The biological activity of cisplatin, was discovered serendipitously about 125 years after the initial report of its synthesis and characterization. Although the synthesis and characterization of cisplatin was first reported by Peyrone in 1845 (**Peyrone, 1845**), its anticancer properties remained unnoticed until the mid-1960s, when Rosenberg and co-workers studied the effects of electric fields on *Escherichia coli* growth **(Rosenberg et al., 1965)**. The platinum electrodes released by redox reactions some platinum complexes which provoked complete stop of cell division in the bacterial rods. Amongst the platinum complexes formed, cisplatin was identified as the main antiproliferative agent (**Rosenberg et al., 1969**). In the next years cisplatin developed into one of the most widely used drugs in cancer chemotherapy.

Cisplatin, usually in combination with other drugs, is commonly used as first line chemotherapy against cancers of the lung, head-and-neck, esophagus, stomach, colon, bladder, testis, ovaries, cervix, uterus and as second line treatment against most other advanced cancers, such as cancers of the breast, pancreas, liver, kidney, prostate as well as against glioblastomas, metastatic melanomas, and peritoneal or pleural mesotheliomas (**Langerak and Dreisbach, 2001**).

Biochemical mechanisms of action of cisplatin

It is generally accepted that binding of CDDP to genomic DNA (gDNA) in the cell nucleus is the main event responsible for its antitumor properties (**González et al., 2001**). Thus, the damage induced upon binding of CDDP to gDNA may inhibit transcription, and/or DNA replication mechanisms. Subsequently, these alterations in DNA processing would trigger cytotoxic processes that lead to cancer cell death. **Fig. 6 shows** the main molecular events in which CDDP is involved before reaching its ultimate target gDNA.

2.2.1.1. Drug accumulation

Once CDDP has been intravenously administered to a patient, it rapidly diffuses into tissues and binds to plasma proteins. Binding of CDDP to plasma proteins is a result of

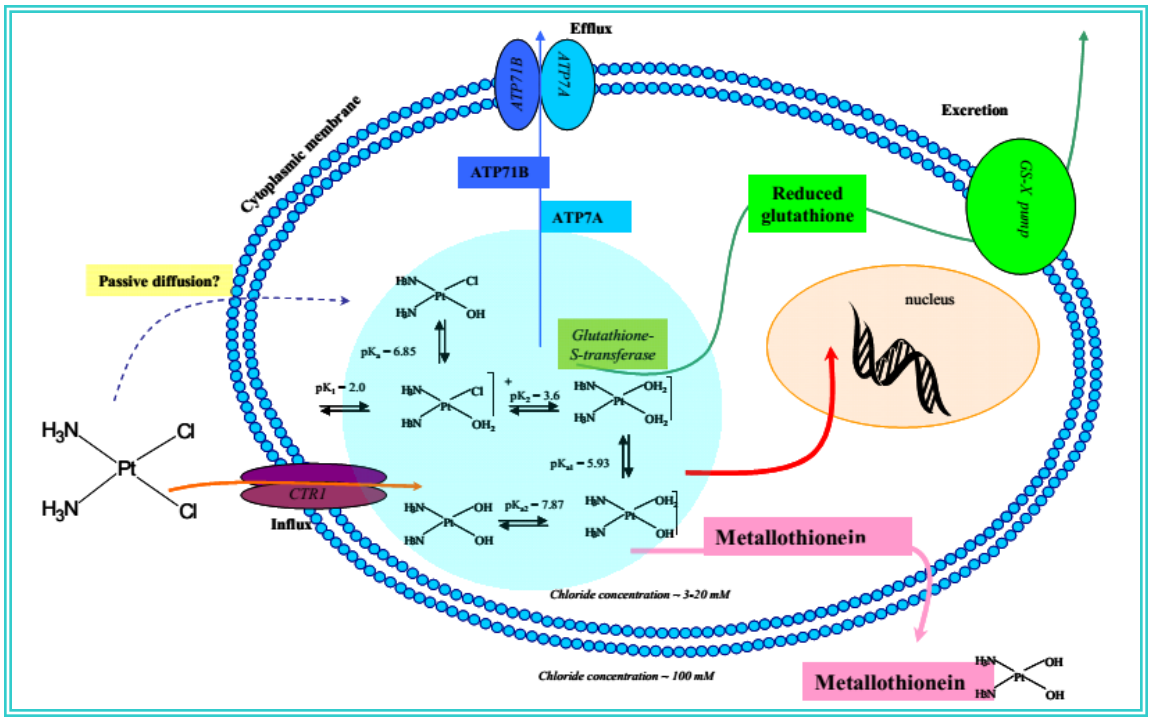

Figure 6: Pharmacokinetic of Cisplatin

the strong reactivity of platinum against sulfur of thiol groups of amino acids such as cysteine. Hence, near 90% of the platinum in the blood is bound to albumin and other plasma proteins leading to inactivation of a great amount of CDDP molecules (**Judson and Kelland, 2000**). Loss of the chloride groups from the CDDP molecule is required before it binds to gDNA. Outside the cell, chloride concentration is around 100 mM. However, within the cell, chloride concentrations range between 2 and 30 mM and

cisplatin aquation occurs. Consequently, water molecules replace one or both chloride leaving groups. The result is the formation of the $[Pt(H_2O)Cl(NH_3)_2]^+$ and $[Pt(H_2O)_2(NH_3)_2]_2^+$ cations. These mono and diaquo species of CDDP are very reactive towards nucleophile centres of biomolecules because H_2O is a much better leaving group than Cl^- (**Jamieson and Lippard, 1999**).

The biochemical mechanism by which CDDP crosses the cell membrane still remains unclear. CDDP, according to a number of studies enters cells through passive diffusion and is independent on an optimum pH **(Binks and Drobota, 1990)**. However, it was also found later that a certain degree of CDDP uptake seemed to be energy dependent and some recent observations point towards a direct connection between the cellular concentrations of copper and platinum, which leads to propose an active transport for CDDP. Thus, experiments with the yeast protein Ctr1 (a high-affinity copper transporter) and CDDP, revealed that mutation or deletion of the *CTR1* gene leads to stronger CDDP resistance and to intracellular reduction of platinum levels in yeast and in mouse cells **(Ishida et al., 2002)**. Interestingly, CDDP accumulation in cells was increased when human *CTR1* gene was over expressed, although the ability of the drug to access its cytotoxic targets was unaltered **(Holzer et al., 2004)**. On the other hand, it has been found that copper-transporting P-type adenosine triphosphate (ATP7B), which regulates copper homeostasis in the cell, has a role in CDDP efflux and is associated with CDDP resistance *in vitro* **(Komatsu et al., 2000)**, and in various cancers.

Hence, expression of ATP7B in human carcinoma cells modulates sensitivity to CDDP and copper through a more efficient efflux of the two agents **(Holzer et al., 2004)**. Another exporter protein implicated in CDDP resistance through drug efflux is the ATP-binding cassette, sub-family C2 (ABCC2 also known as MRP2 or cMOAT) **(Cui et al., 1999)**. Altogether these data indicate that there is a connected transport for copper and CDDP because both copper and CDDP (i) can reduce the uptake of each other, (ii) trigger the degradation and delocalization of CTR1, and (iii) also show bidirectional cross-resistance **(Safaei and Howell, 2005)**.

Cisplatin-induced oxidative stress

Under normal physiological conditions, cells control reactive oxygen species levels by balancing the generation of reactive oxygen species with their elimination by scavenging

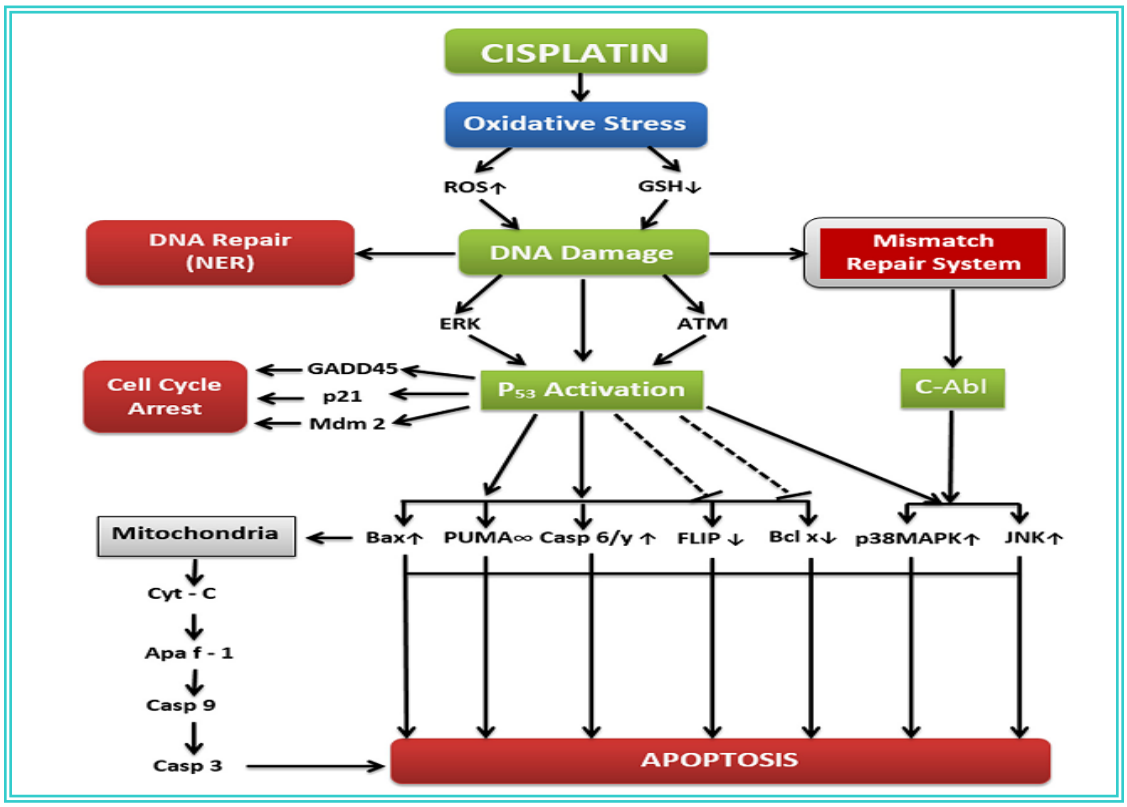

Figure 7: Overview of molecular mechanisms of cisplatin in cancer treatment

system (reduced glutathione-GSH, superoxide dismutase-SOD, and catalase-CAT). But under oxidative stress conditions, excessive reactive oxygen species can damage cellular proteins, lipids and DNA, leading to fatal lesions in cells that contribute to carcinogenesis. Cancer cells exhibit greater reactive oxygen species stress than normal cells do, partly due to oncogenic stimulation, increased metabolic activity and mitochondrial malfunction. Oxidative stress is the one of most important mechanisms involved in CDDP toxicity. The mitochondrion is the primary target for CDDP induced oxidative stress, resulting in loss of mitochondrial protein sulfhydrl group, calcium uptake inhibition and reduction of mitochondrial membrane potential **(Saad et al., 2004)**. Exposure to oxidative stress can upset regular biological functions. CDDP also induces reactive oxygen species that trigger cell death besides DNA damage. Cell death occurs

upon immediate activation of numerous signaling pathways, whereas the definite pathways depend on the (cancer) cell. The formation of reactive oxygen species depends on the concentration of cis-diamminedichloro platinum (II) and the length of exposure. The intracellular redox homeostasis is maintained by the thiol group (–SH) containing molecules. Under certain conditions a thiol group may lead to formation of thiyl radicals that in turn can interact with molecular oxygen, therefore generating reactive oxygen species **(Desoize, 2002)**.

DNA Lesions

Upon entering a cell, all platinating agents become aquated, losing chloride or oxalate

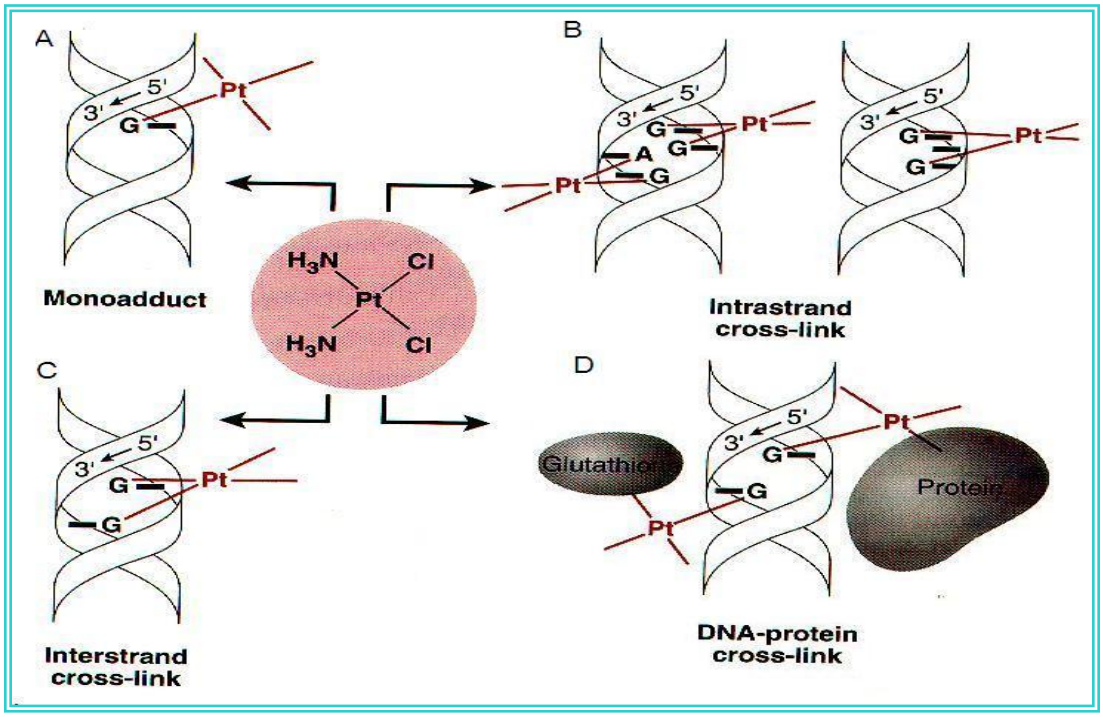

Figure 8: Main adducts formed after binding of CDDP to DNA.
(A) Monofunc- tional adduct (B) 1,2-intrastrand cross-link, (C) Interstrand cross-link, , and (D) Protein-DNA cross-link. The main site of attack of cis -DDP to DNA (N^7 of guanine) is shown in the central panel.

ions, and gaining two water molecules. This positively charged molecule is then able to interact with nucleophilic molecules within the cell, including DNA, RNA, and proteins.

It is generally agreed that DNA is the preferential and cytotoxic target for cisplatin. When binding to DNA, platinating agents favor the N^7 atoms of the imidazole rings of guanosine and adenosine. Three different types of lesions can form on purine bases of DNA: monoadducts, intrastrand crosslinks, and interstrand crosslinks (**Fig. 8**) **(Zorbas and Kepplar, 2005)**.

Monoadducts are first formed as one molecule of water is lost from aquated platinating agents; however, greater than 90% of monoadducts then react to form crosslinks. Almost all of these crosslinks are intrastrand, with the majority being 1, 2-d(GpG) crosslinks. Additional DNA lesions include interstrand crosslinks **(Rabik and Dolan, 2008)**.

Toxicities of cisplatin

Cisplatin interacts with DNA, and forms covalent adduct with purine DNA bases and this platinum compound, interaction is the root cause for cytotoxic effect of cisplatin **(Yousef et al., 2009)**. Cisplatin treatment has been associated with several toxic side effects including nephrotoxicity **(de Jongh et al., 2003)**, hepatotoxicity and cardiotoxicity **(Al-Majed, 2007)**. Decrease in antioxidant defense system is reported due to oxidative stress through the generation of reactive oxygen species, including antioxidant enzymes and non enzymatic molecules, reduced glutathione, are major alterations in the cisplatin toxicity **(Kart et al., 2010)**.

Nephrotoxicity

Nephrotoxicity is primarily due to the renal excretion of cisplatin, the kidney accumulates a higher effective concentration of cisplatin than any other organ. This accumulation preferentially affects the terminal proximal tubule and the distal nephron and can cause either apoptosis or necrosis, depending on exposure time and concentration **(Ikari et al., 2005)**. Low, prolonged doses of cisplatin typically induce apoptosis, whereas necrosis is caused by short exposures to higher concentrations of cisplatin **(Lieberthal et al., 1996)**.

The human organic cation transpoter (hOCT) has been proposed to be involved in potentiating cisplatin-induced nephrotoxicity in the proximal tubule. This transporter is expressed primarily in the kidney **(Gorboulev et al,. 1997)**.

Hepatotoxicity

High dosage of cisplatin may lead to hepatotoxicity **(dos Santos et al., 2007)**. Oxidative stress is the main reason for cisplatin induced toxicity possibly due to depletion of reduced glutathione (GSH), also many studies reported that there were a significant elevation in the hepatic malonaldehyde (MDA) and reduction in the level of antioxidant enzymes in rats treated with cisplatin **(Mansour et al., 2006)**. Observed histopathological changes will be necrosis and degeneration of hepatocytes with inflammatory cells infiltration around portal area with sinusoidal dilatation **(Kart et al., 2010)**.

Ototoxicity

Ototoxicity occurs in approximately 23–54% of patients receiving cisplatin treatment and in greater than half of pediatric patients receiving cisplatin (**Fig. 10**) **(Rybak et al., 2005)**. Bolus higher doses of cisplatin have been shown to be more ototoxic and nephrotoxic than repeated infusions at lower doses in adults **(Reddel et al., 1982)**. In children, however, prolonged infusions are less nephrotoxic than bolus doses but still result in considerable ototoxicity **(Lanvers-Kaminsky et al., 2006)**.

Platinum-based chemotherapeutic agents damage the outer hair cells of the cochlea (inner ear), resulting in functional deficits. The mechanisms underlying these troublesome side effects most likely involve the production of reactive oxygen species (ROS) in the cochlea, which can trigger cell-death pathways. This is thought to be due to activation of the NADPH oxidase isoform nox3, which is expressed only in the inner ear, as kidney cells transfected with the nox3 gene exhibit enhanced superoxide formation upon treatment with cisplatin **(Banfi et al., 2004)**.

Cardiotoxicity

Leakage of lactate dehydrogenase (LDH) and creatine kinase (CK) from cardiac myocytes is due to cardiotoxicity could be a secondary event following cisplatin-induced lipid peroxidation of cardiac membranes. Degeneration and necrosis of cardiac muscle fiber cells with fibrous tissue reaction and vacuolated cytoplasm of many muscle cells and blood vessels are inflated with blood are the histological changes of cisplatin induced toxicology **(Al-Majed et al., 2006)**.

Nerotoxicity

The dorsal root ganglia of the spinal cord are the primary location of cisplatin damage in the central nervous system. This explains the primary sensory neuropathy commonly observed in patients treated with cisplatin **(Meijer et al., 1999)**. Cisplatin-induced neuropathy is characterized by decreased sensory nerve conduction velocity, possibly by acting as a calcium channel blocker **(Hartmann and Lipp, 2003)**.

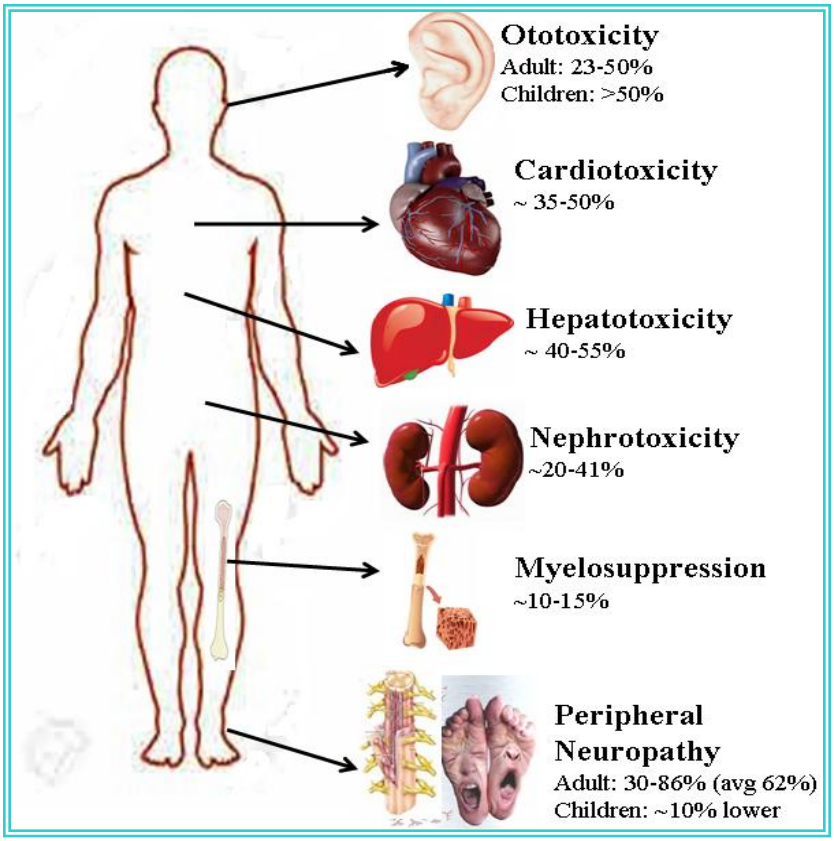

Figure 9: Overview of toxicity of cisplatin on different organ

Myelosuppression

The dose-limiting side effect of cisplatin is myelosuppression, specifically neutropenia and thrombocytopenia (**Fig. 9**). While conventional cisplatin doses result in thrombocytopenia in 20–40% of patients and severe neutropenia in less than 20%, high doses can result in life-threatening toxicity, made more manageable by addition of granulocyte colony stimulating factor (GM-CSF).

Oxidative stress

Free radicals and reactive oxygen species (ROS)

Free radicals were first described by Moses Gomberg more than a century ago **(Gomberg, 1900)**. For a long time they were not considered to present in biological systems due to high reactivity and consequently short living time. More than 30 years later, Leonor Michaelis **(Michaelis, 1939)** proposed that all oxidation reactions involving organic molecules would be mediated by free radicals. Although that statement generally was wrong, it stimulated interest to the role of free radicals in biological processes. In 1950, free radicals were found in biological systems **(Commoner et al., 1954)** and immediately supposed to be involved in diverse pathological processes **(Gerschman, 1954)** an aging **(Harman, 1956)**.

Free radicals can be defined as molecules or molecular fragments containing one or more unpaired electrons in atomic or molecular orbital **(Halliwell & Gutteridge, 1999)**. This unpaired electron(s) usually gives a considerable degree of reactivity to the free radical. Radicals derived from oxygen represent the most important class of radical species generated in living systems **(Miller et al., 1990)**. The most important ROS are the superoxide anion ($O_2^{\bullet -}$), hydroxyl radical ($^{\bullet}OH$), peroxyl radicals ($ROO^{\bullet}$), nitric oxide (NO), hydrogen peroxide (H_2O_2) **(Halliwell and Gutteridge, 1989)**.

Reactive oxygen species (ROS) such as superoxide, hydrogen peroxide and hydroxyl radical are naturally formed because of normal oxygen metabolism. However these free radicals are potentially able to create oxidative damage via interaction with bio-molecules. When there is a pathogen attack, oxidative damage might be beneficial. Obviously, ROS are not only always bad for normal physiology of the cells but

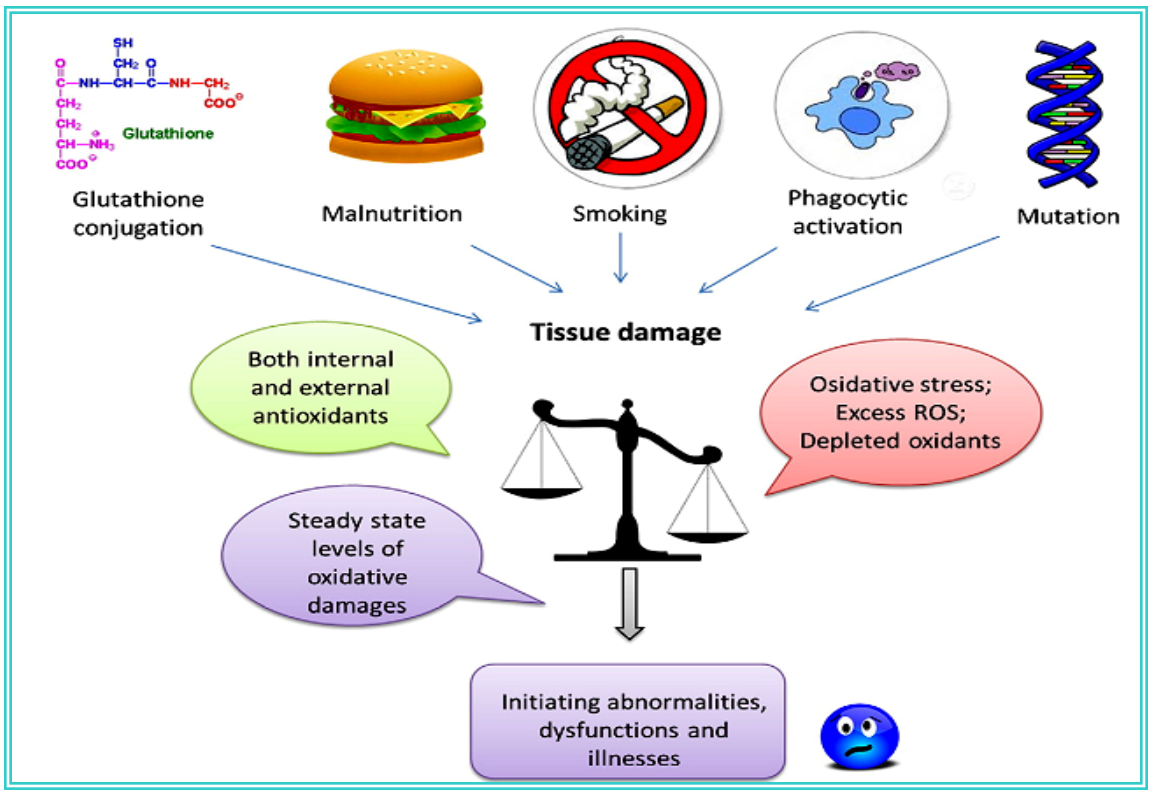

Figure 10: Induction of oxidative stress and consequent damages leading to OSRD; ROS: reactive oxygen species; AOX: antioxidants

sometimes useful. For instance, lower amounts of ROS are produced during mitochondrial activity in normal cells to act as the signaling molecules. The point is that level of oxidants and normal biological antioxidants must be in a balance. If the mentioned balance is interrupted, then toxic oxidative stress may happen (**Fig.10**). This imbalance usually happens during aging (as an example) or it can involve in the pathology of some diseases and also appears as a consequence of the diseases. Normal body contains enzymatic or non-enzymatic antioxidants such as tocopherols or vitamin E, glutathione and ascorbic acid or vitamin C that are involved in above-mentioned process. Among internal antioxidants, the ascorbic acid (AA) and the reduced form of glutathione (GSH) play the main roles in fighting against ROS as well as in maintenance of normal oxidative balance. It seems that AA and GSH are working closely through the ascorbate–glutathione cycle and have sort of cross-talk, although both have their own mechanisms and pathways (**Potters et al., 2004**). As mentioned above, mitochondrial respiration

generates a proton gradient and $O_2^{\bullet-}$ perhaps as a signaling element that might be involved in oxidative stress and alkaline-induced cell death (**Mates et al., 2012**). The creation of $O_2^{\bullet-}$ following irradiation seems to be a main character of cell injury (**Tominaga et al., 2012**). Since manganese superoxide dismutase (Mn-SOD) removes extra $O_2^{\bullet-}$ in the mitochondria to conserve it from oxidative damage, thus over-expression of Mn-SOD reduces the levels of intracellular ROS and protects against cell death (**Mates et al., 2012**).

The role of oxidative stress as a remarkable upstream part is frequently reported in the signaling cascade of inflammation as well as chemo attractant production. Actually in the presence of transition metals, hydrogen peroxide can be converted to the highly reactive hydroxyl radical, which is responsible for most of the oxidative damages to proteins, lipids, sugars, and nucleic acids. Hydroxyl radical is also a hallmark signaling molecule that is able to activate NF-κB (nuclear factor kappa-light-chain-enhancer of activated B cells), an important transcription factor involved in inflammatory responses. Even though hydrogen peroxide can control cell signaling and stimulates cell proliferation at low levels, in higher concentrations it can initiate apoptosis and in very high levels it may create necrosis (**Saeidnia and Abdollahi, 2013**). So far, the role of ROS in cellular damage and death is well documented with implication in a broad range of degenerative alterations (e.g. tissue degradation, carcinogenesis, aging and other oxidative stress related diseases (OSRDs).

Chemistry and biochemistry of reactive nitrogen species (RNS)

Nitric oxide ($NO^{\bullet}$) is an abundant reactive radical that acts as an important oxidative biological signaling molecule in a large variety of diverse physiological processes, including neurotransmission, blood pressure regulation, defence mechanisms, smooth muscle relaxation and immune regulation **(Forstermann et al., 1998)**. This small molecule contains one unpaired electron on the antibonding $2\pi_y^*$ orbital and is, therefore, a radical. $NO^{\bullet}$ is generated in biological tissues by specific nitric oxide synthases (NOSs), which metabolize arginine to citrulline with the formation of $NO^{\bullet}$ via a five-electron oxidative reaction **(Ghafourifar et al., 2005)**. Overproduction of reactive nitrogen species is called nitrosative stress **(Klatt et al., 2000)**. This may occur when the generation of reactive nitrogen species in a system exceeds the system's ability to

neutralize and eliminate them. Nitrosative stress may lead to nitrosylation reactions that can alter the structure of proteins and so inhibit their normal function.

Cells of the immune system produce both the superoxide anion and nitric oxide during the oxidative burst triggered during inflammatory processes. Under these conditions, nitric oxide and the superoxide anion may react together to produce significant amounts of a much more oxidatively active molecule, peroxynitrite anion ($ONOO^-$), which is an oxidizing free radical that can cause DNA fragmentation and lipid oxidation **(Carr et al., 2000)**.

$$NO^{\bullet} + O2^{\bullet -} \rightarrow ONOO^-$$

Nitric oxide readily binds certain transition metal ions; in fact many physiological effects of $NO^{\bullet}$ are exerted as a result of its initial binding to Fe(II)-haem groups in the enzyme guanylate cyclase:

$$Fe\ (II) + NO^{\bullet} \rightarrow Fe(II)–NO$$

Classification of oxidative Stress

Living organisms possess finely regulated systems to maintain very low ROS levels, i.e. their production and elimination are well balanced resulting in certain steady-state ROS level. However, under certain circumstances this balance can be disturbed. There are several reasons for that:

- Increased level of endogenous and exogenous compounds entering autoxidation coupled with ROS production;
- Depletion of reserves of low molecular mass antioxidants;
- Inactivation of antioxidant enzymes;
- Decrease in production of antioxidant enzymes and low molecular mass antioxidants; and, finally,
- Certain combinations of two or more of the listed above factors. Certainly, increase in steady-state ROS level, which results from imbalance between generation and elimination processes, can affect many, if not all living processes.

The consequences of this increase differ and depend on the level and place of ROS generation, efficiency of antioxidant systems, and availability of plastic and energetic resources, and cellular targets they interact with. These processes are presented in **Fig.11**

where inductions of oxidative stress the first definition of which was introduced by Helmut Sies **(Sies, 1985; Sies, 1997).**

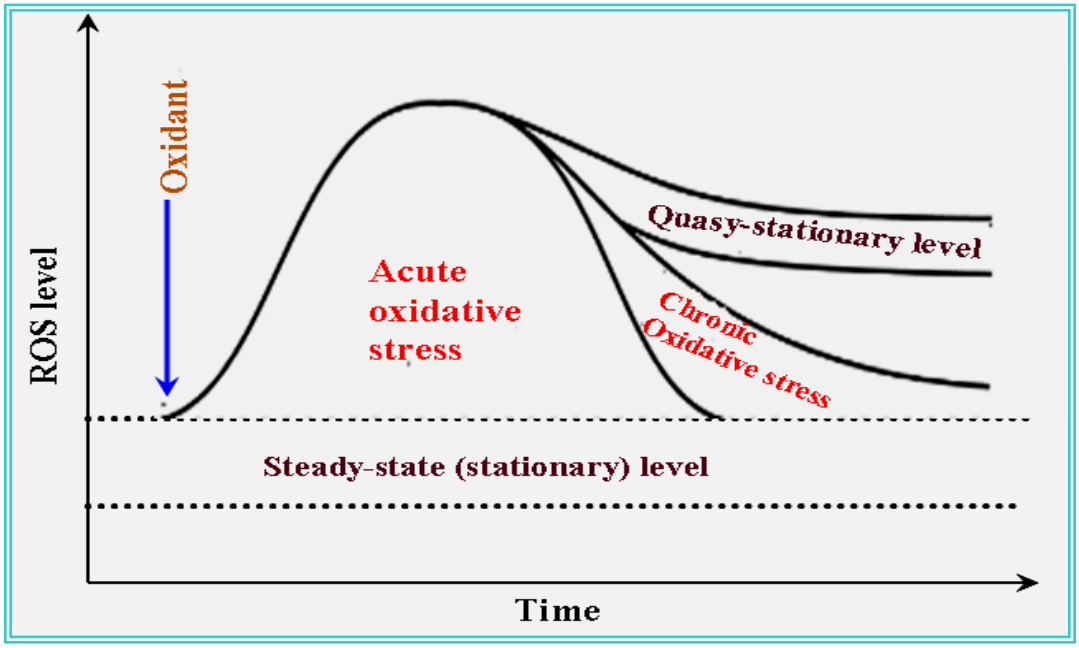

Figure 11: Dynamic of ROS level under control and stressful conditions in biological systems. Steady-state levels of reactive oxygen species fluctuate over certain range under normal conditions. However, under stress ROS levels may increase or decrease beyond the normal range resulting in acute or chronic oxidative or reductive stress. Under some conditions, ROS levels may not return to their initial range and stabilize at a new quasi stationary level

Under normal conditions, ROS level fluctuates in certain range defined by concerted operation of systems of their generation and elimination. Due to some reasons, such as introduction of certain oxidants, ROS level may sharply increase and leave the range of control (rest) conditions. If antioxidant systems are capable adequately cope with enhanced ROS amounts, this level would return into initial corridor. These events may be called ‘‘acute oxidative stress’’ **(Lushchak, 2011)**. In some cases, the cell cannot neutralize enhanced ROS amounts and return ROS level into initial corridor. Even enhanced expression of antioxidant and related enzymes would not be able to do that. Therefore, the ROS level may be slightly enhanced or initial corridor may be extended. Due to that increased ROS level can be stabilized and enhance modification of different cellular components, substantially disturbing homeostasis. This state can be called

‘‘chronic oxidative stress’’. Finally, one more scenario may take place after oxidative boots, or due to change in physiological state of organisms – ROS level may not return into initial corridor and stabilize at new, so-called ‘‘quasistationary level’’ **(Lushchak, 2011)**. This state needs substantial reorganization of whole homeostasis, including ROS one. Several pathologies such as cancer (**Leinonen et al., 2014**), diabetes mellitus **(Yan, 2014)**, cardiovascular **(Feoli et al., 2014)**, and neurodegenerative **(Ahmad et al., 2014)** diseases clearly exemplify the chronic oxidative stress.

Currently the oxidative stress is defined as ‘‘Oxidative stress is a situation when steady-state ROS concentration is transiently or chronically enhanced, disturbing cellular metabolism and its regulation and damaging cellular constituents’’ (**Lushchak, 2011**). This definition includes all mentioned above features and underlines dynamics of the processes involved which is reflected as steady-state (stationary) ROS levels.

Targeting cancer cells by ROS-mediated mechanisms

Mounting evidence suggests that, compared with their normal counterparts, many types of cancer cell have increased levels of reactive oxygen species (ROS) **(Szatrowski et al., 1991)**. A moderate increase in ROS can promote cell proliferation and differentiation **(Boonstra et al., 2004)**, whereas excessive amounts of ROS can cause oxidative damage to lipids, proteins and DNA **(Perry et al., 2000)**. Moreover, as excessive levels of ROS stress can also be toxic to the cells, cancer cells with increased oxidative stress are likely to be more vulnerable to damage by further ROS insults induced by exogenous agents. Therefore, manipulating ROS levels by redox modulation is a way to selectively kill cancer cells without causing significant toxicity to normal cells **(Schumacker et al., 2006)**.

It is worth noting that redox alterations in cancer cells are very complex because of the multiple factors that are involved in the redox regulation and stress response, and that simply adding ROS-generating agents may not always lead to a preferential killing of cancer cells. Under persistent intrinsic oxidative stress, many cancer cells become well-adapted to such stress and develop an enhanced, endogenous antioxidant capacity, which makes the malignant cells resistant to exogenous stress **(Sullivan et al., 2008)**. ROS can

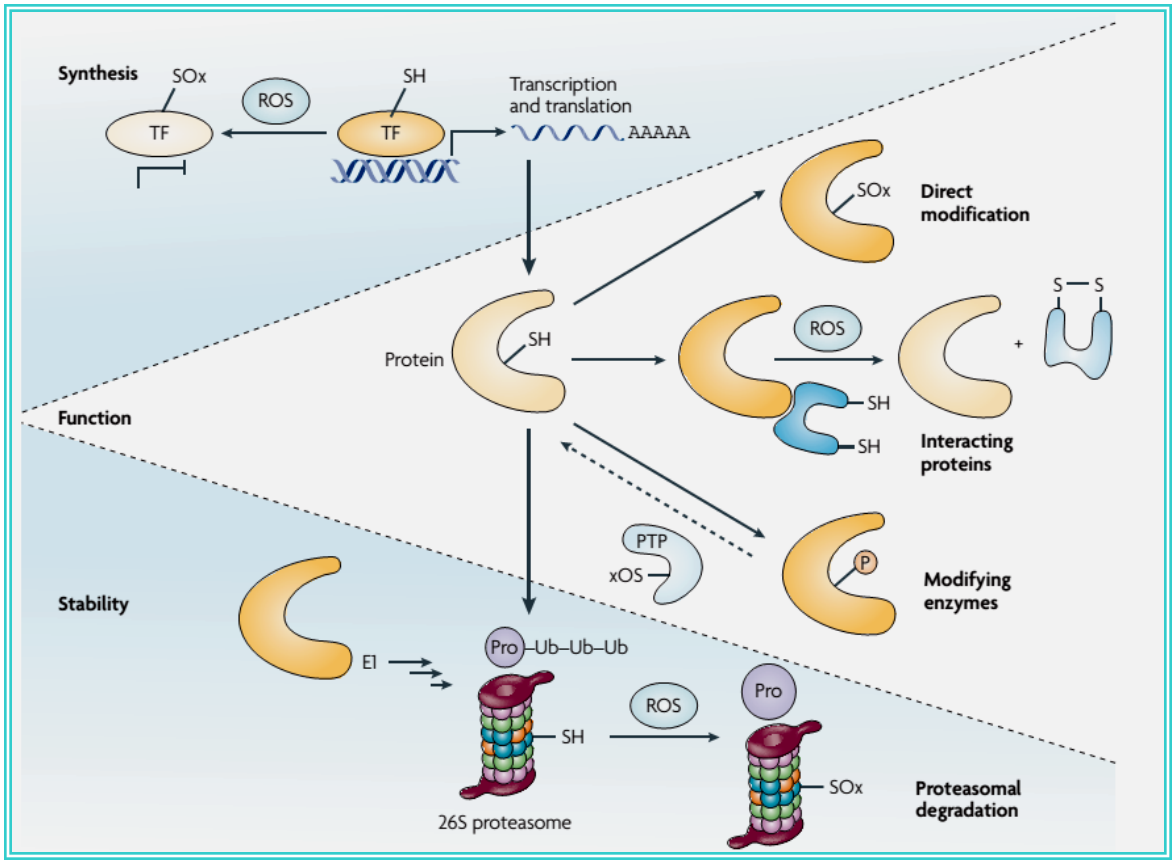

Figure 12: Regulation of protein functions through redox mediated mechanisms Reactive oxygen species (ROS) can affect protein functions through multiple mechanisms, including regulation of protein expression, post-translational modifications and alteration of protein stability.

modulate the activities and expression of many transcription factors and signaling proteins that are involved in the stress response and cell survival through multiple mechanisms **(Trachootham et al., 2008)** (**Fig. 12**). Cancer cells that survive intrinsic oxidative stress may have mobilized a set of adaptive mechanisms, which not only activate ROS-scavenging systems to cope with the stress but also inhibit apoptosis. Recent evidence suggests that such adaptation contributes to malignant transformation, metastasis and resistance to anticancer drugs **(Martinez-Sanchez et al., 2007)**. To effectively kill cancer cells and overcome drug resistance associated with redox adaptation, it is important to understand the complex redox alterations in cancer cells and the underlying mechanisms. Due to the potentially vital roles of stem-like cancer cells in

drug resistance and disease recurrence, it is extremely important to examine the redox status in this subpopulation of malignant cells and to devise therapeutically relevant redox-modulation strategies.

ROS stress in cancer: roles and mechanisms

Compared with normal cells, malignant cells seem to function with higher levels of endogenous oxidative stress in culture and *in vivo* **(Szatrowski et al., 1991)**. Although in some studies the observed increase of oxidative stress might be due to sample handling, analytical artifacts **(Swartz et al., 1977)**, Elevated oxidative stress has been observed in many cancer cell types. For example, leukaemia cells freshly isolated from blood samples from patients with chronic lymphocytic leukaemia or hairy-cell leukaemia showed increased ROS production compared with normal lymphocytes **(Zhou et al., 2003)**. In solid tumors, studies have shown increased levels of oxidative damage products, such as oxidized DNA base (8OHdG), and lipid peroxidation products in clinical tumor specimens **(Patel et al., 2007)**. Moreover, the levels of ROS-scavenging enzymes such as SOD, glutathione peroxidase and peroxiredoxin have been shown to be significantly altered in malignant cells **(Oberley et al., 1997)** and in primary cancer tissues **(Hu et al., 2005)**, suggesting aberrant regulation of redox homeostasis and stress adaptation in cancer cells.

Although the precise pathways leading to ROS stress in cancer cells remain unclear, several intrinsic and extrinsic mechanisms are thought to cause oxidative stress during cancer development and disease progression. Activation of oncogenes, aberrant metabolism, mitochondrial dysfunction and loss of functional p53 are intrinsic factors known to cause increased ROS production in cancer cells **(Rodrigues et al., 2008)**.

At an advanced disease stage, cancer cells usually exhibit genetic instability and show a significant increase in ROS generation, due in part to a ‘vicious cycle’, in which ROS induce gene mutations (especially in the mitochondrial genome) leading to further metabolic malfunction and ROS generation (**(Pelicano et al., 2004)**) (**Fig. 13)**

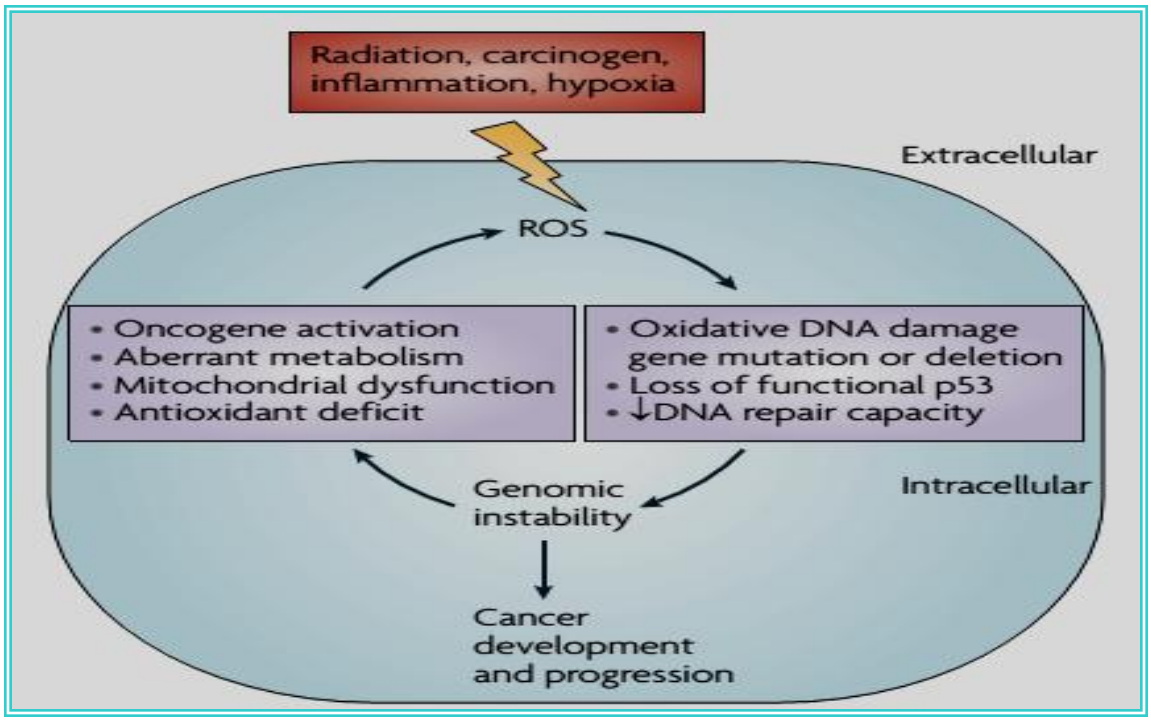

Figure 13: The vicious cycle of ROS stress in cancer**.**

As a genome guardian, the p53 protein has a crucial role in sensing and removing oxidative damage to nuclear DNA and mtDNA, preventing oxidative gene mutations and genetic instability **(Zurer et al., 2004)**. Furthermore, p53 also acts as a transcription factor to regulate the expression of many pro-oxidant and antioxidant genes **(Sablina et al., 2005)**. Loss of functional *p53* is associated with redox imbalance, increased ROS stress, high mutagenesis and aggressive tumor growth **(Attardi et al., 2005)**. This is consistent with the high incidence of *p53* mutation or loss of *p53* function in over 50% of human cancers **(Bourdon, 2007)**, especially in cancer at advanced stages.

Increases in ROS or oxidative DNA and lipid products in some primary cancer cells are associated with a decrease in antioxidants, such as SOD and catalase **(Oberley et al., 1979)**. Increased ROS stress in cancer cells correlates with the aggressiveness of tumors and poor prognosis. Compelling evidence suggests that the increased ROS stress in cancer cells has a pivotal role in the acquisition of the hallmarks of cancer **(Hanahan & Weinberg 2000)**: immortalization and transformation **(Behrend et al., 2003)**, cell proliferation **(Hu et al., 2005)**, and mitogenic signaling **(Irani et al., 1997)**, cell survival and disruption of cell death signaling **(Clerkin et al., 2008)**, epithelial–mesenchymal

transition and metastasis **(Nishikawa, 2008)**, angiogenesis **(Ushio-Fukai & Nakamura 2008)**, and chemoresistance **(Sullivan & Graham 2008)**. Interestingly, in contrast to the tumor-promoting effect, recent work suggests that the high level of ROS has an unexpected role in inducing and maintaining senescence-induced tumour suppression, through sustained activation of the cell-cycle inhibitor *p16* ^{INK4A} **(Takahashi et al., 2006)**. Furthermore, if the increase of ROS reaches a certain threshold level that is incompatible with cellular survival, ROS may exert a cytotoxic effect, leading to the death of malignant cells and thus limiting cancer progression **(Fruehauf et al., 2007)**. These seemingly paradoxical effects raise the important question of how the transformed cells can gain growth and survival benefits under intrinsic ROS stress.

Cancer redox biology: a biological basis for therapeutic selectivity

Reactive oxygen species (ROS) might function as a double-edged sword. A moderate increase of ROS may promote cell proliferation and survival. However, when the increase of ROS reaches a certain level (the toxic threshold), it may overwhelm the antioxidant capacity of the cell and trigger cell death. Under physiological conditions, normal cells maintain redox homeostasis with a low level of basal ROS by controlling the balance between ROS generation (pro-oxidants) and elimination (antioxidant capacity).

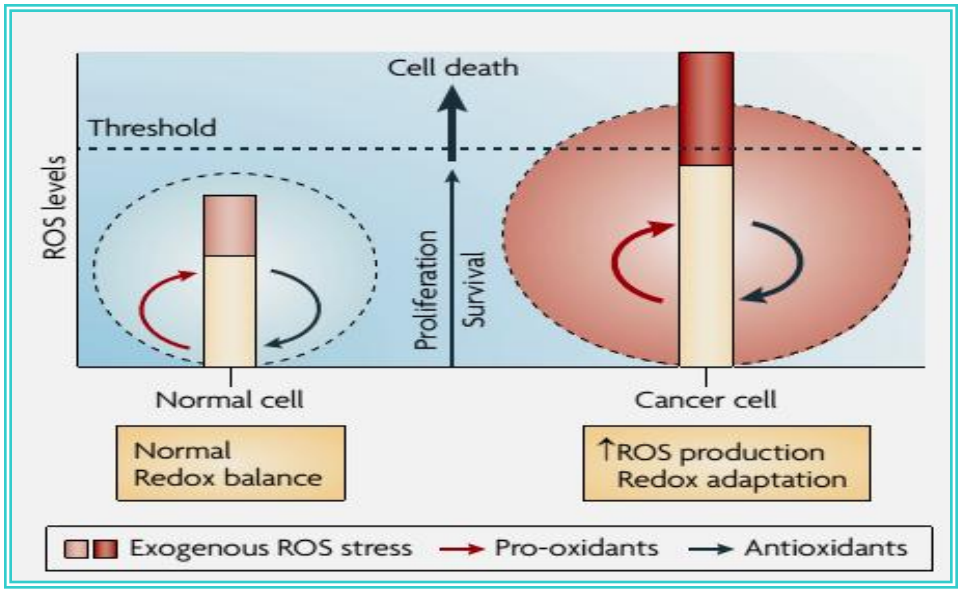

Figure 14: ROS level in between cancer cell and normal cell

Normal cells can tolerate a certain level of exogenous ROS stress owing to their 'reserve' antioxidant capacity, which can be mobilized to prevent the ROS level from reaching the cell-death threshold (horizontal dotted line in figure). In cancer cells, the increase in ROS generation from metabolic abnormalities and oncogenic signalling may trigger a redox adaptation response, leading to an upregulation of antioxidant capacity and a shift of redox dynamics with high ROS generation and elimination to maintain the ROS levels below the toxic threshold. As such, cancer cells would be more dependent on the antioxidant system and more vulnerable to further oxidative stress induced by exogenous ROS-generating agents or compounds that inhibit the antioxidant system. A further increase of ROS stress in cancer cells (red bar) using exogenous ROS-modulating agents is likely to cause elevation of ROS above the threshold level, leading to cell death. This might constitute a biochemical basis to design therapeutic strategies to selectively kill cancer cells using ROS-mediated mechanisms.

Targeting redox alterations in cancer

Therapeutic selectivity is essential in cancer treatment. As cancer cells have elevated ROS generation and are under increased intrinsic oxidative stress, it is conceivable that these malignant cells would be more dependent on antioxidants for cell survival and, therefore, more vulnerable to further oxidative insults induced by ROS-generating agents or by compounds that abrogate the key antioxidant systems in cells. The idea of inducing preferential cancer cell death by a ROS-mediated mechanism based on the different redox states in normal and malignant cells was proposed a decade ago **(Kong et al., 1998)**, but its feasibility has only recently gained momentum **(Fry et al., 2006)**.

Although ROS-generating agents have been found to be effective in many cases **(Soignet et al., 1998)**, low clinical response and resistance to those agents were also reported **(Ramanathan et al., 2005)**. Elevation of certain transcription factors, antioxidants and survival signals as a result of redox adaptation probably explains the drug resistant phenotype **(Soignet et al., 1998)**. To develop effective therapeutic agents, which are selective and able to overcome drug resistance, it will be extremely important to understand the pros and cons of the different redox-modulating strategies and to reconcile the concepts of intrinsic oxidative stress in cancer cells and their redox adaptation.

Cellular redox homeostasis is maintained by the balance between ROS generation and elimination. Exogenous agents that increase ROS generation or decrease antioxidant capacity will shift the redox balance and result in an overall increase in the level of ROS, which when above a cellular tolerability threshold may induce cell death. Approaches to further increase oxidative stress and kill cancer cells are summarized in **Fig. 15.**

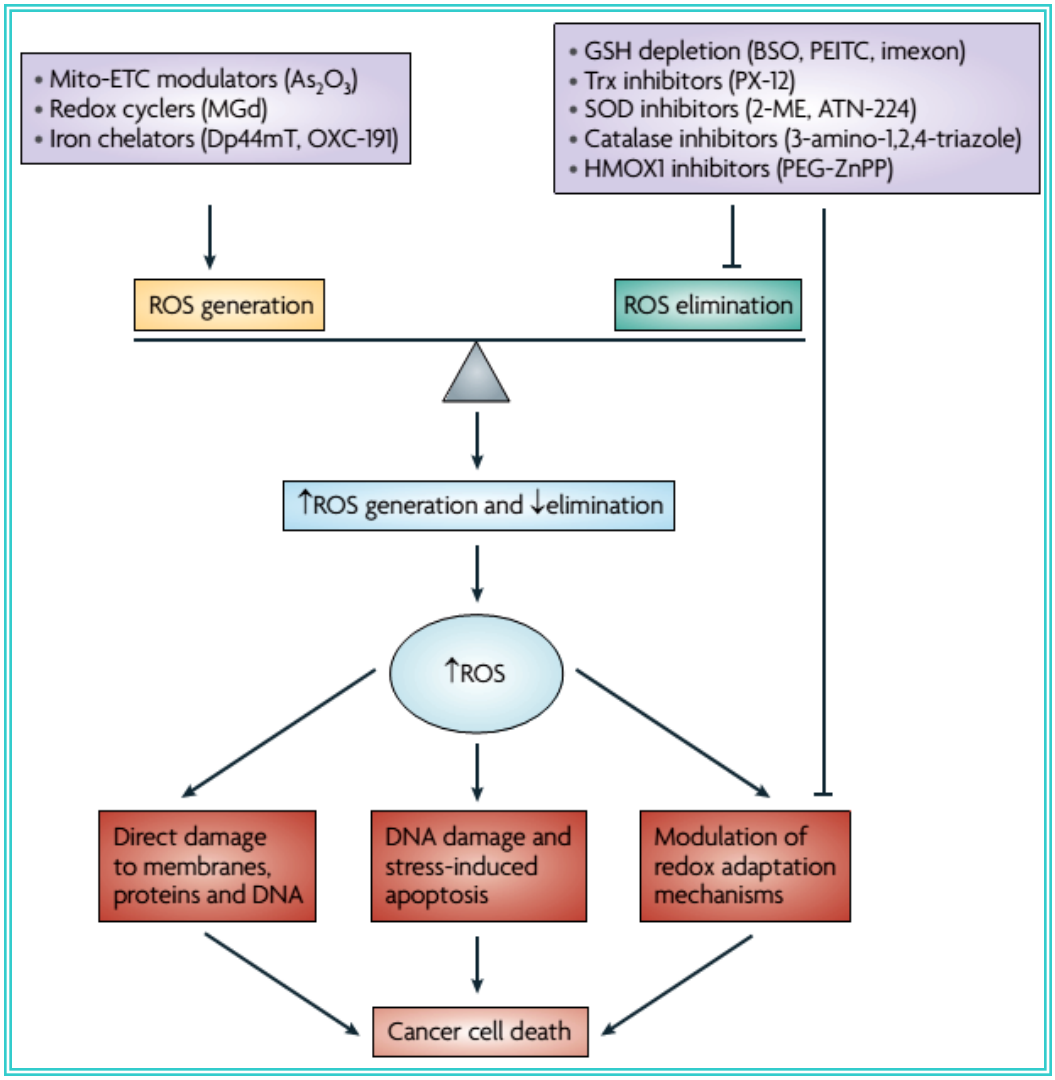

Figure 15: Targeting cancer cells through ROS-mediated mechanisms

Antioxidant defense mechanisms

The effect of reactive oxygen and nitrogen species is balanced by the antioxidant action of non-enzymatic antioxidants, as well as by antioxidant enzymes. Such antioxidant

defenses are extremely important as they represent the direct removal of free radicals (pro-oxidants), thus providing maximal protection for biological sites.

A good antioxidant should: (i) specifically quench free radicals; (ii) chelate redox metals; (iii) interact with (regenerate) other antioxidants within the "antioxidant network"; (iv) have a positive effect on gene expression; (v) be readily absorbed; (vi) have a concentration in tissues and biofluids at a physiologically relevant level; (vii) work in both the aqueous and/or membrane domains. Antioxidants are effective because they can donate their own electrons to free radicals and thereby preventing the chain reaction. In general, an antioxidant in the body may work at three different levels: (a) prevention - keeping formation of reactive species to a minimum, (b) interception - scavenging reactive species either by using catalytic and noncatalytic molecules and (c) repair - repairing damaged target molecules **(Kohen and Nyska, 2002)**.

The most efficient enzymatic antioxidants involve superoxide dismutase, catalase and glutathione peroxidase **(Mates et al., 1999)**. Non-enzymatic antioxidants involve vitamin C, vitamin E, carotenoids, thiol antioxidants (glutathione, thioredoxin and lipoic acid), natural flavonoids, a hormonal product of the pineal gland, melatonin and other compounds **(McCall and Frei, 1999)**. Some antioxidants act in a hydrophilic environment, others in a hydrophobic environment, and some act in both environments of the cell. Certain antioxidants are able to regenerate other antioxidants and thus restore their original function. This process is called an "antioxidant network" **(Sies et al., 2006)**.

Enzymatic antioxidants

Enzyme antioxidants are present in the body and they act as body's first line of defense against free radicals. They convert reactive free radicals into less reactive or inert species **(Fig. 16)**. Enzymatic antioxidants present in the body include superoxide dismutase (SOD), catalase, and glutathione peroxidase (GPx).

Superoxide dismutase (SOD)

One of the most effective intracellular enzymatic antioxidants is superoxide dismutase (SOD). Superoxide dismutase is the antioxidant enzyme that catalyzes the dismutation of $O_2^{\bullet-}$ to O_2 and to the less-reactive species H_2O_2. While this enzyme was isolated as early

as 1939, it was only in 1969 that McCord and Fridovich proved the antioxidant activity of SOD **(Mc Cord and Fridovich, 1969)**.

In humans there are three forms of SOD: (i) cytosolic Cu, Zn-SOD, (ii) mitochondrial Mn-SOD, and (iii) extracellular SOD **(Landis and Tower, 2005)**. SOD destroys $O_2^{\bullet-}$ with remarkably high reaction rates, by successive oxidation and reduction of the transition metal ion at the active site in a "Ping-Pong" type mechanism **(Mates et al., 1999)**. Cu, Zn-SOD specifically catalyzes the dismutation of the superoxide anion to oxygen and water. Mn-SOD is one of the most effective antioxidant enzymes that have anti-tumour activity. A set of studies on different cell lines has confirmed that overexpression of Mn-SOD leads to tumour growth retardation **(Behrend et al., 2003)**. Extracellular superoxide dismutase (EC-SOD) is a secretory, tetrameric, copper and zinc containing glycoprotein, with a high affinity for certain glycosaminoglycans such as heparin and heparin sulphate **(Mates et al., 1999)**. Its regulation in mammalian tissues occurs primarily in a manner coordinated by cytokines, rather than as a response of individual cells to oxidants.

Catalase (CAT)

Catalase is an enzyme present in the cells of plants, animals and aerobic (oxygen requiring) bacteria **(Mates et al., 1999)**. Catalase is located in a cell organelle called the peroxisome. The enzyme very efficiently promotes the conversion of hydrogen peroxide to water and molecular oxygen. Catalase has one of the highest turnover rates for all enzymes: one molecule of catalase can convert ~6 million molecules of hydrogen peroxide to water and oxygen each minute:

$$\mathbf{2\ H_2O_2 \xrightarrow{CAT} H_2O + O_2}$$

The significantly decreased capacity of a variety of tumours for detoxifying hydrogen peroxide is linked to a decreased level of catalase.

Glutathione Peroxidase (GP*x*)

There are two forms of the enzyme glutathione peroxidase, one of which is selenium-independent (glutathione-S-transferase, GST) while the other is selenium- dependent (GP*x*, Glutathione Peroxidase) **(Mates et al., 1999)**. These two enzymes differ in the

number of subunits, the bonding nature of the selenium at the active centre and their catalytic mechanisms. Glutathione metabolism is one of the most essential of antioxidative defence mechanisms.

Humans have four different Se-dependent glutathione peroxidases **(Mates et al., 1999)**. All GPx enzymes are known to add two electrons to reduce peroxides by forming selenoles (Se-OH). The antioxidant properties of these selenoenzymes allow them to eliminate peroxides as potential substrates for the Fenton reaction. GPx acts in conjunction with the tripeptide glutathione (GSH), which is present in cells in high (micromolar) concentrations. The substrate for the catalytic reaction of GPx is H_2O_2, or organic peroxide ROOH. GPx decomposes peroxides to water (or alcohol) while simultaneously oxidizing GSH:

$$\mathbf{2GSH + H_2O_2} \xrightarrow{\mathbf{GPx}} \mathbf{GSSG + 2\ H_2O}$$

$$\mathbf{2GSH + HOOH} \xrightarrow{\mathbf{GPx}} \mathbf{GSSG + ROH + H_2O}$$

Significantly, GPx competes with catalase for H_2O_2 as a substrate and is the major source of protection against low levels of oxidative stress.

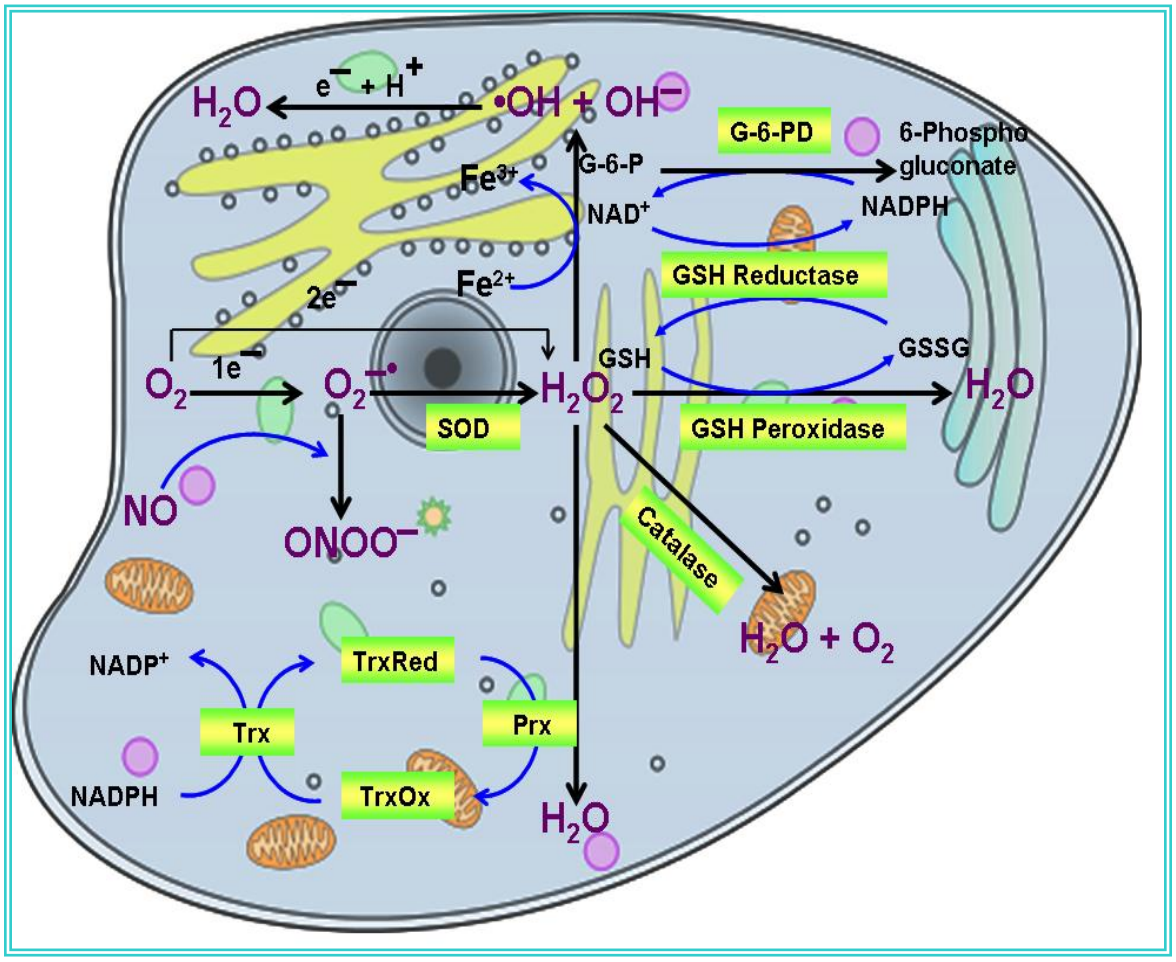

Figure 16: Multiple enzymatic scavengers are utilized by the cell to limit damage from reactive oxygen species. These scavengers include members of the superoxide dismutase (SOD) family, catalase, and glutathione peroxidase.

Thioredoxin reductase (TrxR)

Many cellular processes including antioxidant defense, redox and cell growth regulation as well as selenium metabolism are related to the action of thioredoxin reductase (TrxR). TrxR belongs to a well-known class of homodimeric pyridine nucleotide disulfide oxidoreductases **(Arn´er et al., 2000)**. Three mammalian isoenzymes have been characterised, including the cytosolic TrxR1 **(Gasdaska et al., 1995)**, the mitochondrial TrxR2, and the testis specific thioredoxin glutathione reductase (TrxR3, TGR) **(Miranda-Vizuete et al., 2004)**. The mammalian TrxRs have a higher molecular mass (55 kDa) and a very broad substrate specificity **(Waksman, 1994)**. Mammalian TrxR not only catalyzes reduction of disulfides of thioredoxins (Trx) by NADPH (**Freemerman et**

al, 1999), but also some other protein disulfides or a wide spectrum of oxidized low molecular weight compounds **(Arne´r et al., 1999)**. It should be noted that GSSG and insulin are not substrates for TrxR1, though they can both be efficiently reduced by Trx **(Kanzok et al., 2000)**.

Peroxides, including lipid hydroperoxides and hydrogen peroxide can directly be reduced by TrxR. By this mechanism TrxR could function as an alternative enzymatic pathway for the detoxification of lipid hydroperoxides, otherwise mainly managed by GPx **(Bjo¨rnstedt et al., 1995)**.

Non-enzymatic antioxidants

Thiol antioxidants — glutathione

The major thiol antioxidant is the tripeptide, glutathione. Glutathione (GSH) **(Fig. 17)** is a multifunctional intracellular non-enzymatic antioxidant. It is considered to be the major thiol-disulphide redox buffer of the cell (**Masella et al., 2005**). Glutathione is highly abundant in the cytosol (1–11 mM), nuclei (3–15 mM), and mitochondria (5–11 mM) and is the major soluble antioxidant in these cell compartments **(Masella et al., 2005)**.

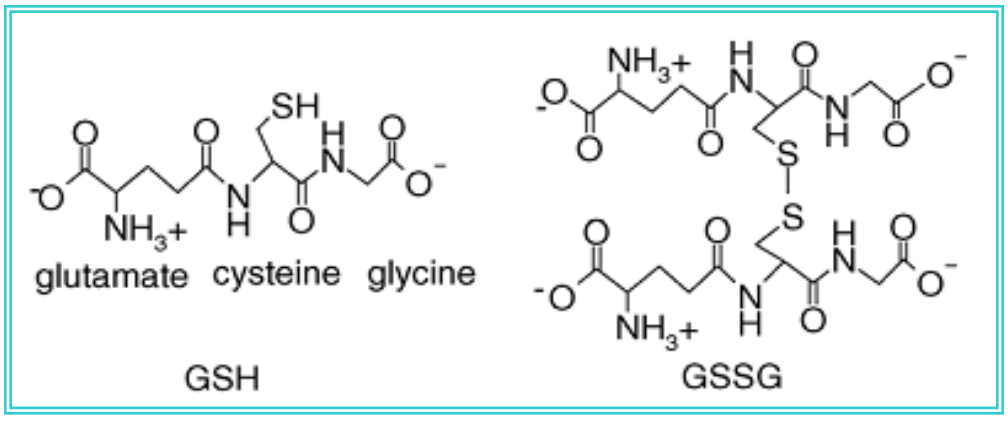

Figure 17: Structures of reduced (GSH) and oxidized (GSSG) glutathione

GSH in the nucleus maintains the redox state of critical protein sulphydryls that are necessary for DNA repair and expression. An oxidative environment leads to rapid modification of protein sulphydryls (protein-SH): twoelectron oxidation yields sulphenic

acids (protein-SOH) and one-electron oxidation yields thiyl radicals (protein-S$^{\bullet}$) **(Ji et al., 1999)**.

Generally, the antioxidant capacity of thiol compounds is due to the sulfur atom which can easily accommodate the loss of a single electron. In addition the lifetime of sulfur radical species thus generated, i.e. a thiyl radical (GS$^{\bullet}$), may be significantly longer than many other radicals generated during the stress. The reaction of glutathione with the radical R$^{\bullet}$ can be described:

$$\mathbf{GSH + R^{\bullet} \rightarrow GS^{\bullet} + RH}$$

Thiyl radicals generated may dimerise to form the nonradical product, oxidized glutathione (GSSG):

$$\mathbf{GS^{\bullet} + GS^{\bullet} \rightarrow GSSG}$$

Oxidized glutathione GSSG is accumulated inside the cells and the ratio of GSH/GSSG is a good measure of oxidative stress of an organism. GSSG can react with protein sulfhydryl groups to produce protein–glutathionemixed disulphides:

$$\mathbf{GSSG + protein\text{-}SH \leftrightarrow protein\text{-}SSG + GSH}$$

The main protective roles of glutathione against oxidative stress are **(Masella et al., 2005)**: that (i) glutathione is a cofactor of several detoxifying enzymes against oxidative stress, e.g. glutathione peroxidase (GPx), glutathione-*S*- transferase and others; (ii) GSH participates in amino acid transport through the plasma membrane; (iii) GSH scavenges hydroxyl radical and singlet oxygen directly, detoxifying hydrogen peroxide and lipid peroxides by the catalytic action of glutathionperoxidase; (iv) glutathione is able to regenerate the most important antioxidants, vitamins C and E back to their active forms; glutathione can reduce the tocopherol radical of vitamin E directly, or indirectly, via reduction of semidehydroascorbate to ascorbate.

Glutathione-*S*-Transferase (GST):

Glutathione transferases (GSTs) are a family of multifunctional proteins capable of detoxifying endogenous and xenobiotic electrophiles by addition of GSH to the electrophiles **(Vanhaelen et. al., 2004)**. This activity is useful in the detoxification of endogenous compounds such as lipids peroxides as well as the metabolism of

xenobiotics. The GSTs catalyze the formation of thioether conjugates between the endogenous tripeptide GSH and xenobiotic compounds **(Jancova et al, 2010).**

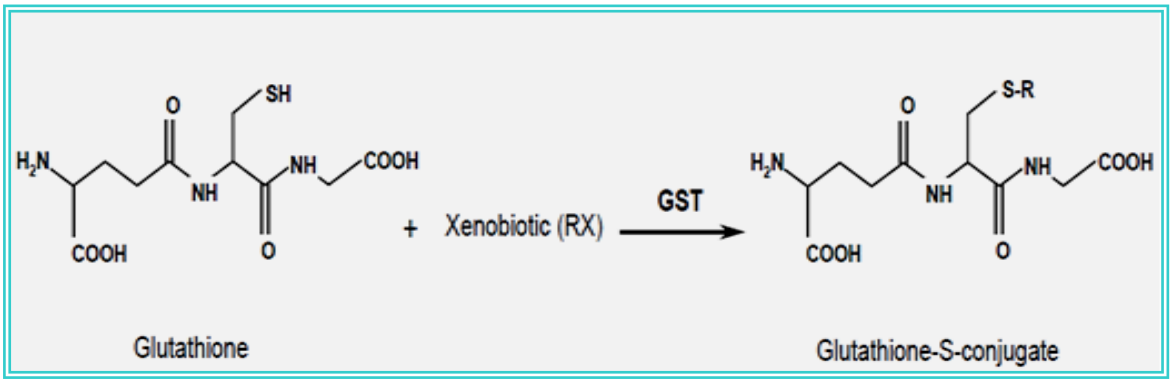

Figure 18: Formation of glutathione conjugate catalyzed by GST

GSTs are induced under conditions of oxidative stress, and alpha, pi, mu, and theta-class GSTs are active in detoxification of organic epoxides, hydroperoxides, and unsaturated aldehydes, including reactive purine and pyrimidine bases and lipid peroxides produced by reactive oxidant damage to DNA and lipids, respectively **(Hayes, 1999)**. The major biological function of GSTs appears to be defense against reactive and electrophiles such as ROS (H_2O_2 and $O_2^{\bullet-}$) that arise through normal metabolic processes **(Jancova et al, 2010)**.

Oxidative damage to DNA, lipids and proteins

At high concentrations, ROS can be important mediators of damage to cell structures, nucleic acids, lipids and proteins **(Valko et al., 2006)**. Mitochondria and nuclei have their own DNA. Mitochondrial DNA is susceptible to oxidative damages because of the lack of protective protein, histones, and close locations to the reactive oxygen species-producing systems. Hydroxyl radical oxidizes guanosine or thymine to 8–hydroxy–2–deoxyguanosine and thymine glycol, respectively, which changes DNA and leads to mutagenesis and carcinogenesis **(Ames et al., 1993).**

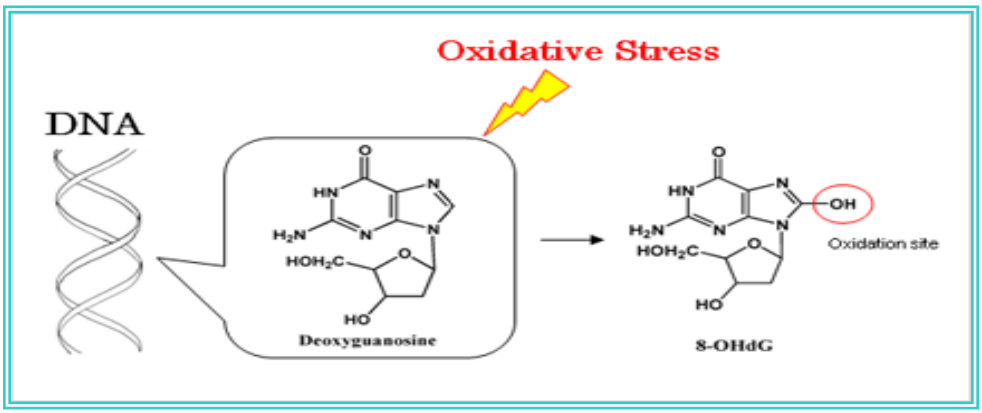

Figure 19: Effect of oxidative stress on DNA

8–hydroxy–2–deoxyguanosine has been used as a biological marker for oxidative stress **(Kasai, 1997).** Altered DNA can be repaired by DNA glycosylase. A low level of oxidative base damage in DNA is found in the cells of a healthy person. However, concentration of oxidized DNA base increases in humans with chronic inflammatory diseases such as rheumatoid arthritis or under oxidative stresses such as smoking **(Halliwell, 1997).** If oxidative stress is too great, the DNA repair system using glycosylase is not enough, and mutagenesis and/or carcinogenesis can be induced.

Besides DNA, lipids are a potential target for reactive free radicals, and lipid peroxidation is one of the most prominent events of oxidative stress. Lipid peroxidation indicates a chain reaction in which membrane lipids are consecutively damaged by the reactive oxygen species (ROS) (**Fig. 20**).

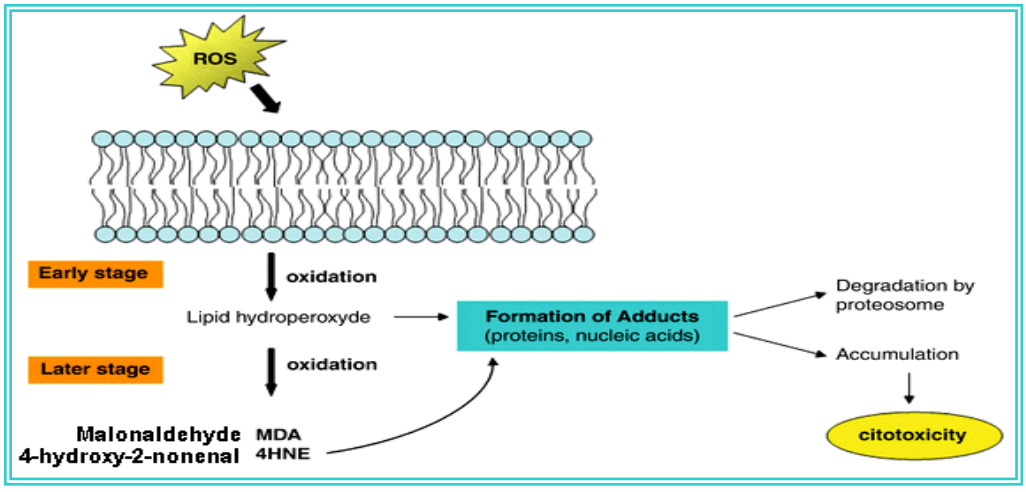

Figure 20: Lipid per-oxidation triggered by reactive oxygen species (ROS) and evolves in subsequent steps with production of aldehyde

The lipid per-oxidation mechanism is didactically subdivided into three consecutive steps: initiation, propagation and termination. As with all other aerobic organism, human being possess several detoxifying mechanism in order to protect cells from toxic effects of oxygen radical and the associated lipid peroxidation **(Felical et al., 2014)**. Malonaldehyde, one of the lipid oxidation products, can react with the free amino group of proteins, phospholipid, and nucleic acids leading to structural modification, which induce dysfunction of immune systems. A high level of lipid oxidation products can be detected in cell degradation after cell injury or disease. The increases of lipid oxidation products are found in diabetes, atherosclerosis, liver disease, apoplexy, and inflammation. Low-density lipoproteins are complicated structures, and oxidative modification of LDLs has been reported to be involved with the development of atherosclerosis and cardiovascular disease **(Frei, 1995)**.

Reactive oxygen species can attack proteins and produce carbonyls and other amino acid modifications, including methionine sulfoxide, 2–oxohistidine, and protein peroxides. Modification of protein is mainly initiated by hydroxyl radicals, leading to the oxidation of amino acid side chains, protein–protein cross linkage, and protein fragmentation (**Stadtman, 2000**). The availability of oxygen, superoxide anion, and its protonated form ($HO_2^{\bullet}$) determines the pathways of protein oxidation processes. Protein oxidation products are usually carbonyls such as aldehydes, and ketones as shown in **Fig. 21.** The consequences of protein damage are loss of enzymatic activity, altered cellular functions such as energy production, and inactivation/activation of transcription factors, changes in the cellular redox potential.

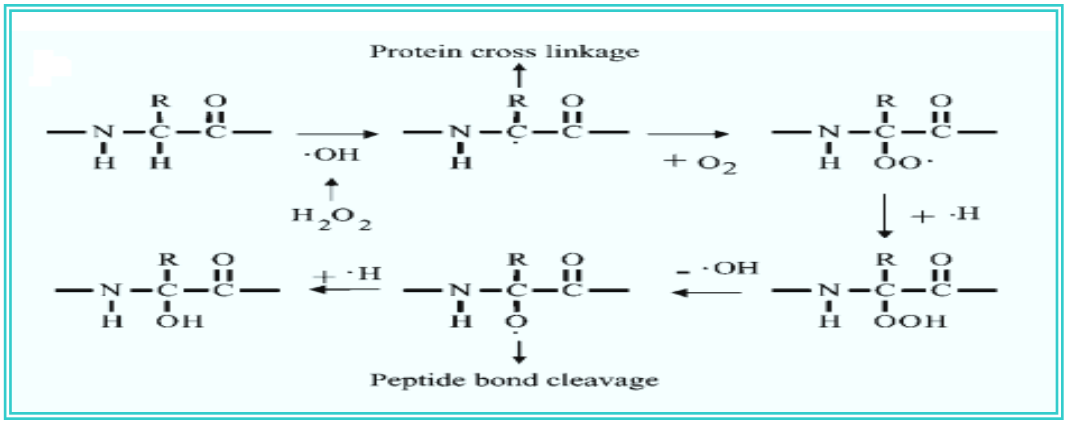

Figure 21: Oxidation mechanisms of proteins by reactive oxygen species (ROS)

Selenium

History of Selenium

Selenium is an essential micronutrient in all forms of life. The word "Selenium" has been derived from a Greek word "selene" which mean "moon". It was discovered by Jons Jacob Berzelius, a Swedish chemist in 1818 **(Berzelius, 1818)**. He identified selenium as a red deposit on the walls of a lead chamber used in the production of sulfuric acid **(Foster and Sumar, 1997)**. Selenium was known as toxic material up to 1957 when Schwarz and Foltz found as essential element for prevention of liver necrosis in vitamin E deficient rats **(Schwarz and Foltz, 1957)** and later the discovery that selenium is the integral part of selenium-dependent glutathione peroxidase enzymes demonstrated a biochemical role for this essential trace element and provided a tool for monitoring its status in animals and humans **(Rotruck et al., 1973)**. In human genome, the sequence SECIS (Sec Insertion Sequence), along with multiple other factors, is employed to insert selenocysteine (Sec) in twenty five of selenoproteins, only few of them are functionally characterized so far **(Sakakibara, 2009)**.

Appearance and characteristics

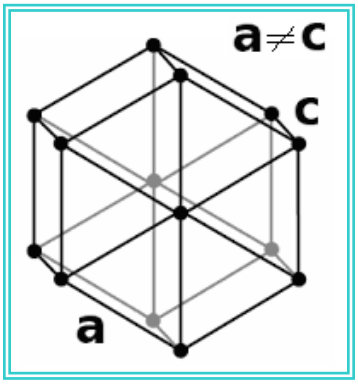

Selenium exists in several allotropic forms. Three are generally recognized. It can be prepared with either an amorphous or crystalline structure. The color of amorphous selenium is either red, in powder form, or black, in vitreous form. Crystalline monoclinic selenium is a deep red; crystalline hexagonal selenium, the most stable variety, is a metallic gray (trigonal form) which is composed of long helical chains of selenium atoms.

4.2. Properties of Selenium

- **Atomic structure of Se:**
  - Atomic radius: 122 Aº
  - Atomic volume: 16.45 cm^3/mol
  - Covalent radius: 1.16 Aº
  - Crystal structure: Hexagonal

- Ionic radius: 0.5 Aº
- Oxidation state: ± 2,4,6
- Electronic configuration: $1s^2s^2p^63s^2p^6d^{10}4s^2p^4$
- Electron per energy level: 2,8,18,6
- Valence electron: $4s^2p^6$

❖ **Chemical Properties:**

- Electrochemical equivalent: 0.7365 g/amp-hr
- Electron work function: 5.9 eV
- Electronegative: 2.55 (pauling)
- Polarizability volume: 3.8 A^{03}
- Heat of fusion: 6.694 kJ/mol
- Ionization potential:
  - First: 9.752
  - Second: 21.19
  - Third: 30.82
- Valence electron potential (eV): 120

❖ **Physical Properties:**

- Atomic mass average: 78.96 amu
- Boiling point: 685 ºC
- Thermal conductivity: 0.0204 W/cmK
- Density: 4.79 g/cc at 300K
- Melting point: 221 ºC
- Physical state (at 20ºC and 1atm): Solid
- Specific heat: 0.32 J/gK

❖ **Elastic Properties:**

- Elastic modulus:
  - Bulk: 8.3/GPa
  - Rigidity: 3.7/GPa
  - Youngs: 58/GPa

❖ **Electrical properties:**

- Electrical resistivity: high (10^{-8} Ωm)

- **Optical Properties:**
  - Refractive Index: 1.000895
  - Reflectivity: no data
- **Typical Reaction:**
  - Reaction with air: Vigorous w/ht, SeO_2
  - Reaction with 15 M HNO_3: mild, H_2SeO_3, NOX
  - Reaction with 6 M HCl: none

Biological aspect of Selenium

Selenium (Se) is a potent nutritional antioxidant, important for various aspects of human health **(Norton and Hoffman, 2012)**. As a constituent of selenoproteins, it plays both structural and enzymatic roles **(Rayman, 2000)**. Also, it is an essential component of the active sites of several enzymes, including glutathione peroxidase (GPx) and thioredoxin reductase, which catalyze reactions, essential to the protection of cellular components against the oxidative stress and free radical damage.

Biochemistry and metabolism

Both inorganic (selenite and selenate) and organic (selenocysteine and selenomethionine) forms of selenium can be used as nutritional sources **(Suzuki et al., 2002)**. The selenoorganic compounds, primarily l- selenomethionine generally are recognized as safe and effective forms of selenium supplementation. It is known that in plants selenium is present predominantly as selenomethionine, whereas in animals selenocysteine is the major form **(Sunde, 1997)**. Although no single marker for selenium status has been identified, a plasma selenium concentration is an indication of recent ingestion. Erythrocytes and platelet GPx activity correlates with selenium supplementation. Urine selenium varies with intake. At very high levels of intake, volatile forms of selenium are exhaled **(Mutanen, 1986)**. Serum selenium was also significantly associated with serum selenoprotein P in both sexes. Also, serum α-tocopherol was positively associated to serum selenium **(Suzuki et al., 2002)**. Serum selenium status and n-3 fatty acids composition were also correlated. This can probably be explained by the association of these fatty acids with fish intake **(Svensson et al., 1992)**.

Food and nutritional sources

Diet is the major source of selenium. Selenium enters the food chain through plants; intake with drinking water is generally negligible. The amount of selenium in foods depends on geographical factors **(Reilly, 2006)**. Selenium levels in soil generally reflect its presence in food and in human populations **(Navarro-Alarcon and Cabrera-Vique, 2008)**. Low availability of selenium may occur in some areas, whereas in seleniferous areas, via plants excessive selenium is taken up **(Levander, 1996)**. Absorption of selenium is not homeostatically controlled, and it depends on the chemical form of selenium. Selenium-selenomethionine (organic form) is more efficiently absorbed and more retained in the body than selenium-selenite (inorganic form). Selenium form in soils also affects selenium bioavailability: selenate is more mobile, soluble and less well adsorbed than selenite **(Fordyce, 2005)**. Selenite, on the other hand, can be effectively used for selenoprotein synthesis, but it cannot be stored in the body. Selenomethionine can act as a storage form of selenium in body proteins from which it can slowly be released by catabolism to maintain Se requirements over a longer period **(Xia et al., 2005)**. Thus, selenium in the form of selenomethionine was almost twice as effective as selenium in the form of selenite in supporting plasma GPx activity **(Rayman et al., 2008a; Rayman, 2008b)**. Furtheremore, selenomethionine is recognized as less toxic than selenite. Many foods as grain products, sea food, meat and poultry are major sources of Se. However, it has been shown recently that selenium in certain plants as corn, soybean, and mushrooms is poorly available, on the other hand in certain foods of animal origin such as beef kidney, Japanese fish, meat, Baltic herring, milk, trout is relatively more available. The reason for the low selenium bioavailability in certain fishes is not clear. It has been suggested that mercury present in fish might complex selenium into unavailable form **(Fairweather et al., 2002)**. Supplementation of selenium with β-carotene or vitamin E enhances the antioxidant system (SOD, GP*x* and glutathione). Serum α-tocopherol and retinol were positively associated to serum selenium **(Patrick, 1999)**.

Selenium intake

In contrast to many other micronutrients, the intake of selenium varies hugely worldwide, ranging from deficient (associated with selenium deficiency diseases) to toxic concentrations **(Fang et al., 2015)**. Selenium status, as measured by plasma or serum selenium, varies by country and corresponds to intake. Intakes are high in Venezuela, Canada, the USA, and Japan, and much lower in Europe, particularly in Eastern Europe. China has areas of both selenium deficiency and excess. Intakes in New Zealand, which were formerly low, have improved after increased importation of high selenium Australian wheat. Selenium intake is mainly in the form of organic compounds ingested in grains, meat, yeast, and vegetables **(Cao et al., 2004)**. The US Food and Nutrition Board (1980) considered to be the Estimated Safe and Adequate Daily Intake for selenium of 50–200µg, being 55µg/day the Recommended Dietary Allowance (RDA) for selenium for both men and women **(Reilly, 2006)**. Reasons for the variability in intake relate not only to the selenium content of the soil on which crops and fodder are grown, but also to factors that determine the availability of selenium to the food chain, including selenium speciation, soil pH and organic matter content, and the presence of ions that can complex with selenium **(Rayman, 2012)**.

Overview of Selenium metabolism

Selenium is an essential trace element, and humans take up selenium predominantly from grains, cereals and meat. A complex reaction cascade may convert inorganic selenium compounds such as selenate and selenite to organic forms and vice versa, **(Fig. 22)** which can be enzymatically catalyzed **(Ip, 1998)**. Hydrogen selenide (H_2Se) plays a central role, formed from glutathione-coupled reactions from selenite (SeO_3^{2-}) via selenodiglutathione (GSSeSG) and glutathione selenopersulfide (GSSeH). H_2Se is generally regarded both as substrate for biosynthesis of selenocysteine (SeCys) by cysteine synthases and as molecule for the transformation into selenophosphate (H_2SePO^{-3}) by selenophosphate synthetase, and both are required for the biosynthesis of selenoproteins. Further metabolism of H_2Se involves sequential methylation to methylselenol (CH_3SeH), dimethylselenide ($(CH_3)_2Se$), and trimethylselenonium ion, the latter both exhaled by breath, and excreted in urine.

Alternatively, selenomethionine (SeMet), which can be incorporated into proteins in place of methionine, converts to selenocysteine through transsulfuration, which in turn is degraded to H_2Se by cysteine lyase **(Birringer et. al., 2002)**.

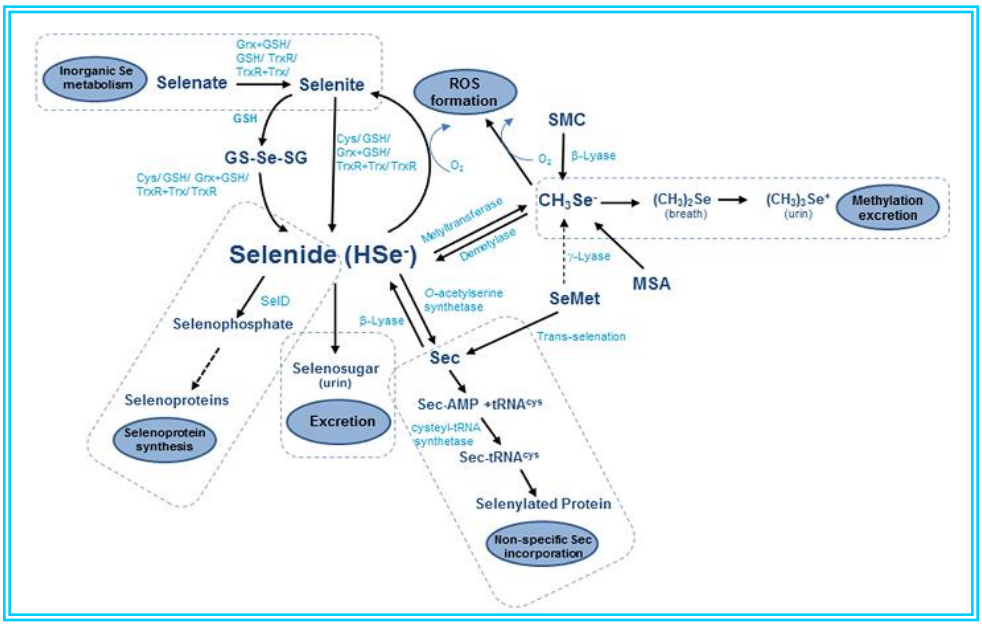

Figure 22: Schematic overview of the selenium metabolism of the most extensively studied selenium compounds.

Selenoprotein

Several selenoproteins have been isolated from mammals (**Table 1).** The human selenoproteome consists of 25 selenoproteins **(Alexander, 2007)**. In selenoproteins, selenium occurs as selenocysteine **(Zhang et al., 1998.)** The main groups are GP*x*, 1-3 thioredoxin reductases, selenoprotein P (Se-P) and other proteins. These are redox enzymes that take advantage of the chemical properties of selenium to catalyze, respectively, removal of hydroperoxides by glutathione, deiodination of thyroid hormones and support of cellular processes requiring reduction of disulfides. Se-P is an extracellular protein that contains most of the selenium in plasma. Approximately 60% of selenium in plasma is incorporated in Se-P which contains 10 selenium atoms

per molecule as selenocysteine and may serve as a transport protein for selenium **(Diplock, 1999)**.

Selenoproteins	Functions
GPx	The four glutathione peroxidase enzymes (classical GPx1, gastrointestinal GPx2, plasma GPx3, phospholipid hydroperoxide GPx4) which represent a major class of functionally important selenoproteins, were first to be characterised Crucial antioxidant enzyme in mammals, remove H_2O_2, thereby protects cellular components from oxidative damage and stress
Selenoprotein P	Approximately 60% of Se in plasma is incorporated in selenoprotein P which contains 10 Se atoms per molecule as selenocysteine, and may serve as a transport protein for Se. However, selenoprotein P is also expressed in many tissues. It may be involved in selenium transport (between the liver and other organs) as well as in the prevention of free radical pathology Development of functional spermatozoa
Selenoprotein W	Isolated from the skeletal muscle of a rat, this selenoprotein is necessary for muscle metabolism
Cytosolic selenoprotein, Prostate epithelial selenoprotein, 15kDa	Found in rat prostate. Seems to have redox function (resemble GPx), perhaps protecting secretuar cells against development of prostate cancer
Selenophosphate synthtase, SPS2	Required for biosynthesis of selenophosphate, the precursor of selenocysteine, and therefore for selenoprotein synthesis
Phospholipid hydroperoxide GPx	Described in porcine heart and liver, it specially reduces lipid peroxides in cell membrane
Sperm mitochondrial capsule selenoprotein	In accordance with the role of mitochondria in assisting sperm motility
Tip I iodothyronine deiodinases	An enzyme necessary for proper thyroid function and conversion of T_4 into T_3, is a selenoprotein containing selenium in the form of selenocysteine
Thioredoxin reductases	Recently identified seleno-cysteine containing enzyme which catalyzes the NADPH dependent reduction of thioredoxin and therefore plays a regulatory role in its metabolic activity. Maintenance of intracellular redox state, critical for cell viability and proliferation, regeneration of antioxidant systems
DNA-bound spermatid selenoprotein, 34kDa	GPx-like activity found in stomach and in nuclei of spermatozoa, may protect developing sperm
18kDa selenoprotein	Important selenoprotein, found in kidney and other tissues preserved in selenium deficiency

Table 1: Selenoprotein types and their functions

Biological role of Selenium in the human body

Cardiovascular disease and selenium

Selenium may be protective against cardiovascular disease. This hypothesis is supported by the ability of GPx to combat the oxidative modification of lipids and to reduce platelet aggregation **(Neve, 1996)**. In cerebral ischemia model, infarct volume was increased three-fold in the GPx knockout mice compared with the wild-type mice **(Crack et al., 2001)**. GPx is required for the metabolism of hydroperoxides produced in eicosanoid synthesis by the lipoxygenase and cyclooxygenase pathways.

In selenium deficiency, a built-up of these hydroperoxides inhibits the enzyme prostacyclin synthetase that is responsible for the production of vasodilatory prostacyclin by the endothelium, but stimulates the production of tromboxane, which is associated with vasoconstriction and platelet aggregation. GPx4 reduces hydroperoxides of phospholipids and cholesteryl esters associated with lipoproteins and may therefore reduce the accumulation of oxidized low-density lipoproteins in the artery wall **(Sattler et al., 1994)**. Suadicani et al. **(Suadicani et al., 1992)** showed that middle-aged and elderly Danish men with serum selenium below 79µg/L had a significantly increased risk of ischaemic heart disease. In one report, ventricular tachycardia resistant to several standard therapeutic agents was normalized after selenium supplementation to the patient. Selenium supplementation may be of benefit in preventing ischemia-reperfusion injury: a selenium enriched diet had a significant effect in preventing reperfusion-induced arrhythmias in an animal model **(Tanguy et al., 1998)**.

Oxidative stress or inflammatory conditions and selenium

Selenium behaves both as an antioxidant and anti inflammatory agent. Its antioxidant role, notably as GP*x*, can reduce hydrogen peroxide, lipid and phospholipids hydroperoxides. Diminishing the production of inflammatory burst was provided with removal of hydrogen peroxide and reduction of superoxide production. Any conditions associated with increased oxidative stress or inflammation might be expected to be influenced by selenium levels, which may be the case in rheumatoid arthritis, pancreatitis, and asthma. In a double-blind randomized trial, a small group of patients with rheumatoid arthritis, supplementation with 200µg selenium as selenium yeast for 3 months, significantly had reduced pain and joint involvement **(Knekt et al., 2000)**. There is an evidence for a protective effect of selenium in pancreatitis, a disorder associated with a high level of oxidative stress. Another small study in intrinsic asthmatics showed significant clinical improvement on supplementation with selenium at 100 µg per day as sodium selenite. However, significant associations between selenium status and prevalence or severity of asthma have not been consistently demonstrated in human studies **(Norton and Hoffman, 2012)**.

Viral Infection and selenium

Selenium deficiency is linked to the occurrence virulence or disease progression of some viral infection. Beck and his group **(Beck, et al., 1995)** have shown that harmless viruses can become virulent in a selenium deficient host. Coxackie virus has been isolated from the blood and tissue of people with Keshan disease, coxackie virus become virulent, and causing myocarditis infection in the host **(Beck et al., 1998)**. In selenium-deficient host, the other RNA viruse infections, such as poliovirus, hepatitis, influenza or HIV infections progresses will be more serious. Selenium also appears to be protective in infection with hepatitis virus B and C against the progression of the condition to liver cancer **(Yu et al., 1999)**. It has been suggested that retroviruses such as HIV and coxsackie B3 have the potential to deplete the host's selenium supply by incorporating the selenium into viral selenoproteins for their own protection, as has been demonstrated for the DNA virus, molluscum contagiosum **(Zhao et al., 2000)**.

Reproduction

Selenium is required for human sperm maturation and sperm motility and may reduce the risk of miscarriage **(Rayman, 2002)**. Barrington and Behne **(Barrington et. al., 1996)** found that testicular morphology and functions are affected by severe selenium deficiency and that the element is necessary for testosterone biosynthesis and the formation and normal development of spermatozoa. Animals fed Se-deficient diets show structural abnormalities in the sperm, thus decreasing the chance of fertilization **(Oldereid et al., 1998)**. The selenoprotein phospholipids hydroperoxide glutathione peroxidase (PHGP*x*) is abundantly expressed in spermatids as active peroxidase, where it is a major constituent of the mitochondrial capsule in the midpiece. Male infertility in selenium-deficient animals, which is characterized by impaired sperm motility and morphological midpiece alterations, is considered to result from insufficient PHGPx content **(Maiorino, 2002)**. In studies by Scott and Macpherson **(Scott and Macpherson, 1998)**, supplementation of subfertile men with 100 µg selenium per day for 3 months significantly increased sperm motility. Se-P is required for development of functional spermatozoa and indicates that it is an

essential component of the selenium delivery pathway for developing germ cells **(Flohé, 2007)**. Selenium supplementation was demonstrated in sub–fertile Scottish men who showed a significant increase in sperm motility when supplemented with 100mg selenium/day for 3 months. There is, however, a suggestion that relatively high intakes (about 300mg/d) may decrease sperm motility **(Hawkes et al., 2001)**. In UK pregnant women with higher selenium status had a significantly lower risk of first-trimester or recurrent miscarriage **(Barrington et al., 1997)**. **Fortier et al., 2012** reported the uterine transfer of selenium to embryos was improved with organic Se-yeast as compared to inorganic sodium selenite (Na_2SeO_3), and this was concomitant with a enhanced selenium-specific antioxidant status and development of embryos.

Moods and selenium

The study in the UK, where a 100µg selenium supplement significantly decreased anxiety, depression, and tiredness, the effect being greatest in those whose diets were low in selenium **(Benton and Cook, 1998)**. There can be no doubt that selenium is important to the brain: animal models of neurodegenerative diseases show enhanced cell loss in selenium depletion.

Thyroid function and selenium

Type I iodothyronine deiodinase, an enzyme necessary for proper thyroid function and conversion of T4 into T3 is a selenoprotein containing selenium in the form of selenocysteine. Selenoenzymes GPx and thioredoxin reductase are crucial to the protection of the thyroid from the hydrogen peroxide (H_2O_2) that is produced there for thyroid hormone synthesis. Selenoenzyme iodothyronine deiodinase is required for the production of active thyroid hormone **(Beckett et al., 2005)**.

Type-2 diabetes

Evidence linking selenium to glucose metabolism is conflicting. High selenium status was associated with reduced diabetes prevalence in three case control studies **(Rajpathak et al., 2005)**. By contrast, high serum selenium concentration was associated with an increased prevalence of diabetes in the large US National Health and Nutrition Examination Surveys **(Bleys et al., 2007)**. The selenoenzyme GPx1 which removes H_2O_2,

a second messenger, produced during insulin signaling might be responsible for increased risk of type-2 diabetes following high selenium intake or supplementation. Another selenoprotein implicated in diabetes risk is SEPP1. It functions as a negative insulin modulator **(Rayman, 2012)**.

Several studies suggest that low levels of expression of GPx1 and other stress related (regulated by the amount of selenium in the diet) selenoproteins are as damaging as high levels of expression with respect to insulin resistance and hyperglycaemia **(Labunskyy et al., 2011)**. Hence a U-shaped association between selenoproteins and type-2 diabetes risk might explain some of the apparently contradictory findings.

Cancer and selenium

Various mechanisms of selenium in cancer prevention

The protective role of selenium in carcinogenesis

It is generally accepted that carcinogen-induced genetic damage via the formation of covalent DNA adducts is necessary, but not sufficient, for the initiation of carcinogenesis. In most of these studies, selenium (as selenite, selenate, 1,4-phenylenebis(methylene)selenocyanate (p-XSC) or diallyl selenide (DASe) have been shown to inhibit the initiation phase of carcinogenesis induced by various carcinogens in mammary, liver, colon and lung tissue in rats **(El-Bayoumy, 2001)**. In experiments with selenium enriched garlic, (**Ip and Lisk, 1994)** reported an inhibition of both the initiation and post-initiation stages of mammary carcinogenesis after dimethylbenz(a)anthracene (DMBA) treatment of rats. The explanation for cancer prevention is that some selenium compounds affect procarcinogen activation and metabolism through inhibition of phase I and induction of phase II enzymes. Phase I enzymes are members of the cytochrome P450 system responsible for converting chemical carcinogens to reactive adducts that can attack to DNA. On the other hand, defense against carcinogenic injury is provided by phase II detoxifying enzymes. The experiments by (**Ip and Lisk, 1997)** showed that increased detoxification of carcinogen via the phase II conjugating enzymes might represent the mechanism of tumor suppression by selenium-enriched garlic. This mechanism has been well documented to be important for the chemopreventive activity of many

thiol-reactive chemopreventive agents, mainly by inhibition of the initiation stage of carcinogenesis **(Zhou et al., 2003)**.

However, suppression of carcinogenesis by selenium compounds in the post-initiation stages of carcinogen treatment in animal models suggests the existence of additional mechanisms for cancer chemoprevention. The ability of selenium compounds to inhibit cell growth and to induce tumor cell apoptosis has now been widely demonstrated and is suggested to be a potential mechanism for cancer chemoprevention **(Sinha and El-Bayoumy, 2004)**. It has been speculated that selenium-induced apoptosis can remove carcinogen-initiated transformed cells and suppress the clonal expansion of such transformed cell population **(Zhou et al., 2003)**.

Many experiments have shown that the chemopreventive effect of selenium is due in part to its inhibitory effect on cell growth, DNA, RNA and protein synthesis in transformed cells **(El-Bayoumy, 2001)**. Although the molecular mechanisms of the cancer chemopreventive activity of the selenium compounds remains largely unknown, changes in stress-related cellular proteins have been implicated in explaining the protective effects of selenium. Because protein kinases play a central role in the regulation of cell growth, tumor promotion and differentiation, several reports have described the inhibitory effect of selenium on kinase activity **(Gopalakrishna et al., 1997)**. Moreover, cell cycle CDK2 or cell signaling protein kinases and/or a number of redox-regulated proteins, including the critical transcription factors, such as AP-1 and NF-κB, have been proposed as targets against which Se exerts its chemopreventive effects **(Zhu et al., 1995)**.

Antioxidant activities of selenium

All living aerobic organisms have developed certain defense mechanisms that provide protection against oxidative damage induced by ROS **(Valko et al., 2004)**. The best known of these antioxidant enzymes is superoxide dismutase **(Davies, 1994)**. Selenium was found to be a component of antioxidant defenses either as agent able to scavenge free radicals, or as a component of a family selenoenzymes. Experimental evidence suggesting its effect in eliminating oxidative stress came in

1973 when selenium was found to be incorporated into the first identified selenoprotein, glutathione peroxidase (GPx) **(Rotruck et al., 1973)**. Members of the GPx family of enzymes are effective in catalyzing the reduction of hydrogen peroxide (H_2O_2) and lipid peroxides. In view of the role of GPx in reducing oxidative stress it was proposed that selenium-dependent GPx provided a plausible mechanism for cancer prevention. However, it was found that GPx activity was maximized in tissues of animals fed normal amounts of selenium and was not elevated as dietary selenium was increased 10-fold at higher levels necessary to achieve chemoprevention. Thus, it seemed that selenium supplements exerted their chemopreventive effect in a manner unrelated to the saturated levels of GPx **(Combs and Gray, 1998)**. Selenium is found to be a component of several other selenoproteins, some of which have important enzymatic functions associated with antioxidant defenses. One of these, thioredoxin reductase is considered to be a key enzyme in selenium metabolism, reducing selenium compounds and controlling the intracellular redox state **(Madeja et al., 2005)**. Additionally, iodothyronine deiodinase, produces the active thyroid hormone, T3 from an inactive precursor T4. Another selenoprotein, selenoprotein P appears to protect endothelial cells against damage from free radicals **(Rayman, 2000)**. Each of these selenoproteins contains selenium in the form of selenocysteine, which is incorporated by the co-translational modification of transfer RNAbound serine at certain loci encoded by a specific UGA codon. As noted above, it has generally been thought that the selenoproteins fulfill only the nutritional requirement for dietary selenium. There was not unambiguous evidence supporting the role of any known selenoprotein in cancer prevention. However, it has recently become clear that optimal expression of some selenoproteins, notably selenoprotein P, requires higher amount of dietary selenium **(Xia et al., 2005)** and that a substantial number of individuals may have a higher selenium requirement for efficient synthesis of selenoproteins **(Rayman, 2005)**. This inter individual variation in selenoprotein expression levels may be accounted for single-nucleotide polymorphisms in selenoproteins genes that determine the efficiency with which individuals can incorporate selenium into selenoproteins **(Apostolou et al., 2004)**. Whether the selenoproteins are crucial to the anticancer

effects needs to be elucidated. The functions of many of the 25 human selenoproteins are as yet unknown, although some of them are involved in antioxidant and anabolic processes **(Hatfield and Gladyshev, 2002)**. Selenoproteins that may be relevant to cancer risk are supposed to be the GPx family, the 15 kDa selenoprotein, selenoprotein P and the thioredoxin reductases, although a beneficial role of thioredoxin reductase in cancer prevention is doubtful (**Rayman, 2005)**.

Role of selenium in apoptosis

Evasion of apoptosis is one of the hallmarks of human cancer. It is responsible for tumor promotion and progression as well as for treatment resistance **(Fulda, 2009)**. It is known that the most cytotoxic agents used in cancer treatment mediate their anticancerogenic effects by induction of apoptosis **(Lowe and Lin, 2000)**. Apoptosis induction is thought to be also one of the mechanisms mediating the anticancer activity of selenium. Apoptosis induced by supranutritional doses of this compound was described in various types of neoplastic cells, including prostate cancer, colon cancer, liver cancer, leukemia and lymphoma. The regulating mechanisms of selenium-induced apoptosis are very complex and involve protein kinases signaling, activation of caspases, p53 phosphorylation and ROS generation **(Sanmartin et al., 2008)**. Importantly, monomethylated selenium compounds, that are direct precursors of putative active anticancer metabolite CH_3SeH, induce apoptosis through biochemical and cellular processes that are distinct from those induced by selenium forms that initially enter the H_2Se pool, such as inorganic selenium **(Zeng and Combs 2008).**

Apoptosis induced by the precursors of H_2Se, such as sodium selenite, seems to be connected with single strand breaks (SSBs) formation and genotoxicity **(Zhou et al., 2003)**. A fact that SOD blocks formation of SSBs and apoptosis, suggests that these effects are directly connected with the redox state of sodium selenite **(Zhong and Oberley, 2001)**. Sodium selenite induced apoptosis in human prostate cancer cells involved O_2^- production that was mainly in or adjacent to mitochondria and therefore triggered apoptosis involved mitochondrial pathway **(Xiang et al., 2009)**. In addition, sodium selenite exposure caused S-phase cell arrest, induced SSBs and caused ROS

induced p53 activation leading to superoxide/p53/Bax mediated activation of mitochondrial pathway in the human p53 proficient LNCaP prostate cancer cells **(Li et al., 2007)**. The phosphorylation of p53 appeared to be important for activating the caspase mediated apoptosis involving both caspase-8 and caspase-9 **(Jiang et al., 2004)**. On the other hand, apoptosis induced by SeL in p53 mutant human DU145 prostate cancer cells and in p53 null HL6O leukemia cells is a caspase independent, and it is accompanied with decreased expression of p27kipl and p2lcipl and increased phosphorylation of AKT, JNKI/2 and p38MAPK **(Zeng et al., 2009)**. It was also found **(Chen and Wong, 2008)** that SeCys, with similar mode of action as sodium selenite, induced apoptosis connected with DSBs formation, p53 phosphorylation and ROS generation in A373 human melanoma cells. In nude mice xenografts, SeCys significantly inhibited tumor growth via induction of apoptosis. Furthermore, it was demonstrated that sodium selenite induced apoptosis is coupled with the activation of ATM/ATR signaling pathway and induction of topoisomerase I and II DNA complexes and DNA damage in HL60 and K562 human leukemia cell lines **(Lopez-Lazaro et al., 2008)**. Thus, DNA damage seems to play an important regulatory role in apoptosis induced by precursors of H_2Se, such as sodium selenite and SeCys.

On the other hand, precursors of CH_3SeH, such as Methylseleninic acid (MSA), induced apoptosis in mammary tumor epithelial cells without induction of DNA strand breaks **(Lu et al., 1995)**. It was demonstrated that a monomethylated selenium compound, MSA, induced apoptosis in human DUI4S prostate cancer **(Jiang et al., 2001)** and HL60 leukemia cells **(Kim et al., 2001)** in a caspase dependent but p53 independent way, as they are p53 mutant and p53 null cells, respectively. MSA induced apoptosis was accompanied by the activation of multiple caspases (caspase-3, 7, 8 and 9), mitochondrial release of cytochrome c, poly (ADP-ribose) polymerase cleavage and DNA fragmentation. Of note, p53 independent MSA induced apoptosis was also observed in human LNCaP prostate cancer cells which, however, contain wild type p53 protein **(Li et al., 2007)**. Recently, it was demonstrated **(Suzuki et al., 2007)** that apoptosis induced by three selenium compounds, SeMet, MeSeCys and sodium selenite, in human HSC 3 and HSC 4 oral squamous cell carcinoma, A549 non-small cell lung adenocarcinoma and MCF7 breast cancer is caspase dependent process that, however, involves complicated

mechanisms. Activation of both the intrinsic apoptotic pathway and endoplasmic stress pathway plays a major and concurrent role, while p53 activation is important only in the case of SeMet. These results suggest that the process of selenium induced apoptosis in cancer cells is very complex and many factors such as chemical form of this compound, type of cells, p53 or androgen signaling status may influence its course.

Selenium and cancer treatment

Numerous evidences have been accumulated over the past decade indicating that Se compounds have potential to be used not only for cancer prevention but also for cancer treatment. The inhibitory effect on cell growth with a preference for tumor cells versus non-transformed cells suggests that Se compounds should belong to drugs modifying and/or inhibiting process of carcinogenesis. Analysis of the gene expression profile in several cancer cells revealed that Se-induced growth inhibition is associated with modulation of the cell cycle, apoptosis and signaling **(Narayanan, 2006)**.

Cancer inhibiting efficacy of selenium depends on its chemical forms. Different chemical forms of selenium metabolize differently in vivo, activate distinct molecular mechanisms and exhibit varying degree of toxicity and possible anticarcinogenity. Selenomethionine (SeMet), methylselenic acid (MSA) and sodium selenite (Na_2SeO_3) are the most frequent forms in which tumor inhibiting potential was tested in cell culture, preclinical and clinical studies. SeMet seems to be less suitable for such studies. The reason is that SeM needs to be metabolized primarily in liver β-lyase to a monomethylated intermediate for the expression of the anticancer activity, and epithelial tissues generally have a low capacity to generate a monomethylated selenium metabolite from SeMet **(Dong et al., 2002)**. MSA might be more appropriate than SeMet as supplements for supporting the production of Se intermediates with potential anticarcinogenic activities such as H_2Se and CH_3SeH or both. A large number of potential selenium-responsive genes were identified after exposure to either 5 or 10 μM MSA for 48 or 72 h in PC-3 human prostate cancer cells **(Dong et al., 2003)**. Na_2SeO_3 is supposed to be a form that has a great chance to be clinically used in cancer therapy. This stems mainly from its prooxidant character and low bioavailability in comparison with SeMet **(Reeves et al., 2005).** The effects of Na_2SeO_3 either on redox regulation of transcription factors or on inhibition of cell growth

seems to be associated with ROS production and alteration of thiol redox balance **(Yan and Spallholz, 1993)**.

Role of oxidative stress

There is duality as to ROS connection with cancer. First, ROS belongs to cancer-promoting factors. $O_2^{\bullet}$ is rapidly dismutated by superoxide dismutase yielding H_2O_2, which can diffuse to the nucleus and give rise to formation of highly toxic •OH radical which attack DNA, thereby contributing to genetic instability **(Brozmanova ´et al., 2001)**. Moreover, the increase in chronic ROS levels may cause accumulation of damage not only in DNA, but also in lipids and proteins causing oxidative stress. Damage of these macromolecules may lead to a variety of pathological consequences, including cancer, neurodegenerative disease and aging **(Maynard et al., 2009)**. Secondly, ROS can suppress cancer progression. It was suggested that cancer cells normally produce more ROS than do normal cells **(Trachootham et al., 2009)**. Moderate levels of ROS in normal cells have been implicated in regulation of diverse cellular functions including intracellular signaling, transcriptional activation, proliferation and survival. Significant elevation of ROS in cancer cells may participate in anomalous signaling pathways and expression of genes that contribute to cancer suppression by preferential induction of apoptosis in affected cells while leaving normal cells intact **(Pan et al., 2009)**. Chemopreventing agents that enhance ROS and/or oxidative stress in transformed cells could drive these cells to elimination via apoptosis and amplifying of oxidative stress in tumor cells by these agents above the threshold level was supposed to be associated with cancer-specific toxicity **(Trachootham et al., 2009)**. Na_2SeO_3 have chemotherapeutic potential by inducing cancer cell apoptosis with minimal side effects to normal cells. This cancer-specific chemotherapeutic potential of Na_2SeO_3 is supposed to be associated with its prooxidant character **(Lipinski, 2005)**. However, precise mechanism by which Na_2SeO_3 stimulates apoptotic machinery in cancer cells is poorly understood yet. More recently, it has been demonstrated that key factor of specific Na_2SeO_3 cytotoxicity is selenium uptake which depends on extracellular environment, namely on extracellular thiols, the level of which is commanded by x_c^{-} cystine/glutamate antiporter widely expressed in different cancer cell lines as well as primary tumors **(Olm et al., 2009).**

Supplementation of selenium during chemotherapy and radiotherapy

Selenium compounds may potentially be beneficial for anticancer therapeutic regimens because they may increase efficiency of therapeutic agents. Such effect was observed in vitro using battery of tumor cell lines including breast, lung, prostate and colon. Supplementation of Se in the form of inorganic selenous acid enhanced chemotherapeutic effects of taxol and doxorubicin in these cells beyond that seen with the chemotherapeutic drugs used alone **(Vadgama et al., 2000)**. Similar results were published for combined effect of Na_2SeO_3 and campthotecin on cervical carcinoma cells when Na_2SeO_3 behaved as a potential modulator and enhancer of campthotecin-based anticancer therapy **(Rudolf et al., 2004)**. Using a panel of human B-cell lymphoma cell lines, it was found that the chemotherapeutic effects of doxorubicin, etopoxide, 4-hydroperoxycyclophosphamide, melphalan and 1-b-D-arabinofuranosylcytosine were increased up to 2.5-fold when combined with minimally toxic concentration of organic selenium compound methylselenic acid. This concentration of methylselenic acid induced DNA strand breaks and 50% decrease in nuclear factor-κB (NF-κB) activity after 5-h exposure. The results suggest that NF-κB pathway is one target for mechanism by which methylselenic acid modulates the activity of cytotoxic drug **(Juliger et al., 2007)**. More recently, it has been shown that poor sensitivity to 5-fluorouracil (5-FU) in certain colorectal cancer cells was adjusted by its combined treatment with selenous acid, thus indicating possible efficacious strategy to overcome 5-FU resistance in certain colorectal cancer cells **(Thant et al., 2008)**. Selenium compounds can also modulate therapeutic effects of ionizing radiation (IR) in tumor cells and tissues **(Dorr, 2006)**. It was demonstrated that pretreatment with sodium selenite sensitized both LAPC-4 and androgen independent DU145 human cancer prostate cells to clinically relevant dose of IR **(Husbeck et al., 2005)**. These observations suggest that sodium selenite might be a novel radiosensitizer for treatment of prostate cancer. Radiosensitizing effect of SeL was also observed in IR exposed C6 rat glioma cells **(Schueller et al., 2004)**. Furthermore, it was exhibited that SeMet exposure resulted in the selective enhancement of sensitivity to IR in human lung cancer cell lines, whereas it has no effect on normal lung cell line **(Shin et al., 2007)**.

Selenium Deficiency

Although selenium deficiency in animals has long been recognized, obvious clinical signs of human selenium deficiency are rare. One of the selenium-deficiency disorders in humans is known as Keshan Disease. Keshan disease was named after an epidemic outbreak in 1935 in Keshan County, China. This disease occurred in the selenium deficient soil areas **(Cheng and Qian, 1990)**. Keshan disease is an endemic cardiomyopathy that occurs with signs of congestive heart failure or stroke from diffuse cardiac thromboses **(Tuomilehto et al., 1994)**. The myocarditic coxsackievirus has been associated with the pathogenesis of this disease. The virus will become virulent in selenium deficient or vitamin E deficient animals **(Beck, 1994)**. Selenium enriched salt supplementation of the diets has reduced significantly the incidence of Keshan disease in selenium deficient areas **(Xia et al., 2005)**.

Another disease found in humans as a result of selenium deficiency is Kashin-Beck disease. Like Keshan disease, Kashin-Beck is most prevalent in areas of the world with selenium deficient soils. A range of bone and joint deformations that develop during childhood and puberty characterizes the disease. The hands and feet are usually affected, and the bones of the wrist and ankles may be smaller in size or sometimes completely absent **(Fairweather et al., 2011)**. Radiographs of these affected individuals have shown that the disease causes a deformation and fragmentation of the epiphyseal plate, uneven mineralization of the extracellular matrix, and an irregular bone surface. One diagnostic feature of Kashin-Beck disease is the broken, blocky or conical shape of the growth apparatus **(Fairweather et al., 2011)**. Histological observations attribute these signs to the necrosis of chondrocytes during bone growth and necrosis of the growth plate. Although, the importance of selenium for bone metabolism is still unknown, the consequences of the disease demonstrate the requirement for selenium in bone metabolism (**Moreno-Reyes et al., 2001)**.

Toxic thresholds of selenium ingestion

All selenium compounds are potentially toxic to animals with the toxicity dependent upon the animal species, the chemical form of the selenium compound, the route of administration and the dose. For selenium compounds, the often quoted statement

attributed to Paracelsus, Father of Modern Medicine, "The dose makes the poison" is particularly apparent and presently apt in view of the recent deaths of the 21 Polo horses in Florida noted above. To date, we know only that selenite was administered to these horses and that liver and blood tissues contained circa 20×the normal levels of selenium. Further details will surely determine the amount of selenium in the formulary and the total amount of selenite selenium administered to the Polo horses.

Selenite selenium along with selenate selenium is a common additive to animal feeds present at 0.1– 0.2 ppm selenium. Experimental rats and mice can tolerate dietary selenite/selenate selenium to about 2 ppm Se, with about 3–5 ppm Se being chronically toxic and 10–15 ppm Se fatal as summarized in (**Table 2).** Organic selenium supplements Se-yeast, selenomethionine and Se-methylselenocysteine are less toxic than the inorganic selenium compounds.

Selenium	μg Se g^{-1} diet (ppm)	Atoms Se g^{-1} diet
Nutritional deficiency	0.05	38 000 000 000 000 000
Nutritional adequacy	0.20	152 000 000 000 000 000
~Oral tolerance	2.00	1 520 000 000 000 000 000
~Oral toxicity	5.00	3 800 000 000 000 000 000
~Oral lethality	15.00	11 400 000 000 000 000 000

Numbers are approximate depending upon species, sex, age and other dietary factors. Given to the author (JES) by the late Dr Douglas Frost, Schenectady, NY.

Table 2: Mathematics of selenium essentiality and toxicity (selenite; rodents)

All selenium compounds are potentially toxic to humans. Although there is much less controlled experimental data, there are some mistakes that have been made with human selenium supplements similar to that which has recently occurred in the Polo horses. There is no reason to suspect that the chemical forms of selenium that are toxic to animals are not similarly toxic to humans. Thus, selenite/selenate selenium probably remains as the most toxic selenium dietary supplement available, with Se-yeast, selenomethionine and methylselenocysteine being much less toxic. Very few reports of selenium toxicity have been reported in humans, but they are not unknown. The most extensive environmental human selenium toxicity occurred in China with keratinous tissues affected, loss of hair and cracked nails as found in horses, cattle and sheep, loss of

mane, hair, wool along with cracked and deformed hooves. Similar symptoms have been reported in Water Buffalo in the Indian Punjab due to high selenium content of ground waters.

The US RDI is 55 µg Se each day for adults from food and/or supplements. The tolerable upper limit (TUL) is 400 µg Se each day and overt selenosis occurs at 15,000 µg selenium each day as observed in China. (**Table 3**) provides dietary intake information about selenium and its effects in humans. The data are presented as it might apply to selenite. The predominant forms of dietary selenium intake from foods are selenomethionine and selenocysteine with much lesser amounts of methylselenocysteine. These latter selenium compounds are less toxic and the tabular data below do not directly apply to the toxic selenium concentrations cited.

Se ($\mu g\ day^{-1}$)	Chemical form	Effect
<11	Dietary	Keshan's disease
20	Dietary	Minimum dietary requirement
40	Dietary	WHO adequate dietary requirement
55	Dietary	Adult US RDI
400	Dietary	TUL, tolerable upper limit
600	Dietary	Individual maximum safe limit
819	Dietary	NOAEL, maximum safe limit
1000	Na_2SeO_3	Personal known intake for years
1540	Dietary	LOAEL, low level toxicity
1600	Dietary	Adverse effective level
5000	Dietary	Selenosis; hair and nail loss
15 000	Dietary	Overt selenosis

Table 3: Selenium essentiality and toxicity in humans

Toxicity of selenium compounds

As noted above, selenium toxicity is initially thought to have been first described in horses by Marco Polo while travelling the "Silk Road" of China. A similar description of toxicity symptoms affecting hooves and mane hair in horses given by Marco Polo was also observed in horses in the western United States in the late 1800s. Its cause was to remain undiscovered until the USDA in South Dakota and the Wyoming Experiment Station in the 1930s determined that the cause of the toxicity was the ingestion of seleniferous range plants containing up to several thousand milligrams of selenium per kg

dry matter. With great sadness, it was the 21 Argentinean Polo horses that succumbed to acute selenium toxicity in Florida in May 2009 resembling "blind staggers".

In the case of selenium toxicity from seleniferous plants and infrequently from cereal grains, toxicity to horses and other livestock is from organic selenium compounds. In contrast, the Polo horses from Argentina succumbed to selenite, inorganic selenium toxicity, with more than 20 times the normal concentration of selenium found in liver and muscle tissues. Inorganic selenium compounds, selenates/selenites, particularly selenites, are infrequent constituents of ground or well water, but more frequent constituents of leaching from concentrated geological formations and commercial mine effluents. These more highly concentrated inorganic selenium sources enter the food chain through algae and other plants and then up the food chain making their way to birds and fish of all kinds. Although selenium is not necessarily concentrated in the food chain by adults, it may be highly concentrated in eggs by female adults. Selenium toxicity is well known to adversely affect unborn fish, birds and perhaps other ovaripids when it is excessively ingested by females during periods of ovogenesis and egg formation. Such embryos are subject to selenium-induced developmental mutations and malformations of chicks and fish **(Hoffman, 2002)**.

Inorganic selenium toxicity

From the time of the association of seleniferous plants with toxicity in the 1930s and the subsequent experimental confirmation of selenite toxicity in laboratory animals, the reason for selenium's toxicity had been debated for years thereafter. At the second International Symposium of Selenium in Biology and Medicine held in Lubbock, Texas in 1980 the major focus of the meeting was the composition, mechanism and role of selenium in glutathione peroxidase. Two presentations were to progress the understanding of the metabolism of inorganic selenium (e.g., toxicity) in biological systems initially pioneered by **Painter (1941)**, and latter by **Tsen and Tappel (1958)**. The first paper by **Kice (1981)**, System Toxicology Approaches for Evaluating Chemical Carcinogenicity, discussed the detailed reaction of Se IV species, selenite/selenium dioxide, with thiols, as first reported by Tsen and Tappel in 1958. In Nanotoxicology of the Symposium, **Bhuyan et al., 1981** described their not-too-distant past work on the generation of bilateral nuclear cataracts in rats, rabbits and guinea pigs from a single

injection of selenite following the finding that these injections did not protect rabbits from cataracts induced by 3-aminotriazole. Cataract induction in animals by 3-aminotriazole had been shown to be due to the generation of reactive oxygen species (ROS), loss of lens protein thiols and lenticular lipid peroxidation. Ascorbic acid (vitamin C) had been shown to protect from 3-aminotriazole cataract formation in animals, but when "other antioxidant" selenium failed to afford protection but rather induced cataratogenesis, insight into selenium's oxidative role in biological systems further emerged. Selenite, by oxidizing thiols, cross-linking disulphides and forming unstable selenotrisulphides, as originally proposed by **Painter (1941)**, was discussed in the context of cataract formation by injections of selenite.

Bhuyan had alluded to in their 1981, Proceedings publication (**Bhuyan et al. 1981**) was the possibility that selenite was generating ROS as the cause of cataract formation. Their supposition could have been more emphatic had they been aware of and cited the paper of (**Misra, 1974)**. The study by Misra describes the auto-oxidation of various thiols, including glutathione, generation of superoxide and the inhibition of nitroblue tetrazolium (NBT) reduction by superoxide dismutase. The authors went on to explain how transitions metals, such as copper, might catalyse thiol oxidation generating superoxide and other ROS. Thus, both (**Kice** and **Bhuyanet al., 1981)** had the selenium chemistry, *in vitro* and *in vivo*, nearly correct. What was missing was the "Misra Connection" to the superoxide generation from the auto-oxidation of glutathione. Selenite selenium was just a catalyst of thiol oxidation, as first demonstrated by (**Levander et al., 1973)** and later shown by (**Seko et al., 1989)**, to produce superoxide. The "Misra Connection" to selenate-accelerated superoxide generation was directly made by (**Seko et al., 1988)** in an unassuming poster presentation at the 4th International Symposium on Selenium in Biology and Medicine in Tubingen, Germany and later published in the Proceedings of the Symposium **(Seko et al., 1989)**. This realization that inorganic selenite generated superoxide and likely other ROS seemed to account for the toxicity of selenite *ex vivo* and *in vivo*. Immediately following the Seko paper in the Proceedings were two papers that, retrospectively, evaluated the superoxide-generating effect of selenium that was generating superoxide. Following the Seko paper was a manuscript by (**Hogberg et al., 1989)** showing that selenite in a dose-dependent manner induced single

stranded DNA fragmentation provided that oxygen was present. Hogberg and coworkers had previously shown that selenite induced cell lysis and speculated that oxidation–reduction (redox) cycles were likely at play contributing to the lysis of hepatic cells. The paper following Hogberg and coworkers, by (**Frankel and Favey, 1989)**, reported that selenite inhibited DNA and RNA polymerases but only in the presence of a thiol. Again, retrospectively, these authors incorrectly concluded that selenite was toxic by forming a seleno trisulphide **(Ganther, 1968)**, selenodiglutathione, which then served to inhibit the polymerases. In their experiments, non-specific cell depletion of all thiols served to inhibit selenite inhibition of the polymerase whereas specific inhibition of glutathione with buthionine sulfoximine did not prevent polymerase inhibition. This suggests that not only selenite but also other thiols such as protein thiols (cysteine residues) oxidize gluthathione to generate superoxide. From more recent research, it is known that selenite *in vivo* targets and oxidizes the protein thiols of mitochondria **(Hail and Lotan, 2009)** decreasing the mitochondrial membrane potential. This is the likely cause of mitochondrial swelling, as first observed by **Levander et al., 1974**, and the inhibition of the mitochondrial permeability transition (MPT) pore followed by the release of cytochrome- *c*. As a cellular oxidizer, selenite oxidation is concentration dependent and does not apparently discriminate among thiols. Most cells encounter selenite toxicity exposed to concentrations of 5–10 μM.

Organic selenium toxicity

Toxicity of organic selenium compounds in comparison with selenite is well known to be far less toxic to cells, particularly as studied with cancer cells *in vitro* **(Fico et al., 1986)** and in mice **(Poirier and Milner, 1983)** as well as in larger animals on a comparative selenium basis **(Tiwary et al., 2006)**. *In vivo*, the study of inorganic and organic selenium metabolism beyond H_2Se formation showed that methylation reactions were the route to selenite and organic selenium detoxification and excretion **(Foster et al., 1986)**. The trimethylselenonium ion is excreted in urine and the methylated intermediate of the trimethylselenonium ion, dimethylselenide, is exhaled via the pulmonary system. The latter route of selenite metabolism and excretion occurs under mild to severe toxic conditions where the methylation pathways appear to be compromised and which

contributes to the "garlicky to horse radish" smell of the breath from dimethylselenide **(Hsieh and Ganther, 1977)**.

When present in tissues or cells we know that all the principal dietary forms of selenium, selenomethionine, selenocysteine and methylselenocysteine, are metabolized by enzymes, methioninase and β-lyases, directly or indirectly in the case of selenocysteine via methylation of H_2Se and on to an common metabolite, methylselenol, CH_3SeH. It is also known that like selenite, methylselenol can react with glutathione and generate superoxide as shown *in vitro* from dimethyldiselenide **(Spallholz et al., 2001)**, and from the methioninase reaction with selenomethionine as substrate **(Spallholz et al., 2004)**. The realization that many organic selenium compounds were toxic because of the same or a similar selenite chemistry generating superoxide immediately became plausible to Spallholz **(Yan et al., 1991)** from the 1988 poster presented at Tubingen. By 1990, the authors knew that in an *in vitro* chemiluminescent (CL) assay that measured superoxide generation, selenite and selenocystine both generated superoxide in the presence of glutathione and other thiols **(Yan et al., 1990)**. Selenate and selenomethionine were not catalytic in the *in vitro* CL assay and were therefore not toxic to cancer cells affecting cell growth at the same concentrations of added selenium compounds. The CL superoxide data and 1991 mammary cancer cell data from these selenium compounds were the same for selenite, selenate, selenocystine and selenomethionine as that reported by (**Greeder and Milner, 1980)** against an ascites cancer in mice. (**Thompson and Ip, 1991)** found that when selenite was injected into Sprague–Dawley rats the hepatic glutathione levels were lowered when measured 2 h later. *In vivo*, feeding 5 ppm Se as selenite in diets increased hepatic glutathione whereas selenomethionine had no effect upon glutathione. It was quite clear that the similarities and differences between the toxicity of selenite and organic selenium compounds to cells in culture, and animals, depended upon the differences in the chemical composition of different organic selenium compounds and how they were being metabolized.

Nanotechnology

Background of Nanotechnology

The prefix "nano" derives from the Greek word for "dwarf". One nanometer (nm) is equal to one-billionth of a meter, or about the width of 6 carbon atoms or 10 water molecules. A human hair is approximately 80,000 nm wide, and a red blood cell is approximately 7000 nm wide. Atoms are smaller than 1 nm, whereas many molecules including some proteins range between 1 nm and larger **(Whitesides, 2003)**.

The conceptual underpinnings of nanotechnologies were first laid out in 1959 by the physicist Richard Feynman in his lecture, "There's plenty of room at the bottom". Feynman explored the possibility of manipulating material at the scale of individual atoms and molecules, imagining the whole of the *Encyclopedia Britannica* written on the head of a pin and foreseeing the increasing ability to examine and control matter at the nanoscale. The term "nanotechnology" was not used until 1974, when Norio Taniguchi, a researcher at the University of Tokyo, used it to refer to the ability to engineer materials precisely at the nanometer level. The primary driving force for miniaturization at that time came from the electronics industry, which aimed to develop tools to create smaller (and therefore faster and more complex) electronic devices on silicon chips. Furthermore, at IBM in the United States, a technique called electron beam lithography was used to create nanostructures and devices as small as 40 to 70 nm in the early 1970s.

Nanotechnology can be defined as the science and engineering involved in the design, synthesis, characterization and application of materials and devices whose smallest functional organization in at least one dimension is on the nanometer scale (one-billionth of a meter) **(Sahoo and Labhasetwar, 2003)**. In the past few years nanotechnology has grown by leaps and bounds, and this multidisciplinary scientific field is undergoing explosive development **(Chan, 2006)**. It can prove to be a boon for human health care, because nanoscience and nanotechnologies have a huge potential to bring benefits in areas as diverse as drug development, water decontamination, information and communication technologies, and the production of stronger, lighter materials. Human health-care nanotechnology research can definitely result in immense health benefits. The genesis of nanotechnology can be traced to the promise of revolutionary advances across medicine, communications, genomics, and robotics. A is too vast and diverse to discuss

in detail, but without doubt, one of the greatest values of nanotechnology will be in the development of new and effective medical treatments complete list of the potential applications of nanotechnology **(Shaffer, 2005**).

Nanoparticle

One of the first and most natural questions asked when starting to deal with nanoparticles is "Why are nanoparticles so interesting? Why work with these extremely small structures that are challenging to handle and synthesize especially when compared with their macroscopic counterparts?" The answer lies in the unique properties possessed by these nanoparticles.

Nanoparticles have a large surface area to volume ratio which leads to an alteration in biological activity compared to the parent bulk materials. In the past two decades, the use of nanoparticles in experimental and clinical settings has risen exponentially due to their small size (1–100 nm), high aspect ratio, reactivity, and freedom to change their surface properties along with their electrical and biochemical properties. [In the pharmaceutical field, however, nanoparticles are considered as being particles ranging between 10 and 1,000 nm **(De Jong and Borm, 2008)**]. This unparalleled freedom gives the opportunity to modify the pharmacokinetic paradigms of a drug such as solubility, diffusivity, blood circulation half-time, immunogenicity, and drug release. Currently, morphological variability of the nanoparticle is also heralding a prime importance for its use in specific applications **(Muro et al., 2008)**. Due to their small size and physical resemblance to physiological molecules, nanoparticles possess the capacity to revolutionise medical imaging, diagnostics and therapeutics as well as carry out functional biological processes. In the last few decades, more than 150 companies have been involved in developing nanoscale therapeutics with the success of 24 nanotechnology-based therapeutic products already in clinical use **(Bose et al., 2014)**.

Entry point

Route of administration

The primary aim when designing a nano-drug is to enhance drug accumulation at the targeted disease site. In order to obtain maximum therapeutic efficiency, efficient crossing of all barriers must be achieved. For decades, drug administration into the

human body has been accomplished by administrating drugs into the human body via various routes: oral, parenteral, topical, inhalation, etc. Of all the routes, oral route is the most conventional route for drug delivery. Although it is the safest method, it suffers from various drawbacks, such as poor bioavailability, fast metabolism, and variable absorption of the drugs, mainly due to the variability of pH conditions and digestion of peptide drugs by proteolytic enzymes present in the intestine. Hence, other important major routes of administration (parenteral, pulmonary, topical, and ocular as illustrated in **Fig. 23)** are gaining administrative importance depending upon the targeted tissue locations. Therefore, the primary challenge while designing a nanosystem is the need to understand which route of nanodrug administration will result in their maximal accumulation at the target site.

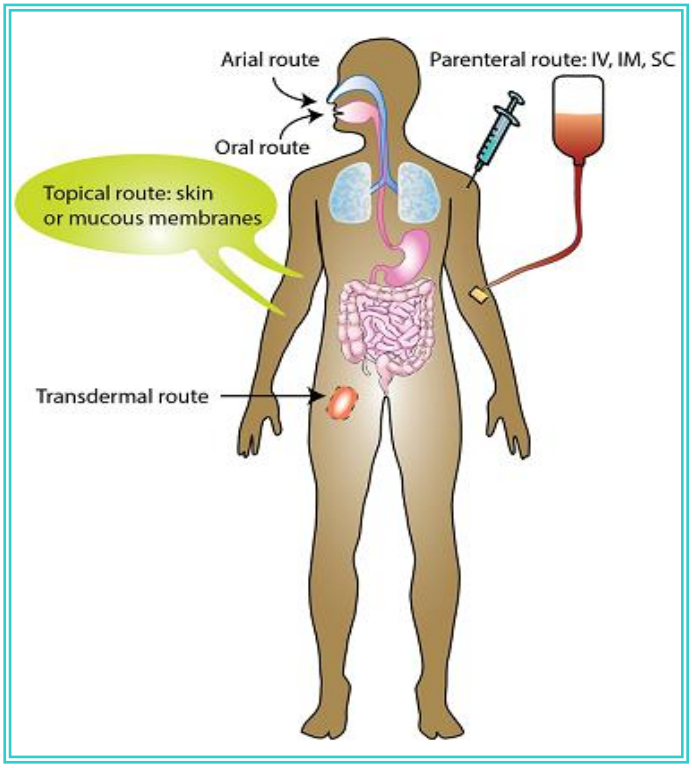

Figure 23: Routes of nano-drug administration

Functional point

In the cancer theranostic field, nanotechnology has gained rapid popularity due to its potential to design, construct, and utilize various functional structures at the nanometer scale (≤100 nm). The prevalent advantage is that the fundamental characteristics of a

given material can be precisely controlled by nanotechnology without changing its chemical composition (i.e., melting point or magnetic properties). Their promising applications in the field of medicine for treatment, diagnosis, monitoring, and control of biological systems have recently been coined as 'nanomedicine' by the National Institute of Health (Bethesda, MD, USA) **(Park et al., 2008)**. In the context of nanomedicine based therapeutics and diagnostics, effective functionality poses the major challenge which requires efficient tissue specificity, long-term systemic retention, and prolonged site-specific release of the drug.

Use of nano-modules as nano-drug for cancer therapy

In spite of the fact that cancer is one of the most studied diseases that has given rise to the development of various therapeutic approaches, such as surgery, radiation therapy, and chemotherapy, the search is still ongoing for an effective and non-recurring solutions for cancer therapy. All of these conventional therapies have major limitations with regards to inefficient target delivery, toxicity to the normal cells, and acquisition of drug resistance by the cancer cells **(Park et al., 2008)**. However, nanomaterials have shown promising results by overcoming many of the drawbacks of conventional therapy, leading to the introduction of many productive drugs for cancer therapy and prevention.

The advent of nanoparticles in cancer research could not have come at a more opportune time. Their small size and subsequent larger surface area endows them with some highly useful characteristics for various applications that can remove current obstacles in cancer therapies **(Harakeh et al., 2010)**. The National Cancer Institute (NCI) has recognized nanotechnology as an emerging field with the potential to revolutionize modern medicine for detection, treatment, and prevention of cancer **(Kawasaki et al., 2005)**.

Paclitaxel (National Cancer Institute, 1967) which was the first and most commonly used chemotherapeutic drug has various limitations, such as hydrophobicity and short blood retention period, etc. (**Chipman et al., 2006)**. Intravenous injection of this poorly soluble drug can cause an embolization of blood vessels due to the accumulation of the insoluble drugs, and often leads to local toxicity due to higher drug concentrations at the site of deposition. Overcoming the above constraint, nanoparticles loaded with Paclitaxel called

AI850 **(Zhang et al., 2008)** have proven successful in cancer treatment, mainly due to its enhanced accumulation at cancerous tissues.

Another serious problem of cancer treatment is the multi-drug resistance (MDR) of the cancerous tissues. This is due to the fact that these tissues have high hydrostatic pressure (unlike normal tissues) which leads to an outward convective interstitial flow that can flush the drug away from the tumor **(Park et al., 2008)**. MDR is mainly characterized by the expression of plasma membrane P-gp (P-glycoprotein) which is capable of repelling drugs from the cell. Several strategies have been developed to avoid the P-gp mediated MDR. One of them is the formulation of the co-administration of P-gp inhibitor on the anti-cancer drug-loaded nanoparticles **(Allen et al.,, 2013)**. Furthermore, angiogenetic molecular factors (e.g., vascular, endothelial, transforming, epidermal growth factor, and angiogenin (**Banerjee et al., 2011**) are targeted to design cancer-specific nanoparticles. To utilize the behavior of cancer cells, nanomedicines are being actively developed to co-administer anti-angiogenetic and chemotherapeutic drugs. For example, a polymer based nuclear nanoparticle within an extra-nuclear PEGylated lipid envelope leads to simultaneous release of anti-angiogenetic as well as chemotherapeutic agent **(Sengupta et al., 2005)**.

Bioactive natural products (bioflavonoids, polyphenols), which have miraculous antitumor properties, remain underutilized as cancer drugs because of their poor water solubility, low oral bioavailability, and inefficient systemic delivery. These problems can be meted out with the application of nanotechnology. Nano formulations of nutraceuticals are based on the general principles of nanotechnology. Some of them have showcased their potential in experimental/human studies.

Genistein covalently attached to iron oxide NPs coated by cross-linked carboxymethylated chitosan has been studied as novel multifunctional, tumor targeting drug delivery system. This nanoconjugate inhibited SGC-7901 cancer cells more significantly than the free genistein, seemingly provision for a multifunctional chemotherapeutic application combining drug release and magnetic hyperthermia **(Nair et al., 2010)**. Nano-EGCG (PLA-PEG NPs encapsulated EGCG), when used against the human prostate cancer cell lines (also in relevant tumor xenograft mouse model), exercised comparable anticancer, proapoptotic, and antiangiogenic effects at 10-fold

lower dose as non-nano-EGCG **(Siddiqui et al., 2009)**. The *in vivo* usage of resveratrol has been limited by its high lipophilicity and rapidity of glucuronation and sulfonation. Various nanoformulations of resveratrol like with chitosan NPs have been shown to have increased bioavailability, proapoptotic, and antioxidative potency than the free resveratrol **(Siddiqui et al., 2012)**.

Exploitation of nanoparticle properties for cancer diagnosis

Diseases need early and accurate diagnostics, coupled with therapy. The major drawbacks of current day diagnostic probes are their poor biodistribution and reduced systemic retention time. Nanomaterials have evolved as a new hope for future diagnostics due to their unique features such as long persistence, better penetration, and near inertness.

Nanoparticle-based carriers have increased the efficiency of diagnostics, largely through passive and active accumulation. Prolong blood retention along with porous and leaky blood vessels enhances passive accumulation of nanoparticles at the disease tissues employing EPR effects **(Barreto et al., 2011)**. The porous and leaky vessels around the tumor tissue enhance nanoparticles accumulation at the tumor site. Moreover, to induce target site accumulation via passive targeting strategies, the advantages of the variation in the pH, temperature, or redox potential of the pathological tumor sites must be taken into consideration. For example, the pH-sensitive polymeric carrier, such as polyvinyl pyrrolidone-co-dimethyl maleic anhydride (PVD) loaded with diagnostic agents (e.g., Tumor Necrosis Factor-a) (fulfills these considerations) showing gradual release in response to changes in pH at the tumor site **(Foulds et al., 2011)**.

Among various molecular imaging technologies, SPECT and PET are the two key nuclear imaging techniques that have revolutionized the clinical practice. Although SPECT and PET exhibit low spatial resolution compared to MRI, they show a high sensitivity in magnitude and widened imaging time window. Thus, they provide much functional information such as the pharmacokinetics and the biodistribution of the drugs. The major drawbacks of conventional imaging probes are their poor biodistribution and reduced systemic retention time. The use of nanoparticles has shown a way to bypass these problems. Target-specific radio-labeled nanoparticles (<100 nm) have maximized

passive and active accumulation by inducing enhanced binding affinity via receptor-specific biomolecules on the target cells of respective tissue **(Hong et al., 2009)**.

Another class of nanoparticles used successfully as image contrast agents is iron oxide nanoparticles. Due to their large magnetic moment, they generally produce enhanced proton relaxation rates than paramagnetic ions (e.g., Gd^{3+}) at a significantly lower dosage. For diagnostic purposes, it is exemplified by radio-nucleotide particles (e.g., F^{18} and Cu^{64} loaded nanoparticles) which are in use for PET imaging **(Jarrett et al., 2008)**. These nanomaterials are profitably used in fluorescent imaging along with MRI or PET imaging. For example, QD conjugated with Gd^{3+} is used for Fluorescence-MRI imaging, whereas Mn^{2+} or Cu^{64} conjugations are used in PET imaging. Furthermore, other contrasting agents such as nano- and macrobubbles are also attracting scientific interest as a probe for the ultrasonography imaging **(Wang et al., 2011)**.

Polymeric fluorescent nanoparticles are promising candidates for both in vitro and in vivo imaging, because of their multiple advantages over dye molecules. Due to its multi-valency and nanometric size, these nanoparticles have shown enhanced target site accumulation, better distribution, and significant increase in the retention time. The fluorescence is greater because a few hundred dye molecules can be encaged within a single nanoparticle. This entrapment helps in protecting the dye from interacting with the biochemical environment thereby significantly reducing photo-bleaching.

Exit point

Excretion criteria for nanoparticles

The route of administration determines the fate of a nanoparticle's accumulation and elimination. If the particle is injected orally, then there is greater likelihood of accumulation in intestinal organs (e.g., liver and spleen), whereas after parenteral or intravenous application, molecules are mostly eliminated via the kidney while traveling through the blood. This is known for fullerene particles applied through the oral and intravenous route. Particles administered through the former route can easily be eliminated through feces, whereas those administered through the latter pathway can be

retained in the body for 1-week. The intravenously injected fullerene particles are mainly (91.7 % of dose) distributed in the liver **(Shinohara et al., 2011)**.

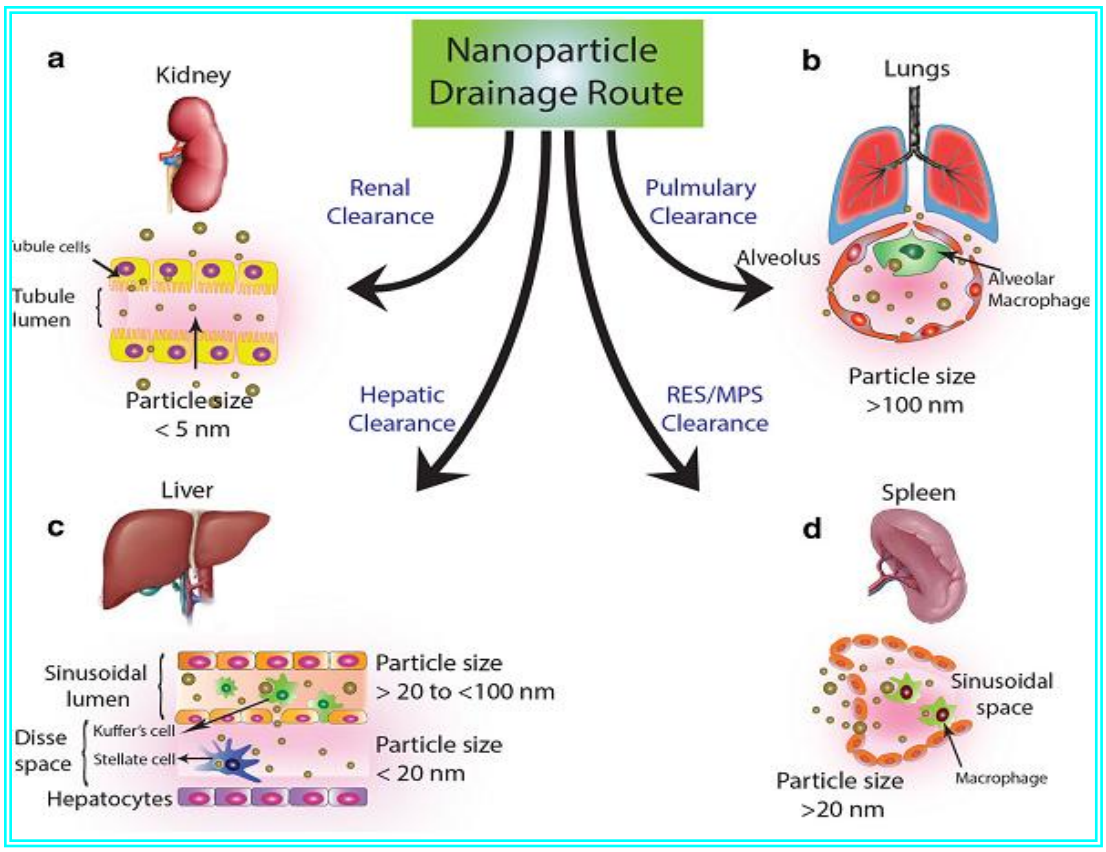

Figure 24: Drainage of nanoparticles through different organs according to their properties

Future Perspective

Nanotechnology is considered one of the greatest man-made engineering marvels in minuscule scale. The technology has grown exponentially in recent years, and it arguably has had the most impact on contemporary science and society since technologies of the Industrial Revolution. Demand for this cutting-edge technology in biomedical fields is growing by more than 17% annually, and is expected to reach approximately $53 billion by 2011 **(The Freedonia Group, 2007)**. One prospective report predicted that in the near future half of pharmaceutical industry products will have some connection with nanotechnology **(Lux Research, 2006)**.

Nanotechnology has already made an impact on cancer detection and therapy. The rapid intrusion of this cutting-edge technology in the current pharmaceutical industry is manifested by Abraxane, a nanomedicine approach to treat metastatic breast cancer. These aluminum-bound paclitaxel nanoparticles also have treatment potential for other cancers with or without the co-presence of other anticancer drugs. Many Nanomaterials like superparamagnetic iron oxide (SPIO) and ultra small superparamagnetic iron oxide (USPIO) nanoparticles are extensively used under various trademarks for imaging of various types of cancers. On the website ClinicalTrials.gov, a registry of federally and privately supported clinical trials conducted in the US and around the world, it is revealed that over 70 nanomedicine approaches are currently in clinical trials for cancer treatment and imaging **(NIH, 2011)**.

Though many of the technologies involving nanoparticles for cancer detection and treatment are mainly in preclinical stages, there is tremendous potential for nanotechnology to enable desperately needed cancer detection in its early stages. Nano-carriers loaded with a chemotherapeutic payload targeting the tumor site can not only eliminate adverse side effects, but may also pave the way for bringing a more effective, specific, and personalized medicine for eradicating cancer and many other complex diseases. Thus, nanotechnology has multifunctional proficiency and enormous potential to detect, treat, and monitor in real time. Nanotechnology applications in cancer detection and treatment have the potential to replace highly invasive conventional cancer detection and treatment, which often includes biopsies, irradiation, and painful therapies; they can become part of a painful past.

Nano-Selenium

The combination of biotechnology and nanotechnology has led to the development of an interdisciplinary area, medical nanotechnology, which shows broad applications in molecular imaging, molecular diagnosis, and targeted therapy **(Nie et al., 2007)**. The basic rationale is that nanoscaled materials have optical, magnetic, or structural properties that are not available from molecules or bulk solids **(Nel et al., 2006)**. Nanoparticles are submicron and sub-cellular in size, they have versatile advantages such as increased surface area and reactivity, increased gastric residence time and permeability, and improved solubility in both aqueous and organic phases. Brownian motion can provide enough energy to keep exceptionally small particles agitated and hence precipitation is less likely to happen with nanoparticle suspension. Therefore, suspensions of nanoparticles are easier to stabilize because precipitation is less likely. Due to their unique physical and chemical properties, nanoparticles have become the focus of many research areas such as applied physics and chemistry, mechanical engineering, pharmaceutical industry and environmental investigations.

Nanoparticle of selenium (Nano-Se) was first synthesized by a group of scientist from Chinese Academy of Science, Hefei, China, in the year 2001 **(Zhang et al., 2001)**. Nano red elemental selenium (Nano-Se) with the size range of 5–100 nm, can be synthesized by reducing selenite in an environment containing bovine serum albumin (BSA) by dialyzing process, which is able to adhere to Se atoms and control the size of their aggregation: thus the sizes of the nanoparticles are dependent on BSA concentration in the preparation system. BSA at higher concentration produces smaller Nano-Se particles, hence a series of Nano-Se particles of different sizes were prepared by varying the concentration of BSA. It is well known that some materials acquire many properties when particle sizes are reduced to the nanometer scale, such as large surface area, quantum effects, and high reactivity. In this new era of nanobiotechnology, bacteria and fungi and plants are also able to produce nano-particles. Nano-Se is also produced microbiologically by using *Pseudomonas alcaliphila* strain with or without addition of poly (vinyl pyrrolidone) (PVP) **(Zhang et al., 2011)**. In the work of Ramamurthy and his colleagues, it's evident that Nano-Se can also be prepared by green synthesis using the reducing power of fenugreek seed extract. This method is capable of producing Nano-Se

in a size range of about 50-150 nm, under ambient conditions **(Ramamurthy et al., 2013)**. In 2010, Dhanjal and Cameotra reported that, microorganisms are exposed to pollutants in the environment, such as metals/metalloids. These metal-microbe interactions have already found an important role in biotechnological applications. Recently microorganisms have been explored as potential biofactories for synthesis of metal/metalloid nanoparticles. Biosynthesis of selenium (Se^0) nanospheres can also be done in aerobic conditions by a bacterial strain isolated from the coalmine soil **(Dhanjal et al., 2010)**. It has been seen in many works that monosaccharide or polysaccharide has been used as a stabilizer in order to produce Nano-Se **(Chen et al., 2012)**.

Advantages of Nano-Se over inorganic and organic selenium compounds

On the basis of toxic profile

Nanomedicine involves utilization of nanotechnology for the benefit of human health and well being. Conventional drugs suffer from major limitations of adverse effects occurring as a result of non specificity of drug action and lack of efficacy due to improper or ineffective dosage formulation. Designing of drugs with greater degree of cell specificity improves efficacy and minimizes adverse effects.

Selenium is being used for quite a long time. It is taken into consideration that selenium has tremendous health aspect against various health issues. Results of epidemiological, preclinical and clinical studies show the importance of Se in case of several diseases such as cancers **(Rayman, 2005**), diabetes **(Wei et al., 2015a)**, cardiovascular disease **(Alehagen et al., 2014)**, infertility **(Pieczyńska et al., 2015)**, neurodegenerative diseases **(Wei et al., 2015b)**, inflammatory bowel disease **(Speckmann et al., 2014)** and osteoporosis **(Pedrera-Zamorano et al., 2012)** which are related to oxidative stress related diseases (OSRDs).

Selenium (Se) is an essential micronutrient with well-known antioxidant characteristics. The antioxidant and prooxidant effects of Se as well as its bioavailability and toxicity depend on its chemical form **(El-Bayoumy and Sinha, 2004)**. The major chemical forms of Se are organic, as selenomethionine (SeMet), selenocysteine (SeCys), and metylselenocysteine (MeSeCys), and inorganic as selenite and selenate **(Letavayová et al., 2006)**. Selenium (Se) occurs in a variety of oxidation states, like selenate (SeO_4^{2-})/

selenite (SeO_3^{2-}) oxyanions, wherein the oxidation states are +6 and +4; elemental selenium (Se^0), and selenide (Se^{2-}) **(Dhanjal et al., 2010)**. The toxicity of these states is related to their degrees of solubility in water and hence their bioavailability. In 1976, The U.S. National Research Council stated that growth inhibition might be the best indicator of toxic effects from selenium. On the basis of this, a comparative study of toxicity has been made between Nano-Se and inorganic as well as organic selenium compound. Zhang **(Zhang et al., 2004)** found large difference in acute toxicity between Nano-Se and selenite. In their study they compared the short-term toxicity of the two Se forms in mice by orally administering high doses of Se. Their results showed that Nano-Se was less toxic than selenite in terms of suppressing growth, liver toxicity, and antioxidant status. Nano-Se has a 7-fold lower acute toxicity than sodium selenite in mice (LD_{50} 113 and 15 mg Se/kg body weight, respectively) **(Clark, 1996)**. Wang **(Wang et al., 2007)** was led to the conclusion based on animal tests that Nano-Se is a very effective antioxidant, devoid of toxicity which is typical for other selenium forms. Nano-Se has at least the same effect on activating glutathione peroxidase (GP*x*) and thioredoxin reductase (TrxR) enzymes as selenoproteins has, however, this form is less toxic, it does not trigger acute liver injury and short term toxicities. Furthermore nano-Se accumulates less in the treated mice and activates glutathione-*S*-transferase (GST) more effectively than selenoproteins, independently from the level of toxication. In another study, Liu et al has reported, acute toxicity of newly synthesized folate (FA)-conjugated selenium nanoparticles (Nano-Se) is much lower compared to SeMet and selenite **(Liu et al., 2015)**.

On the basis of pharmacokinetic profile

Animal studies have demonstrated that liver is not only the organ of metabolism but also main target organ of Se toxicity **(Diskin et al., 1979)** due to the consequence of hyper-accumulation of the absorbed selenium in liver and the fact that selenium generated reactive oxygen species (ROS) formation are the major mechanisms for Se toxicity **(Spallholz et al., 2004)**. The main route of absorption of inorganic selenium, such as selenite, is a passive diffusion from the intestine, and then 50–75% of total ingested Se is excreted in the urine **(Holben et al., 2002)**. This may be the reason of high selenium accumulation in the kidneys **(Shi et al., 2001)**. In contrary to inorganic forms, organic

selenium, such as selenomethionine (SeMet), is utilized in the intestinal wall by active transportation (e.g. by amino acid transport systems) and non-specifically incorporated into body proteins in place of methionine during protein synthesis, providing a means of reversible Se storage in organs and tissues **(Schrauzer, 2000)**. Nanoparticles, such as Nano-Se, are absorbed in the duodenum also by active transportation **(Zhang et al., 2001)**. Otherwise an *in situ* study on the intestinal transport of Se from ligated loop to body showed that the transfer of Nano-Se from the intestinal lumen to the body was higher than that of selenite, while the intestinal retention of Nano-Se was lower compared with selenite **(Hu et al., 2012)**.

In chicken the highest selenium concentrations was found in serum, liver and breast muscle, and it was increased as the dietary Se level increased (0.03 to 1.3 mg/ kg feed), but the magnitude of increase was substantially greater when Nano-Se was fed as compared to sodium selenite **(Hu et al., 2012)**. Moreover, the addition of 1.20 mg/ kg Se from Nano-Se did not cause signs of toxicity which suggest that the range between optimal and toxic dietary levels of Nano-Se was wider than that of sodium selenite (**Hu et al., 2012)**. The possible cause of higher tolerance to selenium in form of Nano-Se is its higher rate of retention in muscle, which may effectively reduce the available Se for inducing selenosis. This hypothesis supported by the study with intravenously administered [^{75}Se]–nano-Se or [^{75}Se]–Na_2SeO_3, which showed that the percentages of Nano-Se in the whole body was much higher than those of selenite **(Hu et al., 2012)**.

In pharmacology, bioavailability is a subcategory of absorption and is the fraction of an administered dose of unchanged drug that reaches the systemic circulation, one of the principal pharmacokinetic properties of drugs. In the view of bioavailability, size of nano-Se plays a pivotal role. Nano-Se has higher bioavailability compared to other selenium compounds **(Wang et al., 2007)**, as it was proven in broiler chicken and goat compared with selenite **(Shi et al., 2001; Zhou et al., 2011)**. These differences may be the result of the differences in lipophilic properties and metabolic pathways of the Se species **(Li et al., 2008)**.

On the basis of haematological profile

Selenium, as the functional component of selenium dependent GP*x* **(Drake, 2006)** protects the neutrophils and other blood components against peroxidative damage **(Bickhardt et al., 1999)**. It was mentioned that selenium deficiency can increase oxygen free radicals in body tissues, the major negative effects of which are on the consistency of biological membranes and Nano-Se with 1 mg/ kg of feed has a positive effect on the consistency of biological membranes and the performance of immune cells **(Lessard et al., 1991)**. In a comparative study of selenium compound with sheep showed that Nano-Se with 1 mg/ kg of feed has a positive effect against peroxidative damage in blood components **(Sadeghian et al., 2012)**. The results revealed that lipid peroxidation was reduced by Nano-Se treatment, but the groups treated with sodium selenite only with more delay, showed the better antioxidant activity of selenium nanoparticles. Otherwise there were no significant differences between the packed cell volume and red blood cell count among the groups. Also, there were significant increases of the neutrophil counts and significant decreases of the lymphocyte counts in the Nano-Se treated group as compared to sodium selenite and control groups. To sum up, in sheep, selenium nanoparticles were found to be more bioactive than selenite.

Rational of the study

Rational of the Study

Chemotherapy-induced reactive oxygen and nitrogen species (ROS/RNS) and their concomitant oxidative damage to proteins, lipids, nucleic acids, and other cellular components are prime suspects in the toxic side effects of acute or chronic chemotherapeutic treatment. In an effort to develop effective alternative strategies that increase the therapeutic efficacy and minimize the systemic toxicity of chemotherapeutic agents, efforts are being directed towards the investigation of dietary supplements and other cytoprotective agents for their synergistic efficacy in combination with anticancer agents. The trace element selenium is well known a chemopreventive and antioxidant agent. It is a structural component of several enzymes with physiological antioxidant properties. The biological and pharmaceutical activities of different selenium compounds are of special interest because it has been associated with the prevention of cancer. Nano particle of selenium (Nano-Se) have substantially greater bioavailability than that of inorganic and organic selenium. More importantly, Nano-Se is usually found to be less toxic than inorganic as well as organic forms of the element. New synthesized nanotechnology based Nano-Se may provide a way to minimize toxicity associated with higher selenium intake. The development of a nontoxic selective chemoprotective agent that preferentially protects normal tissues from chemotherapy induced toxicity, at the same time maintaining the efficacy of the cancer chemotherapeutic agents, is a major challenge in cancer research.

This thesis report is an attempt to evaluate the possible protective action of a nanotechnology based less toxic Nano-Se, as a potential antioxidant and cancer chemoprotective agent against the oxidative stress mediated side effects induced by two well known cancer chemotherapeutic drugs, cyclophosphamide and cisplatin in murine model. It is also aimed to identify the possible influences of the Nano-Se in maintaining the normal cellular oxidant/antioxidant balance that is adversely affected by chemotherapy and cause organ failure.

Chapter I

Synthesis, Characterizations, Dose selection of Nanoparticle of Selenium (Nano-Se) and Comparative Toxicological study with Inorganic and Organic Selenium compound

Synthesis and Characterizations

The Nano-Se was synthesized following a simplified protocol with slight modifications **(Zhang et al., 2004)**.

Chemicals

- Sodium selenite (Na_2SeO_3)
- Reduced glutathione (GSH)
- Bovine serum albumin (BSA)
- Sodium hydroxide (NaOH)

Procedure

Sodium selenite (Na_2SeO_3) is mixed with reduced glutathione (GSH) containing 200mg BSA for the preparations of the Nano-Se

⇩

The pH of the mixture was adjusted to 7.2 with 1.0 M sodium hydroxide; the red Nano-Se and oxidized glutathione (GS-SG) were formed instantly.

⇩

The red solution dialyzed against doubly distilled water for 96 hrs with the water changing every 24 hrs to separate GS-SG from Nano-Se

⇩

The final solution containing Nano-Se and BSA was subjected to centrifugation at 13,000 rpm for 10 min

⇩

The pellet thus recovered was subjected to washing by its re-suspension in de-ionized water followed by centrifugation at 13,000 rpm for 10 min, to remove possible organic contaminations present in the nano particles

Finally, pellet was freeze-dried using a lyophilizer and stored at room temperature

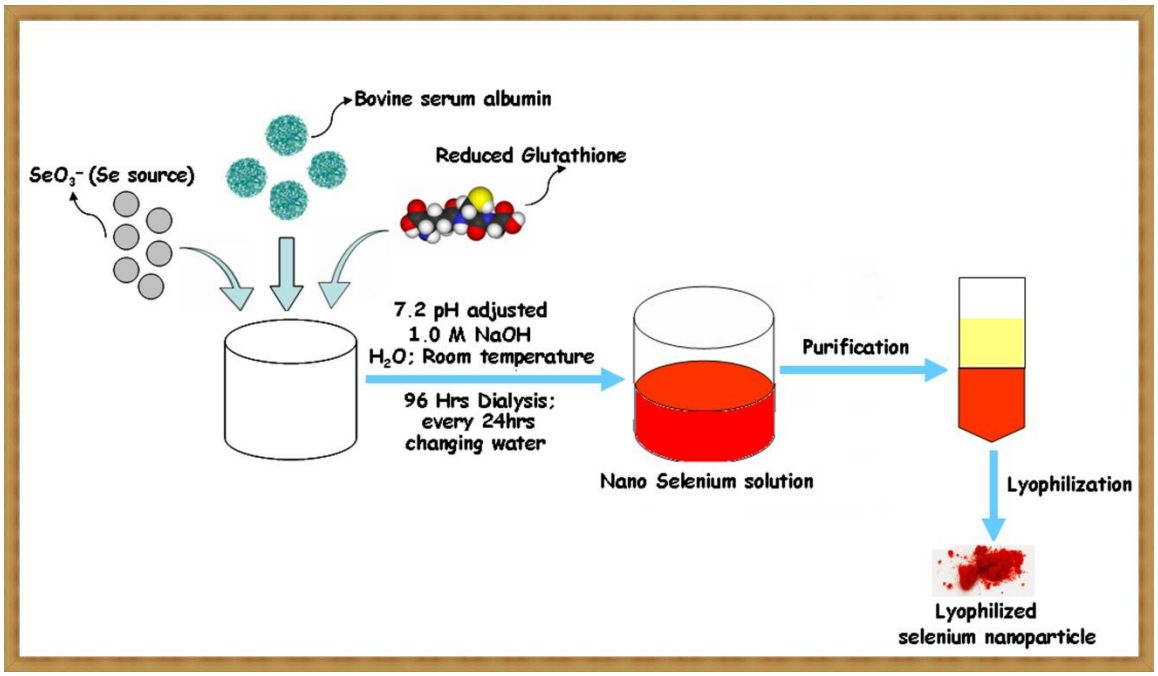

Figure 1: Schematic presentation of preparation and reaction condition of nano particle of selenium (Nano-Se)

Characterization

The properties of Nano-Se were studied by Scanning electron microscope (SEM), Transmission electron microscope (TEM), Dynamic light scattering (DLS) and purity of the substance was confirmed by EDAX analysis.

The synthesized Nano-Se aqueous solution was stable and clear and well dispersed in solution. TEM analysis was carried out at 200 KV accelerating voltage with Techni 20 (Philips, Holland) for size determination. For this purpose, a thin film of the sample was prepared on a carbon-coated copper grid by dropping a very small amount of the sample on to the grid. TEM images **(Fig. 2A)** show that the synthesized Nano-Se presents monodisperse and homogeneous spherical structures with an average diameter of about 23.3 nm.

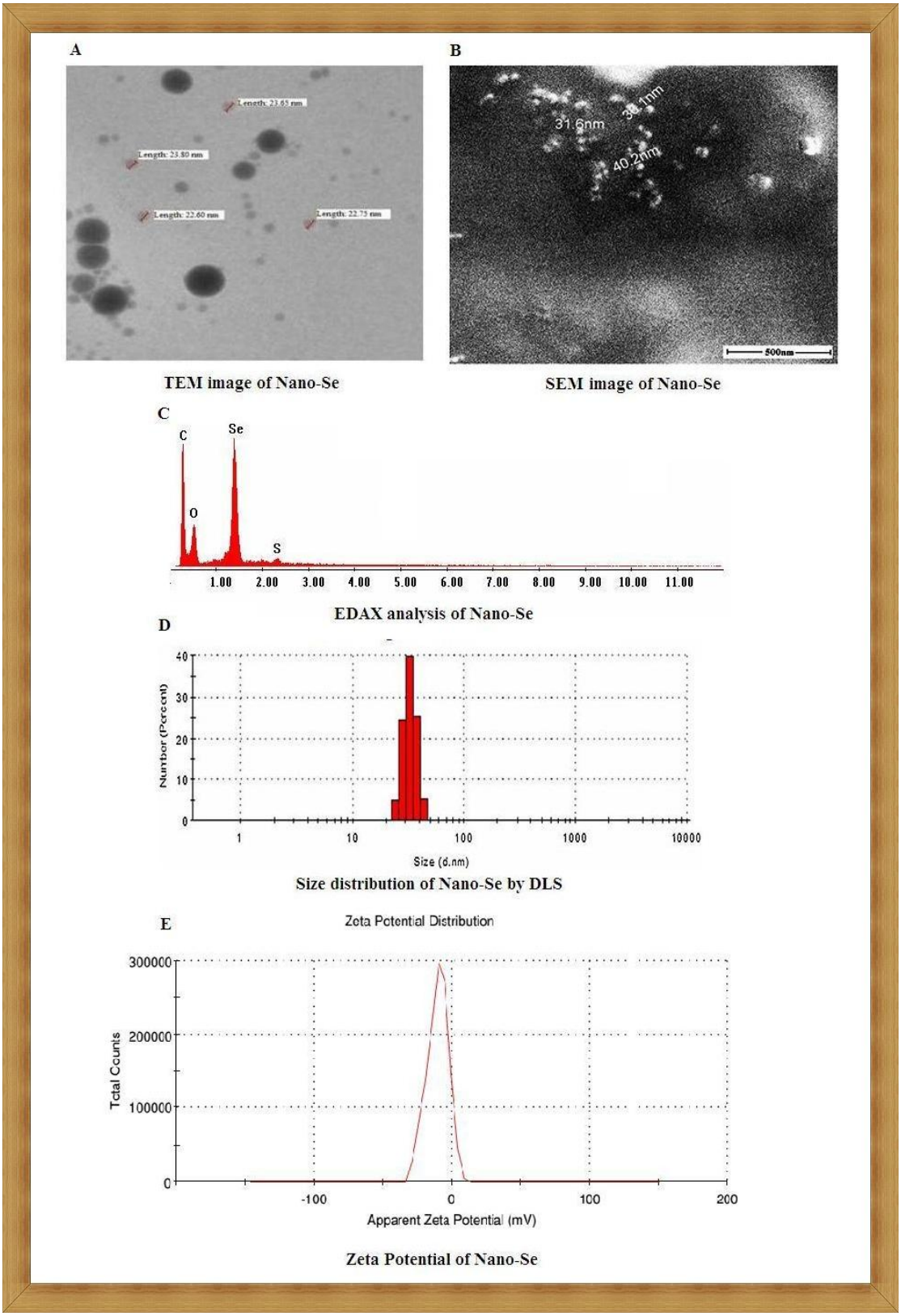

Figure 2: Characterization of selenium nanoparticles (Nano-Se)

The size and morphology of the synthesized Nano-Se were analyzed using a SEM (FEI Quanta—200 MK2). SEM image **(Fig. 2B)** of the Nano-Se revealed an average size of 35 nm; most of the nano particles being in the size range of 30–40 nm.

The spectrum of the energy dispersive X-ray spectroscopy (EDAX) of Nano-Se was carried out using an XL-30 (Philips, Netherlands) operating at 15–25 kV and employed to examine the elemental composition. The EDAX of the nano particle dispersion confirmed the presence of elemental selenium. The analysis revealed the highest proportion of selenium (64.28%) in nano particles followed by carbon (18.03%), oxygen (17.31%), and sulphur (0.38%) **(Fig. 2C)**.

The size distribution and average diameter of Nano-Se in aqueous solution were characterized by Zetasizer Nano ZS (Zen 3690 Zetasizer Nano ZS 90, Version 7.03). A sharper peak in Zetasizer analysis indicates uniform size distribution. The average diameter of Nano-Se was observed to be 33.09 nm **(Fig. 2D)**. Degree of aggregation can be determined by zeta potential values **(Fig. 2E)**. Suspended particles with a large negative or positive zeta potential tend to repel each other and thus do not aggregate. A zeta potential of –10.7mV with a polydispersity index of 0.362 indicates higher stability of the monodispersed suspension.

Determination the non-toxic dose of Nano-Se

Drug preparation

The synthesized Nano-Se was dissolved in saline (0.9%NaCl) and administered orally. It was prepared on each day just before treatment.

Experimental design

Animals

Adult (5–6 weeks) Swiss albino female mice (25 ± 2g), bred in the animal colony of Chittaranjan National Cancer Institute (CNCI) (Kolkata, India), were used for this study. The mice were maintained under standard condition of humidity (45–55%), temperature (23 ± 2ºC), and light (12 h light/12 h dark). Standard food pellets (EPIC rat and mice pellet) from Kalyani Feed Milling Plant, Kalyani, West Bengal, India and drinking water was provided *ad libitum*. The experiments were carried out following strictly the Institute's guideline for the Care and Use of Laboratory Animals.

Experimental groups

Animals were distributed into three groups containing six animals (n=6) in each group.

Vehicle control group (Gr. I): Each animal received saline (0.9% NaCl) orally for 30 days.

Nano selenium treated group (Gr. II): Each animal was given nano selenium (Nano-Se) orally at the dose of 2mg Se/kg b.w. for 30 days as a solution in saline (0.9% NaCl).

Nano selenium treated group (Gr. III): Each animal was given nano selenium (Nano-Se) orally at the dose of 3mg Se/kg b.w. for 30 days as a solution in saline (0.9% NaCl)

Nano selenium treated group (Gr. IV): Each animal was given nano selenium (Nano-Se) orally at the dose of 4mg Se/kg b.w. for 30 days as a solution in saline (0.9% NaCl).

Animals were sacrificed on day 31.

Parameter studied

- Determination of body weight
- Estimation of blood hemoglobin level
- Quantitative estimation microsomal lipid peroxidation level in liver

- Estimation alanine transaminase (ALT) and aspartate transaminase (AST) activity in serum.
- Estimation of renal function markers blood urea nitrogen (BUN) and creatinine levels in serum.
- Histopathological evaluation of liver tissue by hematoxylin/eosin (H & E) staining

Methodologies

❖ **Blood hemoglobin (Hb) level (Sahli, 1909)**

Reagents required

N/10 HCl.

Procedure

In Sahli's tube N/10 HCl was taken up to lowest graduation (0.02 gramme).

⇩

20 µl blood was added into the Sahli's tube.

⇩

Blood and HCl in the tube were stirred with a glass rod for proper mixing.

⇩

The tube was then placed in stand and kept for 3 minutes during which period HCl caused lysis of RBC and released hemoglobin, which on reacting with HCl forms a dark brown colored acid hematin.

⇩

Distilled water was added in the tube drop by drop and stirred with a glass rod.

⇩

The process was continued until the color of the solution exactly matched with that of the standard.

⇩

Finally, the hemoglobinometer was held against good light and the reading was taken.

❖ **Quantitative estimation of lipid peroxidation (LPO) level (Okhawa et al, 1979)**

Spectrophotometric method was applied to estimate the level of LPO in liver and lung microsomes by measuring the formation of lipid peroxides using thiobarbituric acid (TBA) and was expressed as nmTBARS/mg protein.

Reagents required

Normal saline, 1.15% KCl, 8.1% SDS, 20% Acetic acid, 0.8% TBA, n-Butanol and pyridine.

Procedure

Estimation of thiobarbituric acid reactive substances (TBARS)

Liver and lung tissues of the experimental mice were collected after their sacrifice, washed in normal saline and 400 mg of liver and lung tissues were weighed.

⇩

The tissues were then homogenized in 3.6 ml 1.15% KCl using a Teflon homogenizer.

⇩

The homogenates were centrifuged at 12000 g for 10 minutes at 4^{o}C.

⇩

The supernatants (devoid of nuclear debris) were again centrifuged at 10000 g for 10 minutes at 4^{o}C.

⇩

The supernatants (devoid of mitochondria) were centrifuged for third time at 25000 g for 1 hour at 4^{o}C.

⇩

The precipitates (containing microsomal fraction) were suspended in 400 µl 1.15% KCl and the suspensions were used as sample for determining the LPO level.

⇩

In test tubes 200 µl sample, 200 µl SDS, 1.5 ml acetic acid and 1.5 ml TBA were added along with 600 µl distilled water.

⇩

A blank sample was prepared following the same procedure using all the above mentioned reagents except distilled water in place of tissue sample.

The reaction mixtures were then heated at 95°C in water bath for 1 hour.

⇩

The reaction resulted in the development of pink coloration.

⇩

5 ml mixture of butanol and pyridine (15:1; v/v) was added to each sample and each sample was then vortexed thoroughly and centrifuged at 3000 g for 10 minutes.

⇩

Absorbance of the upper pink colored organic layer was measured at 532 nm against the colorless blank sample using the Varian Cary 100 UV–Vis Spectrophotometer.

Assessment

Total protein concentration of each unknown sample was determined from the standard curve prepared by measuring the absorbance of different known concentrations of BSA. The level of LPO was expressed as nmol TBARS formed/mg protein using extinction co-efficient of 1.56×10^5 $M^{-1}cm^{-1}$ as follows:

Absorbance = Extinction coefficient × Concentration × Length (Beer-Lambert Law)

Now, Extinction co-efficient = 1.56×10^5 $M^{-1}cm^{-1}$

Length = 1cm

So, Concentration of TBARS = Absorbance/(1.56×10^5) M

= Absorbance × $10^9/(1.56 \times 10^5)$ nM

Hence, the level of LPO in 200 µl sample was expressed as:

$$\text{nmol TBARS/mg protein} = \frac{\text{Absorbance of TBARS at 532 nm} \times 2}{1.56 \times \text{Protein concentration (mg) in 200 µl sample}}$$

❖ **Hepatic marker enzymes alanine transaminase and aspartate transaminase assay (Reitman and Frankel, 1957)**

Serum alanine transaminase (ALT) and aspartate transaminase (AST) activity were estimated using 2, 4-Dinitrophenyl hydrazine (2,4-DNPH) color method principles as

supplied with the kit (Span Diagnostics, India) following the method of Reitman and Frankel.

- **Estimation of ALT activity**

ALT catalyzes the transfer of α amino group of alanine to α -ketoglutaric acid, producing pyruvate and glutamate. Pyruvate so formed is coupled with 2,4-DNPH to give the corresponding hydrazone, which gives brown color in alkaline medium which can be measured spectrophotometrically.

α-ketoglutarate + L- Alanine ⟷ L-Glutamate + Pyruvate

Reagents required (Supplied in the kit)

Reagent 1: Buffered alanine- α - ketoglutarate substrate, pH 7.4.

Reagent 2: 2, 4-Dinitrophenyl hydrazine (2,4-DNPH) color reagent.

Reagent 3: Sodium hydroxide, 4 N.

Reagent 4: Working pyruvate standard, 2 mM.

Preparation of working solutions

Solution-1: 1 ml Reagent 3 was diluted to 10 ml with double distilled water. Reagents 1, 2, and 4 were ready for use.

Preparation of standard curve

Different known concentrations (250 µl, 225 µl, 200 µl, 175 µl and 150 µl) of reagent 1 were taken sequentially in 5 different test tubes.

⇩

25 µl, 50 µl, 75 µl and 100 µl of reagent 4 were added from 2nd test tube to 5th test tube respectively. Nothing was added in 1st test tube.

⇩

100 µl double distilled water was added to all the test tubes.

⇩

250 µl reagent 2 was added to all the test tubes.

⇩

The reaction mixtures in the test tubes were mixed properly and then allowed to stand at room temperature for 20 minutes.

2.5 ml solution 1 was then added to all the test tubes

⇩

The reactants were then mixed thoroughly and all the test tubes were kept at room temperature for 10 minutes.

⇩

Absorbance was taken immediately at 505 nm using Varian Cary 100 UV–Vis Spectrophotometer against double distilled water as blank.

⇩

The standard curve was then prepared to calculate the ALT enzyme activity of different unknown samples and was expressed as IU/L.

Assay of ALT activity in serum

Isolation of serum

Blood samples were collected from mice by retro orbital puncture and centrifuged at 3000 rpm for 5 minutes for serum separation. The serum samples were stored at 2-8^{o}C.

Enzyme assay

125 µl reagent 1 was taken in test tubes and was incubated at 37^{o}C for 5 minutes.

⇩

50 µl serum sample (diluted 1: 5 times with normal saline) was added to the test tubes.

⇩

The reactants in the test tubes were then mixed well and incubated at 37^{o}C for 30 minutes.

⇩

125 µl reagent 2 was then added to the test tubes.

⇩

Mixing was done properly and the test tubes were allowed to stand at room temperature for 20 minutes.

⇩

1.25 ml solution 1 was then added to the test tubes.

Mixing was done by vortex for 2 minutes and all the test tubes were allowed to stand at room temperature for 10 minutes.

⇩

The absorbance of the reaction mixture from all test tubes was measured immediately at 505 nm in Varian Cary 100 UV–Vis Spectrophotometer against double distilled water as blank.

Assessment

The optical density obtained in the serum sample was extrapolated on the standard curve (on Y-axis) to get the corresponding enzyme activity (on X-axis) and expressed as IU/L. The ALT activity was multiplied with the dilution factor for serum to get the final enzyme activity.

- **Estimation of AST activity**

AST catalyzes the transfer of α amino group of aspartic acid to α-ketoglutaric acid, forming oxaloacetate and glutamate. Oxaloacetate so formed is coupled with 2,4-DNPH to generate the corresponding hydrazone, which gives brown color in alkaline medium which is measured spectrophotometrically.

α-ketoglutarate + L- Aspartate ⟷ L-Glutamate + Oxaloacetate

Reagents required (Supplied in the kit)

Reagent 1: Buffered aspartate- α - ketoglutarate substrate, pH 7.4.

Reagent 2: 2, 4-Dinitrophenyl hydrazine (2,4-DNPH) color reagent.

Reagent 3: Sodium hydroxide, 4 N.

Reagent 4: Working pyruvate standard, 2 mM.

Preparation of working solutions

Solution-1: 1 ml Reagent 3 was diluted to 10 ml with double distilled water. Reagents 1, 2, 4 were ready for use.

Preparation of standard curve

Different concentrations (250 µl, 225 µl, 200 µl, 175 µl and 150 µl) of reagent 1 were taken in 5 consecutive test tubes.

5 µl, 50 µl, 75 µl and 100 µl reagent 4 were added from 2nd test tube to 5th test tube respectively. Nothing was added in 1st test tube.

⇩

50 µl double distilled water was added to all the test tubes.

⇩

250 µl reagent 2 was added to all the test tubes.

⇩

Mixing was done properly and the test tubes were kept at room temperature for 20 minutes.

⇩

2.5 ml solution 1 was then added to all the test tubes.

⇩

The reaction mixtures were then vortexed for 2 minutes and all the test tubes were allowed to stand at room temperature for 10 minutes.

⇩

Absorbance of each reaction mixture was measured immediately at 505 nm in Varian Cary 100 UV–Vis Spectrophotometer against double distilled water as blank.

⇩

The standard curve was then plotted to calculate the AST activity of different samples and was expressed as IU/L.

Assay of AST activity in serum

Isolation of Serum

Blood samples were collected from mice by retro orbital puncture and were centrifuged at 3000 rpm for 5 minutes for serum separation. The serum samples were stored at 2-8^{o}C.

Enzyme assay

250 µl reagent 1 was added in test tubes.

⇩

Incubation was done at 37^{o}C for 5 minutes.

50 µl serum sample (diluted1: 5 times with normal saline) was added to the test tubes.

⇩

The reactants in each test tube were mixed properly and were then incubated at 37^{o}C for 60 minutes.

⇩

250 µl reagent 2 was added to the test tubes.

⇩

Mixing was done properly and the test tubes were kept at room temperature for 20 minutes.

⇩

2.5 ml solution 1 was then added to the test tubes.

⇩

Mixing of the reactants was done by vortex for 2 minutes and all the test tubes were allowed to stand at room temperature for 10 minutes.

⇩

Absorbance of each reaction mixture was taken immediately at 505 nm in Varian Cary 100 UV–Vis Spectrophotometer against double distilled water as blank.

Assessment

The optical density obtained in the serum sample was extrapolated on the standard curve (on Y-axis) to get the corresponding enzyme activity (on X-axis) and expressed as IU/L. The AST enzyme activity was multiplied with the dilution factor for serum to obtain the final enzyme activity.

- **Determination of blood urea nitrogen (BUN) (Carl Allinson, 1944; Mather et al., 1969)**

Urea is hydrolysed in presence of water and urease to produce ammonia and carbon dioxide. Under alkaline conditions, ammonia so formed, reacts with hypochlorite and phenolic chromogen to form colored indophenol, which is measured at 578 nm spectrophotometrically. Sodium nitropruside acts as a catalyst. The intensity of color is

proportional to the concentration of urea in the sample **(Carl Allinson, 1944; Mather et al., 1969)**.

Reagents required

Reagent 1: Urease reagent containing 20 mM phosphate buffer, > 20 U/L urease, 3.2 mM/L Sodium nitropruside, 60 mM/L sodium salicylate.

Reagent 2: Urea chromogen containing 0.2% sodium hypochlorite, 400 mM/L sodium hydroxide.

Reagent 3: Urea standard containing urea preservative, 50 mg/dl.

Reagent 4: Purified ammonia free water.

Preparation of working solution

Solution 1: It was prepared by reconstituting the entire reagent 1 present in the vial with 50 ml of reagent 4.

Solution 2: It was prepared by reconstituting reagent 2 with reagent 4 in 1:5 ratios.

Procedure

10 µl of serum was added to the test tubes.

⇩

In test tubes 1.5 ml of solution 1 was then added.

⇩

Mixing was done properly and incubated at 37^{o}C for 3 minutes.

⇩

1.5 ml of solution 2 was added to each test tube.

⇩

Blank and standard were prepared as above using 10 µl of purified water and 10 µl of reagent 3 (urea standard) instead of serum sample.

⇩

Reagents of each test tube were mixed properly and incubated for 5 minutes.

⇩

Absorbance of standard and test samples was measured at 578 nm against the blank using Varian Cary 100 UV–Vis Spectrophotometer.

Assessment

Serum BUN level was expressed as mg/dl and was calculated using the following formula:

$$\text{Blood Urea Nitrogen (BUN) (mg/dl)} = \frac{\text{Absorbance of test}}{\text{Absorbance of standard}} \times 50 \times 0.467$$

❖ **Estimation of serum creatinine level (Carl Allinson, 1944; Mather et al., 1969)**

Creatinine in a protein free solution reacts with alkaline picrate and produces a red colored complex, which is measured spectrophotometrically at 520 nm.

Reagents required

Reagent 1: Picric acid

Reagent 2: Sodium hydroxide, 0.75 N

Reagent 3: Stock Creatinine standard, 150 mg %

Preparation of working solution

Working standard: It was prepared by adding 9.9 ml of purified water to 0.1 ml of reagent 3 (stock creatinine standard) to make final volume 10 ml and were mixed well. All other reagents were ready for use.

Procedure

A) Deprotenization of test sample

0.5 ml of serum was mixed with 0.5 ml purified water in test tubes.

⇩

3.0 ml of reagent was added to the tubes.

⇩

Mixing was done properly.

⇩

Test tubes were kept in a boiling water bath exactly for one minute

⇩

Test tubes were then cooled immediately under running tap water.

⇩

The material from each test tube was then centrifuged and the supernatant was the protein free sample.

B) Color development

2.0 ml of supernatant was taken in test tubes.

⇩

0.5 ml of reagent 2 was then added in the test tubes and mixed properly.

⇩

The standard sample was prepared by adding 0.5 ml of working standard, 1.5 ml of reagent 1 and 0.5 ml of reagent 2 in a test tube. Blank was prepared like that of working standard, except 0.5 ml of purified water was added in the test tube instead of working standard.

⇩

All the test tubes were allowed to stand exactly for 20 minutes.

⇩

Absorbance of blank, standard and test samples were taken at 520 nm against purified water using Varian Cary 100 UV–Vis Spectrophotometer.

Assessment

Serum creatinine level was expressed as mg/ 100 ml and was calculated using following formula:

$$\text{Serum creatinine (mg/100 ml)} = \frac{\text{Absorbance Test} - \text{Absorbance Blank}}{\text{Absorbance standard} - \text{Absorbance Blank}}$$

❖ **Histopathology (Bancroft et al, 1990; Lillie et al, 1976)**

The purpose of histological staining methods by hematoxylin and eosin is to visualize and differentiate between tissue components in normal and pathological condition. Identification and confirmation of histopathological changes induced by chemotherapy drugs and the protective effect of the test compound was carried out using standard hematoxylin-eosin staining procedure and analysis was done by light microscopy.

Procedure

Tissue collection and fixation

After sacrificing the mice liver and lungs were collected, washed repeatedly in PBS and soaked in blotting paper to remove the blood. Tissues were then placed into fixatives as soon as possible. The death of cells leads to the breakdown of cellular constituents resulting from endogenous enzymes and from damages caused by external agents such as bacteria. The purpose of fixation is to preserve tissues permanently in as life-like a state as possible and it needs to be carried out as soon as possible to prevent autolysis. Tissue is fixed by cross-linkages formed in the proteins particularly between lysine residues. These cross linkages dose not harm the structure of protein significantly. After collection, all tissues were fixed in 10% neutral buffered formalin for 24 hours. Formalin is a fixative of choice for histopathological procedures because it penetrates tissues slowly but properly and prevents acidity that might promote autolysis and cause precipitation of formol-heme pigment in the tissue. After fixation tissues were washed thoroughly in running tap water for about 6 hours followed by a rinse in distilled water for 30 minutes.

Tissue processing

After fixation tissues are processed for the preparation of thin microscopic sections. For This purpose tissues are embedded in paraffin block. Before embedding, tissues are processed through the steps of dehydration and clearing as follows:

Dehydration

Wet and fixed tissues cannot be directly infiltrated with paraffin. Tissues need to be processed through solvents with decreasing water concentrations in order to infiltrate them with paraffin. The fixed tissues were transfer through ascending graded alcoholic solutions, as alcohol is the most common solvent used for dehydration. It was done by keeping the tissues in 50% alcohol (1 hour), 70% alcohol (over night), 90% (2 hours with 2 changes), absolute alcohol (1 hour, with 2 changes).

Clearing

The next step is called 'clearing' where removal of dehydrant with a substance that will be miscible with the embedding medium (paraffin) is carried out. The frequently used clearing agent is xylene. It serves as a transition medium between two immiscible compounds, alcohol and paraffin. So the dehydrated tissues were transferred to xylene for 15 minutes. This procedure increases the refractive index of the tissues, thereby making them transparent. It hardens the tissue if left in too long.

Embedding

The 'embedding' process is very important because the tissues must be aligned or oriented properly in the block of paraffin. The tissue was embedded in paraffin (melting point 58-60^{o}C) by transferring them from xylene to molten paraffin in a porcelain pot for 2 hours which was kept in paraffin bath at 60^{o}C.

Block preparation

After complete impregnation with paraffin, blocks containing the tissues were prepared to facilitate proper sectioning of the material. Molten paraffin was poured in a paper boat to which the tissue was then transferred with hot forceps and oriented properly in the center of depression. Presence of air bubbles in the blocks hinders proper sectioning, so care was taken to remove the bubbles during setting of the paraffin.

Section cutting

The paraffin blocks were sectioned in a rotary microtome to get 4 -5 μm serial sections, which come out in the form of a paraffin ribbon. After having a 6″ ribbon, it was detached from the knife by the help of a scalpel and floated in a tray containing warm water. Small portions of this ribbon with serial sections floated in warm water were placed on glass slide coated with egg albumin and gently stretched using forceps or needles. The glass slides were then placed in a warm oven for about 15 minutes to help the sections to adhere to the slide.

Staining with hematoxylin and eosin

Hematoxylin is extracted from the heartwood of the logwood tree *Haematoxylum campechianum*. When oxidized it forms hematein, a compound that forms strongly colored complexes with certain metal ions, the most notable ones being Fe(III) and Al(III) salts. Metal-hematein complexes are used to stain cell nuclei prior to examination under a microscope. Eosin is an acidic dye with an affinity for cytoplasmic components of the cell. To differentiate the nucleus and cytoplasm, hematoxylin and eosin were used for staining of the tissue sections. The steps described below were followed for staining the slides.

Slides were dipped in xylene for 10 minutes.

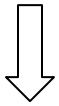

The slides were then dipped in absolute alcohol for 10 minutes.

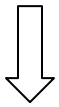

Next, the slides were dipped in 90% alcohol for 10 minutes.

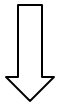

Then the slides were dipped in 70% alcohol for 10 minutes.

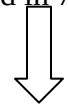

The slides were then dipped in water for 10 minutes.

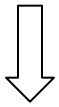

Sections were then stained with hematoxylin for 3-5 minutes.

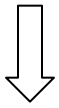

The slides were washed in running tap water for 8-10 minutes. Excess hematoxylin was removed in acid alcohol, so that cytoplasm remains unstained.

Excess acid was removed by putting the slides under running tap water.

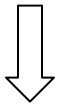

The slides were then dipped in 70% alcohol for 10 minutes.

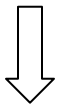

The slides were then dipped in 90% alcohol for 10 minutes.

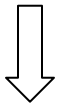

The slides were stained with eosin for 1-2 minutes.

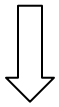

To remove excess stain the slides were washed in 90% alcohol.

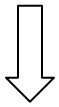

The slides were kept in absolute alcohol for 10 minutes.

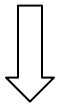

The slides were kept in xylene for 5 minutes and were finally mounted in DPX.

Evaluation

Stained sections were evaluated by observing the arrangement of tissue architecture under a light microscope (Leica DM 1000). Photomicrographs were taken with the software Las EZ.

Statistical analysis

All data were presented as mean ± SD. n = 6 animals per group. One way ANOVA followed by Tukey's Multiple Comparison Test using Graph Pad Prism software was performed for comparisons among groups. Significant difference was indicated when the *P* value was < 0.05.

Results

- **Body weight**

Oral administration of Nano-Se at the dose of 2mg Se/kg b.w. increased body weight significantly by 3.21% in Gr. II in comparison to the vehicle control group (Gr. I) **(Fig. 3)**, whereas oral administration of Nano-Se at the dose of 4mg Se/kg b.w. deceased the body weight significantly by 4.82% in Gr. III in comparison to the vehicle control group (Gr. I).

- **Hemoglobin level**

Oral administration of Nano-Se at the dose of 2mg Se/kg b.w increased blood hemoglobin level significantly by 6.46% in Gr. II in comparison to the vehicle control group (Gr. I) **(Fig. 3)**, whereas oral administration of Nano-Se at the dose of 3 mg Se/kg b.w. and 4mg Se/kg b.w decreased blood hemoglobin level by 3.02% in Gr. III and 4.61% in Gr. IV in comparison to the vehicle control group (Gr. I).

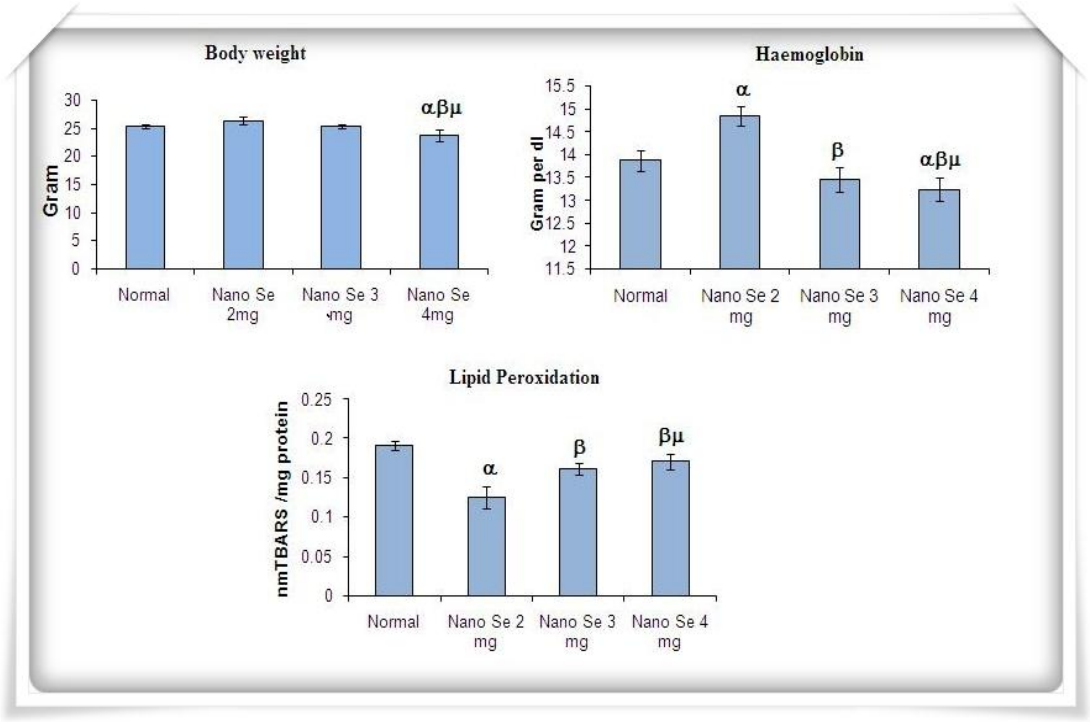

Figure 3: Data were represented as mean ± SD, n = 6. α - significant *(P<0.05)* as compared with Normal; β - significant *(P<0.05)* as compared with Nano-Se 2mg.

- **Lipid peroxidation level**

Oral administration of Nano-Se at the dose of 2mg Se/kg b.w decreased hepatic lipid peroxidation significantly (*P < 0.05*) by 34.21% in Gr. II in comparison to the vehicle control group (Gr. I) **(Fig. 3)**, whereas oral administration of Nano-Se at the dose of 3 mg Se/kg b.w and 4mg Se/kg b.w also decreased hepatic lipid peroxidation non-significantly by 15.78% in Gr. III and by 10.52% in Gr. IV respectively, in comparison to the vehicle control group (Gr. I).

- **ALT activity**

Oral administration of Nano-Se at the dose of 2mg Se/kg b.w decreased serum ALT level significantly (*P < 0.05*) by 23.40% in Gr. II in comparison to the vehicle control group (Gr. I) **(Fig. 4)**, whereas oral administration of Nano-Se the dose of 3 mg Se/kg b.w and 4mg Se/kg b.w also decreased serum ALT level numerically by 7.44 in Gr. III and by 8.51% in Gr. IV respectively, in comparison to the vehicle control group (Gr. I).

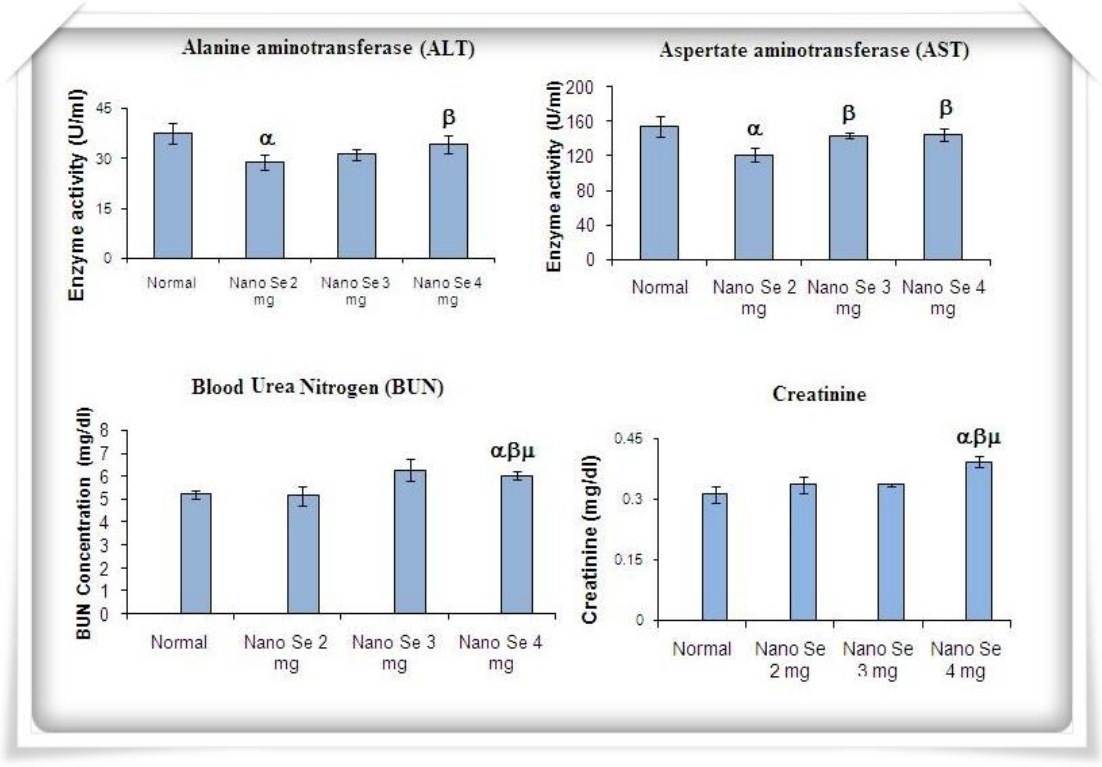

Figure 4: Data were represented as mean ± SD, n = 6. α - significant *(P<0.05)* as compared with Normal; β - significant *(P<0.05)* as compared with Nano Se 2mg.

- **AST activity**

Oral administration of Nano-Se at the dose of 2mg Se/kg b.w decreased serum AST level significantly (*P < 0.05*) by 21.50% in Gr. II in comparison to the vehicle control group (Gr. I)**(Fig. 4)**, whereas oral administration of Nano-Se at the dose of 3 mg Se/kg b.w and 4mg Se/kg b.w also decreased serum AST level numerically by 6.99% in Gr. III and by 6.54% in Gr. IV respectively, in comparison to the vehicle control group (Gr. I).

- **BUN level**

Oral administration of Nano-Se at the dose of 2mg Se/kg b.w decreased serum BUN level numerically by 1.15% in Gr. II in comparison to the vehicle control group (Gr. I)**(Fig. 4)**, in same duration of treatment with Nano-Se at the dose of 3 mg Se/kg b.w increased the serum BUN level numerically by 20.76%, whereas 4mg Se/kg b.w increased the serum BUN level significantly (*P < 0.05*) by 15.96% in comparison to the vehicle control group (Gr. I).

- **Creatinine level**

Oral administration of Nano-Se at the dose of 2mg Se/kg b.w increased serum creatinine level numerically by 7.66% in Gr. II in comparison to the vehicle control group (Gr. I) **(Fig. 4)**, in same duration of treatment with Nano-Se at the dose of 3 mg Se/kg b.w (Gr. III) increased serum creatinine level numerically by 7.34%, whereas oral administration of Nano-Se at the dose of 4mg Se/kg b.w (Gr. IV) increased the serum creatinine level significantly (*P < 0.05*) by 25.55% in comparison to the vehicle control group (Gr. I).

- **Histopathological examination**

Histology of liver from different doses of Nano-Se of mice has been shown in **Fig. 5.** After 30 days of different doses of Nano-Se administration, various histopathological lesions were observed in experimental mice. Dilatation of central vein, formation of pyknotic nuclei and inflammatory cellular infiltration were showed in 4 mg Se/kg b.w Nano-Se treated group. Whereas, no remarkable changes has not been shown in 2 mg Se/kg b.w Nano-Se treated group (Gr. II).

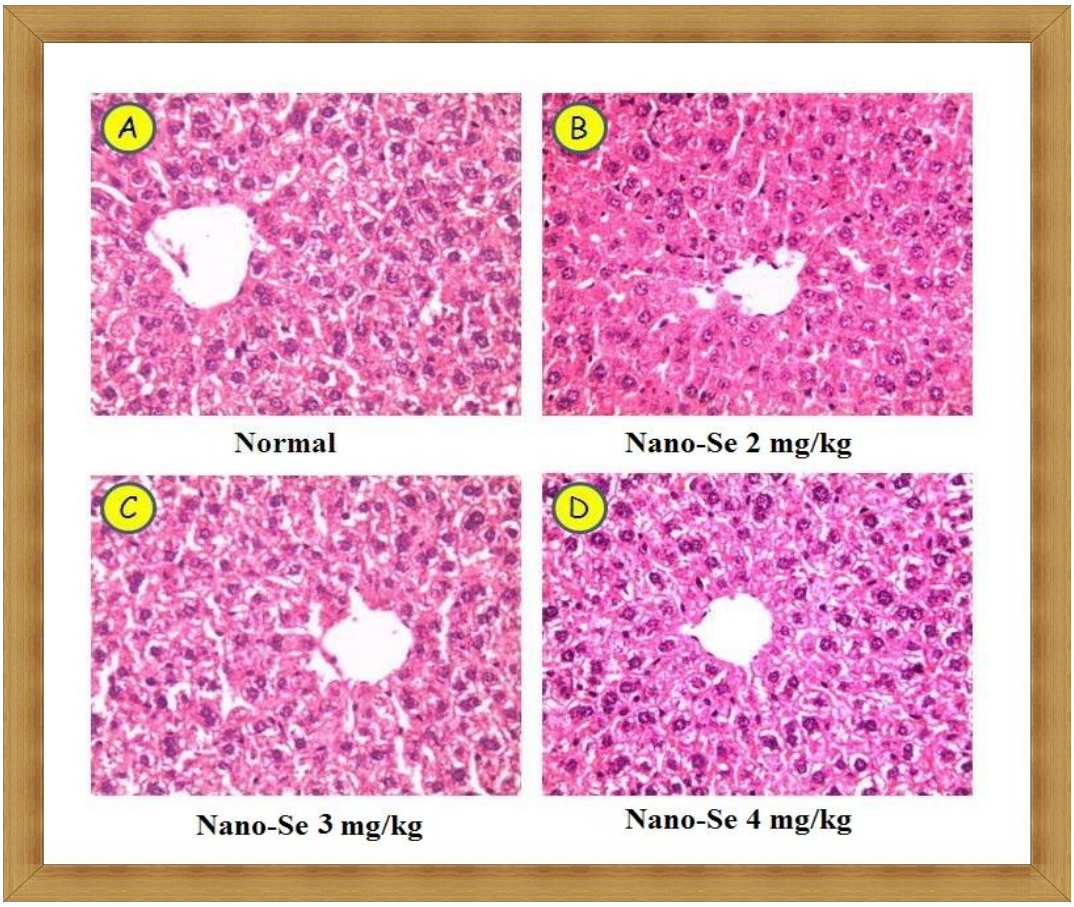

Figure 5: Photograph of liver section of mice stained with hematoxylin and eosin, ×200

Discussion

Determination of appropriate dose to advance into preclinical study is one of the most challenging and important task during drug development. Selecting a high dose may result in unacceptable safety problems, while a low dose may lead to ineffective drugs. Proper estimation of such dose-response profile for relevant safety and efficacy endpoints allows the reliable evaluation of the risk benefit profile of a drug at the end of the dose selection study. The dose selection study of Nano-Se was carried out at different dose intervals on the basis of some toxicity parameters. Liver is aversatile organ involved in drug metabolism and detoxification; hence determination of hepatic toxicity markers, lipid peroxidation level and Histopathological evaluation were performed from liver. He major amount of ingested selenium excreted through the kidneys; hence estimation of

renal toxicity markers study were also performed. The body weight was also estimated as a marker of general health as well as toxicity because the stability of body weight depends on the well being of an individual.

In the dose selection of Nano-Se, the drug was initially administered orally at 2 mg Se/kg b.w., 3 mg Se/kg b.w. and 4 mg Se/kg b.w. to mice for 30 days. The result showed that no significant toxicity was observed at the dose of 3 mg Se/kg b.w. and 4 mg Se/kg b.w. dose. Change of body weight, lipid peroxidation, serum ALT & AST activity, blood hemoglobin level, creatinine and BUN level and histopathological alteration standardized to evaluate the toxicity of different doses against only vehicle control group (Gr .I). Nano-Se treated group at the dose of 2 mg Se/kg b.w (Gr. II) is more effective than Nano-Se treated group at the dose of 3 mg Se/kg b.w. (Gr. III) and 4mg Se/kg b.w. (Gr. IV) respectively. Hence, the oral dose of 2 mg Se/kg b.w. was selected for ongoing preclinical studies of Nano-Se.

Hence, in this study, we have successfully synthesized and characterized Nano-Se with the help of different techniques. Following synthesis, we conducted in vivo studies to evaluate the toxicity profile and effective dose of Nano-Se. The study results proved that Nano-Se at 2 mg Se/kg b.w. oral dose is the most safe and efficacious. Hence, the oral dose of 2 mg Se/kg b.w. was selected for the evaluation of antioxidant and Chemoprotective potential of Nano-Se against chemotherapy induced toxicity.

Comparative Toxicological study with Inorganic and Organic Selenium compound

The main motive of researchers of now a day is to find ways to minimize the toxicity of certain drugs; those have potent therapeutic outcomes against several diseases and disorders. The human body has several mechanisms to counteract oxidative stress by producing antioxidants, which are either naturally produced *in situ*, or externally supplied through foods and/or supplements. Endogenous and exogenous antioxidants act as "free radical scavengers" by preventing and repairing damages caused by ROS and RNS, and therefore can enhance the immune defense and lower the risk of cancer and degenerative diseases **(Ahmadinejad et al., 2017)**.

The first line of endogenous defense against free radicals consists of some selenium containing enzymes. Selenium (Se) is an essential and unique trace element mainly because of the antioxidant effects of these selenoproteins such as glutathione peroxidase (GP*x*) and thioredoxin reductase (TrxR) and plays a crucial role in health and disease (**Fernandes and gandin, 2015**). Being a cofactor of these antioxidant enzymes selenium takes part in scavenging free radicals, thus protecting cells, membranes and cell organelles from lipid peroxidation, enzymes and nucleic acids from the harmful effects of ROS (**Éva Ungvári et al., 2014**). Thus, Se functions in the body as an antioxidant, in thyroid hormone metabolism, redox reactions, reproduction, and immune function **(Valdiglesias et al., 2010)**.). A wide variety of selenium compounds exists, both in organic forms as well as in inorganic forms. In daily life, we ingest these selenicals with our ordinary diet. The US Food and Nutrition Board (1980) considered to be the Estimated Safe and Adequate Daily Intake for Se of 50–200µg, being 55µg/day the Recommended Dietary Allowance (RDA) for Se for adults **(Kieliszek and Błażejak, 2016)**. These data support the importance of proper selenium intake but Se has a narrow therapeutic window (**Rayman, 2012**). 75 to 120µg/L is accepted as the normal range of Se plasma concentration (**Ghaemi et al., 2013**), and 1350µg/L is associated with the risk of selenosis in humans. Other related toxic effects are a disruption of endocrine function, synthesis of thyroid hormones and growth hormones, and an insulin-like growth factor metabolism **(Mullur et al., 2014)**.

Apart from that, depending on chemical form, dose and duration of intake, Se can be toxic, such as invertebrates **(Jaishankar et al., 2014)**. Tolerance for Se toxicity depends on, among other factors, the rate of excretion, and Se excretion depends on the rate of methylation of Se **(Combs GF Jr, 2015)**. Inorganic forms of Se appear to react with tissue thiols, such as glutathione (**Fernandes and gandin, 2015**) to form seleno-trisulphides and those are reacting with other thiols to generate oxygen free radicals, such as superoxide anion ($O_2^{-\bullet}$) by redox catalysis. Organic diselenides (e.g. selenocystine and selenocystamine are converted into selenols (RSeH) in presence of thiols which also results oxygen free radical generation during further reductions catalyzes the formation of superoxide under aerobic conditions in the presence of thiol; this reaction could play a role in the toxicity of diselenides and alkylselenols (**Chaudiere et al. 1992**). Free radical hypothesis of selenium toxicosis is based on the methyl-selenide formation, which also results superoxide radicals and at least oxidative stress. Excess selenium in the form of selenocysteine inhibits the methylation of selenium and increases the amount of intermediary metabolite, hydrogen-selenide, which can also be toxic **(Ganther, 1979).** In order to improve the toxicity of Se, nanotechnology is an emerging technological field with great potential to lead in great breakthroughs that can be applied in real life. Therefore, synthesis and characterization of the nanoparticles gained importance on account of their therapeutic applications **(Kumar et al., 2015)**. The unique characteristics, *viz*. nanosize, large surface to volume ratio and the difference in their properties of surface atom of the nanoparticles invite more attention **(Mousa et al., 2011)**. By exploiting these unique properties, scientists are developing nanodrugs that have an enhanced efficiency over the conventional system in terms of drug delivery, diagnostic, and as imaging agents. In this regard, nanoparticles of selenium (Nano-Se) as a new form of selenium and attracting increasing attention due to their excellent biological activities **(Hosnedlova et al., 2018)**. The present study was designed to establish that Nano-Se is less toxic compared to inorganic and organic selenium yet to more efficacious.

Materials and methods

Experimental animals

Adult (5–6 weeks) Swiss albino female mice (25 ± 2g), bred in the animal colony of Chittaranjan National Cancer Institute (CNCI) (Kolkata, India), were used for this study. The mice were maintained under standard condition of humidity (45–55%), temperature (23 ± 2ºC), and light (12 h light/12 h dark). Standard food pellets (EPIC rat and mice pellet) from Kalyani Feed Milling Plant, Kalyani, West Bengal, India and drinking water was provided *ad libitum*. The experiments were carried out following strictly the Institute's guideline for the Care and Use of Laboratory Animals.

Experimental groups

Animals were distributed into four groups containing six animals (n=6) in each group.

Normal control: Each animal received saline (0.9% NaCl) orally for 30 days.

Inorganic Selenium-treated group: Each animal was given sodium selenite (M.W. 172.94) at 2 mg Se/kg b.w. in distilled water orally for 30 days.

Organic Selenium-treated group: Each animal was given 1, 4 – phenylene –bis (methylene) selenocyanate (M.W. 314.104) at 2 mg Se/kg b.w. as suspension in water orally for 30 days.

Nano Selenium-treated group: Each animal was given Nano-Se at 2 mg Se/kg b.w. in distilled water orally for 30 days. Animals were sacrificed on day 31.

Prameter studied

- Determination of body weight
- Quantitative estimation microsomal lipid peroxidation level in liver, kidney and lungs
- Quantitative estimation of reduced glutathione level, estimation of the activity of phase II detoxifying enzyme glutathione-S-transferase and different antioxidant enzymes like superoxide dismutase, catalase and glutathione peroxidase in liver.
- Estimation alanine transaminase (ALT) and aspartate transaminase (AST) activity in serum.

- Estimation of renal function markers blood urea nitrogen (BUN) and creatinine levels in serum.
- Evaluation of chromosome aberrations by conventional flame dry technique and assessment of DNA damage by comet assay in bone marrow cells.
- Histopathological evaluation of liver, kidney and lungs tissue by hematoxylin/eosin (H & E) staining

Methodologies

❖ **Hematological parameters**

➢ **Blood hemoglobin (Hb) level (Sahli, 1909)**

Blood hemoglobin was measured following **Sahli's method** (Sahli, 1909). Detailed procedure for the estimation of blood hemoglobin level has already been given in Dose selection study.

➢ **Red blood cell count** (**D'Armour et al, 1965**)

Red blood cell (RBC) count was performed using the hemocytometer. This particular instrument possesses a platform with microscopic grid scoring. Rails on either side hold up a cover slip so that a specified quantity of fluid is held. With proper dilution of blood, counting of all cells in specified squares and finally by multiplying the counted RBC with the proper conversion factor, the number of RBC/mm^3 is determined.

Reagents required

RBC diluting fluid containing 1% sodium citrate, formalin and distilled water.

Procedure

Blood was drawn up to the 0.5 mark in a RBC diluting pipette.

⇩

Holding the pipette horizontally, the RBC diluting fluid was drawn up to the 101 mark (Dilution of 1 to 200).

The diluent and blood was mixed properly.

⇩

Holding at an angle of 45^{o}, the pipette tip was positioned at the junction of the cover glass and the counting chamber.

⇩

Diluted blood from the pipette was charged to one chamber of the hemocytometer.
The cells were allowed to settle for about 1 minute.

⇩

RBC counting was done at 400× in each of five fields (each with 16 smallest squares).
The cells touching top and right sides of the squares were ignored.

Calculation

The smallest squares in the large center square (where red cells are counted) have an area of 1/400 mm and are arranged in groups of 16. The volume of fluid in the portion of the hemocytometer which was counted: 1/400 mm^2 (area of smallest square) × 16 (no. of squares/group) × 5 (no. of groups counted) × 1/10 mm (depth of chamber) = 0.02 mm^3. Before being placed in the chamber, blood was diluted by a factor of 200.

So, the number of RBC in 0.02 mm^3 blood

= 200 (dilution factor) × the number of cells counted.

So, the number of RBC in 1 mm^3 blood

= 200 (dilution factor) × the number of cells counted × 50 (volume factor).

RBC count was reported as millions of cells/mm^3.

- **White blood cell count (Wintrobe et al, 1961)**

A sample of whole blood was mixed with a weak acid solution that lyses nonnucleated red blood cells. Following adequate mixing, the specimen was introduced into a counting chamber where the white blood cells (WBCs) in a diluted volume were counted.

Reagent required

WBC diluting fluid containing 2% acetic acid.

Procedure

Blood was sucked up exactly to the 0.5 mark in a WBC diluting pipette.

Excess blood was wiped out from the outside of the pipette to avoid excess transfer of cells to the diluting fluid.

Diluting fluid was immediately drawn to the "11" mark while rotating the pipette between the thumb and forefinger to mix the specimen and diluent.

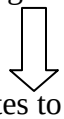

Mixing was done for 3-5 minutes to ensure even distribution of cells.

Holding at an angle of 45^{o}, the pipette tip was positioned at the junction of the cover glass and the counting chamber.

The mixture in the pipette was allowed to flow under the cover glass until the chamber was completely filled. Similarly the opposite chamber of the hemocytometer was also filled.

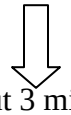

The cells were allowed to settle for about 3 minutes. Under low-power magnification of microscope, the WBCs were counted in the four 1 sq. mm corner areas.

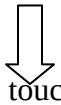

WBCs lying within the square and those touching the upper and right hand center lines were counted and those touching the left hand and bottom lines were not counted.

Calculation

Routinely, blood was drawn to the 0.5 mark and diluted to the 11 mark with WBC diluting fluid. All the blood was washed into the bulb of the pipette (which had a volume

of 10). Therefore, 0.5 volumes of blood were contained in 10 volumes of diluting fluid. The resulting dilution was 1:20.

The depth of the counting chamber was 0.1 mm and the area counted was 4 sq mm (4 squares were counted, each with an area of 1.0 sq mm therefore, 4 × 1.0 sq mm = a total of 4 mm^2). The volume counted was: 4 mm^2 × 0.1 mm = 0.4 mm^3 (area × depth).

Finally, the formula for obtaining the no. of WBC/mm^3 was as follows:

$$\text{WBC/mm}^3 = \frac{\text{Average number of chamber (2) WBCs counted} \times \text{Dilution (20)}}{\text{Volume (0.4)}}$$

- **Spleen Cell Count**

Reagent required

WBC diluting fluid containing 2% acetic acid

Procedure

Whole spleen was isolated from the sacrificed mice.

⇩

The Spleen was put on a Petri dish and was ruptured by flushing with PBS using a hypodermic syringe. The process continued until the entire cells from spleen come out into the dish making the spleen fade.

⇩

The cell suspension was then centrifuged at 2000 rpm at 4^oC for 10 minutes.

⇩

The pellet was resuspended in a measured volume of PBS after removing the supernatant. Nucleated cell count from the spleen cell suspension was done under microscope using hemocytometer as in WBC count.

⇩

Spleen cell count was reported as total numbers of nucleated cells/mm^3.

- **Thymus Cell Count**

Reagent required

WBC diluting fluid containing 2% acetic acid

Procedure

Whole thymus was isolated from the sacrificed mice.

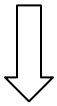

The thymus was put on a Petri dish and was ruptured by flushing with PBS using a hypodermic syringe. The process continued until the entire cells from thymus come out into the dish making the spleen fade.

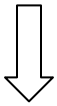

The cell suspension was then centrifuged at 2000 rpm at $4^{o}C$ for 10 minutes.

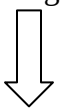

The pellet was resuspended in a measured volume of PBS after removing the supernatant. Nucleated cell count from the spleen cell suspension was done under microscope using hemocytometer as in WBC count.

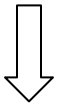

Thymus cell count was reported as total numbers of nucleated cells/mm^3.

- **Bone marrow cell count**

Reagent required

WBC diluting fluid containing 2% acetic acid.

Procedure

Bone marrow was collected from the femur bone of sacrificed mice by flushing with PBS using a hypodermic syringe. The bone marrow in PBS was aspirated well to make a homogeneous suspension.

The cell suspension was then centrifuged at 2000 rpm at 4^{o}C for 10 minutes.

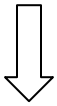

The pellet was resuspended in a measured volume of PBS after removing the supernatant. Nucleated cell count from bone marrow cell suspension was done under microscope using hemocytometer as in WBC count.

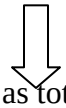

Bone marrow cell count was reported as total numbers of nucleated cells/femur/mm^3.

- **Biochemical parameters**

- **Estimation of protein content in tissue homogenate (Lowry et al, 1951)**

Total protein content in tissue homogenate during biochemical estimation was measured following Lowry method using Folin-Phenol reagent.

Reagents required

2% Na_2CO_3, 1% $CuSO_4$. $5H_2O$, 2% Sodium-potassium tartarate, 1N NaOH, 2% Folin-Phenol reagent and Bovine Serum Albumin (BSA).

Procedure

In microcentrifuge tubes 10 µl unknown tissue sample was added to 100 µl 1N NaOH.

10 µl 1% $CuSO_4$, 10 µl 2% sodium-potassium tartarate and 980 µl 2% Na_2CO_3 were then added in the reaction mixture and kept for 15 minutes.

Next, 300 µl Folin-Phenol reagent (v/v; 1:2 with water) was added and kept for 15 minutes in dark at room temperature.

Development of blue coloration.

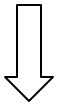

For preparation of blank, all the reagents were used except the tissue sample which was replaced with distilled water.

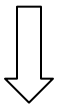

The absorbance of the color was measured against the colorless blank sample at 660 nm using the Varian Cary 100 UV–Vis Spectrophotometer.

Assessment

A standard curve was prepared by measuring the absorbance of different known concentrations of BSA and the total protein concentration of the unknown sample was determined from the standard curve.

- **Quantitative estimation of lipid peroxidation (LPO) level (Okhawa et al, 1979)**

Spectrophotometric method was applied to estimate the level of LPO in liver and lung microsomes by measuring the formation of lipid peroxides using thiobarbituric acid (TBA) and was expressed as nmTBARS/mg protein.

Reagents required

Normal saline, 1.15% KCl, 8.1% SDS, 20% Acetic acid, 0.8% TBA, n-Butanol and pyridine.

Procedure

Estimation of thiobarbituric acid reactive substances (TBARS)

Liver, lung and kidney tissues of the experimental mice were collected after their sacrifice, washed in normal saline and 400 mg of liver and lung tissues were weighed.

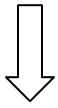

The tissues were then homogenized in 3.6 ml 1.15% KCl using a Teflon homogenizer.

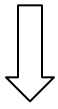

The homogenates were centrifuged at 12000 g for 10 minutes at 4^{o}C.

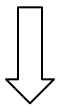

The supernatants (devoid of nuclear debris) were again centrifuged at 10000 g for 10 minutes at 4^{o}C.

The supernatants (devoid of mitochondria) were centrifuged for third time at 25000 g for 1 hour at 4^{o}C.

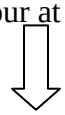

The precipitates (containing microsomal fraction) were suspended in 400 µl 1.15% KCl and the suspensions were used as sample for determining the LPO level.

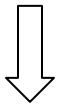

In test tubes 200 µl sample, 200 µl SDS, 1.5 ml acetic acid and 1.5 ml TBA were added along with 600 µl distilled water.

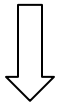

A blank sample was prepared following the same procedure using all the above mentioned reagents except distilled water in place of tissue sample.

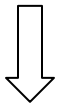

The reaction mixtures were then heated at 95°C in water bath for 1 hour.

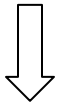

The reaction resulted in the development of pink coloration.

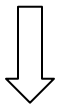

5 ml mixture of butanol and pyridine (15:1; v/v) was added to each sample and each sample was then vortexed thoroughly and centrifuged at 3000 g for 10 minutes.

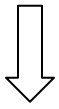

Absorbance of the upper pink colored organic layer was measured at 532 nm against the colorless blank sample using the Varian Cary 100 UV–Vis Spectrophotometer.

Assessment

Total protein concentration of each unknown sample was determined from the standard curve prepared by measuring the absorbance of different known concentrations of BSA. The level of LPO was expressed as nmol TBARS formed/mg protein using extinction co-efficient of 1.56×10^5 $M^{-1}cm^{-1}$ as follows:

Absorbance = Extinction coefficient × Concentration × Length (Beer-Lambert Law)

Now, Extinction co-efficient = 1.56×10^5 $M^{-1}cm^{-1}$

Length = 1cm

So, Concentration of TBARS = Absorbance/(1.56×10^5) M

= Absorbance × $10^9/(1.56 \times 10^5)$ nM

Hence, the level of LPO in 200 µl sample was expressed as:

$$\text{nmol TBARS/mg protein} = \frac{\text{Absorbance of TBARS at 532 nm} \times 2}{1.56 \times \text{Protein concentration (mg) in 200 µl sample}}$$

- **Estimation of reduced glutathione (GSH) level (Mulder et al, 1995; Sedlack et al, 1968)**

Spectrophotometric method was used to evaluate the level of GSH in mouse liver and lung tissue samples. GSH level was measured in tissue cytosol by determination of DTNB reduced by – SH groups, as described by Sedlack and Lindsay and was expressed as nmol/mg protein.

Reagents required

Homogenizing buffer (pH 7.4; 250 mM sucrose, 20 mM Tris-HCl), 0.01 M DTNB dissolved in absolute methanol (prepared fresh before use), 0.4 M Tris buffer (pH 8.9), 0.02 M EDTA, TCA (50% w/v), standard glutathione (1 mg/ml).

Procedure

After sacrifice, 200 mg of liver and lung tissues were collected, washed with normal saline and were then homogenized in 5 volumes (1 ml) of homogenizing buffer, using a Teflon homogenizer.

The homogenates were centrifuged at 35000g for 2 hours at 4^{o}C.

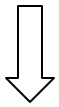

The supernatants (cytosolic fractions) were collected and used as samples for estimation.

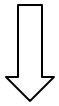

0.1 ml supernatant, 2.4 ml EDTA solution were added in test tubes and kept on ice for 10 minutes.

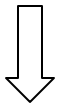

2 ml distilled water and 0.5 ml 50% TCA were then added in each test tube. The test tubes were kept on ice for 10-15 minutes and were then centrifuged at 3000 g for 15 minutes.

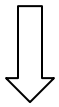

1 ml supernatant from each sample was taken, to which 2 ml Tris buffer was added. Then 0.05 ml DTNB solution (Ellman's reagent) was added and vortexed thoroughly. Instead of supernatant distilled water was used to prepare blank.

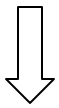

Optical density (OD) of each sample was taken (within 2-3 minutes after the addition of DTNB) at 412 nm using Varian Cary 100 UV–Vis Spectrophotometer against the blank. Standards were run simultaneously.

Assessment

Total protein concentration of the unknown sample was determined from the standard curve prepared by measuring the absorbance of different known concentrations of BSA. The GSH level was determined from the standard curve prepared by measuring the absorbance of different known concentrations of GSH and expressed as nmol/mg protein.

- **Estimation of glutathione-S-transferase (GST) activity (Mulder et al, 1995; Habig et al, 1974)**

GST activity in liver and lung tissues was evaluated using spectrophotometric method. GST activity was measured in tissue cytosolic fractions by determining the increase in absorbance at 340 nm with CDNB as the substrate and the specific activity of the enzyme was expressed as formation of CDNB-GSH conjugate formed/minute/mg protein.

Reagents required

Homogenizing buffer (pH 7.4; 250 mM sucrose, 20 mM Tris-HCl & 1 mM DTT), 0.3 M phosphate buffer (pH 6.5; Na_2HPO_4 & NaH_2PO_4), 30 mM GSH and 30 mM CDNB.

Procedure

Estimation CDNB-GSH conjugates

After sacrifice, 200 mg of liver and lung tissues were collected, washed in normal saline and were then homogenized in 5 volumes (1 ml) of homogenizing buffer, using a Teflon homogenizer.

⇩

The homogenates were centrifuged at 35,000 g for 2 hours at 4^{o}C.

⇩

The supernatants (cytosolic fraction) were collected and used as samples for estimation.

⇩

In test tubes 1 ml 0.3M phosphate buffer, 100 µl CDNB and 100 µl sample were added.

A blank sample was prepared as above using distilled water instead of tissue sample.

⇩

1.7 ml distilled water was then added in each test tube.

⇩

Test tubes were then kept at 30°C for 5 minutes.

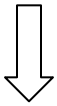

100 µl GSH solution was added to each of the test tube.

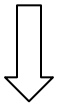

Change in absorbance was measured at 340 nm using Varian Cary 100 UV–Vis Spectrophotometer. The readings were taken for 3 minutes each at 30 seconds interval.

Assessment

Total protein concentration of the unknown sample was determined from the standard curve prepared by measuring the absorbance of different known concentrations of BSA. The activity of GST was expressed as CDNB-GSH conjugate formed/minute/mg protein present in the sample. The enzyme activity was determined according to the following formula

Absorbance = Extinction coefficient × Concentration × Length (Beer-Lambert Law)

Now, Absorbance = Change in Absorbance/minute for 3 minutes, i.e.,

(Change in Absorbance/minute) × 3

Extinction co-efficient = $9.6 \times 10^2\ M^{-1}cm^{-1}$

Length = 1cm

Therefore, Concentration of CDNB-GSH

$= \{(\text{Change in Absorbance/minute}) \times 3\}/(9.6 \times 10^2)$ M

$= \{(\text{Change in Absorbance/minute}) \times 3 \times 10^9\}/ (9.6 \times 10^2)$ nM

Hence, GST activity (in 100 µl sample) was expressed as:

$$\text{CDNB-GSH conjugate formed/minute/mg protein} = \frac{\text{Change in Absorbance/ minute} \times 3 \times 1000}{9.6 \times \text{Protein concentration (mg) in 100 µl sample}}$$

- **Superoxide dismutase activity (SOD) (Marklund et al, 1974; McCord et al, 1969)**

SOD activity was determined by estimating the inhibition of pyrogallol autooxidation by the enzyme. Partial extraction and purification of SOD was done as described by McCord and Fridovich. SOD activity was assayed by the method of Marklund and Marklund.

Reagents required

Homogenizing buffer (pH 7.5; 50 mM Tris-HCl, 2 mM DTPA), pyrogallol solution: stock solution of 20 mM pyrogallol was made in 10 mM HCl. Working solution was prepared fresh by diluting the stock 1:10 with 50 mM Tris-HCl, chloroform and ethanol.

Procedure

100 mg liver and lung tissues were collected from sacrificed mice, washed in normal saline and homogenized in 500 µl homogenizing buffer, using a Teflon homogenizer.

⇩

The homogenates were centrifuged at 10000 g for 30 minutes at 4^{o}C. The supernatants were taken and 250 µl ethanol and 150 µl chloroform were added to the supernatants.

⇩

The mixtures were then vortexed for 5-7 minutes and were centrifuged at 13000g for 15 minutes at 4^{o}C and the supernatants were used as the sample.

⇩

The reaction mixture for autooxidation consisted of 2 ml homogenizing buffer, 0.4 ml 2 mM pyrogallol solution and 1.6 ml distilled water.

⇩

Auto-oxidation of pyrogallol was measured by the increase in absorbance at 420 nm (0.02 min^{-1} and reading was taken at 30 seconds interval for 3 minutes).

⇩

The reaction mixtures for SOD estimation contained 10 µl cytosolic extract, 2 ml homogenizing buffer, 0.4 ml 2mM pyrogallol solution and 1.6 ml distilled water. A blank sample was prepared using 2 ml homogenizing buffer and 2 ml distilled water.

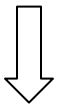

SOD activity was determined by means of inhibition of pyrogallol autooxidation by the enzyme present in the cytosolic fraction at 420 nm and the absorbances were taken at 30 seconds interval for 3 minutes in Varian Cary 100 UV–Vis Spectrophotometer.

Assessment

Total protein concentration of the unknown sample was determined from the standard curve prepared by measuring the absorbance of different known concentrations of BSA. SOD activity was determined by means of inhibition of pyrogallol auto-oxidation by the enzyme. A unit of enzyme is defined as the amount of enzyme that inhibits the reaction by 50%. Specific activity was expressed as unit/mg protein. DTPA acts as a chelator and prevents the interference from Fe^{+2} as well as from Cu^{+2} and Mn^{+2}. SOD activity was calculated by using the following formula:

% Inhibition = 100 – [{(AP–AF- AI)} × 100]/AP

AP= Absorbance of Pyrogallol auto-oxidation, AF= Absorbance final, AI= Absorbance initial

Unit/mg protein= % inhibition/{50 × Protein concentration (mg)}.

- **Catalase activity (CAT) (Luck, 1963)**

CAT catalyzes the break down of H_2O_2 into H_2O and O_2 and competes with the GPx for the common substrate H_2O_2. CAT is considered to be the primary scavenger of intracellular H_2O_2 generated due to oxidative stress. CAT activity in liver and lung cytosol was determined spectrophotometrically at 240 nm and expressed as unit/mg protein, where the unit is the amount of enzyme that liberates half the peroxide oxygen from H_2O_2 in second at 25°C.

Reagents required

M/15 phosphate buffer {(Na_2HPO_4 and NaH_2PO_4) (pH 7.0)}, Homogenizing buffer {M/150 phosphate buffer (pH 7.0)}, H_2O_2 phosphate buffer {0.16 ml H_2O_2 (30%, w/v) was diluted to 100 ml with M/15 phosphate buffer}. H_2O_2 at a concentration of 14.12 mM had an absorbance of approximately 0.50 at 240 nm with 1 cm light path.

Procedure

Mice were sacrificed, 100 mg liver and lung tissues were excised out, washed and homogenized in 500 µl ice-cold M/150 phosphate buffer, using a Teflon homogenizer.

⇩

The homogenates were centrifuged at 2000 g for 10 minutes at 4°C.

⇩

The supernatants were taken for the assay of CAT activity.

⇩

In test tubes 10 µl sample and 3.0 ml H_2O_2 phosphate buffer were taken.

⇩

Time required for 0.05 unit OD change was measured at 240 nm in Varian Cary 100 UV–Vis Spectrophotometer against a blank containing the enzyme source in H_2O_2 free phosphate buffer (H_2O_2 phosphate buffer prepared above had absorbance of 0.50 at 240 nm and after the addition of enzyme, Δt was noted till OD was 0.45). If Δt was longer than 60 seconds, the procedure was repeated with a more concentrated enzyme sample. Reading was taken at every 3 seconds interval.

Assessment

Total protein concentration of the unknown sample was determined from the standard curve prepared by measuring the absorbance of different known concentrations of BSA.

A unit of CAT activity is the amount of enzyme that liberates half the peroxide oxygen from H_2O_2 solution of any concentration in 100 seconds at 25°C

$$\text{Unit/mg protein} = \frac{2.3}{\Delta t} \times \log \frac{\text{E-initial}}{\text{E-final}} \times \frac{1}{6.93\times10^{-3}} \times \frac{1}{\text{Protein concentration}}$$

E= optical density at 240 nm

2.3= conversion factor from ln to log

Δt= time required for a decrease in the OD

- **Estimation of GP*x* activity (Paglia et al, 1967)**

GPx activity was measured spectrophotometrically by NADPH oxidation using a coupled reaction system consisting of reduced glutathione, glutathione reductase and hydrogen peroxide. The enzyme activity was expressed as micromole NADPH utilized/minute/mg protein, using extinction co-efficient of NADPH at 340 nm as 6200 M^{-1} cm^{-1}.

Reagents required

0.25 M potassium phosphate buffer (pH 7.0, containing 2.5 mM EDTA and 2.5 mM sodium azide), glutathione reductase (2.4 units), 10 mM reduced glutathione, 2.5 mM NADPH, 0.1% $NaHCO_3$, 12 mM H_2O_2.

Procedure

From sacrificed mice liver and lung tissues were isolated, washed and weighed (100 mg each).

⇩

Tissues were then homogenized in 5 volumes (500 µl) of homogenizing buffer, using a Teflon homogenizer.

⇩

The homogenates were centrifuged at 13,000 rpm for 10 minutes at 4°C.

The supernatants were considered as the sample for enzyme assay.

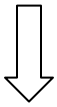

In microcentrifuge tube 200 µl potassium phosphate buffer, 100 µl glutathione reductase, 100 µl GSH, 100 µl NADPH and 100 µl supernatant were added.

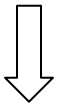

300µl distilled water then was added to the reaction mixture to make the volume 900 µl.

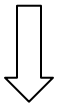

The reaction mixtures were then incubated at 37^{o}C for 10 minutes.

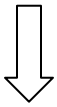

The reaction was started on adding 100 µl 12 mM H_2O_2. Blank was prepared using all the above mentioned reagents except NADPH, H_2O_2 and tissue sample, all of which were replaced by distilled water.

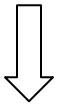

OD was measured at 340 nm at 30 seconds interval for 3 minutes.

Assessment

Total protein concentration of the unknown sample was determined from the standard curve prepared by measuring the absorbance of different known concentrations of BSA. The enzyme activity was expressed as micromol NADPH utilized/minute/mg of protein using molar extinction coefficient of NADPH at 340 nm as 6200 $M^{-1}cm^{-1}$.

- **Estimation of Thioredoxin Reductase Activity (TrxR) (Mustacich and Powis, 2000; Arner et al., 1999)**

TrxR reduces oxidized thioredoxin (Trx) using NADPH as a reducing equivalent to form reduced Trx which in turn spontaneously reduces various biomolecules of the cell like proteins, nucleic acids etc. Mammalian TrxR activity was determined spectrophotometrically following a standard enzymatic method (reduction of DTNB with NADPH to TNB) provided with the commercially available kit. Two moles of 5-thio-2-nitrobenzoic acid (TNB) are formed for every one mole of NADPH oxidized. The assay was performed at room temperature (25°C) and the TNB had an absorption maximum at 412 nm. In crude biological samples, other enzymatic activities, such as glutathione reductase and glutathione peroxidase, also reduce DTNB and increase the observed rate of DTNB reduction. The contribution of these activities to the total DTNB reduction may be estimated by using a specific TrxR inhibitor. In order to determine the DTNB reduction due only to the TrxR activity present in the sample, two assays need to be performed: the first measurement is of the total DTNB reduction by the sample and the second one is the DTNB reduction by the sample in the presence of the TrxR inhibitor solution. The difference between the two results is the DTNB reduction due to TrxR activity.

Reagents required

Assay Buffer 5× for thioredoxin reductase (500 mM potassium phosphate, pH 7.0, containing 50 mM EDTA), TrxR [rat liver TrxR in 50 mM Tris-HCl, pH 7.4, containing 1 mM EDTA, 300 mM NaCl, and 10% glycerol {≥200 µg (protein)/ml}], TrxR inhibitor solution, DTNB, NADPH, dimethyl sulfoxide (DMSO).

Preparation of working solutions

1× Assay Buffer - It was prepared by diluting 2 ml of the Assay Buffer 5× for TrxR to 10 ml with ultrapure water and was kept at room temperature.

DTNB Solution - 39.6 mg of DTNB was dissolved in 1 ml of dimethyl sulfoxide (DMSO). This solution was prepared the day before use and stored at 2–8 °C.

NADPH Solution - 0.625 ml of water was added to the bottle containing 25 mg of NADPH and care was taken for complete dilution of the content.

Working buffer - 10 ml of working buffer was prepared by adding 50 µl of NADPH solution to 2 ml of assay buffer 5× for TrxR and the final volume was brought to 10 ml with ultra pure water. The final concentration of the working buffer was 100 mM potassium phosphate with 10 mM EDTA and 0.24 mM NADPH. The working buffer was kept at room temperature and used within 2 hours.

Diluted Inhibitor Solution - 10 ml of the TrxR Inhibitor Solution was diluted 20-fold with DMSO to a final volume of 200 ml. The solution was kept at room temperature during the assay.

Procedure

Animals were sacrificed and kidneys were isolated, washed in PBS and were weighed (100 mg)

⇩

The tissue was then homogenized with 4 volumes of 0.25× assay buffer Teflon homogenizer

⇩

The homogenate was then centrifuged for 15 minutes at 10,000g at 4oC. The supernatant was used as the enzyme sample.

In 96 well plate 180 µl of working buffer was added

⇩

5 µl of tissue sample was added in each well

⇩

9 µl of 1× assay buffer was added in each well.

⇩

For the inhibition reaction 5 µl of sample, 5 µl of 1× assay buffer, 180 µl of working buffer and 4 µl of diluted inhibitor solution were added and were mixed by inversion

⇩

6 µl of DTNB solution was added to each well and mixed thoroughly

⇩

Reaction started as soon as DTNB was added

The reaction of DTNB and NADPH produces TNB with formation of yellow color. The rate of formation of the yellow color was determined by measuring the increase in absorption per minute for each reaction at 412 nm.

Assessment

Total protein concentration of the unknown sample was determined from the standard curve prepared by measuring the absorbance of different known concentrations of BSA. TrxR activity was expressed as unit/ml/mg protein using the following formula:

$$\text{Unit/ml/mg protein} = \frac{\Delta A_{412}/\text{minute (TrxR)} \times \text{Dil} \times \text{Vol}}{\text{Enzvol} \times \text{Protein concentration in 5 µl sample}}$$

ΔA_{412}/minute (TrxR) = ΔA_{412}/minute (sample) – ΔA_{412}/minute (sample + inhibitor)

Dil = sample dilution factor.

Vol = volume of reaction in ml.

Enzvol = volume of enzyme in ml.

Unit definition: One unit of mammalian TrxR will cause an increase in A_{412} of 1.0 per minute per ml (when measured in a non-coupled assay containing DTNB alone) at pH 7.0 at 25°C.

The calculation of the enzymatic activity in this case needs to be adjusted for the difference in path length between a 1 ml cuvette (1 cm) and the plate used. A standard 96 well polystyrene plate containing 200 ml of liquid will have a path length of ~0.55 cm. The calculated activity obtained with a 96 well plate needs to be divided by 0.55 to be compared to activity determined with a 1 ml cuvette.

- **Hepatic marker enzymes alanine transaminase and aspartate transaminase assay (Reitman and Frankel, 1957)**

Detailed procedure for the estimation of alanine transaminase (ALT) and aspertate transaminase (AST) activity has already been given in Dose selection study.

- **Determination of blood urea nitrogen (BUN) (Urease-Bertholot end point assay) and Creatinine level (Murrary, 1984; Chaney and Marbach, 1962)**

Detailed procedure for the estimation of blood urea nitrogen (BUN) activity and creatinine level has already been given in Dose selection study.

- **Genotoxicity parameters**
- **Detection of DNA damage by alkaline single cell gel electrophoresis (Comet assay) (Singh et al., 1988; Endoh et al., 2002)**

The alkaline single cell gel electrophoresis (SCG) (Comet) assay is a rapid and sensitive procedure for quantitating DNA damage in mammalian cells **(Singh et. al., 1988; Endoh et al., 2002)**. The use of this alkaline SCG assay as a method to detect genotoxicity and cytotoxicity *in vivo* is well documented, and DNA damage thus detected has been used to predict the presence of genotoxic metabolites in specific organs **(Henderson et. al., 1998)**. In this assay, cells are embedded in agarose, lysed in an alkaline buffer, and subjected to an electric current. Relaxed and broken DNA fragments stream further from the nucleus than intact DNA, so the extent of DNA damage can be measured by the length of the stream. This method has several advantages: it is highly sensitive to DNA damage expressed as single strand breaks and alkali-labile sites and disordered DNA fragmentation **(Hartmann et. al., 2003)**, and few cells are required. DNA damage (disorderly DNA fragmentation) induced by differet form of selenium was measured by using this assay under alkaline conditions following a simplified protocol with slight modifications.

Reagents required

1% normal melting agarose in PBS, 1% low melting point agarose in Milli Q water, 0.5% low melting point agarose in PBS, sodium hydroxide (NaOH), Ethylenediaminetetra acetic acid (Na_2EDTA), Ethidium bromide,.

Lysing solution: 2.5 M NaCl, 100 mM EDTA, 10 mM Tris buffer, 1 % Triton X 100, pH was adjusted to 10 with NaOH.

Electrophoresis buffer: 1 mM Na_2EDTA and 0.3 M NaOH (pH>13).

Neutralizing buffer: 0.4 M Tris buffer (pH 7.5).

Staining solution: Ethidium bromide in water (20 µg/ml).

Isolation of bone marrow from femur for comet assay:

Bone marrow cells suspension was prepared from femurs of each animal, where the bone was split longitudinally and the marrow was exposed using forceps and the content of the femur was flushed gently using 2 ml syringe containing PBS (pH 7.4) into a centrifuge tube and centrifugation at 1000 rpm for 10 min at 4ºC. Cell pellets were re-suspended with PBS and the density of cells was adjusted to 10^6cells/slide for the comet assay.

Procedure:

Half frosted microscope slides were coated with 1% normal melting agarose in PBS

⇩

The slides were then allowed to dry at room temperature protected from dust and other particles

⇩

On the day of single cell gel electrophoresis an aliquots of 10µl of freshly prepared cell suspension was mixed with 75µl of 1% low melting point agarose in Milli Q water

⇩

This mixture was then layered on the top of the pre-coated slide and covered with a 24 x 50 mm cover slip and kept on ice to allow the agarose to solidify

⇩

After the agarose had solidified on ice for at least 10-15 min. containing required amount of cells, the cover slip was gently removed and a third layer of 0.5% low melting point agarose was layered on the top of the second layer and covered with a cover slip and kept on ice for 5-10 min.

⇩

After the agarose had solidified, the cover slipwas gently removed and the slides were carefully immersed in a freshly prepared ice-cold lysing solution

After lysis for overnight at 40ºC, cell membrane and cytosol were lysed and isolated nucleus was remain in the agarose. The slides were placed in an electrophoresis unit.

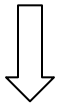

The buffer reservoirs were gently filled with fresh electrophoresis buffer to a level of 0.25 cm above the microscope slides, and incubated for 20min. at 40ºC to allow the unwinding of DNA

Keeping the same temperature, the slides were subjected to electrophoresis (25V, 400 mA) for another 25 min.

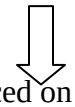

After electrophoresis, the slides were placed on a tray to remove alkali and detergents and neutralized with neutralizing buffer for 10 min.

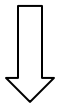

Excess liquid was carefully removed from each slide using a paper towel
The microscope slides were carefully dried at room temperature avoiding dust and other particles and then stored in a sealed container until the day of image analysis

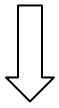

The dried microscope slides were stained with ethidium bromide in water (20µg/ml; 50µl/slide)

Assessment:

The slides with a cover slip were examined at 400X magnification under fluorescence microscope with green filter and photomicrographs of cell were taken. 150-200 randomly selected cells in each slide were counted (4 slides/ animals in each group). The damaged cell (%) was calculated using the following formula:

$$\%\ \text{Cell with damaged DNA} = \frac{\text{Number of damaged cells}}{\text{Total number of cells counted}} \times 100$$

Average tail length due to DNA migration in each group. The parameters analyzed for detection of DNA damage were damaged cell (%) in each group, tail DNA (%), tail length [migration of the DNA from the nucleus (lm)], and Olive tail moment [product of tail length and the fraction of total DNA in the tail (arbitrary units)].

- **Assay of chromosomal aberration**

This assay is a valuable technique for evaluation of damage to chromosomes on the basis of direct observation and classification of chromosomal aberrations. Slides for study of chromosomal aberrations (CA) were prepared from bone marrow cells by the conventional flame drying technique **(Biswas et al, 2004)**.

Reagents required

0.03% colchicines, 1% sodium citrate, Giemsa stain.

Procedure

Mice were injected intraperitoneally with 0.03 % colchicine at the rate of 1 ml/100 g b.w. 90 minutes before sacrifice.

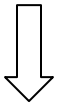

Bone marrow cells were collected from the femur by flushing with warm (37°C) sodium citrate (1%) solution using a hypodermic syringe. Cells were then carefully aspirated to make a suspension.

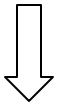

The material was then centrifuged at 2000 rpm for 10 minutes.

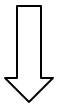

Cell pellet was fixed in acetic acid/ethanol (1:3) and kept for 15 minutes.

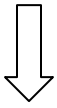

The cell suspension was again centrifuged at 2000 rpm for 15 minutes.

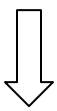

Cell pellet was collected and resuspended in a small volume of fixative (1:3 acetic acid/alcohol) by gentle flushing until a cloudy suspension resulted.

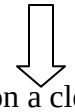

The cell suspension was then dropped on a clean slide chilled for one day in 50% ethanol

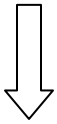

Slides were then burnt on a flame for a while, air dried.

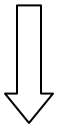

On the next day slides were stained with Giemsa.

Assessment

Slides were analyzed a light microscope (Leica DM 1000). Photomicrographs were taken with the software Las EZ. CA of various natures like stretching, terminal association, break, fragment, ring formation etc. were analyzed. A total of 300 bone marrow cells were observed, 50 from each of 6 mice of a set.

- **Histopathology (Bancroft et al, 1990; Lillie et al, 1976)**

Histopathological evaluation of various organs was done by conventional hematoxylin-eosin staining method details of which have already been mentioned in Dose selection study.

Statistical analysis

All data were presented as mean ± SD. n = 6 animals per group. One way ANOVA followed by Tukey's Multiple Comparison Test using Graph Pad Prism software was performed for comparisons among groups. Significant difference was indicated when the *P* value was < 0.05.

Results

- **Body weight**

Oral administration of inorganic (Gr. II) and organic selenium (Gr. III) at the dose of 2 mg Se/kg b.w. decreased body weight significantly by 22.13% and 6.32% respectively, in comparison to the vehicle control group (Gr. I), where as oral administration of Nano-Se (Gr. IV) at the same dose *i.e.*, 2 mg Se/kg b.w. increased body weight significantly by 9.32%.

- **LPO level**

Oral administration of inorganic selenium compound (Gr. II) significantly ($P < 0.05$) elevated LPO level by 200% in liver and by 265.2% in kidney and by 114.77% in lungs, compared to the vehicle treated group (Gr. I) **Fig. 6**. A further significant elevation in LPO level in liver, kidney and lungs were observed after administration of organic selenium compound. Whereas chronic administration of Nano-Se at the dose of 2 mg Se/kg b.w. negligible elevation of LPO level ($P < 0.05$) compared to the vehicle treated group (Gr. I).

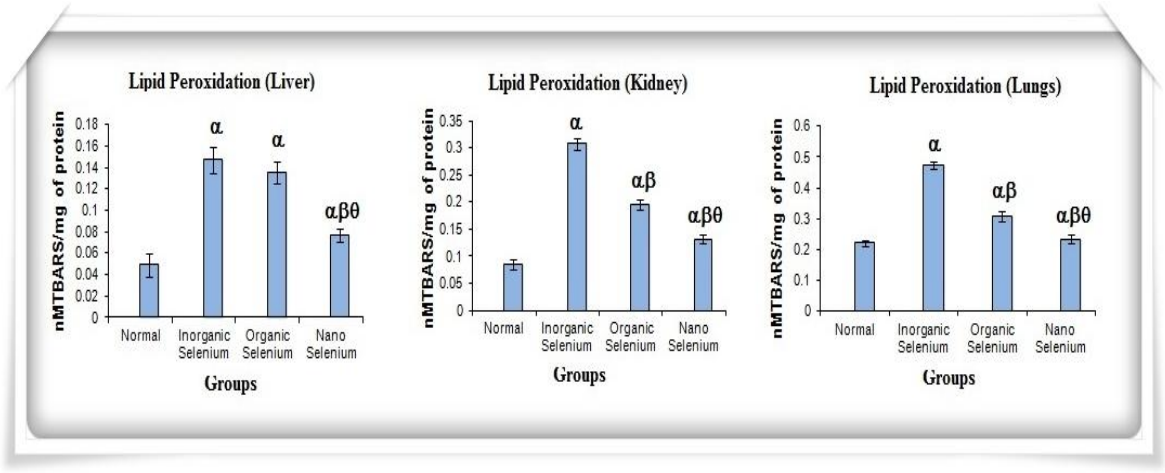

Figure 6: Data were represented as mean ± SD, n=6. α - significant *(P<0.05)* as compared with Normal; β - significant *(P<0.05)* as compared with Inorganic selenium; θ - significant *(P<0.05)* as compared with Organic selenium.

- **GSH level**

The GSH content was found to incline by 4.17% and 8.57% in liver after treating with inorganic and organic selenium compound respectively, compared to the vehicle treated group (Gr. I), yet this elevation is not significant **Fig. 7**. Whereas, oral administration of Nano-Se resulted in a significant ($P < 0.05$) elevation of GSH content by 65.24% as compared to the vehicle treated group (Gr. I).

- **GST activity**

Chronic oral administration of inorganic and organic form of selenium compound enhances the hepatic GST activity by 2.45% and 5.78% respectively, compared to the vehicle treated group (Gr. I) **Fig. 7**. When the same dose of Nano-Se in same duration administered caused a significant ($P < 0.05$) increment of GST activity by 23.49%, as compared to the vehicle treated group (Gr. I).

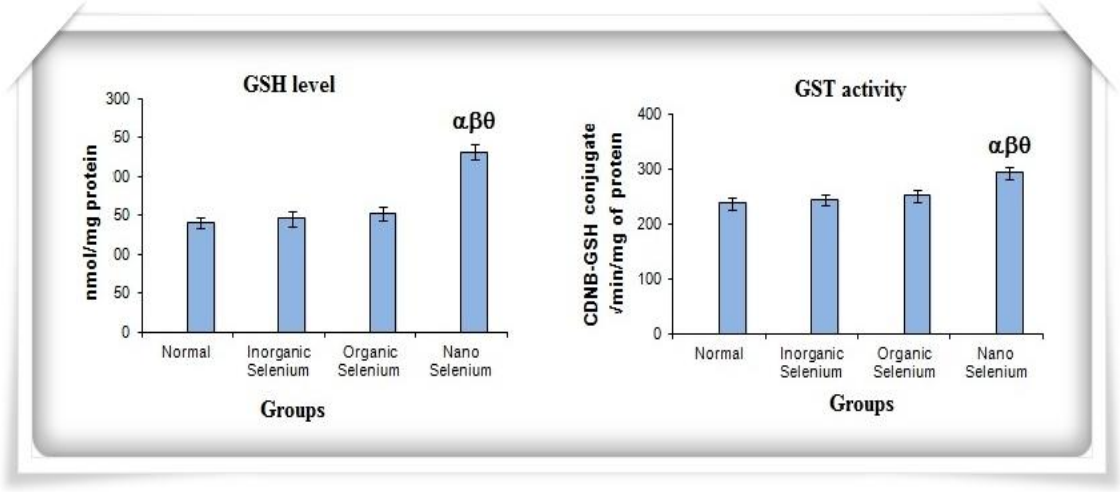

Figure 7: Data were represented as mean ± SD, n=6. α - significant *(P<0.05)* as compared with Normal; β - significant *(P<0.05)* as compared with Inorganic selenium; θ - significant *(P<0.05)* as compared with Organic selenium.

- **SOD activity**

The hepatic SOD activity increased significantly ($P < 0.05$) by 16.04% after oral administration of organic selenium compound compared to the vehicle treated group (Gr. I) **Fig. 8**. SOD activity was numerically increased when treated with inorganic selenium but that was not statistically significant ($P > 0.05$) as compared with the vehicle control group. At the dose of 2 mg Se/kg b.w. oral administration of Nano-Se resulted in a significant ($P < 0.05$) elevation of SOD activity by 46.5%, in comparison to the vehicle control group.

- **CAT activity**

The hepatic CAT activity was found to increase by 12.5% and 16.6% in liver after treating with inorganic and organic selenium compound respectively, compared to the vehicle treated group (Gr. I), yet this elevation is not significant ($P > 0.05$) **Fig. 8**. Whereas, oral administration of Nano-Se resulted in a significant ($P < 0.05$) elevation of CAT content by 33.87% as compared to the vehicle treated group (Gr. I).

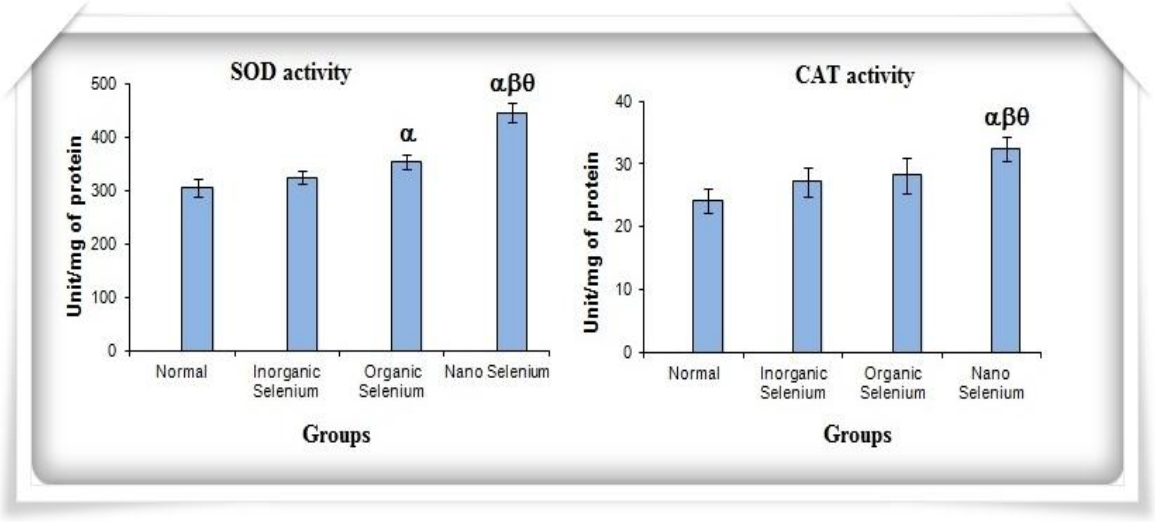

Figure 8: Data were represented as mean ± SD, n=6. α - significant *(P<0.05)* as compared with Normal; β - significant *(P<0.05)* as compared with Inorganic selenium; θ - significant *(P<0.05)* as compared with Organic selenium.

- **GP*x* activity**

Chronic oral administration of inorganic and organic form of selenium compound enhances the hepatic GP*x* activity by 3.6% and 15% respectively, compared to the vehicle treated group (Gr. I) **Fig. 9**. Whereas, oral administration of Nano-Se resulted in a significant ($P < 0.05$) elevation of GP*x* activity by 22.29% as compared to the vehicle treated group (Gr. I).

- **TrxR activity**

The TrxR activity was found to incline by 10.65% and 24.69% in liver after treating with inorganic and organic selenium compound respectively, compared to the vehicle treated group (Gr. I) **Fig. 9**. Whereas, oral administration of Nano-Se resulted in a significant ($P < 0.05$) elevation of TrxR activity by 37.53% as compared to the vehicle treated group (Gr. I).

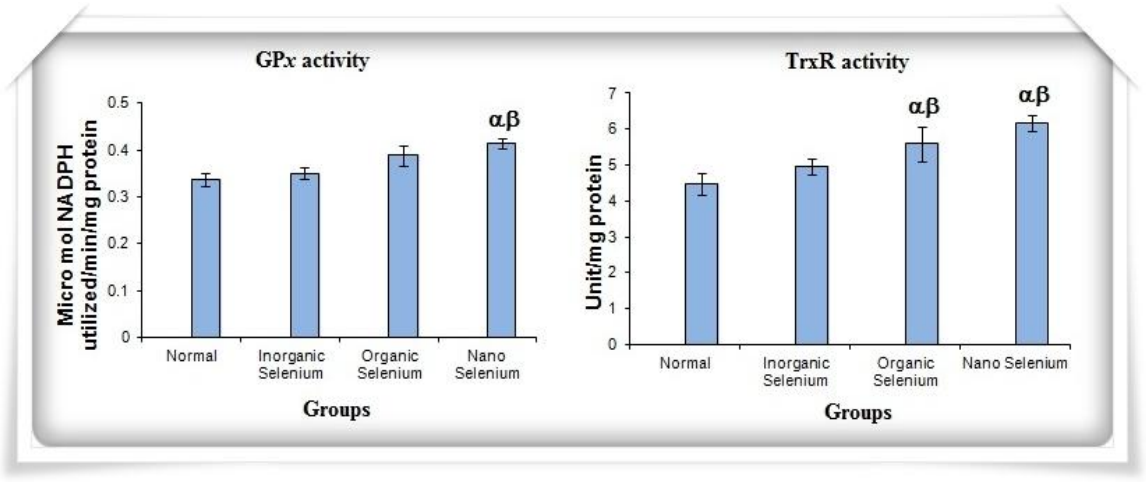

Figure 9: Data were represented as mean ± SD, n=6. α - significant *(P<0.05)* as compared with Normal; β - significant *(P<0.05)* as compared with Inorganic selenium; θ - significant *(P<0.05)* as compared with Organic selenium.

- **Serum ALT, AST and ALP activity**

The serum ALT, AST and ALP activity was increased significantly (*P < 0.05*) by 77.21%, 113.13% and 57.65% respectively, in inorganic selenium treated group (Gr. II) and by 57.59%, 48.72% and 35.78% respectively, in organic selenium compound treated group (Gr. III)) in comparison to the vehicle treated group (Gr. I). At the dose of 2 mg Se/kg b.w. oral administration of Nano-Se resulted in a non-significant (*P* > 0.05) elevation of serum ALT, AST and ALP activity by 10.12%, 9.74% and 5.28% respectively, in comparison to the vehicle control group **(Table 1)**.

Groups	ALT (IU/L)	AST (IU/L)	ALP (IU/L)
Vehicle control (Gr. I)	31.6 ± 3.28	94.4 ± 6.38	56.20 ± 3.15
Inorganic Selenium (Gr. II)	$56 \pm 3.74^{\alpha}$	$201.2 \pm 7.69^{\alpha}$	$88.61 \pm 3.27^{\alpha}$
Organic Selenium (Gr. III)	$49.8 \pm 3.63^{\alpha\beta}$	$140.4 \pm 6.54^{\alpha\beta}$	$76.32 \pm 3.14^{\alpha\beta}$
Nano-Se (Gr. IV)	$34.8 \pm 2.28^{\beta\theta}$	$103.6 \pm 7.12^{\beta\theta}$	$59.17 \pm 4.59^{\beta\theta}$

Table 1: Data were represented as mean ± SD, n=6. α - significant *(P<0.05)* as compared with Normal; β - significant *(P<0.05)* as compared with Inorganic selenium; θ - significant *(P<0.05)* as compared with Organic selenium.

- **Serum BUN and creatinine**

Renal functions were impaired as illustrated by considerable increase in BUN and creatinine levels. BUN and creatinine levels were significantly *(P < 0.05)* raised by 109.7% and 375.97% respectively, in inorganic selenium treated group (Gr. II) and by 36.69% and by 326.42% respectively, in organic selenium compound treated group (Gr. III)) in comparison to the vehicle treated group (Gr. I). These two levels was numerically

increased when treated with Nano-Se but that was not statistically significant (*P > 0.05*) as compared with the vehicle control group **(Table 2)**.

Groups	BUN (mg/dl)	Creatinine (mg/dl)
Vehicle control (Gr. I)	10.45 ± 0.21	0.40 ± 0.03
Inorganic Selenium (Gr. II)	$16.63 \pm 0.41^{\alpha}$	$1.95 \pm 0.07^{\alpha}$
Organic Selenium (Gr. III)	$12.52 \pm 0.40^{\alpha\beta}$	$1.74 \pm 0.04^{\alpha\beta}$
Nano-Se (Gr. IV)	$8.47 \pm 0.24^{\beta\theta}$	$0.45 \pm 0.02^{\beta\theta}$

Table 2: Data were represented as mean ± SD, n=6. α - significant *(P<0.05)* as compared with Normal; β - significant *(P<0.05)* as compared with Inorganic selenium; θ - significant *(P<0.05)* as compared with Organic selenium.

- **Hematological parameters and bone marrow and spleen cellularity**

The hemoglobin level in blood decreased significantly by 8.58% in inorganic selenium treated group (Gr. II) in comparison to the vehicle treated group (Gr. I)**.** In organic selenium treated group (Gr. III) hemoglobin level in blood also decreased significantly by 6.60% in comparison to the vehicle treated group (Gr. I)**.** Nano-Se at the dose of 2 mg Se/kg b.w. (Gr. IV) hemoglobin level increased in blood significantly (*P* < 0.05) by 7.92% in comparison to the vehicle treated group (Gr. I)**.**

The exposure of inorganic selenium resulted in a significant (*P > 0.05*) decline in RBC and WBC counts. In addition to this, bone marrow as well as splenic cell counts also decreased significantly (*P < 0.05*) after chronic administration of inorganic as well organic selenium. This decreased cell counts in both the primary and secondary immune organs were significantly (*P < 0.05*) prevented on oral administration of Nano-Se in prolonged treatment **(Table 3)**.

Groups	Hb (gm/dl)	RBC (10^6/mm^3)	WBC (10^6/mm^3)	Splenic Cell ($\times10^6$)	Thymus Cell ($\times10^6$)	Bone Marrow cell ($\times10^6$)
Vehicle control (Gr. I)	12.12 ± 0.60	6.96 ± 0.40	6.66 ± 0.37	66.31 ± 2.83	62.51 ± 3.24	26.16 ± 2.25
organic Selenium (Gr. II)	11.08 ± 0.72	6.14 ± 1.09	7.19 ± 0.41	$54.23 \pm 4.30^{\alpha}$	62.04 ± 2.75	23.56 ± 1.92
rganic Selenium (Gr. III)	11.32 ± 0.96	6.95 ± 0.32	7.05 ± 0.59	$63.69 \pm 3.64^{\beta}$	65.87 ± 2.44	26.01 ± 2.26
Nano-Se (Gr. IV)	$13.08 \pm 0.38^{\beta\theta}$	$7.44 \pm 0.69^{\beta}$	$7.73 \pm 0.51^{\alpha}$	$84.64 \pm 4.90^{\alpha\beta\theta}$	$74.87 \pm 3.93^{\alpha\beta\theta}$	$32.23 \pm 2.43^{\alpha\beta\theta}$

Table 3: Data were represented as mean ± SD, n=6. α - significant *(P<0.05)* as compared with Normal; β - significant *(P<0.05)* as compared with Inorganic selenium; θ - significant *(P<0.05)* as compared with Organic selenium.

- **Comet assay findings**

Comet assay was carried out to examine the selenium induced DNA damage in bone marrow **(Fig. 10)** and for this purpose percentage of damaged cells and the average tail length was measured.

Percentage of damaged cells in each group

The frequency of damaged bone marrow was 9.10% in Gr. I **(Table 4)**. An inorganic and organic selenium compound administration caused a significant ($P < 0.05$) increase in the percentage of bone marrow cells by 19.41% and 16.52% respectively in Gr. II and in Gr III. In case of Nano-se treated group (Gr. IV), the percentages of damaged bone marrow cells was increased to 10.78%, yet this elevation is not significant *($P > 0.05$).*

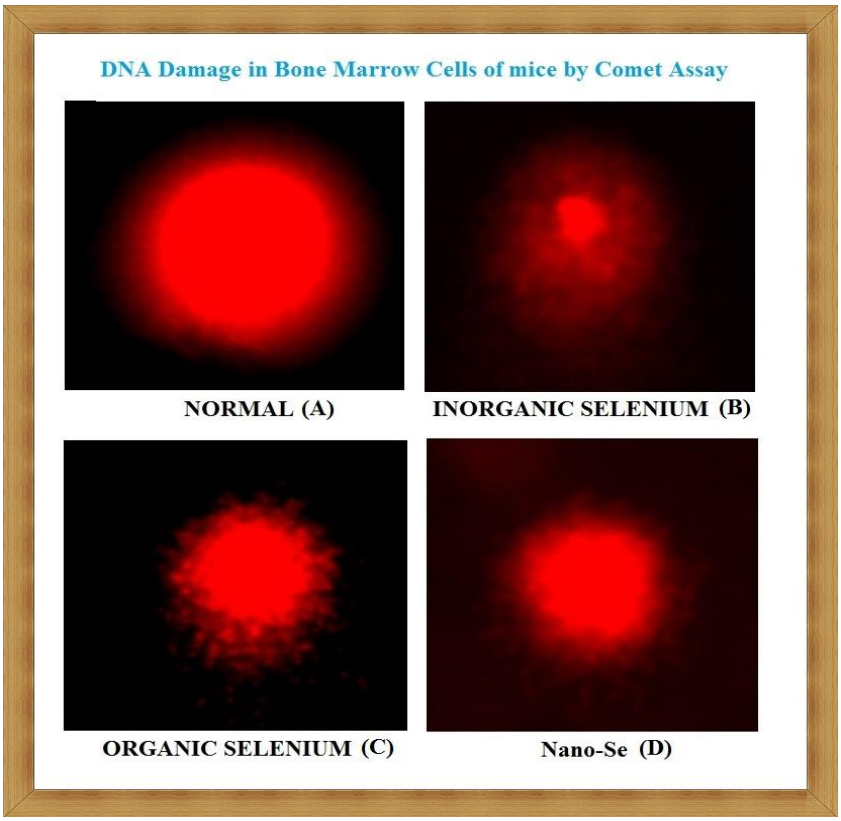

Figure 10: Microphotograph of bone marrow: (A) vehicle treated (no DNA damage), (B) Inorganic Selenium treated fewer DNA migrations (C) Organic Selenium treated showing slightly migrated DNA with scattered comet tail, (D) Nano-Se treatment (less or very fewer migrated DNA]

Average Tail Length due to DNA Migration in each group

The magnitudes of average tail length was 7.89 ± 0.86 µm in bone marrow cells in Gr. I. Inorganic selenium compound caused a marked increase in the magnitude of tail length to 20.23 ± 1.75 µm in bone marrow cells in Gr. III (**Table 4**). Oral administration of organic selenium compound and Nano-Se resulted in the induction of average tail length to 18.34 ± 2.24 µm and 8.97 ± 1.51 µm respectively.

Groups	Bone Marrow Cell	
	Damaged cells showing comet (%)	Average tail length (µm)
Vehicle control (Gr. I)	9.10 ± 0.81	7.89 ± 0.86
Inorganic Selenium (Gr. II)	$19.4 \pm 1.69^{\alpha}$	$20.23 \pm 1.75^{\alpha}$
Organic Selenium (Gr. III)	$16.5 \pm 1.20^{\alpha\beta}$	$18.34 \pm 2.24^{\alpha}$
Nano-Se (Gr. IV)	$10.7 \pm 1.55^{\alpha\beta\theta}$	$8.97 \pm 1.51^{\beta\theta}$

Table 4: Data were represented as mean ± SD, n=6. α - significant *(P<0.05)* as compared with Normal; β - significant *(P<0.05)* as compared with Inorganic selenium; θ - significant *(P<0.05)* as compared with Organic selenium.

- **Chromosomal aberrations**

The magnitude of chromosomal aberrations was estimated to be 14.17% in vehicle treated group (Gr. I). Due to the administration of inorganic selenium compound (Gr. II), the proportion of CA was raised significantly ($P < 0.05$) to 26.06%. But when treated with Nano-Se CA was increased numerically in comparison to the vehicle control animals but this increment is not statistically significant ($P > 0.05$) **Fig. 11**.

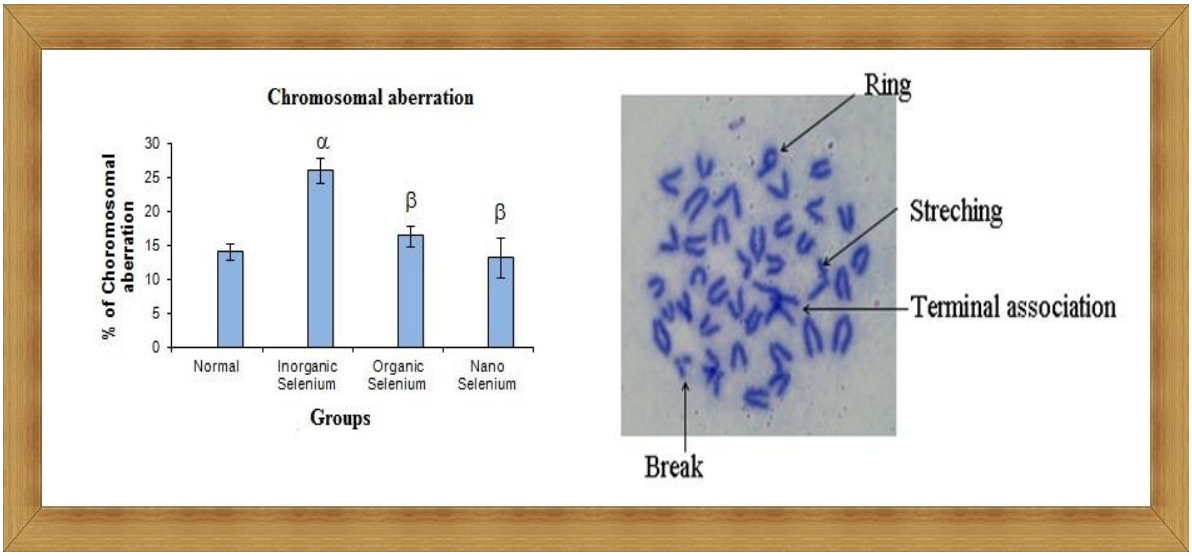

Figure 11: Data were represented as mean ± SD, n=6. α - significant *(P<0.05)* as compared with Normal; β - significant *(P<0.05)* as compared with Inorganic selenium; θ - significant *(P<0.05)* as compared with Organic selenium.

Metaphase complements showing stretching (STR), and Ring formation (R), Break (B) and Terminal association.

- **Histopathology**

Histology of liver, kidney and lung from different groups of mice has been shown in **Fig. 12.** Histopahtological examination of selected organs from both and vehicle control and Nano-Se treated animals showed normal architecture, suggesting no detrimental changes or morphological disturbances resulted from the administration of Nano-Se for 30 days. The overall cellular structure remains unaltered with no necrosis, inflammation or other significant lesion. Whereas inorganic selenium supplementation resulted in infiltration of mononuclear cells in both liver and kidney tissues.

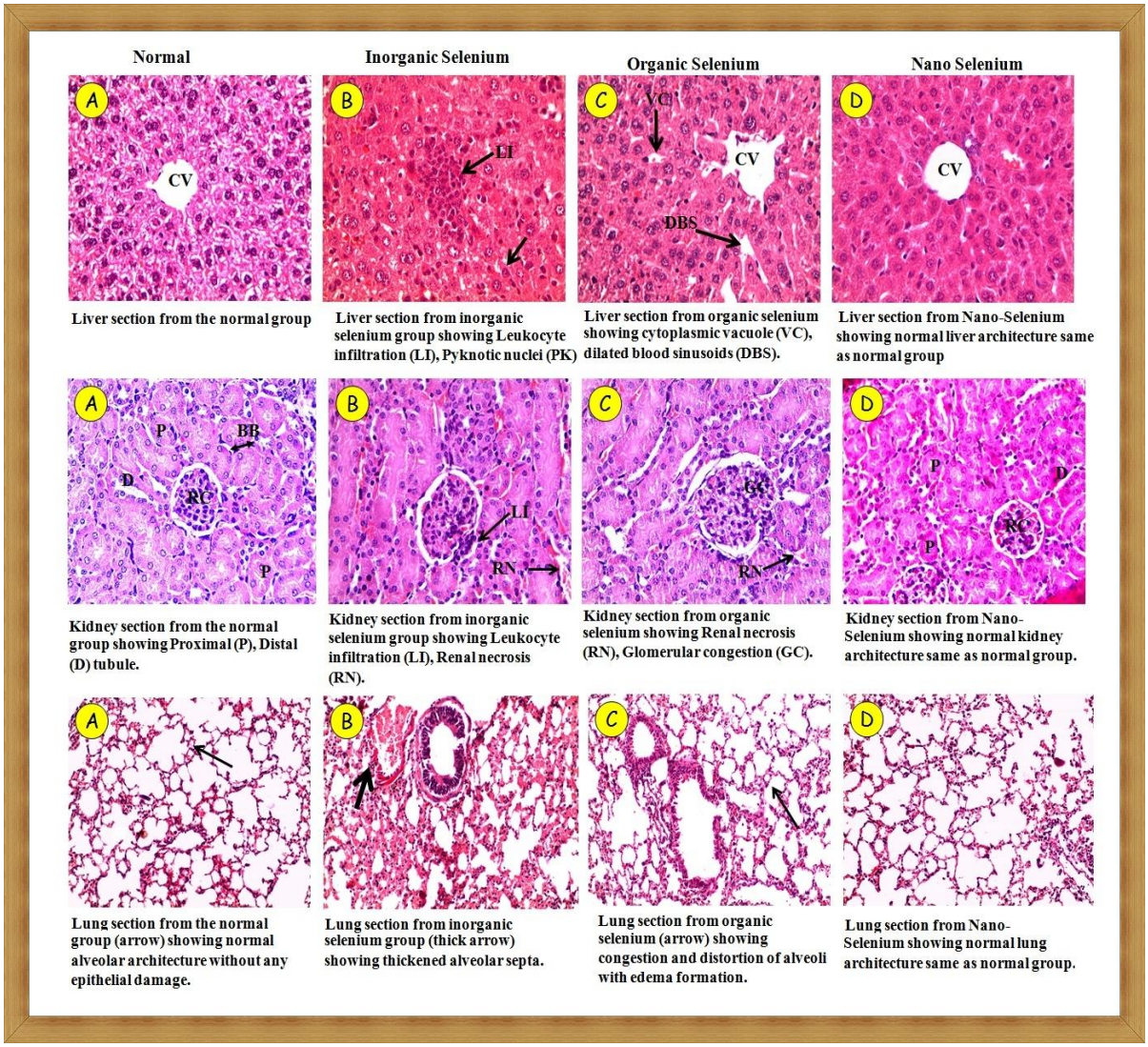

Figure 12: Photograph of liver, kidney and lungs section of mice stained with hematoxylin and eosin, ×200

Discussion:

The objective of this study is to synthesize a non toxic form of selenium which has efficient protective activity. Because of the very narrow range between the toxic dose and the adequate dose for the organism, not only the dose volume but also the form of Se supplemented is evenly important. Compared with inorganic and organic form of selenium, one of the most noticeable features of this comparative study is that Nano-Se has lower toxicity and possesses equal efficacy in increasing the activities of seleno enzymes.

Se compounds show cancer chemopreventive property at doses which are much higher than the nutritional requirement. Due to toxicity of selenium at high doses, Se compounds have limited doses used in chemoprevention study. Literature survey reveals that most of the experimental works for evaluation of Se as cancer chemopreventive agent were carried out using inorganic Se and organic Se compounds as the Se source **(Hosnedlova et al., 2018)**. Studies also indicated that inorganic and organic Se compounds have been found to be toxic due to their pro-oxidant ability to catalyze the oxidation of thiols and simultaneous generation of superoxide ($O_2^{\bullet-}$) that can damage cellular components **(Wang et al., 2007)**. Therefore, there has been a growing interest in the synthesis of less toxic form of selenium and could be used as antioxidants, enzyme inhibitors, neuroprotective, anti-infectious and cancer chemopreventive agents and immunomodulators.

Se intoxication has been extensively studied in animals. Growth retardation has long been known to be a major characteristic in selenium-intoxicated animals. Se causes growth retardation through reduction in growth hormone and somatomedin C production **(Thorlacius-Ussing, 1990)**. The U.S. National Research Council concluded in 1976 that growth inhibition might be the best indicator of toxic effects from selenium **(Ørskov and Flyvbjerg, 2000)**. In the present study, we found that there has been no significant decrease in body weight amongst Nano-Se treated group and daily food intake was normal and there was no diarrhea or excessive salivation. These observations together with the no loss in the body weight indicated that Nano-Se had no negative effects on the growth of mice.

Animal studies have demonstrated that the liver is the major target organ of Se toxicity **(Poole et al., 2017)**. In the present study, we found both inorganic and organic selenium compound caused liver injury, but inorganic selenium compound was more potent as evidenced by serum levels of ALT, AST and ALP and the changes of liver architecture. Generally high levels of transaminases such as ALT, AST and ALP are good indication of hepatic damage **(Basu et al., 2015)**. LPO is also used as biomarker to show the index of oxidative stress and causes cell membrane damage resulting in gradual loss of membrane fluidity, decrease membrane potential and increased permeability to ions **(Basu et al., 2016)**. Both inorganic and organic selenium forms caused MDA increase, but its accumulation and duration in liver tissues of inorganic selenium treated mice was higher and longer than that for Nano-Se. Same observation was also found in kidney and lungs tissues. Blood urea nitrogen (BUN) measures the amount of urea nitrogen, a waste product of protein metabolism, in the blood and creatinine is chiefly filtered out of the blood by the kidneys. If the filtering of the kidney is deficient, blood levels rise. In the present study nephrotoxicity markers BUN and creatinine showed significant increase in inorganic and organic selenium treated group. Hence, it is clear that Nano-Se have no adverse effect on kidney function.

Reactive oxygen species (ROS) such as superoxide anion or hydroxy radicals are known to destroy key biological components and cause damage to cell membranes. These reactive species are involved in the initiation, propagation and maintenance of both acute and chronic inflammatory processes **(Halliwell et al., 1982)**. There is a requirement for cellular defense against reactive oxygen species to protect cell membranes and other cellular component fromoxidative damage and living organisms have evolved a number of defense mechanisms to cope with this oxidative stress. Oxygen handling cells have antioxidant and detoxifying enzymes (GST, GP*x*, SOD, CAT, TrxR) which are the first line of cellular defense against oxidative injury, decomposing O_2 and H_2O_2 before they interact to form more reactive hydroxide radicals, SOD mainly act by quenching of superoxide and active oxygen free radical, produced in different aerobic metabolism **(Khan et al., 2017)**. GP*x* is the first mammalian enzyme characterized which contains the unusual amino acid selenocysteine in its catalytic center **(Snider et al., 2013)**. The role of the enzyme glutathione peroxidase is to reduce hydrogen peroxide via its selenocysteine

containing active site, selenol, through a redox cycle in which two equivalents of glutathione are oxidized to the disulfide and water, while the hydroperoxide is reduced to the corresponding alcohol **(Lubos et al., 2011)**. Another selenoenzyme, TRxR, which exerts its antioxidant action through catalyzing the reduction of oxidized thioredoxin by using NADPH as the electron donor. It is a key enzyme in Se metabolism, reducing Se compounds and thereby providing selenide to synthesis of all selenoproteins. Additionally, TrxR possesses a number of other antioxidant functions and directly scavenging lipid peroxides and hydrogen peroxide **(Ren et al., 2017)**. Nano-Se was found to be efficient enhancer of host antioxidant defense system such as SOD, CAT, GST, GSH, GP*x,* and TRxR. GP*x* and TRxR level were also increased when treated with inorganic and organic selenium compound but the increment was not that much as it was observed in case of Nano-Se.

Development of total chromosomal aberrations (CA) has often been used as sensitive biological indicator in the mutagenic bioassays of a drug **(Leme et al., 2008)**. In this present study no marked chromosomal aberration was observed when treated with Nano-Se with respect to the vehicle control group which supports the non mutagenic character of Nano-Se.

The organ sparing property of Nano-Se is also confirmed by histological assessment. Histopathological examination of selected organs (liver, kidney and lungs) from Nano-Se treated animals showed normal architecture, suggesting no detrimental changes or morphological disturbances. The overall cellular structure remains unaltered with no necrosis, inflammation or other significant lesion. Where as inorganic and organic selenium compound supplementation resulted in infiltration of mononuclear cells in liver and kidney and in lungs pulmonary congestion, pulmonary inflammation, thickened alveolar septa, and distortion of alveoli were observed.

In summary, based on chemoprevention-related responses in animals, as compared with inorganic as well as organic selenium compound, Nano-Se possesses much more efficacy and ability to modulate the antioxidative defense system by modulating the antioxidant enzyme levels especially GP*x* and TRxR., but has much lower toxicity, suggesting that Nano-Se can serve as a potential chemopreventive agent with significantly reduced risk of selenium toxicity.

Chapter II

Protective effect of Nano-Se against the toxicities induced by a cancer chemotherapeutic agent cyclophosphamide in Swiss albino mice

Introduction

Cancer chemotherapy is an integral part of modern day treatment regimen, but anticancer drugs fail to demarcate between cancerous and normal cells thereby causing severe form of systemic toxicity to multiple organ. These adverse effects affect the quality of life of cancer patients **(Sarkar et al., 2006)**. Cyclophosphamide (CP) is a well-known bi-functional alkylating agent widely used in cancer chemotherapy and in organ transplantation as an immunosuppressant **(Rehman et al., 2012)**. According to the International Agency for Research on Cancer (IARC), CP is widely used as reference mutagen and has been classified as carcinogenic for both animals and humans **(IARC, 2012)**. It shows no activity against cancer cells *in vitro* until it undergoes metabolic activation catalyzed by liver cytochrome P450 enzymes **(Wang et al., 2007)**, to produce reactive metabolites such as 4-hydroxy-CP, acrolein, and phosphoramide mustard. These metabolites can alkylate nucleophilic sites in DNA, RNA, and protein such as –SH, –COOH, $–NH_2$ which cause cellular toxicity, genotoxicity, and mutagenic effects (**Ponticelli, 1991)**. Acrolein, a toxic metabolite of CP, is responsible for chemically alkylation of DNA as well as protein, producing cross-links and thereby inducing cytotoxicity **(Nafees et al., 2012)**. Acrolein interferes with the tissue antioxidant defense system **(Arumugam, 1997)**, produces high amount of reactive oxygen free radicals and is mutagenic to mammalian cells **(Mythili et al, 2004)**. However, despite the fact that its use causes severe cytotoxicity to normal cells in experimental animals and humans **(Gokhale et al., 2003)**, clinicians prescribe it as the first line of treatment for the cancer patients. CP produces carbonium ions that react with the electron-rich centres of nucleic acids and proteins. It is known to cause mutations, DNA damage, micronuclei induction as well as the production of reactive oxygen species (ROS). The high reactivity of free radicals causes cellular damage through various mechanisms **(Nafees et al., 2012)**.

Experimental evidence suggests that the development of oxidative stress after CP administration leads to decrease in the activities of antioxidant enzymes and increase in the level of lipid peroxidation (LPO) in liver and lungs of mice **(Basu et al., 2014)**.

In view of the drawbacks of chemotherapeutic agents, there is a critical need to develop new treatment strategies that minimize or antagonize the toxicity of CP which would protect the normal tissue from chemotherapy-induced toxicity without tumor protection and tumor growth stimulation properties.

Selenium (Se) is an essential micronutrient for higher animals and humans with well known antioxidant characteristics **(Darke, 2006)**. The best-known biological roles of selenium are linked to its presence as the functional component in selenoenzymes such as glutathione peroxidase (GPx) and thioredoxin reductase (TrxR). Se is involved in maintaining normal liver function, protein synthesis and protects against toxic minerals. Results of epidemiological, preclinical and clinical studies have shown Se decreases the risk of a series of cancers **(Gandin, 2015)**. Pharmacologically, consumption of 200µg Se per day by cancer patients reduces mortality and decreases the incidence of many diseases including lung, colorectal, and prostate cancers **(Pagmantidis et al., 2008)**. Studies suggest that low Se status may increase the risk of oxidative damage and cancer **(Rayman, 2000)**. The antioxidant and pro-oxidant effects of Se as well as its bioavailability and toxicity depend on its chemical form **(El-Bayoumy and Sinha, 2004)**. In spite of that, the use of inorganic Se (sodium selenite) as well as naturally occurring Se (such as selenomethionine and selenocystein) is often restricted due to its toxic effects **(Ip C, 1998; Narajji et al., 2007)**. The toxicity of selenium is now mainly thought to be mediated through its pro-oxidant capability to catalyze the oxidation of thiols and simultaneous generation of superoxide ($O^{\bullet -}$) that can damage cellular components **(Spallholz, 1994)**.

In this regard, nanotechnology based nanoparticles provides the extensive awareness of applied science and technology to organize the matter on the atomic and molecular scale **(Prathna et al., 2011)**. Due to their unique physical and chemical properties, nanomaterials have become the focus of many research areas such as applied physics and chemistry, mechanical engineering, electrical engineering, industrial applications and environmental investigations. Various nanoparticles, such as titanium oxide, silver, gold,

cadmium selenide and carbon nanoparticles are already being used in catalysis, stain-resistant clothing, sunscreens, cosmetics, and electronics **(Jeevanandam et al., 2018)**. A selenium nanoparticle (Nano-Se) is drawing wide attention due to their excellent bioavailability, broad range of biological activity, excellent anticancer activities and low toxicity **(Zhang et al., 2008)**. Nano-Se has a sevenfold lower acute toxicity than sodium selenite in mice (LD_{50} 113 and 15 mg Se/kg body weight, respectively) **(Clark et al., 1996)**. The toxicity reported for elemental selenium (Se^0) at nano size is lower than the toxicity of selenate (Se^{+2}) or selenite (Se^{+4}) ions; therefore, selenium nano particle (Nano-Se) may be a good candidate to replace other forms of selenium in nutritional supplements or pharmaceutical dosage forms **(Zhang et al., 2008)**.

The present study was undertaken to evaluate the chemoprotective potential of Nano-Se against CP induced toxicity in Swiss albino mice. To explore this aspect we studied the effect of Nano-Se in combination with CP on certain biochemical, hematological and genotoxic parameters.

Materials and methods

Experimental animals

Adult (5–6 weeks) Swiss albino female mice (25 ± 2g), bred in the animal colony of Chittaranjan National Cancer Institute (CNCI) (Kolkata, India), were used for this study. The mice were maintained under standard condition of humidity (45–55%), temperature (23 ± 2ºC), and light (12 h light/12 h dark). Standard food pellets (EPIC rat and mice pellet) from Kalyani Feed Milling Plant, Kalyani, West Bengal, India and drinking water was provided *ad libitum*. The experiments were carried out following strictly the Institute's guideline for the Care and Use of Laboratory Animals.

Chemicals

CP was obtained from Cadila Pharmaceuticals (Bhat, Ahmedabad, India). 1-Chloro-2, 4-dinitrobenzene (CDNB), ethylene diamine tetraacetic acid (EDTA), reduced glutathione (GSH), pyrogallol, 5,5´-dithio-bis (2-nitro benzoic acid) (DTNB), sodium dodecyl sulphate (SDS), bovine serum albumin (BSA), β-nicotinamide adenine dinucleotide phosphate (reduced), glutathione reductase, normal melting agarose, low melting point

agarose, ethidium bromide, sodium azide (NaN_3), HEPES, 2´,7´ - dichloro fluorescence diacetate (DCFH-DA), dihydroethidium (DHE), dimethyl sulphoxide (DMSO), vanadium chloride (VCl_3), phenylmethanesulfonyl fluoride (PMSF), Triton-X 100, Giemsa stain and acridine orange were obtained from Sigma-Aldrich Chemicals Private Limited, Bangalore, India. Hydrogen peroxide 30% (H_2O_2), thioberbituric acid (TBA), propylene glycol, sodium carbonate, copper sulfate, sodium hydroxide, potassium-sodium tartrate, sucrose, TRIS, dithiothreitol, calcium chloride, di-sodium hydrogen phosphate, sodium di-hydrogen phosphate, acetic acid, n-butanol, pyridine, hematoxylin, and eosin were obtai ned from Merck (India) Limited, Mumbai, India. Chloroform and Folin-phenol reagent were purchased from Sisco Research Laboratories Private Limited, Mumbai, India. Magnesium chloride was purchased from Glaxo laboratories (India) Ltd, Bombay. Diethyl ether, dipotassium hydrogen phosphate, and potassium dihydrogen phosphate were obtained from Spectrochem Private Limited, Mumbai, India. Serum alanine transaminas (ALT) and aspartate transaminase (AST) assay kits were obtained from Span Diagnostics Ltd, Udhna, Surat, India.

Experimental design

Experimental groups

Animals were distributed into five groups containing six animals (n=6) in each group. The day of beginning of CP administration was considered as day 1.

Vehicle treated group (Group I): Each animal was given oral administration of saline (0.9% NaCl) from day 1 to day 10.

Nano Selenium treated group (Group II): Animals were treated orally with Nano-Se only at a dose of 2 mg Se/kg b.w. throughout the experimental period.

CP-treated group (Group III): CP was administered intraperitoneally at a dose of 25 mg/kg b.w. in water for 10 days.

Concomitant treatment group (Group IV): Nano-Se was administered orally at a dose of 2 mg Se/kg b.w. for 10 days and CP was given as in Gr. III.

Pretreatment group (Group V): Nano-Se was administered orally at a dose of 2 mg Se/kg b.w. seven days prior to the CP treatment and then continued along with CP for 10 days.

The mice were sacrificed on day 11, 24 hours after the last treatment and the parameters described below were studied. The treatment schedule has been schematically presented in F**ig. 1**.

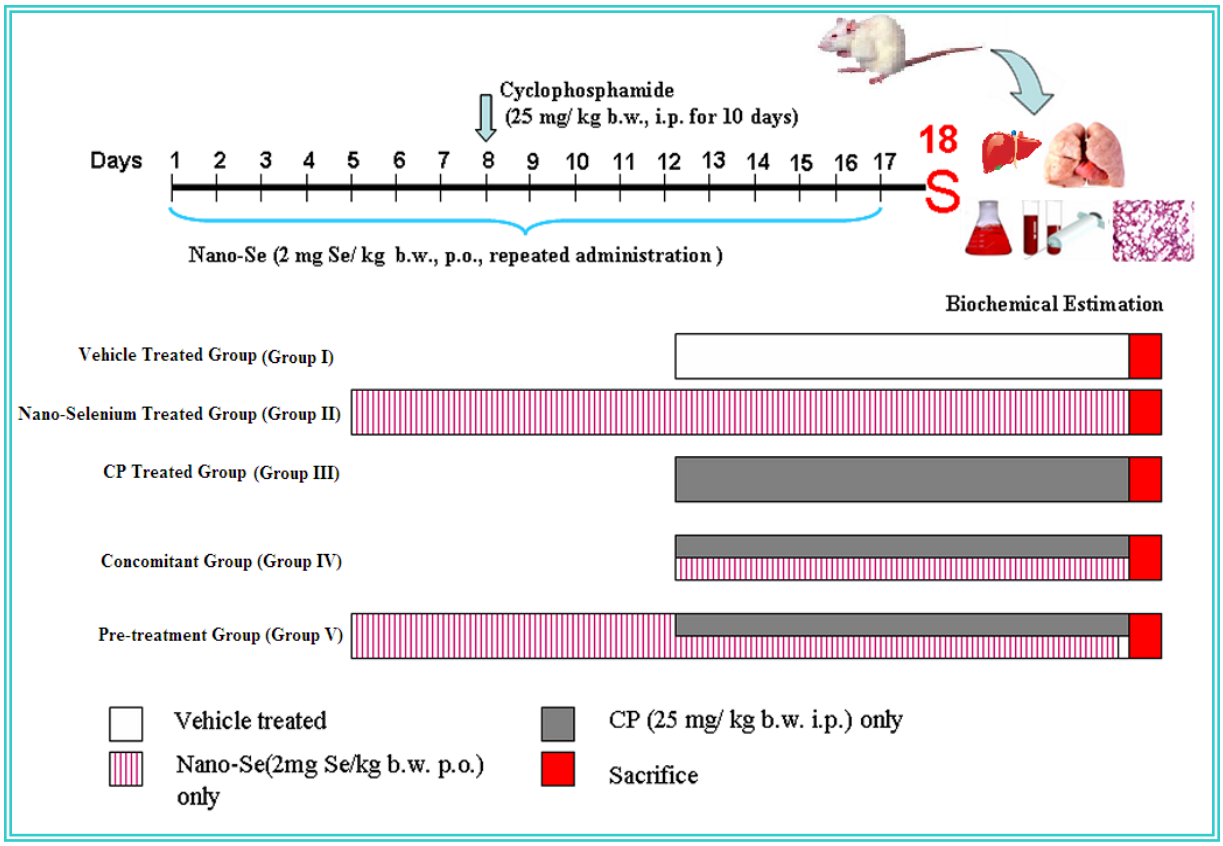

Figure 1: Treatment schedule

Parameter studied

Set A

It was designed for the assessment of the following parameters:

- Quantitative estimation microsomal lipid peroxidation level in liver and lung tissue sample.
- Biochemical estimation of reactive oxygen species levels in liver and lung tissue sample.
- Measurement of nitric oxide (NO) production in liver and lung tissue sample.

Set B

- Estimation of reduced glutathione (GSH) level and phase II detoxifying/antioxidant enzymes like glutathione-*S*-transferase (GST), glutathione peroxidase (GP*x*), catalase (CAT), and superoxide dismutase (SOD) activity in liver and lung tissue sample.
- Estimation of alanine transaminase (ALT) and aspartate transaminase (AST) activity in serum.
- Estimation of blood hemoglobin level, RBC and WBC count, bone marrow cell and spleen cell counts.

Set C

- Biochemical estimation of reactive oxygen species levels in bone marrow cells
- Detection of DNA damage in lymphocytes, broncho alveolar lavage fluid (BALF) and bone marrow by alkaline single cell gel electrophoresis (Comet Assay).
- The assay of important cytogenetic parameters like chromosome aberration (CA) in bone marrow cells.
- Determination of percentage of DNA fragmentation by diphenylamine (DPA assay) in bone marrow cells.
- Detection of apoptosis of bone marrow cells by using Acridine orange (AO)/ Ethidium bromide (EtBr).
- Histopathological evaluation of liver and lung tissue.

Methodologies

❖ **Biochemical parameters**

➢ **Estimation of protein content in tissue homogenate (Lowry et al, 1951)**

Total protein content in tissue homogenate during biochemical estimation was measured following Lowry method using Folin-Phenol reagent.

Reagents required

2% Na_2CO_3, 1% $CuSO_4$. $5H_2O$, 2% Sodium-potassium tartarate, 1N NaOH, 2% Folin-Phenol reagent and Bovine Serum Albumin (BSA).

Procedure

In microcentrifuge tubes 10 µl unknown tissue sample was added to 100 µl 1N NaOH.

⇩

10 µl 1% $CuSO_4$, 10 µl 2% sodium-potassium tartarate and 980 µl 2% Na_2CO_3 were then added in the reaction mixture and kept for 15 minutes.

⇩

Next, 300 µl Folin-Phenol reagent (v/v; 1:2 with water) was added and kept for 15 minutes in dark at room temperature.

⇩

Development of blue coloration.

⇩

For preparation of blank, all the reagents were used except the tissue sample which was replaced with distilled water.

⇩

The absorbance of the color was measured against the colorless blank sample at 660 nm using the Varian Cary 100 UV–Vis Spectrophotometer.

Assessment

A standard curve was prepared by measuring the absorbance of different known concentrations of BSA and the total protein concentration of the unknown sample was determined from the standard curve.

- **Quantitative estimation of lipid peroxidation (LPO) level (Okhawa et al., 1979)**

Spectrophotometric method was applied to estimate the level of LPO in liver and lung microsomes by measuring the formation of lipid peroxides using thiobarbituric acid (TBA) and was expressed as nmTBARS/mg protein.

Reagents required

Normal saline, 1.15% KCl, 8.1% SDS, 20% Acetic acid, 0.8% TBA, n-Butanol and pyridine.

Procedure

Estimation of thiobarbituric acid reactive substances (TBARS)

Liver and lung tissues of the experimental mice were collected after their sacrifice, washed in normal saline and 400 mg of liver and lung tissues were weighed.

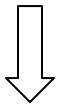

The tissues were then homogenized in 3.6 ml 1.15% KCl using a Teflon homogenizer.

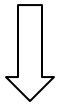

The homogenates were centrifuged at 12000 g for 10 minutes at 4^{o}C.

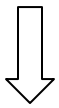

The supernatants (devoid of nuclear debris) were again centrifuged at 10000 g for 10 minutes at 4^{o}C.

The supernatants (devoid of mitochondria) were centrifuged for third time at 25000 g for 1 hour at 4^{o}C.

The precipitates (containing microsomal fraction) were suspended in 400 µl 1.15% KCl and the suspensions were used as sample for determining the LPO level.

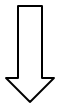

In test tubes 200 µl sample, 200 µl SDS, 1.5 ml acetic acid and 1.5 ml TBA were added along with 600 µl distilled water.

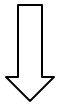

A blank sample was prepared following the same procedure using all the above mentioned reagents except distilled water in place of tissue sample.

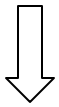

The reaction mixtures were then heated at 95°C in water bath for 1 hour.

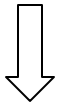

The reaction resulted in the development of pink coloration.

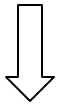

5 ml mixture of butanol and pyridine (15:1; v/v) was added to each sample and each sample was then vortexed thoroughly and centrifuged at 3000 g for 10 minutes.

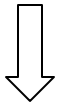

Absorbance of the upper pink colored organic layer was measured at 532 nm against the colorless blank sample using the Varian Cary 100 UV–Vis Spectrophotometer.

Assessment

Total protein concentration of each unknown sample was determined from the standard curve prepared by measuring the absorbance of different known concentrations of BSA. The level of LPO was expressed as nmol TBARS formed/mg protein using extinction co-efficient of 1.56×10^5 $M^{-1}cm^{-1}$ as follows:

Absorbance = Extinction coefficient × Concentration × Length (Beer-Lambert Law)

Now, Extinction co-efficient = 1.56×10^5 $M^{-1}cm^{-1}$

Length = 1cm

So, Concentration of TBARS = Absorbance/(1.56×10^5) M

= Absorbance × $10^9/(1.56 \times 10^5)$ nM

Hence, the level of LPO in 200 µl sample was expressed as:

$$\text{nmol TBARS/mg protein} = \frac{\text{Absorbance of TBARS at 532 nm} \times 2}{1.56 \times \text{Protein concentration (mg) in 200 µl sample}}$$

- **Estimation of ROS production**

ROS generation in liver and lung homogenate was measured spectrofluorimetrically with slight modifications using two probes, DCFH-DA and DHE.

- **DCFH-DA assay for determination of hydrogen peroxide level (Shinomol and Muralidhara, 2007):**

DCFH-DA is a nonfluorescent probe that is hydrolyzed by mitochondrial esterase to form 2',7'-dichlorodihydrofluorescein (DCFH), which is then oxidized by ROS to form the fluorescent compound 2',7'-dichlorofluorescein (DCF) which is measured spectrofluorimetrically (excitation 485 nm/emission 530 nm).

Reagents required

Locke's Buffer (pH 7.4 containing 140 mM NaCl, 5 mM KCl, 10 mM HEPES, 1 mM $CaCl_2$, 1 mM $MgCl_2$, 10 mM glucose), 10 µM DCFH-DA, PBS.

Procedure

Liver and lung tissues were collected from sacrificed mice, washed in normal saline and were then weighed (50 mg).

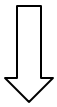

Tissues were then homogenized in 1 ml Locke's buffer.

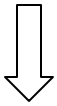

In test tubes 250 µl tissue homogenate in whole and 30 µl 10 µM DCFH-DA were added.

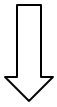

Locke's buffer was then added in the test tubes to make the total volume of the reaction mixture 3 ml.

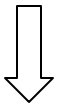

Test tubes were incubated in dark at 37°C for 45 minutes to allow formation of DCF.

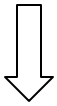

Samples were then analyzed for fluorescence (excitation 485 nm/emission 530 nm) using spectrofluorimeter (Varian Cary Eclipse).

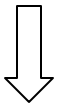

Values were expressed as fluorescence intensity/mg protein.

- **DHE assay for determination of superoxide level (Zou et al., 2001)**.

DHE is a non-fluorescent dye and freely permeable to the cell. Upon oxidation by superoxide anions (O^{2-}) forms the red fluorescent product ethidium which is measured spectrofluorimetrically (excitation 475 nm/emission 610 nm).

Reagents required

HEPES buffer (pH 7.4, containing 25 mM HEPES, 1 mM EDTA and 0.1 mM PMSF), 10µM DHE, PBS.

Procedure

Liver and lung tissues were collected from sacrificed mice, washed in normal saline and were then weighed (50 mg).

⇩

Tissues were then homogenized in 1 ml HEPES buffer.

⇩

In test tubes 150 µl tissue homogenate in whole and 30 µl 10 µM DHE were added.

⇩

HEPES buffer was then added in the test tubes to make the total volume of the reaction mixture 3 ml.

⇩

Test tubes were incubated in dark at 37°C for 30 minutes to allow formation of ethidium.

⇩

Samples were then analyzed for fluorescence (excitation 475 nm/emission 610 nm) using spectrofluorimeter (Varian Cary Eclipse).

⇩

Values were expressed as fluorescence intensity/mg protein.

- **Estimation of NO production (Green et al., 1982)**

Tissue nitrite (NO_2^-) was estimated as an index of NO production. NO_2^- is one of two primary, stable and nonvolatile breakdown products of NO. This assay was accomplished through diazotization reaction using Griess reagent system which includeed sulfanilamide and N-1-napthylethylenediamine dihydrochloride under acidic (phosphoric acid) conditions. Total NO_2^- levels in tissue homogenates were measured spectrophotometrically at 545 nm after the reduction of NO_3^- to NO_2^- by VCl_3.

Reagents required

PBS (pH 7.5), 0.3 (M) NaOH, 10% (w/v) $ZnSO_4$, VCl_3 (0.05 M), Griess reagent (1% sulphanilamide, 5% phosphoric acid, sodium nitrite ($NaNO_3$), 0.1% N-(1-naphthyl)ethylenediamine dihydrochloride (NEDD).

Procedure

Liver and lung tissues were collected from sacrificed mice, washed and weighed (200 mg).

⇩

Tissues were then homogenized in 1 ml PBS and centrifuged at 2000 g for 5 minutes at 4^oC.

⇩

500 µl supernatant and 250 µl 0.3 (M) NaOH were added in micro-centrifuge tubes.

⇩

The reaction mixture was then incubated at room temperature for 5 minutes.

⇩

250 µl 10% (w/v) $ZnSO_4$ was then added in the micro-centrifuge tubes and mixed well.

⇩

Reaction mixtures from each micro-centrifuge tubes were centrifuged at 14000 g for 5 minutes.

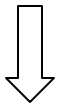

Supernatant was considered as sample.

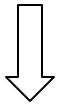

In microtitre plate 100 µl supernatant, 100 µl VCl_3 were added and then incubated at room temperature for 2 minutes.

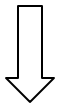

100 µl Griess reagent was added.

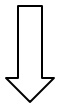

Incubation was done at room temperature for 5 minutes.

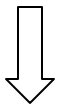

Absorbance was taken at 545 nm.

Calculation

A NO_2^- standard reference curve was prepared using 6 serial twofold dilutions of $NaNO_3$ (100, 50, 25, 12.5, 6.25, 3.13 and 1.56 µM). The absorbance of each concentration of the NO_2^- standard was plotted as a function of "Y" with nitrite concentration as a function of "X". After absorbance of each experimental sample was obtained, concentration of each sample was determined by comparison to the nitrite standard reference. Nitrite levels were expressed as micro mol/mg protein.

- **Estimation of reduced glutathione (GSH) level (Sedlack et al, 1968)**

Spectrophotometric method was used to evaluate the level of GSH in mouse liver and lung tissue samples. GSH level was measured in tissue cytosol by determination of DTNB reduced by – SH groups, as described by Sedlack and Lindsay and was expressed as nmol/mg protein.

Reagents required

Homogenizing buffer (pH 7.4; 250 mM sucrose, 20 mM Tris-HCl), 0.01 M DTNB dissolved in absolute methanol (prepared fresh before use), 0.4 M Tris buffer (pH 8.9), 0.02 M EDTA, TCA (50% w/v), standard glutathione (1 mg/ml).

Procedure

After sacrifice, 200 mg of liver and lung tissues were collected, washed with normal saline and were then homogenized in 5 volumes (1 ml) of homogenizing buffer, using a Teflon homogenizer.

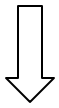

The homogenates were centrifuged at 35000g for 2 hours at 4^{o}C.

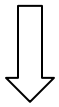

The supernatants (cytosolic fractions) were collected and used as samples for estimation.

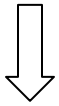

0.1 ml supernatant, 2.4 ml EDTA solution were added in test tubes and kept on ice for 10 minutes.

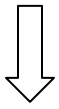

2 ml distilled water and 0.5 ml 50% TCA were then added in each test tube. The test tubes were kept on ice for 10-15 minutes and were then centrifuged at 3000 g for 15 minutes.

1 ml supernatant from each sample was taken, to which 2 ml Tris buffer was added. Then 0.05 ml DTNB solution (Ellman's reagent) was added and vortexed thoroughly. Instead of supernatant distilled water was used to prepare blank.

⇩

Optical density (OD) of each sample was taken (within 2-3 minutes after the addition of DTNB) at 412 nm using Varian Cary 100 UV–Vis Spectrophotometer against the blank. Standards were run simultaneously.

Assessment

Total protein concentration of the unknown sample was determined from the standard curve prepared by measuring the absorbance of different known concentrations of BSA. The GSH level was determined from the standard curve prepared by measuring the absorbance of different known concentrations of GSH and expressed as nmol/mg protein.

- **Estimation of glutathione-S-transferase (GST) activity (Habig et al, 1974)**

GST activity in liver and lung tissues was evaluated using spectrophotometric method. GST activity was measured in tissue cytosolic fractions by determining the increase in absorbance at 340 nm with CDNB as the substrate and the specific activity of the enzyme was expressed as formation of CDNB-GSH conjugate formed/minute/mg protein.

Reagents required

Homogenizing buffer (pH 7.4; 250 mM sucrose, 20 mM Tris-HCl & 1 mM DTT), 0.3 M phosphate buffer (pH 6.5; Na_2HPO_4 & NaH_2PO_4), 30 mM GSH and 30 mM CDNB.

Procedure

Estimation CDNB-GSH conjugates

After sacrifice, 200 mg of liver and lung tissues were collected, washed in normal saline and were then homogenized in 5 volumes (1 ml) of homogenizing buffer, using a Teflon homogenizer.

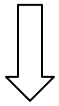

The homogenates were centrifuged at 35,000 g for 2 hours at 4^{o}C.

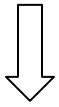

The supernatants (cytosolic fraction) were collected and used as samples for estimation.

In test tubes 1 ml 0.3M phosphate buffer, 100 µl CDNB and 100 µl sample were added. A blank sample was prepared as above using distilled water instead of tissue sample.

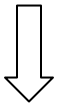

1.7 ml distilled water was then added in each test tube.

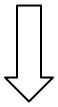

Test tubes were then kept at 30°C for 5 minutes.

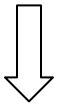

100 µl GSH solution was added to each of the test tube.

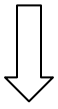

Change in absorbance was measured at 340 nm using Varian Cary 100 UV–Vis Spectrophotometer. The readings were taken for 3 minutes each at 30 seconds interval.

Assessment

Total protein concentration of the unknown sample was determined from the standard curve prepared by measuring the absorbance of different known concentrations of BSA. The activity of GST was expressed as CDNB-GSH conjugate formed/minute/mg protein present in the sample. The enzyme activity was determined according to the following formula

Absorbance = Extinction coefficient × Concentration × Length (Beer-Lambert Law)

Now, Absorbance = Change in Absorbance/minute for 3 minutes, i.e.,

(Change in Absorbance/minute) × 3

Extinction co-efficient = 9.6×10^2 $M^{-1}cm^{-1}$

Length = 1cm

Therefore, Concentration of CDNB-GSH

= {(Change in Absorbance/minute) × 3}/(9.6×10^2) M

= {(Change in Absorbance/minute) × 3 × 10^9}/ (9.6×10^2) nM

Hence, GST activity (in 100 µl sample) was expressed as:

$$\text{CDNB-GSH conjugate formed/minute/mg protein} = \frac{\text{Change in Absorbance/ minute} \times 3 \times 1000}{9.6 \times \text{Protein concentration (mg) in 100 µl sample}}$$

- **Superoxide dismutase activity (SOD) (Marklund et al, 1974; McCord et al, 1969)**

SOD activity was determined by estimating the inhibition of pyrogallol autooxidation by the enzyme. Partial extraction and purification of SOD was done as described by McCord and Fridovich. SOD activity was assayed by the method of Marklund and Marklund.

Reagents required

Homogenizing buffer (pH 7.5; 50 mM Tris-HCl, 2 mM DTPA), pyrogallol solution: stock solution of 20 mM pyrogallol was made in 10 mM HCl. Working solution was prepared fresh by diluting the stock 1:10 with 50 mM Tris-HCl, chloroform and ethanol.

Procedure

100 mg liver and lung tissues were collected from sacrificed mice, washed in normal saline and homogenized in 500 µl homogenizing buffer, using a Teflon homogenizer.

⇩

The homogenates were centrifuged at 10000 g for 30 minutes at 4^{o}C. The supernatants were taken and 250 µl ethanol and 150 µl chloroform were added to the supernatants.

⇩

The mixtures were then vortexed for 5-7 minutes and were centrifuged at 13000g for 15 minutes at 4^{o}C and the supernatants were used as the sample.

⇩

The reaction mixture for autooxidation consisted of 2 ml homogenizing buffer, 0.4 ml 2 mM pyrogallol solution and 1.6 ml distilled water.

⇩

Auto-oxidation of pyrogallol was measured by the increase in absorbance at 420 nm (0.02 min^{-1} and reading was taken at 30 seconds interval for 3 minutes).

⇩

The reaction mixtures for SOD estimation contained 10 µl cytosolic extract, 2 ml homogenizing buffer, 0.4 ml 2mM pyrogallol solution and 1.6 ml distilled water. A blank sample was prepared using 2 ml homogenizing buffer and 2 ml distilled water.

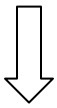

SOD activity was determined by means of inhibition of pyrogallol autooxidation by the enzyme present in the cytosolic fraction at 420 nm and the absorbances were taken at 30 seconds interval for 3 minutes in Varian Cary 100 UV–Vis Spectrophotometer.

Assessment

Total protein concentration of the unknown sample was determined from the standard curve prepared by measuring the absorbance of different known concentrations of BSA. SOD activity was determined by means of inhibition of pyrogallol auto-oxidation by the enzyme. A unit of enzyme is defined as the amount of enzyme that inhibits the reaction by 50%. Specific activity was expressed as unit/mg protein. DTPA acts as a chelator and prevents the interference from Fe^{+2} as well as from Cu^{+2} and Mn^{+2}. SOD activity was calculated by using the following formula:

% Inhibition = 100 – [{(AP–AF- AI)} × 100]/AP

AP= Absorbance of Pyrogallol auto-oxidation, AF= Absorbance final, AI= Absorbance initial

Unit/mg protein= % inhibition/{50 × Protein concentration (mg)}.

- **Catalase activity (CAT) (Luck, 1963)**

CAT catalyzes the break down of H_2O_2 into H_2O and O_2 and competes with the GPx for the common substrate H_2O_2. CAT is considered to be the primary scavenger of intracellular H_2O_2 generated due to oxidative stress. CAT activity in liver and lung cytosol was determined spectrophotometrically at 240 nm and expressed as unit/mg protein, where the unit is the amount of enzyme that liberates half the peroxide oxygen from H_2O_2 in second at 25°C.

Reagents required

M/15 phosphate buffer {(Na_2HPO_4 and NaH_2PO_4) (pH 7.0)}, Homogenizing buffer {M/150 phosphate buffer (pH 7.0)}, H_2O_2 phosphate buffer {0.16 ml H_2O_2 (30%, w/v) was diluted to 100 ml with M/15 phosphate buffer}. H_2O_2 at a concentration of 14.12 mM had an absorbance of approximately 0.50 at 240 nm with 1 cm light path.

Procedure

Mice were sacrificed, 100 mg liver and lung tissues were excised out, washed and homogenized in 500 µl ice-cold M/150 phosphate buffer, using a Teflon homogenizer.

⇩

The homogenates were centrifuged at 2000 g for 10 minutes at 4^oC.

⇩

The supernatants were taken for the assay of CAT activity.

⇩

In test tubes 10 µl sample and 3.0 ml H_2O_2 phosphate buffer were taken.

⇩

Time required for 0.05 unit OD change was measured at 240 nm in Varian Cary 100 UV–Vis Spectrophotometer against a blank containing the enzyme source in H_2O_2 free phosphate buffer (H_2O_2 phosphate buffer prepared above had absorbance of 0.50 at 240 nm and after the addition of enzyme, Δt was noted till OD was 0.45). If Δt was longer than 60 seconds, the procedure was repeated with a more concentrated enzyme sample. Reading was taken at every 3 seconds interval.

Assessment

Total protein concentration of the unknown sample was determined from the standard curve prepared by measuring the absorbance of different known concentrations of BSA. A unit of CAT activity is the amount of enzyme that liberates half the peroxide oxygen from H_2O_2 solution of any concentration in 100 seconds at 25°C.

$$\text{Unit/mg protein} = \frac{2.3}{\Delta t} \times \log \frac{\text{E-initial}}{\text{E-final}} \times \frac{1}{6.93\times10^{-3}} \times \frac{1}{\text{Protein concentration}}$$

E= optical density at 240 nm

2.3= conversion factor from ln to log

Δt= time required for a decrease in the OD

- **Estimation of GP*x* activity (Paglia et al, 1967)**

GPx activity was measured spectrophotometrically by NADPH oxidation using a coupled reaction system consisting of reduced glutathione, glutathione reductase and hydrogen peroxide. The enzyme activity was expressed as micromole NADPH utilized/minute/mg protein, using extinction co-efficient of NADPH at 340 nm as 6200 M^{-1} cm^{-1}.

Reagents required

0.25 M potassium phosphate buffer (pH 7.0, containing 2.5 mM EDTA and 2.5 mM sodium azide), glutathione reductase (2.4 units), 10 mM reduced glutathione, 2.5 mM NADPH, 0.1% $NaHCO_3$, 12 mM H_2O_2.

Procedure

From sacrificed mice liver and lung tissues were isolated, washed and weighed (100 mg each).

⇩

Tissues were then homogenized in 5 volumes (500 µl) of homogenizing buffer, using a Teflon homogenizer.

⇩

The homogenates were centrifuged at 13,000 rpm for 10 minutes at 4^oC.

⇩

The supernatants were considered as the sample for enzyme assay.

⇩

In micreocentrifuge tube 200 µl potassium phosphate buffer, 100 µl glutathione reductase, 100 µl GSH, 100 µl NADPH and 100 µl supernatant were added.

⇩

300µl distilled water then was added to the reaction mixture to make the volume 900 µl.

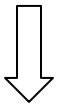

The reaction mixtures were then incubated at 37^{o}C for 10 minutes.

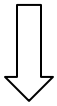

The reaction was started on adding 100 µl 12 mM H_2O_2. Blank was prepared using all the above mentioned reagents except NADPH, H_2O_2 and tissue sample, all of which were replaced by distilled water.

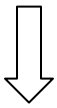

OD was measured at 340 nm at 30 seconds interval for 3 minutes.

Assessment

Total protein concentration of the unknown sample was determined from the standard curve prepared by measuring the absorbance of different known concentrations of BSA. The enzyme activity was expressed as micromol NADPH utilized/minute/mg of protein using molar extinction coefficient of NADPH at 340 nm as 6200 $M^{-1}cm^{-1}$.

- **Hepatic marker enzymes alanine transaminase and aspartate transaminase assay (Reitman and Frankel, 1957)**

Serum alanine transaminase (ALT) and aspartate transaminase (AST) activity were estimated using 2, 4-Dinitrophenyl hydrazine (2,4-DNPH) color method principles as supplied with the kit (Span Diagnostics, India) following the method of Reitman and Frankel.

2.5.1.10.1. Estimation of ALT activity

ALT catalyzes the transfer of α amino group of alanine to α -ketoglutaric acid, producing pyruvate and glutamate. Pyruvate so formed is coupled with 2,4-DNPH to give the corresponding hydrazone, which gives brown color in alkaline medium which can be measured spectrophotometrically.

α-ketoglutarate + L- Alanine ⟷ L-Glutamate + Pyruvate

Reagents required (Supplied in the kit)

Reagent 1: Buffered alanine- α - ketoglutarate substrate, pH 7.4.

Reagent 2: 2, 4-Dinitrophenyl hydrazine (2,4-DNPH) color reagent.

Reagent 3: Sodium hydroxide, 4 N.

Reagent 4: Working pyruvate standard, 2 mM.

Preparation of working solutions

Solution-1: 1 ml Reagent 3 was diluted to 10 ml with double distilled water. Reagents 1, 2, and 4 were ready for use.

Preparation of standard curve

Different known concentrations (250 µl, 225 µl, 200 µl, 175 µl and 150 µl) of reagent 1 were taken sequentially in 5 different test tubes.

⇩

25 µl, 50 µl, 75 µl and 100 µl of reagent 4 were added from 2nd test tube to 5th test tube respectively. Nothing was added in 1st test tube.

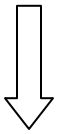

100 µl double distilled water was added to all the test tubes.

250 µl reagent 2 was added to all the test tubes.

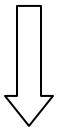

The reaction mixtures in the test tubes were mixed properly and then allowed to stand at room temperature for 20 minutes.

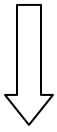

2.5 ml solution 1 was then added to all the test tubes

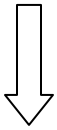

The reactants were then mixed thoroughly and all the test tubes were kept at room temperature for 10 minutes.

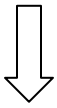

Absorbance was taken immediately at 505 nm using Varian Cary 100 UV–Vis Spectrophotometer against double distilled water as blank.

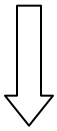

The standard curve was then prepared to calculate the ALT enzyme activity of different unknown samples and was expressed as IU/L.

Assay of ALT activity in serum

Isolation of serum

Blood samples were collected from mice by retro orbital puncture and centrifuged at 3000 rpm for 5 minutes for serum separation. The serum samples were stored at 2-8^{o}C.

Enzyme assay

125 µl reagent 1 was taken in test tubes and was incubated at 37^{o}C for 5 minutes.

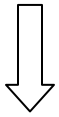

50 µl serum sample (diluted 1: 5 times with normal saline) was added to the test tubes.

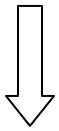

The reactants in the test tubes were then mixed well and incubated at 37^{o}C for 30 minutes.

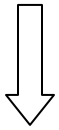

125 µl reagent 2 was then added to the test tubes.

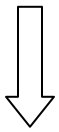

Mixing was done properly and the test tubes were allowed to stand at room temperature for 20 minutes.

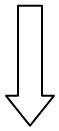

1.25 ml solution 1 was then added to the test tubes.

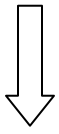

Mixing was done by vortex for 2 minutes and all the test tubes were allowed to stand at room temperature for 10 minutes.

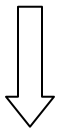

The absorbance of the reaction mixture from all test tubes was measured immediately at 505 nm in Varian Cary 100 UV–Vis Spectrophotometer against double distilled water as blank.

Assessment

The optical density obtained in the serum sample was extrapolated on the standard curve (on Y-axis) to get the corresponding enzyme activity (on X-axis) and expressed as IU/L.

The ALT activity was multiplied with the dilution factor for serum to get the final enzyme activity.

- **Serum aspartate transaminase (AST) activity**

AST catalyzes the transfer of α amino group of aspartic acid to α-ketoglutaric acid, forming oxaloacetate and glutamate. Oxaloacetate so formed is coupled with 2,4-DNPH to generate the corresponding hydrazone, which gives brown color in alkaline medium which is measured spectrophotometrically.

α-ketoglutarate + L- Aspartate ⟷ L-Glutamate + Oxaloacetate

Reagents required (Supplied in the kit)

Reagent 1: Buffered aspartate- α - ketoglutarate substrate, pH 7.4.

Reagent 2: 2, 4-Dinitrophenyl hydrazine (2,4-DNPH) color reagent.

Reagent 3: Sodium hydroxide, 4 N.

Reagent 4: Working pyruvate standard, 2 mM.

Preparation of working solutions

Solution-1: 1 ml Reagent 3 was diluted to 10 ml with double distilled water. Reagents 1, 2, 4 were ready for use.

Preparation of standard curve

Different concentrations (250 µl, 225 µl, 200 µl, 175 µl and 150 µl) of reagent 1 were taken in 5 consecutive test tubes.

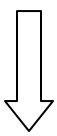

25 µl, 50 µl, 75 µl and 100 µl reagent 4 were added from 2nd test tube to 5th test tube respectively. Nothing was added in 1st test tube.

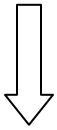

50 µl double distilled water was added to all the test tubes.

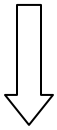

250 µl reagent 2 was added to all the test tubes.

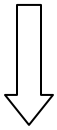

Mixing was done properly and the test tubes were kept at room temperature for 20 minutes.

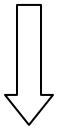

2.5 ml solution 1 was then added to all the test tubes.

The reaction mixtures were then vortexed for 2 minutes and all the test tubes were allowed to stand at room temperature for 10 minutes.

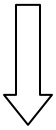

Absorbance of each reaction mixture was measured immediately at 505 nm in Varian Cary 100 UV–Vis Spectrophotometer against double distilled water as blank.

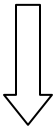

The standard curve was then plotted to calculate the AST activity of different samples and was expressed as IU/L.

Assay of AST activity in serum

Isolation of Serum

Blood samples were collected from mice by retro orbital puncture and were centrifuged at 3000 rpm for 5 minutes for serum separation. The serum samples were stored at 2-8^{o}C.

Enzyme assay

250 µl reagent 1 was added in test tubes.

⇩

Incubation was done at 37^{o}C for 5 minutes.

⇩

50 µl serum sample (diluted1: 5 times with normal saline) was added to the test tubes.

⇩

The reactants in each test tube were mixed properly and were then incubated at 37^{o}C for 60 minutes.

⇩

250 µl reagent 2 was added to the test tubes.

⇩

Mixing was done properly and the test tubes were kept at room temperature for 20 minutes.

⇩

2.5 ml solution 1 was then added to the test tubes.

⇩

Mixing of the reactants was done by vortex for 2 minutes and all the test tubes were allowed to stand at room temperature for 10 minutes.

⇩

Absorbance of each reaction mixture was taken immediately at 505 nm in Varian Cary 100 UV–Vis Spectrophotometer against double distilled water as blank.

Assessment

The optical density obtained in the serum sample was extrapolated on the standard curve (on Y-axis) to get the corresponding enzyme activity (on X-axis) and expressed as IU/L. The AST enzyme activity was multiplied with the dilution factor for serum to obtain the final enzyme activity.

- **Hematological parameters**
- **Blood hemoglobin (Hb) level (Sahli, 1909)**

Reagents required

N/10 HCl.

Procedure

In Sahli's tube N/10 HCl was taken up to lowest graduation (0.02 gramme).

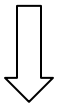

20 µl blood was added into the Sahli's tube.

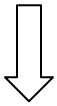

Blood and HCl in the tube were stirred with a glass rod for proper mixing.

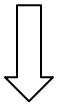

The tube was then placed in stand and kept for 3 minutes during which period HCl caused lysis of RBC and released hemoglobin, which on reacting with HCl forms a dark brown colored acid hematin.

Distilled water was added in the tube drop by drop and stirred with a glass rod.

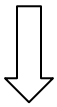

The process was continued until the color of the solution exactly matched with that of the standard.

⇩

Finally, the hemoglobinometer was held against good light and the reading was taken.

- **Red blood cell count (D'Armour et al, 1965)**

Red blood cell (RBC) count was performed using the hemocytometer. This particular instrument possesses a platform with microscopic grid scoring. Rails on either side hold up a cover slip so that a specified quantity of fluid is held. With proper dilution of blood, counting of all cells in specified squares and finally by multiplying the counted RBC with the proper conversion factor, the number of RBC/mm^3 is determined.

Reagents required

RBC diluting fluid containing 1% sodium citrate, formalin and distilled water.

Procedure

Blood was drawn up to the 0.5 mark in a RBC diluting pipette.

⇩

Holding the pipette horizontally, the RBC diluting fluid was drawn up to the 101 mark (Dilution of 1 to 200).

⇩

The diluent and blood was mixed properly.

⇩

Holding at an angle of 45^o, the pipette tip was positioned at the junction of the cover glass and the counting chamber.

⇩

Diluted blood from the pipette was charged to one chamber of the hemocytometer. The cells were allowed to settle for about 1 minute.

⇩

RBC counting was done at 400× in each of five fields (each with 16 smallest squares). The cells touching top and right sides of the squares were ignored.

Calculation

The smallest squares in the large center square (where red cells are counted) have an area of 1/400 mm and are arranged in groups of 16. The volume of fluid in the portion of the hemocytometer which was counted: 1/400 mm^2 (area of smallest square) × 16 (no. of squares/group) × 5 (no. of groups counted) × 1/10 mm (depth of chamber) = 0.02 mm^3. Before being placed in the chamber, blood was diluted by a factor of 200.

So, the number of RBC in 0.02 mm^3 blood

= 200 (dilution factor) × the number of cells counted.

So, the number of RBC in 1 mm^3 blood

= 200 (dilution factor) × the number of cells counted × 50 (volume factor).

RBC count was reported as millions of cells/mm^3.

- **White blood cell count (Wintrobe et al, 1961)**

A sample of whole blood was mixed with a weak acid solution that lyses nonnucleated red blood cells. Following adequate mixing, the specimen was introduced into a counting chamber where the white blood cells (WBCs) in a diluted volume were counted.

Reagent required

WBC diluting fluid containing 2% acetic acid.

Procedure

Blood was sucked up exactly to the 0.5 mark in a WBC diluting pipette.

⇩

Excess blood was wiped out from the outside of the pipette to avoid excess transfer of cells to the diluting fluid.

⇩

Diluting fluid was immediately drawn to the "11" mark while rotating the pipette between the thumb and forefinger to mix the specimen and diluent.

⇩

Mixing was done for 3-5 minutes to ensure even distribution of cells.

⇩

Holding at an angle of 45°, the pipette tip was positioned at the junction of the cover glass and the counting chamber.

⇩

The mixture in the pipette was allowed to flow under the cover glass until the chamber was completely filled. Similarly the opposite chamber of the hemocytometer was also filled.

⇩

The cells were allowed to settle for about 3 minutes. Under low-power magnification of microscope, the WBCs were counted in the four 1 sq. mm corner areas.

⇩

WBCs lying within the square and those touching the upper and right hand center lines were counted and those touching the left hand and bottom lines were not counted.

Calculation

Routinely, blood was drawn to the 0.5 mark and diluted to the 11 mark with WBC diluting fluid. All the blood was washed into the bulb of the pipette (which had a volume of 10). Therefore, 0.5 volumes of blood were contained in 10 volumes of diluting fluid. The resulting dilution was 1:20.

The depth of the counting chamber was 0.1 mm and the area counted was 4 sq mm (4 squares were counted, each with an area of 1.0 sq mm therefore, 4 × 1.0 sq mm = a total of 4 mm^2). The volume counted was: 4 mm^2 × 0.1 mm = 0.4 mm^3 (area × depth).

Finally, the formula for obtaining the no. of WBC/mm^3 was as follows:

$$\text{WBC/mm}^3 = \frac{\text{Average number of chamber (2) WBCs counted} \times \text{Dilution (20)}}{\text{Volume (0.4)}}$$

- **Bone marrow cell count (Ghosh et al, 1999)**

Reagent required

WBC diluting fluid containing 2% acetic acid.

Procedure

Bone marrow was collected from the femur bone of sacrificed mice by flushing with PBS using a hypodermic syringe. The bone marrow in PBS was aspirated well to make a homogeneous suspension.

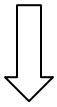

The cell suspension was then centrifuged at 2000 rpm at $4^{o}C$ for 10 minutes.

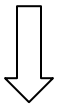

The pellet was resuspended in a measured volume of PBS after removing the supernatant. Nucleated cell count from bone marrow cell suspension was done under microscope using hemocytometer as in WBC count.

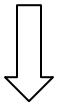

Bone marrow cell count was reported as total numbers of nucleated cells/femur/mm^3.

- **Spleen Cell Count**

Reagent required

WBC diluting fluid containing 2% acetic acid

Procedure

Whole spleen was isolated from the sacrificed mice.

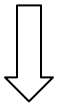

The Spleen was put on a Petri dish and was ruptured by flushing with PBS using a hypodermic syringe. The process continued until the entire cells from spleen come out into the dish making the spleen fade.

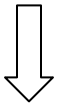

The cell suspension was then centrifuged at 2000 rpm at $4^{o}C$ for 10 minutes.

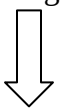

The pellet was resuspended in a measured volume of PBS after removing the supernatant. Nucleated cell count from the spleen cell suspension was done under microscope using hemocytometer as in WBC count.

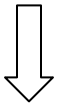

Spleen cell count was reported as total numbers of nucleated cells/mm^3.

❖ **Genotoxicity parameters**

➢ **Estimation of ROS in bone marrow cell**

ROS generation in bone marrow cells was measured spectrofluorimetrically using DCFH-DA following a simplified protocol with slight modifications **(Huang et al., 2008)**. DCFH-DA is a nonfluorescent probe that is hydrolyzed by mitochondrial esterase to form 2',7'-dichlorodihydrofluorescein (DCFH), which is then oxidized by ROS to form the fluorescent compound 2',7'-dichlorofluorescein (DCF) is measured by spectrofluorimeter (excitation 485 nm/emission 530 nm). Values were expressed as fluorescence intensity/10^7 cell.

Reagents required

Locke's Buffer (pH 7.4 containing 140 mM NaCl, 5 mM KCl, 10 mM HEPES, 1 mM $CaCl_2$, 1 mM $MgCl_2$, 10 mM glucose), 10 µM DCFH-DA, PBS.

Procedure

In test tubes 1 ml of PBS containing 1×10^7 bone marrow cells from each sample was added in test tubes, to which 30 µl of 10 µM DCFH-DA was added.

⇩

2 ml of Locke's buffer was then added in the test tubes.

⇩

Test tubes were incubated in dark at 37°C for 30 minutes to allow the formation of DCF.

⇩

Samples were then analyzed for fluorescence (excitation 485 nm/emission 530 nm) using spectrofluorimeter (Varian Cary Eclipse).

⇩

Values were expressed as fluorescence intensity/10^7 cells.

- **Detection of DNA damage by alkaline single cell gel electrophoresis (Comet assay) (Singh et al., 1988; Endoh et al., 2002)**

The alkaline single cell gel electrophoresis (SCG) (Comet) assay is a rapid and sensitive procedure for quantitating DNA damage in mammalian cells **(Singh et. al., 1988; Endoh et al., 2002)**. The use of this alkaline SCG assay as a method to detect genotoxicity and cytotoxicity *in vivo* is well documented, and DNA damage thus detected has been used to predict the presence of genotoxic metabolites in specific organs **(Henderson et. al., 1998)**. In this assay, cells are embedded in agarose, lysed in an alkaline buffer, and subjected to an electric current. Relaxed and broken DNA fragments stream further from the nucleus than intact DNA, so the extent of DNA damage can be measured by the length of the stream. This method has several advantages: it is highly sensitive to DNA damage expressed as single strand breaks and alkali-labile sites and disordered DNA fragmentation and few cells are required. DNA damage (disorderly DNA fragmentation) induced by CP was measured by using this assay under alkaline conditions following a simplified protocol with slight modifications.

Reagents required

1% normal melting agarose in PBS, 1% low melting point agarose in Milli Q water, 0.5% low melting point agarose in PBS, sodium hydroxide (NaOH), Ethylenediaminetetra acetic acid (Na_2EDTA), Ethidium bromide,.

Lysing solution: 2.5 M NaCl, 100 mM EDTA, 10 mM Tris buffer, 1 % Triton X 100, pH was adjusted to 10 with NaOH.

Electrophoresis buffer: 1 mM Na_2EDTA and 0.3 M NaOH (pH>13).

Neutralizing buffer: 0.4 M Tris buffer (pH 7.5).

Staining solution: Ethidium bromide in water (20 µg/ml).

Isolation of lymphocytes from blood for comet assay:

After 10 days of CP treatment mice were sacrificed following the guideline of our Institute and blood was collected from each mouse of all groups. Lymphocytes were isolated from samples of blood by standard centrifugation over a cushion of histopaque, washed with isotonic phosphate buffered saline solution, and centrifuged. The pellet was resuspended in isotonic phosphate buffered saline solution. The cell viability in each

group was measured by the trypan blue exclusion method and approximately 10^4 cells /slide were taken for the assay.

Isolation of bronchoalveolar lavage fluid (BALF) from lung for comet assay:

Lungs were removed and BALF was collected using the method of Henderson et al., 1985, with some modifications. Lungs were lavaged five times with 7 mL saline and the lavage fluids were centrifuged at 300 g for 20 min at 4ºC to separate the cells and the supernatants. The cell viability in each group was measured by 0.1 % trypan blue with hemocytometer in phosphate-buffered saline and density of cells was adjusted to 10^5 cells/slide for the comet assay.

Isolation of bone marrow from femur for comet assay:

Bone marrow cells suspension was prepared from femurs of each animal, where the bone was split longitudinally and the marrow was exposed using forceps and the content of the femur was flushed gently using 2 ml syringe containing PBS (pH 7.4) into a centrifuge tube and centrifugation at at 1000 rpm for 10 min at 4ºC. Cell pellets were re-suspended with PBS and the density of cells was adjusted to 10^6cells/slide for the comet assay.

Procedure:

Half frosted microscope slides were coated with 1% normal melting agarose in PBS

⇩

The slides were then allowed to dry at room temperature protected from dust and other particles

⇩

On the day of single cell gel electrophoresis an aliquots of 10µl of freshly prepared cell suspension was mixed with 75µl of 1% low melting point agarose in Milli Q water

⇩

This mixture was then layered on the top of the pre-coated slide and covered with a

24 x 50 mm cover slip and kept on ice to allow the agarose to solidify

⇩

After the agarose had solidified on ice for at least 10-15 min. containing required amount of cells, the cover slip was gently removed and a third layer of 0.5% low melting point agarose was layered on the top of the second layer and covered with a cover slip and kept on ice for 5-10 min.

⇩

After the agarose had solidified, the cover slipwas gently removed and the slides were carefully immersed in a freshly prepared ice-cold lysing solution

⇩

After lysis for overnight at 40ºC, cell membrane and cytosol were lysed and isolated nucleus was remain in the agarose. The slides were placed in an electrophoresis unit.

⇩

The buffer reservoirs were gently filled with fresh electrophoresis buffer to a level of 0.25 cm above the microscope slides, and incubated for 20min. at 40ºC to allow the unwinding of DNA

⇩

Keeping the same temperature, the slides were subjected to electrophoresis (25V, 400 mA) for another 25 min.

⇩

After electrophoresis, the slides were placed on a tray to remove alkali and detergents and neutralized with neutralizing buffer for 10 min.

⇩

Excess liquid was carefully removed from each slide using a paper towel
The microscope slides were carefully dried at room temperature avoiding dust and other particles and then stored in a sealed container until the day of image analysis

The dried microscope slides were stained with ethidium bromide in water (20µg/ml; 50µl/slide)

Assessment:

The slides with a cover slip were examined at 400X magnification under fluorescence microscope with green filter and photomicrographs of cell were taken. 150-200 randomly selected cells in each slide were counted (4 slides/ animals in each group). The damaged cell (%) was calculated using the following formula:

$$\% \text{ Cell with damaged DNA} = \frac{\text{Number of damaged cells}}{\text{Total number of cells counted}} \times 100$$

Average tail length due toDNA migration in each group. The parameters analyzed for detection of DNA damage were damaged cell (%) in each group, tail DNA (%), tail length [migration of the DNA from the nucleus (lm)], and Olive tail moment [product of tail length and the fraction of total DNA in the tail (arbitrary units)].

- **Assay of chromosomal aberration**

This assay is a valuable technique for evaluation of damage to chromosomes on the basis of direct observation and classification of chromosomal aberrations. Slides for study of chromosomal aberrations (CA) were prepared from bone marrow cells by the conventional flame drying technique **(Biswas et al, 2004)**.

Reagents required

0.03% colchicine, 1% sodium citrate, Giemsa stain.

Procedure

Mice were injected intraperitoneally with 0.03 % colchicine at the rate of 1 ml/100 g b.w. 90 minutes before sacrifice.

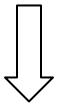

Bone marrow cells were collected from the femur by flushing with warm (37°C) sodium citrate (1%) solution using a hypodermic syringe. Cells were then carefully aspirated to make a suspension.

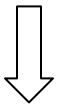

The material was then centrifuged at 2000 rpm for 10 minutes.

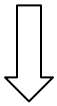

Cell pellet was fixed in acetic acid/ethanol (1:3) and kept for 15 minutes.

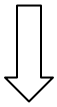

The cell suspension was again centrifuged at 2000 rpm for 15 minutes.

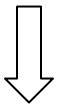

Cell pellet was collected and resuspended in a small volume of fixative (1:3 acetic acid/alcohol) by gentle flushing until a cloudy suspension resulted.

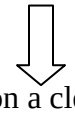

The cell suspension was then dropped on a clean slide chilled for one day in 50% ethanol

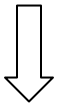

Slides were then burnt on a flame for a while, air dried.

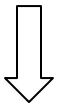

On the next day slides were stained with Giemsa.

Assessment

Slides were analyzed a light microscope (Leica DM 1000). Photomicrographs were taken with the software Las EZ. CA of various natures like stretching, terminal association, break, fragment, ring formation etc. were analyzed. A total of 300 bone marrow cells were observed, 50 from each of 6 mice of a set.

- **DNA fragmentation by diphenylamine (DPA assay) (Zhivotovsky et al., 2001)**

DNA fragmentation is a key feature of apoptosis, a type of programmed cell death. The discovery of the internucleosomal fragmentation of DNA to regular repeating oligonucleosomal fragments generated by Ca/Mg-dependent endonuclease is accepted as one of the best-characterized biochemical markers of apoptosis (programmed cell death).

Reagent required

Lysis buffer (pH 8.0 containing 5 mM Tris–HCl, 20 mM EDTA and 0.5 % Triton X-100), 10 and 5 % of trichloroacetic acid (TCA), diphenylamine (DPA).

Procedure

Bone marrow was collected from the femur bone of sacrificed mice by flushing with PBS using a hypodermic syringe. The bone marrow in PBS was aspirated well to make a homogeneous suspension.

⇩

2×10^6 bone marrow cells lysed in lysis buffer for 30 min at 4ºC

⇩

The cell lysate were centrifuged at 15,000g for 15 min at 4ºC

⇩

The supernatant containing small DNA fragments was separated from the pellet containing large pieces of DNA.

⇩

The supernatant and pellet were re-suspended in 10 and 5 % of trichloroacetic acid (TCA), respectively, and kept overnight.

⇩

Then both samples were heated at 95ºC for 15 min and centrifuged at 2500g for 5 min to remove proteins.

⇩

Supernatant fractions were reacted with DPA for 4 h at 37ºC and the developing blue color was measured at 600 nm

Assessment

DNA fragmentation in samples was expressed as percentage of total DNA appearing in the supernatant fraction.

$$\% \text{ Fragmented DNA} = \frac{\text{Absorbance of the supernatant}}{\text{Absorbance of supernatant} + \text{pellet}} \times 100$$

- **Detection of apoptosis of bone marrow cell by using Acridine orange (AO)/ Ethidium bromide (EtBr) (Shylesh et al. 2005)**

Acridine orange/ethidium bromide (AO/EB) staining is used to visualize nuclear changes and apoptotic body formation that are characteristic of apoptosis. Cells are viewed under a fluorescence microscope and counted to quantify apoptosis.

Reagent required

Acridine orange, Ethidium bromide, PBS

Procedure

Bone marrow was collected from the femur bone of sacrificed mice by flushing with PBS using a hypodermic syringe. The bone marrow in PBS was aspirated well to make a homogeneous suspension.

⇩

The cell suspension was centrifuged at 2000 rpm for 15 minutes.

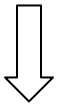

Cell pellet was collected and resuspended in a small volume of PBS (100 µl) and smeared on a glass slide fixed with methanol: acetic acid (3:1) and air dried in humidified chamber.

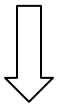

The cells were hydrated with PBS and stained with 4 µl dye mixture of acridine orange (1 mg/ml): ethidium bromide (1 mg/ml) in ratio (1:1)

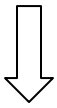

The cells were visualized immediately under a fluorescence microscope.

Assessment

The slides with a cover slip were examined under fluorescence microscope (Model: Leica DM 4000B) using a blue and green filter and photomicrographs (Leica FW 4000) were taken at 400× magnification. Viable cell's nucleus stain green due to permeability of only AO whereas, apoptotic cells appear yellow–red due to co-staining of both stains.

❖ **Histopathology (Bancroft et al, 1990; Lillie et al, 1976)**

The purpose of histological staining methods by hematoxylin and eosin is to visualize and differentiate between tissue components in normal and pathological condition. Identification and confirmation of histopathological changes induced by chemotherapy drugs and the protective effect of the test compound was carried out using standard hematoxylin-eosin staining procedure and analysis was done by light microscopy.

Procedure

Tissue collection and fixation

After sacrificing the mice liver and lungs were collected, washed repeatedly in PBS and soaked in blotting paper to remove the blood. Tissues were then placed into fixatives as soon as possible. The death of cells leads to the breakdown of cellular constituents resulting from endogenous enzymes and from damages caused by external agents such as bacteria. The purpose of fixation is to preserve tissues permanently in as life-like a state as possible and it needs to be carried out as soon as possible to prevent autolysis. Tissue is fixed by cross-linkages formed in the proteins particularly between lysine residues. These cross linkages dose not harm the structure of protein significantly. After collection, all tissues were fixed in 10% neutral buffered formalin for 24 hours. Formalin is a fixative of choice for histopathological procedures because it penetrates tissues slowly but properly and prevents acidity that might promote autolysis and cause precipitation of formol-heme pigment in the tissue. After fixation tissues were washed thoroughly in running tap water for about 6 hours followed by a rinse in distilled water for 30 minutes.

Tissue processing

After fixation tissues are processed for the preparation of thin microscopic sections. For This purpose tissues are embedded in paraffin block. Before embedding, tissues are processed through the steps of dehydration and clearing as follows:

Dehydration

Wet and fixed tissues cannot be directly infiltrated with paraffin. Tissues need to be processed through solvents with decreasing water concentrations in order to infiltrate them with paraffin. The fixed tissues were transfer through ascending graded alcoholic solutions, as alcohol is the most common solvent used for dehydration. It was done by keeping the tissues in 50% alcohol (1 hour), 70% alcohol (over night), 90% (2 hours with 2 changes), absolute alcohol (1 hour, with 2 changes).

Clearing

The next step is called 'clearing' where removal of dehydrant with a substance that will be miscible with the embedding medium (paraffin) is carried out. The frequently used clearing agent is xylene. It serves as a transition medium between two immiscible compounds, alcohol and paraffin. So the dehydrated tissues were transferred to xylene for 15 minutes. This procedure increases the refractive index of the tissues, thereby making them transparent. It hardens the tissue if left in too long.

Embedding

The 'embedding' process is very important because the tissues must be aligned or oriented properly in the block of paraffin. The tissue was embedded in paraffin (melting point 58-60^{o}C) by transferring them from xylene to molten paraffin in a porcelain pot for 2 hours which was kept in paraffin bath at 60^{o}C.

Block preparation

After complete impregnation with paraffin, blocks containing the tissues were prepared to facilitate proper sectioning of the material. Molten paraffin was poured in a paper boat to which the tissue was then transferred with hot forceps and oriented properly in the center of depression. Presence of air bubbles in the blocks hinders proper sectioning, so care was taken to remove the bubbles during setting of the paraffin.

Section cutting

The paraffin blocks were sectioned in a rotary microtome to get 4 -5 µm serial sections, which come out in the form of a paraffin ribbon. After having a 6″ ribbon, it was detached from the knife by the help of a scalpel and floated in a tray containing warm water. Small portions of this ribbon with serial sections floated in warm water were placed on glass slide coated with egg albumin and gently stretched using forceps or needles. The glass slides were then placed in a warm oven for about 15 minutes to help the sections to adhere to the slide.

Staining with hematoxylin and eosin

Hematoxylin is extracted from the heartwood of the logwood tree *Haematoxylum campechianum*. When oxidized it forms hematein, a compound that forms strongly colored complexes with certain metal ions, the most notable ones being Fe(III) and Al(III) salts. Metal-hematein complexes are used to stain cell nuclei prior to examination under a microscope. Eosin is an acidic dye with an affinity for cytoplasmic components of the cell. To differentiate the nucleus and cytoplasm, hematoxylin and eosin were used for staining of the tissue sections. The steps described below were followed for staining the slides.

Slides were dipped in xylene for 10 minutes.

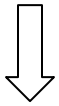

The slides were then dipped in absolute alcohol for 10 minutes.

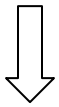

Next, the slides were dipped in 90% alcohol for 10 minutes.

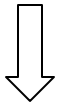

Then the slides were dipped in 70% alcohol for 10 minutes.

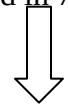

The slides were then dipped in water for 10 minutes.

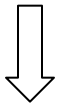

Sections were then stained with hematoxylin for 3-5 minutes.

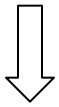

The slides were washed in running tap water for 8-10 minutes. Excess hematoxylin was removed in acid alcohol, so that cytoplasm remains unstained.

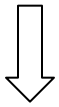

Excess acid was removed by putting the slides under running tap water.

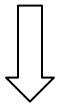

The slides were then dipped in 70% alcohol for 10 minutes.

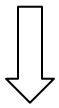

The slides were then dipped in 90% alcohol for 10 minutes.

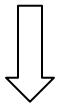

The slides were stained with eosin for 1-2 minutes.

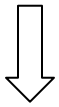

To remove excess stain the slides were washed in 90% alcohol.

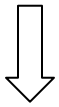

The slides were kept in absolute alcohol for 10 minutes.

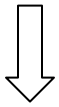

The slides were kept in xylene for 5 minutes and were finally mounted in DPX.

Evaluation

Stained sections were evaluated by observing the arrangement of tissue architecture under a light microscope (Leica DM 1000). Photomicrographs were taken with the software Las EZ.

Statistical analysis

All data were presented as mean ± SD. n = 6 animals per group. One way ANOVA followed by Tukey's Multiple Comparison Test using Graph Pad Prism software was performed for comparisons among groups. Significant difference was indicated when the *P* value was < 0.05.

Results

Nano selenium (Nano-Se) did not produce any significant change in the parameters investigated when administered alone as compared to the vehicle treated group.

➢ LPO level

Intraperitoneal administration of cyclophosphamide (Gr. III) significantly ($P < 0.05$) elevated LPO level by 47.51% in liver and by 145.12% in lung, compared to the vehicle treated group (Gr. I) **(Fig. 2A & B)**. Concomitant treatment (Gr. IV) with Nano-Se significantly ($P < 0.05$) reduced the LPO level by 17.73% in liver and by 20.89% in lung, where as pretreatment (Gr. V) with the same compound inhibited LPO level much more significantly ($P < 0.05$) by 26.24% in liver and by 36.31% in lung in comparison to the CP treated group (Gr. III).

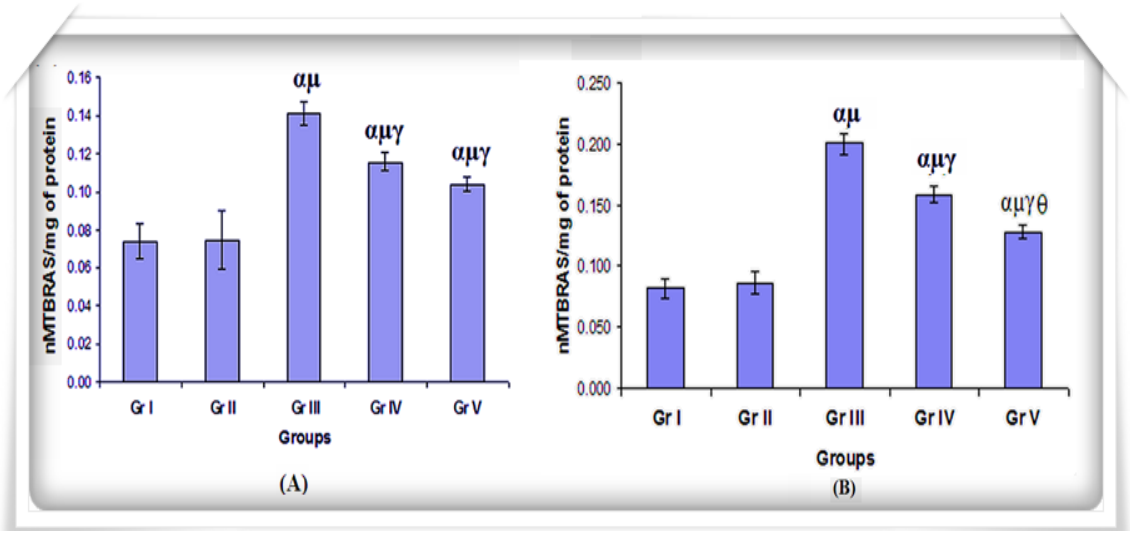

Figure 2: Data were represented as mean ± SD (n=6). α - significant *(P < 0.05)* as compared with Gr. I; μ - significant *(P < 0.05)* as compared with Gr. II; γ - significant *(P < 0.05)* as compared with Gr. III; θ - significant (*P < 0.05)* as compared with Gr. IV.

➢ **ROS level**

- **Hydrogen peroxide level by using DCFH-DA**

Intraperitoneal administration of CP significantly (*P < 0.05*) elevated H_2O_2 level in liver, lung and in bone marrow cells by 52.8%, 122% and 63.03% respectively in Gr. III as compared to the vehicle treated group (Gr. I) **(Fig. 3A, B, C)**. Concomitant treatment (Gr. IV) and pretreatment (Gr. V) with Nano-Se caused a sharp reduction in H_2O_2 level in liver, lungs as well as in bone marrow cells. Concomitant treatment (Gr. IV) with Nano-Se significantly (*P* < 0.05) reduced H_2O_2 level in liver by 13.73%, in lungs by 29.95% and in bone marrow cells by 37.80% respectively, but on 7 days pretreatment (Gr.V) with the same inhibited the H_2O_2 level much more significantly (*P* > 0.05) by 43.49% in liver, by 45.16% in lungs and by 52.76% in bone marrow cells in comparison to the CP treated group (Gr. III).

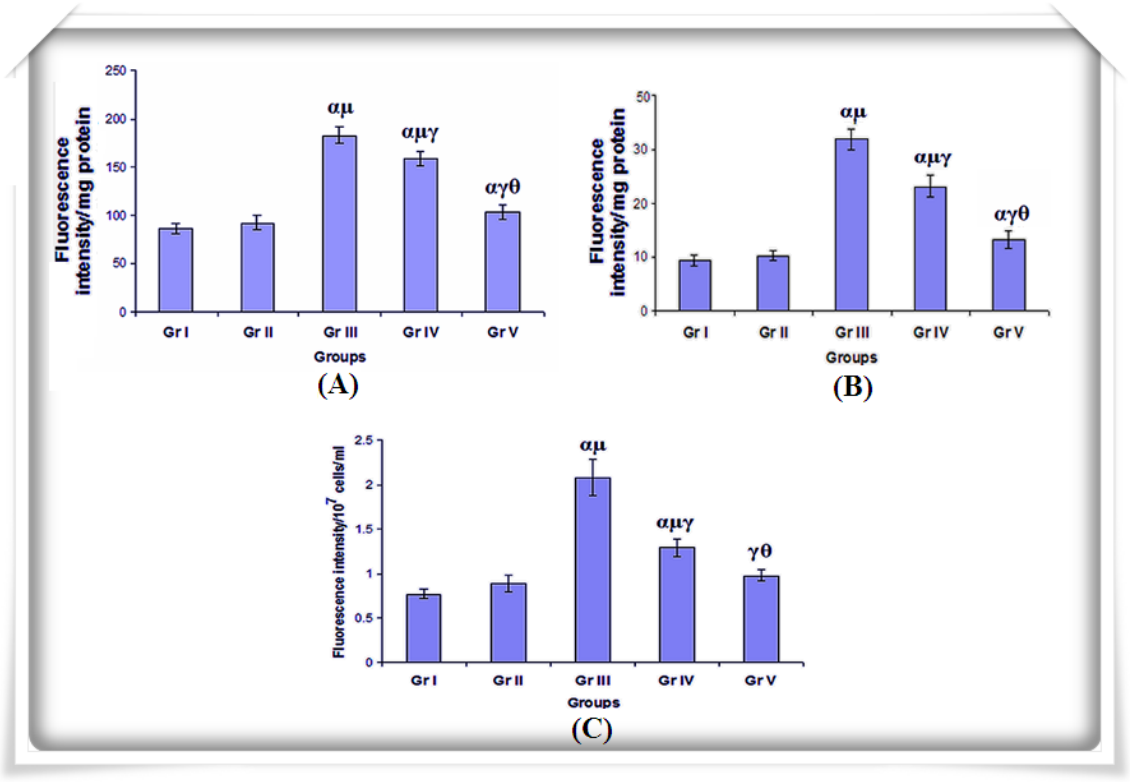

Figure 3: Data were represented as mean ± SD (n=6). α - significant (*P < 0.05*) as compared with Gr. I; μ - significant (*P < 0.05*) as compared with Gr. II; γ - significant (*P < 0.05*) as compared with Gr. III; θ - significant (*P < 0.05*) as compared with Gr. IV.

- **Superoxide level by using DHE**

The super oxide level in liver, lung tissues and bone marrow cells were found to increase significantly ($P < 0.05$) by 288.93%, 237.71% and 273.48% respectively, after the administration of CP (Gr. III), compared to the vehicle treated group (Gr. I) (**Fig. 4A, B, C**). Concomitant treatment (Gr. IV) with Nano-Se significantly ($P < 0.05$) reduced superoxide level in liver by 33.84%, in lungs by 27.22% and in bone marrow cells by 36.79% respectively, but on 7 days pretreatment (Gr. V) with the same inhibited the superoxide level much more significantly ($P < 0.05$) by 53.07% in liver, by 58.31% in lungs and by 61.32% in bone marrow cells in comparison to the CP treated group (Gr. III).

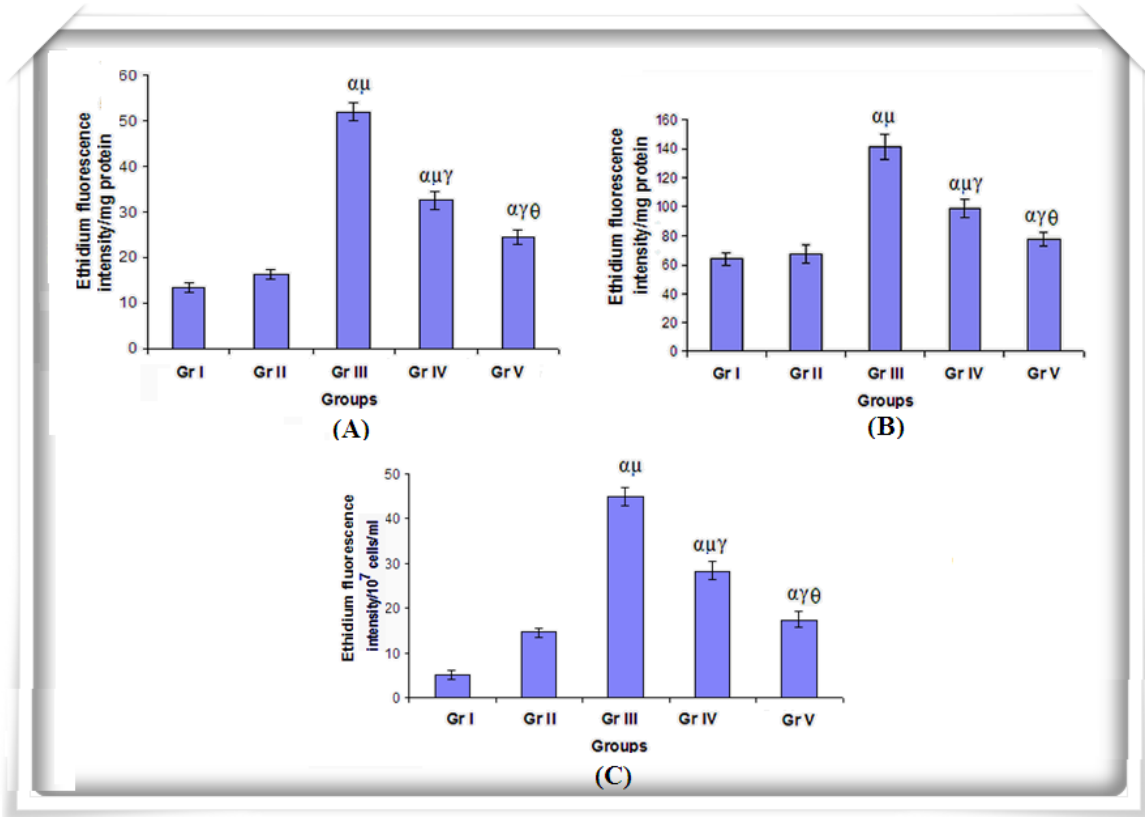

Figure 4: Data were represented as mean ± SD (n=6). α - significant ($P < 0.05$) as compared with Gr. I; μ - significant ($P < 0.05$) as compared with Gr. II; γ - significant ($P < 0.05$) as compared with Gr. III; θ - significant ($P < 0.05$) as compared with Gr. IV.

➢ **Nitric oxide (NO) level**

Intraperitoneal administration of cyclophosphamide (Gr. III) significantly (*P<0.05*) elevated NO level by 154.72% in liver and by 67.69% in lung, compared to the vehicle treated group (Gr. I) **(Fig. 5A & B)**. Concomitant treatment (Gr. IV) with Nano-Se significantly ($P < 0.05$) reduced the NO level by 56.23% in liver and by 16.36% in lung, where as pretreatment (Gr. V) with the same compound inhibited NO level much more significantly ($P < 0.05$) by 58.88% in liver and by 25.84% in lung in comparison to the CP treated group (Gr. III).

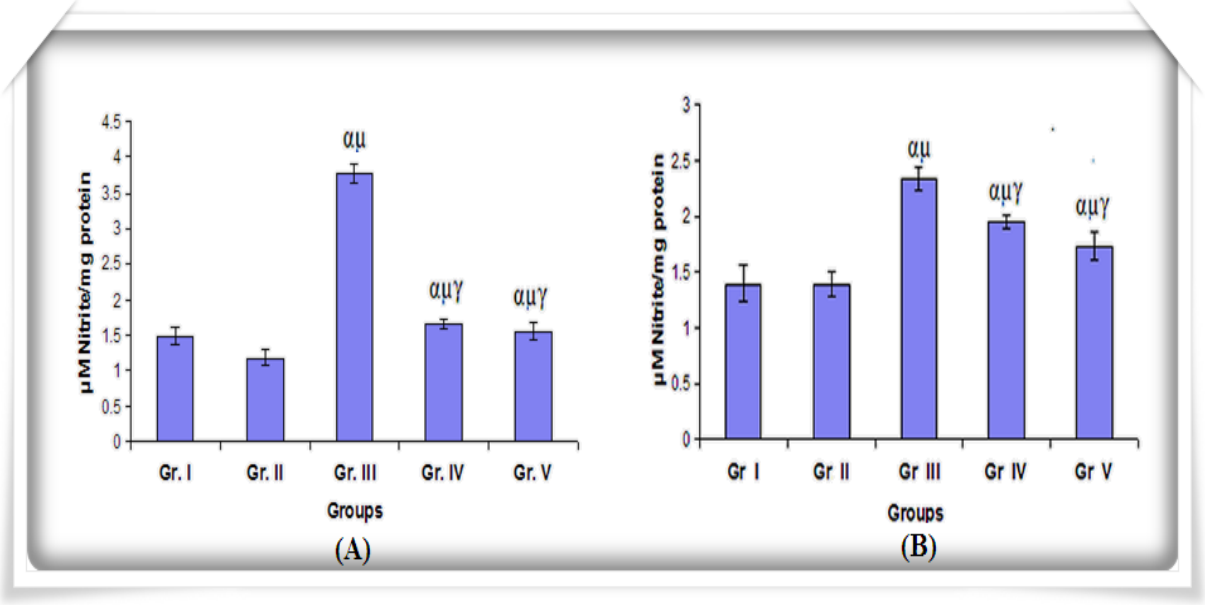

Figure 5: Data were represented as mean ± SD (n=6). α - significant (*P < 0.05*) as compared with Gr. I; µ - significant (*P < 0.05*) as compared with Gr. II; γ - significant (*P < 0.05*) as compared with Gr. III; θ - significant (*P < 0.05*) as compared with Gr. IV.

- **GSH level**

The GSH content was found to decline significantly (*P<0.05*) by 44.9% & 56.64% respectively in liver and lung after CP administration (Gr. III) as compared to the vehicle treated group (Gr. I) **(Fig. 6A & B)**. Concomitant treatment (Gr. IV) and pretreatment (Gr. V) with the Nano-Se resulted in a significant (*P* < 0.05) elevation of GSH content by 34.23% & 43.18% respectively in liver and by 38.16% & 76.29% respectively in lung in comparison to the CP treated group(Gr. III).

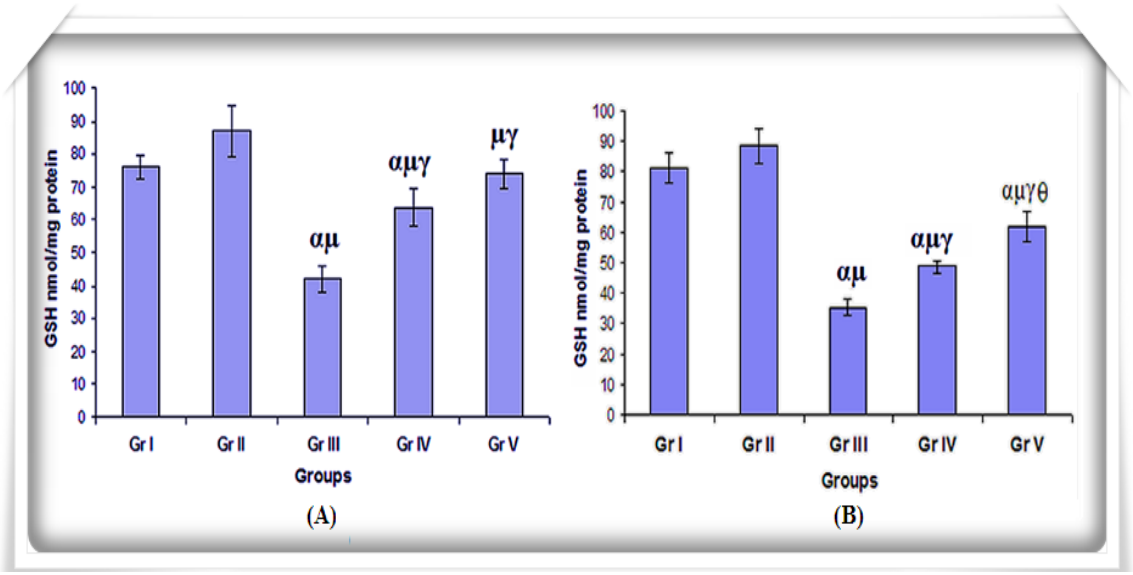

Figure 6: Data were represented as mean ± SD (n=6). α - significant (*P < 0.05*) as compared with Gr. I; μ - significant (*P < 0.05*) as compared with Gr. II; γ - significant (*P < 0.05*) as compared with Gr. III; θ - significant (*P < 0.05*) as compared with Gr. IV.

- **GST activity**

A significant (*P<0.05*) reduction of GST activity by 42.53% in liver and by 36.2% in lung was observed in CP treated group (Gr. III) in comparison to the vehicle treated group (Gr. I) **(Fig. 7A & B)**. Concomitant administration of Nano-Se (Gr. IV) significantly (*P* < 0.05) increased the GST activity in liver by 29.33% and in lung by 31.46% compared to the CP treated group (Gr. III). In pretreatment schedule (Gr. V), the same compound raised the enzyme activity in liver by 37.85% and in lung by 52.18% in comparison to the CP treated group (Gr. III).

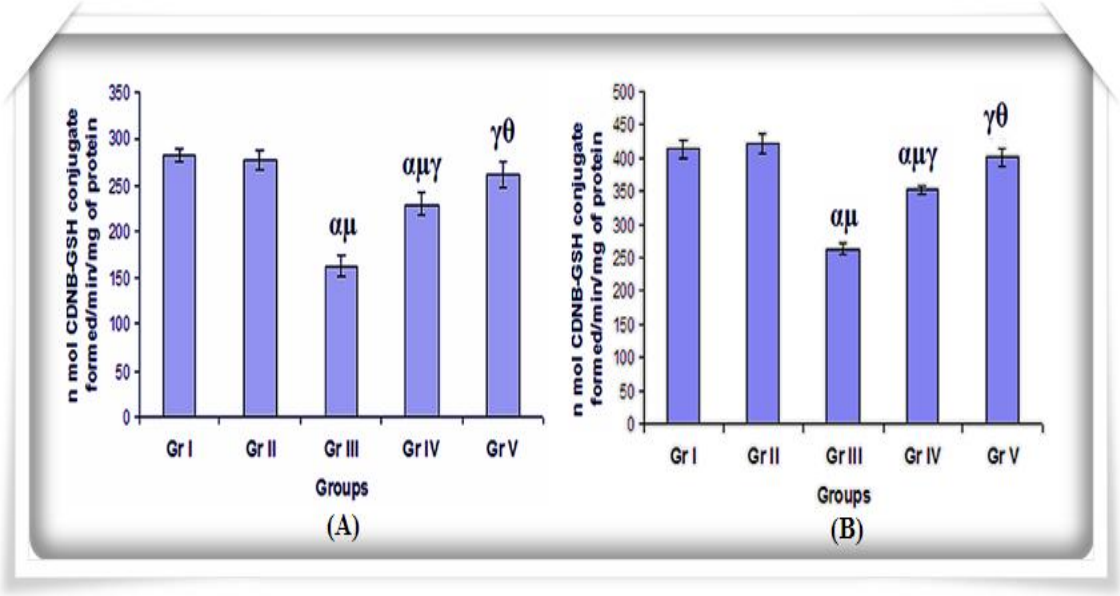

Figure 7: Data were represented as mean ± SD (n=6). α - significant (*P < 0.05*) as compared with Gr. I; μ - significant (*P < 0.05*) as compared with Gr. II; γ - significant (*P < 0.05*) as compared with Gr. III; θ - significant (*P < 0.05*) as compared with Gr. IV.

- **SOD activity**

Intraperitoneal administration of CP (Gr. III) significantly (*P<0.05*) decreased the SOD activity by 63.25% in liver and by 75.09% in lung, as compared to the vehicle treated group (Gr. I) **(Fig. 8A & B)**. Concomitant treatment (Gr. IV) with Nano-Se significantly ($P < 0.05$) enhanced the SOD activity by 30.42% in liver and by 73.95% in lung, while pretreatment (Gr. V) with the same compound increased the SOD activity much more significantly ($P < 0.05$) by 50.47% in liver and by 171.1% in lung in comparison to the CP treated group(Gr. III).

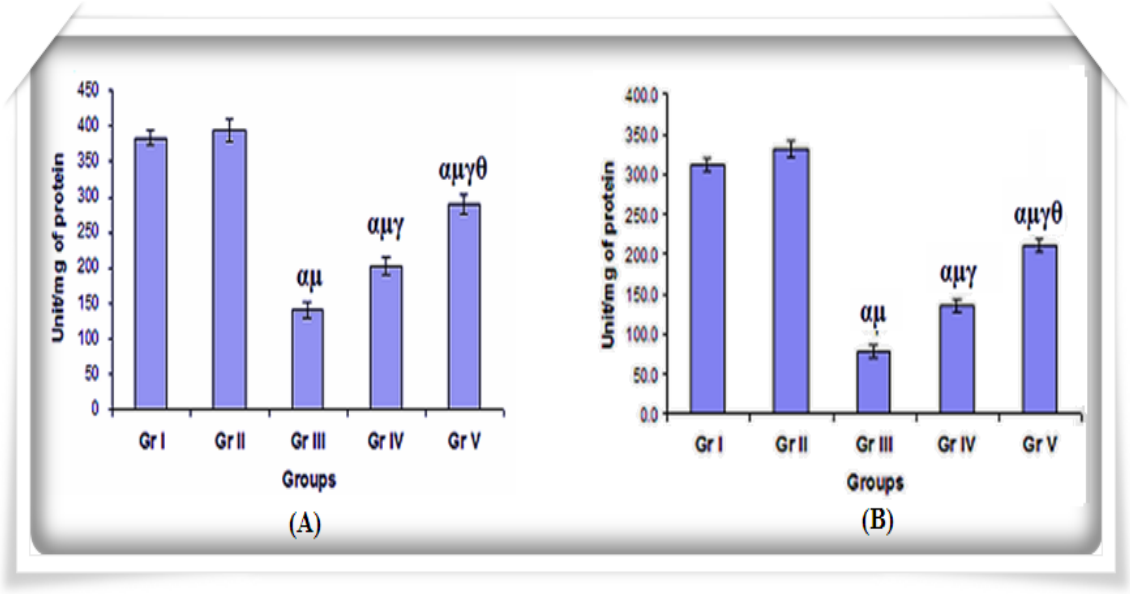

Figure 8: Data were represented as mean ± SD (n=6). α - significant (*P < 0.05*) as compared with Gr. I; μ - significant (*P < 0.05*) as compared with Gr. II; γ - significant (*P < 0.05*) as compared with Gr. III; θ - significant (*P < 0.05*) as compared with Gr. IV.

- **CAT activity**

The hepatic and pulmonary CAT activity was found to decrease significantly (*P < 0.05*) by 50.64% & 54.03% in CP treated group (Gr. III) in comparison to the vehicle treated group (Gr. I) **(Fig. 9A & B)**. Concomitant administration of Nano-Se (Gr. IV) resulted in a significant (*P* < 0.05) enhancement in hepatic CAT activity by 41.49% and pulmonary CAT activity by 51.4% in comparison to the CP treated group (Gr. III). Pretreatment (Gr. V) with the same compound increased the CAT activity significantly (*P* < 0.05) by 46.23% and 77.75% respectively in liver and lung as compared to the CP treated group (Gr. III).

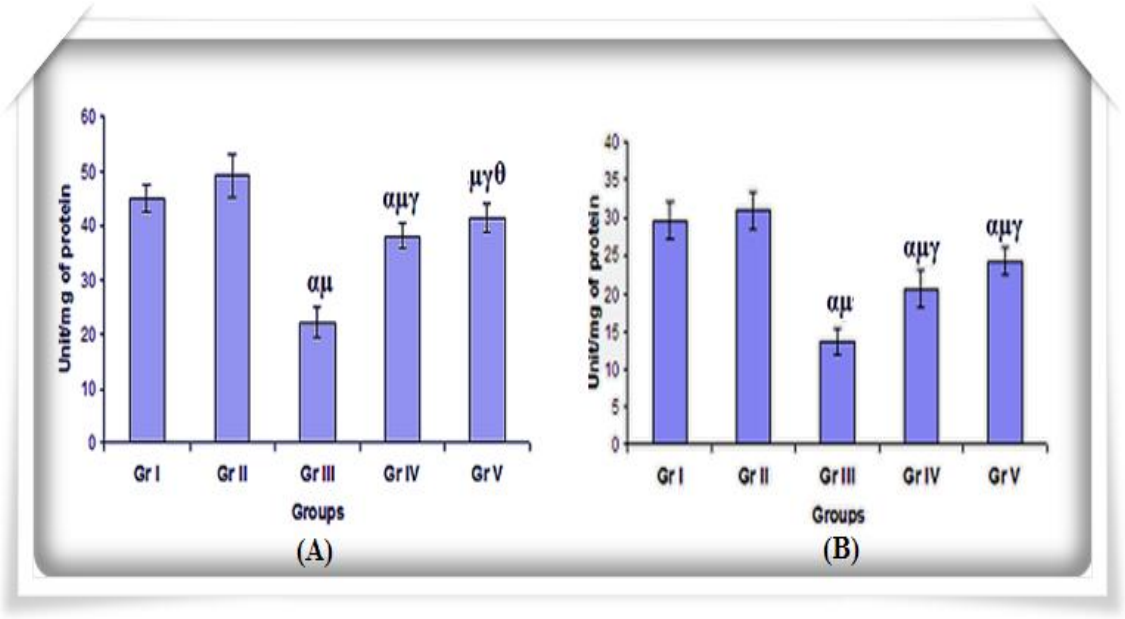

Figure 9: Data were represented as mean ± SD (n=6). α - significant (*P < 0.05*) as compared with Gr. I; μ - significant (*P < 0.05*) as compared with Gr. II; γ - significant (*P < 0.05*) as compared with Gr. III; θ - significant (*P < 0.05*) as compared with Gr. IV.

- **GP*x* activity**

Intraperitonial administration of CP (Gr. III) caused a significant ($P < 0.05$) reduction in GP*x* activity by 69.49% in liver and by 74.71% in lung in comparison to the vehicle treated group (Gr. I) **(Fig. 10A & B)**. Nano-Se in concomitant treatment schedule (Gr. IV) resulted in a significant enhancement of GP*x* activity by 32.39% in hepatocytes and by 69.46% in pneumocytes in comparison to the CP treated group (Gr. III), while in pretreatment schedule (Gr. V), the same compound significantly ($P < 0.05$) elevated the hepatic GP*x* activity by 65.33% and the pulmonary GP*x* activity by 241.22%, as compared to the CP treated group (Gr. III).

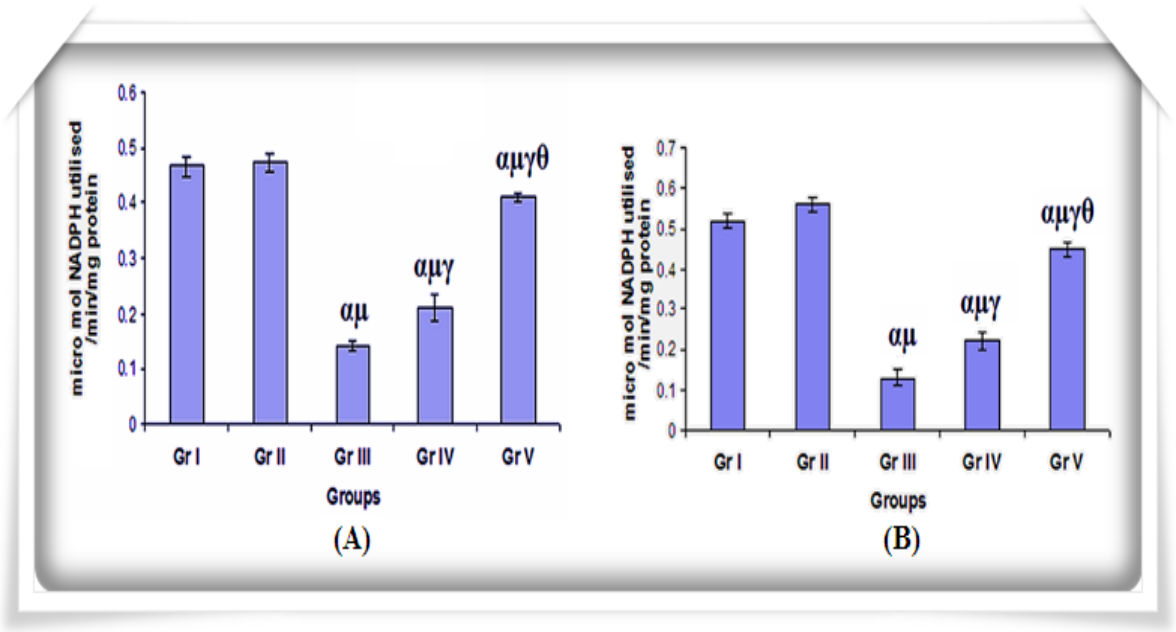

Figure 10: Data were represented as mean ± SD (n=6). α - significant ($P < 0.05$) as compared with Gr. I; μ - significant ($P < 0.05$) as compared with Gr. II; γ - significant ($P < 0.05$) as compared with Gr. III; θ - significant ($P < 0.05$) as compared with Gr. IV.

- **Serum ALT and AST activity**

The serum ALT and AST activity was increased significantly ($P < 0.05$) by 59.47% and by 44.28% in the CP treated group (Gr. III) in comparison to the vehicle treated group (Gr. I) **(Table. 1)**. Concomitant and pretreatment with Nano-Se along with CP (Gr. IV & Gr. V) significantly ($P < 0.05$) reduced the ALT activity by 47.71% & 58.82% and AST activity by 29.14% & 41.71% in comparison to the CP treated group (Gr. III).

Groups	ALT (U/ml)	AST (U/ml)
I	24.8 ± 2.28	156.0 ± 3.16
II	24.4 ± 2.96	154.0 ± 5.83
III	61.2 ± 3.03$^{\alpha\mu}$	280.4 ± 7.97$^{\alpha\mu}$
IV	32.0 ± 2.44$^{\alpha\mu\gamma}$	198.4 ± 8.76$^{\alpha\mu\gamma}$
V	25.2 ± 2.28$^{\gamma\theta}$	163.2 ± 3.63$^{\gamma\theta}$

Table 1: Data were represented as mean ± SD (n=6). α - significant ($P < 0.05$) as compared with Gr. I; μ - significant ($P < 0.05$) as compared with Gr. II; γ - significant ($P < 0.05$) as compared with Gr. III; θ - significant ($P < 0.05$) as compared with Gr. IV.

- **Hematological parameters and bone marrow and spleen cellularity**

The hemoglobin level in blood decreased significantly by 25.73% in CP treated group (Gr. II) in comparison to the vehicle treated group (Gr. I)**.** Concomitant treatment (Gr. III) and pretreatment (Gr. IV) with Nano-Se along with CP increased the hemoglobin level in blood significantly ($P < 0.05$) by 19.57% and 23.27% respectively as compared to the CP treated group (Gr. II).

The exposure of CP resulted in a significant ($P > 0.05$) decline in RBC and WBC counts. In addition to this, bone marrow as well as splenic cell counts also decreased significantly ($P < 0.05$) after CP treatment. This decreased cell counts in both the primary and secondary immune organs were significantly ($P < 0.05$) prevented on oral administration of Nano-Se in concomitant and pretreatment schedule.

Groups	Haemoglobin (mg/dl)	RBC (10^6/mm^3)	WBC (10^3/mm^3)	Bone Marrow cell count (x 10^6)	Splenic cell count (x 10^6)
I	14.38 ± 0.52	6.27 ± 0.33	6.61 ± 0.32	28.6 ± 1.76	89.44 ± 1.6
II	13.44 ± 1.21	6.37 ± 0.26	6.53 ± 0.49	29.45 ± 0.7	96.01 ± 1.09
III	10.68 ± 1.41$^{\alpha\mu}$	4.05 ± 0.49$^{\alpha\mu}$	3.22 ± 0.11$^{\alpha\mu}$	5.87 ± 0.87$^{\alpha\mu}$	15.47 ± 1.52$^{\alpha\mu}$
IV	13.28 ± 0.46$^{\gamma}$	4.67 ± 0.37$^{\alpha\mu\gamma}$	4.55 ± 0.21$^{\alpha\mu\gamma}$	10.07 ± 0.55$^{\alpha\mu\gamma}$	36.73 ± 1.04$^{\alpha\mu\gamma}$
V	13.92 ± 0.87$^{\gamma}$	5.75 ± 0.26$^{\gamma\theta}$	5.47 ± 0.19$^{\alpha\mu\gamma\theta}$	20.37 ± 1.73$^{\alpha\mu\gamma\theta}$	47.0 ± 1.12$^{\alpha\mu\gamma\theta}$

Table 2: Data were represented as mean ± SD (n=6). α - significant ($P < 0.05$) as compared with Gr. I; μ - significant ($P < 0.05$) as compared with Gr. II; γ - significant ($P < 0.05$) as compared with Gr. III; θ - significant ($P < 0.05$) as compared with Gr. IV.

- **Comet assay findings**

Comet assay was carried out to examine the CP induced DNA damage in lymphocytes **(Fig. 11A-E),** broncho alveolar lavage fluid (BALF) **(Fig. 12A-E)** and bone marrow **(Fig. 13A-E)** and for this purpose percentage of damaged cells and the average tail length was measured.

- **Percentage of damaged cells in each group**

The frequency of damaged lymphocytes, bronchoalveolar lavage cells and bone marrow were 12.65%, 7.8%, 10.02% respectively in Gr. I **(Table 3)**. The CP administration caused a significant ($P < 0.05$) increase in the percentage of damaged lymphocytes, bronchoalveolar lavage cells and bone marrow cells by 53.69%, 60.05% and 49.51% respectively in Gr. III. In case of concomitant group (Gr. IV), the percentages of damaged cells were reduced to 42.41% in lymphocyte, 36.4% in bronchoalveolar lavage cells and 34.95% in bone marrow cells respectively. However pretreatment (Gr. V) with Nano-Se sharply decreased the percentage of damaged cells to 32.21%, 28.07% and 26.58% respectively, in lymphocytes, bronchoalveolar lavage cells and bone marrow cells.

- **Average Tail Length due to DNA Migration in each group**

The magnitudes of average tail length were 15.69 ± 1.67 µm, 7.13 ± 1.06 µm and 7.29 ± 1.30 µm respectively, in lymphocyte, bronchoalveolar lavage cells and bone marrow cells in Gr. I. CP caused a marked increase in the magnitude of tail length to 66.72 ± 2.89 µm in lymphocyte, 50.04 ± 3.70 µm in bronchoalveolar lavage cells and 55.39 ± 3.83 µm in bone marrow cells in Gr. III (**Table 3**). Oral administration of Nano-Se in concomitant (Gr. IV) and pretreatment (Gr. V) schedule, resulted in the reduction of average tail length to 42.13 ± 1.55 µm and 23.07 ± 1.04 µm respectively, in case of lymphocytes, in bronchoalveolar lavage cells 30.55 ± 1.94 µm and 21.27 ± 2.94 µm respectively and 21.45 ± 2.45 µm and 11.8 ± 1.81 µm, respectively in bone marrow cells.

Groups	Peripheral Lymphocyte		Bronchoalveolar lavage cells		Bone Marrow	
	Damaged cells showing comet (%)	Average tail length (µm)	Damaged cells showing comet (%)	Average tail length (µm)	Damaged cells showing comet (%)	Average tail length (µm)
I	12.65 ± 0.83	15.69 ± 1.67	7.8 ± 1.38	7.13 ± 1.06	10.02 ± 1.90	7.29 ± 1.30
II	11.77 ± 1.45	14.03 ± 1.42	10.2 ± 1.34	8.15 ± 1.12	9.95 ± 1.08	6.99 ± 0.74
III	$53.69 \pm 1.18^{\alpha\mu}$	$66.72 \pm 2.89^{\alpha\mu}$	$60.05 \pm 2.87^{\alpha\mu}$	$50.04 \pm 3.70^{\alpha\mu}$	$49.51 \pm 3.55^{\alpha\mu}$	$55.39 \pm 3.83^{\alpha\mu}$
IV	$42.41 \pm 2.54^{\alpha\mu\gamma}$	$42.13 \pm 1.55^{\alpha\mu\gamma}$	$36.42 \pm 2.34^{\alpha\mu\gamma}$	$30.55 \pm 1.94^{\alpha\mu\gamma}$	$34.95 \pm 3.23^{\alpha\mu\gamma}$	$21.45 \pm 2.45^{\alpha\mu\gamma}$
V	$32.21 \pm 1.29^{\alpha\mu\gamma\theta}$	$23.07 \pm 1.04^{\alpha\mu\gamma\theta}$	$28.07 \pm 1.87^{\alpha\mu\gamma\theta}$	$21.27 \pm 2.94^{\alpha\mu\gamma\theta}$	$26.58 \pm 3.03^{\alpha\mu\gamma\theta}$	$11.8 \pm 1.81^{\alpha\mu\gamma\theta}$

Table 3: Data were represented as mean ± SD (n=6). α - significant ($P < 0.05$) as compared with Gr. I; µ - significant ($P < 0.05$) as compared with Gr. II; γ - significant ($P < 0.05$) as compared with Gr. III; θ - significant ($P < 0.05$) as compared with Gr. IV.

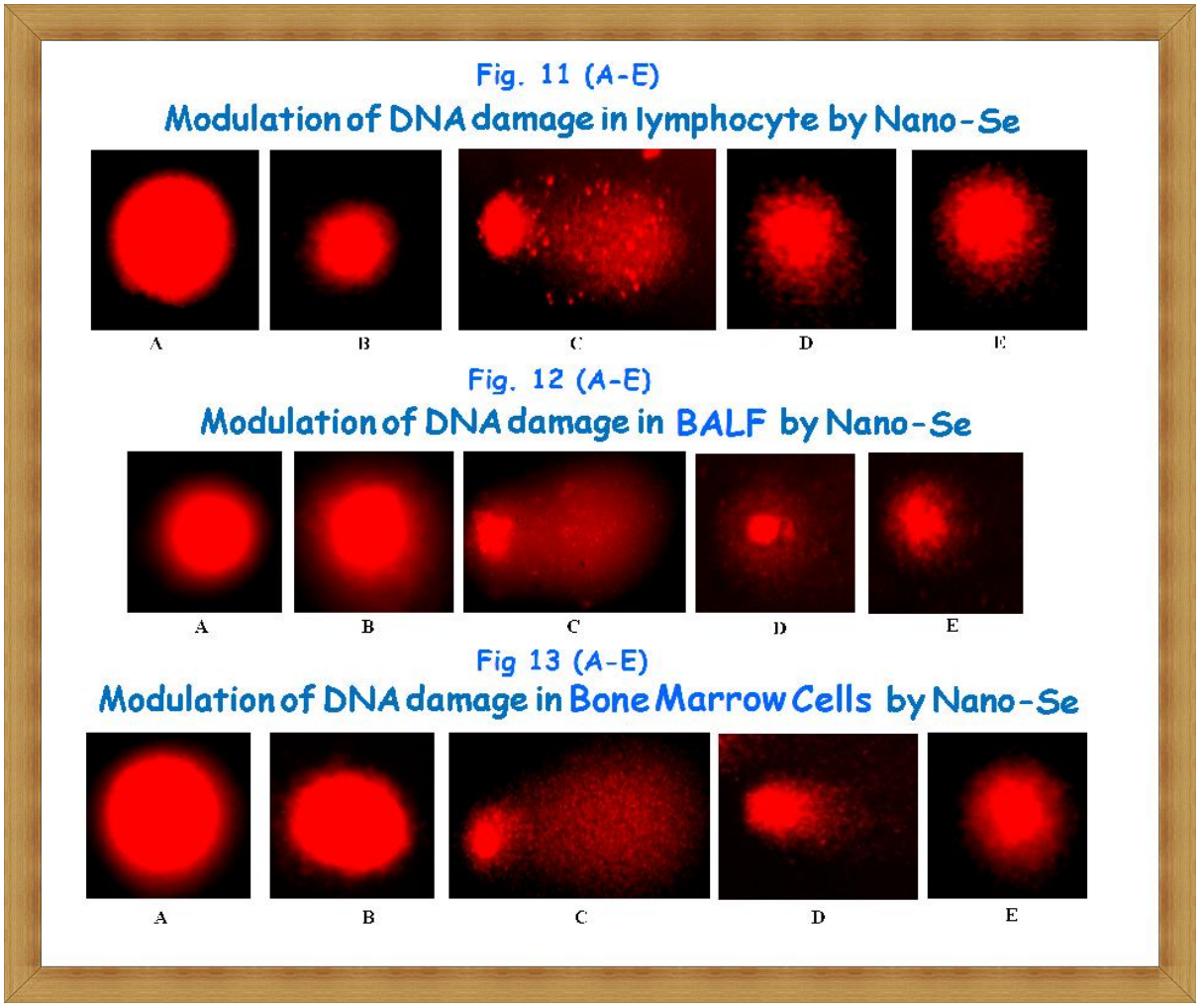

Figure 11, 12, 13: Microphotograph of lymphocyte **(11: A-E)**; bronchoalveolar fluids **(12: A-E)**; bone marrow **(13: A-E)**: (A) vehicle treated (no DNA damage), (B) Nano-Se treated very fewer DNA migrations (C) Cyclophosphamide treated (showing highly migrated DNA with scattered comet tail), (D) Concomitant treatment (less migrated DNA) and (E) Pretreatment (showing no marked DNA migration)

- **Chromosomal aberrations**

The magnitude of chromosomal aberrations was estimated to be 12.67% in vehicle treated group (Gr. I) **(Fig. 14A)**. Due to the administration of CP (Gr. III), the proportion of CA was raised significantly ($P < 0.05$) to 41.13%. The Nano-Se provided significant ($P < 0.05$) protection against the genotoxicity imparted by CP, and the frequency of CA was reduced to 27.85% in case of concomitant treatment group (Gr. IV) and to 21.24% in case of pretreatment group (Gr. V). Different types of CA have been shown in **Fig. 14B.**

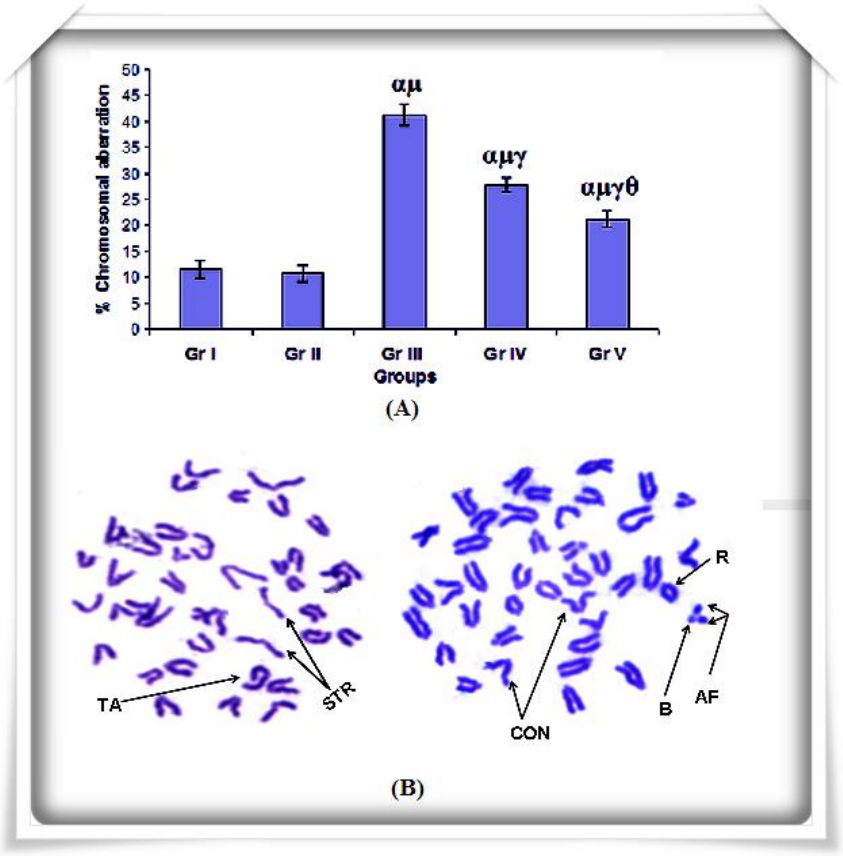

Figure 14 A: Data were represented as mean ± SD (n=6). α - significant ($P < 0.05$) as compared with Gr. I; μ - significant ($P < 0.05$) as compared with Gr. II; γ - significant ($P < 0.05$) as compared with Gr. III; θ - significant ($P < 0.05$) as compared with Gr. IV.

Figure 14 B: Metaphase complements showing stretching (STR), Terminal association (TA with arrow) and Ring formation (R), Constriction (CON), Break (B) and Acentric fragment (AF).

➢ **DNA fragmentation**

Genomic DNA fragmentation in bone marrow cells was found 6.71% in vehicle treated group (Gr. I). CP administration caused a significantly ($P < 0.05$) greater rate (52.55%) of DNA fragmentation in CP treated group (Gr. III) of mice. In case of concomitant and 7 days pretreatment, the percentages of DNA fragmentation were reduced to 39.08% (G. IV) and 24.56% (Gr. V), respectively **(Fig. 15)**.

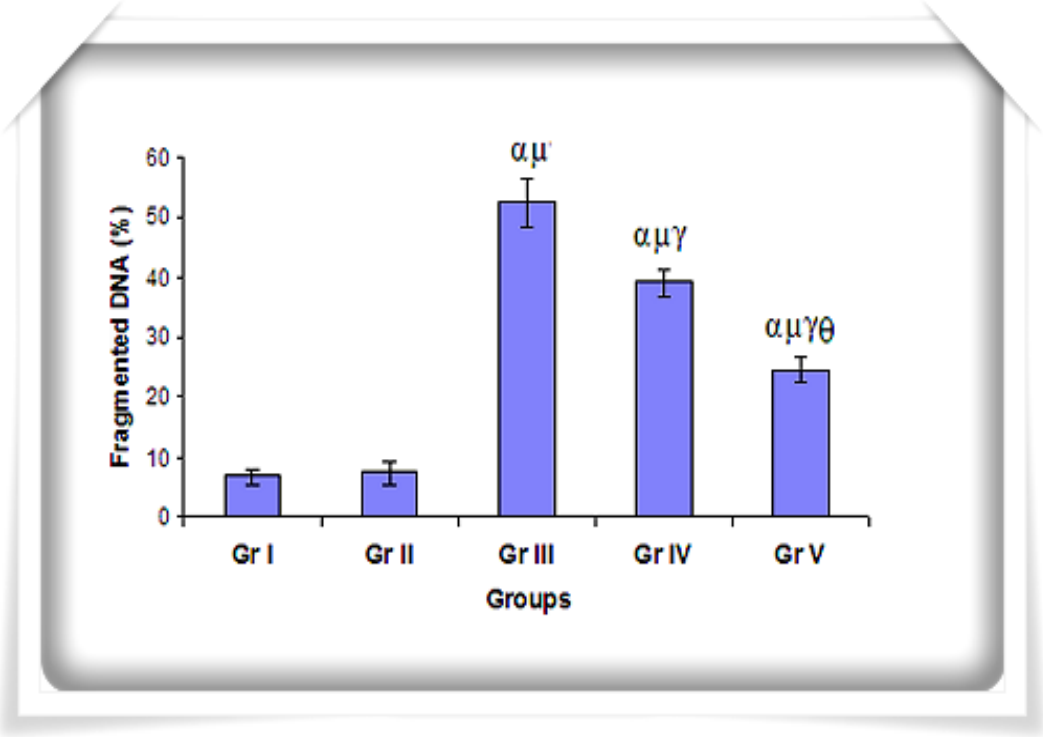

Figure 15: Data were represented as mean ± SD (n=6). α - significant ($P < 0.05$) as compared with Gr. I; μ - significant ($P < 0.05$) as compared with Gr. II; γ - significant ($P < 0.05$) as compared with Gr. III; θ - significant ($P < 0.05$) as compared with Gr. IV.

- **Apoptosis in bone marrow cells**

The results obtained from the acridine orange–ethidium bromide double staining are shown in **(Fig. 16A-B)**. Acridine orange is a vital dye that stains both live and dead cells, whereas ethidium bromide will stain only those cells that have lost their membrane integrity. Cells stained green represents viable cells, whereas yellowish–red staining represents apoptotic cells. The cells in CP treated group, due to the increase in cell membrane permeability, showed green and red fluorescence. The cells pre-treated with Nano-Se before CP administration, showed green and slight red fluorescence with few apoptotic cells and nucleus fragmented or apoptotic bodies. In contrast, the cells in vehicle control and Nano-Se groups all showed green fluorescence and normal structures.

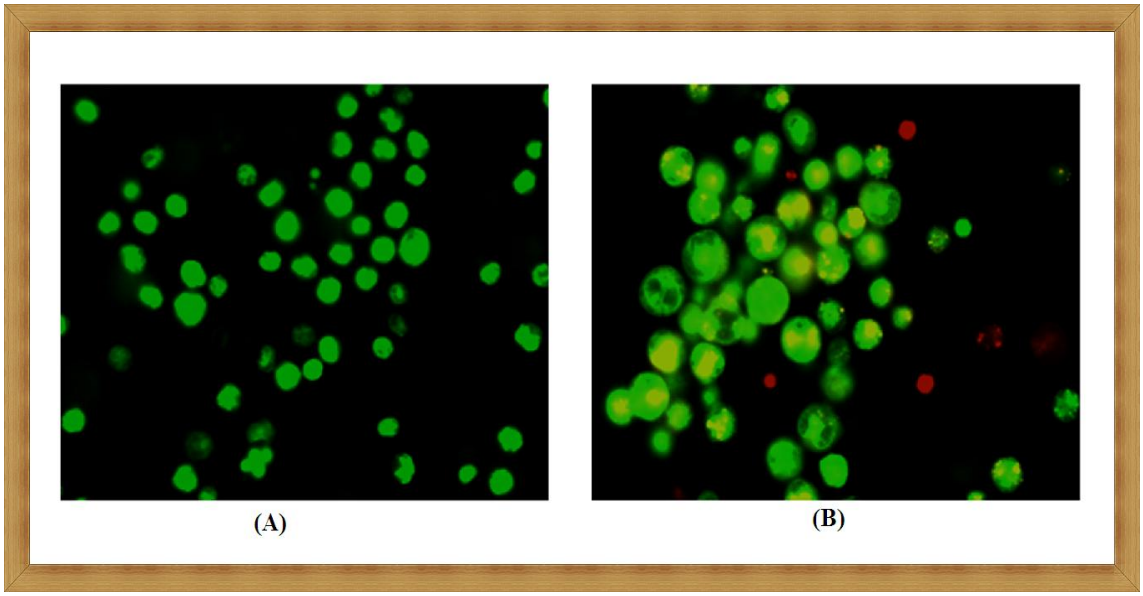

Figure 16A-B: Effect of Nano-Se against CP-induced cell morphological changes with fluorescence microscope in mouse bone marrow cells. (A) Cells were stained green and showed normal structure, (B) Cell structure was damaged, the cells are not only stained with AO and EB, but the fragmented or apoptotic bodies could be seen clearly

- **Histopathological examination**

Histology of liver and lung from different groups of mice has been shown in **Fig. 17-18**. Histopathological evaluation was used as confirmatory diagnostic test to prove the hepatotoxic and pulmonary toxic effect of CP and hapatoprotective and pulmonary protective potential of the Nano-Se. After 10 days of CP administration, various histopathological lesions were observed in experimental mice. In case of liver, dilatation of central vein, necrosis of hepatocytes and inflammatory cellular infiltration were showed. In another organ like lung, when treated with CP, the lung of experimental mice showed various histopathological lesions like pulmonary fibrosis, thickened alveolar septa, pulmonary congestion, pulmonary inflammation and distortion of alveoli. Such lesions were successfully attenuated by the administration of Nano-Se, where the most effective attenuation was exerted by the administration of test compound in the pretreatment schedule.

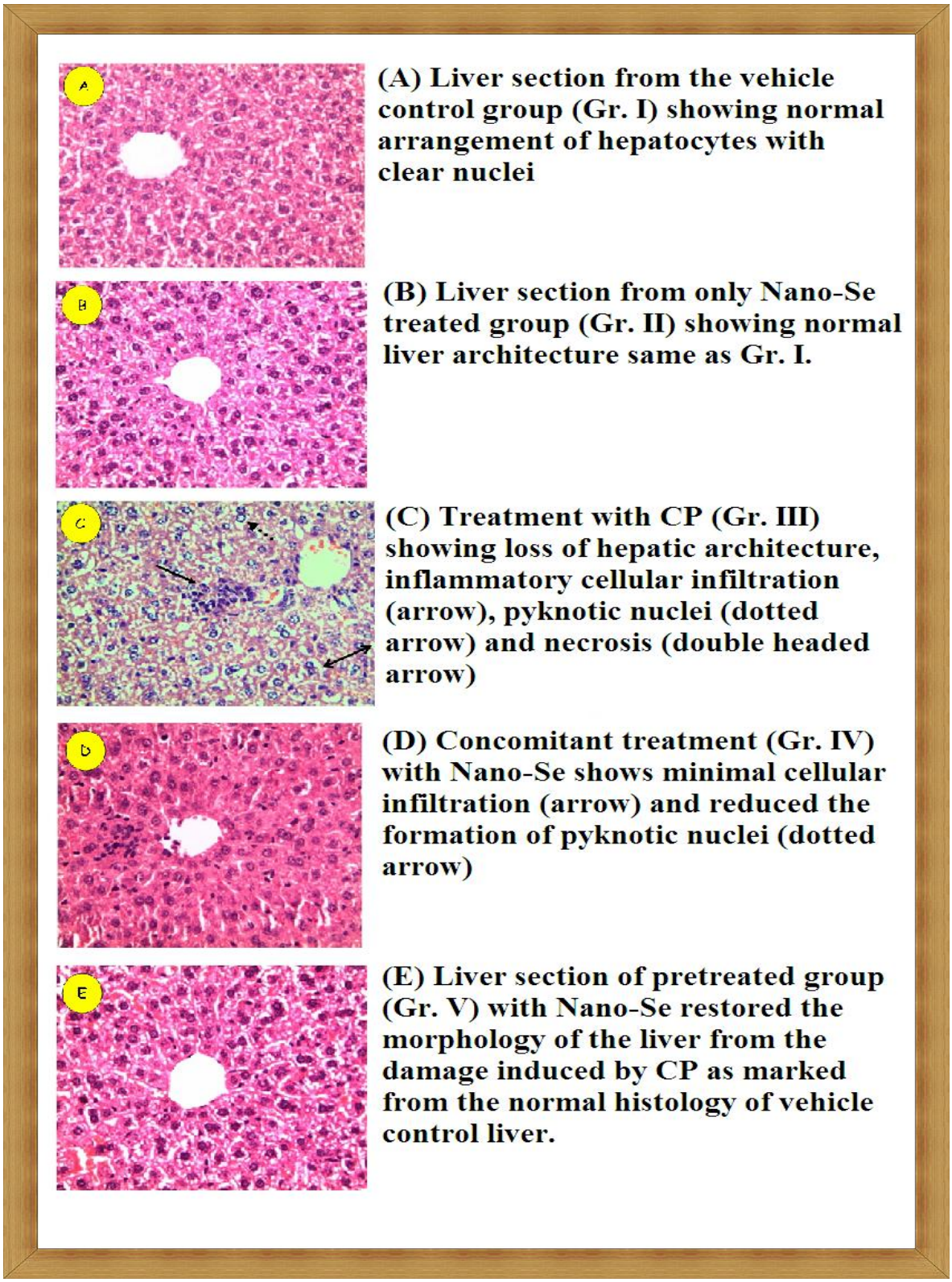

Figure 17: Photograph of liver section of mice stained with hematoxylin and eosin, ×200

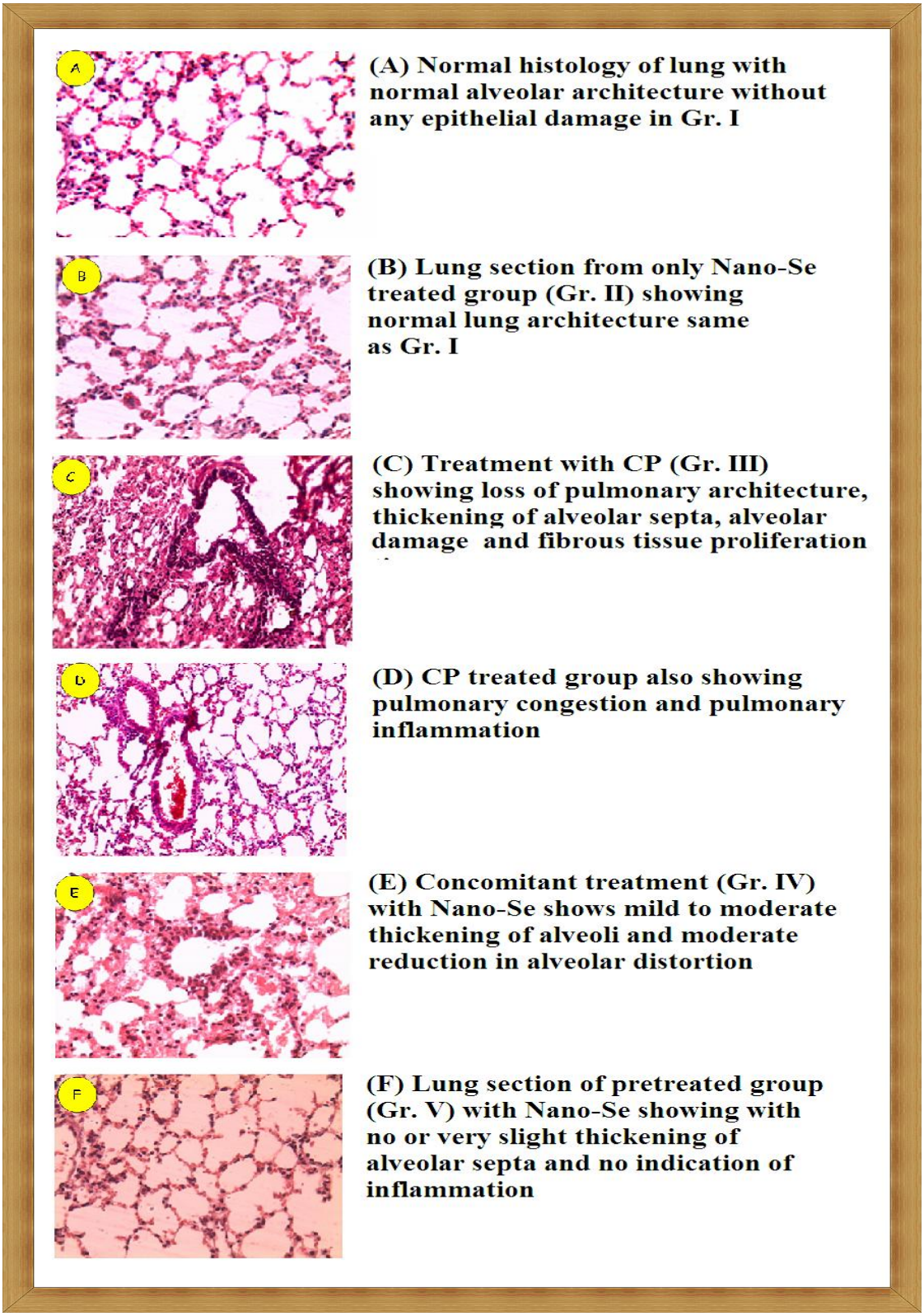

Figure 18: Photograph of lung section of mice stained with hematoxylin and eosin, ×200

Discussion

Despite the ever increasing population of chemotherapeutic agents, including several anti-cancer drugs cyclophosphamide, the clinical outcome of treatments with these agents is severely limited, mostly due to their toxicity to normal tissues. Such commonly used anticancer agents fail to discriminate normal cells from cancerous cells. It is well known that the redox balance of a cell is disturbed during the production of ROS, causing oxidative stress, DNA damage and finally the cell death **(Matés 1999)**. During the metabolism of CP, ROS are produced and catalysed by cytochrome P450, peroxidases and lipooxygenases **(Kanekal et al. 1994)**. Biotransformation of cyclophosphamide mainly occurs in the liver; it is metabolized by cytochrome P450 to yield 4-hydroxy-CP, phosphoramide mustard, and acrolein. These metabolites can alkylate nucleophilic sites in DNA, RNA, and protein such as –SH, –COOH, $–NH_2$, and –OH **(Fraiser et al. 1991)** which cause cellular toxicity, genotoxicity and mutagenic effects **(Zhang et al., 2008)**. The present investigation was carried out to evaluate the chemoprotective potential of Nano-Se against oxidative stress mediated cellular toxicity induced by CP in Swiss albino mice.

CP has a pro-oxidant character and its treatment is associated with induction of oxidative stress through the generation of free radicals **(Basu t al., 2015)**. LPO is used as a biomarker to show the index of oxidative stress, produces cell membrane damage, gradual loss of cell membrane fluidity, decreases membrane potential and increases permeability to ions **(Das et al., 2013)**. In the process of LPO, malonaldehyde (MDA) is formed by the conversion of polyunsaturated fatty acid or lipid peroxides. Increased free radical production stimulates LPO and is the sources for the degradation of DNA, lipids and carbohydrates **(Ghosh et al., 2015)**. In the present study, due to the induction of LPO by CP, the level of TBARS was found to increase in liver and lung tissues of experimental mice. This might be due to the increased production of free radicals or decreased antioxidant status. Following the administration of Nano-Se, the levels of TBARS were maintained to near normal status which indicates the reduced level of LPO. From this, it may be concluded that inhibition of CP-induced lipid peroxidation could be attributed to the free radical quenching activity of Nano-Se and thus protecting against oxidative membrane damage in mice.

Several mechanisms have been proposed to explain the adverse health effects of chemotherapeutic drug. ROS production and the generation of oxidative stress have received the most attention. ROS, such as superoxide, hydrogen peroxide, hydroxyl and other oxygen radicals, are capable of directly oxidizing the DNA, proteins, and lipids **(Yoshida et al., 2004)**. DCFH-DA is a nonfluorescent probe that is hydrolyzed by mitochondrial esterase to form 2',7'-dichlorodihydrofluorescein (DCFH), which is then oxidized by ROS to form the fluorescent compound 2',7'-dichlorofluorescein (DCF). Another one, DHE is a non-fluorescent dye and freely permeable to the cell. **(Basu et al., 2014)**. The oxidation of DHE to fluorescent compound ethidium is mainly modulated by superoxide anion whereas, DCFH-DA as a cell permeable specific dye probe fluoresces to 2′, 7′-dichlorofluorescein (DCF) which is mainly regulated by H_2O_2 **(Halliwell et al., 2004)**. In this study, CP treatment substantially elevated H_2O_2 and superoxide levels in hepatic and lung as well as bone marrow cells of experimental mice as measured by DCFH-DA and DHE, respectively. Treatment with Nano-Se prevented elevation of CP induced ROS generation which could be attributed to free radical scavenging activity of the test compound.

Reactive nitrogen species (RNS), including nitric oxide (NO), peroxynitrite ($ONOO^-$) and nitrogen dioxide, which are released from neutrophils and macrophages, play an important role in the pathogenesis of lung diseases as well as hepatic disorders **(Boyaci et al., 2006)**. NO is synthesized from L-arginine by the enzyme nitric oxide synthase (NOS). NO reacts spontaneously with available superoxide radical to form the more potent and versatile oxidant peroxynitrite (ONOO-) which can damage DNA, initiate membrane lipid peroxidation **(Radi et. al., 1991)**, depleted antioxidant enzyme activity and reduce glutathione content **(Luperchio et. al., 1996)**. In the present study, the hepatic and pulmonary NO levels were found to increase after administration of CP. The Nano-Se successfully ameliorated this enhancement in hepatic as well as pulmonary NO levels. This result suggests the ability of Nano-Se in preventing CP-induced nitrosative stress.

Non-enzymatic antioxidants like glutathione (GSH) is considered as second line of defense and protect the cells against oxidative stress mediated cellular injury either by scavenging free radicals or by converting the toxic radicals to non-toxic end products **(Basu et al., 2016)**. CP metabolism produces highly reactive electrophiles. The decreased

level of GSH in CP treated group most probably due to the electrophilic burden on the cells and also due to the formation of acrolein, which deplete GSH content **(Yousefipour et al., 2005)**. GSH depletion leads to lowering of cellular defense against free radical induced cellular injury resulting in necrotic cell death **(Srivastava et al., 2010)**. In the present study, the result showed that the mechanism of protection by Nano-Se against CP induced hepatic toxicity and pulmonary damage involves suppression of oxidative stress by preventing GSH depletion.

GSH metabolizing enzyme GST, catalyses the detoxification of endogenous compounds such as lipid peroxide, as well as the metabolites of xenobiotics like acrolein, a metabolite of CP, through conjugation of GSH via the sulfhydryl group **(Jagetia et al., 2011)**. GST activity has been shown to be decreased significantly by CP administration, treatment with Nano-Se restored the activity near to vehicle treated group both in liver and lung and making the cells more effective with respect to detoxification of toxic metabolites. Moreover the elevated level of GSH could effectively provide thiol group for the possible GST mediated detoxification reactions.

The selenium-containing glutathione peroxidase (GP*x*) contains a single selenocysteine (Sec) residue, which is essential for enzyme activity **(Talas et al., 2010)**. GP*x* catalyses the reduction of hydroperoxides utilizing GSH, thereby protecting mammalian cells against oxidative damage. In fact, glutathione metabolism is one of the most essential antioxidative defense mechanisms **(Sigalov et al., 1998)**. The decreased activity of the antioxidant enzyme GP*x* in this study after administration of CP may be either due to the decreased level of GSH as a substrate or inability of organ (liver and lung) to produce this enzyme. Treatment with Nano-Se prevented the depletion of GP*x* activity in liver and lung; thus providing protection of biomembrane from oxidative attack.

Cellular antioxidant defences involving the enzymes, SOD and CAT play an important role against ROS generation during oxidative stress and protect tissues including liver and lung from oxidative damage **(Das et al., 2013)**. SOD catalyzes dismutation of the superoxide anion to H_2O_2 and O_2. The harmful H_2O_2 is further detoxified to water by CAT. Therefore, the activity of theses antioxidant enzymes is a vital protection against oxidative stress. In this study, the activities of the antioxidant enzymes SOD and CAT in the mice liver and lung were significantly reduced by CP administration indicating

pronounced oxidative stress. SOD activity was drastically reduced which was corroborated with elevated superoxide anion level in the liver and lungs of CP treated mice. On the other hand, depletion of the activities of CAT resulted in enhanced level of H_2O_2 found in this study. Nano-Se administration produced a significant protection against CP induced changes in antioxidant enzyme activity by restoring them to normal by preventing the induction of oxidative stress and enhancing the hepatic as well as pulmonary antioxidant defenses involving SOD and GSH-dependant enzymes.

ALT and AST are the most sensitive biomarkers directly implicated in the extent of hepatic damage and toxicity. Elevated levels of serum enzymes are indicative of cellular damages and loss of functional integrity of cell membrane in liver **(El-Demerdash, 2004**). Damage to liver cells cause release of cellular enzymes in to serum. Hepatic activation of CP leading to the formation of toxic metabolites caused damage to the liver tissues as shown by increased ALT and AST levels. Treatment with Nano-Se resulted in significant reduction in the level of these transaminase activities. The most common problems encountered in cancer chemotherapy are myelosuppression and anemia **(Groopman, 1991)**.

Chemotherapy inevitably leads to the decrease in bone marrow function that reflects by a substantial decrease in the mature blood elements **(Blackwell, 1994)**. This is because chemotherapeutic drugs kill rapidly dividing cells in the body, including cancer cells and normal cells which include red blood and white blood cells at the same time suppress bone marrow ability to produce new ones, resulting in decrease in blood Hb level. In this study, treatment with CP reduced the blood Hb level which was also attenuated by the treatment with Nano-Se.

Various cytogenic biomarkers have been used to determine cellular DNA damage. The Comet assay or single cell gel electrophoresis (SCGE) is a widely used technique for measuring and analysing DNA breakage in individual cells **(Singh et. al., 1988)**. It combines the simplicity of biochemical techniques for detecting DNA single strand breaks (strand breaks and incomplete excision repair sites), alkali labile sites, and cross-links, with the single cell approach typical of cytogenetic assays. CP can induce DNA–DNA and DNA–protein crosslinks and also generate reactive species, for damaging DNA (**Basu et al., 2016**). In the present study, the percentage of affected cells showing a comet

tail significantly increased after CP treatment in blood lymphocytes, bronchoalveolar lavage fluid (BALF) as well as in bone marrow cells, whereas treatment with Nano-Se significantly decreased DNA damage in peripheral lymphocyte cells, BALF and also in bone marrow cells, which clearly indicated the potential role of Nano-Se in protecting DNA damage.

CP, an indirect-acting mutagen, damages chromosomes through generation of free radicals and alkylating DNA thereby producing mutation **(Słoczyńska et al., 2014)**. Genotoxic activity of CP resulted from metabolic activation to the highly reactive metabolite phosphoramide mustard. CP produces chromosome damage and micronuclei formation in the erythropoietic system of rats, mice, and Chinese hamsters via production of highly active carbonium ions **(Young et al., 2013)**. In the present investigation, animals treated with CP presented a significant increase in total number of CA in bone marrow cells when compared to the vehicle treated animals. Treatment with Nano-Se produced significant reduction of CA in bone marrow cells. Some studies suggest that CP induced apoptosis, as indicated by the derivatives of CP to stimulate outer membrane blebbing and DNA fragmentation **(Tan et al., 2014)**. In this study, percentage of DNA fragmentation assay and apoptosis were performed in murine bone marrow cells. CP administration, at a dose of 25 mg/kg b.w triggered the percentage of DNA fragmentation in bone marrow cells. The AO/EB staining assay further demonstrated that CP increased the number of apoptotic cells in the bone marrow. Taken together, it is clear that CP can cause DNA damage and apoptosis in non-tumor cells, which can potentially lead to the secondary mutagenesis and carcinogenesis when it is used for chemotherapy **(Ferguson, 1996)**. Treatment with Nano-Se reduced the percentage of DNA fragmentation and number of apoptotic cells in bone marrow cells.

Hepatic and pulmonary damages in CP treated mice were also established by histopathological evaluation. When the liver of the mice is exposed to CP following abnormalities were visible such as, inflammatory cellular infiltration in between degenerated hepatocytes, formation of pyknotic nuclei, and hepatocellular necrosis. In the same way, lung tissues of CP-treated animals showed distinct cellular and architectural changes including pulmonary congestion, pulmonary inflammation, thickened alveolar septa, and distortion of alveoli. These observations indicated marker changes in the

overall histoarchitecture of liver as well as of lungs in response to CP, which could be due to its toxic effects primarily by the generation of reactive oxygen species causing damage to the various membrane components of the cell. Nano-Se treatment alone induced no remarkable alteration in lung histology. However, Nano-Se when administered in combination with CP either in concomitant or pretreatment schedule, a protective effect of Nano-Se was revealed, where the most effective protection was exerted by the administration of test compound in the pretreatment schedule.

This study demonstrates for the first time that Nano-Se has a protective role in the abatement of CP-induced hepatic and pulmonary toxicity and the subsequent DNA damage in both the peripheral blood and the bone marrow cells of mice. In conclusion, the present studies further demonstrated that CP may induce oxidative stress, genotoxicity, and trigger apoptosis in lungs and in bone marrow cells also. Nano-Se, a pharmacologically active and less toxic new form of selenium reduced CP-induced functional and histological damage in liver, lung as well as genotoxicity. Furthermore, Nano-Se suppressed the generation of ROS, lipid peroxidation, and oxidative stress. This protective effect resides, at least in part, in its radical scavenger activity. The improvement of anti-genotoxic activity on bone marrow cells of animal pre-treated with Nano-Se against CP toxicity may focus attention on the beneficial effect of Nano-Se to overcome one of the serious problems in cancer chemotherapy, namely the bone marrow suppression and related immunosuppression. Therefore, Nano-Se can be a promising chemoprotective agent and may be useful to avert secondary malignancy and to reduce the risk for abnormal reproductive outcomes in cancer patients and medical personnel exposed to CP.

Chapter III

Chemoprotective and chemoenhacing properties of Nano–Se against cyclophosphamide induced cellular toxicities without compromising its antitumor properties in Swiss albino mice bearing Ehrlich ascites carcinoma cells

Introduction

Nanotechnology and nanoengineering stand to produce significant scientific and technological advances in diverse fields including pathology and medicine. The combination of cancer biology and nanotechnology has led to the development of an interdisciplinary area, cancer nanotechnology, which shows broad applications in molecular imaging, molecular diagnosis, and targeted therapy **(Nie et al., 2007)**. The excellent performance of bionanomaterials opens novel horizons for diagnosis and therapy of diseases such as malignant neoplasms that have traditionally been recognized as incurable via basic therapies or surgical methods **(Rozhkova et al., 2009)**.

Cancer chemotherapy is the major therapeutic modalities used for the treatment of a large number of cancer patients. However, in many cases, chemotherapy alone cannot achieve a satisfactory therapeutic outcome, namely the complete remission of tumors, and induction of severe form of toxicity at therapeutically effective doses. Most of the commonly used anticancer drugs currently used in chemotherapy are nonspecific in action; hence cytotoxic to normal cells, leading to unwanted adverse effects. Chemotherapy associated adverse effects in cancer patients have been linked to generation of oxidative stress in normal organs and tissues **(Conklin, 2004)**. CP is a bifunctional alkylating agent and has been in the clinic since the late-1950s, indicated for various form of malignancies in combination with other chemotherapeutic drugs **(kim et al., 2014)**. Although the broad-spectrum clinical applications of cyclophosphamide for tumor treatment, as a double-edged sword, severe toxic side effects, hemopoetic suppression, hepatotoxicity, immunotoxicity, mutagenicity, urotoxicity, cardiotoxicity, teratogenicity and carcinogenicity **(Basu et al., 2015)**. In view of the drawbacks of

chemotherapy agents, there is an urgent need for a sensitizing agent which can selectively exert its cytotoxic effect towards cancer cells when used alone or in combination with other chemotherapeutic agents, at the same time protecting the normal cells.

Selenium (Se) is one of the essential trace elements present in the body and has great importance in maintaining physiological homeostasis **(Ghosh et al., 2015)**. High levels of selenium in blood plasma have been correlated with prevention of several types of cancers, several cardiovascular diseases, muscle disorders, and, to a certain extent, diabetes mellitus **(Navarro-Alarcón and López-Martínez, 2000)**. The role of selenocompounds as chemopreventive and chemotherapeutic agents has been supported by a large number of epidemiological, preclinical and clinical studies **(Gao et al., 2014)**. Results from epidemiologic, ecological and clinical studies have shown Se has the potential to reduce the incidence of some cancers, such as prostate, lung and colon cancers **(Kong et al., 2011)**. Accumulative evidences have suggested that the dose and the chemical form (structure) are determinants for anticancer activities of selenocompounds **(El-Bayoumy et al., 2004)**. Several different kinds of Se compounds, such as selenomethionine (SeMet), sodium selenite, monomethylated Se etc, had been tested for their chemotherapeutic activity **(Fernandes and Gandin, 2015)**. They are more effective at high dosage, however high dosage of these compounds incurs some side effects **(Whanger et al., 1996)**. Se occurs in a variety of oxidation states, like selenate (SeO_4^{2-})/ selenite (SeO_3^{2-}) oxyanions, wherein the oxidation states are +6 and +4; elemental selenium (Se^0), and selenide (Se^{2-}) **(Dhanjal et al., 2010)**. The toxicity of these states is related to their degrees of solubility in water and hence their bioavailability. In recent times, there has been increasing interest in medicinal importance of nanoparticles using biological systems leading to the development of various biomimetic approaches. Nano-sized particles exhibit unique properties that arise from their larger surface/volume ratio and higher surface energy **(Prasad et al., 2013)**. Recently, the introduction of nanosize elemental selenium produces a highly effective molecular compound in medical diagnostics and therapy. It showed similar efficacy in increasing antioxidant GP*x* activity while displaying lower toxicity when compared to SeMet **(Wang et al., 2015)**. These nanoparticles also show better biological activity due to good adsorptive ability as a

result of interaction between the nanoparticles and NH, C=O, COO– and C-N groups of proteins present in the cell membrane **(Hassanin et al., 2013)**.

The present study was designed to examine the antitumor efficacy of synthesized Nano-Se in the tumor bearing Swiss albino mice. In this study design, Nano-Se was administered along with a widely used broad spectrum chemotherapeutic agent CP to investigate the 'chemoprotective' (protection against chemotherapeutic drug induced toxicity) and 'chemosensitization' (potentiation of cytotoxicity of chemotherapeutic drugs towards tumor cells) efficacy of Nano-Se.

Materials and methods

Experimental animals

Adult (5–6 weeks) Swiss albino female mice (25 ± 2g), bred in the animal colony of Chittaranjan National Cancer Institute (CNCI) (Kolkata, India), were used for this study. The mice were maintained under standard condition of humidity (45–55%), temperature (23 ± 2ºC), and light (12 h light/12 h dark). Standard food pellets (EPIC rat and mice pellet) from Kalyani Feed Milling Plant, Kalyani, West Bengal, India and drinking water was provided *ad libitum*. The experiments were carried out following strictly the Institute's guideline for the Care and Use of Laboratory Animals.

Chemicals

Cyclophosphamide was obtained from Cadila Pharmaceuticals (Bhat, Ahmedabad, India). 1-Chloro-2, 4-dinitrobenzene (CDNB), ethylene diamine tetraacetic acid (EDTA), reduced glutathione (GSH), pyrogallol, 5,5´-dithio-bis (2-nitro benzoic acid) (DTNB), sodium dodecyl sulphate (SDS), bovine serum albumin (BSA), β-nicotinamide adenine dinucleotide phosphate (reduced), glutathione reductase, normal melting agarose, low melting point agarose, ethidium bromide, sodium azide (NaN_3), HEPES, 2´,7´- dichloro fluorescence diacetate (DCFH-DA), dimethyl sulphoxide (DMSO), Triton-X 100 and Giemsa stain were obtained from Sigma-Aldrich Chemicals Private Limited, Bangalore, India. Hydrogen peroxide 30% (H_2O_2) and thiobarbituric acid (TBA), propylene glycol, sodium carbonate, copper sulfate, sodium hydroxide, potassium-sodium tartarate, sucrose, TRIS, dithiothreitol, calcium chloride, di-sodium hydrogen phosphate, sodium di-hydrogen phosphate, acetic acid, n-butanol, pyridine, hematoxylin and eosin were

obtained from Merck (India) Limited, Mumbai, India. Chloroform and Folin-phenol reagent were purchased from Sisco Research Laboratories Private Limited, Mumbai, India. Magnesium chloride was purchased from Glaxo laboratories (India) Ltd, Bombay. Diethyl ether, dipotassium hydrogen phosphate and potassium dihydrogen phosphate were obtained from Spectrochem Private Limited, Mumbai, India. Serum alanine transaminas (ALT) and aspartate transaminase (AST) assay kits were obtained from Span Diagnostics Ltd, Udhna, Surat, India. In situ cell detection kit and Mouse Total MMP-9 ELISA Kit were purchased from Roche Molecular and R&D system USA respectively.

Experimental design

Tumor cells

EAC cells were maintained in Swiss albino mice by weekly intraperitoneal (i.p.) transplantation of 1×10^6 viable tumor cells suspended in phosphate buffer saline (PBS).

Experimental groups

Animals were distributed into seven groups Gr. (I-VII) each group consisting of eighteen animals. Six animals from each group were taken for the study of biochemical and hematological parameters, histopathological evaluation and for cytogenetic evaluation. The second set, consisting of six animals from each group was taken for studying some parameters to evaluate the anti-tumor activity of Nano-Se, for detection of apoptosis of tumor cells and level of MMP9 in serum and tumor cells. The third set, consisting of six animals from each group was stipulated to determine the mean survival time of animals in each group. Animals of Gr. (II-VII) were injected with EAC cells (1×10^6 cells/mouse) intraperitoneally. The day of EAC cell inoculation was counted as day zero. No treatment was given on the day of EAC cell inoculation. The groups were treated as follows:

Vehicle control (VC) (Group I): Each animal was given oral administration of saline (0.9% NaCl) from day 1 to day 10 and was kept as normal.

EAC control (E) (Group II): Animals were given saline (0.9% NaCl) by oral gavages from day 1 to day 10.

Only CP treated group (EC) (Group III): Animals were received CP at a dose of 25 mg/kg b.w. in water by intraperitoneal administration from day 1 to day 10.

Only Nano-Se concomitant treated group (ED) (Group VI): Animals were treated only with Nano-Se at a dose of 2 mg Se/kg. b.w. 24 hr after tumor inoculation from day 1 to day 10.

Only Nano-Se pretreated group (PED) (Group V): Animals were pretreated with the Nano-Se at a dose of 2 mg Se/kg. b.w. 7 days prior to tumor inoculation and the treatment was continued 24 hr after tumor inoculation from day 1 to day 10. (The day of EAC cell inoculation was count as day zero.)

Concomitant treatment with CP and Nano-Se (ECD) (Group VI): Nano-Se was administered orally at a dose of 2 mg Se/kg. b. w along with CP (25 mg/kg b.w.) from day 1 to day 10.

Pretreatment with CP and Nano-Se (PECD) (Group VII): Animals were given Nano-Se orally at a dose of 2 mg Se/kg b.w. 7 days prior to tumor inoculation and the treatment was continued from day 1 to day 10 starting from 24 hr after tumor inoculation along with CP (25 mg/kg b.w.).

The mice were sacrificed on day 11, 24 hours after the last treatment and the parameters described below were studied. The treatment schedule has been schematically presented in **Fig. 1**.

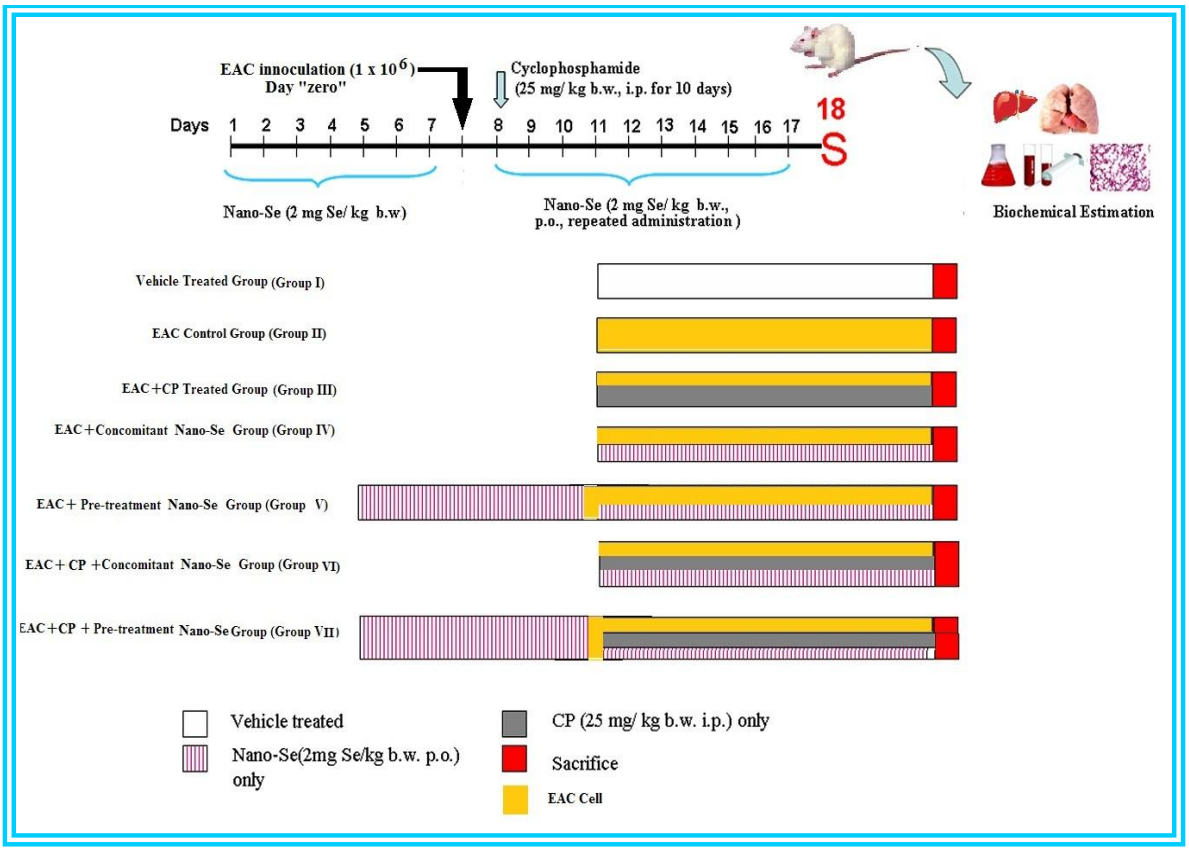

Figure 1: Treatment schedule

Parameter studied

Set A

Following parameters were assessed from Set A

- Quantitative estimation microsomal lipid peroxidation level in liver.
- Biochemical estimation of reactive oxygen species (ROS) level in hepatic, bone marrow and in EAC cells
- Quantitative estimation of reduced glutathione level, estimation of the activity of phase II detoxifying enzyme glutathione-S-transferase and different antioxidant enzymes like superoxide dismutase, catalase and glutathione peroxidase in liver.
- Estimation of hepatic marker enzymes alanine transaminase and aspartate transaminase in serum.
- Estimation of blood hemoglobin level, RBC and WBC count.

- Evaluation of chromosome aberrations by conventional flame dry technique and assessment of DNA damage by comet assay in blood lymphocyte and in tumor cells.
- Histopathological evaluation of liver tissue.

Set B

Following parameters were assessed from Set B

- Measurement of tumor volume, packed cell volume of EAC cells and viable EAC cell count.
- Detection of apoptosis of EAC cells by TUNEL assay.
- Estimation of MMP9 level in serum as well as in EAC cells.

Set C

Following parameters were assessed from Set C

- Determination of mean survival time and percentage increase in life span.

Methodologies

❖ **Biochemical assay**

Detailed procedures regarding the biochemical parameters and others parameters have already been mentioned in Chapter II.

➢ **Estimation of protein content in the tissue homogenate (Lowry et al., 1951)**

Total protein content in tissue homogenate during biochemical analysis assay was measured through Lowry method using Folin-Phenol reagent.

➢ **Quantitative estimation of lipid peroxidation (LPO) level (Ohkawa et al., 1979)**

Spectrophotometric method was applied to estimate the level of lipid peroxidation in liver microsomes by measuring the formation of lipid peroxides using thiobarbituric acid (TBA) and was expressed as nm TBARS/mg protein.

➢ **Estimation of ROS production (Shinomol and Muralidhara, 2007)**

ROS generation in liver homogenate was measured spectrofluorimetrically with slight modifications using probe *i.e.,* DCFH-DA which is hydrolyzed by mitochondrial esterase

to form 2',7'-dichlorodihydrofluorescein (DCFH) then it is oxidized by ROS to form the fluorescent compound 2',7'-dichlorofluorescein (DCF) which is measured spectrofluorimetrically (excitation 485 nm/emission 530 nm).

- **Estimation of reduced glutathione (GSH) level (Mulder et al., 1995; Sedlack et al., 1968)**

GSH level was estimated in liver cytosol spectrophotometrically by determination of dithiobis (2-nitro) - benzoic acid (DTNB) reduced by –SH groups by measuring the absorbance at 412 nm. The level of GSH was expressed as nmol/mg protein.

- **Estimation of glutathione-S-transferase (GST) activity (Mulder et al., 1995; Habig et al., 1974)**

Spectrophotometric method was adopted to evaluate the activity of GST in liver tissue. GST activity was measured in tissue cytosolic fractions by determining the increase in absorbance at 340 nm with 1-chloro-2,4-dinitrobenzene (CDNB) as the substrate and the specific activity of the enzyme was expressed as CDNB-GSH conjugate formed/minute/mg protein.

- **Superoxide dismutase activity (SOD) (Marklund et al., 1974; McCord et al., 1969)**

SOD was determined by means of inhibition of pyrogallol auto-oxidation by the enzyme. Partial extraction and purification of SOD was done as described by McCord and Fridovich. SOD activity was assayed by the method of Marklund and Marklund.

- **Catalase activity (CAT) (Luck, 1963)**

CAT catalyzes the breakdown of H_2O_2 into H_2O and O_2 and competes with the GP*x* for the common substrate H_2O_2. CAT has been considered to be the primary scavenger of intracellular H_2O_2 generated due to oxidative stress. Activity of CAT in liver tissue sample was determined spectrophotometrically at 240 nm and expressed as unit/mg protein where the unit is the amount of enzyme that liberates half the peroxide oxygen from H_2O_2 in seconds at 25^oC.

- **Estimation of GP*x* activity (Paglia et al., 1967)**

GP*x* activity was measured by NADPH oxidation using a coupled reaction system consisting of reduced glutathione, glutathione reductase and hydrogen peroxide. The enzyme activity was expressed as micromol NADPH utilized/minute/mg protein using extinction coefficient of NADPH at 340 nm as 6200 $M^{-1}cm^{-1}$.

- **Hepatic marker enzymes alanine transaminase and aspartate transaminase assay (Reitman and Frankel, 1957)**

Serum alanine transaminase (ALT) and aspartate transaminase (AST) activity were estimated using 2, 4-Dinitrophenyl hydrazine (2, 4-DNPH) color method principles as supplied with the kit (Span Diagnostics, India) following the method of Reitman and Frankel.

❖ **Hematological parameters**

- **Blood hemoglobin (Hb) level (Sahli, 1909)**

Blood hemoglobin was measured following **Sahli's method** (Sahli, 1909). Detailed procedure for the estimation of blood hemoglobin level has already been given in chapter II.

- **Red blood cell count** (**D'Armour et al., 1965**)

Red blood cell (RBC) count was performed using the haemocytometer. Detailed procedure for the count of red blood cell has already been given in chapter II.

- **White blood cell count** (**Wintrobe et al., 1961**)

A sample of whole blood was mixed with a weak acid solution that lyses nonnucleated red blood cells. The specimen was introduced into a counting chamber where the white blood cells (WBCs) in a diluted volume were counted. Detailed procedure for the count of white blood cell has already been given in chapter II.

❖ **Genotoxicity parameters**

Assay of chromosomal aberration

For the study of chromosomal aberrations (CA), slides were prepared from bone marrow cells by the conventional flame drying technique **(Biswas et al., 2004)**. Detailed procedure has already been given in chapter II.

➢ **Detection of DNA damage by alkaline single cell gel electrophoresis (Comet assay) (Singh et al., 1988; Endoh et al., 2002)**

The alkaline single cell gel electrophoresis (SCG) (Comet) assay is a rapid and sensitive procedure for quantitating DNA damage in mammalian cells **(Singh et. al., 1988; Endoh et al., 2002)**. The use of this alkaline SCG assay as a method to detect genotoxicity and cytotoxicity *in vivo* is well documented, and DNA damage thus detected has been used to predict the presence of genotoxic metabolites in specific organs **(Henderson et. al., 1998)**. In this assay, cells are embedded in agarose, lysed in an alkaline buffer, and subjected to an electric current. Relaxed and broken DNA fragments stream further from the nucleus than intact DNA, so the extent of DNA damage can be measured by the length of the stream. This method has several advantages: it is highly sensitive to DNA damage expressed as single strand breaks and alkali-labile sites and disordered DNA fragmentation **(Hartmann et. al., 2003)**, and few cells are required. DNA damage (disorderly DNA fragmentation) induced by CP was measured by using this assay under alkaline conditions following a simplified protocol with slight modifications.

Reagents required

1% normal melting agarose in PBS, 1% low melting point agarose in Milli Q water, 0.5% low melting point agarose in PBS, sodium hydroxide (NaOH), Ethylenediaminetetra acetic acid (Na_2EDTA), Ethidium bromide,.

Lysing solution: 2.5 M NaCl, 100 mM EDTA, 10 mM Tris buffer, 1 % Triton X 100, pH was adjusted to 10 with NaOH.

Electrophoresis buffer: 1 mM Na_2EDTA and 0.3 M NaOH (pH>13).

Neutralizing buffer: 0.4 M Tris buffer (pH 7.5).

Staining solution: Ethidium bromide in water (20 µg/ml).

Procedure:

Half frosted microscope slides were coated with 1% normal melting agarose in PBS

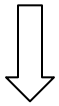

The slides were then allowed to dry at room temperature protected from dust and other particles

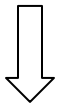

On the day of single cell gel electrophoresis an aliquots of 10µl of freshly prepared cell suspension was mixed with 75µl of 1% low melting point agarose in Milli Q water

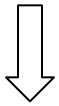

This mixture was then layered on the top of the pre-coated slide and covered with a 24 x 50 mm cover slip and kept on ice to allow the agarose to solidify

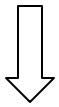

After the agarose had solidified on ice for at least 10-15 min. containing required amount of cells, the cover slip was gently removed and a third layer of 0.5% low melting point agarose was layered on the top of the second layer and covered with a cover slip and kept on ice for 5-10 min.

After the agarose had solidified, the cover slipwas gently removed and the slides were carefully immersed in a freshly prepared ice-cold lysing solution

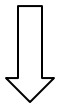

After lysis for overnight at 40ºC, cell membrane and cytosol were lysed and isolated nucleus was remain in the agarose. The slides were placed in an electrophoresis unit.

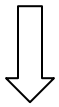

The buffer reservoirs were gently filled with fresh electrophoresis buffer to a level of 0.25 cm above the microscope slides, and incubated for 20min. at 40ºC to allow the

unwinding of DNA

⇩

Keeping the same temperature, the slides were subjected to electrophoresis (25V, 400 mA) for another 25 min.

⇩

After electrophoresis, the slides were placed on a tray to remove alkali and detergents and neutralized with neutralizing buffer for 10 min.

⇩

Excess liquid was carefully removed from each slide using a paper towel

⇩

The microscope slides were carefully dried at room temperature avoiding dust and other particles and then stored in a sealed container until the day of image analysis

⇩

The dried microscope slides were stained with ethidium bromide in water (20µg/ml; 50µl/slide)

Assessment:

The slides with a cover slip were examined at 400X magnification under fluorescence microscope with green filter and photomicrographs of cell were taken. 150-200 randomly selected cells in each slide were counted (4 slides/ animals in each group). The damaged cell (%) was calculated using the following formula:

$$\%\ \text{Cell with damaged DNA} = \frac{\text{Number of damaged cells}}{\text{Total number of cells counted}} \times 100$$

Average tail length due toDNA migration in each group. The parameters analyzed for detection of DNA damage were damaged cell (%) in each group, tail DNA (%), tail

length [migration of the DNA from the nucleus (lm)], and Olive tail moment [product of tail length and the fraction of total DNA in the tail (arbitrary units)].

- **Estimation of ROS in bone marrow cell**

ROS generation in bone marrow cells was measured spectrofluorimetrically using DCFH-DA following a simplified protocol with slight modifications **(Huang et al., 2008)**. Detailed procedure has already been given in chapter II.

- **Histopathology (Bancroft et al., 1990; Lillie et al., 1976)**

Histopathological evaluation of liver tissues was done by conventional hematoxylin-eosin staining method detail of which already mentioned in chapter II.

- **Tumor growth response (Mazumder et al., 1997; Gupta et al., 2000)**

The anti-tumor effect of CP along with Nano-Se was assessed by measuring the changes in ascites tumor volume, packed cell volume and viable tumor cell count. Mean survival time (MST) of each group containing six mice was monitored and percentage increase in life span (% ILS) was calculated using following equation. MST= (Day of first death + Day of last death)/2. ILS (%) = [(Mean survival time of treated group/Mean survival time of control group)–1] × 100.

- **Detection of apoptosis by terminal deoxynucloeotidyl transferase dUTP nick end labeling (TUNEL) technique (Caderni et al., 2000)**

To identify individual apoptotic cells TUNEL method is a fast and simple non radioactive technique. Cleavage of genomic DNA during apoptosis may yield double-stranded, low molecular weight DNA fragments (mono- and oligonucleosomes) as well as single strand breaks (“nicks”) in high molecular weight DNA. Those DNA strand breaks can be identified by labeling free 3′-OH termini with modified nucleotides in an enzymatic reaction. In this technique, the DNA strand breaks are labeled by free terminal deoxynucleotidyl transferase (TdT), which catalyzes polymerization of labeled nucleotide to free 3′-OH DNA ends in a template independent manner. The apoptotic cells are identified by the fluorescence they emit.

Reagents required

Enzyme solution: Terminal deoxynucleotidyl transferase (TdT) from calf thymus.

Labeling solution: Nucleotide mixture (DUTP).

Fixation solution: 4% Paraformaldehyde in PBS, pH 7.4.

Permiabilisation solution: 0.1% Triton-X-100 in 0.1% Sodium citrate.

PBS.

Procedure

Smears of EAC cell suspension from each group of mice were taken on glass slides and air dried.

⇩

The samples were then fixed with a freshly prepared fixation solution for 1hr at 15-25°C.

⇩

Slides were then rinsed with PBS followed by incubation in permiabilisation solution for 2 minutes on ice (Solution of Triton-X-100 and sodium citrate).

⇩

After 2 minutes, slides were again rinsed twice with PBS and the area around sample on each slide was dried.

⇩

TUNEL reaction mixture containing TdT and flurescein-DUTP (Enzyme solution and label solution were mixed in 1:9 ratios) was then added on the cell smear on each slide.

⇩

The slides were then covered with cover slip and incubated in a humidified chamber for 1 hour at 37ºC in dark.

⇩

Finally, the slides were washed 3 times in PBS and the slides were analyzed in a drop of PBS under a fluorescence microscope.

Evaluation

The cells with DNA strand breaks were fluorescently labeled and the cells with apoptosis were identified by their fluorescence. Number of labeled and unlabeled cells was counted. The Apoptotic Index (AI) was determined as the percentage of the labeled cells with respect to the total number of cells counted.

$$\text{Apoptotic Index} = \frac{\text{Number of labeled cells}}{\text{Total number of cells counted}} \times 100$$

- **Matrix metalloproteinase-9 (MMP-9) Immunoassay (Van Wart and Birkedal-Hansen, 1990)**

MMP-9 level in serum and in EAC cells were measured following a method provided in the commercially available kit. This assay employs the quantitative sandwich enzyme immunoassay technique. A monoclonal antibody specific for mouse MMP-9 is pre-coated onto a microplate. Standards, control, and samples are pipetted into the wells and any mouse MMP-9 present in the sample is bound by the immobilized antibody. After washing away any unbound substances, an enzyme-linked polyclonal antibody specific for mouse MMP-9 is added to the wells. Following a wash to remove any unbound antibody-enzyme reagent, a substrate solution is added to the wells and the color develops in proportion to the amount of mouse MMP-9 bound in the initial step. The color development is stopped and the intensity of the color is measured.

Reagents required

Mouse MMP-9 (total) Microplate: 96 well polystyrene microplate coated with a rat monoclonal antibody specific for mouse MMP-9.

Mouse MMP-9 (total) Conjugate: Polyclonal antibody against mouse MMP-9 conjugated to horseradish peroxidase.

Mouse MMP-9 (total) Standard: Recombinant mouse MMP-9 in a buffered protein base.

Mouse MMP-9 (total) Control: Recombinant mouse MMP-9 in a buffered protein base.

Assay Diluent: Buffered protein solution.

Calibrator Diluent: Buffered protein solution.

Wash Buffer Concentrate: 25-fold concentrated solution of buffered surfactant.

Color Reagent A: Stabilized hydrogen peroxide.

Color Reagent B: Stabilized chromogen (tetramethylbenzidine).

Stop Solution: Diluted hydrochloric acid.

Reagent preparation

All the reagents must be brought to room temperature before use.

Mouse MMP-9 (total) Control - The control was reconstituted with 1.0 ml distilled water and the control was assessed undiluted.

Wash Buffer - Wash buffer concentrate was diluted with distilled water to prepare 500 ml of Wash Buffer.

Substrate Solution - Color reagents A and B was mixed together in equal volumes within to prepare substrate solution.

Mouse MMP-9 (total) Standard - The mouse MMP-9 (total) standard was reconstituted with 2 ml calibrator dilutent to produce a stock solution of 5 ng/ml. Mix the standard to ensure complete reconstitution and allow the standard to sit for a minimum of 15 minutes with gentle agitation prior to making dilutions. Pipette 200 L of the Calibrator Diluent RD5-10 into each tube. Use the Stock solution to produce a 2-fold dilution series (below). Mix each tube thoroughly before the next transfer. The 5 ng/mL standard serves as the high standard. Calibrator Diluent RD5-10 serves as the zero standards (0 ng/mL).

Sample Collection

Separation of serum and isolation of EAC cells have been described previously in detail.

Procedure

96 well antibody coated microplate was taken from the foil pouch. Excess microplate strips were removed from the plate frame and were returned to the foil pouch and was resealed.

⇩

50 µl assay diluent was added to each well.

50 µl serum (diluted 50 fold with calibrator diluent) or 50 µl EAC cell suspension containing 1×10^6 cells were added per well. The plate was then gently tapped to ensure thorough mixing. Plate was then covered with the adhesive strip provided and incubated for 2 hours at room temperature.

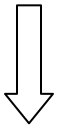

Each well was aspirated and washed four times with 400 µl wash buffer. Complete removal of liquid at each step is essential for good performance. After the last wash, any remaining wash buffer was removed by aspirating or decanting. The plate was wiped out against clean paper towels.

In each well 100 µl mouse MMP-9 (total) conjugate was added. Plate was covered with a new adhesive strip and incubated for 2 hours at room temperature.

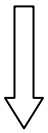

Aspiration and washing were done as in step 4.

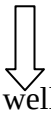

100 µl substrate solution was added to each well and incubated for 30 minutes at room temperature. The plate was protected from light.

100 µl stop solution was added to each well. To ensure thorough mixing the plate was gently tapped.

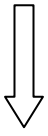

Optical density of each well was determined within 30 minutes, using Tecan ELISA reader set to 450 nm. The readings at 540 nm were subtracted from the readings at 450 nm. This subtraction corrects for optical imperfections in the plate. A duplicate reading was taken for each sample.

Calculation

A standard curve was prepared using the reagent mouse MMP-9 (total) standard provided in the kit. From this stock solution, a 2-fold dilution series (5 ng/ml, 2.5 ng/ml, 1.25 ng/ml, 0.625 ng/ml, 0.312 ng/ml, 0.156 ng/ml, 0.078 ng/ml) of the reagent standard was prepared. Calibrator diluent was served as the zero standards (0 ng/ml). Optical density of this dilution series was taken after completing all the reaction steps described above. The standard curve was constructed by plotting the mean absorbance (obtained by taking the average of the duplicate reading) for each standard on the y-axis against the concentration on the x-axis and a best fit curve was drawn through the points on the graph. The concentration of MMP-9 of each sample was determined by plotting the absorbance of each experimental sample on the standard curve for MMP-9 and the MMP-9 level was expressed as ng/ml.

- **Peritoneal angiogenesis**

To determine the angiogenic response, the tumor-bearing mice were sacrificed and the peritoneum was opened after dissection. The inner lining of the peritoneal cavity was examined for angiogenesis in both tumor control and treated groups and photographed.

Statistical analysis

All data were presented as mean ± SD. n = 6 animals per group. One way ANOVA followed by Tukey's Multiple Comparison Test using Graph Pad Prism software was performed for comparisons among groups. Significant difference was indicated when the *P* value was < 0.05.

Results

- **LPO level**

The level of LPO was increased significantly ($P < 0.05$) by 105.69% in liver tissues in the EAC control group (Gr. II) compared to the vehicle control group (Gr. I) **(Fig. 2)**. A further significant elevation in LPO level in liver by 90.17% was observed after administration of CP in tumor bearing mice (Gr. III) in comparison to the EAC control group (Gr. II). Treatment with Nano-Se alone decreased the LPO level significantly by 43.57% (Gr. IV) & by 45.84% (Gr. V) in liver, compared to the EAC control group (Gr. II). Concomitant administration of Nano-Se along with CP (Gr. VI) significantly diminished the LPO level in liver by 61.19% in comparison to the CP treated group (Gr. III). Pretreatment with Nano-Se along with CP reduced the LPO level in liver by 68.34% in comparison to the CP treated group (Gr. III).

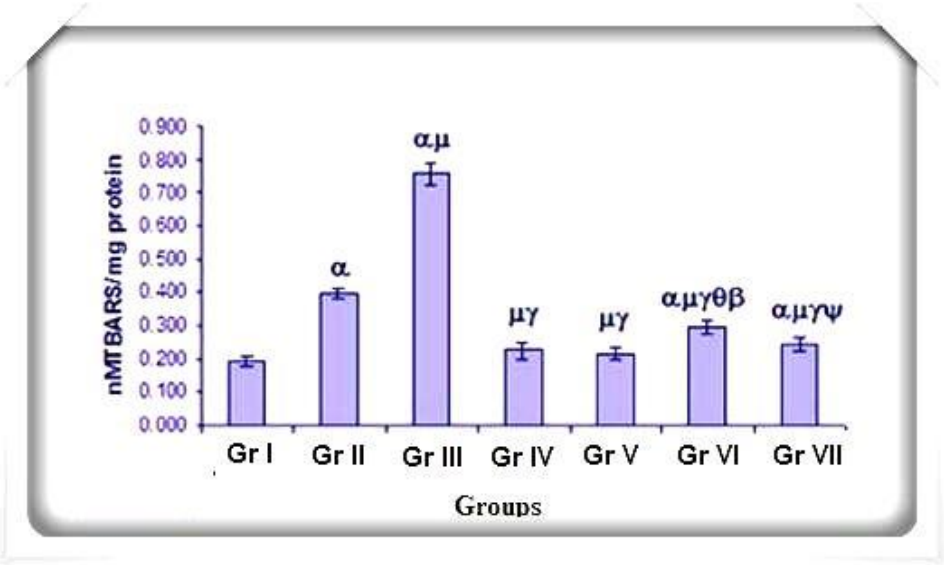

Figure 2: Data were represented as mean ± Standard deviation (SD) (n=6). α - significant ($P < 0.05$) as compared with Gr. I; μ - significant ($P < 0.05$) as compared with Gr. II; γ - significant ($P < 0.05$) as compared with Gr. III; θ - significant ($P < 0.05$) as compared with Gr. IV; β - significant ($P < 0.05$) as compared with Gr. V; ψ - significant ($P < 0.05$) as compared with Gr. VI.

- **ROS Level**

- **Hydrogen peroxide level by using DCFH-DA in hepatic and bone marrow cells**

The ROS level in liver and bone marrow cells increased significantly ($P < 0.05$) by 61.53% and 207.37% in the EAC control group (Gr. II) as compared to the vehicle control (Gr. I) **(Fig. 3A & B)**. Intraperitoneal administration of CP in tumor bearing mice (Gr. III) resulted in an additional significant enhancement of ROS level by 53.23% and 32.01% respectively in liver and bone marrow cells, in comparison to the EAC control group (Gr. II). Treatment with Nano-Se on its own decreased the ROS level significantly in liver by 20.61% (Gr. IV) and 31.12% (Gr. V) and in bone marrow by 40.47% (Gr. IV) and 52.28% (Gr. V) as compared with EAC control group (Gr. II). Concomitant and pretreatment of Nano-Se along with CP decreased the ROS level significantly in liver by 33.75% and 44.53% respectively in Gr. VI and Gr. VII and in bone marrow by 37.28% and 47.1% respectively in Gr. VI and Gr. VII in comparison to the CP treated group (Gr. III).

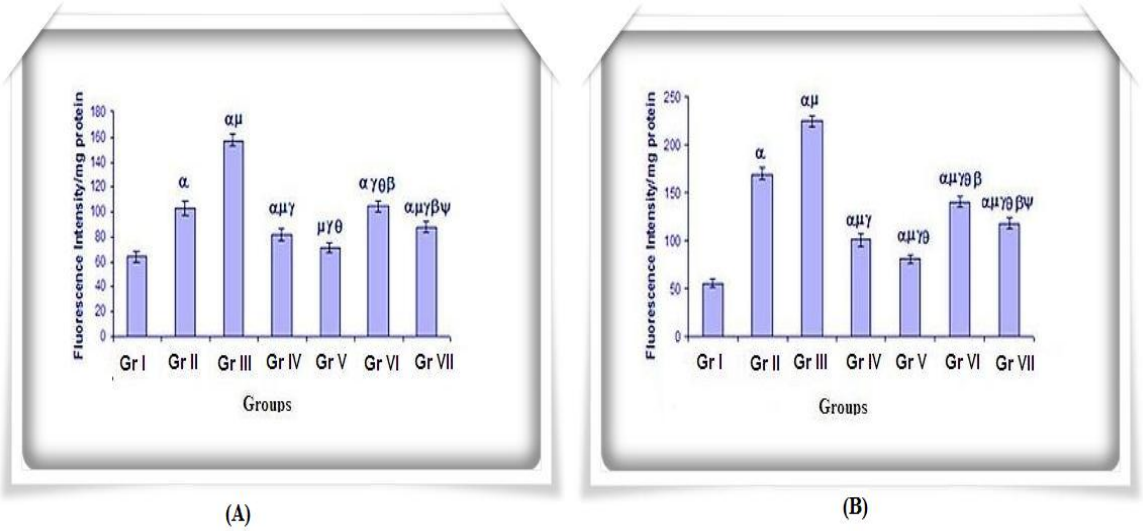

Figure 3: Data were represented as mean ± Standard deviation (SD) (n=6). α - significant ($P < 0.05$) as compared with Gr. I; μ - significant ($P < 0.05$) as compared with Gr. II; γ - significant ($P < 0.05$) as compared with Gr. III; θ - significant ($P < 0.05$) as compared with Gr. IV; β - significant ($P < 0.05$) as compared with Gr. V; ψ - significant ($P < 0.05$) as compared with Gr. VI.

- **Hydrogen peroxide level by using DCFH-DA in tumor cell**

To evaluate the mechanism of cell death on the basis of ROS production DCFH-DA assay was done in tumor cells **(Fig. 4)**. Intraperitoneal administration of CP in tumor bearing mice (Gr. III) resulted in significant enhancement of ROS level by 194.05% in comparison to the EAC control group (Gr. II). Treatment with Nano-Se on its own increased the ROS level significantly ($P < 0.05$) in tumor cells by 60.48% (Gr. IV) and 123.19% (Gr. V) in comparison to the EAC control group (Gr. II). In addition, when Nano-Se was used along with chemotherapeutic drug CP in combination regimen ROS in the tumor cells was boosted up by 21.12% in case of concomitant treatment (Gr. VI) and by 64.48% in case of pretreatment (Gr. VII) compared to the CP control group (Gr. III).

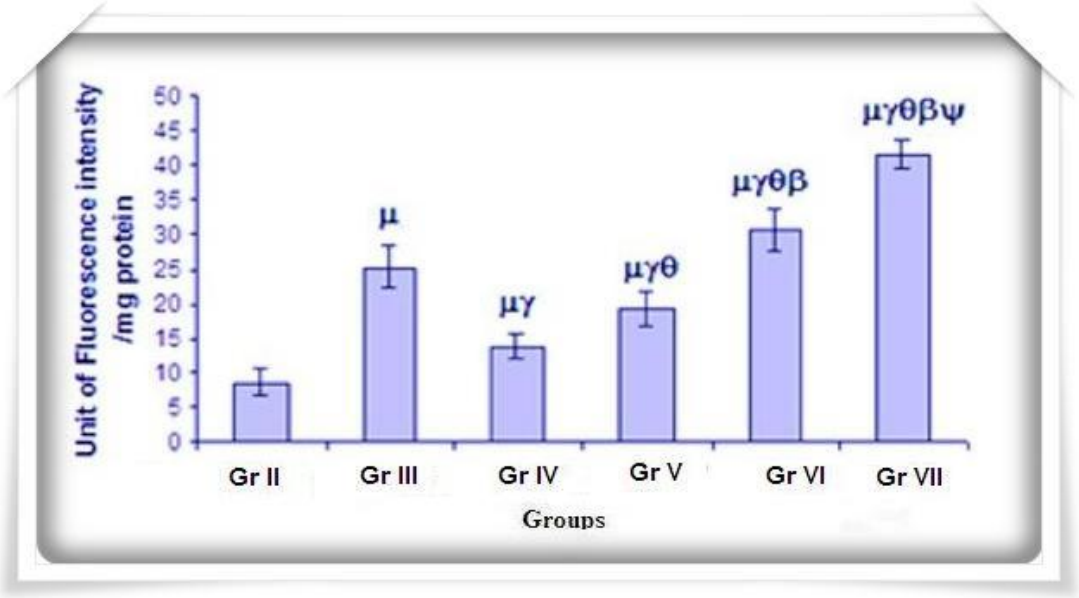

Figure 4: Data were represented as mean ± Standard deviation (SD) *(n=6)*. μ - significant (*P < 0.05*) as compared with Gr. II; γ - significant (*P < 0.05*) as compared with Gr. III; θ - significant (*P < 0.05*) as compared with Gr. IV; β - significant (*P < 0.05*) as compared with Gr. V; ψ - significant (*P < 0.05*) as compared with Gr. VI.

- **GSH level**

The GSH content was found to decrease significantly ($P < 0.05$) by 56.22% in liver after tumor inoculation in Gr. II, compared to the vehicle control group (Gr. I) **(Fig. 5)**. After intraperitoneal administration of CP (Gr. III), GSH content was decreased for a second time by 45.39% in liver in comparison to the EAC control group (Gr. II). Sole application of Nano-Se caused a significant increment in the hepatic GSH level by 31.57 % & 43.85% respectively in Gr. IV & Gr. V, compared to the EAC control group (Gr. II). Combined application of Nano-Se in concomitant and pretreatment schedule with CP (Gr. VI & Gr. VII) augmented the GSH content in liver significantly by 127.26% & 228.71% in comparison to the CP treated group (Gr. III).

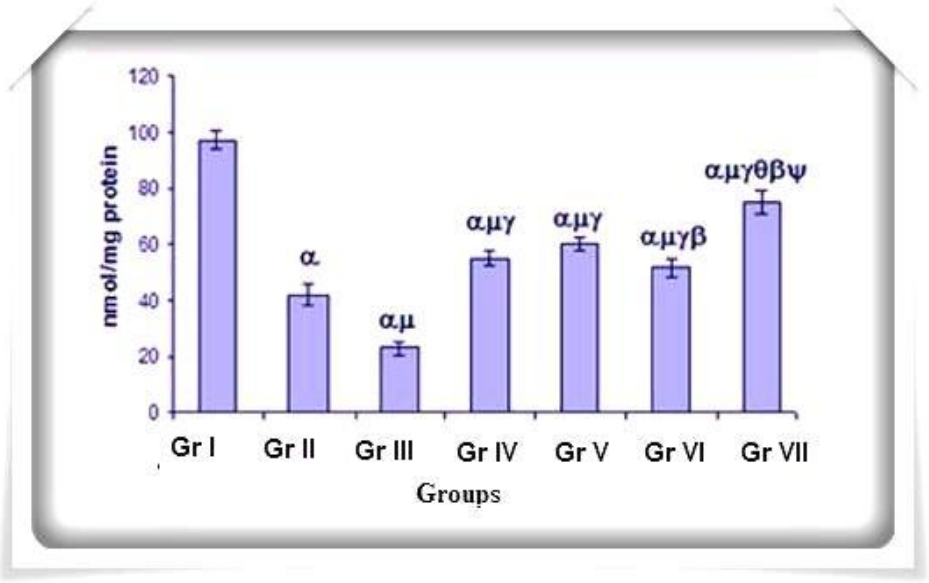

Figure 5: Data were represented as mean ± Standard deviation (SD) (n=6). α - significant ($P < 0.05$) as compared with Gr. I; μ - significant ($P < 0.05$) as compared with Gr. II; γ - significant ($P < 0.05$) as compared with Gr. III; θ - significant ($P < 0.05$) as compared with Gr. IV; β - significant ($P < 0.05$) as compared with Gr. V; ψ - significant ($P < 0.05$) as compared with Gr. VI.

- **GST activity**

It was observed that tumor inoculation resulted in a significant ($P < 0.05$) reduction in GST activity by 47.22% in liver (Gr. II), compared to the vehicle control group (Gr. I) **(Fig. 6)**. GST activity reduced significantly by 16.12% in liver once again when CP was given in tumor inoculated mice (Gr.III) in comparison to the EAC control group (Gr. II). The Nano-Se alone (Gr. IV & Gr. V) significantly enhanced the GST activity in liver by 13.71% & 35.92% in comparison to the EAC control group (Gr. II). Concomitant and pretreatment of Nano-Se along with CP (Gr. VI & Gr. VII) significantly increased the GST activity in liver by 28.2% & 80.57% in comparison to the CP treated group (Gr. III).

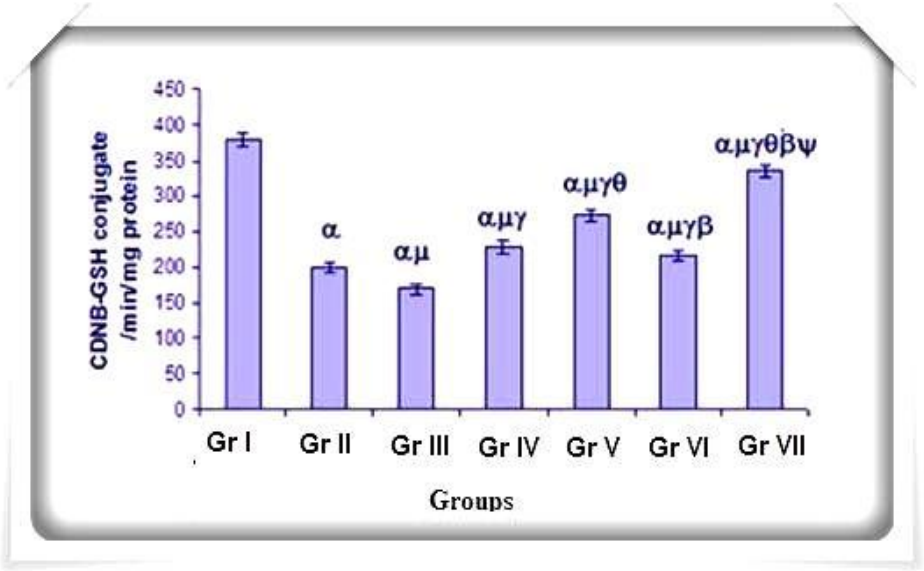

Figure 6: Data were represented as mean ± Standard deviation (SD) (n=6). α - significant ($P < 0.05$) as compared with Gr. I; μ - significant ($P < 0.05$) as compared with Gr. II; γ - significant ($P < 0.05$) as compared with Gr. III; θ - significant ($P < 0.05$) as compared with Gr. IV; β - significant ($P < 0.05$) as compared with Gr. V; ψ - significant ($P < 0.05$) as compared with Gr. VI.

- **SOD activity**

The SOD activity decreased significantly ($P < 0.05$) by 44.84% in liver in the EAC control group (Gr. II) in comparison to the vehicle control group (Gr. I) **(Fig. 7)**. SOD activity was further significantly diminished after intraperitoneal administration of CP (Gr. III) in liver by 18.52% in comparison to the EAC control group (Gr. II). Nano-Se alone (Gr. IV & Gr. V) increased the SOD activity in liver by 15.21% & 25.63% compared to the EAC control group (Gr. II). When the same dose of Nano-Se was applied in combination with CP in concomitant and pretreatment schedule (Gr. VI & Gr. VII), enhancement in the SOD activity was 38.34% & 72.91% in liver in comparison to the CP treated group (Gr. III).

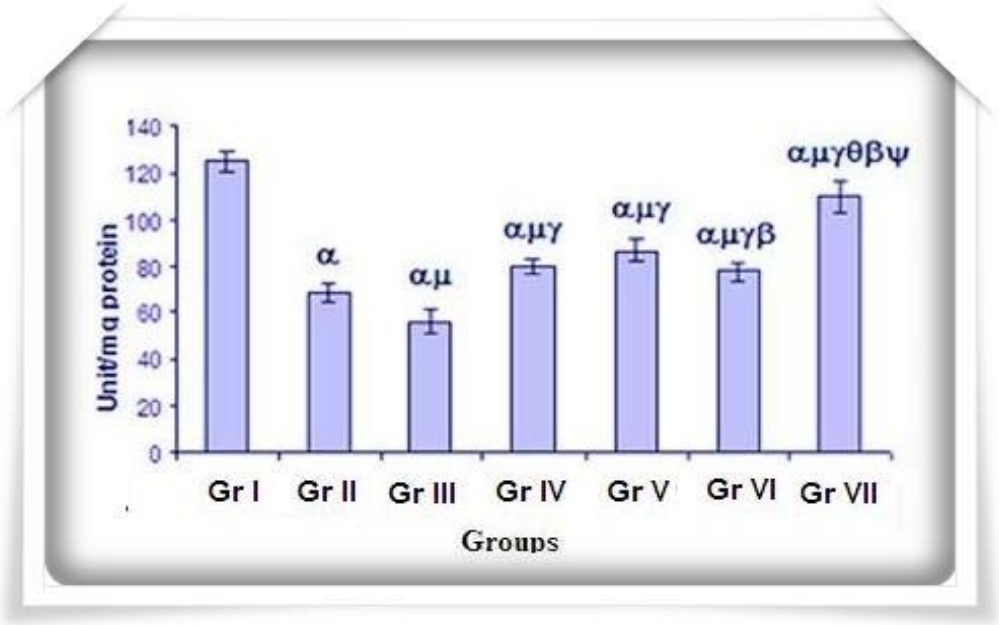

Figure 7: Data were represented as mean ± Standard deviation (SD) (n=6). α - significant ($P < 0.05$) as compared with Gr. I; μ - significant ($P < 0.05$) as compared with Gr. II; γ - significant ($P < 0.05$) as compared with Gr. III; θ - significant ($P < 0.05$) as compared with Gr. IV; β - significant ($P < 0.05$) as compared with Gr. V; ψ - significant ($P < 0.05$) as compared with Gr. VI.

- **CAT activity**

Tumor inoculation caused a significant ($P < 0.05$) reduction in the CAT activity in liver by 52.43% in the EAC control group (Gr. II), compared to the vehicle control group (Gr. I) **(Fig. 8)**. When CP was administered in tumor inoculated mice (Gr. III), CAT activity reduced significantly for a second time in liver by 28.86% in comparison to the EAC control group (Gr. II). Nano-Se when administered alone in tumor bearing mice (Gr. IV & Gr. V), it resulted in a significant augmentation of CAT activity in liver by 35.86% & 68.03% in comparison to the EAC control group (Gr. II). Concomitant and pretreatment of Nano-Se along with CP (Gr. VI & Gr. VII) increased the CAT activity in liver significantly by 71.93% & 87.98% in comparison to the CP treated group (Gr. III).

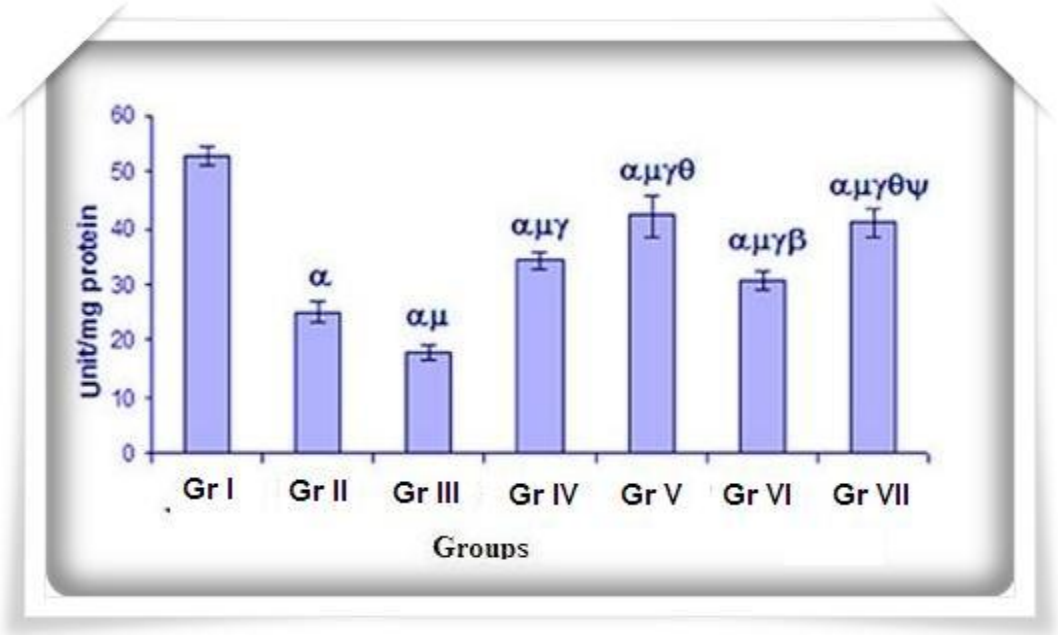

Figure 8: Data were represented as mean ± Standard deviation (SD) (n=6). α - significant ($P < 0.05$) as compared with Gr. I; μ - significant ($P < 0.05$) as compared with Gr. II; γ - significant ($P < 0.05$) as compared with Gr. III; θ - significant ($P < 0.05$) as compared with Gr. IV; β - significant ($P < 0.05$) as compared with Gr. V; ψ - significant ($P < 0.05$) as compared with Gr. VI.

- **GP*x* activity**

A significant ($P < 0.05$) depletion in GP*x* activity by 55.03% in liver was noticed in the EAC control group (Gr. II) compared to the vehicle control group (Gr. I) **(Fig. 9)**. Administration of CP in tumor bearing mice (Gr. III) resulted in an additional reduction of GP*x* activity in liver by28.35% in comparison to the EAC control group (Gr. II). The Nano-Se itself (Gr. IV & Gr. V) increased the GP*x* activity in liver by 20.39% & 34.82% in comparison to the EAC control group (Gr. II). Concomitant administration of Nano-Se along with CP (Gr. VI) significantly enhanced the GP*x* activity in liver by 53.47% in comparison to the CP treated group (Gr. III). Pretreatment with Nano-Se along with CP raised the GP*x* activity in liver by 159.72% in comparison to the CP treated group (Gr. III).

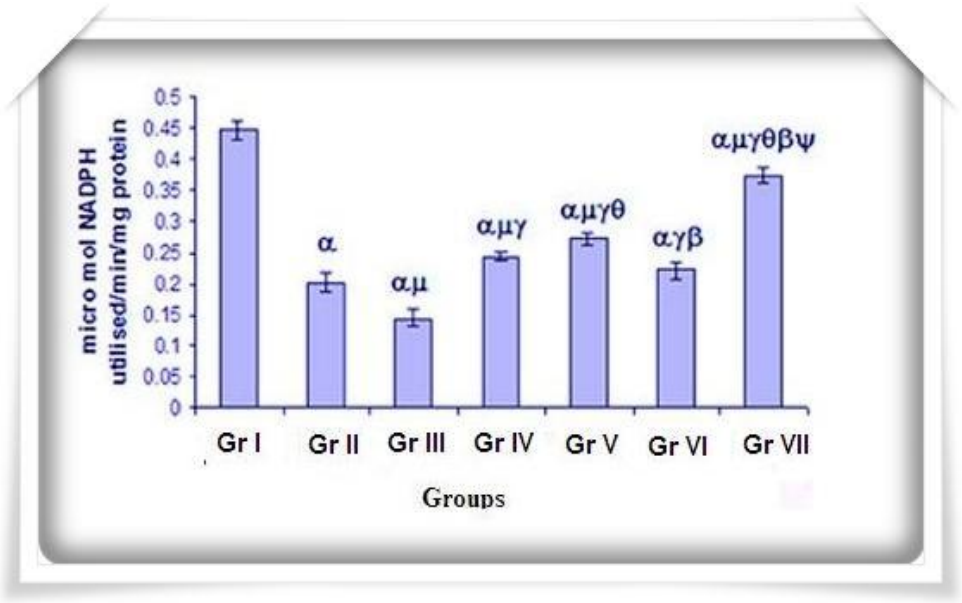

Figure 9: Data were represented as mean ± Standard deviation (SD) (n=6). α - significant ($P < 0.05$) as compared with Gr. I; μ - significant ($P < 0.05$) as compared with Gr. II; γ - significant ($P < 0.05$) as compared with Gr. III; θ - significant ($P < 0.05$) as compared with Gr. IV; β - significant ($P < 0.05$) as compared with Gr. V; ψ - significant ($P < 0.05$) as compared with Gr. VI.

- **ALT and AST activity**

The ALT and AST activity in serum increased significantly ($P < 0.05$) by 28.16% and by 45.17% in the EAC control group (Gr. II) in comparison to the vehicle control group (Gr. I) **(Fig. 10A & B)**. After intraperitoneal administration of CP (Gr. III), ALT and AST activity again increased significantly by 31.57% and 59.97% respectively, in comparison to the EAC control group (Gr. II). The Nano-Se itself (Gr. IV & Gr. V) significantly decreased the ALT activity by 14.47% & 26.71%, and AST activity by 25% & 29.89% in comparison to the EAC control group (Gr. II). Concomitant and pretreatment with the Nano-Se along with CP (Gr. VI & Gr. VII) significantly reduced the ALT activity by 20% & 28% and AST activity by 30.97% & 49.89% in comparison to the CP treated group (Gr. III).

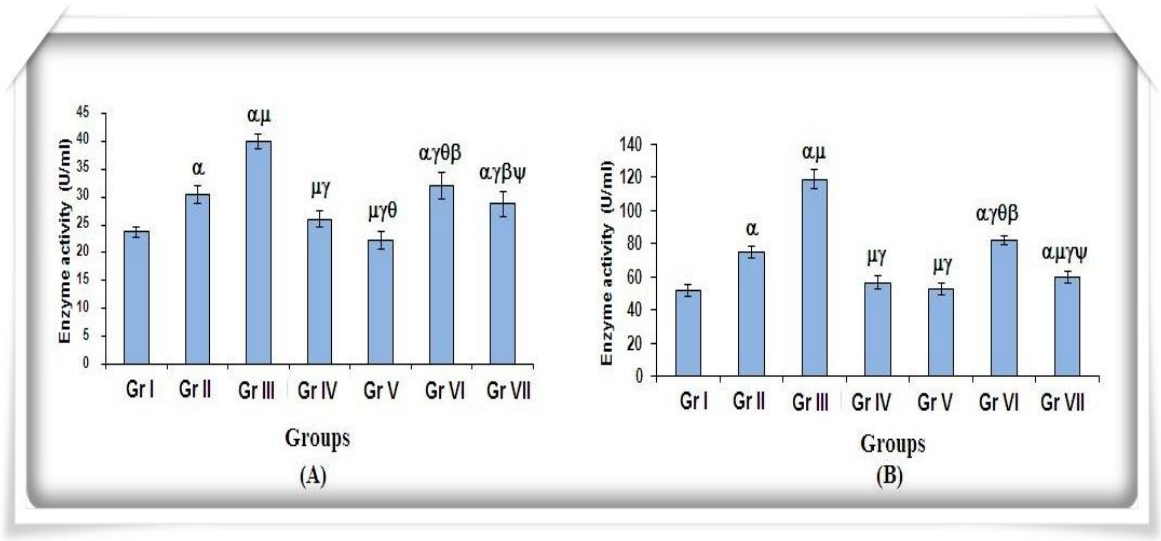

Figure 10: Data were represented as mean ± Standard deviation (SD) (n=6). α - significant ($P < 0.05$) as compared with Gr. I; μ - significant ($P < 0.05$) as compared with Gr. II; γ - significant ($P < 0.05$) as compared with Gr. III; θ - significant ($P < 0.05$) as compared with Gr. IV; β - significant ($P < 0.05$) as compared with Gr. V; ψ - significant ($P < 0.05$) as compared with Gr. VI.

- **Hematological parameters**

Tumor growth was associated with significant ($P < 0.05$) decline in hemoglobin and RBC values with concomitant rise in WBC count **(Table 1)** in the EAC control group (Gr. II) compared to the vehicle control group (Gr. I). Treatment for consecutive 10 days of CP further declined the Hb level and RBC count significantly ($P < 0.05$) by 30.52 and 28 %, respectively, compared to EAC control group (Gr. II). Treatment with Nano-Se along with CP in concomitant (Gr. VI) and in pretreatment (Gr. VII) scheme increased the Hb level by 69.36 % (Gr. VI), 52.6 % (Gr. VII), and RBC count by 55 % (Gr. VI), 77.25 % (Gr. VII), respectively. Besides EAC inoculation radically increased the WBC count compared to the vehicle control group (Gr. I). Administration of CP led to a huge fall in WBC count. Treatment with Nano-Se in CP-treated mice in concomitant (Gr. VI) and pretreatment (Gr. VII) schedule, rose the WBC count significantly ($P > 0.05$) compared to the CP control group (Gr. III). However, monotherapy with Nano-Se in concomitant (Gr. IV) and pre-treatment (Gr. V) scheme declined the WBC count significantly ($P > 0.05$) compared to the EAC control group.

Groups	Haemoglobin (mg/dL)	RBC (10^6/mm^3)	WBC (10^3/mm^3)
I	14.38 ± 0.52	10.08 ± 0.54	6.52 ± 0.46
II	$9.96 \pm 0.57^{\alpha}$	$7.08 \pm 0.27^{\alpha}$	$14.32 \pm 0.69^{\alpha}$
III	$6.92 \pm 0.67^{\alpha\mu}$	$5.1 \pm 0.23^{\alpha\mu}$	$4.18 \pm 0.5^{\alpha\mu}$
IV	$11.4 \pm 1.06^{\alpha\mu\gamma}$	$8.18 \pm 0.48^{\alpha\mu\gamma}$	$9.62 \pm 0.42^{\alpha\mu\gamma}$
V	$12.28 \pm 0.48^{\alpha\mu\gamma}$	$9.88 \pm 0.52^{\mu\gamma\theta}$	$8.46 \pm 0.46^{\alpha\mu\gamma\theta}$
VI	$11.72 \pm 0.46^{\alpha\mu\gamma}$	$7.92 \pm 0.52^{\alpha\mu\gamma\beta}$	$5.6 \pm 0.61^{\mu\gamma\theta\beta}$
VII	$13.6 \pm 0.4^{\mu\gamma\theta\beta\psi}$	$9.04 \pm 0.47^{\alpha\mu\gamma\theta\beta\psi}$	$7.28 \pm 0.42^{\mu\gamma\theta\beta\psi}$

Table 1: Data were represented as mean ± Standard deviation (SD) (n=6). α - significant ($P < 0.05$) as compared with Gr. I; μ - significant ($P < 0.05$) as compared with Gr. II; γ - significant ($P < 0.05$) as compared with Gr. III; θ - significant ($P < 0.05$) as compared with Gr. IV; β - significant ($P < 0.05$) as compared with Gr. V; ψ - significant ($P < 0.05$) as compared with Gr. VI.

- **Chromosomal aberration**

EAC inoculation (Gr. II) showed significantly (P < 0.05) high proportion of chromosomal aberration of 54.2 % compared to the vehicle treated group (Gr. I) **(Fig. 11A)**. After administration of CP treatment was given to EAC-inoculated animals (Gr. III), it showed further more rise in chromosomal aberration of about 67.36 %. The frequency of CA reduced to 31.1% in Gr. IV and to 25.86% in Gr. V after administration of the Nano-Se alone. The same Nano-Se exerted a significant protection against CP induced genotoxicity when the compound was given in combination therapy schedule with CP and the frequency of CA reduced to 49.26% in Gr. VI and 38.02% in Gr. VII. Different types of chromosomal aberrations have been shown in Fig. **11 B**.

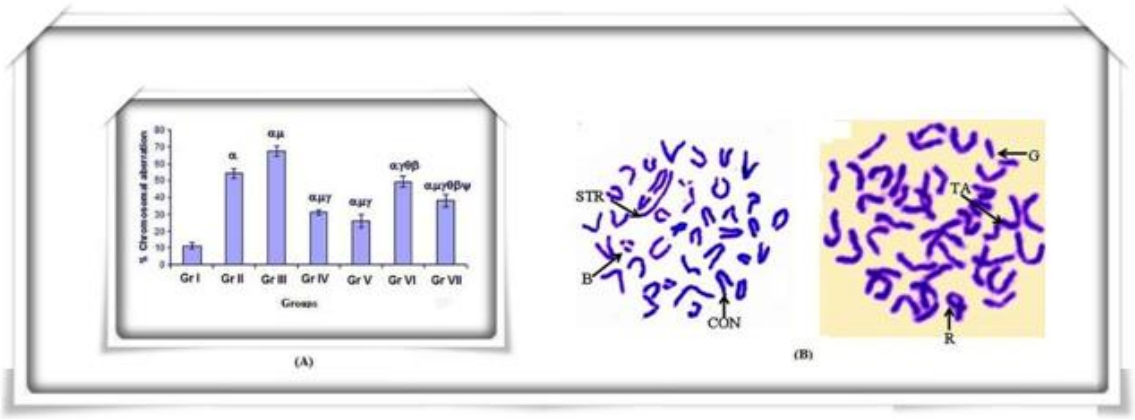

Figure 11A: Data were represented as mean ± Standard deviation (SD) (n=6). α - significant ($P < 0.05$) as compared with Gr. I; μ - significant ($P < 0.05$) as compared with Gr. II; γ - significant ($P < 0.05$) as compared with Gr. III; θ - significant ($P < 0.05$) as compared with Gr. IV; β - significant ($P < 0.05$) as compared with Gr. V; ψ - significant ($P < 0.05$) as compared with Gr. VI.

Figure 11B: 7 Photographs of metaphase chromosomes of bone marrow cells from treated and untreated EAC bearing mice. Arrows indicate stretching (STR), break (B), constriction (CON), ring (R), terminal association (TA) and gap (G)

- **Comet assay findings**

Single cell gel electrophoresis assay (comet assay) was performed to find out induction of genotoxicity by CP at DNA level in peripheral lymphocyte **(Fig. 12 A-G)** and EAC cells **(Fig. 13 A-F)** of experimental mice and two parameters namely percentage of damaged cells and the average tail length were measured.

- **Percentage of damaged cells in each group**

The frequency of damaged lymphocyte cells was estimated to be 9.14 % in Gr. I (Table 3). In EAC control group the frequency of cells with damaged DNA was increased significantly ($P < 0.05$) to 44.46%. CP treatment resulted in further significant increase in the proportion of damaged cells (76.04%) in Gr. III **(Table 2)**. When Nano-Se was given singly in tumor bearing mice in concomitant (Gr. IV) and pretreatment (Gr. V) schedule, the frequency of damaged cells reduced respectively to 19.37% & 35.74%. In combination therapy with both CP and Nano-Se, the percentages of damaged cells were reduced to 33.41% (Gr. VI) and 23.75% (Gr. VII).

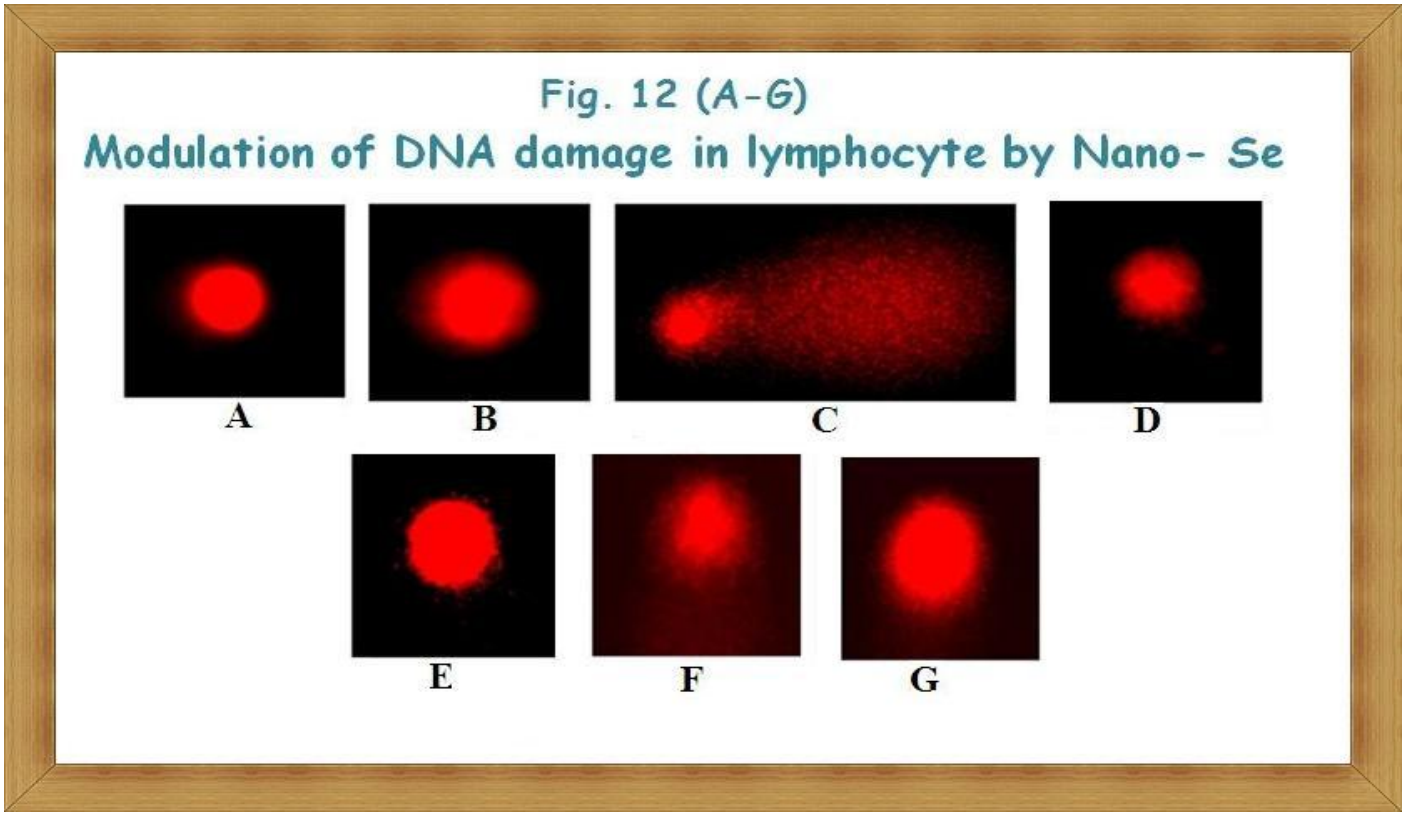

Figure 12 (A - G): Microphotograph of comet of lymphocyte, (A). vehicle treated (no DNA damage), (B and C) EAC control and CP treated group) showed highly migrated DNA with distinct scattered comet tail; Concomitant treatment (D) and pretreatment (E) with Nano-Se capable to reduce the migration of DNA and less diffused comet tail; Combined treatment with Nano-Se and CP (F and G) showed no or very less migrated DNA.

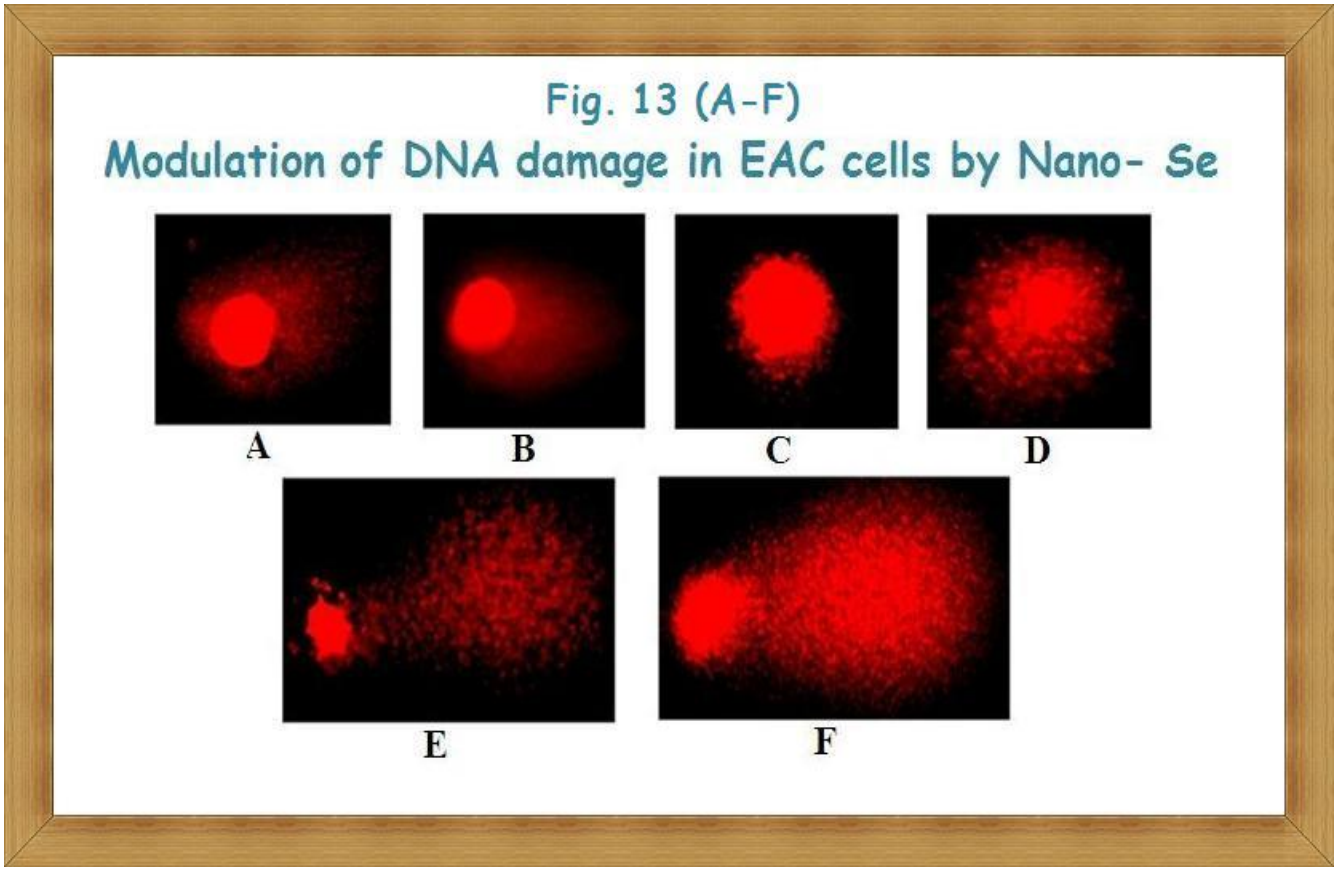

Figure 13 (A - F): Microphotograph of comet of EAC cell, EAC inoculation (A) showed less migrated DNA with less diffused comet tail. Treatment with CP (B) showed highly migrated DNA with distinct scattered comet tail. Monotherapy with the Nano-Se able to induce the DNA damage (C and D). Combined treatment with Nano-Se with CP showed extremely migrated DNA with distinct scattered comet tail (E and F).

- **Average Tail Length of peripheral lymphocyte due to DNA Migration in each group**

The magnitude of average tail length was 7.88±0.75 µm in Gr. I. With inoculation of tumor, the magnitude of tail length increased significantly ($P < 0.05$) to 64.1±1.42 µm in Gr. II. The tail length further increased significantly to 96.7±1.25 µm after administration of CP in Gr. III **(Table 2)**. Oral administration of Nano-Se resulted in reduction of average tail length of cells both to 29.4±1.26 µm in Gr. IV and to 22.3±2.24µm in Gr. V. Significant reduction in tail length of lymphocyte was also observed in Gr. VI (58.1±1.21 µm) and in Gr. VII (37.9±1.99 µm), where CP and Nano-Se were given together.

- **Average Tail Length of tumor cells due to DNA Migration in each group**

The magnitude of average tail length was 8.19±2.07 µm in EAC control group (Gr. II). CP administration caused a marked increase in the magnitude of tail length to 32.15±2.63 µm (Gr. III) **(Table 2)**. Oral administration of Nano-Se itself in concomitant (Gr. IV) and pretreatment (Gr. V) schedule, resulted in the enhancement of average tail length to 16.57±2.98 µm and 26.78±2.67 µm, respectively. However, the combination management caused enormous enhancement of average tail length to 41.89±2.08 µm in concomitant (Gr. VI) and 56.41±6.10 µm in pretreatment (Gr. VII) group, respectively.

Groups	Peripheral Lymphocyte		Tumor cell	
	Damaged cells showing comet (%)	Average tail length (µm)	Damaged cells showing comet (%)	Average tail length (µm)
I	9.14 ± 0.47	7.88 ± 0.75	–	–
II	$44.46 \pm 3.08^{\alpha}$	$64.1 \pm 1.42^{\alpha}$	13.64 ± 2.44	8.19 ± 2.07
III	$76.04 \pm 2.39^{\alpha\mu}$	$96.71 \pm 1.25^{\alpha\mu}$	$56.29 \pm 2.14^{\mu}$	$32.15 \pm 2.63^{\mu}$
IV	$19.37 \pm 2.15^{\alpha\mu\gamma}$	$29.42 \pm 1.26^{\alpha\mu\gamma}$	$21.6 \pm 1.89^{\mu\gamma}$	$16.57 \pm 2.98^{\mu\gamma}$
V	$15.74 \pm 1.04^{\alpha\mu\gamma\theta}$	$22.3 \pm 2.24^{\alpha\mu\gamma\theta}$	$35.99 \pm 3.16^{\mu\gamma\theta}$	$26.78 \pm 2.67^{\mu\theta}$
VI	$33.41 \pm 0.9^{\alpha\mu\gamma\theta\beta\psi}$	$58.19 \pm 1.21^{\alpha\mu\gamma\theta\beta}$	$66.29 \pm 2.65^{\mu\gamma\theta\beta}$	$41.89 \pm 2.08^{\mu\gamma\theta\beta\epsilon}$
VII	$23.75 \pm 2.39^{\alpha\mu\gamma\theta\beta\psi}$	$37.91 \pm 1.99^{\alpha\mu\gamma\theta\beta\psi}$	$72.35 \pm 4.35^{\mu\gamma\theta\beta}$	$56.41 \pm 6.1^{\mu\gamma\theta\beta\psi}$

Table 2: Data were represented as Mean ± SD *(n=6)*. α - significant (*P < 0.05*) as compared with Gr. I; µ - significant (*P < 0.05*) as compared with Gr. II; γ - significant (*P < 0.05*) as compared with Gr. III; θ - significant (*P < 0.05*) as compared with Gr. IV; β - significant (*P < 0.05*) as compared with Gr. V; ψ - significant (*P < 0.05*) as compared with Gr. VI

- **Effect of Nano-Se with CP on tumor growth, MST and % ILS**

Enhancement of therapeutic efficacy of CP by Nano-Se was examined by evaluating the parameters like tumor volume, packed cell volume, viable tumor cell count, MST, % ILS in tumor inoculated mice **(Table 3)**. The mean (±SD) tumor volume and PCV of EAC control group (Gr. II) after 10 days of tumor inoculation were found to be 4.84 ± 0.47 ml and 2.32 ± 0.22 ml respectively. After the treatment with CP (Gr. III), Nano-Se (Gr. IV & Gr. V) and after a combined treatment with both the CP and Nano-Se (Gr. VI & Gr. VII), tumor volume was estimated to be 1.36 ± 0.16 ml, 2.96 ± 0.32 ml & 2.32 ± 0.3 ml, 0.80 ± 0.14 ml & 0.60 ± 0.15 ml respectively and PCV was estimated to be 0.80 ± 0.24 ml, 1.84 ± 0.35 ml & 1.28 ± 0.22 ml, 0.36 ± 0.15 ml & 0.26 ± 0.08 ml respectively. The result

clearly showed that combined treatment with CP and Nano-Se was most effective in reducing tumor volume and PCV, compared to other treatment groups. The mean (±SD) value of tumor cell count was 55.12 ± 3.42 (in million) in EAC control group (Gr. II). After the administration of CP (Gr. III), Nano-Se (Gr. IV & Gr. V) and a combined application of both CP and Nano-Se (Gr. VI & Gr. VII), the mean (± SD) tumor cell count (in million) was 18.66 ± 2.24, 34.88 ± 3.88 & 26.12 ± 1.67, 12.20 ± 1.14 & 8.64 ± 1.55 respectively, the maximum reduction in tumor cell count was observed in the CP plus Nano-Se combined treatment groups. MST of the animals in the EAC control group was 22.10 ± 1.83 days. The survival time significantly ($P < 0.05$) increased to 41.90 ± 2.26 days in case of CP only treated group (Gr. III), 27.55 ± 2.61 days & 33.05 ± 2.19 days in case of Nano-Se only treated groups (Gr. IV & Gr. V). The survivability further significantly ($P < 0.01$) increased to 52.45 ± 2.47 days & 62.85 ± 3.46 days for the animals receiving combine treatment of CP & Nano-Se (Gr. VI & Gr. VII). The increase in life span of tumor bearing mice treated with only CP and only Nano-Se was 89.5% (Gr. III) and 24% (Gr. IV) & 49.5% (Gr. V). Combined treatment with CP and Nano-Se increased the life span by 153.16% (Gr. VI) & 184.38% (Gr. VII).

Groups	Tumor volume (ml)	Packed cell volume (ml)	Tumor cellcount ($\times 10^6$)	Mean survivability (days)	Increasing life span (%)
II	4.84 ± 0.47	2.32 ± 0.22	55.12 ± 3.42	22.1 ± 1.83	–
III	1.36 ± 0.16$^{\mu}$	0.8 ± 0.24$^{\mu}$	18.66 ± 2.24$^{\mu}$	41.9 ± 2.26$^{\mu}$	89.5
IV	2.96 ± 0.32$^{\mu\gamma}$	1.84 ± 0.35$^{\mu\gamma}$	34.88 ± 3.88$^{\mu\gamma}$	27.55 ± 2.61$^{\mu\gamma}$	24
V	2.32 ± 0.3$^{\mu\gamma\theta}$	1.28 ± 0.22$^{\mu\gamma\theta}$	26.12 ± 1.67$^{\mu\gamma\theta}$	33.05 ± 2.19$^{\mu\gamma\theta}$	49.5
VI	0.8 ± 0.14$^{\mu\gamma\theta\beta}$	0.36± 0.15$^{\mu\gamma\theta\beta}$	12.2± 1.14$^{\mu\gamma\theta\beta}$	52.45 ± 2.47$^{\mu\gamma\theta\beta}$	153.16
VII	0.6 ± 0.15$^{\mu\gamma\theta\beta}$	0.26 ± 0.08$^{\mu\gamma\theta\beta}$	8.64± 1.55$^{\mu\gamma\theta\beta}$	62.85 ± 3.46$^{\mu\gamma\theta\beta\psi}$	184.38

Table 3: Data were represented as Mean ± SD *(n=6)*. μ - significant (*P < 0.05*) as compared with Gr. II; γ- significant (*P < 0.05*) as compared with Gr. III; θ - significant (*P < 0.05*) as compared with Gr. IV; β- significant (*P < 0.05*) as compared with Gr. V; ψ - significant (*P < 0.05*) as compared with Gr. VI.

➢ **Evaluation of apoptotic index of EAC cells by TUNEL assay**

To confirm the nature of cell death, TUNEL assay was performed in which as result of apoptosis FITC-conjugated dUTP was incorporated into the DNA strand breaks in the presence of the enzyme terminal deoxynucleotidyl transferase. Apoptotic index (AI) from this assay was measured.

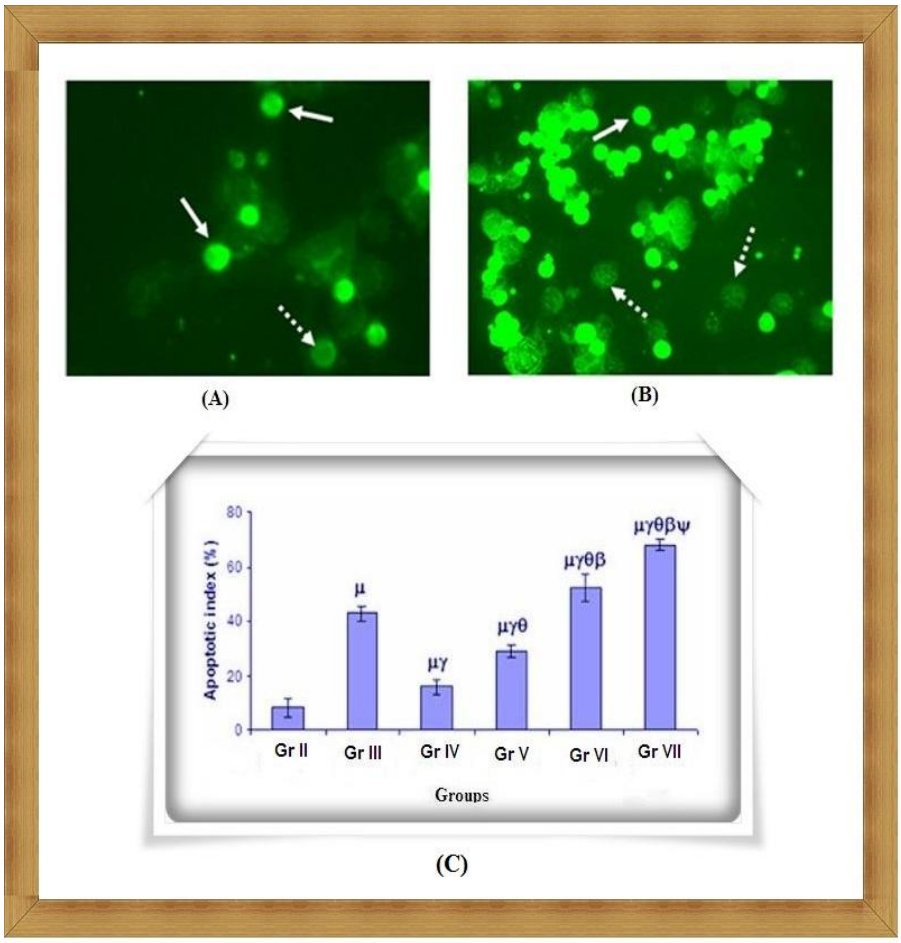

Figure 14: Photomicrographs of TUNEL assay performed in tumor cells. Apoptotic cells (TUNEL label cells) are indicated by white arrows whereas non-apoptotic cells are indicated by white broken arrows (A) and (B); C: Effect of Nano-Se alone or in combination with CP on Apoptotic index of tumor cells.

Data were represented as Mean ± SD *(n=6)*. μ - significant (*P < 0.05*) as compared with Gr. II; γ- significant (*P < 0.05*) as compared with Gr. III; θ - significant (*P < 0.05*) as compared with Gr. IV; β- significant (*P < 0.05*) as compared with Gr. V; ψ - significant (*P < 0.05*) as compared with Gr. VI.

AI in the EAC control group was estimated to be 8.01% (Gr. II), which was increased markedly after treatment with CP (Gr. III) to 42.73% **(Fig. 14C)**. The Nano-Se alone increased the AI value to 15.73% in concomitant treatment schedule (Gr. IV) and to 28.92% in pretreatment schedule (Gr. V). The most effective enhancement in the value of AI was observed in Gr. VI in Gr. VII, where CP and Nano-Se were given in a combination therapy and the values were 52.17% in Gr. VI and 67.96% in Gr. VII.

- **MMP-9 level and neo-vascularization of blood vessels**

Untreated mice bearing Ehrlich tumor elicited a highly significant ($P < 0.05$) increase of serum MMP-9 level (546.01 ng/ml) **(Fig. 15A)**, which was reduced in mice treated with either CP alone (422.41 ng/ml in Gr. III) or with Nano-Se alone (476.33 ng/ ml in Gr. IV & 457.48 ng/ml in Gr. V) or with both CP and Nano-Se (383.71 ng/ml in Gr. VI & 335.77 ng/ml in Gr. VII). The result showed that combined treatment with CP and Nano-Se brought serum MMP-9 level close to the normal mice serum level. It was also found that the individual treatment each with CP or Nano-Se and combined treatment significantly reduced the MMP-9 values at cellular level in mice bearing EAC, compared to untreated mice **(Fig. 15B)**.

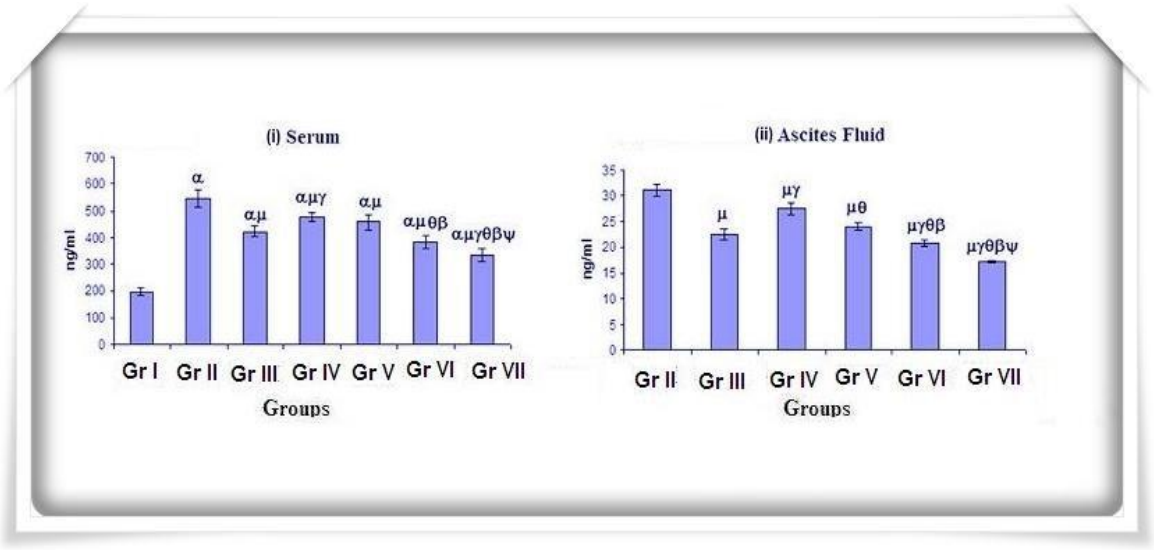

Figure 15: Data were represented as Mean ± SD *(n=6)*. α - significant (*P < 0.05*) as compared with Gr. I; μ - significant (*P < 0.05*) as compared with Gr. II; γ - significant (*P < 0.05*) as compared with Gr. III; θ - significant (*P < 0.05*) as compared with Gr. IV; β - significant (*P < 0.05*) as compared with Gr. V; ψ - significant (*P < 0.05*) as compared with Gr. VI

The peritoneum of EAC bearing mice was rich in blood vessels **(Fig. 16 A-E)** when compared to that of normal mice due to angiogenesis. This enables the delivery of oxygen and nutrients essential for growth and metastasis of tumor. However, reduction in sprouting due to inhibition of the neovasculature in peritoneal angiogenesis was observed in mice that were treated with Nano-Se during concomitant and pretreatment schedule.

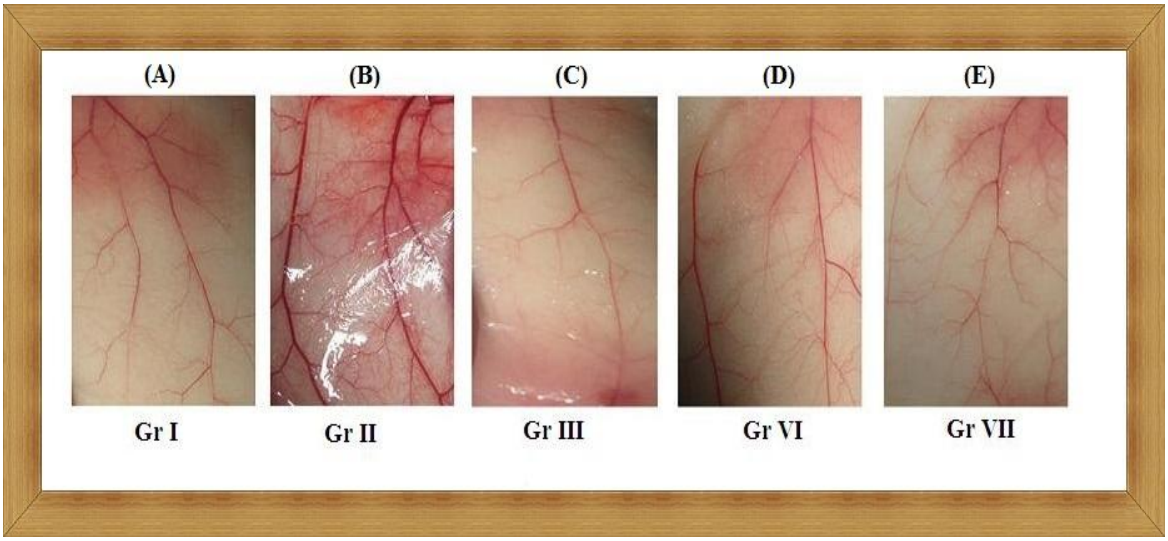

Figure 16: Photograph of peritoneal lining of tumor bearing animals. (Gr. I) shows normal architecture of peritoneal lining of vehicle control group. (Gr. II) Shows sprouting of new capillaries and leaky blood vessels of the peritoneal membrane in EAC control groups. Treatment with CP (Gr. III) showed reduction in the peritoneal vasculature and treatment with Nano-Se along with CP in concomitant (Gr. VI) and pretreatment (Gr. VII) scheme showed markedly reduced peritoneal vasculature and normalization of blood vessels.

- **Histopathological examination**

The liver section of vehicle control mice (Gr. I) appeared to be formed of the classical hepatic lobules. Each lobule showed radially arranged hepatocytes forming cords around the central veins (CV). Portal vein (PV) also was normal in architecture, without any congestion. The liver sections of the EAC-inoculated animals showed several changes in hepatic tissue and showed severe dilatation of both CV and PV and congestion of blood vessels in CV as well as in PV. Hepatocytes showed vacuolar degeneration (hydropic changes) with deeply stained pyknotic nuclei, mononuclear cellular infiltration around the congested CV and necrosis were seen after

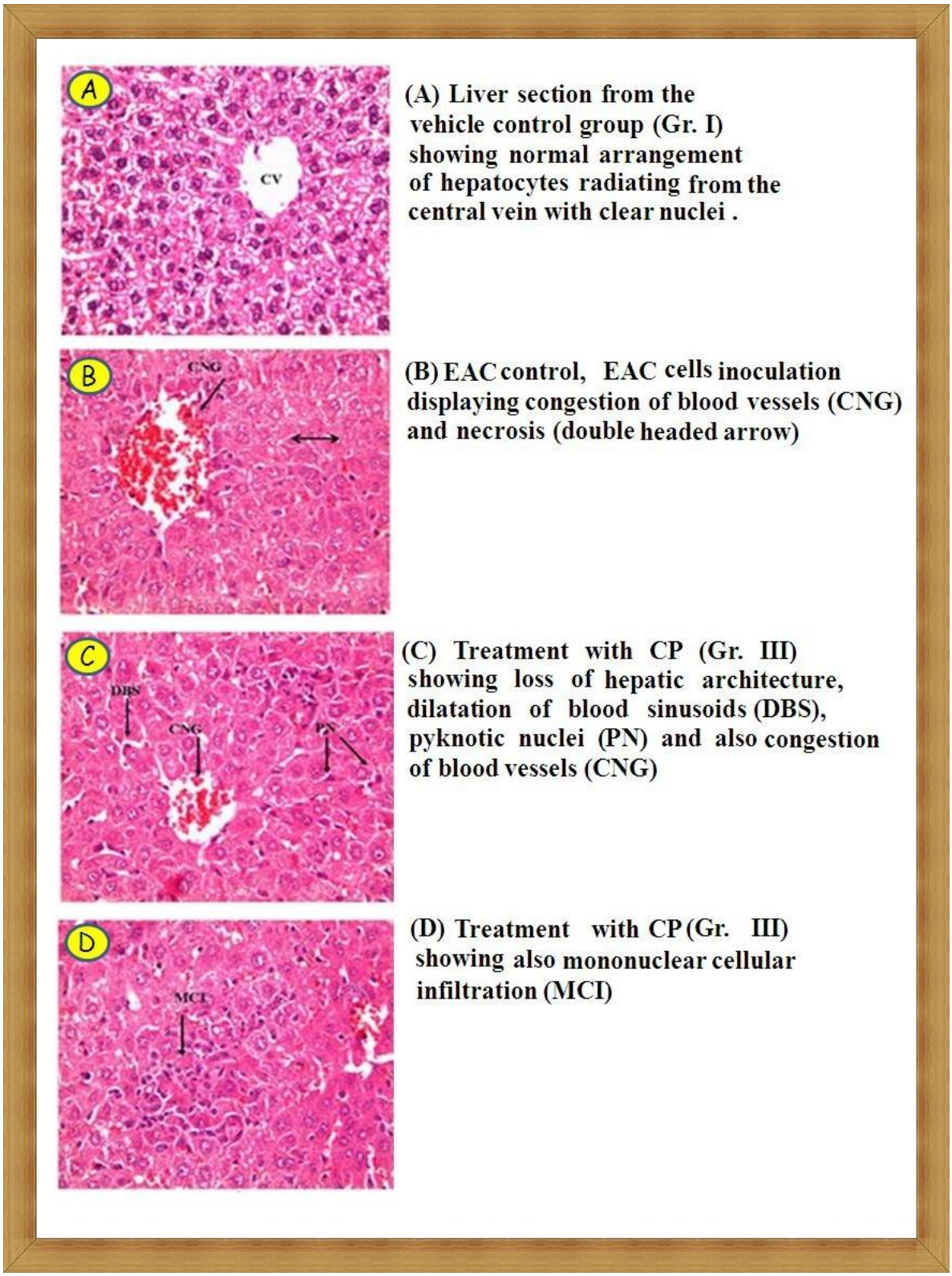

Figure 17 (A- D): Photograph of liver section of mice stained with hematoxylin and eosin, ×200

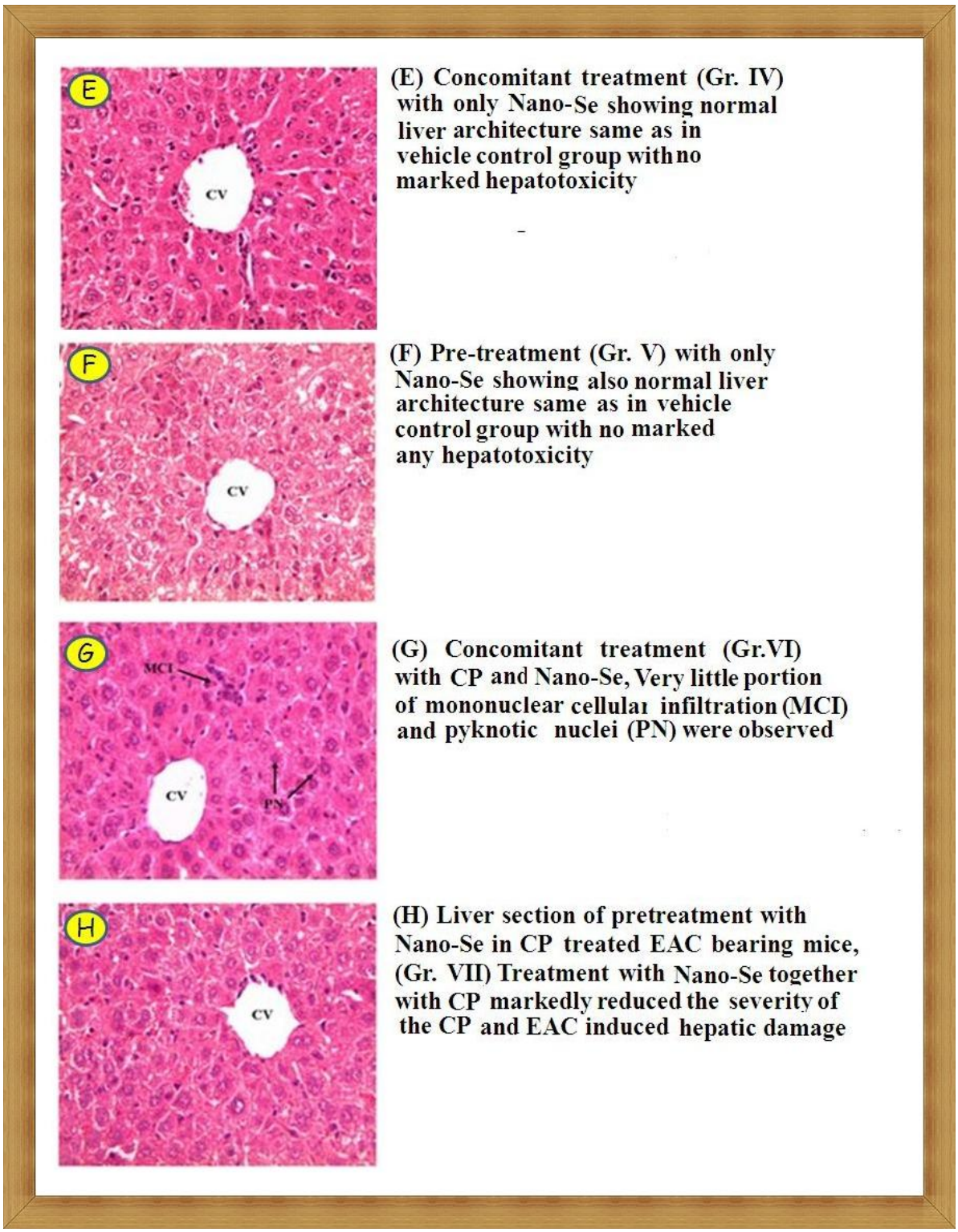

Figure 17 (E- H): Photograph of liver section of mice stained with hematoxylin and eosin, ×200

10 days of EAC inoculation. These pathological changes became more severe when EAC inoculated mice treated with chemotherapeutic drug CP and revealed the loss of normal appearance which includes congestion of CV, mononuclear cellular infiltration, dilatation of blood sinusoids and formation of pyknotic nuclei and hepatocellular necrosis. A great deal of prevention of these pathological alterations in liver was observed after the administration of the Nano-Se, either alone or combination with CP. Whereas, the concomitant treatment with the Nano-Se exerted a moderate reversion of the pathological changes of the hepatic tissue, maximum protection of the hepatic tissue was obtained by pretreatment with the same. Histology of liver from animals of different groups has been shown in (**Fig. 17 A-H)**.

Discussion

The use of antioxidant supplements by patients with cancer is estimated between 13% and 87%. This wide range of percentages might be attributed to the variability of definitions of complementary and alternative medicine used in the different studies, and to differences in the cancer types, age, education, economic status, and ethnicity of the groups assessed **(Block et al., 2007)**. Patients may take different types of supplements while undergoing chemotherapy to help alleviate side effects from toxic chemotherapies and to increase the efficacy of chemotherapy **(Ladas et al., 2004)**, as it enable patients to tolerate chemotherapy during the full course of treatment and possibly at higher doses. As a result, patients may have better tumor response rates and improved quality of life.

Antineoplastic agents have been shown to produce multi-organ toxicity mainly due to drug induced oxidative stress in patients **(Conklin, 2004)**. Chemotherapeutic drugs mostly kill rapidly dividing cells in the body, targeting cancer cells as well as normal cells originating from bone marrow **(Szatrowski et al., 1991)**. In the present study, a noticeable decrease of hemoglobin (Hb) level, WBC count and RBC count was observed in the CP treated tumor bearing mice compared to untreated tumor bearing mice. Treatment with Nano-Se brought back the hemoglobin level, RBC, and WBC count to near normal levels, indicating the protective effects of Nano-Se on the hemopoietic system.

Cancer cells can generate large amounts of hydrogen peroxide which may contribute to their ability to mutate and damage normal tissues, and moreover, facilitate tumor growth and invasion **(Pelicano et al., 2004)**. Many chemopreventive and chemotherapeutic agents have been found to induce cancer cell apoptosis through upregulation of intracellular ROS generation **(Nilsonne et al., 2006)**. Growing evidences suggest that ROS generation acts as an important cellular event induced by Se compounds and resulted in cell apoptosis **(Ghosh et al., 2015)**. Results obtained from the present study indicated that CP treatment increased ROS production in the liver cytosol as well as in bone marrow cells as measured by the DCFH-DA assay. In the present study, Nano-Se significantly inhibited CP induced ROS formation in liver cytosol and also in bone marrow cells and at the same time significantly enhanced the intracellular ROS level in EAC cells, suggesting the involvement of ROS as a critical mediator in Nano-Se-induced apoptosis in tumor cells and protection in normal cells.

Thiobarbituric acid reactive substance such as malondialdehyde (MDA), a degradation product of lipid hydroperoxides is considered as an index of lipid peroxidation, which was reported to be higher in cancer tissues than in non-diseased organ **(Liu et al., 2012)**. Metabolism of CP results in production of acrolein which is a toxic metabolite responsible for production of ROS and enhancement of LPO **(Matés, 2000)**. The present study showed increased lipid peroxidation in the liver of CP treated mice which was associated with hepatic damage. Concomitant and pretreatment with Nano-Se effectively inhibited the CP induced hepatic LPO level. It means that Nano-Se evoked an antioxidant action and eliminated peroxides such as hydrogen peroxide and lipid peroxide. This proves the protective role of the Nano-Se in preventing lipid peroxidation and in maintaining the integrity and normal function of the liver cells.

In the current study, liver function was significantly impaired after EAC inoculation which was further appended by CP treatment. ALT and AST are marker enzymes for assessment of liver functions. Elevated levels of transaminase enzymes are indicative of cellular damages and loss of functional integrity of cell membrane in liver **(Gong et al., 2014)**. Damage to liver cells causes release of these enzymes into serum. Hepatic activation of CP leads to the formation of toxic metabolites which further cause damage

to the liver tissues as shown by increased AST and ALT levels. Treatment with Nano-Se resulted in significant reduction in the level of these transaminase activities in both EAC control and also in CP treated EAC bearing mice indicating hepatocellular protection.

GSH acts as a multifunctional intracellular non-enzymatic antioxidant and protects cells against several toxic oxygen-derived chemical species. It is considered to be an important scavenger of free radicals and a cofactor of several detoxifying enzymes against oxidative stress, e.g., glutathione-S-transferase, glutathione peroxidase and others **(Bhattacharyya et al., 2007)**. Several studies demonstrated that EAC inoculation induced a decrease in hepatic glutathione (GSH) content associated with inhibition of hepatic glutathione peroxidase (GP*x*) and superoxide dismutase (SOD) activity **(Yousefipour et al., 2004)**. In this present study we found that EAC inoculation significantly reduced the GSH level, this level was further suppressed by CP treatment. The depletion of GSH level caused due to CP treatment could be attributed to the direct conjugation metabolites of CP with GSH, thereby reducing its cellular level which leads to induction of oxidative stress **(Srivastava et al., 2010)**. GSH depletion leads to lowered cellular defense against free radicals induced cellular injury resulting in necrotic cell death **(Kaya et al., 1999)**. Our study shows that the mechanism of hepatoprotection by Nano-Se against CP toxicity and hepatic damage involves suppression of oxidative stress by preventing GSH depletion. Very recently, it has been reported that meat from lamb supplemented with Nano-Se enriched diet has the ability to protect 7, 12-dimethyl-benz(a)anthracene (DMBA)-induced oxidative stress injury in mice **(Ungvári et al., 2014)**.

Antioxidant enzyme GST catalyzes the detoxification of endogenous compounds such as lipid peroxide, as well as the metabolites of xenobiotics like acrolein from CP through conjugation of GSH via the sulfhydryl group with these toxic compounds. Several reports suggest that increased ROS generation after CP treatment reduced the GSH level and GST activity in several organs including liver **(Ghosh et al., 2014)**. The hepatic GST activity was decreased significantly by EAC inoculation which was further diminished by CP treatment. Treatment with Nano-Se invariably increased the GST activity and reduced the CP mediated oxidative stress in liver cells.

SOD, CAT, and GP*x* are involved in the clearance of superoxide and hydrogen peroxide (H_2O_2). SOD catalyses the diminution of superoxide into H2O2, which has to be eliminated by CAT and/or GP*x*. The balance between the dismutation of superoxide anion (by SOD) and its conversion to molecular oxygen and water (by CAT or GP*x*) may be critical to maintain cellular antioxidant defense **(Basu et al., 2015)**. CP-induced hepatotoxicity is associated with oxidative stress caused by the reduction in these antioxidant enzymes activities **(Bhattacharjee et al., 2014)**. Further, it has been reported that a decrease in SOD activity in EAC bearing mice may be due to loss of Mn^{2+} containing SOD activity in EAC cells and loss of mitochondria, leading to a decrease in total SOD activity in the liver **(Di Bucchianico et al., 2014)**. Similar findings were observed in our present study in EAC bearing and also in CP treated mice. Treatment with Nano-Se invariably increased the SOD, CAT and GP*x* activity and reduced the CP mediated stress in liver cells. It may be possible that treatment with Nano-Se increased the activity of antioxidant selenoenzyme GP*x* which, in turn, upregulated the other antioxidant enzyme systems.

Histopathological studies also provided clear evidence for the protective effect of Nano-Se on CP-induced hepatotoxicity in EAC bearing mice. In the liver sections of the EAC-inoculated animals, hepatocytes showed vacuolar degeneration (hydropic changes), pyknotic nuclei and necrosis. This may be due to the accumulation of hemorrhagic ascetic fluid within the peritoneal cavity in which the cells proliferate and move to invade the internal organs; these activities were further suppressed by CP treatment. Nano-Se effectively diminished EAC and CP induced hepatopathological alterations.

DNA is probably the most biologically significant target of oxidative attack, and it is widely thought that continuous oxidative damage to DNA is a significant contributor for the development of major cancers. Excessive production of ROS might be the prime cause of severe DNA damage as observed from the comet assay of lymphocytes **(Ghosh et al., 2012)**. Phosphoramide and acrolein are the major metabolites of CP, induces DNA strand breaks, cessation of DNA synthesis, DNA-protein cross-links and DNA adducts formation. This DNA damage ultimately leads to the secondary tumors in humans. In the present study, it was observed that percentage of damaged cells of lymphocytes showed a

significant increase of the comet tail after treatment with CP in tumor bearing mice. Administration of Nano-Se before and during CP treatment ameliorated the DNA damages induced by EAC inoculation and CP treatment. This anti-genotoxic effect of Nano-Se might be due to its antioxidant and chemoprotective activity. On the other hand, striking observation was found. The comet tail length of tumor cells were significantly enhanced after administration of Nano-Se along with CP in pre and concomitant treatment respectively in the same mice.

Oxidative stress can induce chromosomal aberrations through oxidative base damage and strand breaks in DNA contributing to mutagenesis **(Sanderson et al., 1996)**. Such genetic damage caused by CP is not cancer cell specific, as it may also occur in the normal tissues leading to gene mutations. It has been reported that mutations may lead to the formation of secondary tumors if they occur in somatic cells **(Selvakumar et al., 2006)**. In the present investigation, mice treated with CP presented a marked increase in percentage of chromosomal aberrations in bone marrow cells in tumor bearing mice. Restoration of these levels toward normal after Nano-Se treatment in tumor bearing CP-treated mice suggests an antigenotoxic efficacy of Nano-Se. This might be in part due to the direct scavenging activity of Nano-Se against the ROS, which is one of the major causes of DNA damage and chromosomal aberration.

Ascitic fluid is the essential nutritional source for proliferation of tumor cells and a rapid increase in ascitic fluid with tumor growth would provide the essential nutritional requirement of tumor cells **(Gupta et al., 2000)**. In this study, the antitumor effect of Nano-Se on Ehrlich ascites carcinoma was demonstrated. When the Nano-Se when used alone to treat tumor bearing mice, showed moderate antitumor efficacy without any toxicity on normal tissue compared to the CP monotherapy. The advantage of combination therapy significantly reduced the tumor volume, packed cell volume and the viable number of tumor cells, as well as it also increased the mean survival time and life span of tumor bearing host. Prolongation of life span of animals and enhancing the quality of health are a reliable standard for evaluating the outcome of chemotherapy. Thus, it may be conceivable that, Nano-Se exerts its antitumor effect by decreasing viable

tumor cells counts and consequently decreased ascetic volume and increased the life span of EAC-bearing mice.

It has been reported that chemotherapy induced ROS generation diminish the efficacy of the cancer treatment by interfering with anticancer drug induced apoptosis, which is important for chemotherapeutic agents to exert their optimal effect on cancer cells **(Conklin, 2004)**. In this study, we demonstrate that Nano-Se is capable of inducing apoptosis in EAC cells. The morphological hallmarks of apoptosis such as nuclear fragmentation, membrane blebbing and inter nucleosomal fragmentation of DNA. So an agent which can selectively modulate the ability of antineoplastic drugs to induce apoptosis may enhance treatment efficacy, and prevent tissue damaging inflammatory response. In this present study, it was observed that the percentage of apoptotic cells increased after the treatment with Nano-Se alone or in combination with CP. However, the exact mechanism of cell death has not been determined fully. But from the above discussion it can be inferred that the Nano-Se can generate ROS in tumor cell which sensitized them to apoptosis.

Tumor growth and metastasis are dependent on angiogenesis **(Ushio et al., 2004)**. Increased neovasculature may allow not only an increase in tumor growth but also enhances hematogenous tumor embolization. It is well known that ascites tumor growth including EAC cell are angiogenesis dependent **(Saraswati et al., 2013)**. Thus inhibiting tumor angiogenesis may halt the tumor growth and decrease metastatic potential of tumors. Inhibition of angiogenesis by Nano-Se is thought to be another major effecter in enhancing the therapeutic efficacy of cyclophosphamide. It has been reported that selenium metabolite, CH_3SH is the key inhibitor of angiogenic switching in early lesions and in tumor **(Nagy et al., 1995)**. Here the angiostatic property of Nano-Se was established by substantial reduction of the neovascularization in the peritoneum lining of tumor bearing mice. Furthermore, to strongly claim the angiostatic property of Nano-Se, we have measured the MMP-9 level in serum as well as in ascites fluid of tumor bearing mice. MMP-9 is a mediator of angiogenesis which in turn, causes tumor growth and metastasis **(Yoon et al., 2002)**. In the present investigation, we have found that with the combined treatment of Nano-Se and CP there is a highly significant reduction of MMP-9

level in serum and ascites fluid. Various report suggested that antiangiogenic compound regularize the blood flow in dilated, chaotic, hemorrhagic and leaky tumor vasculatures, ensuring proper homogenous delivery of anticancer drugs to the tumor bed. In combination with anticancer drugs, antiagiogenic compounds enhance their antitumor efficacy by diffusing the chemotherapeutic drugs to the distant tumor cells **(Lu et al., 2001)**. The results clearly demonstrated that Nano-Se does not interfere with the antitumor efficacy of CP on the other hand administration of Nano-Se in CP treated animals synergistically enhanced the therapeutic efficacy of CP.

In conclusion, the mechanism of such selective protection of normal cells over the tumor cells by Nano-Se against CP induced toxicity is exactly not known. It was suggested that dietary antioxidants may act as an antioxidant to normal cells and as a prooxidant to cancer cells **(Gupta et al., 2004)**. The prooxidant activity of an antioxidant may be the reason for the antitumor activity of many antioxidants **(Caderni et al., 2000)**. Nevertheless, the mechanisms of action of Nano-Se, either via a prooxidant pathway, as seen in cytotoxicity and apoptosis, or via an antioxidant pathway, as proposed in cancer chemoprevention, are still unclear but intriguing. Further investigations are required to fully explore the exact molecular mode of action of Nano-Se on CP induced toxicity and antitumour efficacy.

Chapter IV

Protective effect of Nano -Se against the toxicities induced by a cancer chemotherapeutic agent cisplatin in Swiss albino mice

Introduction

Cancer treatment using chemotherapeutic drugs has unfolded new prospect to improve the quality of life of cancer patients. Unfortunately, numerous anticancer agents have been considered to be carcinogenic in clinical experimental application systems **(Ansari, 2017)**. Cisplatin (CDDP), a typical platinum-based agent during "the war on cancer", is widely used to treat many types of cancers within the effective dose range, including cervical, ovarian, head, neck and non-small cell lung carcinoma. It is particularly effective in testicular cancer, with a cure rate of more than 90% **(Abdel Moneim et al., 2014)**. The ability of CDDP to react with nucleophilic bases in DNA and form intra and interstrand cross-links has been suggested to be main mechanism behind its anticancer activity **(Florea et al., 2011)**. However, full therapeutic efficacy of CDDP is limited due to the development of drug resistance **(Li et al., 2016),** and the dose limiting side effects, which includes nausea, vomiting, nephrotoxity **(Hoek et al., 2016),** peripheral neuropathy **(Ferreira et al., 2018)**, mutagenecity **(Basu et al., 2015)**, embryotoxicity **(Ongio et al., 2006)** and ototoxicity **(Kim et al., 2017)**. Approximately one-third of patients who were treated with CDDP experienced nephrotoxic renal injury **(Guo et al., 2018)**. The nephrotoxic injury typically affects the S3 segment of the proximal tubule in the outer stripe of the outer medulla including a thinning or local loss of brush border, cellular swelling and condensation of the nuclear chromatin and focal areas of necrosis **(Bland et. al., 2017)**. Reports suggested that CDDP induced nephrotoxicity is related to oxidative stress, inflammation and apoptosis **(Ning et al., 2018)**. Copper transporter 1 and organic cation transporter 2 transport CDDP to renal tubules and proximal tubules, then induce mitochondrial dysfunction **(Oh et al., 2014)**. The level of reactive oxygen species (ROS), an important factor that modulates oxidative stress, is related to the facilitation of some side effects **(Abdal et al., 2017)**. Nitric oxide is an indispensable factor in CDDP induced nephrotoxicity. Many other ROS such as hydrogen peroxide and superoxide

anion are also important **(Qi et al., 2017)**. Peroxynitrite must exist in the kidney if excessive CDDP affects cells that produce both superoxide and nitric oxide **(Ratliff et al., 2016)**. The excessive expression of ROS and reactive nitrogen species causes oxidation reactions, enzyme inactivation, protein nitration, the generation of pro-inflammation factors, cell dysfunction and the activation of apoptosis signalling pathways, which eventually leads to cell death **(Qi et al., 2017)**. Experimental evidence suggested that alteration of kidney function after CDDP administration are characterized by signs of injury, such as changes in body weight; increase of lipid peroxidation products in kidney; level of antioxidative enzyme's status; morphological destruction of intracellular organelles; cellular necrosis; and a significant elevation in serum creatinine and urea levels **(Basu et al., 2015)**. Cisplatin is highly mutagenic, inducing chromosomal aberrations (CA) in peripheral blood lymphocytes in patients and in rat bone marrow cells **(Attia, 2010)**. The genotoxic potential of CDDP has become of great interest because of its serious effects on the DNA of non-tumour cells **(Basu et al., 2015)**.

As a result, the search for nontoxic chemoprotective agent that can efficiently antagonize CDDP-induced toxicities, without altering the chemotherapeutic efficacy is the need of the hour.

Selenium is an essential micronutrient mainly because of the antioxidant effects of these selenoproteins. Functionally there are at least two different enzyme families of selenoproteins: glutathione peroxidases (GP*x*) and thioredoxin reductases (TrxR). Being a cofactor of these anti-oxidant enzymes selenium takes part in scavenging free radicals, thus protecting cells, membranes and cell organelles from lipid peroxidation, enzymes and nucleic acids from the harmful effects of ROS **(Zoidis et al., 2018)**. Se effectively improves the therapeutic efficacy and selectivity of anti-cancer drugs by increasing the chemotherapeutic window distinguishing cancer cells from normal cells, there is strong evidence which confirms it. Se is reported to be the first agent that significantly improves the therapeutic index of anticancer drugs. It has been proved regarding selectivity that, Se protects normal tissues from dose limiting toxicity of DNA-damaging chemotherapeutics and thus facilitates the delivery of higher chemotherapeutic doses **(Gandin et al., 2018)**. In this regard, Se compounds have been found to attenuate CDDP-toxicities in target/non-target organs without affecting its antitumor activity

(Wrobel et al., 2016), but there is yet a level of concern on Se potential toxicity even at the pharmacological doses **(Li et al., 2012)**. The limiting factors for using Se are its bioavailability and toxicity. For example, sodium selenite appears to have little potential as a preventive agent against CDDP toxicities **(Li et al., 2012)** and additionally, it can be metabolized into hydrogen selenide which is a highly toxic Se compound **(Tarze et al., 2007)**. Thus, it is more reasonable to use a different Se form with significantly lower toxicity and higher efficacy. Nanotechnology holds a future promise for medication and nutrition because materials at the nanometer dimension exhibit novel properties different from those of both isolated atom and bulk material **(Rasmussen et al., 2010)**. Thus as a result nano particle of selenium (Nano-Se) are increasingly drawing attention due to their excellent biological activities and low toxicity **(Zhang et al., 2008; Wang et al., 2007)**. Likely, the development of Nano-Se with higher chemoprotective and renoprotective efficacy is attracting the interest of the researcher. The toxicity reported for elemental selenium (Se^0) at nano-size is lower than selenite (Se^{+2} or Se^{+4}) ions; therefore, selenium nanoparticles may be a good candidate to replace other types of selenium in nutritional supplements or pharmaceutical dosage types **(Chang et al., 2017)**. To explore this aspect However, there have been no reports on the nephroprotective activity of Nano-Se against CDDP-induced renal toxicity. Hence, we conducted this study to investigate the Nano-Se nephroprotective potential using a murine model of CDDP-induced nephrotoxicity.

Materials and methods

Experimental animals

Adult (5–6 weeks) Swiss albino female mice (25 ± 2g), bred in the animal colony of Chittaranjan National Cancer Institute (CNCI) (Kolkata, India), were used for this study. The mice were maintained under standard condition of humidity (45–55%), temperature (23 ± 2ºC), and light (12 h light/12 h dark). Standard food pellets (EPIC rat and mice pellet) from Kalyani Feed Milling Plant, Kalyani, West Bengal, India and drinking water was provided *ad libitum*. The experiments were carried out following strictly the Institute's guideline for the Care and Use of Laboratory Animals.

Chemicals

Cisplatin was purchased from Cadila Health Care Limited, Kundaim Industrial Estate, Ponda, Goa, India. 1-Chloro-2, 4- dinitrobenzene (CDNB), ethylene diamine tetraacetic acid (EDTA), reduced glutathione (GSH), pyrogallol, 5,5´-dithio-bis (2-nitro benzoic acid) (DTNB), sodium dodecyl sulphate (SDS), bovine serum albumin (BSA), β-nicotinamide adenine dinucleotide phosphate (reduced), glutathione reductase, normal melting agarose, low melting point agarose, ethidium bromide, sodium azide (NaN3), HEPES, 2´,7´ - dichloro fluorescence diacetate (DCFH-DA), dihydroethidium (DHE), dimethyl sulphoxide (DMSO), vanadium chloride (VCl_3), phenylmethanesulfonyl fluoride (PMSF), Triton-X 100, Giemsa stain acridine orange and thioredoxin reductase (ThxR) assay kit were obtained from Sigma-Aldrich Chemicals Private Limited, Bangalore, India. Hydrogen peroxide 30% (H2O2), thioberbituric acid (TBA), propylene glycol, sodium carbonate, copper sulfate, sodium hydroxide, potassium-sodium tartrate, sucrose, TRIS, dithiothreitol, calcium chloride, di-sodium hydrogen phosphate, sodium di-hydrogen phosphate, acetic acid, n-butanol, pyridine, hematoxylin, and eosin were obtained from Merck (India) Limited, Mumbai, India. Chloroform and Folin-phenol reagent were purchased from Sisco Research Laboratories Private Limited, Mumbai, India. Magnesium chloride was purchased from Glaxo laboratories (India) Ltd, Bombay. Diethyl ether, dipotassium hydrogen phosphate, and potassium dihydrogen phosphate were obtained from Spectrochem Private Limited, Mumbai, India. Urea Berthelot Test Kit and Creatinine Test Kit were obtained from Span Diagnostics Ltd, Sachin (Surat), India.

Experimental design

Experimental groups

Animals were distributed into five groups containing six animals (n = 6) in each group. The day of beginning of CDDP administration was considered as day 1.

Vehicle treated group (Group I): Each animal was given oral administration of saline (0.9% NaCl) from day 1 to day 9.

Nano Selenium treated group (Group II): Animals were treated orally with Nano-Se only at a dose of 2 mg Se/kg b.w. throughout the experimental period.

CDDP-treated group (Group III): CDDP was administered intraperitoneally at a dose of 5 mg/kg b.w. in water for consecutive 5 days (day 1 to day 5).

Concomitant treatment group (Group IV): Nano-Se was administered orally at a dose of 2 mg Se/kg b.w. for 9 days and CDDP was given as in Gr. III.

Pretreatment group (Group V): Nano-Se was administered orally at a dose of 2 mg Se/kg b.w. seven days prior to the CDDP treatment and then continued along with CDDP for 9 days.

The mice were sacrificed 4 days after last injection of CDDP, and the parameters described below were studied. The treatment schedule has been schematically presented in **Fig. 1.**

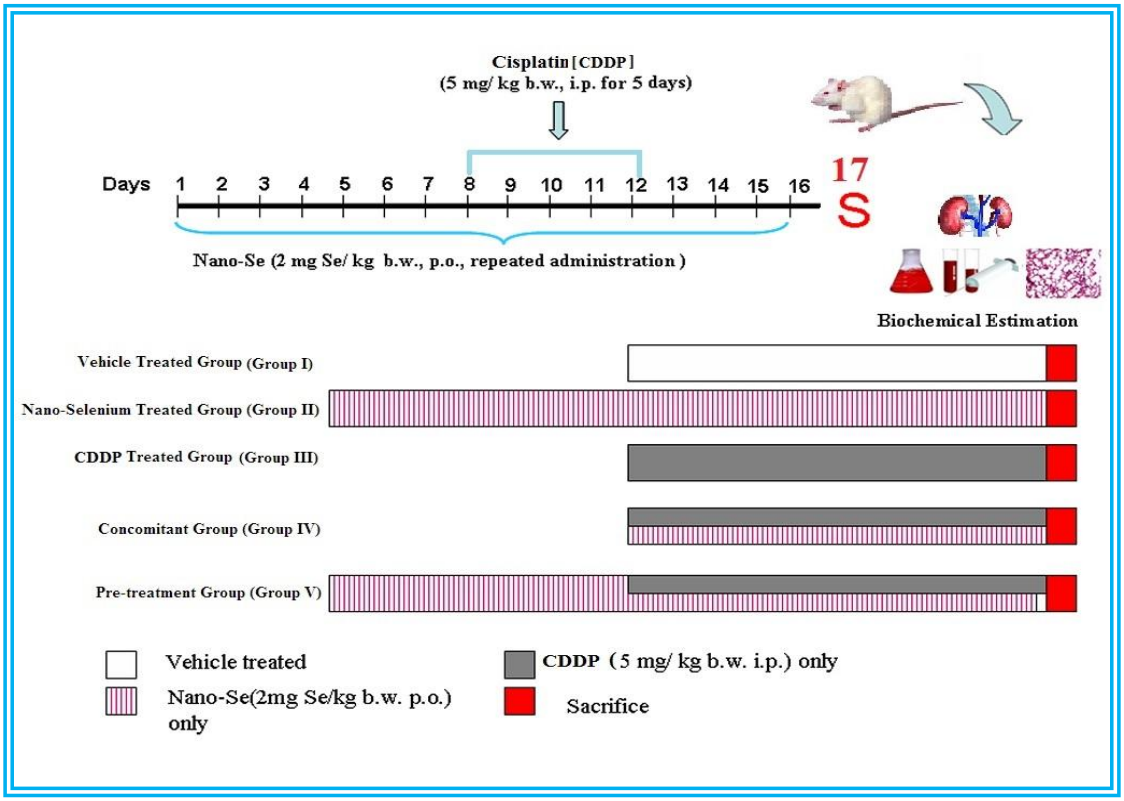

Figure 1: Treatment schedule

Parameter studied

Set A

It was designed for the assessment of the following parameters:

- Quantitative estimation microsomal lipid peroxidation level in kidney tissue and bone marrow cell sample.
- Biochemical estimation of reactive oxygen species levels in kidney and bone marrow sample.
- Measurement of nitric oxide (NO) production in kidney tissue and bone marrow cell sample.

Set B

- Estimation of reduced glutathione (GSH) level and phase II detoxifying/antioxidant enzymes like glutathione-*S*-transferase (GST), glutathione peroxidase (GP*x*), thioredoxine reductase (TrxR), catalase (CAT), and superoxide dismutase (SOD) activity in kidney tissue sample.
- Estimation of renal function markers namely blood urea nitrogen and creatinine levels in serum.

Set C

- Detection of DNA damage in lymphocytes and bone marrow by alkaline single cell gel electrophoresis (Comet Assay).
- The assay of important cytogenetic parameters like chromosome aberration (CA) in bone marrow cells.
- Detection of micronuclei (MN) assay in bone marrow cells.
- Determination of percentage of DNA fragmentation by diphenylamine (DPA assay) in bone marrow cells.
- Detection of apoptosis of bone marrow cells by using TUNEL method
- Determination of *in situ* cell proliferation using BrdU Labeling
- Histopathological evaluation of kidney tissue.

Methodologies

❖ Biochemical parameters

Detailed procedures regarding the biochemical parameters (except that for thioredoxin reductase) already have been mentioned in Chapter I and Chapter II.

➢ Estimation of protein content in the tissue homogenate (Lowry et al, 1951)

Total protein content in tissue homogenate during biochemical analysis assay was measured through Lowry method using Folin-Phenol reagent.

➢ Quantitative estimation of lipid peroxidation (LPO) level (Ohkawa et al, 1979)

Spectrophotometric method was applied to estimate the level of lipid peroxidation in kidney microsomes and bone marrow cells by measuring the formation of lipid peroxides using thiobarbituric acid (TBA) and was expressed as nmTBARS/mg protein.

➢ Estimation of reactive oxygen species (ROS) production

ROS generation in kidney homogenate and bone marrow cells were measured spectrofluorimetrically with slight modifications using two probes, DCFH-DA and DHE.

- **DCFH-DA assay for determination of hydrogen peroxide level**

ROS generation in kidney homogenate and bone marrow cells were measured spectrofluorimetrically using DCFH-DA following a simplified protocol with slight modifications **(Lu et al, 2010; Shinomol and Muralidhara, 2007)**. DCFH-DA is a non-fluorescent probe that is hydrolyzed by mitochondrial esterase to form 2',7'-dichlorodihydrofluorescein (DCFH), which is then oxidized by ROS to form the fluorescent compound 2',7'-dichlorofluorescein (DCF) which is measured spectrofluorimetrically (excitation 485 nm/emission 530 nm).

- **DHE assay for determination of superoxide level (Zou et al., 2001)**

DHE is a non-fluorescent dye and freely permeable to the cell. Upon oxidation by superoxide anions (O^{2-}) forms the red fluorescent product ethidium which is measured spectrofluorimetrically (excitation 475 nm/emission 610 nm).

- **Estimation of NO production (Green et al., 1982)**

Tissue nitrite (NO_2^-) was estimated as an index of NO production. NO_2^- is one of two primary, stable and nonvolatile breakdown products of NO. This assay was accomplished through diazotization reaction using Griess reagent system which includeed sulfanilamide and N-1-napthylethylenediamine dihydrochloride under acidic (phosphoric acid) conditions. Total NO_2^- levels in tissue homogenates were measured spectrophotometrically at 545 nm after the reduction of NO_3^- to NO_2^- by VCl_3.

- **Estimation of glutathione peroxidase (GP*x*) activity (Paglia et al., 1967)**

GPx activity in kidney was measured by NADPH oxidation using a coupled reaction system consisting of reduced glutathione, glutathione reductase and hydrogen peroxide. The enzyme activity was expressed as micromol NADPH utilized/minute/mg protein using extinction coefficient of NADPH at 340 nm as 6200 $M^{-1}cm^{-1}$.

- **2.5.1.6. Estimation of Thioredoxin Reductase Activity (TrxR) (Mustacich et al., 2000)**

TrxR reduces oxidized thioredoxin (Trx) using NADPH as a reducing equivalent to form reduced Trx which in turn spontaneously reduces various biomolecules of the cell like proteins, nucleic acids etc. Mammalian TrxR activity was determined spectrophotometrically following a standard enzymatic method (reduction of DTNB with NADPH to TNB) provided with the commercially available kit. Two moles of 5-thio-2-nitrobenzoic acid (TNB) are formed for every one mole of NADPH oxidized. The assay was performed at room temperature (25°C) and the TNB had an absorption maximum at 412 nm. In crude biological samples, other enzymatic activities, such as glutathione reductase and glutathione peroxidase, also reduce DTNB and increase the observed rate

of DTNB reduction. The contribution of these activities to the total DTNB reduction may be estimated by using a specific TrxR inhibitor. In order to determine the DTNB reduction due only to the TrxR activity present in the sample, two assays need to be performed: the first measurement is of the total DTNB reduction by the sample and the second one is the DTNB reduction by the sample in the presence of the TrxR inhibitor solution. The difference between the two results is the DTNB reduction due to TrxR activity.

Reagents required

Assay Buffer 5× for thioredoxin reductase (500 mM potassium phosphate, pH 7.0, containing 50 mM EDTA), TrxR [rat liver TrxR in 50 mM Tris-HCl, pH 7.4, containing 1 mM EDTA, 300 mM NaCl, and 10% glycerol {≥200 μg (protein)/ml}], TrxR inhibitor solution, DTNB, NADPH, dimethyl sulfoxide (DMSO).

Preparation of working solutions

1× Assay Buffer - It was prepared by diluting 2 ml of the Assay Buffer 5× for TrxR to 10 ml with ultrapure water and was kept at room temperature.

DTNB Solution - 39.6 mg of DTNB was dissolved in 1 ml of dimethyl sulfoxide (DMSO). This solution was prepared the day before use and stored at 2–8 °C.

NADPH Solution - 0.625 ml of water was added to the bottle containing 25 mg of NADPH and care was taken for complete dilution of the content.

Working buffer - 10 ml of working buffer was prepared by adding 50 μl of NADPH solution to 2 ml of assay buffer 5× for TrxR and the final volume was brought to 10 ml with ultra pure water. The final concentration of the working buffer was 100 mM potassium phosphate with 10 mM EDTA and 0.24 mM NADPH. The working buffer was kept at room temperature and used within 2 hours.

Diluted Inhibitor Solution - 10 ml of the TrxR Inhibitor Solution was diluted 20-fold with DMSO to a final volume of 200 ml. The solution was kept at room temperature during the assay.

Procedure

Animals were sacrificed and kidneys were isolated, washed in PBS and were weighed (100 mg)

⇩

The tissue was then homogenized with 4 volumes of 0.25× assay buffer Teflon homogenizer

⇩

The homogenate was then centrifuged for 15 minutes at 10,000g at 4oC. The supernatant was used as the enzyme sample.

In 96 well plate 180 µl of working buffer was added

⇩

5 µl of tissue sample was added in each well

⇩

9 µl of 1× assay buffer was added in each well.

⇩

For the inhibition reaction 5 µl of sample, 5 µl of 1× assay buffer, 180 µl of working buffer and 4 µl of diluted inhibitor solution were added and were mixed by inversion

⇩

6 µl of DTNB solution was added to each well and mixed thoroughly

⇩

Reaction started as soon as DTNB was added

⇩

The reaction of DTNB and NADPH produces TNB with formation of yellow color. The rate of formation of the yellow color was determined by measuring the increase in absorption per minute for each reaction at 412 nm.

Assessment

Total protein concentration of the unknown sample was determined from the standard curve prepared by measuring the absorbance of different known concentrations of BSA. TrxR activity was expressed as unit/ml/mg protein using the following formula:

$$\text{Unit/ml/mg protein} = \frac{\Delta A_{412}/\text{minute (TrxR)} \times \text{Dil} \times \text{Vol}}{\text{Enzvol} \times \text{Protein concentration in 5 µl sample}}$$

ΔA_{412}/minute (TrxR) = ΔA_{412}/minute (sample) – ΔA_{412}/minute (sample + inhibitor)

Dil = sample dilution factor.

Vol = volume of reaction in ml.

Enzvol = volume of enzyme in ml.

Unit definition: One unit of mammalian TrxR will cause an increase in A_{412} of 1.0 per minute per ml (when measured in a non-coupled assay containing DTNB alone) at pH 7.0 at 25°C.

The calculation of the enzymatic activity in this case needs to be adjusted for the difference in path length between a 1 ml cuvette (1 cm) and the plate used. A standard 96 well polystyrene plate containing 200 ml of liquid will have a path length of ~0.55 cm. The calculated activity obtained with a 96 well plate needs to be divided by 0.55 to be compared to activity determined with a 1 ml cuvette.

- **Estimation of reduced glutathione (GSH) level (Mulder et al., 1995; Sedlack et al., 1968)**

GSH level was estimated in kidney cytosol spectrophotometrically by determination of dithiobis (2-nitro) - benzoic acid (DTNB) reduced by –SH groups by measuring the absorbance at 412 nm. The level of GSH was expressed as nmol/mg protein.

- **Estimation of glutathione-S-transferase (GST) activity (Mulder et al, 1995; Habig et al., 1974)**

Spectrophotometric method was adopted to evaluate the activity of GST in kidney tissue. GST activity was measured in tissue cytosolic fractions by determining the increase in absorbance at 340 nm with 1-chloro-2, 4-dinitrobenzene (CDNB) as the substrate and the

specific activity of the enzyme was expressed as CDNB-GSH conjugate formed/minute/mg protein.

- **Superoxide dismutase activity (SOD) (Marklund et al., 1974; McCord et al., 1969)**

SOD activity in kidney was determined by means of inhibition of pyrogallol auto-oxidation by the enzyme. Partial extraction and purification of SOD was done as described by McCord and Fridovich. SOD activity was assayed by the method of Marklund and Marklund.

- **Catalase activity (CAT) (Luck, 1963)**

CAT catalyzes the breakdown of H_2O_2 into H_2O and O_2 and competes with the GP*x* for the common substrate H_2O_2. CAT has been considered to be the primary scavenger of intracellular H_2O_2 generated due to oxidative stress. Activity of CAT in kidney tissue sample was determined spectrophotometrically at 240 nm and expressed as unit/mg protein where the unit is the amount of enzyme that liberates half the peroxide oxygen from H_2O_2 in seconds at 25^oC.

- **Determination of blood urea nitrogen (BUN) and Creatinine levels (Carl Allinson, 1944; Mather et al., 1969)**

Blood samples were collected from mice and centrifuge at 2,000 × g for 5 min for serum preparation. Then BUN and creatinine levels were measured spectrophotometrically by standard enzymatic method using commercial kits.

❖ **Genotoxicity parameters**

➢ **Detection of DNA damage by alkaline single cell gel electrophoresis (comet assay) (Hartmann et al., 2003; Endoh et al., 2002)**

Possible DNA damage induced by CDDP was detected in blood lymphocytes using the alkaline single cell gel electrophoresis (comet) assay following a simplified protocol with slight modifications. For separation of lymphocytes from whole blood, the mice were anesthetized and blood samples were collected from by retroorbital puncture. Lymphocytes were isolated from samples of blood by standard centrifugation over a cushion of histopaque, washed with isotonic PBS and centrifuged. The pellet was resuspended in isotonic PBS. The cell viability in each group was measured by the trypan blue exclusion method and approximately 10^4 cells /slide were taken for the assay. Rest of the procedure is same as that for bone marrow cells which has been described in details in chapter II. The results were expressed as:

1. Percentage of cells with tail in each group and
2. Average tail length due to DNA migration in each group.

➢ **Assay of chromosomal aberration**

For the study of chromosomal aberrations (CA), slides were prepared from bone marrow cells by the conventional flame drying technique **(Biswas et al, 2004)**. Detailed procedure has already been given in chapter II.

➢ **Detection of mouse bone marrow micronucleus assay (Klein et al., 2001)**

Procedure

The bone marrow cells were collected in 1 ml 0.075 M KCl solution and incubated at 37 °C for 10 min

⇩

The tubes were centrifuged at 500 g for 10 min and the pellet was carefully resuspended in, as little supernatant as possible

⇩

Two smears of bone marrow were prepared from each mouse

After air-drying, the smears were fixed in absolute methanol and stained by May-Grunwald-Giemsa

The slides were examined for the presence of MN at 1,000× magnification (DM1000, Leica)

Calculation

The number of MN were scored in ≥1000 non-overlapping, differentiated, uniformly stained bone marrow cells/slide and expressed as:

$$\text{MN (\%)} = \frac{\text{Numer of micronucleated cells}}{\text{Total number of cells counted}} \text{ x } 100$$

- **DNA fragmentation by diphenylamine (DPA assay) (Zhivotovsky et al., 2001)**

2×10^6 bone marrow cells were lysed in lysis buffer (pH 8.0 containing 5 mM Tris-HCl, 20 mM EDTA and 0.5% Triton X-100) for 30 min at 4°C. The cell lysate were centrifuged at 15,000 g for 15 min at 4 °C. Then, the supernatant containing small DNA fragments was separated from the pellet containing large pieces of DNA. The supernatant and pellet were re-suspended in 10 % and 5% of trichloroacetic acid (TCA), respectively, and kept overnight. Then both samples were heated at 95 °C for 15 min and centrifuged at 2,500 g for 5 min to remove proteins. Supernatant fractions were reacted with DPA for 4 hr at 37 °C and the developing blue color was measured at 600 nm and expressed as:

Assessment

DNA fragmentation in samples was expressed as percentage of total DNA appearing in the supernatant fraction.

$$\text{\% Fragmented DNA} = \frac{\text{Absorbance of the supernatant}}{\text{Absorbance of supernatant} + \text{pellet}} \times 100$$

- **Detection of apoptosis of bone marrow cells by using TUNEL method**

Apoptosis of bone marrow cells were determined by using the TUNEL method with the help of in situ cell death detection kit, according to the manufacturer's instructions.

Procedure:

Fix air dried slides with methanol at $15^0 – 25^0$C for 1h.

⇩

Rinse slides with 1X PBS for 10 minutes.

⇩

Incubate in permiabilisation solution (0.1% Triton X-100 in 0.1% sodium citrate) at 4^0C for 15 minutes.

⇩

Rinse slides twice with 1X PBS.

⇩

Dry area around sample.

⇩

Add 50µl TUNEL reaction mixture on sample.

⇩

Put coverslip on slide.

⇩

Add lid and incubate for 1 h at 37^0C in a humidified atmosphere in the dark.

⇩

Rinse slides three times with 1X PBS.

⇩

Samples can be analyzed in a droplet of PBS under a fluorescence microscope.

⇩

Use an excitation wavelength in the range of 450-500 nm and detect in the range of 515-565 nm. The slides were then analysed under a fluorescence microscope ×400 magnification.

Assessment

Randomly selected 80–120 cells from 5-6 zones/slide were counted to determine the number of apoptotic cells. The apoptotic index (AI) was determined by following formula:

$$AI\ (\%) = \frac{\text{Numbered of labeled cells}}{\text{Total number of celss counted}} \times 100$$

- **Determination of *in situ* cell proliferation using *BrdU* Labeling**

Cell proliferation was measured using BrdU labeling with 5-bromo-2′-deoxyuridine Labeling and Detection Kit II.

Procedure

Add 10 µM BrdU into cells (approximately 10^6) in pre-warmed (37°C) cell culture medium for 1h (37°C, 5% CO_2).

⇩

Smear and air dry the cells after collecting the cells by centrifugation (3000g for 5 min).

⇩

Fix air dried slides with methanol at 15^0 – 25^0C for 1h.

⇩

Wash the glass slide thrice with 1X PBS and carefully dry the peripheral zone.

⇩

Then anti-BrdU monoclonal antibody was added followed by incubation at 37°C for 30 min in humid atmosphere.

⇩

Wash the glass slide thrice with 1X PBS and carefully dry the peripheral zone.

Then alkaline phosphatase conjugated anti mouse-immunoglobulin antibody (anti-mouse-Ig- AP) was added followed by incubation at 37°C for 30 min in humid atmosphere.

⇩

Wash the glass slide thrice with 1X PBS and carefully dry the peripheral zone.

⇩

Then freshly prepared substrate solution (BCIP/NBT) was added to the cells followed by incubation at 25°C for 30 min in humid atmosphere.

⇩

Wash the glass slide thrice with 1X PBS and carefully dry the peripheral zone.

⇩

After drying the cells were visualized under light microscope.

Assessment

Randomly selected 80-120 cells from 5-6 zones/slide were counted to determine the number of proliferating cells. The BrdU labeling index (BrdU LI) was determined by the following formula:

$$\text{BrdU LI (\%)} = \frac{\text{Numbered of labeled cells}}{\text{Total number of celss counted}} \times 100$$

Histopathology (Bancroft et al, 1990; Lillie et al, 1976)

Histopathological evaluation of kidney tissues was done by conventional hematoxylin-eosin staining method details of which have already been mentioned in chapter II.

Statistical analysis

All data were presented as mean ± SD. $n = 6$ animals per group. One way ANOVA followed by Tukey's Multiple Comparison Test using Graph Pad Prism software was performed for comparisons among groups. Significant difference was indicated when the P value was < 0.05.

Results

Nano selenium (Nano-Se) did not produce any significant change in the parameters investigated when administered alone as compared to the vehicle treated group.

- **LPO level**

Intraperitoneal administration of CDDP (Gr. III) significantly *(P < 0.05)* elevated LPO level by 44.36% in kidney and by 61.45% in bone marrow, compared to the vehicle treated group (Gr. I) **(Fig. 2A & B)**. Concomitant treatment (Gr. IV) with Nano-Se significantly *(P < 0.05)* reduced the LPO level by 19.34% in kidney and by 34.37% in bone marrow, where as pretreatment (Gr. V) with the same Nano-Se inhibited LPO level much more significantly *(P < 0.05)* by 30.07% in kidney and by 50.34% in bone marrow in comparison to the CDDP treated group (Gr. III).

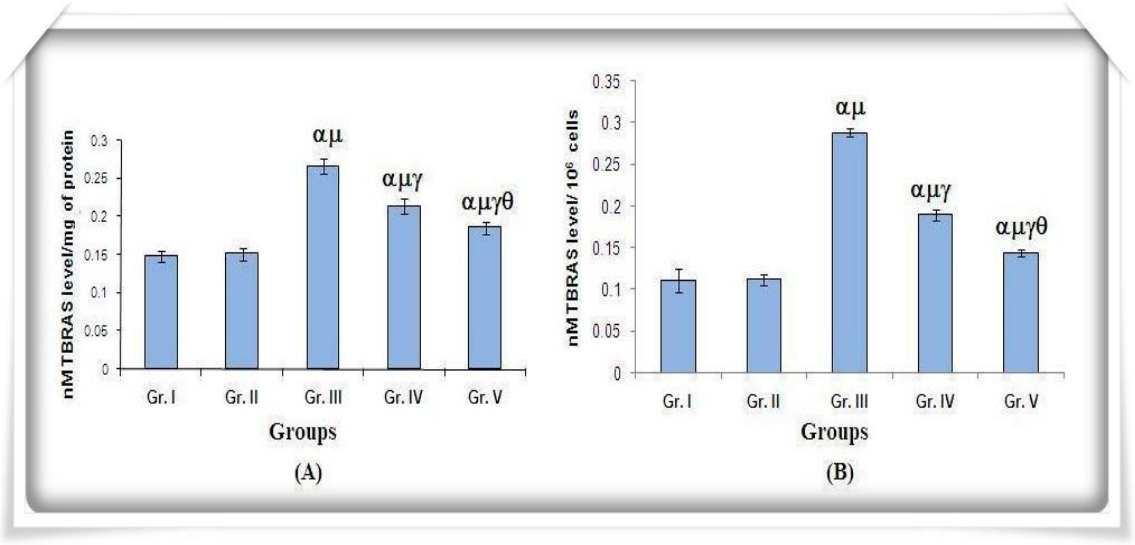

Figure 2: Data were represented as mean ± SD (n=6). α - significant (*P < 0.05*) as compared with Gr. I; μ - significant (*P < 0.05*) as compared with Gr. II; γ - significant (*P < 0.05*) as compared with Gr. III; θ - significant (*P < 0.05*) as compared with Gr. IV.

- **ROS level**

- **Hydrogen peroxide level by using DCFH-DA**

Intraperitoneal administration of CDDP significantly *(P < 0.05)* elevated H_2O_2 level in kidney and in bone marrow cells by 43.23% and 54.78% respectively in Gr. III as compared to the vehicle treated group (Gr. I) **(Fig. 3A & B)**. Concomitant treatment (Gr. IV) and pretreatment (Gr. V) with Nano-Se caused a sharp reduction in H_2O_2 level in kidney as well as in bone marrow cells. Concomitant treatment (Gr. IV) with Nano-Se significantly *(P < 0.05)* reduced H_2O_2 level in kidney by 11.84% and in bone marrow cells by 29.05% respectively, but on 7 days pretreatment (Gr.V) with the same inhibited the H_2O_2 level much more significantly *(P > 0.05)* by 31.07% in kidney and by 43.7% in bone marrow cells in comparison to the CDDP treated group (Gr. III).

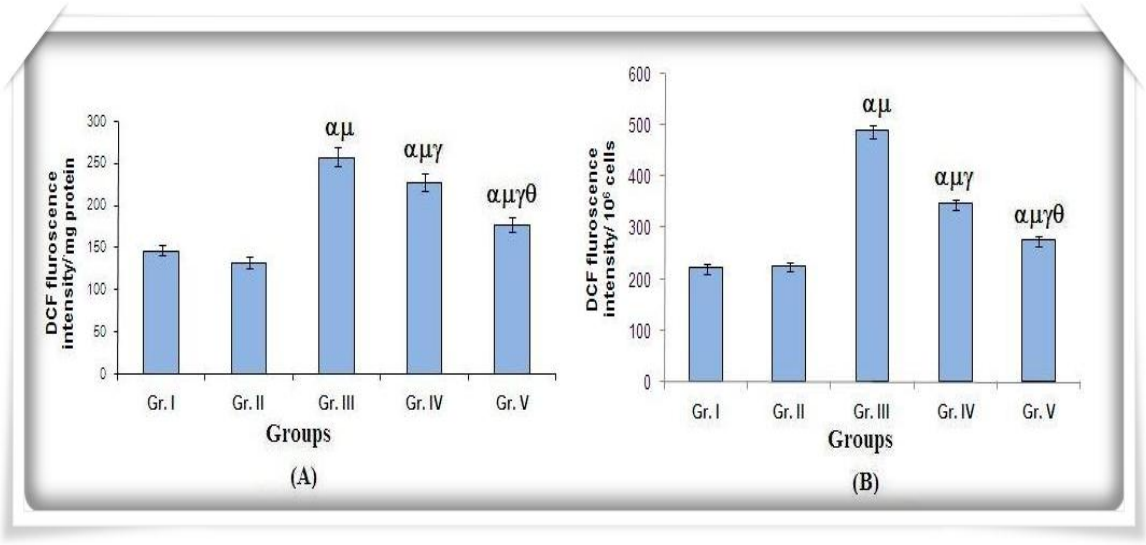

Figure 3: Data were represented as mean ± SD (n=6). α - significant (*P < 0.05*) as compared with Gr. I; μ - significant (*P < 0.05*) as compared with Gr. II; γ - significant (*P < 0.05*) as compared with Gr. III; θ - significant (*P < 0.05*) as compared with Gr. IV.

- **Superoxide level by using DHE**

The super oxide level in kidney and bone marrow cells were found to increase significantly ($P < 0.05$) by 76.67% and 62.56% respectively, after the administration of CDDP (Gr. III), compared to the vehicle treated group (Gr. I) (**Fig. 4A & B**). Concomitant treatment (Gr. IV) with Nano-Se significantly ($P < 0.05$) reduced superoxide level in kidney by 46.68% and in bone marrow cells by 28.93% respectively, but on 7 days pretreatment (Gr.V) with the same inhibited the superoxide level much more significantly ($P < 0.05$) by 55.62% in kidney and by 45.21% in bone marrow cells in comparison to the CDDP treated group (Gr. III).

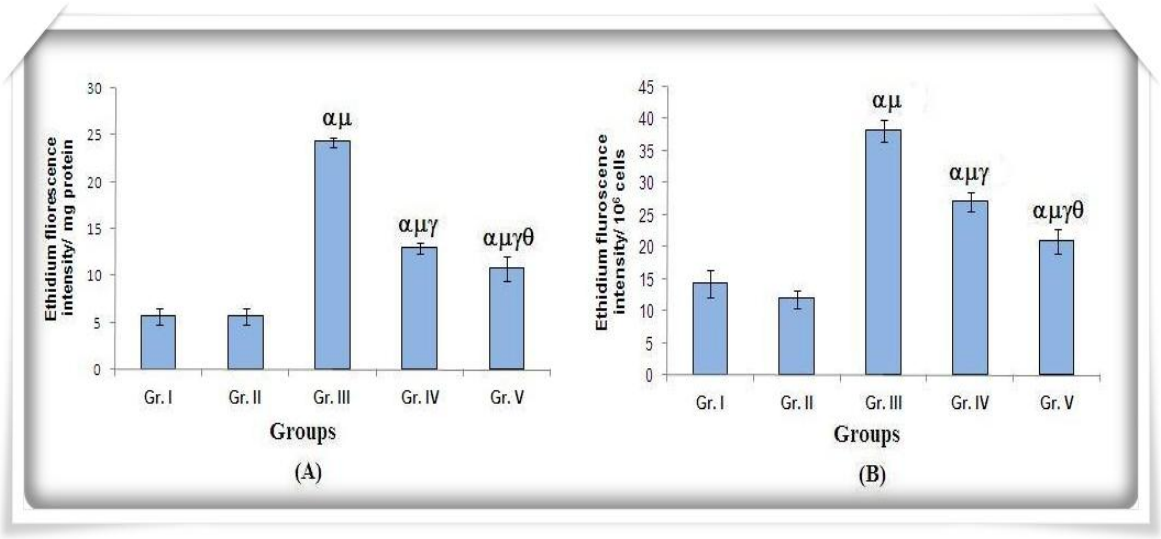

Figure 4: Data were represented as mean ± SD (n=6). α - significant (*P < 0.05*) as compared with Gr. I; μ - significant (*P < 0.05*) as compared with Gr. II; γ - significant (*P < 0.05*) as compared with Gr. III; θ - significant (*P < 0.05*) as compared with Gr. IV.

- **Nitric oxide (NO) level**

Intraperitoneal administration of CDDP (Gr. III) significantly (*P<0.05*) elevated NO level by 47.86% in kidney and by 51.5% in bone marrow, compared to the vehicle treated group (Gr. I) **(Fig. 5A & B)**. Concomitant treatment (Gr. IV) with Nano-Se significantly ($P < 0.05$) reduced the NO level by 26.02% in kidney and by 29.58% in bone marrow, where as pretreatment (Gr. V) with the same Nano-Se inhibited NO level much more significantly ($P < 0.05$) by 38.29% in kidney and by 37.73% in bone marrow in comparison to the CDDP treated group (Gr. III).

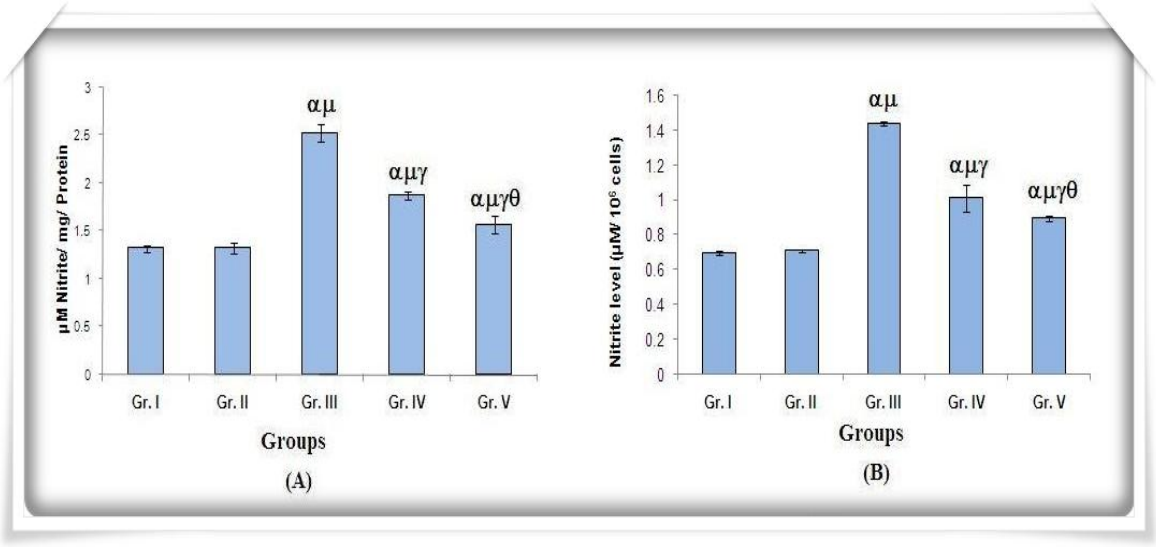

Figure 5: Data were represented as mean ± SD (n=6). α - significant (*P < 0.05*) as compared with Gr. I; µ - significant (*P < 0.05*) as compared with Gr. II; γ - significant (*P < 0.05*) as compared with Gr. III; θ - significant (*P < 0.05*) as compared with Gr. IV.

- **GSH level**

The GSH content was found to decline significantly *(P<0.05)* by 64.16% in kidney after CDDP administration (Gr. III) as compared to the vehicle treated group (Gr. I) **(Fig. 6)**. Concomitant treatment (Gr. IV) and pretreatment (Gr. V) with the Nano-Se resulted in a significant *(P < 0.05)* elevation of GSH content by 15.98% and 55.57% respectively in kidney in comparison to the CDDP treated group (Gr. III).

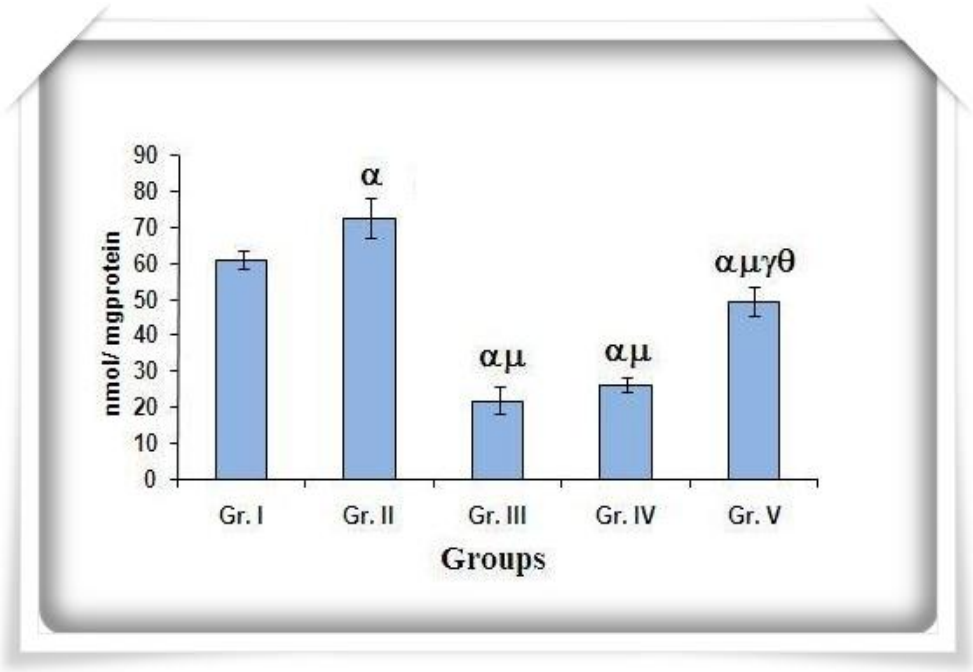

Figure 6: Data were represented as mean ± SD (n=6). α - significant (*P < 0.05*) as compared with Gr. I; μ - significant (*P < 0.05*) as compared with Gr. II; γ - significant (*P < 0.05*) as compared with Gr. III; θ - significant (*P < 0.05*) as compared with Gr. IV.

- **GST activity**

A significant *(P<0.05)* reduction of GST activity by 57.2% in kidney was observed in CDDP treated group (Gr. III) in comparison to the vehicle treated group (Gr. I) **(Fig. 7)**. Concomitant administration of Nano-Se (Gr. IV) significantly *(P < 0.05)* increased the GST activity in kidney by 31.05% compared to the CDDP treated group (Gr. III). In pretreatment schedule (Gr. V), Nano-Se raised the enzyme activity in kidney by 50.19% in comparison to the CDDP treated group (Gr. III).

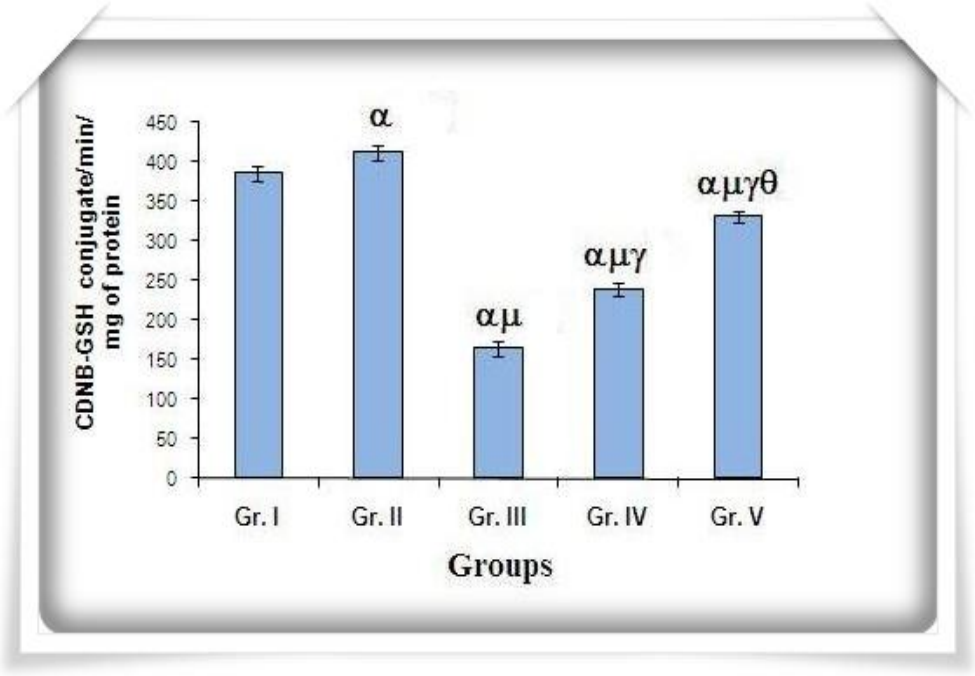

Figure 7: Data were represented as mean ± SD (n=6). α - significant (*P < 0.05*) as compared with Gr. I; μ - significant (*P < 0.05*) as compared with Gr. II; γ - significant (*P < 0.05*) as compared with Gr. III; θ - significant (*P < 0.05*) as compared with Gr. IV.

- **SOD activity**

Intraperitoneal administration of CDDP (Gr. III) significantly (*P<0.05*) decreased the SOD activity by 72.98% in kidney as compared to the vehicle treated group (Gr. I) **(Fig. 8)**. Concomitant treatment (Gr. IV) with Nano-Se significantly ($P < 0.05$) enhanced the SOD activity by 33.02%, while pretreatment (Gr. V) with Nano-Se increased the SOD activity much more significantly ($P < 0.05$) by 55.74% in comparison to the CDDP treated group (Gr. III).

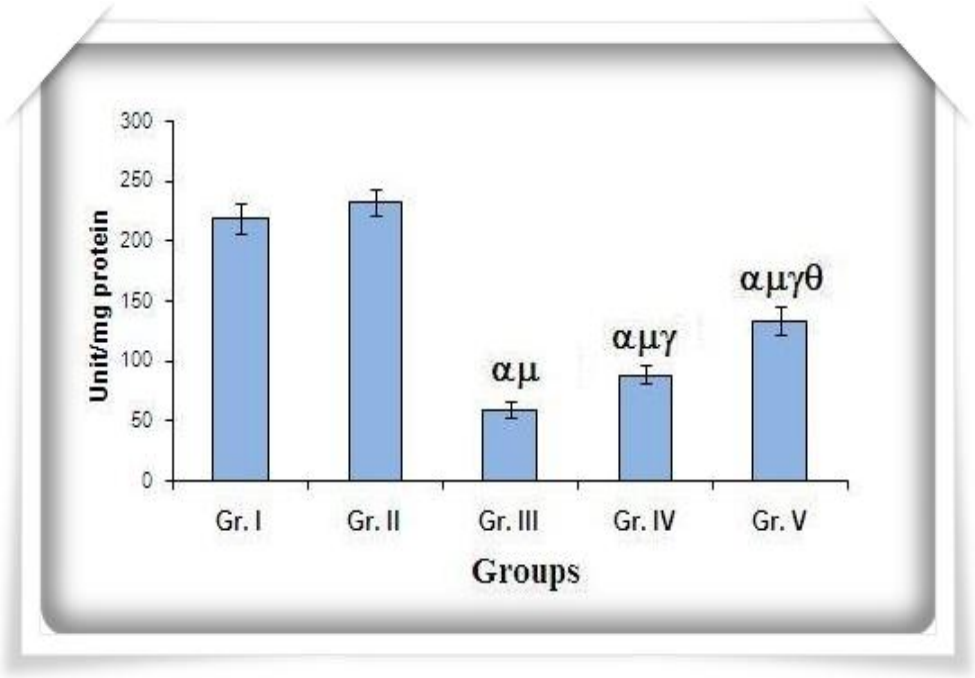

Figure 8: Data were represented as mean ± SD (n=6). α - significant (*P < 0.05*) as compared with Gr. I; μ - significant (*P < 0.05*) as compared with Gr. II; γ - significant (*P < 0.05*) as compared with Gr. III; θ - significant (*P < 0.05*) as compared with Gr. IV.

- **CAT activity**

The renal CAT activity was found to decrease significantly (*P < 0.05*) by 55.42% in CDDP treated group (Gr. III) in comparison to the vehicle treated group (Gr. I) **(Fig. 9)**. Concomitant administration of Nano-Se (Gr. IV) resulted in a significant (*P* < 0.05) enhancement in renal CAT activity by 34.84% in comparison to the CDDP treated group (Gr. III). Pretreatment (Gr. V) with Nano-Se increased the CAT activity significantly (*P* < 0.05) by 48.35% as compared to the CDDP treated group (Gr. III).

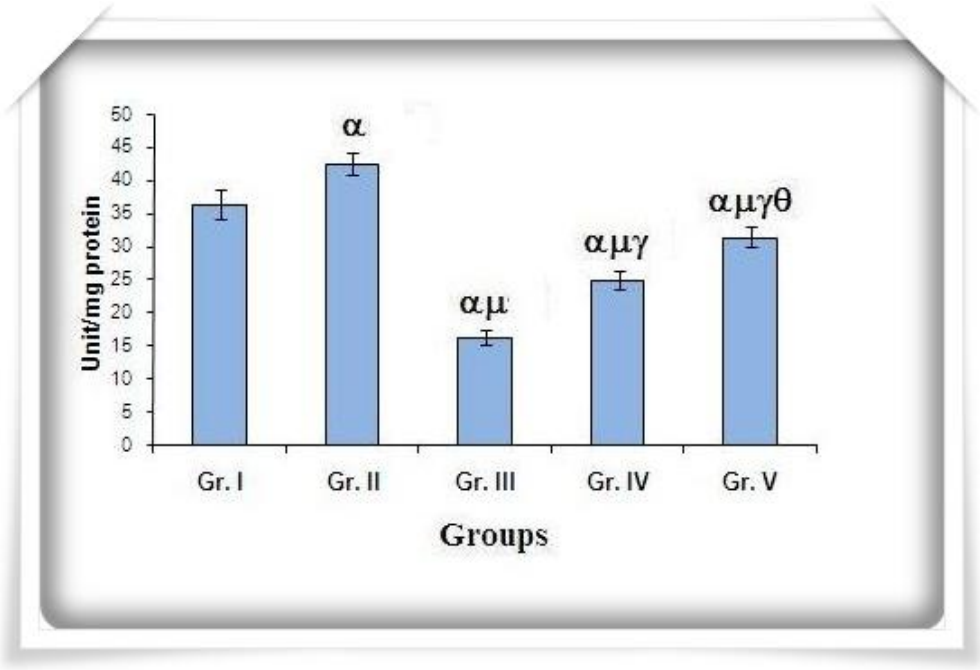

Figure 9: Data were represented as mean ± SD (n=6). α - significant (*P < 0.05*) as compared with Gr. I; μ - significant (*P < 0.05*) as compared with Gr. II; γ - significant (*P < 0.05*) as compared with Gr. III; θ - significant (*P < 0.05*) as compared with Gr. IV.

- **GP*x* activity**

Intraperitonial administration of CDDP (Gr. III) caused a significant (*P < 0.05*) reduction in GP*x* activity by 51.14% in kidney in comparison to the vehicle treated group (Gr. I) **(Fig. 10)**. Nano-Se in concomitant treatment schedule (Gr. IV) resulted in a significant enhancement of GP*x* activity by 27.79% in renal cell in comparison to the CDDP treated group (Gr. III), while in pretreatment schedule (Gr. V), the same compound significantly (*P* < 0.05) elevated the GP*x* activity by 43.19%, as compared to the CDDP treated group (Gr. III).

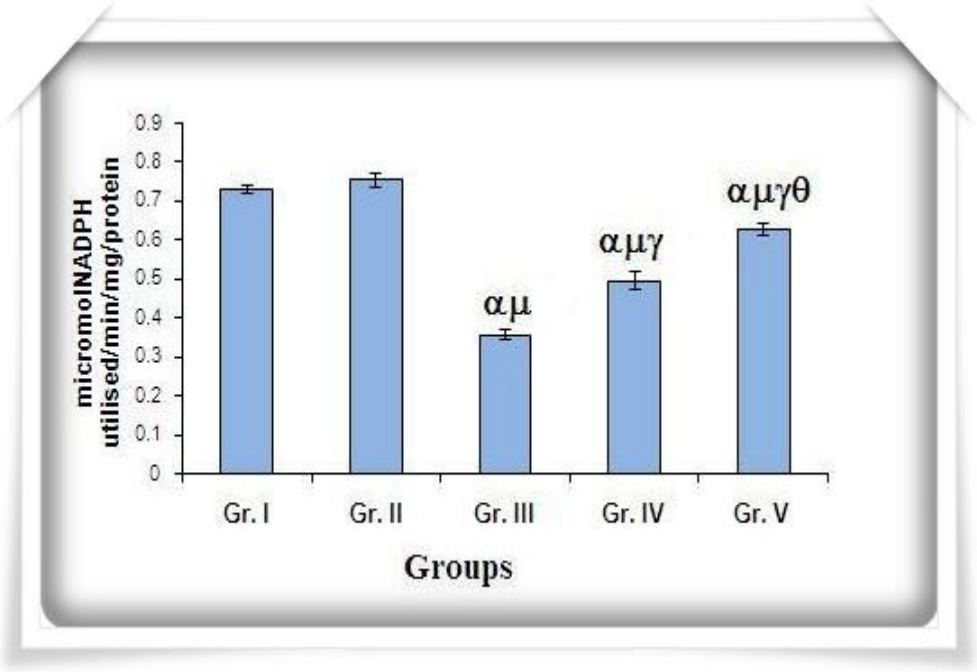

Figure 10: Data were represented as mean ± SD (n=6). α - significant (*P < 0.05*) as compared with Gr. I; μ - significant (*P < 0.05*) as compared with Gr. II; γ - significant (*P < 0.05*) as compared with Gr. III; θ - significant (*P < 0.05*) as compared with Gr. IV.

- **TrxR activity**

Intraperitonial administration of CDDP (Gr. III) caused a significant *(P < 0.05)* reduction in kidney TrxR activity by 65.73% in comparison to the vehicle treated group (Gr. I) **(Fig. 11)**. Treatment with the Nano-Se resulted in a rise in renal TrxR activity by 42.83% and 57.06% in concomitant (Gr. IV) and pretreatment (Gr. V) schedule respectively in comparison to the CDDP treated group (Gr. III).

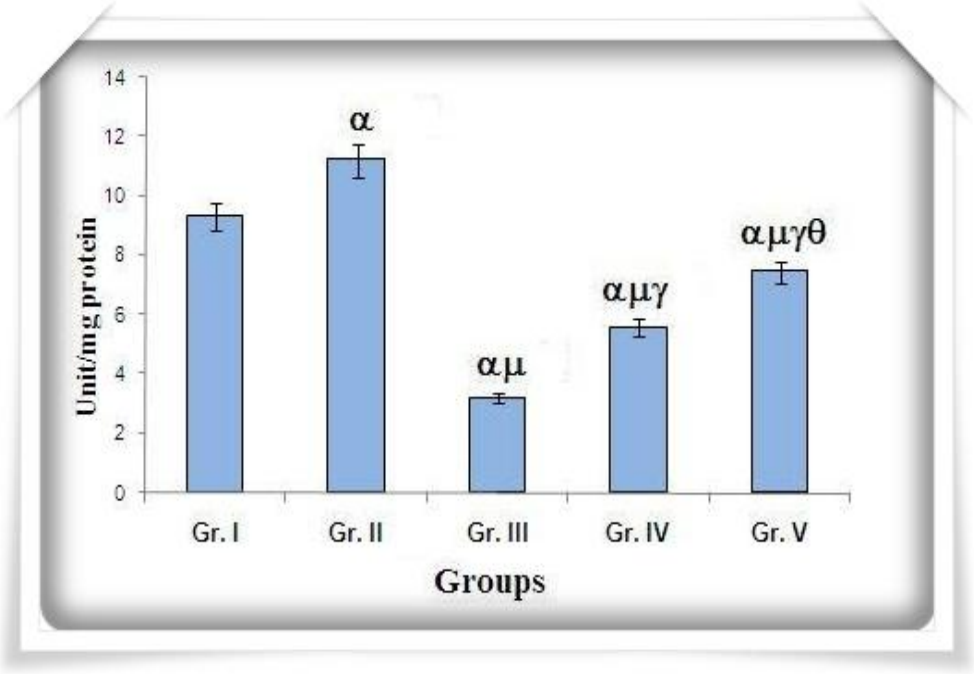

Figure 11: Data were represented as mean ± SD (n=6). α - significant (*P < 0.05*) as compared with Gr. I; μ - significant (*P < 0.05*) as compared with Gr. II; γ - significant (*P < 0.05*) as compared with Gr. III; θ - significant (*P < 0.05*) as compared with Gr. IV.

- **BUN and creatinine levels**

Renal functions were impaired severely by CDDP administration, as illustrated by considerable increase in BUN and creatinine levels **(Table 1)**. BUN and creatinine levels were significantly *(P < 0.05)* raised by 53.60% and 70.27% respectively in CDDP treated group (Gr. III) compared compared to the vehicle treated group (Gr. I). Concomitant treatment (Gr. IV) with Nano-Se reduced the increased levels of BUN and creatinine by 15.09% and 24.22% respectively in comparison to the CDDP treated group (Gr. III). Administration of Nano-Se in pretreatment schedule (Gr. V) reduced the BUN and creatinine levels by 44.18% and 64.58% respectively, as compared to the CDDP treated group (Gr. III).

Groups	BUN (mg/dl)	Creatinine (mg/dl)
I	20.24 ± 0.88	0.16 ± 0.008
II	22.79 ± 1.35	0.17 ± 0.008
III	$43.63 \pm 1.24^{\alpha\mu}$	$0.54 \pm 0.007^{\alpha\mu}$
IV	$36.69 \pm 0.50^{\alpha\mu\gamma}$	$0.41 \pm 0.018^{\alpha\mu\gamma}$
V	$24.35 \pm 0.86^{\alpha\mu\theta}$	$0.19 \pm 0.01^{\alpha\mu\theta}$

Table 1: Data were represented as mean ± SD (n=6). α - significant (*P < 0.05*) as compared with Gr. I; μ - significant (*P < 0.05*) as compared with Gr. II; γ - significant (*P < 0.05*) as compared with Gr. III; θ - significant (*P < 0.05*) as compared with Gr. IV.

➢ **Comet assay findings**

Comet assay was carried out to examine the CDDP induced DNA damage in lymphocytes **(Fig. 11A-E)** and bone marrow **(Fig. 12A-E)** and for this purpose percentage of damaged cells and the average tail length was measured.

- **Percentage of damaged cells in each group**

The frequency of damaged lymphocytes and bone marrow were 11.73% and 9.52% respectively in vehicle treated group (Gr. I) **(Table 2)**. The CDDP administration caused a significant (*P < 0.05*) increase in the percentage of damaged lymphocyte and bone marrow cells by 54.23% and 52.32% respectively in Gr. III. In case of concomitant group (Gr. IV), the percentages of damaged cells were reduced to 32.31% in lymphocytes and 28.29% in bone marrow cells respectively. However pretreatment (Gr. V) with Nano-Se sharply decreased the percentage of damaged cells to 21.47% and 20.92% respectively, in lymphocytes and bone marrow cells.

Groups	Peripheral Lymphocyte		Bone marrow	
	Damaged cells showing comet (%)	Average tail length (µm)	Damaged cells showing comet (%)	Average tail length (µm)
I	11.73 ± 1.23	9.22 ± 1.79	9.52 ± 1.59	11.74 ± 1.68
II	11.44 ± 1.21	10.62 ± 2.31	10.83 ± 1.67	$16.72 \pm 1.52^{\alpha}$
III	$54.23 \pm 2.61^{\alpha\mu}$	$75.4 \pm 2.35^{\alpha\mu}$	$52.32 \pm 2.62^{\alpha\mu}$	$81.14 \pm 3.36^{\alpha\mu}$
IV	$32.31 \pm 2.54^{\alpha\mu\gamma}$	$27.84 \pm 2.16^{\alpha\mu\gamma}$	$28.29 \pm 2.65^{\alpha\mu\gamma}$	$35.61 \pm 2.65^{\alpha\mu\gamma}$
V	$21.47 \pm 1.91^{\alpha\mu\gamma\theta}$	$21.69 \pm 1.10^{\alpha\mu\gamma\theta}$	$20.92 \pm 1.57^{\alpha\mu\gamma\theta}$	$28.05 \pm 2.75^{\alpha\mu\gamma\theta}$

Table 2: Data were represented as mean ± SD (n=6). α - significant (*P < 0.05*) as compared with Gr. I; µ - significant (*P < 0.05*) as compared with Gr. II; γ - significant (*P < 0.05*) as compared with Gr. III; θ - significant (*P < 0.05*) as compared with Gr. IV.

- **Average Tail Length due to DNA Migration in each group**

The magnitudes of average tail length were 9.22 ± 1.79 µm and 11.74 ± 1.68 µm respectively, in lymphocytes and bone marrow cells in Gr. I. CDDP caused a marked increase in the magnitude of tail length to 75.40 ± 2.35 µm in lymphocytes and 81.14 ± 3.36 µm in bone marrow cells in Gr. III (**Table 2**). Oral administration of Nano-Se in concomitant (Gr. IV) and pretreatment (Gr. V) schedule, resulted in the reduction of average tail length to 27.84 ± 2.16 µm and 21.69 ± 1.10 µm respectively, in case of lymphocytes and 35.61 ± 2.65 µm and 28.05 ± 2.75 µm, respectively in bone marrow cells.

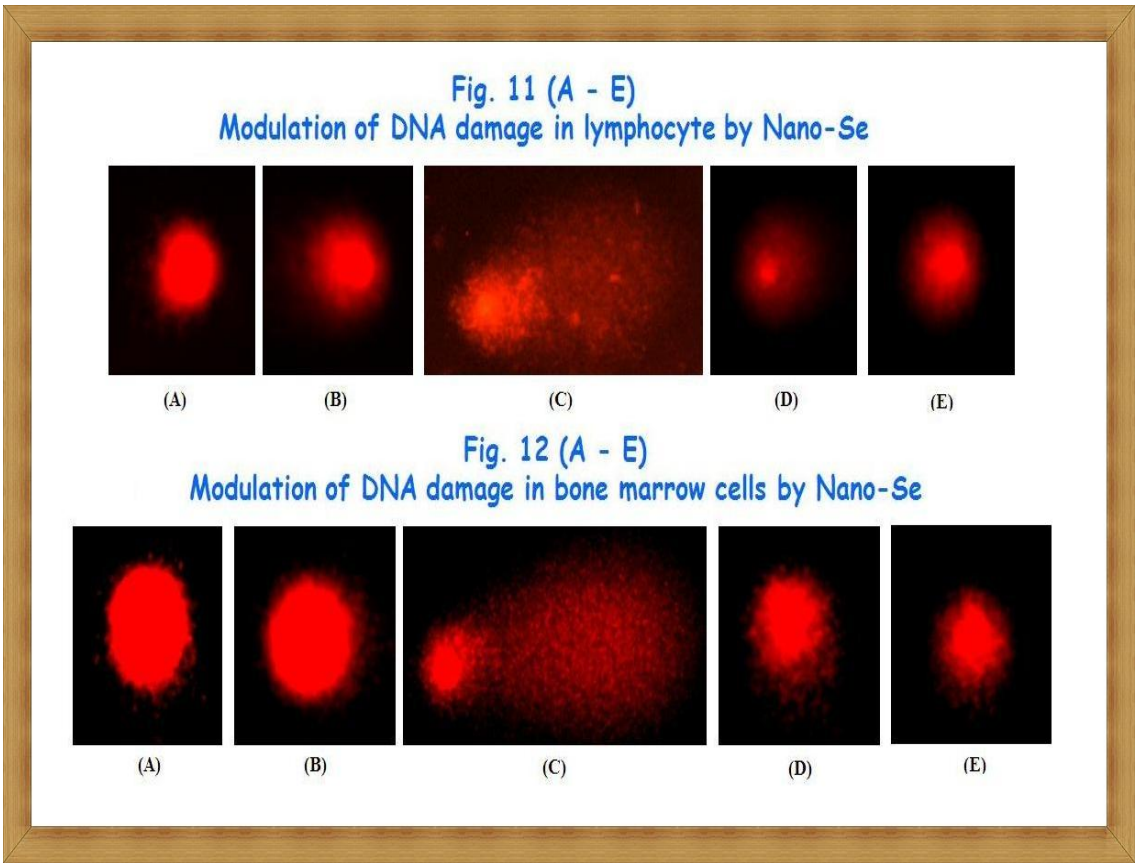

Figure 11 & 12: Microphotograph of lymphocyte **(11: A-E)**; bone marrow **(12: A-E)**: (A) vehicle treated (no DNA damage), (B) Nano-Se treated very fewer DNA migrations (C) Cisplatin treated (showing highly migrated DNA with scattered comet tail), (D) Concomitant treatment (less migrated DNA) and (E) Pretreatment (showing no marked DNAmigration)

- **Chromosomal aberrations**

The magnitude of chromosomal aberrations was estimated to be 9.56% in vehicle treated group (Gr. I) **(Fig. 13A)**. Due to the administration of CDDP (Gr. III), the proportion of CA was raised significantly (*P < 0.05*) to 42.11%. The Nano-Se provided significant (*P* < 0.05) protection against the genotoxicity imparted by CDDP, and the frequency of CA was reduced to 30.10% in case of concomitant treatment group (Gr. IV) and to 19.21% in case of pretreatment group (Gr. V). Different types of CA have been shown in **Fig. 13B.**

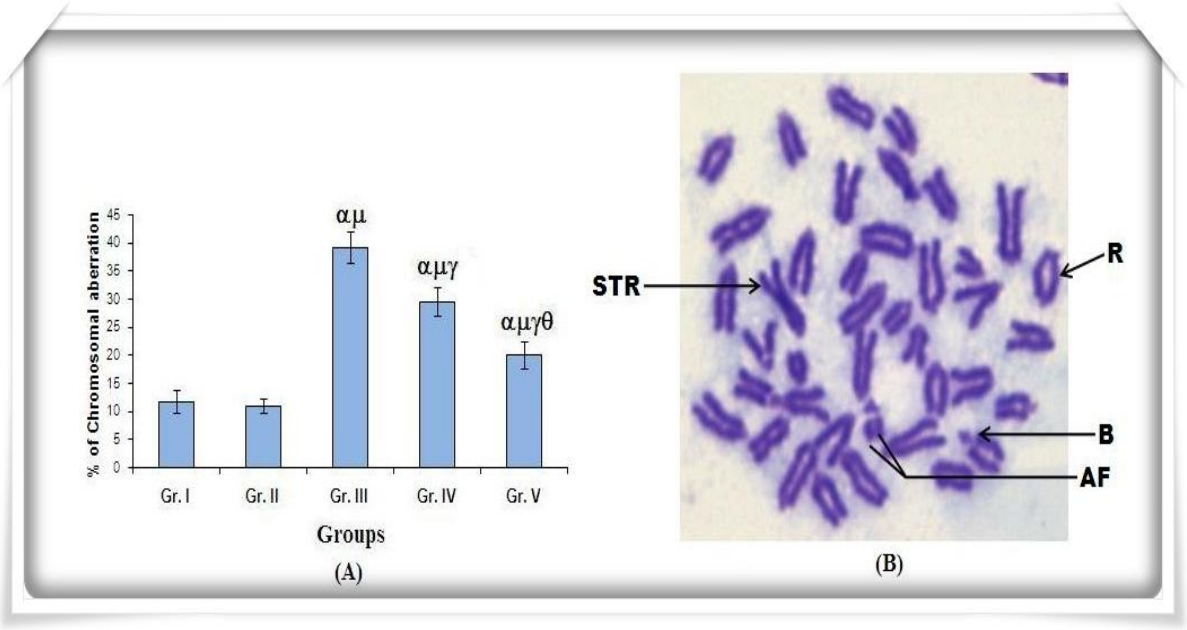

Figure 13 A: Data were represented as mean ± SD (n=6). α - significant (*P < 0.05*) as compared with Gr. I; μ - significant (*P < 0.05*) as compared with Gr. II; γ - significant (*P < 0.05*) as compared with Gr. III; θ - significant (*P < 0.05*) as compared with Gr. IV.

Figure 13 B: Metaphase complements showing stretching (STR), and Ring formation (R), Break (B) and Acentric fragment (AF).

- **Micronuclei assay**

Mice intoxicated with CDDP showed significantly *(P < 0.05)* high MN frequency of 1.29 ± 0.04 compared to vehicle treated group (Gr. I) mice (0.21 ± 0.01) **(Fig. 14)**. Treatment with Nano-Se in concomitant (Gr. III) and pretreatment (Gr. IV) schedule was able to minimize MN frequency to a significant *(P < 0.05)* level of about 0.68±0.03 and 0.53±0.01, respectively, compared to CDDP-treated mice (Gr. III).

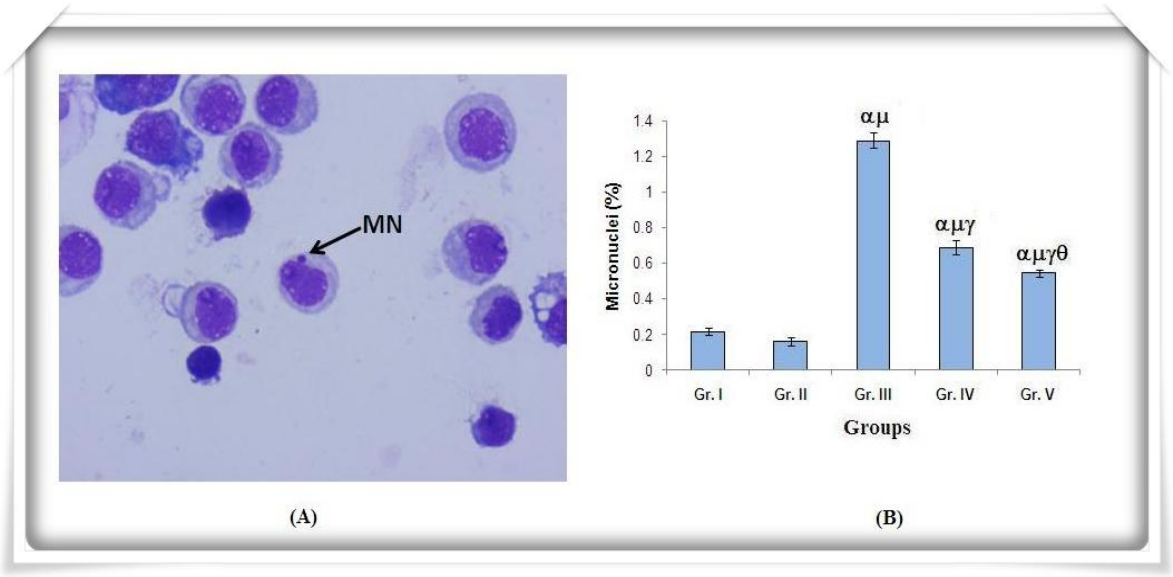

Figure 14A: Representative photomicrograph of Giemsa-stained bone marrow slide showing MN (indicated by black arrow), ×1000 magnification

Figure 14B: Data were represented as mean ± SD (n=6). α - significant *(P < 0.05)* as compared with Gr. I; μ - significant *(P < 0.05)* as compared with Gr. II; γ - significant *(P < 0.05)* as compared with Gr. III; θ - significant *(P < 0.05)* as compared with Gr. IV.

- **DNA fragmentation**

Genomic DNA fragmentation in bone marrow cells was found 9.05% in vehicle treated group (Gr. I). CDDP administration caused a significantly (*P < 0.05*) greater rate (50.29%) of DNA fragmentation in CDDP treated group (Gr. III) of mice. In case of concomitant and 7 days pretreatment, the percentages of DNA fragmentation were reduced to 26.38% (G. IV) and 19.39% (Gr. V), respectively **(Fig. 15)**.

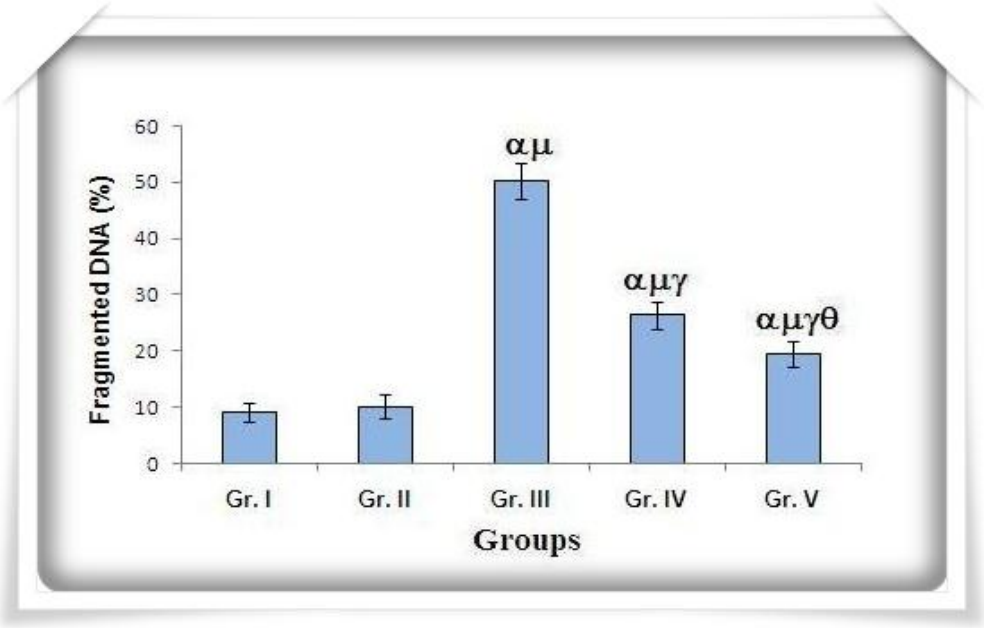

Figure 15: Data were represented as mean ± SD (n=6). α - significant (*P < 0.05*) as compared with Gr. I; μ - significant (*P < 0.05*) as compared with Gr. II; γ - significant (*P < 0.05*) as compared with Gr. III; θ - significant (*P < 0.05*) as compared with Gr. IV.

- **Apoptosis in bone marrow cells by TUNEL assay**

To confirm the nature of cell death, TUNEL assay was performed in which as result of apoptosis FITC-conjugated dUTP was incorporated into the DNA strand breaks in the presence of the enzyme terminal deoxynucleotidyl transferase. AI in the vehicle treated group was estimated to be 4.22% (Gr. I), which was increased markedly after treatment with CDDP (Gr. III) to 40.44%. The Nano-Se significantly *(P < 0.05)* inhibited CDDP-induced apoptotic cell death to 18.23 % in concomitant treatment (Gr. IV) schedule and to 12.04 % in pretreatment (Gr. V) schedule. **(Fig. 16A-B).**

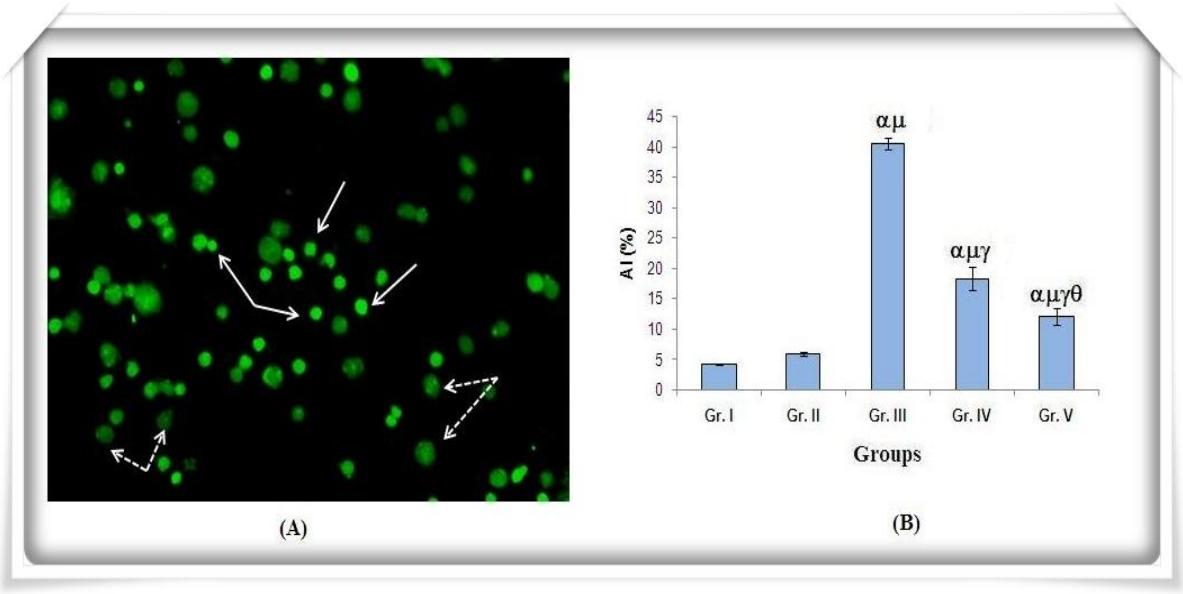

Figure 16A: Apoptotic cells (TUNEL label cells) are indicated by white arrows whereas non-apoptotic cells indicated by white broken arrows, × 200 magnifications

Figure 16B: Data were represented as mean ± SD (n=6). α - significant (*P < 0.05*) as compared with Gr. I; μ - significant (*P < 0.05*) as compared with Gr. II; γ - significant (*P < 0.05*) as compared with Gr. III; θ - significant (*P < 0.05*) as compared with Gr. IV.

➢ **Bone marrow cell proliferation by *BrdU* LI assay**

BrdU LI (%) in the bone marrow cells of vehicle treated group (Gr. I) was found to be 59.83% (**Fig. 17A-B & C**), which was decreased distinctly after administration of CDDP (Gr. III) to 26.29%. Treatment with Nano-Se significantly *(P < 0.05)* reversed CDDP-induced inhibitory effect on cellular proliferation to 39.92% in concomitant treatment schedule (Gr. IV) and to 46.99% in pretreatment schedule (Gr. V).

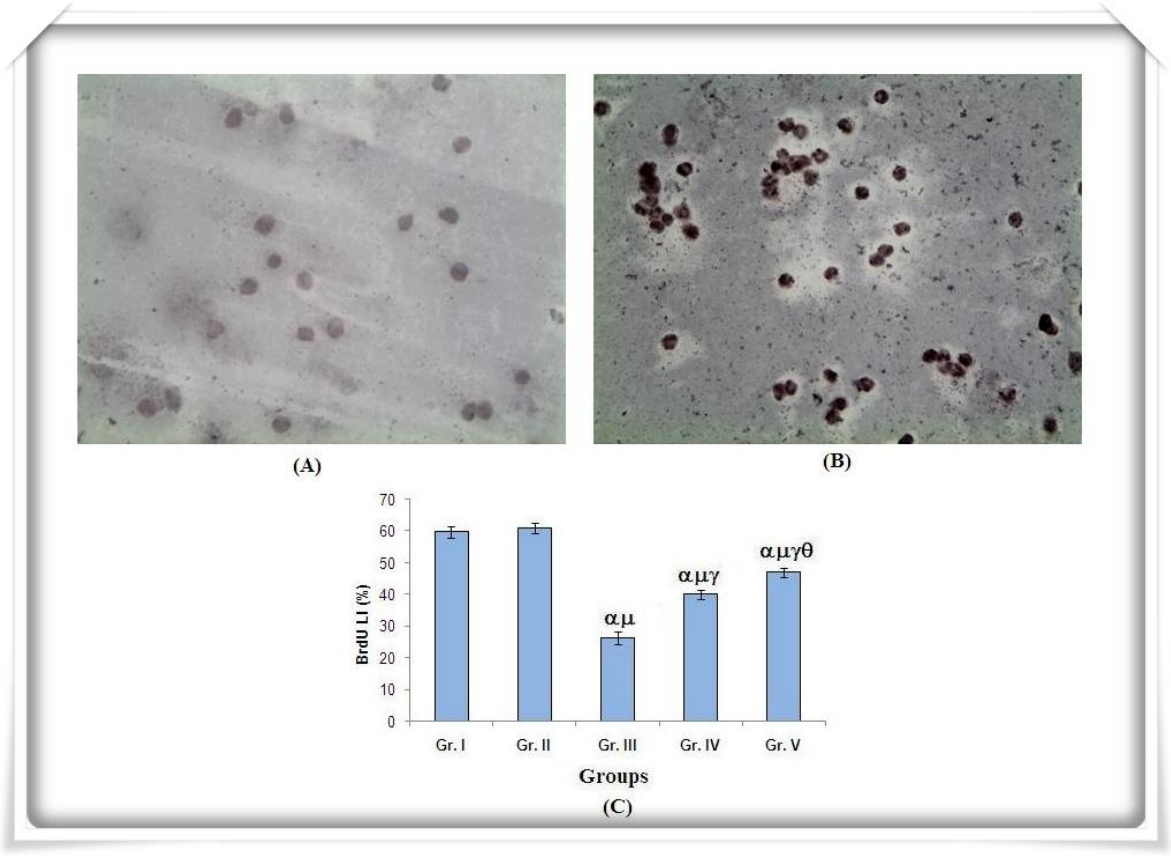

Figure 17 A & B: Non-proliferating cells and proliferating cells (indicated by BCIP/NBT staining), ×400 magnification

Figure 17C: Data were represented as mean ± SD (n=6). α - significant *(P < 0.05)* as compared with Gr. I; μ - significant *(P < 0.05)* as compared with Gr. II; γ - significant *(P < 0.05)* as compared with Gr. III; θ - significant *(P < 0.05)* as compared with Gr. IV.

- **Histopathological examination**

The photomicrograph of vehicle treated (Gr. I) and Nano-Se treated (Gr. II) mice showed normal architecture of renal cortex having glomerulus, distal convoluted tubule and proximal convoluted tubule **(Fig. 17)**. The kidney histology of CDDP treated (Gr. III) mice showed tubular dilatation, glomerular degeneration and loss of brush border of tubular epithelial cells. In addition, interstitial hemorrhage, atrophy and inflammatory cell infiltration was also observed upon CDDP administration. Co-treatment with Nano-Se in both concomitant (Gr. IV) and pre-treatment schedule (Gr. V) effectively ameliorated CDDP-induced histopathological lesions of which pre-treatment group showed better result.

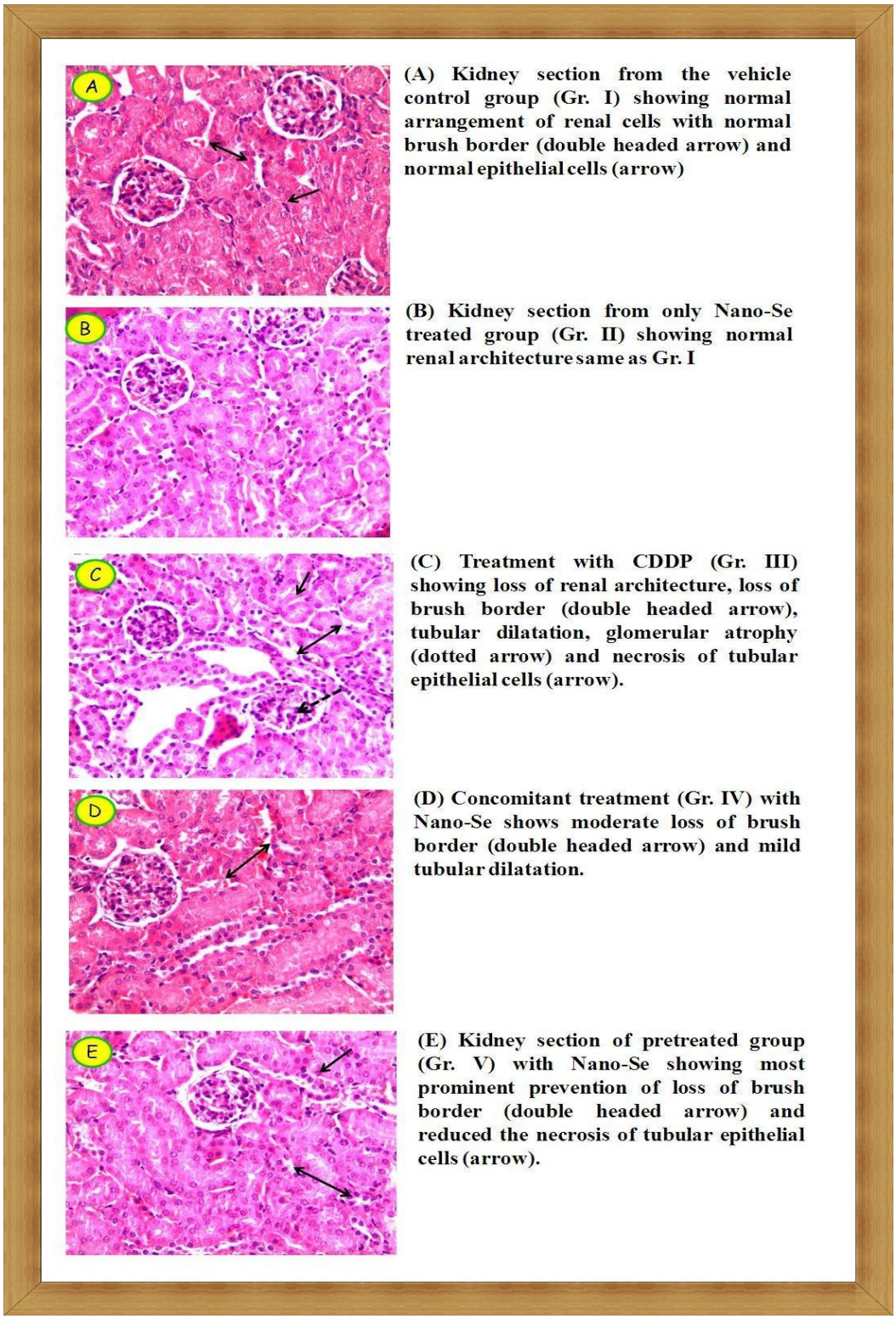

Figure 18: Photograph of kidney section of mice stained with hematoxylin and eosin, ×200.

Discussion

Nephrotoxicity arises when renal tissue fails to detoxify and properly excrete wastes due to the destruction of renal function by toxicants. Approximately 20% of nephrotoxicity cases are caused by drugs, although therapy for the elderly has increased the incidence of nephrotoxicity to 66% **(Ansari, 2017).** About 25% of most commonly used drugs in intensive care units (ICUs) are potentially nephrotoxic and are recognized as considerable health and economic burden worldwide **(Sanchez-Gonzalez et al., 2011)**. Amongst them cisplatin (CDDP), widely used broad-spectrum antineoplastic drug when used in cancer chemotherapy, induces renal impairment and acute renal failure by induction of reactive oxygen species **(Sahu et al., 2011)**.

LPO is one of the main manifestations of oxidative damage and has been found to play an important role in the toxicity of many xenobiotics by altering the physiological and biological characteristics of biological systems **(Rao et al., 2017)**. Free radical induced LPO has been suggested to alter the membrane structure and function causing cellular abnormalities such as mutations and cell death **(Basu et al., 2015)**. Increased free radical production stimulates LPO and is the sources for the degradation of DNA, lipids and carbohydrates **(Zhang et al., 2016)**. In the present study, due to the induction of LPO by CDDP, the level of TBARS was found to increase in kidney and bone marrow tissues of experimental mice. This might be due to the increased production of free radicals or decreased antioxidant status. Following the administration of Nano-Se, the levels of TBARS were maintained to near normal status which indicates the reduced level of LPO. From this, it may be concluded that inhibition of CDDP-induced lipid peroxidation could be attributed to the free radical quenching activity of Nano-Se and thus protecting against oxidative membrane damage in mice.

ROS is primarily produced endogenously through cellular respiration in mitochondria. Oxidase accepts electron released from an organic substrate through membrane carriers, such as ubiquinone and cytochrome *c* to form superoxide anion **(Quijano al., 2016)**. Molecular oxygen can accept a total of four electrons, one at a time, and the corresponding number of protons to generate two molecules of water. During this process, different oxygen radicals are successively formed as intermediate products, including superoxide ($O_2^{\bullet -}$); peroxide ($O_2^{=}$), which normally exists in cells as hydrogen

peroxide (H_2O_2); and the hydroxyl radical ($^{\bullet}OH$). Superoxide, peroxide, and the hydroxyl radical are considered the primary ROS and have sparked major research on the role of free radicals in biology and medicine **(Halliwell, 1999)**. The cell-permeant 2', 7'-dichlorodihydrofluorescein diacetate (H2DCFDA) (also known as dichlorofluores cin diacetate) is a chemically reduced form of fluorescein used as an indicator for ROS in cells. Another one, DHE is a non-fluorescent dye and freely permeable to the cell. **(Basu et al., 2014)**. The oxidation of DHE to fluorescent compound ethidium is mainly modulated by superoxide anion whereas, DCFH-DA as a cell permeable specific dye probe fluoresces to 2′, 7′-dichlorofluorescein (DCF) which is mainly regulated by H_2O_2 **(Halliwell et al., 2004)**. In this study, CDDP treatment substantially elevated H_2O_2 and superoxide levels in renal and bone marrow cells of experimental mice as measured by DCFH-DA and DHE, respectively. Treatment with Nano-Se prevented elevation of CDDP induced ROS generation which could be attributed to free radical scavenging activity of the test compound.

Reactive nitrogen species (RNS) play a pivotal role in the pathophysiology of several diseases. $ONOO^-$ is formed by coupling of $O_2^{\bullet -}$ and NO when they are simultaneously generated by phagocytes that invade the renal parenchyma **(Rutkowski al., 2007)**. $ONOO^-$ generation is accelerated in cells and tissues that lack an endogenous defense system able to detoxify this noxious and highly reactive oxidant molecule **(Nita et al., 2016)**. Another factor contributing to the enhanced generation of $ONOO^-$ is simultaneous production of NO and $O_2^{\bullet -}$ by activated leukocytes **(Kalogeris et al., 2014)**. Therefore, it is pertinent to note that genetic ablation of inducible nitric oxide synthase or treatments with chemical catalysts of $ONOO^-$ decomposition prevent the CDDP-induced renal tissue damage **(Kezic et al., 2016)**. In the present study, the renal and bone marrow NO levels were found to increase after administration of CDDP. The Nano-Se successfully ameliorated this enhancement in renal as well as bone marrow NO levels. This result suggests the ability of Nano-Se in preventing CDDP-induced nitrosative stress.

GSH is a pivotal endogenous antioxidant molecule that maintains redox homeostasis in cells and tissues and protects biomolecules from oxidative tissue damage by scavenging ROS **(Kurutas, 2016)**, in addition to its conjugating ability owing to nucleophilic center and its involvement in detoxification of xenobiotics that cause toxicity and

carcinogenicity. Such a mechanism would decrease the level of reactive electrophiles available to bind DNA, reducing the likelihood of DNA damage and possible induction of carcinogenic process **(Lobe et al., 2008)**. GSH can react chemically with singlet oxygen, superoxide and hydroxyl radicals and therefore function directly as a free radical scavenger. GSH may stabilize membrane structure by removing acyl peroxides formed by lipid peroxidation reactions **(Blokhina et al., 2003)**. In the present investigation, administration of CDDP caused a significant depletion in renal GSH level, reflecting its accumulation in the kidney cells. Treatment with Nano-Se brought the renal GSH level towards that of vehicle control group. GST catalyzes the conjugation of reduced glutathione to electrophilic centers on a wide variety of substrates **(Allocati et al., 2018)**. This activity detoxifies endogenous compounds such as peroxidized lipids **(Leaver and George, 1998)**, as well as breakdown of xenobiotics. It was observed in our experiment that CDDP treatment lowered the renal GST activity. Treatment with Nano-Se significantly elevated the GST activity in renal tissues suggesting its role in modulating the host defense system through GST mediated neutralization of lipid peroxides and other active oxygen species that ultimately helps in cellular protection.

Following prolonged exposure, CDDP lowers the activity of the selenoenzymes GP*x* and TrxR via covalent reaction with the selenol group of the selenocysteine residue **(Ungvári et al., 2014)**. GP*x* is involved in reducing both H_2O_2 and lipid peroxides, thereby limiting the detrimental effects of oxidative stress. The resulting decrease in GP*x* activity due to CDDP administration in turn reduces GSH level as GP*x* is a part of GSH redox cycle which makes cells further prone to oxidative damage. Another selenoenzyme, TrxR is a potential molecular target of anticancer agents including CDDP **(Nordberg and Arner, 2001).** In normal cells the inhibition of TrxR could be deleterious due to an inhibition of the whole thioredoxin system which affects many important cellular functions as TrxR is involved in supplying reducing equivalents to the thioredoxin/thioredoxin peroxidase systems, direct reduction of H_2O_2 and lipid peroxides **(Mustachich et al., 2000)**. In the present experiment, administration of Nano-Se normalized the CDDP induced depleted activity of both these selenoenzymes in kidney. Selenium supplementation in the form of nanosize probably facilitated the incorporation of elemental selenium into the amino acid cysteine instead of sulfur during cysteine metabolism to yield selenocysteine residues and

subsequent insertion of the selenocysteine residues to the selenoproteins which is critical to the catalytic activity of GP*x* and TrxR **(Allan et al., 1999; Holben et al., 1999)**.

Cellular antioxidant defences involving the enzymes SOD and CAT which detoxify the oxygen free radicals and the consequent oxidative burst **(Basu et al., 2014)**. The enzyme SOD catalyzes dismutation of the O_2^- into H_2O_2, which is then detoxified to H_2O by CAT **(Sofo et al., 2015)**. It has also been reported that after administration of CDDP the SOD activity is reduced probably due to the loss of copper and zinc which are essential for the enzyme activity. This decreased SOD activity is insufficient to scavenge the O_2^- produced during the chemotherapy **(Aprioku, 2013)** and ultimately results into the initiation and propagation of LPO **(Ajith et al., 2007)**. Therefore, the activity of theses antioxidant enzymes is a vital protection against oxidative stress. Inhibition of antioxidant enzymes by CDDP makes the cells more prone to oxidative damage. In the present study, administration of Nano-Se protects CDDP induced nephrotoxicity by preventing the induction of oxidative stress and enhancing the renal antioxidant defenses involving SOD and CAT.

Blood urea nitrogen (BUN) measures the amount of urea nitrogen, a waste product of protein metabolism, in the blood. Urea is formed by the liver and carried by the blood to the kidneys for excretion. Because urea is cleared from the blood stream by the kidneys, a test measuring how much urea nitrogen remains in the blood can be used as a test of renal function. Diseased or damaged kidneys cause an elevated BUN because the kidneys are less able to clear urea from the bloodstream. Creatinine is a spontaneously formed cyclic derivative of creatine. Creatinine is chiefly filtered out of the blood by the kidneys. If the filtering of the kidney is deficient, blood levels rise. Therefore, creatinine levels in blood may be used to calculate the creatinine clearance, which reflects the glomerular filtration rate (GFR). The GFR is clinically important because it is a measurement of renal function. A decreased GFR as evidenced by increased plasma creatinine levels has been observed following CDDP administration **(Bami et al., 2017)**. In the present study functional nephrotoxicity indicates such as BUN and serum creatinine levels were elevated after administration of CDDP, which indicate intrinsic acute renal failure. Treatment with nano-Se provided significant protection against CDDP induced nephrotoxicity which was evident from the lowered BUN and creatinine levels.

The bone marrow is the primary site of the body where hematopoietic stem cells and more mature blood cells lineage progenitors reside and differentiate in an adult cell population **(Ho et al., 2015)**. Due to the proliferating nature, the bone marrow cells are very much sensitive to clastogenic chemicals and susceptible to DNA damage **(Antunes et al., 1999)**. This damage, particularly in such undifferentiated cell population of bone marrow, is dangerous because it can lead to mutations and genetic rearrangements. If such cells survive and proliferate, the risk of secondary cancer such as leukaemia increases **(Attia, 2012)**. *In vitro* and *in vivo* studies have indicated that CDDP can induce various types of genotoxic damage, of which DNA cross-linking is the most important one. Direct breakage of the DNA strands occurs when ROS interact with DNA **(Basu et al., 2015)**. In the present study, the percentage of affected cells showing a comet tail significantly increased after CDDP treatment in blood lymphocytes and in bone marrow cells, whereas treatment with Nano-Se significantly decreased DNA damage in peripheral lymphocyte and also in bone marrow cells, which clearly indicated the potential role of Nano-Se in protecting DNA damage and also reduced fragmented DNA (%) in bone marrow. Being highly mutagenic, CDDP may induce chromosomal aberrations and micronuclei formation in mouse bone marrow cells. Developments of CA and MN have been commonly used as sensitive indicators in the clastogenic assays of a drug **(Attia, 2012)**. During proliferation if a clastogenic agent is administered it may act during the cell division and cause chromosomal damage, such as break **(Arafa et al., 2008)**. The mitotic plate of CDDP-treated mice showed high incidence of aberrations; among which most common were stretching, chromatid break and gap. CDDP administration in mice also showed high MN frequency in bone marrow cells. This suggests increased rate of chromosome loss or fragmentation during earlier nuclear division upon CDDP treatment. Treatment with Nano-Se significantly minimized the incidence of CA and MN in the bone marrow niche. These observations clearly suggest the preventive role of Nano-Se against the clastogenic potential of CDDP.

Inhibition of cell proliferation is one of the major causes of CDDP-induced myelotoxicity and related complications. In this study, cell proliferation was markedly suppressed by CDDP as reflected by BrdU labeling assay. In this assay, BrdU gets incorporated into DNA in place of thymidine and BrdU-labeled cells serve as a measure of DNA synthesis

or cell proliferation **(Das et al., 2005)**. Treatment with Nano-Se effectively reversed CDDP-induced inhibition of bone marrow cell proliferation. This indicates that Nano-Se may provide protection to the early progenitor cells and pluripotent stem cells of the bone marrow niche. In this experiment, apoptotic cell death was evaluated by means of TUNEL assay. This assay has been designed to detect cells that undergo internucleosomal DNA cleavage which is a hallmark of apoptosis **(Geske et al., 2000)**. CDDP-treated mice showed high proportion of TUNEL-positive cells. This may be due to the direct cytotoxicity or extensive induction of DNA damage that leads to cell death **(Rjiba-Touati et al., 2012)**. Treatment with Nano-Se diminished this apoptotic cell death and conferred cytoprotection to the host.

Finally, CDDP induced nephrotoxicity was evaluated in this study by histopathological assessment. The toxic effect of chronic CDDP administration was confirmed by the detection of morphologic alterations in kidney slices of treated animals are characterized by sloughing and necrosis of tubular epithelial cells and loss of brush border which could be due to its toxic effects primarily by the generation of reactive oxygen species causing damage to the various membrane components of the cell. Nano-Se treatment alone induced no remarkable alteration in histology. However, Nano-Se when administered combination with CDDP either in concomitant or pretreatment schedule, resulted in excellent protection against nephrotoxicity induced by cisplatin and showed predominant normal kidney morphology.

In conclusion, a plausible mechanism of the protective action of Nano-Se may be at least partly due to its free radical scavenging activity. Overall, these studies suggest the protective potential of Nano-Se against CDDP-induced genotoxicity and nephropathy; however, future studies need to be conducted at the molecular level to determine if Nano-Se can effectively inhibit the ability of CDDP to induce genetic damage in normal cells without interfering with the antitumor efficacy of CDDP. Experiments at the molecular level will reveal the actual mechanism of action of Nano-Se, and its use may thus increase the therapeutic window of CDDP in cancer patients.

Chapter V

Chemoprotective and chemoenhacing properties of Nano-Se against cisplatin induced cellular toxicities without compromising its antitumor properties in Swiss albino mice bearing Ehrlich ascites carcinoma cells

Introduction

Nanomedicine involves utilization of nanotechnology for the benefit of human health and well being. The use of nanotechnology in various sector of therapeutics has revolutionized the field of medicine where nanoparticle of dimensions ranging from 1-100 nm are designed and used for diagnostics, therapeutics and as biomedical tools for research **(Basavaraj et al., 2012)**. The application of nanomedicine to the diagnosis and treatment of cancer has been ongoing for over 20 years, although its clinical utility has yet to be fully realized **(Kim et al., 2013)**.

Cisplatin (CDDP) is an inorganic antineoplastic drug, used extensively for the treatment of variety of human cancers including that of testis, ovary, head and neck, cervix, lungs, breast and bladder **(Dasari et al., 2014)**. Its neoplastic use is limited by development of moderate to severe nephrotoxicity, ototoxicity and neurotoxicity **(Callejo et al., 2015)**. Clinical studies have revealed that approximately 30–50% of the patients treated with CDDP could develop hearing loss and 14–57% experienced neurotoxicity. Furthermore, 70% of the patients treated with CDDP experienced nephrotoxicity **(Dasari et al., 2014)**. Nephrotoxicity has been shown to develop primarily in the S3 segment of the proximal tubule, which impair the patient's quality of life and can even be life-threatening in preexisting conditions **(Ansari et al., 2017)**. CDDP-induced nephrotoxicity can manifest with various types of symptoms such as acute kidney injury, hypomagnesemia, Fanconi-like syndrome, distal renal tubular acidosis, hypocalcemia, renal salt wasting, the renal concentrating defect, hyperuricemia, transient proteinuria, and erythropoietin deficiency **(Miller et al., 2010)**.The most serious and life-threatening side effect is acute kidney injury, which occurs in 20–30% of the patients treated with CDDP **(Oh et al., 2014)**. The renal damage associated with CDDP is multifactorial and includes adduct formation, oxidative stress, nitrosative stress, biotransformation and inflammation **(Ansari et al.,**

2017). Experimental evidence suggested that the role of reactive oxygen and reactive nitrogen species (ROS/RNS) in increasing lipid peroxide formation and decreasing the activity of antioxidant enzymes in CDDP-induced renal injuries **(Meo et al., 2016).** In such a clinical condition, discontinuation of CDDP remains the only option to prevent further renal damage in affected patients. Presently, no effective treatment regimen is available that can completely prevent renal damage due to CDDP. Therefore, there is an unmet need to develop agents that can confer renoprotection without compromising the anticancer activity of CDDP.

Several trials have suggested that chemopreventive antioxidants mitigate toxicity and increase survival times and tumour responses **(Rahman et al., 2010)**. Selenium (Se) is an essential trace element required for animals and humans for its possible role as a potent antioxidant against oxidative stress induced by xenobiotic compounds of diverse nature **(Kurutas, 2016)**. Se is a vital component of several enzymes such as glutathione peroxidase, thioredoxin reductase and selenoprotein P, which contains selenium as selenocysteine **(Saha, 2017)**. Researchers have reported that excessive intake of selenium could lead to gastrointestinal disturbances, hair and nail changes, and neurologic manifestations including acroparesthesias, weakness, convulsions, and decreased cognitive function **(Li et al., 2008)**. In the last few years, nanotechnology known as science of using nanometer dimensions of materials, has become a great interest in biomedical field due to their utility for the efficient medical diagnosis, treatment, and prevention of diseases **(Zhang et al., 2016)**. Recently, selenium nanoparticles (Nano-Se), a unique type of elemental selenium of nano defined size with bright red appearance, have aroused worldwide attention due to its distinguished properties and excellent biological activities **(Wang et al., 2007; Zhang et al., 2005)**. It is able to scavenge free radicals *in vitro* **(Huang et al., 2003)** and to improve growth performance, serum oxidant status and Se retention *in vivo* **(Hu et al., 2012)**. Amazingly, compared with other Se compounds such as selenite **(Zhang et al., 2005)**, selenomethionine **(Navarro-Alarcon, 2008)**, Se-yeast **(Shi et al., 2010)** and Se-methylselenocysteine **(Zhang et al., 2008)**, Nano-Se exhibit much lower acute toxicity while increasing the activities of selenoenzymes. In addition, Nano-Se can inhibit the growth of microorganisms **(Hosnedlova et al., 2018)**, and it also exhibits antitumor activities both *in vivo*

(Ramamurthy et al., 2013) and *in vitro* **(Yazdi et al., 2013)**. Therefore Nano-Se is regarded as a prospective Se formulation due to its potential in nutritional supplement use, chemoprevention and chemical therapy against cancer.

The present study was designed to examine the antitumor efficacy of synthesized Nano-Se in the tumor bearing Swiss albino mice. In this study design, Nano-Se was also administered along with a widely used broad spectrum chemotherapeutic agent CDDP to investigate the 'chemoprotective' (protection against chemotherapeutic drug induced toxicity) and 'chemosensitization' (potentiation of cytotoxicity of chemotherapeutic drugs towards tumor cells) efficacy of Nano-Se.

Materials and methods

Experimental animals

Adult (5–6 weeks) Swiss albino female mice (25 ± 2g), bred in the animal colony of Chittaranjan National Cancer Institute (CNCI) (Kolkata, India), were used for this study. The mice were maintained under standard condition of humidity (45–55%), temperature (23 ± 2ºC), and light (12 h light/12 h dark). Standard food pellets (EPIC rat and mice pellet) from Kalyani Feed Milling Plant, Kalyani, West Bengal, India and drinking water was provided *ad libitum*. The experiments were carried out following strictly the Institute's guideline for the Care and Use of Laboratory Animals.

Chemicals

Cisplatin was purchased from Cadila Health Care Limited, Kundaim Industrial Estate, Ponda, Goa, India. HEPES, 2',7'-dichlorodihydrofluorescein diacetate (DCFH-DA), vanadium chloride (VCl3), 1-chloro-2,4-dinitrobenzene (CDNB), ethylene diamine tetraacetic acid (EDTA), reduced glutathione (GSH), pyrogallol, 5,5´ -dithio-bis (2-nitro benzoic acid) (DTNB), sodium dodecyl sulphate (SDS), bovine serum albumin (BSA), β -nicotinamide adenine dinucleotide phosphate (reduced) (NADPH), glutathione reductase, sodium azide (NaN_3), colchicine, giemsa stain, normal melting agarose (NMA), low melting point agarose (LMPA), Histopaque, Triton-X 100, ethidium bromide, were obtained from Sigma-Aldrich Chemicals Private Limited, Bangalore, India. Hydrogen peroxide 30% (H_2O_2), thiobarbituric acid (TBA), propylene glycol, sodium carbonate, copper sulfate, sodium hydroxide, potassium-sodium tartrate, sucrose,

TRIS, dithiothreitol (DTT), di-sodium hydrogen phosphate, sodium di-hydrogen phosphate, acetic acid, n-butanol, pyridine, formaldehyde (37%), paraffin (58°C - 60°C), calcium chloride, ortho-phosphoric acid, xylene and DPX mounting medium were obtained from Merck (India) Limited, Mumbai, India. Chloroform, methanol, zinc sulphate (ZnSO4), sodium bicarbonate, glucose and Folin-phenol reagent were purchased from Sisco Research Laboratories Private Limited Mumbai, India. Dipotassium hydrogenphosphate and potassium dihydrogenphosphate were obtained from Spectrochem Private Limited, Mmbai, India. Sodium citrate and magnesium chloride ($MgCl_2$) were purchased from Glaxo laboratories (India) Ltd, Mumbai. Urea Berthelot Test Kit and Creatinine Test Kit were obtained from Span Diagnostics Ltd, Sachin (Surat), India. Hematoxylin and Eosin stains were obtained from Qualigens Limited, India. Egg albumin was prepared in our laboratory. Conventional microscope slides, end frosted microscope slides (75 mm × 25 mm with 19 mm frosted end) and cover glass (No.1, 24 × 60 mm) were purchased from Blue Star, India. *In situ* cell death detection Kit II, AP was purchased from Roche Molecular Biochemicals, Manheim, Germany.

Experimental design

Tumor cells

EAC cells were maintained in Swiss albino mice by weekly intraperitoneal (i.p.) transplantation of 1×10^6 viable tumor cells suspended in phosphate buffer saline (PBS).

Experimental groups

Animals were distributed into seven groups Gr. (I-VII) each group consisting of eighteen animals. Six animals from each group were taken for the study of biochemical and hematological parameters, histopathological evaluation and for cytogenetic evaluation. The second set, consisting of six animals from each group was taken for studying some parameters to evaluate the anti-tumor activity of Nano-Se, for detection of apoptosis of tumor cells and DNA damage comet assay in tumor cells. The third set, consisting of six animals from each group was stipulated to determine the mean survival time of animals in each group. Animals of Gr. (II-VII) were injected with EAC cells (1×10^6 cells/mouse) intraperitoneally. The day of EAC cell inoculation was counted as day zero.

No treatment was given on the day of EAC cell inoculation. The groups were treated as follows:

Vehicle control (VC) (Group I): Each animal was given oral administration of saline (0.9% NaCl) from day 1 to day 9 and was kept as normal.

EAC control (E) (Group II): Animals were given saline (0.9% NaCl) by oral gavages from day 1 to day 9.

Only CDDP treated group (EC) (Group III): Animals were received CDDP at a dose of 5 mg/kg b.w. by intraperitoneal administration from day 1 to day 5.

Only Nano-Se concomitant treated group (ED) (Group VI): Animals were treated only with Nano-Se at a dose of 2 mg Se/kg. b.w. 24 hr after tumor inoculation from day 1 to day 9.

Only Nano-Se pretreated group (PED) (Group V): Animals were pretreated with the Nano-Se at a dose of 2 mg Se/kg. b.w. 7 days prior to tumor inoculation and the treatment was continued 24 hr after tumor inoculation from day 1 to day 9. (The day of EAC cell inoculation was count as day zero.)

Concomitant treatment with CDDP and Nano-Se (ECD) (Group VI): Nano-Se was administered orally at a dose of 2 mg Se/kg. b. w along with CDDP (5 mg/kg b.w.) from day 1 to day 9.

Pretreatment with CDDP and Nano-Se (PECD) (Group VII): Animals were given Nano-Se orally at a dose of 2 mg Se/kg b.w. 7 days prior to tumor inoculation and the treatment was continued from day 1 to day 9 starting from 24 hr after tumor inoculation along with CDDP (5 mg/kg b.w.).

The mice were sacrificed on day 10, 24 hours after the last treatment and the parameters described below were studied. The treatment schedule has been schematically presented in **Fig. 1**

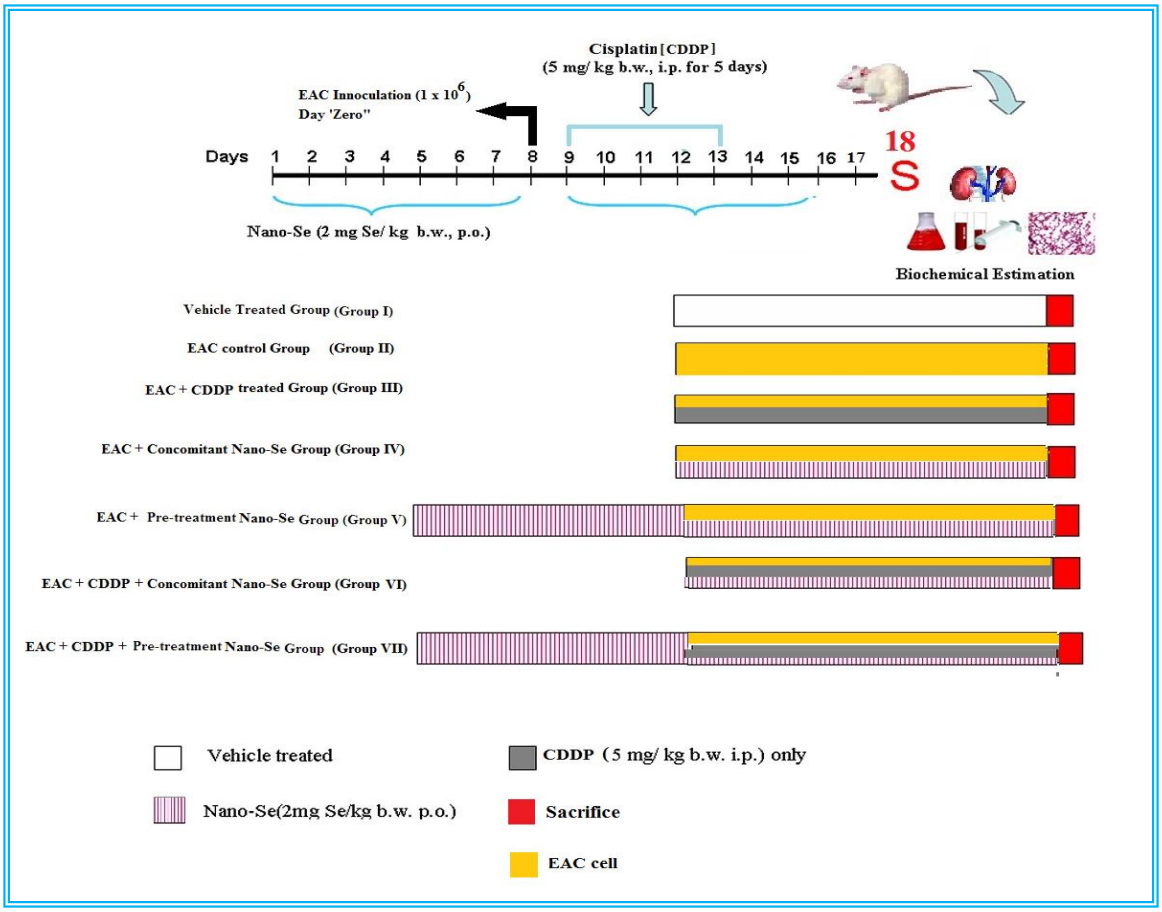

Figure 1: Treatment schedule

Parameter studied

Set A

Following parameters were assessed from Set A

- Quantitative estimation microsomal lipid peroxidation level in kidney.
- Biochemical estimation of reactive oxygen species (ROS) level in kidney and in EAC cells
- Quantitative estimation of reduced glutathione level, estimation of the activity of phase II detoxifying enzyme glutathione-S-transferase and different antioxidant enzymes like superoxide dismutase, catalase and glutathione peroxidase in kidney.

- Estimation of renal function markers namely blood urea nitrogen and creatinine levels in serum.
- Evaluation of chromosome aberrations by conventional flame dry technique and assessment of DNA damage by comet assay in blood lymphocyte.
- Histopathological evaluation of kidney tissue.

Set B

Following parameters were assessed from Set B

- Measurement of tumor volume, packed cell volume of EAC cells and viable EAC cell count.
- Detection of apoptosis of EAC cells by TUNEL assay.

Set C

Following parameters were assessed from Set C

- Determination of mean survival time and percentage increase in life span

Methodologies

❖ **Biochemical assay**

Detailed procedures regarding the biochemical parameters and others parameters have already been mentioned in Chapter II.

➢ **Estimation of protein content in the tissue homogenate (Lowry et al., 1951)**

Total protein content in tissue homogenate during biochemical analysis assay was measured through Lowry method using Folin-Phenol reagent.

➢ **Quantitative estimation of lipid peroxidation (LPO) level (Ohkawa et al., 1979)**

Spectrophotometric method was applied to estimate the level of lipid peroxidation in kidney microsomes by measuring the formation of lipid peroxides using thiobarbituric acid (TBA) and was expressed as nm TBARS/mg protein.

- **Estimation of ROS production (Shinomol and Muralidhara, 2007)**

ROS generation in kidney homogenate was measured spectrofluorimetrically with slight modifications using probe *i.e.,* DCFH-DA which is hydrolyzed by mitochondrial esterase to form 2',7'-dichlorodihydrofluorescein (DCFH) then it is oxidized by ROS to form the fluorescent compound 2',7'-dichlorofluorescein (DCF) which is measured spectrofluorimetrically (excitation 485 nm/emission 530 nm).

- **Estimation of reduced glutathione (GSH) level (Mulder et al., 1995; Sedlack et al., 1968)**

GSH level was estimated in kidney cytosol spectrophotometrically by determination of dithiobis (2-nitro) - benzoic acid (DTNB) reduced by –SH groups by measuring the absorbance at 412 nm. The level of GSH was expressed as nmol/mg protein.

- **Estimation of glutathione-S-transferase (GST) activity (Mulder et al., 1995; Habig et al., 1974)**

Spectrophotometric method was adopted to evaluate the activity of GST in kidney tissue. GST activity was measured in tissue cytosolic fractions by determining the increase in absorbance at 340 nm with 1-chloro-2,4-dinitrobenzene (CDNB) as the substrate and the specific activity of the enzyme was expressed as CDNB-GSH conjugate formed/minute/mg protein.

- **Superoxide dismutase activity (SOD) (Marklund et al., 1974; McCord et al., 1969)**

SOD was determined by means of inhibition of pyrogallol auto-oxidation by the enzyme. Partial extraction and purification of SOD was done as described by McCord and Fridovich. SOD activity was assayed by the method of Marklund and Marklund.

- **Catalase activity (CAT) (Luck, 1963)**

CAT catalyzes the breakdown of H_2O_2 into H_2O and O_2 and competes with the GP*x* for the common substrate H_2O_2. CAT has been considered to be the primary scavenger of intracellular H_2O_2 generated due to oxidative stress. Activity of CAT in kidney tissue

sample was determined spectrophotometrically at 240 nm and expressed as unit/mg protein where the unit is the amount of enzyme that liberates half the peroxide oxygen from H_2O_2 in seconds at 25^oC.

- **Estimation of GP*x* activity (Paglia et al., 1967)**

GP*x* activity was measured by NADPH oxidation using a coupled reaction system consisting of reduced glutathione, glutathione reductase and hydrogen peroxide. The enzyme activity was expressed as micromol NADPH utilized/minute/mg protein using extinction coefficient of NADPH at 340 nm as 6200 $M^{-1}cm^{-1}$.

- **Determination of blood urea nitrogen (BUN) (Urease-Bertholot end point assay)**

Urea is hydrolysed in presence of water and urease to produce ammonia and carbon dioxide. Under alkaline conditions, ammonia so formed, reacts with hypochlorite and phenolic chromogen to form colored indophenol, which is measured at 578 nm spectrophotometrically. Sodium nitropruside acts as a catalyst. The intensity of color is proportional to the concentration of urea in the sample **(Murrary, 1984; Chaney and Marbach, 1962).**

- **Estimation of serum creatinine level (Bonses and Taussky, 1945)**

Creatinine in a protein free solution reacts with alkaline picrate and produced a red colored complex, which is measured spectrophotometrically at 520 nm.

- **Genotoxicity parameters**

- **Assay of chromosomal aberration**

For the study of chromosomal aberrations (CA), slides were prepared from bone marrow cells by the conventional flame drying technique **(Biswas et al, 2004)**. Detailed procedure has already been given in chapter II.

- **Detection of DNA damage by alkaline single cell gel electrophoresis (comet assay)**

Possible DNA damage induced by CDDP was detected in blood lymphocytes using the alkaline single cell gel electrophoresis (comet) assay following a simplified protocol with slight modifications. For separation of lymphocytes from whole blood, the mice were anesthetized and blood samples were collected from by retro orbital puncture. Lymphocytes were isolated from samples of blood by standard centrifugation over a cushion of histopaque, washed with isotonic PBS and centrifuged. The pellet was resuspended in isotonic PBS. The cell viability in each group was measured by the trypan blue exclusion method and approximately 104 cells /slide were taken for the assay. Rest of the procedure is same as that for bone marrow cells which has been described in details in chapter II. The results were expressed as:

1. Percentage of cells with tail in each group and
2. Average tail length due to DNA migration in each group.

- **Histopathology (Bancroft et al., 1990; Lillie et al., 1976)**

Histopathological evaluation of kidney tissues was done by conventional hematoxylin-eosin staining method detail of which already mentioned in chapter II.

- **Tumor growth response (Mazumder et al, 1997; Gupta et al, 2000)**

The anti-tumor effect of CDDP along with the test compound was assessed by measuring the changes in ascites tumor volume, packed cell volume (PCV) and viable tumor cell count. Mean survival time (MST) of each group containing six mice was monitored and percentage increase in life span (% ILS) was calculated using following equation. MST= (Day of first death + Day of last death)/2. ILS (%) = [(Mean survival time of treated group/Mean survival time of control group)–1] × 100.

- **Detection of apoptosis by terminal deoxynucloeotidyl transferase dUTP nick end labeling (TUNEL) technique (Caderni et al, 2000)**

Individual apoptotic cells were identified by TUNEL assay. It is a fast and simple non radioactive technique. Cleavage of genomic DNA during apoptosis may yield double-

stranded, low molecular weight DNA fragments (mono- and oligonucleosomes) as well as single strand breaks ("nicks") in high molecular weight DNA. Those DNA strand breaks can be identified by labeling free 3′-OH termini with modified nucleotides in an enzymatic reaction. In this technique, the DNA strand breaks are labeled by free terminal deoxynucleotidyl transferase (TdT), which catalyzes polymerization of labeled nucleotide to free 3′-OH DNA ends in a template independent manner. The apoptotic cells are identified by the fluorescence they emit. Number of labeled and unlabeled cells was counted. The Apoptotic Index (AI) was determined as the percentage of the labeled cells with respect to the total number of cells counted.

$$\text{Apoptotic Index} = \frac{\text{Number of labeled cells}}{\text{Total number of cells counted}} \times 100$$

Detailed procedure regarding the TUNEL assay has already been described in Chapter II.

Statistical analysis

All data were presented as mean ± SD. n = 6 animals per group. One way ANOVA followed by Tukey's Multiple Comparison Test using Graph Pad Prism software was performed for comparisons among groups. Significant difference was indicated when the *P* value was < *0.05*.

Results

- **LPO level**

The level of LPO was increased significantly *(P < 0.05)* by 25.28% in kidney tissues in the EAC control group (Gr. II) compared to the vehicle control group (Gr. I) **(Fig. 2)**. A further significant *(P < 0.05)* elevation in LPO level in kidney by 76.45% was observed after administration of CDDP in tumor bearing mice (Gr. III) in comparison to the EAC control group (Gr. II). Treatment with Nano-Se alone decreased the LPO level significantly *(P < 0.05)* by 15.47% (Gr. IV) & by 27.35% (Gr. V) in kidney, compared to the EAC control group (Gr. II). Concomitant administration of Nano-Se along with CDDP (Gr. VI) significantly *(P < 0.05)* diminished the LPO level in kidney by 46.5% in comparison to the CDDP treated group (Gr. III). Pretreatment with Nano-Se along with CDDP reduced the LPO level in kidney by 51.96% in comparison to the CDDP treated group (Gr. III).

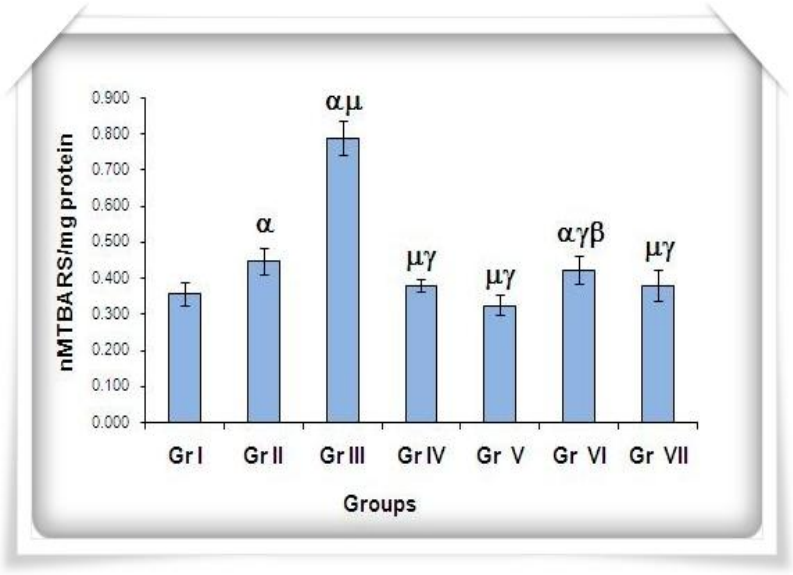

Figure 2: Data were represented as mean ± Standard deviation (SD) (*n*=6). α - significant (*P < 0.05*) as compared with Gr. I; μ - significant (*P < 0.05*) as compared with Gr. II; γ - significant (*P < 0.05*) as compared with Gr. III; θ - significant (*P < 0.05*) as compared with Gr. IV; β - significant (*P < 0.05*) as compared with Gr. V; ψ - significant (*P < 0.05*) as compared with Gr. VI.

- **ROS Level**

- **Hydrogen peroxide level by using DCFH-DA in kidney**

The ROS level in kidney increased significantly *(P < 0.05)* by 191.93% in the EAC control group (Gr. II) as compared to the vehicle control (Gr. I) **(Fig. 3)**. Intraperitoneal administration of CDDP in tumor bearing mice (Gr. III) resulted in an additional significant *(P < 0.05)* enhancement of ROS level by 13.86%, in comparison to the EAC control group (Gr. II). Treatment with Nano-Se on its own decreased the ROS level significantly *(P < 0.05)* by 6.94% (Gr. IV) and 13.75% (Gr. V) as compared with EAC control group (Gr. II). Concomitant and pretreatment of Nano-Se along with CDDP decreased the ROS level significantly *(P < 0.05)* by 48.16% and 50.66% respectively in Gr. VI and Gr. VII in comparison to the CDDP treated group (Gr. III).

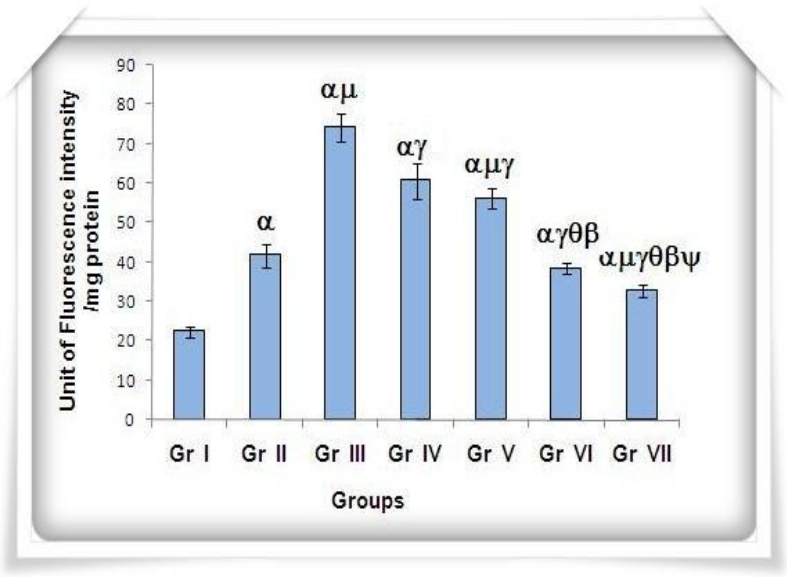

Figure 3: Data were represented as mean ± Standard deviation (SD) (*n*=6). α - significant (*P < 0.05*) as compared with Gr. I; μ - significant (*P < 0.05*) as compared with Gr. II; γ - significant (*P < 0.05*) as compared with Gr. III; θ - significant (*P < 0.05*) as compared with Gr. IV; β - significant (*P < 0.05*) as compared with Gr. V; ψ - significant (*P < 0.05*) as compared with Gr. VI.

- **Hydrogen peroxide level by using DCFH-DA in tumor cell**

To evaluate the mechanism of cell death on the basis of ROS production DCFH-DA assay was done in tumor cells **(Fig. 4)**. Intraperitoneal administration of CDDP in tumor bearing mice (Gr. III) resulted in significant *(P < 0.05)* enhancement of ROS level by 278.33% in comparison to the EAC control group (Gr. II). Treatment with Nano-Se on its own increased the ROS level significantly *(P < 0.05)* in tumor cells by 100.62% (Gr. IV) and 194.45% (Gr. V) in comparison to the EAC control group (Gr. II). In addition, when Nano-Se was used along with chemotherapeutic drug CDDP in combination regimen ROS in the tumor cells was boosted up by 21.10% in case of concomitant treatment (Gr. VI) and by 55.95% in case of pretreatment (Gr. VII) compared to the CDDP control group (Gr. III).

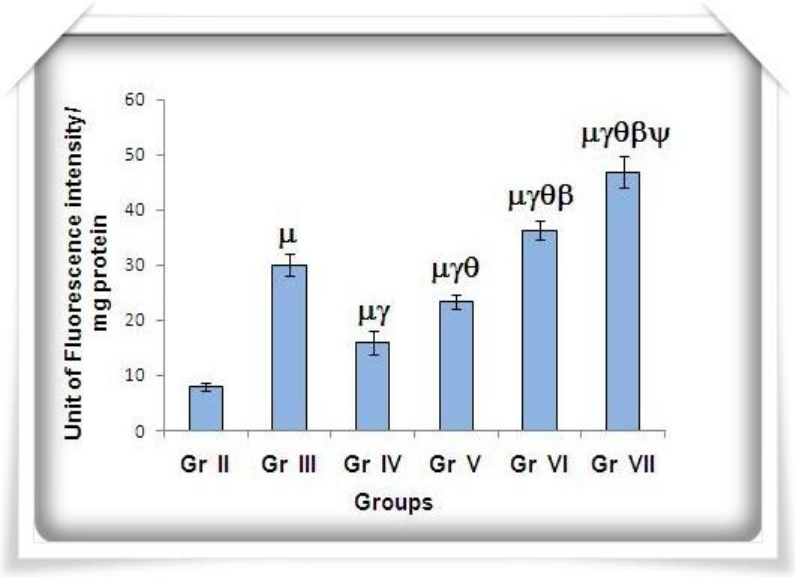

Figure 4: Data were represented as mean ± Standard deviation (SD) *(n=6)*. μ - significant (*P < 0.05*) as compared with Gr. II; γ - significant (*P < 0.05*) as compared with Gr. III; θ - significant (*P < 0.05*) as compared with Gr. IV; β - significant (*P < 0.05*) as compared with Gr. V; ψ - significant (*P < 0.05*) as compared with Gr. VI.

- **GSH level**

The GSH content was found to decrease significantly ($P < 0.05$) by 60.34% in kidney after tumor inoculation in Gr. II, compared to the vehicle control group (Gr. I) **(Fig. 5)**. After intraperitoneal administration of CDDP (Gr. III), GSH content was decreased for a second time by 32.10% in kidney in comparison to the EAC control group (Gr. II). Sole application of Nano-Se caused a significant ($P < 0.05$) increment in the nephrotic GSH level by 58.99 % & 8.15% respectively in Gr. IV & Gr. V, compared to the EAC control group (Gr. II). Combined application of Nano-Se in concomitant and pretreatment schedule with CDDP (Gr. VI & Gr. VII) augmented the GSH content in kidney significantly by 86.3% & 190.07% in comparison to the CDDP treated group (Gr. III).

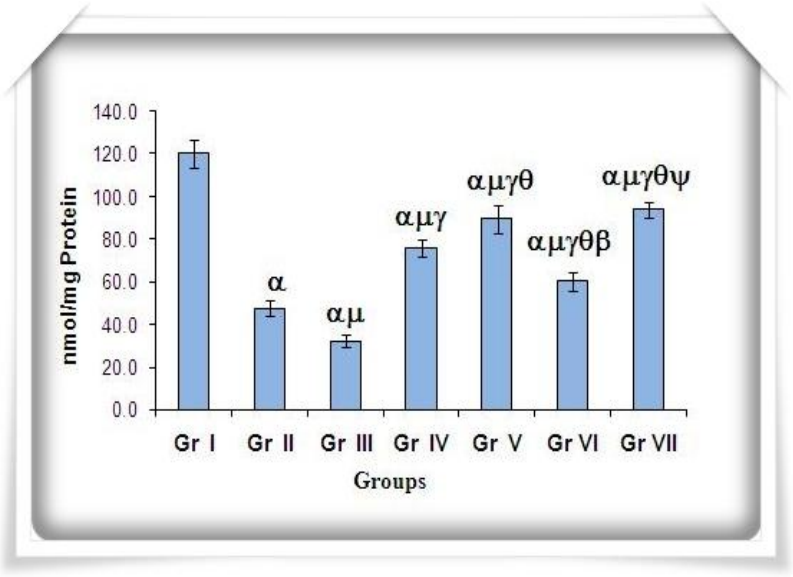

Figure 5: Data were represented as mean ± Standard deviation (SD) (n=6). α - significant ($P < 0.05$) as compared with Gr. I; μ - significant ($P < 0.05$) as compared with Gr. II; γ - significant ($P < 0.05$) as compared with Gr. III; θ - significant ($P < 0.05$) as compared with Gr. IV; β - significant ($P < 0.05$) as compared with Gr. V; ψ - significant ($P < 0.05$) as compared with Gr. VI

- **GST activity**

It was observed that tumor inoculation resulted in a significant ($P < 0.05$) reduction in GST activity by 42.68% in kidney (Gr. II), compared to the vehicle control group (Gr. I) **(Fig. 6)**. GST activity reduced significantly by 25.68% in kidney once again when CDDP was given in tumor inoculated mice (Gr.III) in comparison to the EAC control group (Gr. II). The Nano-Se alone (Gr. IV & Gr. V) significantly enhanced the GST activity in kidney by 14.7% & 46.12% in comparison to the EAC control group (Gr. II). Concomitant and pretreatment of Nano-Se along with CDDP (Gr. VI & Gr. VII) significantly increased the GST activity in kidney by 51.21% & 79.88% in comparison to the CDDP treated group (Gr. III).

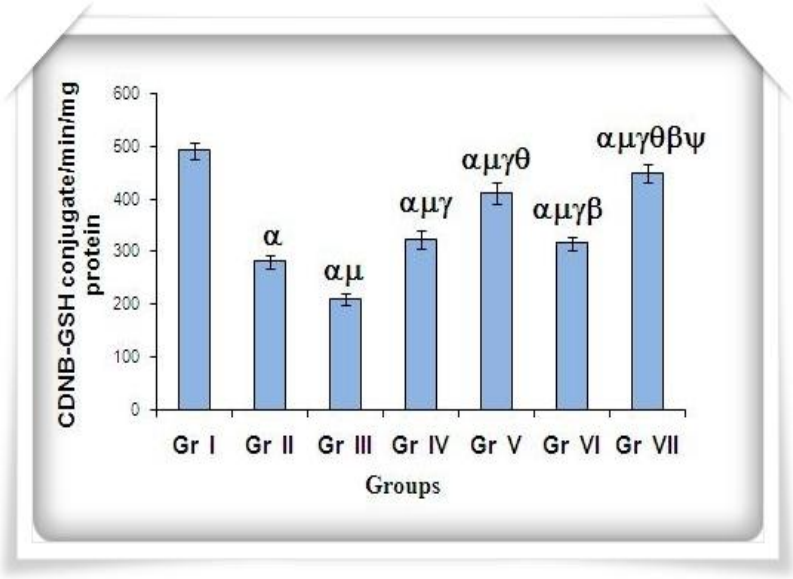

Figure 6: Data were represented as mean ± Standard deviation (SD) (n=6). α - significant ($P < 0.05$) as compared with Gr. I; μ - significant ($P < 0.05$) as compared with Gr. II; γ - significant ($P < 0.05$) as compared with Gr. III; θ - significant ($P < 0.05$) as compared with Gr. IV; β - significant ($P < 0.05$) as compared with Gr. V; ψ - significant ($P < 0.05$) as compared with Gr. VI.

- **SOD activity**

The SOD activity decreased significantly ($P < 0.05$) by 46.07% in kidney in the EAC control group (Gr. II) in comparison to the vehicle control group (Gr. I) **(Fig. 7)**. SOD activity was further significantly diminished after intraperitoneal administration of CDDP (Gr. III) in kidney by 20.76% in comparison to the EAC control group (Gr. II). Nano-Se alone (Gr. IV & Gr. V) increased the SOD activity in kidney by 16.37% & 36.21% compared to the EAC control group (Gr. II). When the same dose of Nano-Se was applied in combination with CDDP in concomitant and pretreatment schedule (Gr. VI & Gr. VII), enhancement in the SOD activity was 38.31% & 64.06% in kidney in comparison to the CDDP treated group (Gr. III).

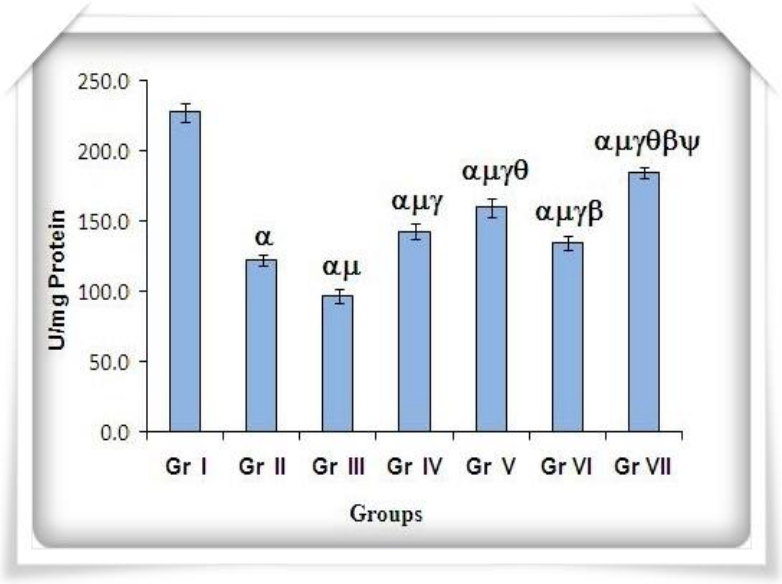

Figure 7: Data were represented as mean ± Standard deviation (SD) (n=6). α - significant ($P < 0.05$) as compared with Gr. I; μ - significant ($P < 0.05$) as compared with Gr. II; γ - significant ($P < 0.05$) as compared with Gr. III; θ - significant ($P < 0.05$) as compared with Gr. IV; β - significant ($P < 0.05$) as compared with Gr. V; ψ - significant ($P < 0.05$) as compared with Gr. VI.

- **CAT activity**

Tumor inoculation caused a significant ($P < 0.05$) reduction in the CAT activity in kidney by 52.43% in the EAC control group (Gr. II), compared to the vehicle control group (Gr. I) **(Fig. 8)**. When CDDP was administered in tumor inoculated mice (Gr. III), CAT activity reduced significantly for a second time in kidney by 28.86% in comparison to the EAC control group (Gr. II). Nano-Se when administered alone in tumor bearing mice (Gr. IV & Gr. V), it resulted in a significant ($P < 0.05$) augmentation of CAT activity in kidney by 35.86% & 68.03% in comparison to the EAC control group (Gr. II). Concomitant and pretreatment of Nano-Se along with CDDP (Gr. VI & Gr. VII) increased the CAT activity in kidney significantly by 71.93% & 87.98% in comparison to the CDDP treated group (Gr. III).

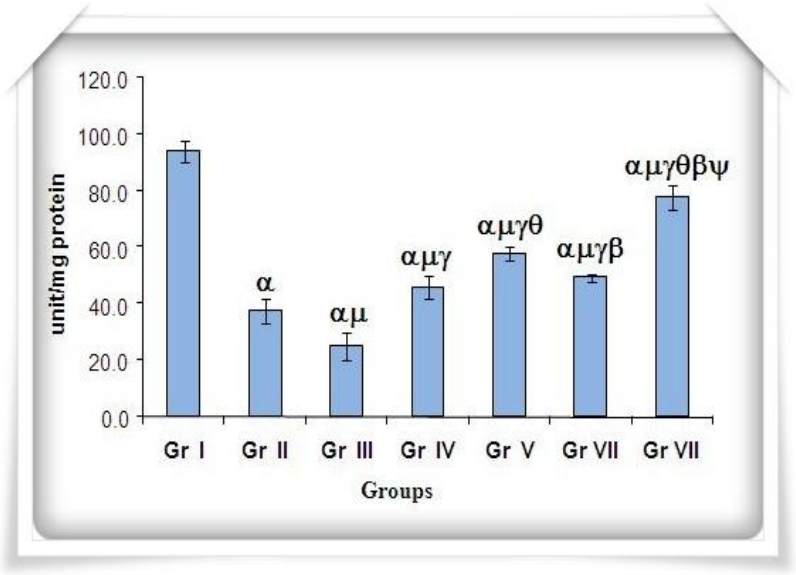

Figure 8: Data were represented as mean ± Standard deviation (SD) (n=6). α - significant ($P < 0.05$) as compared with Gr. I; μ - significant ($P < 0.05$) as compared with Gr. II; γ - significant ($P < 0.05$) as compared with Gr. III; θ - significant ($P < 0.05$) as compared with Gr. IV; β - significant ($P < 0.05$) as compared with Gr. V; ψ - significant ($P < 0.05$) as compared with Gr. VI.

- **GP*x* activity**

A significant ($P < 0.05$) depletion in GP*x* activity by 63.96% in kidney was noticed in the EAC control group (Gr. II) compared to the vehicle control group (Gr. I) **(Fig. 9)**. Administration of CDDP in tumor bearing mice (Gr. III) resulted in an additional reduction of GP*x* activity in kidney by 28.26% in comparison to the EAC control group (Gr. II). The Nano-Se itself (Gr. IV & Gr. V) increased the GP*x* activity in kidney by 50.72% & 87.68% in comparison to the EAC control group (Gr. II). Concomitant administration of Nano-Se along with CDDP (Gr. VI) significantly ($P < 0.05$) enhanced the GP*x* activity in kidney by 80.80% in comparison to the CDDP treated group (Gr. III). Pretreatment with Nano-Se along with CDDP raised the GP*x* activity in kidney by 174.74% in comparison to the CDDP treated group (Gr. III).

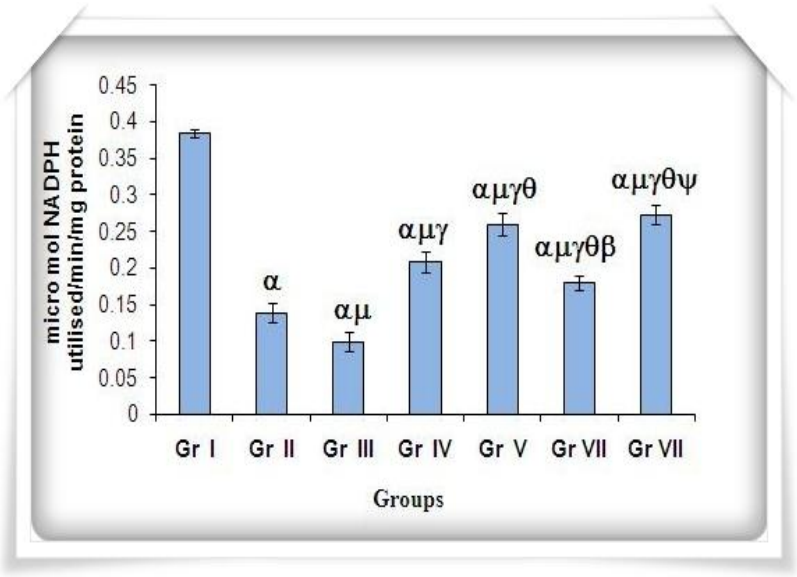

Figure 9: Data were represented as mean ± Standard deviation (SD) (n=6). α - significant ($P < 0.05$) as compared with Gr. I; μ - significant ($P < 0.05$) as compared with Gr. II; γ - significant ($P < 0.05$) as compared with Gr. III; θ - significant ($P < 0.05$) as compared with Gr. IV; β - significant ($P < 0.05$) as compared with Gr. V; ψ - significant ($P < 0.05$) as compared with Gr. VI.

- **BUN and creatinine levels**

The BUN and creatinine level in serum increased significantly ($P < 0.05$) by 140.03% and by 160.4% in the EAC control group (Gr. II) in comparison to the vehicle control group (Gr. I) **(Table 1)**. After intraperitoneal administration of CDDP (Gr. III), BUN and creatinine level again increased significantly by 33.58% and 66.21% respectively, in comparison to the EAC control group (Gr. II). The Nano-Se itself (Gr. IV & Gr. V) significantly decreased the BUN by 38.49% & 50.13%, and creatinine level by 35.15% & 46.11% in comparison to the EAC control group (Gr. II). Concomitant and pretreatment with the Nano-Se along with CDDP (Gr. VI & Gr. VII) significantly reduced the BUN by 33.59% & 44.68% and creatinine level by 39.01% & 54.67% in comparison to the CDDP treated group (Gr. III).

Groups	BUN (mg/dl)	Creatinine (mg/dl)
Gr. I	26.2 ± 1.72	0.84 ± 0.01
Gr. II	$62.8 \pm 2.35^{\alpha}$	$2.19 \pm 0.13^{\alpha}$
Gr. III	$84.0 \pm 1.84^{\alpha\mu}$	$3.62 \pm 0.15^{\alpha\mu}$
Gr. IV	$38.6 \pm 1.57^{\alpha\mu\gamma}$	$1.42 \pm 0.08^{\alpha\mu\gamma}$
Gr. V	$31.3 \pm 1.17^{\alpha\mu\gamma\theta}$	$1.18 \pm 0.13^{\alpha\mu\gamma\theta}$
Gr.VI	$55.79 \pm 3.36^{\alpha\mu\gamma\theta\beta}$	$2.22 \pm 0.18^{\alpha\gamma\theta\beta}$
Gr. VII	$46.4 \pm 3.41^{\alpha\mu\gamma\theta\beta\psi}$	$1.65 \pm 0.09^{\alpha\mu\gamma\theta\beta\psi}$

Table 1: Data were represented as mean ± Standard deviation (SD) (n=6). α - significant ($P < 0.05$) as compared with Gr. I; μ - significant ($P < 0.05$) as compared with Gr. II; γ - significant ($P < 0.05$) as compared with Gr. III; θ - significant ($P < 0.05$) as compared with Gr. IV; β - significant ($P < 0.05$) as compared with Gr. V; ψ - significant ($P < 0.05$) as compared with Gr. VI.

➢ **Chromosomal aberration**

EAC inoculation (Gr. II) showed significantly (P < 0.05) high proportion of chromosomal aberration of 53.86% compared to the vehicle treated group (Gr. I) **(Fig. 11A)**. After administration of CDDP treatment was given to EAC-inoculated animals (Gr. III), it showed further more rise in chromosomal aberration of about 69.52%. The frequency of CA reduced to 32.66% in Gr. IV and to 25.07% in Gr. V after administration of the Nano-Se alone. The same Nano-Se exerted a significant protection against CDDP induced genotoxicity when the compound was given in combination therapy schedule with CDDP and the frequency of CA reduced to 46.5% in Gr. VI and 39.91% in Gr. VII. Different types of chromosomal aberrations have been shown in **Fig. 11B**.

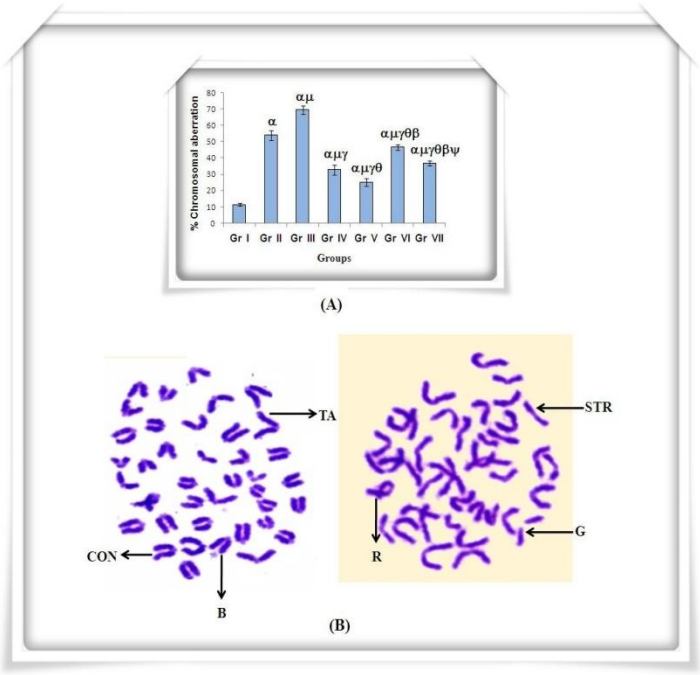

Figure 11A: Data were represented as mean ± Standard deviation (SD) (n=6). α - significant ($P < 0.05$) as compared with Gr. I; μ - significant ($P < 0.05$) as compared with Gr. II; γ - significant ($P < 0.05$) as compared with Gr. III; θ - significant ($P < 0.05$) as compared with Gr. IV; β - significant ($P < 0.05$) as compared with Gr. V; ψ - significant ($P < 0.05$) as compared with Gr. VI.

Figure 11B: 7 Photographs of metaphase chromosomes of bone marrow cells from treated and untreated EAC bearing mice. Arrows indicate stretching (STR), break (B), constriction (CON), ring (R), terminal association (TA) and gap (G)

- **Comet assay findings**

Single cell gel electrophoresis assay (comet assay) was performed to find out induction of genotoxicity by CDDP at DNA level in peripheral lymphocyte **(Fig. 12 A-G)** of experimental mice and two parameters namely percentage of damaged cells and the average tail length were measured.

- **Percentage of damaged cells in each group**

The frequency of damaged lymphocyte cells was estimated to be 8.92% in Gr. I (Table 3). In EAC control group the frequency of cells with damaged DNA was increased significantly ($P < 0.05$) to 48.75%. CDDP treatment resulted in further significant increase in the proportion of damaged cells (85.33%) in Gr. III **(Table 2)**. When Nano-Se was given singly in tumor bearing mice in concomitant (Gr. IV) and pretreatment (Gr. V) schedule, the frequency of damaged cells reduced respectively to 24.45% & 20.39%. In combination therapy with both CDDP and Nano-Se, the percentages of damaged cells were reduced to 38.35% (Gr. VI) and 32.37% (Gr. VII).

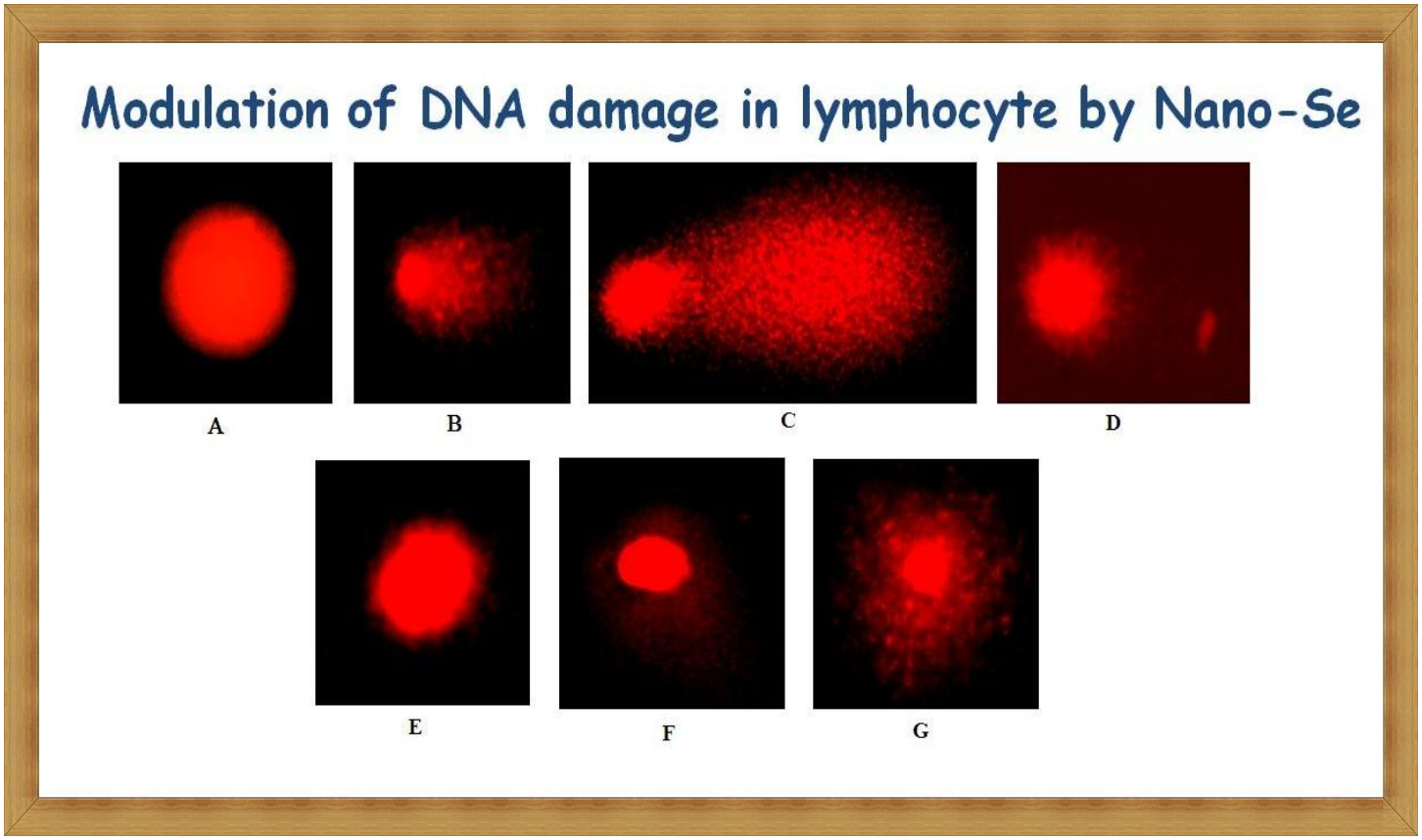

Figure 12 (A - G): Microphotograph of comet of lymphocyte, (A). vehicle treated (no DNA damage), (B and C) EAC control and CP treated group) showed highly migrated DNA with distinct scattered comet tail; Concomitant treatment (D) and pretreatment (E) with Nano-Se capable to reduce the migration of DNA and less diffused comet tail; Combined treatment with Nano-Se and CP (F and G) showed no or very less migrated DNA.

- **Average Tail Length of peripheral lymphocyte due to DNA Migration in each group**

The magnitude of average tail length was 7.39±0.91 µm in Gr. I. With inoculation of tumor, the magnitude of tail length increased significantly ($P < 0.05$) to 70.08±1.72 µm in Gr. II. The tail length further increased significantly to 94.15±3.40 µm after administration of CDDP in Gr. III **(Table 2)**. Oral administration of Nano-Se resulted in reduction of average tail length of cells both to 33.79±1.85 µm in Gr. IV and to 25.12±0.66 µm in Gr. V. Significant reduction in tail length of lymphocyte was also observed in Gr. VI (58.21±1.57 µm) and in Gr. VII (42.31±2.11 µm), where CDDP and Nano-Se were given together.

Groups	Peripheral Lymphocyte	
	Damaged cells showing comet (%)	Average tail length (µm)
I	8.92 ± 0.70	7.39 ± 0.91
II	$48.75 \pm 3.68^{\alpha}$	$70.08 \pm 1.72^{\alpha}$
III	$85.33 \pm 4.12^{\alpha\mu}$	$94.15 \pm 3.40^{\alpha\mu}$
IV	$26.45 \pm 1.54^{\alpha\mu\gamma}$	$33.79 \pm 1.85^{\alpha\mu\gamma}$
V	$20.39 \pm 2.06^{\alpha\mu\gamma\theta}$	$25.12 \pm 0.66^{\alpha\mu\gamma\theta}$
VI	$38.35 \pm 1.31^{\alpha\mu\gamma\theta\beta}$	$58.21 \pm 1.57^{\alpha\mu\gamma\theta\beta}$
VII	$32.37 \pm 2.48^{\alpha\mu\gamma\theta\beta\psi}$	$42.31 \pm 2.11^{\alpha\mu\gamma\theta\beta\psi}$

Table 2: Data were represented as Mean ± SD *(n=6)*. α - significant (*P < 0.05*) as compared with Gr. I; µ - significant (*P < 0.05*) as compared with Gr. II; γ - significant (*P < 0.05*) as compared with Gr. III; θ - significant (*P < 0.05*) as compared with Gr. IV; β - significant (*P < 0.05*) as compared with Gr. V; ψ - significant (*P < 0.05*) as compared with Gr. VI

- **Effect of Nano-Se with CDDP on tumor growth, MST and % ILS**

Enhancement of therapeutic efficacy of CDDP by Nano-Se was examined by evaluating the parameters like tumor volume, packed cell volume, viable tumor cell count, MST, % ILS in tumor inoculated mice **(Table 3)**. The mean (±SD) tumor volume and PCV of EAC control group (Gr. II) after 10 days of tumor inoculation were found to be 4.95 ± 0.19 ml and 2.5 ± 0.11 ml respectively. After the treatment with CDDP (Gr. III), Nano-Se (Gr. IV & Gr. V) and after a combined treatment with both the CDDP and Nano-Se (Gr. VI & Gr. VII), tumor volume was estimated to be 2.05 ± 0.19 ml, 3.85 ± 0.25 ml & 2.95 ± 19 ml, 1.7 ± 0.11 ml & 1.05 ± 0.19 ml respectively and PCV was estimated to be 1.25 ± 0.1 ml, 2.1 ± 0.2 ml & 1.6 ± 0.16 ml, 0.95 ± 0.19 ml & 0.6 ± 0.23 ml respectively. The result clearly showed that combined treatment with CDDP and Nano-Se was most effective in reducing tumor volume and PCV, compared to other treatment groups. The mean (±SD) value of tumor cell count was 27.7 ± 0.65 (in million) in EAC control group (Gr. II). After the administration of CDDP (Gr. III), Nano-Se (Gr. IV & Gr. V) and a combined application of both CDDP and Nano-Se (Gr. VI & Gr. VII), the mean (± SD) tumor cell count (in million) was 11.4 ± 0.99, 21.3 ± 1.15 & 18.0 ± 2.05, 6.21 ± 0.45 & 4.73 ± 0.64 respectively, the maximum reduction in tumor cell count was observed in the CDDP plus Nano-Se combined treatment groups. MST of the animals in the EAC control group was 21.5 ± 2.49 days. The survival time significantly ($P < 0.05$) increased to 46.06 ± 3.52 days in case of CDDP only treated group (Gr. III), 34.81 ± 3.82 days & 37.81 ± 3.41 days in case of Nano-Se only treated groups (Gr. IV & Gr. V). The survivability further significantly ($P < 0.01$) increased to 57.8 ± 2.26 days & 70.6 ± 3.3 days for the animals receiving combine treatment of CDDP & Nano-Se (Gr. VI & Gr. VII). The increase in life span of tumor bearing mice treated with only CDDP and only Nano-Se was 86.32% (Gr. III) and 54.18% (Gr. IV) & 64.78% (Gr. V). Combined treatment with CDDP and Nano-Se increased the life span by 168.33% (Gr. VI) & 228.37% (Gr. VII).

Groups	Tumor volume (ml)	Packed cell volume (ml)	Tumor cell count ($\times 10^6$)	Mean survivability (days)	Increasing life span (%)
II	4.95 ± 0.19	2.5 ± 0.11	27.7 ± 0.65	21.5 ± 2.49	–
III	$2.05 \pm 0.19^{\mu}$	1.25 ± 0.1	$11.4 \pm 0.99^{\mu}$	$46.06 \pm 3.52^{\mu}$	86.32
IV	$3.85 \pm 0.25^{\mu\gamma}$	$2.1 \pm 0.2^{\mu\gamma}$	$21.3 \pm 1.15^{\mu\gamma}$	$34.81 \pm 3.82^{\mu\gamma}$	54.18
V	$2.95 \pm 0.19^{\mu\gamma\theta}$	$1.6 \pm 0.16^{\mu\gamma\theta}$	$18.0 \pm 2.05^{\mu\gamma\theta}$	$37.81 \pm 3.41^{\mu\gamma}$	64.78
VI	$1.7 \pm 0.11^{\mu\gamma\theta\beta}$	$0.95 \pm 0.19^{\mu\theta\beta}$	$6.21 \pm 0.45^{\mu\gamma\theta\beta}$	$57.8 \pm 2.26^{\mu\gamma\theta\beta}$	168.83
VII	$1.05 \pm 0.19^{\mu\gamma\theta\beta\psi}$	$0.6 \pm 0.23^{\mu\gamma\theta\beta\psi}$	$4.73 \pm 0.64^{\mu\gamma\theta\beta}$	$70.6 \pm 3.3^{\mu\gamma\theta\beta\psi}$	228.37

Table 3: Data were represented as Mean ± SD *(n=6)*. μ - significant (*P < 0.05*) as compared with Gr. II; γ- significant (*P < 0.05*) as compared with Gr. III; θ - significant (*P < 0.05*) as compared with Gr. IV; β- significant (*P < 0.05*) as compared with Gr. V; ψ - significant (*P < 0.05*) as compared with Gr. VI.

- **Evaluation of apoptotic index of EAC cells by TUNEL assay**

To confirm the nature of cell death, TUNEL assay was performed in which as result of apoptosis FITC-conjugated dUTP was incorporated into the DNA strand breaks in the presence of the enzyme terminal deoxynucleotidyl transferase. Apoptotic index (AI) from this assay was measured **(Fig. 14)**.

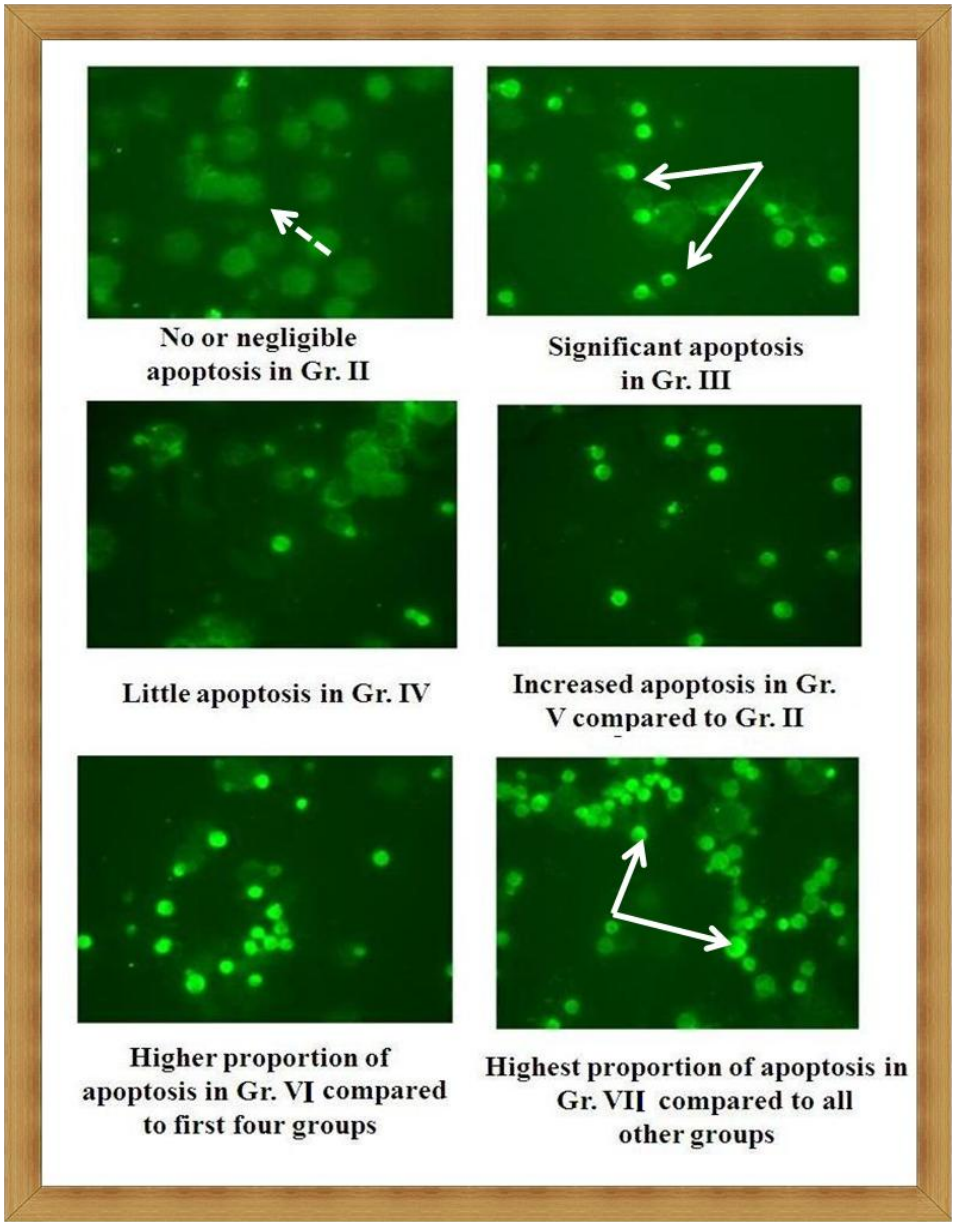

Figure 14: Photomicrographs of TUNEL assay performed in tumor cells. Apoptotic cells (TUNEL label cells) are indicated by white arrows whereas non-apoptotic cells are indicated by white broken arrows.

AI in the EAC control group was estimated to be 7.91% (Gr. II), which was increased markedly after treatment with CDDP (Gr. III) to 45.95% **(Fig. 15)**. The Nano-Se alone increased the AI value to 18.02% in concomitant treatment schedule (Gr. IV) and to 29.65% in pretreatment schedule (Gr. V). The most effective enhancement in the value of AI was observed in Gr. VI in Gr. VII, where CDDP and Nano-Se were given in a combination therapy and the values were 57.05% in Gr. VI and 69.47% in Gr. VII.

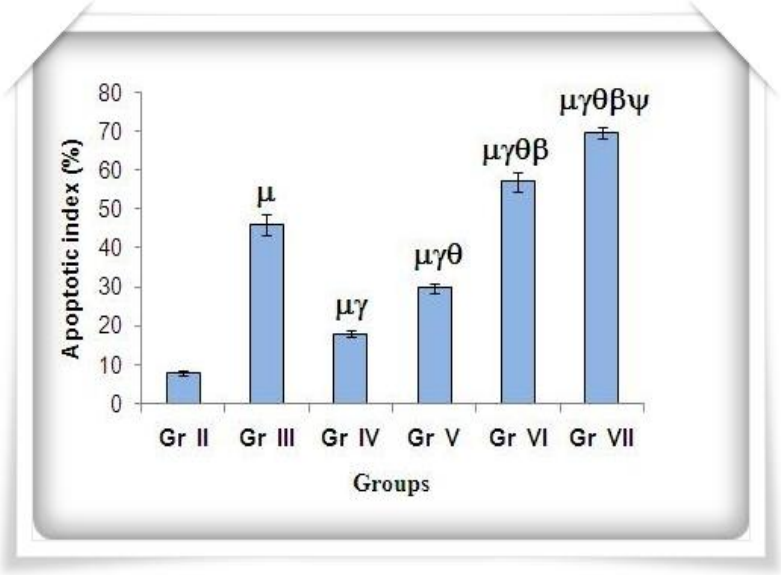

Figure 15: Data were represented as Mean ± SD *(n=6)*. μ - significant (*P < 0.05*) as compared with Gr. II; γ- significant (*P < 0.05*) as compared with Gr. III; θ - significant (*P < 0.05*) as compared with Gr. IV; β- significant (*P < 0.05*) as compared with Gr. V; ψ - significant (*P < 0.05*) as compared with Gr. VI.

- **Histopathological examination**

Kidney histomicrograph of vehicle treated mice showed normal structural design. The renal corpuscles were formed of lobulated glomeruli surrounded by Bowman's spaces. The proximal convoluted tubules appeared to be lined by a single layer of cuboidal epithelium enclosing a narrow lumen. The distal convoluted tubules were lined by cubical cells surrounding wider lumen **(Fig. 16-17)**. After tumor inoculation, pathological lesions like large areas of interstitial hemorrhage and glomerular degeneration were seen. In addition to interstitial hemorrhage and glomerular degeneration, CDDP administration caused loss of brush border, vacuolization and acute tubular necrosis. Nano-Se successfully attenuated both the tumor mediated and CDDP induced histological alterations in kidney when administered alone or in combination with CDDP.

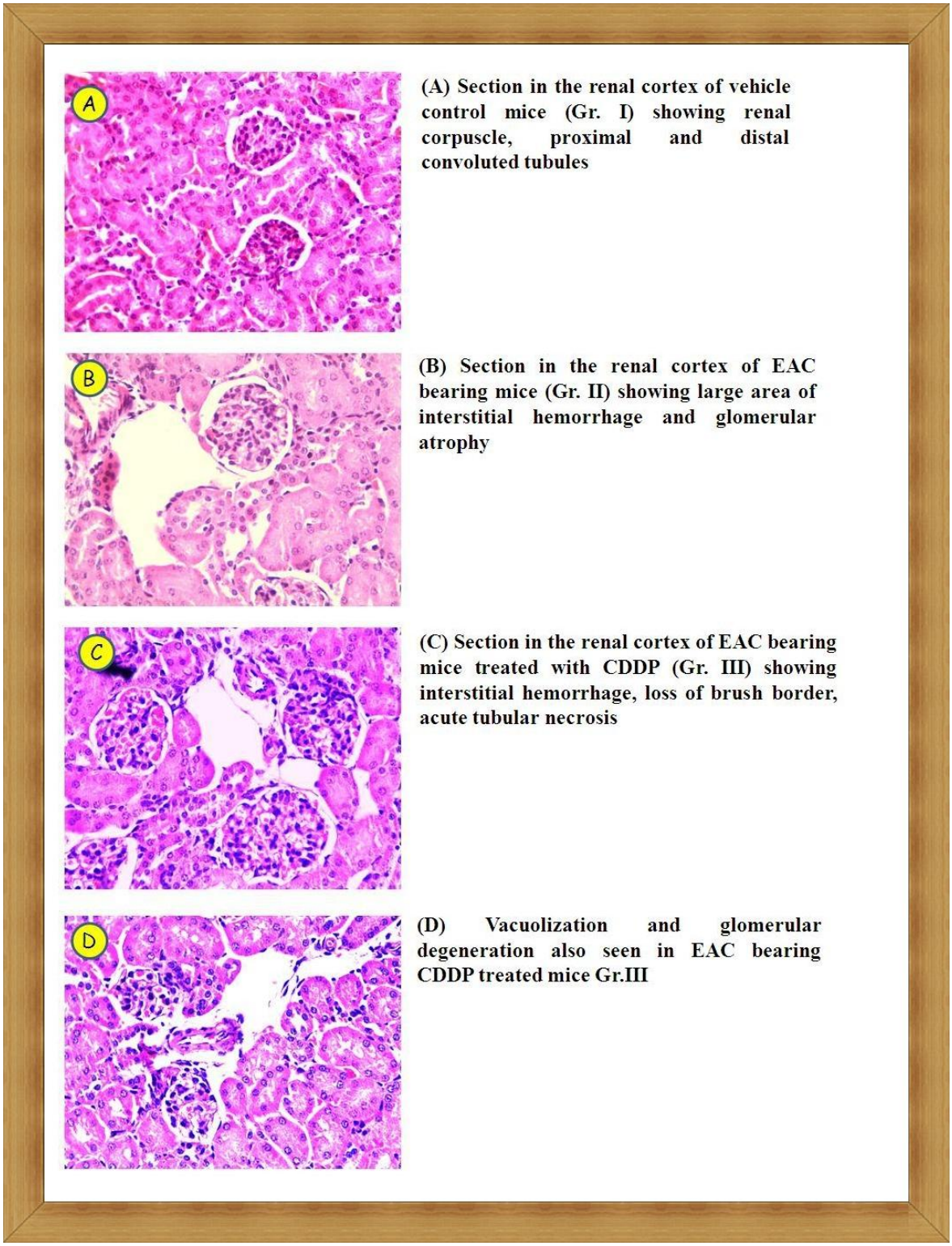

Figure 16 (A- D): Photograph of kidney section of mice stained with hematoxylin and eosin, ×200

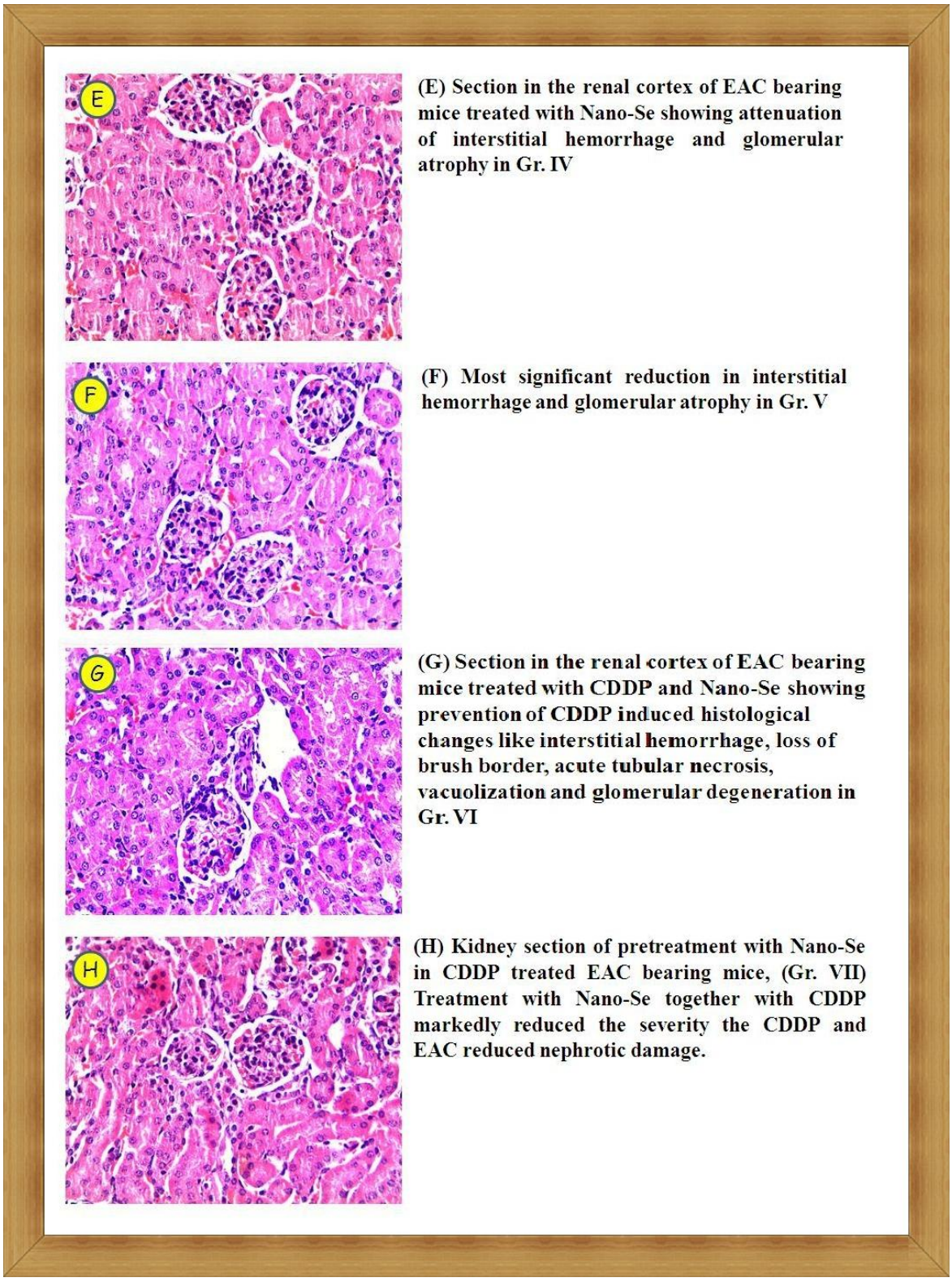

Figure 17 (E- H): Photograph of kidney section of mice stained with hematoxylin and eosin, ×200

Discussion

Nephrotoxicity arises when renal tissue fails to properly detoxify and excrete wastes due to the destruction of renal function by toxicants **(Ansari, 2017)**. Approximately 20% of nephrotoxicity cases are caused by drugs, although therapy for the elderly has increased the incidence of nephrotoxicity to 66% **(Kim et al., 2012)**. Oxidative stress has been implicated in the etiology of several toxic effects causing by many anticancer drugs. Cisplatin is a widely used broad-spectrum antineoplastic drug for the treatment of several malignancies **(Miller et al., 2010)**. Selective accumulation of cisplatin in the renal cortex may cause nephrotoxicity; therefore, its use has been constrained **(Mohamad et al., 2015)**. Thus strategies for cancer treatment using combined therapies or combined agents with distinct molecular mechanisms are considered to be more promising for higher efficacy and /or lower toxicity, thereby resulting in superior survival rates.

Cancer treatment by chemotherapeutic agents depends largely on ROS generation to destroy malignant cells by inducing apoptosis. However, disproportionate generation of ROS poses a serious problem to bodily homeostasis and causes oxidative tissue damage. One of the characteristics of tumor growth and invasion is the increased flux of oxy-radicals and loss of cellular redox homeostasis. Cancer cells can generate large amounts of hydrogen peroxide, which may contribute to their ability to mutate, damage normal tissues and invade other tissues. This suggests that there is a direct correlation between changes in the rate of cancer cell proliferation and changes in the antioxidant machinery. Administration of CDDP cause further reduction in the activity of tissue antioxidant enzymes and GSH level through the generation of ROS **(Bhattacharyya et al., 2014)**. CDDP induces mitochondrial dysfunctions, particularly inhibition of the electron transfer system, resulting in the enhanced production of superoxide anions (O_2^-), hydrogen peroxide (H_2O_2) and hydroxyl radicals (•OH) **(Bolisetty et al., 2014)**. MDA, the end product of lipid peroxidations was reported to be higher in carcinomatous tissue than that in the non diseased organs. The level of MDA reflects the extent of membrane lipid peroxidation and hence cell membrane damage and correlated with advanced clinical stages and the impairment is related to tumor progression. Moreover, it has been claimed that MDA acts as a tumor promoter and co-carcinogenic agent because of its high cytotoxicity and inhibitory action on protective enzymes. Low levels of MDA indicate

inhibition of lipid peroxidation. The biochemical determination of MDA serves to indicate lipid peroxide formation **(Eissa et al., 2014)**. In the present study, the renal concentrations of ROS and malondialdehyde (MDA), the end product of LPO was found to increase after tumor inoculation. CDDP treatment at 5 mg/kg b.w. resulted in further elevation in the level of ROS and MDA in kidney. The levels of these oxidative stress indices in renal tissues were down regulated after administration of Nano-Se. This finding suggested that Nano-Se by direct scavenged ROS and reduced the free radical level in renal tissue of the experimental mice. This effect of the Nano-Se was culminated in the suppression of oxidative stress and subsequent reduction in the oxidative damages to the cellular membrane as well as various important biomolecules.

Glutathione is one of the essential components for maintaining cell integrity because of its reducing properties and participation in the cell metabolism **(Nita et al., 2016)**. The thiol portion is very reactive with several chemical compounds, mainly with alkylating agents such as cisplatin **(Zanotto et al., 2016).** The depletion in renal GSH has been observed in rats in response to oxidative stress by CDDP treatment **(Soliman et al., 2016)** and this depleted renal GSH level can markedly increase the toxicity of CDDP **(Cheng et al., 2018)**. In the current study, renal GSH content was found to decrease in CDDP treated tumor bearing mice. Nano-Se successfully restored the CDDP induced depleted level of renal GSH. The observed depletion of GSH level in CDDP treated mice may be due to the enhanced LPO formation by CDDP, and the excessive LPO caused increased GSH utilization **(Longchar, 2016)**. Restoration of GSH level by Nano-Se alone and also when used along with CDDP suggests its protective role against oxidative damage of membrane lipid which in turn facilitated the enhancement of GSH content. GST represents an integral part of the detoxification system and protects cells against oxidative and chemical-induced toxicity and stress by catalyzing the S-conjugation between the thiol group of GSH and the electrophilic moiety of toxic substrates including cisplatin **(Allocati et al., 2018)**. Cisplatin-GSH complexes have been proposed to be ejected from the cells in an ATP-dependent process by the glutathione S-conjugate export pump **(Khynriam, 2003)**. This activity is useful in the detoxification of endogenous compounds such as peroxidised lipids, as well as the metabolism of xenobiotics **(Cederbaum, 2015)**. Several reports suggest that increased ROS generation after CDDP

treatment reduced the GSH level and GST activity in several organs including kiney **(Ghosh et al., 2014)**. The renal GST activity was decreased significantly by EAC inoculation which was further diminished by CDDP treatment. Treatment with Nano-Se invariably increased the GST activity and reduced the CDDP mediated oxidative stress in liver cells.

The enzyme SOD catalyzes dismutation of the O_2^- into H_2O_2, which is then detoxified to H_2O by CAT **(Sofo et al., 2015)**. CDDP has been found to induce loss of copper and zinc in the kidneys **(Ansari, 2017)**. Tumor growth has been found to cause inhibition of SOD and CAT activities **(Sznarkowska et al., 2017)**. It has also been reported that after administration of CDDP the SOD activity is reduced probably due to the loss of copper and zinc which are essential for the enzyme activity. This decreased SOD activity is insufficient to scavenge the $O_2^{\cdot-}$ produced during the chemotherapy **(Ghosh et al., 2015)** and ultimately results into the initiation and propagation of LPO **(Ajith et al., 2007)**. In the present study depletion in the activity of SOD and CAT was found with the tumor growth and treatment with CDDP caused an additional reduction in their activity, depicting markedly lower renal antioxidant status. Administration of Nano-Se alone and also when used along with CDDP restored their activity. This result reflects that NanoSe protects against CDDP induced nephrotoxicity by preventing the induction of oxidative stress and enhancing the renal antioxidant defenses involving SOD, CAT and GSH-dependant enzymes.

GP*x* are selenoenzymes involved in antioxidant defense and redox regulation and modulation. GP*x* provide protection against oxidative damage and aid in the maintenance of membrane integrity by using GSH as a cofactor to catalyze reduction of hydrogen peroxide, forming oxidized glutathione (GS-SG) in the process **(Raymond et al., 2014)**. The decrease of GP*x* activity induced by CDDP may be attributable to a direct inhibitory oxidative effect on the enzyme. The inhibition of GP*x* by CDDP may result in the accumulation of H_2O_2 with subsequent oxidation of the lipids. In fact, the GSH redox cycle is a major source of protection against low levels of oxidant stress, whereas CAT becomes more significant in protecting against severe oxidant stress **(Kurutas et al., 2016)**. In the present study, depletion in the activity of GP*x* was found with the tumor growth and treatment with CDDP caused an additional reduction in their activity,

depicting markedly lower renal antioxidant status. Administration of Nano-Se alone and in combination with CDDP restored their activity. This result reflects that the Nano-Se protects against CDDP induced renal injury by preventing the induction of oxidative stress and enhancing the performance of renal antioxidant system.

BUN and creatinine are two renal function markers and their levels in serum are elevated when the kidneys are damaged and fail to function properly. Several studies have shown that CDDP administration caused an increase in serum BUN and creatinine levels in rats due to glomerular and tubular damage **(Bami et al., 2017)** which clearly indicated the intrinsic acute renal failure. The current study showed obvious renal dysfunction with increased serum BUN and creatinine levels in cisplatin administered toxicity group. The lowered serum BUN and creatinine levels observed after administration of Nano-Se signifying its protective role against CDDP induced nephrotoxicity.

The detection of chromosomal aberration (CA) and DNA damage are the indications of genotoxicity **(Akyıl et al., 2015)**. CDDP has been demonstrated to have the potential for initiating genetic modifications in non-tumor cells in humans and animals, **Aly et al. (2003)** reported that, the genotoxicity of CDDP is due to its ability to bind with DNA, block and prolong the cell division in the G2 phase of the cell cycle. The blockage of cells in the G2 phase is related to the inhibition of chromatin condensation. It was shown that CDDP can cause a dose and time dependent increase in the number of cells with DNA damage **(Chen et al., 2016)**. In the present investigation CDDP administration caused significant increments in the proportion of CA in bone marrow cells and in the percentage of cells with damaged DNA in lymphocyte. Oral application of Nano-Se provided significant protection against CDDP induced genotoxicity as indicated by considerable reduction in the frequency of CA in bone marrow and the degree of DNA damage in lymphocyte. This anti-clastogenic effect of Nano-Se might be due to its antioxidant and chemoprotective activity.

In the histological study, it was found that CDDP administration caused various types of alterations in the histological architecture of the kidney tissue. Due to its low molecular weight, CDDP permeates the glomerular basal membrane easily and accumulates in the proximal tubular inner medulla and outer cortices **(Akca et al., 2018)**. The pathophysiological effect of CDDP on the kidneys is exerted in the form of apoptosis and

necrosis in proximal tubule cells via oxidative stress, inflammation and vasoconstriction of the renal vascular structure. Tubular cell death was identified as the main underlying histopathological characteristic of nephrotoxicity in one experimental study **(Oh et al., 2014)**. Histological study of kidney tissue from different groups of mice finally established the fact that Nano-Se provided an effective shield against the tumor induced and CDDP induced histological alterations like hemorrhage, glomerular degeneration, and loss of brush border, vacuolization, and tubular necrosis.

Anchorage independent growth and increased cell migration are two major hallmarks of cancer **(Pickup et al., 2014)**. Ascitic fluid is the direct nutritional source of tumor growth; it meets the nutritional requirements of tumor cell **(Kumar et al., 2011)**. Treatment with CDDP alone or in combination with Nano-Se inhibited the tumor volume, PCV, viable tumor cell count. This result confirms that Nano-Se does not interfere the therapeutic efficacy of CDDP rather protects the host from the obvious cellular damage of chemotherapy. Simultaneously, the life span of tumor bearing mice was increased by CDDP treatment which was further elongated by the adjuvant treatment with Nano-Se.

Apoptosis is a process of gene mediated programmed cell death essential for the elimination of unwanted cells in various biological systems and is the key mechanism of chemotherapeutic agents **(Baig et al., 2016)**. Apoptotic cell death is generally characterized by a morphologically homogeneous entity **(Inoue et al., 2014)**. The chief morphological feature of apoptosis is shrinkage of nuclei, nuclear chromatin condensation, cytoplasmic shrinkage, dilated endoplasmic reticulum and membrane blebbing **(Hotchkiss et al., 2009)**. In this study, the TUNEL assay unambiguously showed that Nano-Se alone and also in combination with CDDP, caused apoptosis of the EAC cells which was reflected in the reduced tumor volume and decreased viable tumor cell count and subsequent prolongation of life span. Prolongation of life span of animals and enhancing the quality of health are a reliable standard for evaluating the outcome of chemotherapy. So an agent which can selectively modulate the ability of antineoplastic drugs to induce apoptosis may enhance treatment efficacy, and prevent tissue damaging inflammatory response. Apart from this, it can be seen that Nano-Se enhances the ROS

generation in cancerous cells. Thus it can also be affirmed that the rise in apoptosis index may also be due to the increase of ROS.

This is the first report which shows that supplementation with Nano-Se resulted in protection of chemotherapy induced nephrotoxicity. In conclusion, the results of the present study revealed that oxidative stress play an important role in pathogenesis of CDDP nephrotoxicity. Based on all the information mentioned regarding the role of Nano-Se it is clear that it has less toxicity and has more bioavailability than the other forms of Se, act as an effective chemoprotector and tumor growth inhibitor by inhibiting the generation of ROS and onset of LPO, up regulating the cellular antioxidants in kidney, decreasing the DNA damage and chromosomal aberrations and prevented CDDP induced oxidative stress mediated nephrotoxicity and genotoxicity. Furthermore, by enhancing apoptosis of tumor cells Nano-Se boosted the cytotoxic efficacy of CDDP towards the tumor cells. These results indicate that Nano-Se exhibit chemoprotective effect as well as chemosensitizing effect on CDDP activity and it may find use as an adjunct in the cancer chemotherapy in which CDDP is used as first line of treatment.

Conclusion and Future perspectives

The trace element selenium (Se) is important for health of humans and animals. For example, selenium compounds exhibit potent chemopreventive activities against cancer and selenium supplementation can reduce the cancer mortality and incidence, especially for several major cancers, including prostate, lung, colon and liver cancers. Some molecular Se compounds, such as selenomethionine, sodium selenite, methylselenocysteine etc, have more effective anticancer activity at high dosage. However, high doses of selenite give rise to great concerns about its toxicity. These facts motivated us to develop a non-toxic form of nanoparticle base selenium (Nano-Se) as an adjuvant along with standard chemotherapeutic drugs in order to alleviate chemotherapy induced toxicity and to augment chemotherapeutic outcomes.

At the end, the concluding remarks of the entire study are as follows:

1. The synthesized nanoparticle of selenium (Nano-Se) at the dose of 2 mg Se/kg b.w is non-toxic and is less toxic than inorganic and organic selenium compounds, at the same dose.
2. Nano-Se could provide satisfactory protection towards host organs through mitigation of oxidative and nitrosative stress and enhancement of the activities of antioxidant and detoxifying enzyme.
3. Nano-Se could also inhibit chemotherapeutic drugs-induced cellular toxicities and myelosuppression and to reduce the risk for abnormal reproductive outcomes in cancer patients and medical personnel exposed to chemotherapy.
4. In tumor bearing mice, Nano-Se showed moderate cytotoxic efficacy towards the tumor cells at their non-toxic dose to the host organ and tissues.
5. In combination with chemotherapeutic drugs, Nano-Se enhanced the survivability of tumor bearing host by sensitizing tumor cells towards chemotherapeutic drug induced apoptosis.
6. Inhibition of angiogenesis was another mechanism by which Nano-Se exhibit their selective antitumor modulatory efficacy.

From this study, it is clear that Nano-Se act differentially in normal cells and cancer cells. From the results it has been observed that Nano-Se exert its chemoprotection by reducing CP and cisplatin derived oxidative stress by upregulating the activity of

antioxidant enzymes, GSH and down regulating lipid peroxidation level and also normalizing the hematological parameters and also by inhibiting clastogenic damage to host genome. In contrast, Nano-Se act as prooxidant in cancer cells by elevating reactive oxygen species, inducing DNA damage. Nano-Se has been found to induce apoptosis of EAC cell during tumor growth and increased the life span of the animals. The tumor growth response indicated that Nano-Se does not interfere with the antitumor efficacy of CP or cisplatin on the other hand administration of Nano-Se in CP or cisplatin treated animals had a synergistic action on the tumor growth.

Future work still remains to be done to extend the Chemoprotective and chemo potentiating efficacy of the Nano-Se we reported here. The following points are necessary to investigate:

1. The protective efficacy of Nano-Se against other standard chemotherapeutic drugs such as paclitaxel, doxorubicin, gemcitabine are required to be explored.
2. The experimental model discussed in this study required to be extended to other animal tumor models including tumor xenograft models.
3. The exact mechanism behind the chemoprotective and chemosensitizing properties of Nano-Se needs to be explored.
4. Another interesting future direction of research pharmacokinetic profile of Nano-Se are required to be explored.

In this study, adjuvant therapy with Nano-Se leads to minimization of toxic effects as well as potentiation of therapeutic outcome. Hence, this thesis established selenium based Nano-Se as a new class of ‘chemoprotective’ and ‘chemoenhancement’ agent. Scientific exploration must continue to elucidate the mechanism of action of this Nano-Se in a varied assortment of observed phenomenon; which in turn will define the contribution of this Nano-Se in the patients receiving chemotherapy.

Bibliography

Abdal Dayem A, Hossain MK, Lee SB, Kim K, Saha SK, Yang GM, Choi HY, Cho SG. (2017) The Role of Reactive Oxygen Species (ROS) in the Biological Activities of Metallic Nanoparticles. Int J Mol Sci. 18.

Abdel Moneim AE, Othman MS, Aref AM. (2014) Azadirachta indica attenuates cisplatin-induced nephrotoxicity and oxidative stress. Biomed Res Int. 2014: 647131.

Ahmad F, Nidadavolu P, Durgadoss L, Ravindranath V. (2014) Critical cysteines in Akt1 regulate its activity and proteasomal degradation: implications for neurodegenerative diseases. Free Radic Biol Med 74: 118-28.

Ahmadinejad F, Geir Møller S, Hashemzadeh-Chaleshtori M, Bidkhori G, Jami MS. (2017) Molecular Mechanisms behind Free Radical Scavengers Function against Oxidative Stress. Antioxidants (Basel). 6; (3).

Ahmed LA, Shehata NI, Abdelkader NF, Khattab MM. (2014) Tempol, a Superoxide Dismutase Mimetic Agent, Ameliorates Cisplatin-Induced Nephrotoxicity through Alleviation of Mitochondrial Dysfunction in Mice. PLoS One. 9: e108889.

Ajith TA, Usha S, Nivitha V. (2007) Ascorbic acid and alpha-tocopherol protect anticancer drug cisplatin induced nephrotoxicity in mice: a comparative study. Clin Chim Acta. 375: 82-6.

Akca G, Eren H, Tumkaya L, Mercantepe T, Horsanali MO, Deveci E, Dil E, Yilmaz A. The protective effect of astaxanthin against cisplatin-induced nephrotoxicity in rats. Biomed Pharmacother. 100: 575-582.

Akyıl D, Konuk M. (2015) Detection of genotoxicity and mutagenicity of chlorthiophos using micronucleus, chromosome aberration, sister chromatid exchange, and Ames tests. Environ Toxicol. 30: 937-45.

Alehagen U, Aaseth J. (2014) Selenium and coenzyme Q10 interrelationship in cardiovascular diseases - A clinician's point of view. J Trace Elem Med Biol. doi: 10.1016/j.jtemb.2014.

Alexander J. (2007) Selenium. Novartis Found Symp. 282: 143-9.

Allan C, Lacourciere G, Stadtman T (1999) Responsiveness of selenoproteins to dietary selenium. Annu Rev Nutr 19:1–16.

Allen TM, Cullis PR. (2013) Liposomal drug delivery systems: from concept to clinical applications. Adv Drug Deliv Rev 65: 36–48.

Allocati N, Masulli M, Di Ilio C, Federici L. (2018) Glutathione transferases: substrates, inihibitors and pro-drugs in cancer and neurodegenerative diseases. Oncogenesis. 7: 8.

Al-Majed AA (2007) Carnitine deficiency provokes cisplatin-induced hepatotoxicity in rats. Basic Clin Pharmacol Toxicol 100: 145–150.

Al-Majed AA, Sayed-Ahmed MM, Al-Yahya AA, Aleisa, AM, Al-Rejaie SS, Al-Shabanah OA (2006) Propionyl-L-carnitine prevents the progression of cisplatin-induced cardiomyopathy in a carnitine-depleted rat model. Pharmacol Res 53: 278–286.

Aly HA, Lightfoot DA, El-Shemy HA. () Modulatory role of lipoic acid on lipopolysaccharide-induced oxidative stress in adult rat Sertoli cells in vitro. Chem Biol Interact. 182: 112-8.

American Cancer Society. Cancer Facts & Figures 2014. Atlanta: American Cancer Society; 2014.

Ames BN, Shigenaga MK, Hagen TM. (1993) Oxidants, antioxidants, and the degenerative diseases of aging. Proc Natl Acad Sci. 90: 7915–22.

Amudha G, Josephine A, Sudhahar V, Varalakshmi P. (2007) Protective effect of lipoic acid on oxidative and peroxidative damage in cyclosporine A-induced renal toxicity. Int Immunopharmacol. 7: 1442-9.

Ansari MA. (2017) Sinapic acid modulates Nrf2/HO-1 signaling pathway in cisplatin-induced nephrotoxicity in rats. Biomed Pharmacother. 93: 646-653.

Antunes LM G, Darin J DC. and Bianchi M. A. de. P. (1999) Anticlastogenic effect of vitamin C on cisplatin in vivo. Genet Mol Biol. 22: 415−417.

Apostolou S, Klein JO, Mitsuuchi Y, Shetler JN, Poulikakos PI, Jhanwar SC, Kruger WD, Testa JR. (2004) Growth inhibition and induction of apoptosis in mesothelioma cells by selenium and dependence on selenoprotein SEP15 genotype. Oncogene. 23: 5032–5040.

Aprioku JS. (2013) Pharmacology of free radicals and the impact of reactive oxygen species on the testis. J Reprod Infertil. 14: 158-72.

Arafa S A, AboEl-Ela M M, Kassem H S. and Kassem H S. (2008) Study of the genotoxic effect of cyclophosphamide on albino mice bone marrow polychromatic erythrocytes and the protective effect of captopril. Bull Alex Fac Med. 44: 821−828.

Arn´er ES, Holmgren A. (2000) Physiological functions of thioredoxin and thioredoxin reductase. Eur J Biochem. 267: 6102–9.

Arne´r ESJ, Zhong L, Holmgren A. (1999) Preparation and assay of mammalian thioredoxin and thioredoxin reductase. Methods Enzymol. 300: 226–239.

Arnon J, Meirow D, Lewis-Roness H, Ornoy A. (2001) Genetic and teratogenic effects of cancer treatments on gametes and embryos. Hum Reprod Update. 7: 394-403.

Arumugam N, Sivakumar V, Thanislass J, Devaraj H. (1997) Effects of acrolein on rat liver antioxidant defense system. Indian J Exp Biol. 35: 1373-4.

Attardi LD, & Donehower LA. (2005) Probing p53 biological functions through the use of genetically engineered mouse models. Mutat. Res. 576, 4–21.

Attia SM. (2010) The impact of quercetin on cisplatin-induced clastogenesis and apoptosis in murine marrow cells. Mutagenesis. 25: 281-8.

Attia SM. (2012) Influence of resveratrol on oxidative damage in genomic DNA and apoptosis induced by cisplatin. Mutat Res. 74: 22-31.

Attia SM. (2012) Influence of resveratrol on oxidative damage in genomic DNA and apoptosis induced by cisplatin. Mutat Res. 741: 22–31.

Baig S, Seevasant I, Mohamad J, Mukheem A, Huri HZ, Kamarul T1. (2016) Potential of apoptotic pathway-targeted cancer therapeutic research: Where do we stand? Cell Death Dis. 7: e2058.

Bami E, Ozakpınar OB, Ozdemir-Kumral ZN. (2017) Protective effect of ferulic acid on cisplatin induced nephrotoxicity in rats. Environ Toxicol Pharmacol. 54: 105-111.

Bancroft JD, Stevens A. (1990) Theory and practice of histological techniques, 3rd ed. Churchill-Livingstone, Edinburgh.

Banerjee D, Harfouche R, Sengupta S. (2011) Nanotechnologymediated targeting of tumor angiogenesis. Vasc Cell. 3: 3.

Banfi B et al. (2004) NOX3, a superoxide-generating NADPH oxidase of the inner ear. J Biol Chem. 279: 46065–72.

Barreto JA, O'Malley W, Kubeil M, Graham B, Stephan H, Spiccia L. (2011) Nanomaterials: applications in cancer imaging and therapy. Adv Mater. 23: H18–H40.

Barrington JW, Lindsay P, James D, Smith S, Roberts A. (1996) Selenium deficiency and miscarriage: a possible link? Br J Obstet Gynaecol. 103: 130-2.

Barrington JW, Taylor M, Smith S, Bowen-Simpkins P. (1997) Selenium and recurrent miscarriage. J Obstet Gynaecol. 17: 199-200.

Basavaraj KH. (2012) Nanotechnology in medicine and relevance to dermatology: present concepts. Indian J Dermatol. 57: 169-74.

Basu A, Bhattacharjee A, Roy SS et al (2014) Vanadium as a chemoprotectant: effect of vanadium(III)-L-cysteine complex against cyclophosphamide-induced hepatotoxicity and genotoxicity in Swiss albino mice. J Biol Inorg Chem 19:981-996.

Basu A, Bhattacharjee A, Samanta A, Bhattacharya S. (2015) Prevention of cyclophosphamide-induced hepatotoxicity and genotoxicity: Effect of an l-cysteine based oxovanadium(IV) complex on oxidative stress and DNA damage. Environ Toxicol Pharmacol. 40: 747-57.

Basu A, Ghosh P, Bhattacharjee A, Patra AR, Bhattacharya S. (2015) Prevention of myelosuppression and genotoxicity induced by cisplatin in murine bone marrow cells: effect of an organovanadium compound vanadium(III)-l-cysteine. Mutagenesis. 30: 509-17.

Basu A, Singha Roy S, Bhattacharjee A, Bhuniya A, Baral R, Biswas J, Bhattacharya S. (2016) Vanadium(III)-L-cysteine protects cisplatin-induced nephropathy through activation of Nrf2/HO-1 pathway. Free Radic Res. 50(1):39-55.

Beck MA, Esworty RS, Ho YS, Chu FF. (1998) Glutathione peroxidase protects mice from viral-induced myocarditis. FASEB J.12: 1143-9.

Beck MA, Shi Q, Morris VC, Levander OA. (1995) Rapid genomic evolution of a nonvirulent coxsackievirus B3 in selenium-deficient mice results in selection of identical virulent isolates. Nat Med. 1: 433-6.

Beck MA. (1997) Increased virulence of coxsackievirus B3 in mice due to vitamin E or selenium deficiency. J Nutr. 127: 966S-970S.

Beckett GJ, Arthur JR. (2005) Selenium and endocrine systems. J Endocrinol. 184: 455-65.

Behrend L, Henderson G, & Zwacka RM. (2003) Reactive oxygen species in oncogenic transformation. Biochem Soc Trans 31, 1441–1444.

Behrend L, Henderson G, Zwacka RM. (2003) Reactive oxygen species in oncogenic transformation, Biochem. Soc. Trans. 31: 1441–1444.

Benton D, Cook R. (1991) The impact of selenium supplementation on mood. Biol Psychiatry. 29: 1092-8.

Berzelius JJ. (1818) Letter from Mr Berzelius to Mr Berthollet on two new metals. Ann Phys (Paris) 7: 199–206.

Bhatia U, Danishefsky K, Traganos F, Darzynkiewicz Z. (1995) Induction of apoptosis and cell cycle-specific change in expression of p^{53} in normal lymphocytes and MOLT-4 leukemic cells by nitrogen mustard. Clin Cancer Res. 1: 873-80.

Bhattacharjee A, Basu A, Biswas J, Bhattacharya S (2015) Nano-Se attenuates cyclophosphamide-induced pulmonary injury through modulation of oxidative stress and DNA damage in Swiss albino mice. Mol Cell Biochem 405:243–256.

Bhattacharyya A, Chattopadhyay R, Mitra S, Crowe SE. (2014) Oxidative stress: an essential factor in the pathogenesis of gastrointestinal mucosal diseases. Physiol Rev. 94: 329-54.

Bhattacharyya A, Mandal D, Lahiry L, Bhattacharyya S, Chattopadhyay S, Ghosh UK et al. (2007) Black tea-induced amelioration of hepatic oxidative stress through antioxidative activity in EAC-bearing mice. J Environ Pathol Toxicol Oncol 26:245-54

Bhuyan KC, Bhuyan DK, Podos SM. (1981) Selenium-induced cataract: Biochemical mechanism. InSelenium in Biology and Medicine, Spallholz JE, Martin JL, Ganther HE (eds). AVI Publishing Co.: Westport, CT; 403–412.

Bickhardt K, Ganterm M, Sallmann P. (1999) Investigation of the manifestation of vitamin E and selenium deficiency in sheep and goats. Deut Tierarztl Woch. 106: 242–247.

Binks SP, Dobrota M (1990) Kinetics and mechanism of uptake of platinum-based pharmaceuticals by the rat small intestine. Biochem Pharmacol. 40: 1329-36.

Birringer M. Pilawa S, Flohe L. (2002) Trends in selenium biochemistry. Nat Prod Rep. 19: 693–718.

Biswas SJ, Pathak S and Khuda Bukhsh AR. (2004) Assessment of the genotoxic and cytotoxic potential of an antiepileptic drug Phenobarbital, in mice: a time course study. Mutat Res. 563: 1–11.

Bjo¨rnstedt M, Hamberg M, Kumar S, Xue J, Holmgren A. (1995) Human thioredoxin reductase directly reduces lipid hydroperoxides by NADPH and selenocystine strongly stimulates the reaction via catalytically generated selenols. J Biol Chem. 270: 11761–11764.

Blackwell S, Crawford J (1994) Filgrastim (r-metHuG-CSF) in the chemotherapy setting, in: G. Morstyn, T.M. Dexter, M. Foote (Eds.), Filgrastim (r-metHuGCSF) in Clinical Practice, Marcel Dekker, New York, pp. 103-106

Bland SK, Schmiedt CW, Clark ME, DeLay J, Bienzle D. (2017) Expression of Kidney Injury Molecule-1 in Healthy and Diseased Feline Kidney Tissue. Vet Pathol. 54: 490-510.

Bleys J, Navas-Acien A, Guallar E. (2007) Selenium and diabetes: more bad news for supplements. Ann Intern Med. 147: 271-2.

Block KI, Koch AC, Mead MN, Tothy PK, Newman RA, Gyllenhaal C (2007) Impact of antioxidant supplementation on chemotherapeutic efficacy: a systematic review of the evidence from randomized controlled trials. Cancer Treat Rev 33:407-18

Blokhina O, Virolainen E, Fagerstedt KV. (2003) Antioxidants, oxidative damage and oxygen deprivation stress: a review. Ann Bot. 9: 179-94.

Boddy AV, Furtun Y, Sardas S, Sardas O, Idle JR. (1992) Individual variation in the activation and inactivation of metabolic pathways of cyclophosphamide. J Natl Cancer Inst. 84: 1744-8.

Bolisetty S, Jaimes EA. (2013) Mitochondria and reactive oxygen species: physiology and pathophysiology. Int J Mol Sci. 14: 6306-44.

Boonstra J & Post JA (2004) Molecular events associated with reactive oxygen species and cell cycle progression in mammalian cells. Gene 337, 1–13.

Bose P, Latawiec D, Mondal PP, Mondal S. (2014) Overview of nano-drugs characteristics for clinical application: the journey from the entry to the exit point. J Nanopart Res. 16: 2527.

Boulikas T. (2007) Molecular mechanisms of cisplatin and its liposomally encapsulated form, Lipoplatin™. Lipoplatin™ as a chemotherapy and antiangiogenesis drug. Cancer Ther 5: 351-376.

Bourdon JC. (2007) p53 and its isoforms in cancer. Br. J. Cancer 97, 277–282.

Boyaci H, Maral H, Turan G, Başyiğit I, Dillioğlugil MO, Yildiz F, Tugay M, Pala A, Erçin C (2006) Effects of erdosteine on bleomycin-induced lung fibrosis in rats. Mol Cell Biochem 281:129-37.

Brock N, Pohl J. (1986) Prevention of urotoxic side effects by regional detoxification with increased selectivity of oxazaphosphorine cytostatics. IARC Sci Publ. 78: 269-79.

Brock N, Stekar J, Pohl J, Niemeyer U, Scheffler G. (1979) Acrolein, the causative factor of urotoxic side-effects of cyclophosphamide, ifosfamide, trofosfamide and sufosfamide. Arzneimittelforschung. 29: 659-61.

Brozmanova´ J, Duda´sˇ A, Henriques JA. (2001) Repair of oxidative DNA damage-an important factor reducing cancer risk. Minireview. Neoplasma. 48: 85–93.

Bruce WR, Meeker BE, Valeriote FA. (1966) Comparison of the sensitivity of normal hematopoietic and transplanted lymphoma colony-forming cells to chemotherapeutic agents administered *in vivo*. J Natl Cancer Inst. 37: 233-45.

Bruggemann SK, Kisro J, Wagner T. (1997) Ifosfamide cytotoxicity on human tumor and renal cells: role of chloroacetaldehyde in comparison to 4-hydroxyifosfamide. Cancer Res. 57: 2676-80.

Brydøy M, Fosså SD, Dahl O, Bjøro T. (2007) Gonadal dysfunction and fertility problems in cancer survivors. Acta Oncol. 46: 480-9.

Caderni G, De Filippo C, Luceri C, Salvadori M, Giannini A, Biggeri A, Remy S, Cheynier V, Dolara P (2000) Effects of black tea, green tea and wine extracts on intestinal carcinogenesis induced by azoxymethane in F344 rats. Carcinogenesis 21:1965-9

Callejo A, Sedó-Cabezón L, Juan ID, Llorens J. (2015) Cisplatin-Induced Ototoxicity: Effects, Mechanisms and Protection Strategies. Toxics. 3: 268-293.

Cao S, Durrani FA, Rustum YM. (2004) Selective modulation of the therapeutic eYcacy of anticancer drugs by selenium containing compounds against human tumor xenografts. Clin Cancer Res. 10: 2561–2569.

Carl Allinson MJ (1945) A specific enzymatic method for the determination of creatine and creatinine in blood. J Biol Chem 157:169–172.

Carr AC, McCall MR, Frei B. (2000) Oxidation of LDL by myeloperoxidase and reactive nitrogen species — reaction pathways and antioxidant protection. Arterioscl Thromb Vasc Biol. 20: 1716–1723.

Cederbaum AI. (2015) Molecular mechanisms of the microsomal mixed function oxidases and biological and pathological implications. Redox Biol. 4: 60-73.

Chan WC. (2006) Bionanotechnology progress and advances. Biol Blood Marrow Transplant. 12: 87 - 91.

Chang Y, He L, Li Z, Zeng L, Song Z, Li P, Chan L, You Y, Yu XF, Chu PK, Chen T. (2017) Designing Core-Shell Gold and Selenium Nanocomposites for Cancer Radiochemotherapy. ACS Nano. 11: 4848-4858.

Chaudiere J, Courtin O, Leclaire J. (1992) Glutathione oxidase activity of selenocystamine: a mechanistic study. Arch Biochem Biophys. 296: 328-36.

Chen CS, Lin JT, Goss KA, He YA, Halpert JR, Waxman DJ. (2004) Activation of the anticancer prodrugs cyclophosphamide and ifosfamide: identification of cytochrome P450 2B enzymes and site-specific mutants with improved enzyme kinetics. Mol Pharmacol. 65: 1278-85.

Chen S, Chen X, Xie G, He Y, Yan D, Zheng D, Li S, Fu X, Li Y, Pang X, Hu Z, Li H, Tan W, Li J. (2016) Cdc6 contributes to cisplatin-resistance by activation of ATR-Chk1 pathway in bladder cancer cells. Oncotarget. 7: 40362-40376.

Chen T, Wong YS, Zheng W, Bai Y, Huang L. (2012) Selenium nanoparticles fabricated in Undaria pinnatifida polysaccharide solutions induce mitochondria-mediated apoptosis in A375 human melanoma cells. Colloids Surf. B. 67: 26-31.

Chen T, Wong YS. (2008) Selenocystine induces caspase-independent apoptosis in MCF-7 human breast carcinoma cells with involvement of p53 phosphorylation and reactive oxygen species generation. Int J Biochem Cell Biol. 41: 666–676.

Cheng TC, Hsu YW, Lu FJ, Chen YY, Tsai NM, Chen WK, Tsai CF. (2018) Nephroprotective effect of electrolyzed reduced water against cisplatin-induced kidney toxicity and oxidative damage in mice. J Chin Med Assoc. 81: 119-126.

Cheng YY, Qian PC. (1990) The effect of selenium-fortified table salt in the prevention of Keshan disease on a population of 1.05 million. Biomed Environ Sci. 3: 422-8.

Chipman SD, Oldham FB, Pezzoni G, Singer JW. (2006) Biological and clinical characterization of paclitaxel poliglumex (PPX, CT-2103), a macromolecular polymer-drug conjugate. Int J Nanomed. 1: 375–383.

Clark LC, Combs GF Jr, Turnbull BW et al (1996) Effects of selenium supplementation for cancer prevention in patients with carcinoma of the skin. A randomized controlled trial. Nutritional Prevention of Cancer Study Group. JAMA 276:1957-63

Clark LC, Combs GF Jr, Turnbull BW et al. (1996) Effects of selenium supplementation for cancer prevention in patients with carcinoma of the skin. A randomized controlled trial. Nutritional Prevention of Cancer Study Group. JAMA. 276: 1957-63.

Clerkin JS, Naughton R, Quiney C, & Cotter TG. (2008) Mechanisms of ROS modulated cell survival during carcinogenesis. Cancer Lett. 266, 30–36.

Colvin M, Brundrett RB, Kan MN, Jardine I, Fenselau C. (1976) Alkylating properties of phosphoramide mustard. Cancer Res. 36: 1121-6.

Colvin OM. (1999) An overview of cyclophosphamide development and clinical applications. Curr Pharm Des. 5: 555-60.

Combs GF Jr. (2015) Biomarkers of selenium status. Nutrients. 7: 2209-36.

Combs Jr GF, Gray WP. (1998) Chemopreventive agents: selenium. Pharmacol Ther. 79: 179–192.

Commoner B, Townsend J, Pake GE. (1954) Free radicals in biological materials. Nature. 174: 689–691.

Conklin KA. (2004) Chemotherapy-associated oxidative stress: impact on chemotherapeutic effectiveness.Integr Cancer Ther. 3: 294–300.

Crack PJ, Taylor JM, Flentjar NJ, (2001) Increased infarct size and exacerbated apoptosis in the glutathione peroxidase-1 (Gpx- 1) knockout mouse brain in response to ischemia/reperfusion injury. J Neurochem. 78: 1389-99.

Crook TR, Souhami RL, McLean AE. (1986) Cytotoxicity, DNA crosslinking, and single strand breaks induced by activated cyclophosphamide and acrolein in human leukemia cells. Cancer Res. 46: 5029-34.

Cui Y, König J, Buchholz JK, Spring H, Leier I, Keppler D (1999) Drug resistance and ATP-dependent conjugate transport mediated by the apical multidrug resistance protein, MRP2, permanently expressed in human and canine cells. Mol Pharmacol. 55: 929-37.

D Felical C, Signorini C, Liocini S, *et .al.*, (2014) Biomarkers of Lipid Oxidative Damage in Rett Syndrome. Comprehensive Guide to Autism. pp 2617- 2632.

D'Armour FE, Blood FR, Belden DA (1965) The Manual for Laboratory Work in Mammalian Physiology, third ed., The University of Chicago Press, Chicago

Das JK, Sarkar S, Hossain SU, Bhattacharya S (2013) Diphenylmethyl selenocyanate attenuates malachite green induced oxidative injury through antioxidation and inhibition of DNA damage in mice. Indian J Med Res 137: 1163-1173

Das RK, Hossain SK. and Bhattacharya S. (2005) Diphenylmethyl selenocyanate inhibits DMBA-croton oil induced two-stage mouse skin carcinogenesis by inducing apoptosis and inhibiting cutaneous cell proliferation. Cancer Lett. 230: 90–101.

Dasari S, Tchounwou PB. (2014) Cisplatin in cancer therapy: molecular mechanisms of action. Eur J Pharmacol. 740: 364-78.

Davies KJA. (1994) Oxidative stress: the paradox of aerobic life. Biochem Soc Symp. 61: 1–31.

De Flora, Izzotti A, D'Agostini F, Balansky RM, Noonan D, Albini A. (2001) Multiple points of intervention in the prevention of cancer and other mutation related diseases. Mutat Res 480–481: 9–22.

De Flora, Ramel C. (1998) Mechanisms of inhibitors of mutagenesis and carcinogenesis. Classification and overview. Mutat Res 202: 285–306.

De Jong WH, Borm PJ. (2008) Drug delivery and nanoparticles:applications and hazards. Int J Nanomedicine. 3: 133-49.

de Jongh, FE, van Veen RN, Veltman SJ, de WR, van der, Burg ME, van den Bent MJ, Planting AS, Graveland WJ, Stoter G, Verweij J (2003) Weekly high-dose cisplatin is a feasible treatment option: analysis on prognostic factors for toxicity in 400 patients. Br J Cancer 88: 1199–1206.

DeLeve LD. (1996) Cellular target of cyclophosphamide toxicity in the murine liver: role of glutathione and site of metabolic activation. Hepatology. 24: 830-7.

Desoize B (2002) Cancer and metals and metal compounds: part I–carcinogenesis. Crit Rev Oncol Hematol. 42: 1–3.

DeVita VT, Chu E (2008) A History of Cancer Chemotherapy. Cancer Res. 68: 8643-53.

Dhanjal S, Cameotra SS (2010) Aerobic biogenesis of selenium nanospheres by Bacillus cereusisolated from coalmine soil. Microb Cell Fact 9: 52

Dhanjal S, Cameotra SS. (2010) Aerobic biogenesis of selenium nanospheres by Bacillus cereus isolated from coalmine soil. Microb. Cell. Fact. 9: 52.

Di Bucchianico S, Fabbrizi MR, Cirillo S (2014) Aneuploidogenic effects and DNA oxidation induced in vitro by differently sized gold nanoparticles. Int J Nanomedicine 9:2191–2204.

Di Meo S, Reed TT, Venditti P, Victor VM. (2016) Role of ROS and RNS Sources in Physiological and Pathological Conditions. Oxid Med Cell Longev.2016: 1245049.

Dimopoulos MA, Hamilos G, Zomas A, *et al.* (2004) Pulsed cyclophosphamide, thalidomide and dexamethasone: an oral regimen for previously treated patients with multiple myeloma. Hematol J. 5: 112-7.

Diplock AT. (1994) Antioxidants and disease prevention. Mol Aspects Med. 15: 293-376.

Dirven HA, Venekamp JC, van Ommen B, van Bladeren PJ. (1994) The interaction of glutathione with 4-hydroxycyclophosphamide and phosphoramide mustard, studied by 31P nuclear magnetic resonance spectroscopy. Chem Biol Interact. 93: 185-96.

Diskin CJ, Tomasso CL, Alper JC, Glaser ML, Fliegel SE. (1979) Long-term selenium exposure. Arch Intern Med. 139: 824-6.

Dong Y, Ganther HE, Stewart C, Ip C. (2002) Identification of molecular targets associated with selenium-induced growth inhibition in human breast cells using cDNA microarrays. Cancer Res. 62: 708–714.

Dong Y, Zhang H, Hawthorn L, Ganther HE, Ip C. (2003) Delineation of the molecular basis for selenium-induced growth arrest in human prostate cancer cells by oligonucleotide array. Cancer Res. 63: 52–59.

Dorr W. (2006) Effects of selenium on radiation responses of tumor cells and tissue. Strahlenther Onkol. 182: 693–695.

dos Santos NA, Martins NM, Curti C, Pires Bianchi ML, dos Santos AC (2007) Dimethylthiourea protects against mitochondrial oxidative damage induced by cisplatin in liver of rats. Chem Biol Interact. 170: 177–186.

Doyle C, Kushi LH, Byers T, Courneya KS, Demark-Wahnefried W, Grant B, McTiernan A, Rock CL, Thompson C, Gansler T. & Andrews KS. (2006) Nutrition and Physical Activity During and After Cancer Treatment: An American Cancer Society Guide for Informed Choices, CA Cancer J Clin 56: 323-353.

Drake EN. (2006) Cancer chemoprevention: selenium as a prooxidant, not an antioxidant. Med Hypotheses. 67: 318–322.

Eissaa LA, Habibb SA, ohammed, Latif MM. (2014) Inhibitory effect of the partially purified protein from Raphnus sativus roots and low-molecular-weight heparin on Ehrlich ascites carcinoma bearing mice. Egyp Jour of Bas and Appl Sci. 1: 88-96.

El-Bayoumy K, Sinha R (2004) Mechanisms of mammary cancer chemoprevention by organoselenium compounds. Mutat Res 551: 181–197.

El-Bayoumy K, Sinha R (2004) Mechanisms of mammary cancer chemoprevention by organoselenium compounds. Mutat Res 551:181–197

El-Bayoumy K, Sinha R. (2004) Mechanisms of mammary cancer chemoprevention by organoselenium compounds. Mutat Res 551: 181–197.

El-Bayoumy K. (2001) The protective role of selenium on genetic damage and on cancer. Mutat Res 475, 123–139.

El-Demerdash FM. (2004) Antioxidant effect of vitamin E and selenium on lipid peroxidation, enzyme activities and biochemical parameters in rats exposed to aluminium. J Trace Elem Med Biol. 18: 113–121.

Endoh D, Okui T, Ozawa S. (2002) Protective effect of a lignan-containing flaxseed extract against CCl_4-induced hepatic injury. J Vet Med Sci. 64: 761–765.

Escalon MP, Liu NS, Yang Y, *et al.* (2005) Prognostic factors and treatment of patients with T-cell non-Hodgkin lymphoma. Cancer. 103: 2091-8.

Faghihi T, Radfar M, Barmal M, Amini P, Qorbani M, Abdollahi M, Larijani B. (2013) A randomized, placebo-controlled trial of selenium supplementation in patients with type 2 diabetes: effects on glucose homeostasis, oxidative stress, and lipid profile. Am. J. Ther. 29.

Fairweather-Tait SJ, Bao Y, Broadley MR, Collings R, Ford D, Hesketh JE, Hurst R. (2011) Selenium in human health and disease. Antioxid Redox Signal. 14: 1337-83.

Fairweather-Tait SJ, Dainty J. (2002) Use of stable isotopes to assess the bioavailability of trace elements: a review. Food Addit Contam.19: 939-47.

Fang LQ, Goeijenbier M, Zuo SQ, Wang LP, Liang S. (2015) The association between hantavirus infection and selenium deficiency in mainland China. Viruses.20; 7: 333-51.

Feoli AM, Macagnan FE, Piovesan CH, Bodanese LC, Siqueira IR. (2014) Xanthine oxidase activity is associated with risk factors for cardiovascular disease and inflammatory and oxidative status markers in metabolic syndrome: effects of a single exercise session. Oxid Med Cell Longev. 2014-ID 587083.

Ferguson LR, Pearson AE (1996) The clinical use of mutagenic anticancer drugs. Mutat Res 355:1–12

Ferguson LR, Philpott M, Karunasinghe N. (2004) Dietary cancer and prevention using antimutagens. Toxicol. 198: 147–159.

Fernandes AP, Gandin V (2015) Selenium compounds as therapeutic agents in cancer. Biochim Biophys Acta 1850:1642-1660

Fernandes AP, Gandin V. (2014) Selenium compounds as therapeutic agents in cancer. Biochim Biophys Acta. 1850: 1642-60.

Ferreira RS, Dos Santos NAG, Martins NM, Fernandes LS, Dos Santos AC. (2018) Caffeic Acid Phenethyl Ester (CAPE) Protects PC12 Cells from Cisplatin-Induced Neurotoxicity by Activating the NGF-Signaling Pathway. Neurotox Res. 34: 32-46.

Fico ME, Poirier KA, Watrach AM, Watrach MA, Milner JA. (1986) Differential effects of selenium on normal and neoplastic canine mammary cells. Cancer Res. 46: 3384– 3388.

Flohé L. (2007) Selenium in mammalian spermiogenesis. Biol Chem. 388: 987-95.

Florea AM, Büsselberg D. (2011) Cisplatin as an anti-tumor drug: cellular mechanisms of activity, drug resistance and induced side effects. Cancers (Basel). 3: 1351-71.

Fordyce FM. (2005) Selenium Deficiency and Toxicity in the Environment. In: Selinus O, 5th ed, Essentials of medical geology. Academic Press, London: Elsevier. pp. 373-415.

Forstermann U, Boissel JP, Kleinert H. (1998) Expressional control of the 'constitutive' isoforms of nitric oxide synthase (NOS Iand NOS III). FASEB J. 12: 773–790.

Fortier ME, Audet I, Giguère A, Laforest JP, Bilodeau JF, Quesnel H, Matte JJ. (2012) Effect of dietary organic and inorganic selenium on antioxidant status, embryo development and reproductive performance in hyperovulatory first-parity gilts. J Anim Sci. 90: 231-40.

Foster LH, Sumar S. (1997) Selenium in health and disease: a review. Crit Rev Food Sci Nutr. 37: 211-28.

Foster SJ, Kraus RJ, Ganther HE. (1986) The metabolism of selenomethionine, Se-methylselenocysteine, their selenonium derivatives, and trimethylselenonium in the rat. Arch Biochem Biophys. 251: 77–86.

Foulds PG, Mitchell JD, Parker A, Turner R, Green G, Diggle P, Hasegawa M, Taylor M, Mann D, Allsop D. (2011) Phosphorylated alpha-synuclein can be detected in blood plasma and is potentially a useful biomarker for Parkinson's disease. FASEB J. 25: 4127–4137.

Fraiser LH, Kanekal S and Kehrer JP. (1991) Cyclophosphamide toxicity. Drugs 42: 781–795.

Frankel GD, Favey D. (1989) Involvement of cellular sulfhydryal compounds in the inhibition of DNA and RNA sunthesis by selenite. In Selenium in Biology and Medicine, Wendel A (ed). Springer-Verlag: Berlin; 79–82.

Freemerman AJ, Gallegos A, Powis G. (1999) Nuclear factor kappaB transactivation is increased but is not involved in the proliferative effects of thioredoxin overexpression in MCF-7 breast cancer cells. Cancer Res. 59: 4090-4.

Frei B. (1995) Cardiovascular disease and nutrient antioxidants: role of low-density lipoprotein oxidation. Crit Rev Food Sci Nutr. 35: 83–98.

Friedman HS, Pegg AE, Johnson SP, et al. (1999) Modulation of cyclophosphamide activity by O6-alkylguanine-DNA alkyltransferase. Cancer Chemother Pharmacol. 43: 80-5.

Fruehauf JP. & Meyskens F. L. Jr. (2007) Reactive oxygen species: a breath of life or death? Clin. Cancer Res 13, 789–794.

Fry FH & Jacob C. (2006) Sensor/effector drug design with potential relevance to cancer. Curr. Pharm. Des 12, 4479 – 4499.

Fulda S. (2009) Tumor resistance to apoptosis. Int J Cancer. 124: 511–515.

Gamcsik MP, Dolan ME, Andersson BS, Murray D. (1999) Mechanisms of resistance to the toxicity of cyclophosphamide. Curr Pharm Des. 5: 587-605.

Gandin V, Fernandes AP. (2015) Selenium compounds as therapeutic agents in cancer. Biochim Biophys Acta. 1850: 1642-60.

Gandin V, Khalkar P, Braude J, Fernandes AP. (2018) Organic selenium compounds as potential chemotherapeutic agents for improved cancer treatment. Free Radic Biol Med. 8.

Ganther HE. (1968) Seleno trisulfides. Formation by reaction of thiols with selenious acid. Biochemistry. 7: 2898–2905.

Ganther HE. (1979) Metabolism of hydrogen selenide and methylated selenides. In Draper HH (ed): "Advances in Nutritional Research," vol 2. New York: Plenum Press, pp107– 128.

Gao F, Yuan Q, Gao L, Cai P, Zhu H, Liu R, Wang Y, Wei Y, Huang G, Liang J, Gao X (2014) Cytotoxicity and therapeutic effect of irinotecan combined with selenium nanoparticles. Biomaterials 35:8854-66

Gasdaska PY, Gasdaska JR, Cochran S, Powis G. (1995) Cloning and sequencing of a human thioredoxin reductase. FEBS Lett. 373: 5–9.

Gerschman R, Gilbert DL, Nye SW, Dwyer P, Fenn WO. (1954) Oxygen poisoning and X-irradiation: a mechanism in common. Science. 119: 62362–62366.

Geske FJ, Nelson AC, Lieberman R, Strange R, Sun T, Gerschenson LE. (2000) DNA repair is activated in early stages of p53-induced apoptosis. Cell Death Differ. 7: 393–401.

Ghaemi SZ, Forouhari S, Dabbaghmanesh MH, Sayadi M, Bakhshayeshkaram M, Vaziri F, Tavana Z. (2013) A prospective study of selenium concentration and risk of preeclampsia in pregnant Iranian women: a nested case-control study. Biol Trace Elem Res. 152: 174-9.

Ghafourifar P, Cadenas E. (2005) Mitochondrial nitric oxide synthase. Trends Pharmacol Sci. 26: 190–195.

Ghosh M, MJ, Sinha S, Chakraborty A, Mallick SK, Bandyopadhyay M, Mukherjee A (2012) *In vitro* and *in vivo* genotoxicity of silver nanoparticles. Mutat Res 749:60-9

Ghosh P, Bhattacharjee A, Basu A, Roy SS, Bhattacharya S (2014) Attenuation of cyclophosphamide-induced pulmonary toxicity in Swiss albino mice by naphthalimide-based organoselenium compound 2-(5- selenocyanatopentyl)-benzo[de]isoquinoline 1,3- dione. Pharm Biol 4:1–9

Ghosh P, Bhattacharjee A, Basu A, Roy SS, Bhattacharya S. (2014) Attenuation of cyclophosphamide-induced pulmonary toxicity in Swiss albino mice by naphthalimide-based organoselenium compound 2-(5-selenocyanatopentyl)-benzo[de]isoquinoline 1,3- dione. Pharm Biol 4:1–9.

Ghosh P, Singha SR, Basu A, Bhattacharjee A, Bhattacharya S (2015) Sensitization of cisplatin therapy by a naphthalimide based organoselenium compound through modulation of antioxidant enzymes and p53 mediated apoptosis. Free Radic Res 49:453-71.

GLOBOCAN 2008 onlinehttp://globocan.iarc.fraccessed on Dec 23’2010.

Gokhale NR, Mahajan PM, Sule RR, Belgaumkar VA, Jain SM. (2003) Treatment of pemphigus with intravenous pulse cyclophosphamide. Indian J Dermatol Venereol Leprol. 69: 334-7.

Gomberg M. (1900) An instance of trivalent carbon: triphenylmethyl. J Am Chem Soc. 22: 757–771.

Goncalves A, Braud AC, Viret F, *et al.* (2005) High-dose alkylating agents with autologous hematopoietic stem cell support and trastuzumab in ERBB2 overexpressing metastatic breast cancer: a feasibility study. Anticancer Res. 25: 663-7.

Gong P, Chen FX, Wang L, Wang J, Jin S, Ma YM (2014) Protective effects of blueberries (*Vaccinium corymbosum L.*) extract against cadmium-induced hepatotoxicity in mice. Environ Toxicol Pharmacol 37:1015–1027

Gonzalez VM, Fuertes MA, Alonso C, Perez JM. Is cisplatin-induced cell death always produced by apoptosis? Mol Pharmacol. 59: 657-63.

Gopalakrishna R, Chen ZH, Gundimeda U. (1997) Selenocompounds induce a redox modulation of protein kinase C in the cell, compartmentally independent from cytosolic glutathione: its role in inhibition of tumor promotion. Arch Biochem Biophys 348: 37–48.

Gorboulev V et al. (1997) Cloning and characterization of two human polyspecific organic cation transporters. DNA Cell Biol. 16: 871–81.

Greeder GA, Milner JA. (1980) Factors influencing the inhibitory effect of selenium on mice inoculated with ehrlich ascites tumor cells. Science. 209: 825–827.

Green LC, Wagner DA, Glogowski J, Skipper PL, Wishnok JS, Tannenbaum SR. (1982) Analysis of nitrate, nitrite, and [15N] nitrate in biological fluids. Anal Biochem. 126(1):131-8.

Groopman JE and Itri LM. (1999) Chemotherapy-induced anemia in adults: incidence and treatment. J Natl Cancer Inst. 91: 1616–1634.

Guo Y, Wang M, Mou J, Zhao Z, Yang J, Zhu F, Pei G, Zhu H, Wang Y, Xu G, Zeng R, Yao Y. (2018) Pretreatment of Huaiqihuang extractum protects against cisplatin-induced nephrotoxicity. Sci Rep. 8: 7333.

Gupta M, Mazumder UK, Kumar RS, Kumar TS (2004) Antitumor activity and antioxidant role of *Bauhinia racemosa* against Ehrlich ascites carcinoma in Swiss albino mice [corrected]. Acta Pharmacol Sin 25:1070-6.

Gupta M, Mazumder UK, Rath N, Mukhopadhyay DK (2000) Antitumor activity of methanolic extract of Cassia fistula L. seed against Ehrlich ascites carcinoma. J Ethnopharmacol 72:151-6.

Gurtoo HL, Hipkens JH, Sharma SD. (1981) Role of glutathione in the metabolism-dependent toxicity and chemotherapy of cyclophosphamide. Cancer Res. 41: 3584-91.

Haas JF, Kittelmann B, Mehnert WH, *et al.* (2002) Risk of leukaemia in ovarian tumour and breast cancer patients following treatment by cyclophosphamide. Br J Cancer. 55: 213-8.

Habig WH, Pabst MJ, Jacoby WB (1974) Glutathione S-transferases, the first enzymatic step in marcapturic acid formation. J Biol Chem 249:7130–7139

Hail N, Lotan R. (2009) Cancer chemoprevention and mitochondria: targeting apoptosis in transformed cells via the disruption of mitochondrial bioenergetics/redox state. Mol. Nutr Food Res. 53: 49–67.

Halliwell B and Gutteridge JMC. (1999) Free Radicals in Biology and Medicine (3rd ed.). Oxford University Press.

Halliwell B, Gutteridge JMC. (1989) Free Radical Biology and Medicine. Oxford, UK: Oxford University Press.

Halliwell B. (1997) Antioxidants and human disease: a general introduction. Nutr Rev. 55: S44–9.

Halliwell, B. and Whiteman, M (2004) Measuring reactive species and oxidative damage in vivo and in cell culture: how should you do it and what do the results mean? Br J Pharmacol 142:231–255

Hanahan D & Weinberg RA. (2000) The hallmarks of cancer. Cell 100, 57–70.

Hanahan D, Weinberg RA. (2000) The hallmarks of cancer. Cell. 7: 100: 57-70.

Harakeh S, Abdel-Massih RM, Gil PR, Sperling RA, Meinhardt A, Niedwiecki A, Rath M, Parak WJ, Baydoun E. (2010) The effect of PEG-coated gold nanoparticles on the anti-proliferative potential of Specific Nutrient Synergy. Nanotoxicology. 4: 177-85.

Harman D. (1956) Aging: a theory based on free radical and radiation chemistry. J Gerontol. 11: 298–300.

Hartmann JT, Lipp HP (2003) Toxicity of platinum compounds. Expert Opin Pharmacother. 4: 889–901.

Hassanin KM, Abd El-Kawi SH, Hashem KS (2013) The prospective protective effect of selenium nanoparticles against chromium-induced oxidative and cellular damage in rat thyroid. Int J Nanomedicine 8:1713-20

Hatfield DL, Gladyshev VN. (2002) How selenium has altered our understanding of the genetic code. Mol Cell Biol. 22: 3565–3576.

Hawkes WC, Turek PJ. (2001) Effects of dietary selenium on sperm motility in healthy men. J Androl. 22: 764-72.

Hayes JD, McLellan LI. (1999) Glutathione and glutathione-dependent enzymes represent a co-ordinately regulated defence against oxidative stress. Free Radic Res. 31: 273–300.

Henderson RF, Benson JM, Hahn FF, Hobbs CH et al (1985) New approaches for the evaluation of pulmonary toxicity: bronchoalveolar lavage fluid analysis. Fundam Appl Toxicol 5:451–458

Hermans IF, Chong TW, Palmowski MJ, Harris AL, Cerundolo V. (2003) Synergistic effect of metronomic dosing of cyclophosphamide combined with specific antitumor immunotherapy in a murine melanoma model. Cancer Res. 63: 8408-13.

Hijiya N, Hudson MM, Lensing S, Zacher M, Onciu M, Behm FG et al., (2007) Cumulative incidence of secondary neoplasms as a first event after childhood acute lymphoblastic leukemia. JAMA. 297: 1207-15.

Ho MS, Medcalf RL, Livesey SA, Traianedes K. (2015) The dynamics of adult haematopoiesis in the bone and bone marrow environment. Br J Haematol. 170: 472-86.

Hobdy EM, Kraut E, Masters G, *et al.* (2004) A phase II study of topotecan and cyclophosphamide with G-CSF in patients with advanced small cell lung cancer. Cancer Biol Ther. 3: 89-93.

Hoek J, Bloemendal KM, van der Velden LA, van Diessen JN, van Werkhoven E, Klop WM, Tesselaar ME. (2016) Nephrotoxicity as a Dose-Limiting Factor in a High-Dose Cisplatin-Based Chemoradiotherapy Regimen for Head and Neck Carcinomas. Cancers (Basel). 16: 8.

Hoffman DJ. (2002) Role of selenium toxicity and oxidative stress in aquatic birds, Aquat Toxicol. 57: 11–26.

Hogberg J, Garberg P, Stahal A. (1989) Studies on selenite induced DNA fragmentation and the role of poly (ADP-ribose) polymerase in selenite toxicity. In Selenium in Biology and Medicine, Wendel A (ed). Springer-Verlag: Berlin; 74–78.

Holben D, Smith A (1999) The diverse role of selenium within selenoproteins: a review. J Am Dietetic Assoc 99:836–843.

Holben DH, Smith AM, Ilich JZ, Landoll JD, Holcomb JP, Matkovic V. (2002) Selenium intakes, absorption, retention, and status in adolescent girls. J Am Diet Assoc. 102: 1082-7.

Holzer AK, Samimi G, Katano K, Naerdemann W, Lin X, Safaei R, Howell SB (2004) The copper influx transporter human copper transport protein 1 regulates the uptake of cisplatin in human ovarian carcinoma cells. Mol Pharmacol. 66: 817-23.

Hong H, Zhang Y, Sun J, Cai W. (2009) Molecular imaging and therapy of cancer with radiolabeled nanoparticles. Nano today. 4: 399–413.

Honjo I, Suou T, Hirayama C. (1988) Hepatotoxicity of cyclophosphamide in man: pharmacokinetic analysis. Res Commun Chem Pathol Pharmacol. 61: 149-65.

Hosnedlova B, Kepinska M, Skalickova S, Fernandez C, Ruttkay-Nedecky B, Peng Q. (2018) Nano-selenium and its nanomedicine applications: a critical review. Int J Nanomedicine. 13: 2107-2128.

Hotchkiss RS, Strasser A, McDunn JE, Swanson PE. (2009) Cell death. N Engl J Med. 361: 1570-83.

Hsieh HS, Ganther HE. (1977) Biosynthesis of dimethylselenide from sodium selenite in rat liver and kidney cell-free systems. Biochim Biophys Acta. 497: 205–217.

http://dtp.nci.nih.gov/index.html

Hu CH, Li YL, Xiong L, Zhang HM, Song J, Xia MS. (2012) Comparative effects of nano elemental selenium and sodium selenite on selenium retention in broiler chickens. Anim Feed Sci Technol. 177: 204– 210.

Hu Y. et al. (2005) Mitochondrial manganese-superoxide dismutase expression in ovarian cancer: role in cell proliferation and response to oxidative stress. J. Biol. Chem. 280, 39485–39492.

Huang B, Zhang J, Hou J, et al. (2003) Free radical scavenging efficiency of Nano-Se in vitro.Free Radic Biol Med. 35: 805–813.

Huang W, Xing W, Li D. (2008) Microcystin-RR induced apoptosis in tobacco BY-2 suspension cells is mediated by reactive oxygen species and mitochondrial permeability transition pore status.Toxicol *in Vitro*. 22: 328–337.

Huang Z, Roy P, Waxman DJ. (2000) Role of human liver microsomal CYP3A4 and CYP2B6 in catalyzing N-dechloroethylation of cyclophosphamide and ifosfamide. Biochem Pharmacol. 59: 961-72.

Husbeck B, Peehl DM, Knox SJ. (2005) Redox modulation of human prostate carcinoma cells by selenite increases radiation-induced cell killing. Free Radic Biol Med. 38: 50–57.

Hwang C, Sinskey AJ, Lodish HF. (1992) Oxidized redox state of glutathione in the endoplasmic-reticulum. Science. 57: 1496–1502.

IARC (2012) IARC Working Group on the evaluation of Carcinigenic Risks to Human, Pharmaceuticals, Volume 100 A, A review of human carcinogenesis, IACR Monogr. Eval Crcinog. Risks. Hum. 100: 1-401.

Ikari A (2005) Sodium-dependent glucose transporter reduces peroxynitrite and cell injury caused by cisplatin in renal tubular epithelial cells. Biochim Biophys Acta. 1717: 109–17.

Inoue H, Nagata N, Kurokawa H, Yamanaka S. (2016) iPS cells: a game changer for future medicine. EMBO J. 33: 409-17.

Ip C, Lisk DJ. (1994) Enrichment of selenium in allium vegetables for cancer prevention. Carcinogenesis 15: 1881–1885.

Ip C, Lisk DJ. (1997) Modulation of phase I and phase II xenobiotics metabolizing enzymes by selenium-enriched garlic in rats. Nutr Cancer 28: 184–188.

Ip C. Lessons from basic research in selenium and cancer prevention.J Nutr1998; 128: 1845–1854.

Irani K. et al. (1997) Mitogenic signaling mediated by oxidants in Ras-transformed fibroblasts. Science 275, 1649–1652.

Ishida S, Lee J, Thiele DJ, Herskowitz I (2002) Uptake of the anticancer drug cisplatin mediated by the copper transporter Ctr1 in yeast and mammals. Proc Natl Acad Sci U S A. 99: 14298-302.

Jagetia GC, Reddy TK. (2011) Alleviation of iron induced oxidative stress by the grape fruit flavanone naringin in vitro. Chem Biol Interact. 190: 121-8.

Jaishankar M, Tseten T, Anbalagan N, Mathew BB, Beeregowda KN. (2014) Toxicity, mechanism and health effects of some heavy metals. Interdiscip Toxicol. 7: 60-72.

Jamieson ER, Lippard SJ (1999) Structure, Recognition, and Processing of Cisplatin-DNA Adducts. Chem Rev. 99: 2467-98.

Jancova P, Anzenbacher P, Anzenbacherova E. (2010) Phase II drug metabolizing enzymes. Biomed Pap Med Fac Univ Palacky Olomouc Czech Repub. 154: 103-16.

Jarrett BR, Gustafsson B, Kukis DL, Louie AY. (2008) Synthesis of 64Cu-labeled magnetic nanoparticles for multimodal imaging. Bioconjug Chem. 19: 1496–1504.

Jeevanandam J, Barhoum A, Chan YS, Dufresne A, Danquah MK. (2018) Review on nanoparticles and nanostructured materials: history, sources, toxicity and regulations. Beilstein J Nanotechnol. 9: 1050-1074.

Ji YB, Akerboom TPM, Sies H, Thomas JA. (1999) S-nitrosylation andS-glutathiolation of protein sulfhydryls by S-nitroso glutathione, Arch Biochem Biophys. 362: 67–78.

Jiang C, Hu H, Malewicz B, Wang Z, Lu J. (2004) Selenite-induced p53 Ser-15 phosphorylation and caspase-mediated apoptosis in LNCaP human prostate cancer cells. Mol Cancer Ther. 3: 877–884.

Jiang C, Wang Z, Ganther H, Lu J. (2001) Caspases as key executors of methyl selenium-induced apoptosis (anoikis) of DU-145 prostate cancer cells. Cancer Res. 61: 3062–3070.

Judson I, Kelland LR (2000) New developments and approaches in the platinum arena. Drugs. 2000; 59: 29-36.

Juliger S, Goenaga-Infante H, Lister TA, Fitzgibbon J, Joel SP. (2007) Chemosensitization of B-cell lymphomas by methylseleninic acid involves nuclear factor-kappaB inhibition and the rapid generation of other selenium species. Cancer Res. 67: 10984–10992.

Kalogeris T, Bao Y, Korthuis RJ. (2014) Mitochondrial reactive oxygen species: a double edged sword in ischemia/reperfusion vs preconditioning. Redox Biol. 2: 702-14.

Kanekal S, Kehrer JP. (1994) Metabolism of cyclophosphamide by lipoxygenases. Drug Metab Dispos. 22: 74-8.

Kanzok SM, Schirmer RH, Turbachova I, Iozef R, Becker K. (2000) The thioredoxin system of the malaria parasite Plasmodium falciparum. Glutathione reduction revisited. J Biol Chem.275: 40180–40186.

Kart A, Cigremis Y, Karaman M, Ozen H (2010) Caffeic acid phenethyl ester (CAPE) ameliorates cisplatin-induced hepatotoxicity in rabbit. Exp Toxicol Pathol 62: 45–52.

Kart A, Cigremis Y, Karaman M, Ozen H (2010) Caffeic acid phenethyl ester (CAPE) ameliorates cisplatin-induced hepatotoxicity in rabbit. Exp Toxicol. Pathol 62: 45–52.

Kasai H. (1997) Analysis of a form of oxidative DNA damage, 8-hydroxy-2′-deoxyguanosine, as a marker of cellular oxidative stress during carcinogenesis. Mutat Res. 387: 147–63.

Kawasaki ES, Player A. (2005) Nanotechnology, nanomedicine, and the development of new, effective therapies for cancer. Nanomedicine. 1: 101-9.

Kaya H, Oral B, Ozgüner F, Tahan V et al. (1999) The effect of melatonin application on lipid peroxidation during cyclophosphamide therapy in female rats. Zentralbl Gynakol 121:499-502

Kelloff GJ, Hawk ET, Sigman CC (Eds.). Cancer Chemoprevention: Promising Cancer Chemopreventive Agents, vol. 1, Humana Press, Totowa, NJ, 2004, pp. 697.

Kelloff GJ. (2000) Perspectives on cancer chemoprevention research and drug development. Adv. Cancer Res. 78: 199–334.

Kezic A, Spasojevic I, Lezaic V, Bajcetic M. (2016) Mitochondria-Targeted Antioxidants: Future Perspectives in Kidney Ischemia Reperfusion Injury. Oxid Med Cell Longev. 2016: 2950503.

Khan MN, Mobin M, Abbas ZK, AlMutairi KA, Siddiqui ZH. (2017) Role of nanomaterials in plants under challenging environments. Plant Physiol Biochem. 110: 194-209.

Khynriam D, Prasad SB (2003) Changes in endogenous tissue glutathione level in relation to murine ascites tumor growth and the anticancer activity of cisplatin. Braz J Med Biol Res. 36: 53-63.

Kice J. (1981) The mechanism of the reaction of thiols with selenite and other Se(IV) species. In Selenium in Biology and Medicine, Spallholz JE, Martin JL, Ganther HE (eds). AVI Publishing Co.: Westport, CT; 17–32.

Kieliszek M, Błażejak S. (2016) Current Knowledge on the Importance of Selenium in Food for Living Organisms: A Review. Molecules. 21.

Kim JW, Galanzha EI, Zaharoff DA, Griffin RJ, Zharov VP. (2013) Nanotheranostics of circulating tumor cells, infections and other pathological features in vivo. Mol Pharm. 10: 813-30.

Kim SH, Lee IC, Baek HS, Shin IS, Moon C, Bae CS, Kim SH, Kim JC, Kim HC (2014) Mechanism for the protective effect of diallyl disulfide against cyclophosphamide acute urotoxicity in rats. Food Chem Toxicol 64:110-118

Kim SJ, Park C, Lee JN, Park R. (2018) Protective roles of fenofibrate against cisplatin-induced ototoxicity by the rescue of peroxisomal and mitochondrial dysfunction. Toxicol Appl Pharmacol. 353: 43-54.

Kim SY, Moon A. (2012) Drug-induced nephrotoxicity and its biomarkers. Biomol Ther (Seoul). 20: 268-72.

Kim T, Jung U, Cho DY, Chung AS. (2001) Se-methylselenocysteine induces apoptosis through caspase activation in HL-60 cells. Carcinogenesis. 22: 559–565.

Kiremidjian-Schumacher L, Roy M, Wishe HI, Cohen MW, Stotzky G. (1994) Supplementation with selenium and human immune cell functions. II. Effect on cytotoxic lymphocytes and natural killer cells. Biol Trace Elem Res.41: 115- 27.

Klatt P, Lamas S. (2000) Regulation of protein function by Sglutathiolation in response to oxidative and nitrosative stress. Eur J Biochem. 267: 4928–4944.

Klein EA. (2004) Selenium: epidemiology and basic science. J Urol. 171: S50-3 [discussion S53].

Klein, C. B., Broday, L. and Costa, M. (2001) Mutagenesis assays in mammalian cells. Curr. Protoc. Toxicol. Chapter 3, Unit3.3.

Knekt P, Heliovaara M, Aho K, Alfthan G, Marniemi J, Aromaa A. (2000) Serum selenium, serum alpha-tocopherol and the risk of rheumatoid arthritis. Epidemiology. 11: 402-5.

Kohen R, Nyska A. (2002) Oxidation of biological systems: oxidative stress phenomena, antioxidants, redox reactions, and methods for their quantification. Toxicol Pathol. 30: 620-50.

Kohn KW, Hartley JA, Mattes WB. (1987) Mechanisms of DNA sequence selective alkylation of guanine-N7 positions by nitrogen mustards. Nucleic Acids Res. 15: 10531-49.

Komatsu M, Sumizawa T, Mutoh M, Chen ZS, Terada K, Furukawa T, Yang XL, Gao H, Miura N, Sugiyama T, Akiyama S (2000) Copper-transporting P-type adenosine triphosphatase (ATP7B) is associated with cisplatin resistance. Cancer Res. 60: 1312-6.

Kong L, Yuan Q, Zhu H, Li Y, Guo Q, Wang Q, Bi X, Gao X. (2011) The suppression of prostate LNCaP cancer cells growth by Selenium nanoparticles through Akt/Mdm2/AR controlled apoptosis. Biomaterials. 32: 6515-22.

Kong Q & Lillehei KO. (1998) Antioxidant inhibitors for cancer therapy. Med. Hypotheses 51, 405–409.

Kumar S, Tomar MS, Acharya A. (2015) Carboxylic group-induced synthesis and characterization of selenium nanoparticles and its anti-tumor potential on Dalton's lymphoma cells. Colloids Surf B Biointerfaces. 126: 546-52.

Kurutas EB. (2016) The importance of antioxidants which play the role in cellular response against oxidative/nitrosative stress: current state. Nutr J. 15: 71.

Labunskyy VM, Lee BC, Handy DE, Loscalzo J, Hatfield DL, Gladyshev VN. (2011) Both maximal expression of selenoproteins and selenoprotein deficiency can promote development of type 2 diabetes-like phenotype in mice. Antioxid Redox Signal. 14: 2327-36.

Ladas EJ, Jacobson JS, Kennedy DD, et al. (2004) Antioxidants and cancer therapy: a systematic review. J Clin Oncol. 22: 517–28.

Landis GN, Tower J. (2005) Superoxide dismutase evolution and life span regulation, Mech. Ageing Dev. 126: 365–379.

Langerak AD, Dreisbach LP. (2001) Chemotherapy Regimens and Cancer Care. Landes Bioscience; Georgetown, Texas.

Lanvers-Kaminsky C et al. (2006) Continuous or repeated prolonged cisplatin infusions in children: A prospective study on ototoxicity, platinum concentrations, and standard serum parameters. Pediatr Blood Cancer. 47: 183–93.

Leaver MJ, George SG (1998) A piscine glutathione S-transferase which efficiently conjugates the end-products of lipid peroxidation. Mar Environ Res 46:71–74.

Leinonen HM, Kansanen E, Pölönen P, Heinäniemi M, Levonen AL. (2014) Role of the keap1-nrf2 pathway in cancer. Adv Cancer Res. 122: 281–320.

Leme DM, Marin-Morales MA. (2008) Chromosome aberration and micronucleus frequencies in Allium cepa cells exposed to petroleum polluted water--a case study. Mutat Res.650: 80

Lessard M, Yang WC, Elliott GS, Rebar AH, Van Vleet JF, Deslauriers N, Brisson GJ, Schultz RD. (1991) Cellular immune responses in pigs fed a vitamin E- and selenium-deficient diet. J Anim Sci. 69: 1575-82.

Letavayová L, Vlcková V, Brozmanová J. (2006) Selenium: from cancer prevention to DNA damage. Toxicology. 227:1–14.

Levander OA, Morris VC, Higgs DJ. (1973) Selenium as a catalyst for the reduction of cytochrome c by glutathione. Biochemistry. 12: 4591–4592.

Levander OA, Morris VC, Higgs DJ. (1974) Selenium catalysis of swelling of rat liver mitochondria and reduction of cytochrome c by sulfur compounds. Adv Cirrhosis Hyperammonemia and Hepatic Encephalopathy. 48: 405–423.

Levander OA, Whanger PD. (1996) Deliberations and evaluations of the approaches, endpoints and paradigms for selenium and iodine dietary recommendations. J Nutr. 126(9 Suppl): 2427S-34S.

Lheureux S, Clarisse B, Launay-Vacher V, Gunzer K, Delcambre-Lair C, BouhierLeporrier K, et al. (2011) Evaluation of current practice: management of chemotherapy-related toxicities. Anti-Cancer Drug. 22: 919-25.

Li GX, Hu H, Jiang C, Schuster T, Lu J. (2007) Differential involvement of reactive oxygen species in apoptosis induced by two classes of selenium compounds in human prostate cancer cells. Int J Cancer. 120: 2034–2043.

Li H, Zhang J, Wang T, Luo W, Zhou Q, Jiang G. (2008) Elemental selenium particles at nano-size (Nano-Se) are more toxic to Medaka (*Oryzias latipes*) as a consequence of hyper-accumulation of selenium: a comparison with sodium selenite. Aquat Toxicol. 89: 251-6.

Li J, Sun K, Ni L, Wang X, Wang D, Zhang J. (2012) Sodium selenosulfate at an innocuous dose markedly prevents cisplatin-induced gastrointestinal toxicity. Toxicol Appl Pharmacol 258: 76–83.

Li Y, Qi K, Zu L, Wang M, Wang Y, Zhou Q. (2016) Anti-apoptotic brain and reproductive organ-expressed proteins enhance cisplatin resistance in lung cancer cells via the protein kinase B signaling pathway. Thorac Cancer. 7: 190-8.

Lieberthal W, Triaca V, Levine J (1996) Mechanisms of death induced by cisplatin in proximal tubular epithelial cells: apoptosis vs. necrosis. Am J Physiol. 270: F700–8.

Lillie RD, Fullmer HM. (1976) Histological technique and practical histochemistry, 4th edition. Mc Graw-Hill, New York.

Lipinski B. (2005) Rationale for the treatment of cancer with sodium selenite. Med Hypotheses. 64: 806–810.

Lissoni P, Tancini G, Barni S, Paolorossi F, Ardizzoia A, Conti A, Maestroni G. (1997) Treatment of cancer chemotherapy-induced toxicity with the pineal hormone melatonin. Support Care Cancer. 5: 126-9.

Liu F, Li XL, Lin T, He DW, Wei GH, Liu JH, Li LS (2012) The cyclophosphamide metabolite, acrolein, induces cytoskeletal changes and oxidative stress in Sertoli cells. Mol Biol Rep 39:493-500

Liu T, Zeng L, Jiang W, Fu Y, Zheng W, Chen T. (2015) Rational design of cancer-targeted selenium nanoparticles to antagonize multidrug resistance in cancer cells. Nanomedicine. DOI: 10.1016/j.nano.2015.01.009.

Lodish H, Berk A, Zipursky SL, et al. (2000) Proto-Oncogenes and Tumor-Suppressor Genes. Molecular Cell Biology. 4th edition. Section 24.2.

Loeb LA, Harris CC. (2008) Advances in chemical carcinogenesis: a historical review and prospective. Cancer Res. 68: 6863-72.

Longchar A and Prasad SB. (2016) Ascorbic Acid (Vitamin C)-Mediated Protection on Mutagenic Potentials of Cisplatin in Mice Bearing Ascites Dalton's Lymphoma. Research Journal of Mutagenesis, 6: 1-21.

Lopez-Lazaro M, Willmore E, Elliott SL, Austin CA. (2008) Selenite induces topoisomerase I and II-DNA complexes in K562 leukemia cells. Int J Cancer. 123: 2217–2221.

Lowe SW, Lin AW. (2000) Apoptosis in cancer. Carcinogenesis. 21: 485–495.

Lowry OH, Rosenbrough NJ, Farr AL, Randall RJ (1951) Protein measurement with the folin phenol reagent. J Biol Chem 193:265–276

Lu J, Jiang C (2001) Antiangiogenic activity of selenium in cancer chemoprevention: metabolite-specific effects. Nutr Cancer 40:64-73

Lu J, Jiang C, Kaeck M, Ganther H, Vadhanavikit S, Ip C, Thompson H. (1995) Dissociation of the genotoxic and growth inhibitory effects of selenium. Biochem Pharmacol. 50: 213–219.

Lubos E, Loscalzo J, Handy DE. (2011) Glutathione peroxidase-1 in health and disease: from molecular mechanisms to therapeutic opportunities. Antioxid Redox Signal. 15: 1957-97.

Luck HA (1963) Spectrophotometric method for estimation of catalase. In: Bergmeyer HV (ed) Methods of enzymatic analysis. Academic Press, New York, pp. 886–888

Ludeman SM. (1999) The chemistry of the metabolites of cyclophosphamide. Curr Pharm Des. 5: 627-43.

Luperchio S, Tamir S, Tannenbaum SR. (1996) NO-induced oxidative stress and glutathione metabolism in rodent and human cells. Free Radic Biol Med. 21: 513-9.

Lushchak VI. (2011) Environmentally induced oxidative stress in aquatic animals. Aquat Toxicol. 101: 13–30.

Lux Research. The Nanotech Report™2006: Investment Overview and Market Research for Nanotechnology; Lux Research: New York, NY, USA, 2006.

Madeja Z, Sroka J, Nystrom C, (2005) The role of thioredoxin reductase activity in selenium-induced cytotoxicity. Biochem Pharmacol. 69: 1765–1772.

Maiorino M, Ursini F. (2002) Oxidative stress, spermatogenesis and fertility. Biol Chem. 383: 591-7.

Mansour HH, Hafez HF, Fahmy NM (2006) Silymarin modulates Cisplatin-induced oxidative stress and hepatotoxicity in rats. J Biochem Mol Biol. 396: 356-61.

Marklund S, Marklund G (1974) Involvement of the superoxide anion radical in autooxidation of pyrogallol and a convenient assay for superoxide dismutase. Eur J Biochem 47:469–474.

Martinez-Sanchez G & Giuliani A. (2007) Cellular redox status regulates hypoxia inducible factor-1 activity. Role in tumour development. J. Exp. Clin. Cancer Res. 26, 39–50.

Masella R, Di Benedetto R, Vari R, Filesi C, Giovannini C. (2005) Novel mechanisms of natural antioxidant compounds in biological systems: involvement of glutathione and glutathione-related enzymes, J Nutr Biochem. 16: 577–586.

Mate´s JM. (1999) Antioxidant enzymes and human diseases. Clin Biochem. 32: 595–603.

Mates JM, Perez-Gomez C, De Castro IN. (1999) Antioxidant enzymes and human diseases, Clin. Biochem. 32: 595–603.

Mates JM, Segura JA, Alonso FJ, Marquez J. (2012) Oxidative stress in apoptosis and cancer: an update. Arch Toxicol. 86: 1649–1665.

Matés JM. Effects of antioxidant enzymes in the molecular control of reactive oxygen species toxicology. Toxicology 153:83-104

Mather A, Roland D (1969) The automated thiosemicarbazidediacetyl monoxime method for plasma urea. Clin Chem 15:393–396.

Maynard S, Schurman SH, Harboe C, Souza-Pinto NC, Bohr VA. (2009) Base excision repair of oxidative DNA damage and association with cancer and aging. Carcinogenesis. 30: 2–10.

Mazumdar UK, Gupta M, Maiti S, Mukherjee D (1997) Antitumor activity of *Hygrophila spinosa* on Ehrlich ascites carcinoma and sarcoma-180 induced mice. Indian J Exp Biol 35:473-7

Mc Cord JM, Fridovich I. (1969) Superoxide dismutase an enzymic function for erythrocuprein (hemocuprein), J. Biol. Chem. 244: 60409–60455.

McCall MR, Frei B. (1999) Can antioxidant vitamins materially reduce oxidative damage in humans? Free Rad. Biol. Med. 26: 1034–1053.

McCord JM, Fridovich I (1969) Superoxide dismutase: an enzymatic function for erythrocuprein (hemoprotein). J Biol Chem 244:6049–6055

Meijer C et al. (1999) Cisplatin-induced DNA-platination in experimental dorsal root ganglia neuronopathy. Neurotoxicology. 20: 883–7.

Michaelis L. (1939) Free radicals as intermediate steps of oxidation-reduction, Cold Spring Harb Symp. Quant Biol. 7: 33–49.

Miller DM, Buettner GR and Aust SD. (1990) Transition metals's catalysts of "autoxidation" reactions. Free Radic Biol Med.8: 95-108.

Miller RP, Tadagavadi RK, Ramesh G, Reeves WB. (2010) Mechanisms of Cisplatin nephrotoxicity. Toxins (Basel). 2: 2490-518.

Miranda-Vizuete A, Sadek CM, Jimenez A, Krause M, Sutovsky P, Oko R. (2004) The mammalian testis-specific thioredoxin system. Antioxid Redox Signal. 6: 25–40.

Misra HP. (1974) Generation of superoxide free radical during auto-oxidation of thiols. J Biol Chem. 249: 2151–2155.

Mohamed F, Endre ZH, Buckley NA. (2015) Role of biomarkers of nephrotoxic acute kidney injury in deliberate poisoning and envenomation in less developed countries. Br J Clin Pharmacol. 80: 3-19.

Moreb JS, Gabr A, Vartikar GR, Gowda S, Zucali JR, Mohuczy D. (2005) Retinoic acid down-regulates aldehyde dehydrogenase and increases cytotoxicity of 4-hydroperoxycyclophosphamide and acetaldehyde. J Pharmacol Exp Ther. 312: 339-45.

Moreno-Reyes R, Egrise D, Nève J, Pasteels JL, Schoutens A. (2001) Selenium deficiency-induced growth retardation is associated with an impaired bone metabolism and osteopenia. J Bone Miner Res.16: 1556-63.

Morgan RJ, Doroshow JH, Leong L, *et al.* (2001) Phase II trial of highdose intravenous doxorubicin, etoposide, and cyclophosphamide with autologous stem cell support in patients with residual or responding recurrent ovarian cancer. Bone Marrow Transplant. 28: 859-63.

Mousa SA, Bharali DJ. (2011) Nanotechnology-based detection and targeted therapy in cancer: nano-bio paradigms and applications. Cancers (Basel). 3: 2888-903.

Mullur R, Liu YY, Brent GA. (2014) Thyroid hormone regulation of metabolism. Physiol Rev. 94: 355-82.

Muro S, Garnacho C, Champion JA, (2008) Control of endothelial targeting and intracellular delivery of therapeutic enzymes by modulating the size and shape of ICAM-1-targeted carriers. Mol Ther. 16: 1450–1458.

Mustacich D, Powis G (2000) Thioredoxin Reductase. Biochem J 346:1–8

Mutanen M. (1986) Bioavailability of selenium. Ann Clinical Research. 18: pp. 48-54.

Mythili Y, Sudharsan PT, Selvakumar E, Varalakshmi P. (2004) Protective effect of DL-alpha-lipoic acid on cyclophosphamide induced oxidative cardiac injury. Chem Biol Interact. 151: 13-9.

Nafees S, Ahmad ST, Arjumand W, Rashid S, Ali N, Sultana S (2012) Modulatory effects of gentisic acid against genotoxicity and hepatotoxicity induced by cyclophosphamide in Swiss albino mice. J Pharm Pharmacol 64:259-67.

Nafees S, Rashid S, Ali N, Hasan SK, Sultana S. (2015) Rutin ameliorates cyclophosphamide induced oxidative stress and inflammation in Wistar rats: role of NFκB/MAPK pathway. Chem Biol Interact. 231: 98–107.

Nagy JA, Morgan ES, Herzberg KT, Manseau EJ, Dvorak AM, Dvorak HF (1995) Pathogenesis of ascites tumor growth: angiogenesis, vascular remodeling, and stroma formation in the peritoneal lining. Cancer Res 55:376-385

Nair HB, Sung B, Yadav VR, Kannappan R, Chaturvedi MM, Aggarwal BB. (2010) Delivery of anti-inflammatory nutraceuticals by nanoparticles for the prevention and treatment of cancer. Biochem Pharmacol. 80: 1833–1843.

Narajji C, Karvekar MD and Das AK. (2007) Biological importance of organoselenium compounds. Ind J Pharm Sci. 69: 344–351.

Narayanan BA. (2006) Chemopreventive agents alters global gene expression pattern: predicting their mode of action and targets. Curr Cancer Drug Targets. 6: 711–727.

Navarro-Alarcon M, Cabrera-Vique C. (2008) Selenium in food and the human body: A review. Sci Total Environ.1;4 00: 115-41.

Navarro-Alarcón M, López-Martínez MC (2000) Essentiality of selenium in the human body: relationship with different diseases. Sci Total Environ 249:347-71.

Nel A, Xia T, Madler L, Li N. (2006) Toxic potential of materials at the nano level. Science. 311: 622-627.

Neve J. (1996) Selenium as a risk factor for cardiovascular diseases. J Cardiovasc Risk. 3:42-7.

Nicolini A, Mancini P, Ferrari P, *et al.* (2004) Oral low-dose cyclophosphamide in metastatic hormone refractory prostate cancer (MHRPC). Biomed Pharmacother. 58: 447-50.

Nie S, Xing Y, Kim GJ, Simons JW (2007) Nanotechnology applications in cancer. Annu Rev Biomed Eng 9:257-88.

Nie S, Xing Y, Kim GJ, Simons JW. (2007) Nanotechnology applications in cancer. Annu Rev Biomed Eng.9: 257-88.

NIH. ClinicalTrials.gov. Available online: http://clinicaltrials.gov/ (accessed on July 14, 2011).

Nilsonne G, Sun X, Nyström C, Rundlöf AK, Potamitou FA, Björnstedt M, Dobra K (2006) Selenite induces apoptosis in sarcomatoid malignant mesothelioma cells through oxidative stress. Free Radic Biol Med 41:874-85

Ning Y, Shi Y, Chen J, Song N, Cai J, Fang Y, Yu X, Ji J, Ding X. (2018) Necrostatin-1 Attenuates Cisplatin-Induced Nephrotoxicity Through Suppression of Apoptosis and Oxidative Stress and Retains Klotho Expression. Front Pharmacol. 9: 384.

Nishikawa M. (2008) Reactive oxygen species in tumor metastasis. Cancer Lett. 266, 53–59.

Nita M, Grzybowski A. (2016) The Role of the Reactive Oxygen Species and Oxidative Stress in the Pathomechanism of the Age-Related Ocular Diseases and Other Pathologies of the Anterior and Posterior Eye Segments in Adults. Oxid Med Cell Longev. 2016: 3164734.

Nordberg J, Arner ESJ (2001) Reactive oxygen species, antioxidants, and the mammalian thioredoxin system. Free Radic Biol Med 31:1287–1312.

Norton RL, Hoffmann PR. (2012) Selenium and asthma. Mol Aspects Med. 33: 98-106.

Øarskov H, Flyvbjerg A. (2000) Selenium and human health. Lancet 356: 942–943.

Oberley LW & Buettner GR. (1979) Role of superoxide dismutase in cancer: a review. Cancer Res. 39, 1141–1149.

Oberley TD & Oberley LW. (1997) Antioxidant enzyme levels in cancer. Histol. Histopathol. 12, 525–535.

Ognio E, Chiavarina B, Peterka M, Mariggiò MA, Viale M. (2006) Study of feasibility of the treatment with procainamide hydrochloride and cisplatin in pregnant mice. Chem Biol Interact. 164: 232-40.

Oh GS, Kim HJ, Shen A, Lee SB, Khadka D, Pandit A, So HS. (2014) Cisplatin-induced Kidney Dysfunction and Perspectives on Improving Treatment Strategies. Electrolyte Blood Press. 12: 55-65.

Okhawa H, Ohishi N, Yagi K (1979) Assay for lipid peroxides in animal tissues by thiobarbituric acid reaction. Annal Biochem 95:351–358

Oldereid NB, Thomassen Y, Purvis K. (1998) Selenium in human male reproductive organs. Hum Reprod. 13: 2172-6.

Olm E, Fernandes AP, Hebert C, Rundlo¨f AK, Larsen EH, Danielsson O, Bjo¨rnstedt M. (2009a) Extracellular thiol-assisted selenium uptake dependent on the x(c)-cystine transporter explains the cancer-specific cytotoxicity of selenite. Proc Natl Acad Sci USA. 106: 11400–11405.

O'Regan R M, Von Roenn JH, Carlson RW, *et al.* (2005) Final results of a Phase II trial of preoperative TAC (docetaxel/doxorubicin/cyclophosphamide) in stage III breast cancer. Clin Breast Cancer 6: 163-8.

Paglia DE, Valentine WN (1967) Studies on the quantitative and qualitative characterization of erythrocyte glutathione peroxidase. J Lab Clin Med 70:158–169

Pagmantidis V, Meplan C, van Schothorst EM, Keijer J, Hesketh JE (2008) Supplementation of healthy volunteers with nutritionally relevant amounts of selenium increases the expression of lymphocyte protein biosynthesis genes. Am J Clin Nutr 87:181-9

Painter EP. (1941) The chemistry and toxicity of selenium compounds with special reference to the selenium problem. Chem Rev.28: 179–213.

Pan JS, Hong MZ, Ren JL. (2009) Reactive oxygen species: a double edged sword in oncogenesis. World J Gastroenterol. 15: 1702–1707.

Park JH, Lee S, Kim J-H, Park K, Kim K, Kwon IC. (2008) Polymeric nanomedicine for cancer therapy. Prog Polym Sci. 33: 113–137.

Patel BP et al. (2007) Lipid peroxidation, total antioxidant status, and total thiol levels predict overall survival in patients with oral squamous cell carcinoma. Integr. Cancer Ther. 6, 365–372.

Patrick L. (1999) Nutrients and HIV. Part one. Beta carotene and selenium. Altern Med Rev. 4: 403-13.

Pedrera-Zamorano JD, Calderon-García JF, Roncero-Martin R, Mañas-Nuñez P, Moran JM, Lavado-Garcia JM. (2012) The protective effect of calcium on bone mass in postmenopausal women with high selenium intake. J Nutr Health Aging. 16: 743-8.

Pelicano H, Carney D, Huang P (2004) ROS stress in cancer cells and therapeutic implications. Drug Resist Updat 7:97-110

Perry G et al. (2000) How important is oxidative damage? Lessons from Alzheimer's disease. Free Radic Biol Med. 28, 831–834.

Peters WP, Stuart A, Klotman M, *et al.* (1989) High-dose combination cyclophosphamide, cisplatin, and melphalan with autologous bone marrow support. A clinical and pharmacologic study. Cancer Chemother Pharmacol. 23: 377-83.

Peyrone M. (1845) Ueber die Einwirkung des Ammoniaks auf Platinchlorür'[On the Influence of Ammonia on Platinum Chloride]. Ann Chem Pharm. 51: 1.

Pickup MW, Mouw JK, Weaver VM. (2014) The extracellular matrix modulates the hallmarks of cancer. EMBO Rep. 15: 1243-53.

Pieczyńska J, Grajeta H. (2015) The role of selenium in human conception and pregnancy. J Trace Elem Med Biol. 29: 31-8.

Poirier KA, Milner JA. (1983) Factors influencing the antitumorigeneic properties of selenium in mice. J Nutr. 113: 2147–2154.

Ponticelli C and Passerini P. (1991) Alkylating agents and purine analogues in primary glomerulonephritis with nephrotic syndrome. Nephrol Dial Transplant. 6: 381–388.

Poole LG, Dolin CE, Arteel GE. (2017) Organ-Organ Crosstalk and Alcoholic Liver Disease. Biomolecules. 7: 3.

Potters G, Horemans N, Bellone S, Caubergs RJ, Trost P, Guisez Y, Asard H. (2004) Dehydroascorbate influences the plant cell cycle through a glutathione-independent reduction mechanism. Plant Physiol. 134: 1479–1487.

Prasad KS, Patel H, Patel T, Patel K, Selvaraj K (2013) Biosynthesis of Se nanoparticles and its effect on UV-induced DNA damage. Colloids Surf B Biointerfaces 103:261-6

Prathna TC, Chandrasekaran N, Raichur AM, Mukherjee A (2011) Biomimetic synthesis of silver nanoparticles by Citrus limon (lemon) aqueous extract and theoretical prediction of particle size. Colloids Surf B Biointerfaces 82:152-9

Pritchard KI, Paterson AH, Fine S, et al. (1997) Randomized trial of cyclophosphamide, methotrexate, and fluorouracil chemotherapy added to tamoxifen as adjuvant therapy in postmenopausal women with node-positive estrogen and/or progesterone receptor-positive breast cancer: a report of the National Cancer Institute of Canada Clinical Trials Group. Breast Cancer Site Group. J Clin Oncol. 15: 2302-11.

Qi ZL, Wang Z, Li W, Hou JG, Liu Y, Li XD, Li HP, Wang YP. (2017) Nephroprotective Effects of Anthocyanin from the Fruits of *Panax ginseng* (GFA) on Cisplatin-Induced Acute Kidney Injury in Mice. Phytother Res. 31: 1400-1409.

Quijano C, Trujillo M, Castro L, Trostchansky A. (2016) Interplay between oxidant species and energy metabolism. Redox Biol. 8: 28-42.

Rabik CA, Dolan ME (2008) Molecular mechanisms of resistance and toxicity associated with platinating agents. Cancer Treat Rev. 33: 9-23.

Radi R, Turrens JF, Chang LY, Bush KM, Crapo JD, Freeman BA. (1991) Detection of catalase in rat heart mitochondria. J Biol Chem. 266: 22028-34.

Rahman I, Biswas SK, Kirkham PA. (2006) Regulation of inflammation and redox signaling by dietary polyphenols. Biochem Pharmacol. 72: 1439–1452.

Rahman MA, Amin AR, Shin DM. (2010) Chemopreventive potential of natural compounds in head and neck cancer. Nutr Cancer. 62: 973-87.

Rajpathak S, Rimm E, Morris JS, Hu F. (2005) Toenail selenium and cardiovascular disease in men with diabetes. J Am Coll Nutr. 24: 250-6.

Ramamurthy Ch, Sampath KS, Arunkumar P, Kumar MS, Sujatha V, Premkumar K, Thirunavukkarasu C. (2013) Green synthesis and characterization of selenium nanoparticles and its augmented cytotoxicity with doxorubicin on cancer cells. Biopr and Biosy Eng. 36: 1131-9.

Ramanathan B et al. (2005) Resistance to paclitaxel is proportional to cellular total antioxidant capacity. Cancer Res. 65, 8455–8460.

Ramu K, Fraiser LH, Mamiya B, Ahmed T, Kehrer JP. (1995) Acrolein mercapturates: synthesis, characterization, and assessment of their role in the bladder toxicity of cyclophosphamide. Chem Res Toxicol. 8: 515-24.

Rao CV, Pal S, Mohammed A, Farooqui M, Doescher MP, Asch AS, Yamada HY. (2017) Biological effects and epidemiological consequences of arsenic exposure, and reagents that can ameliorate arsenic damage in vivo. Oncotarget. 8: 57605-57621.

Rao R, Shammo JM, Enschede SH, *et al.* (2005) The combination of fludarabine, cyclophosphamide, and granulocyte-macrophage colony-stimulating factor in the treatment of patients with relapsed chronic lymphocytic leukemia and low-grade non-Hodgkin's lymphoma. Clin Lymphoma. 6: 26-30.

Rasmussen JW, Martinez E, Louka P, Wingett DG. (2010) Zinc oxide nanoparticles for selective destruction of tumor cells and potential for drug delivery applications. Expert Opin Drug Deliv. 7: 1063-77.

Ratliff BB, Abdulmahdi W, Pawar R, Wolin MS. (2016) Oxidant Mechanisms in Renal Injury and Disease. Antioxid Redox Signal. 25: 119-46.

Rayman MP (2000) The importance of selenium to human health. Lancet. 356: 233-41.

Rayman MP, Infante HG, Sargent M. (2008a) Foodchain selenium and human health: spotlight on speciation. Br J Nutr.; 100: 238–53

Rayman MP, Rayman MP. (2002) The argument for increasing selenium intake. Proc Nutr Soc. 61: 203-15.

Rayman MP. (2005) Selenium in cancer prevention: a review of the evidence and mechanism of action. Proc Nutr Soc. 64: 527–542.

Rayman MP. (2008b) Food-chain selenium and human health: emphasis on intake. Br J Nutr. 100: 254-68.

Rayman MP. (2012) Selenium and human health. Lancet. 379: 1256-68.

Raymond LJ, Deth RC, Ralston NV. (2014) Potential Role of Selenoenzymes and Antioxidant Metabolism in relation to Autism Etiology and Pathology. Autism Res Treat. 2014: 164938.

Reddel RR et al. (1982) Ototoxicity in patients receiving cisplatin: importance of dose and method of drug administration. Cancer Treat Rep; 66: 19–23.

Reeves PG, Leary PD, Gregoire BR, Finley JW, Lindlauf JE, Johnson LK. (2005) Selenium bioavailability from buckwheat bran in rats fed a modified AIN-93G torula yeast-based diet. J Nutr. 135: 2627–2633.

Rehman MU, Tahir M, Ali F, Qamar W, Lateef A, Khan R, Quaiyoom A, Oday-O-Hamiza, Sultana S (2012) Cyclophosphamide-induced nephrotoxicity, genotoxicity, and damage in kidney genomic DNA of Swiss albino mice: the protective effect of Ellagic acid. Mol Cell Biochem 365:119–127

Reilly C. (2006) Selenium in Food and Health. 2nd ed. Springer, New York, pp. 25-86.

Reitman S, Frankel S. (1957) A colorimetric method for the determination of serum glutamic oxalacetic and glutamic pyruvic transaminases. Am J Clin Pathol. 28: 56-63.

Ren S, Yang JS, Kalhorn TF, Slattery JT. (1997) Oxidation of cyclophosphamide to 4-hydroxycyclophosphamide and deschloroethylcyclophosphamide in human liver microsomes. Cancer Res. 57: 4229-35.

Ren X, Zou L, Zhang X, Branco V. (2017) Redox Signaling Mediated by Thioredoxin and Glutathione Systems in the Central Nervous System. Antioxid Redox Signal. 27: 989-1010.

Richardson MA, Sanders T, Palmer JL, Greisinger A, Singletary SE. (2000) Complementary/ Alternative medicine use in a comprehensive cancer centre and the implication for oncology. J Clin Oncol, 18: 2505-14.

Rjiba-Touati, K, Ayed-Boussema I, Skhiri H, Belarbia A, Zellema D, Achour A, Bacha H. (2012) Induction of DNA fragmentation, chromosome aberrations and micronuclei by cisplatin in rat bone-marrow cells: protective effect of recombinant human erythropoietin. Mutat Res. 747: 202–206.

Rodrigues MS, Reddy MM & Sattler M. (2008) Cell cycle regulation by oncogenic tyrosine kinases in myeloid neoplasias: from molecular redox mechanisms to health implications. Antioxid. Redox Signal. 10, 1813–1848.

Rosenberg B, VanCamp L, Krigas T (1965) Inhibition of Cell Division in Escherichia coli by Electrolysis Products from a Platinum Electrode. Nature. 205: 698 – 699.

Rosenberg B, VanCamp L, Trosko JE. & Mansour VH. (1969). Platinum compounds: a new class of potent antitumour agents. Nature, Land. 222: 385-386.

Rotruck JT, Pope AL, Ganther HA, Swanson AB, Hafeman DG, Hoekstra WG (1973) Selenium: Biochemical role as a component of glutathione peroxidase. Science 179: 588-590.

Rozhkova EA, Ulasov I, Lai B, Dimitrijevic NM, Lesniak MS, Rajh T (2009) A high performance nanobio photocatalyst for targeted brain cancer therapy. Nano Lett 9:3337-42

Rudolf E, Radocha J, Cervinka M, Cerman J. (2004) Combined effect of sodium selenite and campthotecin on cervical carcinoma cells. Neoplasma. 51:127–135.

Rutkowski R1, Pancewicz SA, Rutkowski K, Rutkowska J. (2007) Reactive oxygen and nitrogen species in inflammatory process. Pol Merkur Lekarski. 23: 131-6.

Rybak LP, Whitworth CA (2005) Ototoxicity: therapeutic opportunities. Drug Discov Today. 10: 1313–21.

Saad SY, Najjar TA, Alashari M (2004) Role of non-selective adenosine receptor blockade and phosphodiesterase inhibition in cisplatin-induced nephrogonadal toxicity in rats. Clin Exp Pharmacol Physiol. 31: 862–867.

Saba Khan S, Parvez S, Chaudhari B, Ahmad F, Anjum S, Raisuddin S. (2013) Ellagic acid attenuates bleomycin and cyclophosphamide-induced pulmonary toxicity in Wistar rats. Food Chem Toxicol 58: 210–9.

Sablina AA. et al. (2005) The antioxidant function of the p53 tumor suppressor. Nature Med. 11, 1306–1313.

Sadeghian S, Kojouri GA, Mohebbi A. (2012) Nanoparticles of selenium as species with stronger physiological effects in sheep in comparison with sodium selenite. Biol Trace Elem Res. 146: 302-8.

Saeidnia S, Abdollahi M. (2013) Antioxidants: friends or foe in prevention or treatment of cancer: the debate of the century. Toxicol Appl Pharmacol. 271: 49-63.

Saeidnia S, Abdollahi M. (2013) Antioxidants; friends or foe in prevention or treatment of cancer; the debate of the century. Toxicol Appl Pharmacol. 271: 49–63.

Safaei R, Howell SB (2005) Copper transporters regulate the cellular pharmacology and sensitivity to Pt drugs. Crit Rev Oncol Hematol. 53:1 3-23.

Saha KS. (2017) Selenium: a vital element in soil-pant-animal/human continuum. J Agric Sci Bot. 1: 1-3.

Sahil H. Klinische Untersuchungsmethoden. 5th ed. Leipsic and Vienna. 1909: 845

Sahoo SK, Labhasetwar V. (2003) Nanotech approaches to drug delivery and imaging. Drug Discov Today. 8: 1112 - 20.

Sahu BD, Reddy KKR, Putcha UK, Kuncha M, Naidu VGM, Sistla R. (2011) Carnosic acid attenuates renal injury in an experimental model of rat cisplatin induced nephrotoxicity. Food Chem Toxi. 49: 3090–3097.

Sakakibara I, Fujino T, Ishii M, (2009) "Fasting-Induced Hypothermia and Reduced Energy Production in Mice Lacking Acetyl-CoA Synthetase 2," vol. 9, pp. 191-202.

Sanchez-Gonzalez PD, Lopez-Hernandez PJ, Perez-Barriocanal F, Morales A, Lopez-Novoa JM. (2011) Quercetin reduces cisplatin nephrotoxicity in rats without compromising its anti-tumour activity. Nephrology Dialysis Trans-plantation. 26: 3484–3495.

Sanderson BJ, Shield AJ (1996) Mutagenic damage to mammalian cells by therapeutic alkylating agents. Mutat Res 355:41-57.

Sanmartin C, Plano D, Palop JA. (2008) Selenium compounds and apoptotic modulation: a new perspective in cancer therapy. Mini Rev Med Chem. 8: 1020–1031.

Saraswati S, Agrawal SS, Alhaider AA (2013) Ursolic acid inhibits tumor angiogenesis and induces apoptosis through mitochondrial-dependent pathway in Ehrlich ascites carcinoma tumor. Chem Biol Interact 206:153-65.

Sarkar FH and Li Y. (2006) Using chemopreventive agents to enhance the efficacy of cancer therapy.Cancer Res. 66: 3347–3350.

Sattler W, Maiorino M, Stocker R. (1994) Reduction of HDL- and LDL-associated cholesterylester and phospholipid hydroperoxides by phospholipid hydroperoxide glutathione peroxidase and Ebselen (PZ 51). Arch Biochem Biophys. 309: 214-21.

Schrauzer GN. (2000) Selenomethionine: a review of its nutritional significance, metabolism and toxicity. J Nutr. 130: 1653-6.

Schueller P, Puettmann S, Micke O, Senner V, Schaefer U, Willich N. (2004) Selenium influences the radiation sensitivity of C6 rat glioma cells. Anticancer Res. 24: 2913–2917.

Schumacker PT. (2006) Reactive oxygen species in cancer cells: live by the sword, die by the sword. Cancer Cell 10, 175–176.

Schwartz PS, Waxman DJ. (2001) Cyclophosphamide induces caspase 9-dependent apoptosis in 9L tumor cells. Mol Pharmacol. 60: 1268-79.

Schwarz K, Foltz CM. (1957) Selenium as an integral part of factor 3 against dietary liver degeneration. J Am Chem Soc. 79: 3292-3293.

Scott R, Macpherson A. (1998) The effect of oral selenium supplementation on human sperm motility. Br J Urol. 82: 76-80.

Sedlack J, Lindsay RN (1968) Estimation of total protein bound and non-protein sulfhydryl groups in tissue with ellman's reagent. Annal Biochem 25:192–205

Seko Y, Saito Y, Kitara J, Imura N. (1989) Active oxygen generation by the reaction of selenite with reduced GSH *in vivo*. In Selenium in Biology and Medicine, Wendel A (ed). Springer Verlag: Berlin; 70–73.

Selvakumar E, Prahalathan C, Mythili Y, Varalakshmi P. (2006) Mitigation of oxidative stress in cyclophosphamide-challenged hepatic tissue by DL-a-lipoic acid. Mol Cell Biochem 272: 179–85.

Selvakumar E, Prahalathan C, Varalakshmi P. (2006) Modification of cyclophosphamide-induced clastogenesis and apoptosis in rats by alpha-lipoic acid. Mutat Res 606:85-91

Sengupta S, Eavarone D, Capila I, Zhao G, Watson N, Kiziltepe T, Sasisekharan R. (2005) Temporal targeting of tumour cells and neovasculature with a nanoscale delivery system. Nature 436: 568–572.

Senthil Kumar R, Rajkapoor B, Perumal P, Dhanasekaran T, Alvin Jose M, Jothimanivannan C. (2011) Antitumor Activity of Prosopis glandulosa Torr. on Ehrlich Ascites Carcinoma (EAC) Tumor Bearing Mice. Iran J Pharm Res. 10: 505-10.

Shaffer C. (2005) Nanomedicine transforms drug delivery. Drug Discov Today. 10:1581 – 2.

Shi L, Xun W, Yue W, Zhang C, Ren Y, Shi L, Wang Q, Yang R, Lei F. (2011) Effect of sodium selenite, Se-yeast and nano-elemental selenium on growth performance, Se concentration and antioxidant status in growing male goats. Small Rumin Res. 96: 49–52.

Shin SH, Yoon MJ, Kim M, Kim JI, Lee SJ, Lee YS, Bae S. (2007) Enhanced lung cancer cell killing by the combination of selenium and ionizing radiation. Oncol Rep. 17: 209–216.

Shinohara N, Gamo M, Nakanishi J. (2011) Fullerene c60: inhalation hazard assessment and derivation of a periodlimited acceptable exposure level. Toxicol Sci. 123: 576–589.

Shinomol GK and Muralidhara. (2007) Differential induction of oxidative impairments in brain regions of male mice following sub chronic consumption of Khesari dhal (Lathyrus sativus) and detoxified Khesari dhal. Neurotoxicology. 28: 798–806.

Shylesh BS, Nair SA, Subramoniam A (2005) Induction of cell specific apoptosis and protection from Dalton's lymphoma challenge in mice by an active fraction from Emilia Sonchifolia. Indian J Pharmacol 37:232–7

Siddiqui IA, Adhami VM, Bharali DJ, Hafeez BB, Asim M, Khwaja SI, et al. (2009) Introducing nanochemo-prevention as a novel approach for cancer control: proof of principle with green tea polyphenol epigallocatechin-3-gallate. Cancer Res. 69: 1712–1716.

Siddiqui IA, Adhami VM, Christopher J, Chamcheu, Mukhtar H. (2012) Impact of nanotechnology in cancer: emphasis on nanochemoprevention. Int J Nanomed. 7: 591–605.

Sies H (1985) Oxidative stress: introductory remarks, in: H. Sies (Ed.), Oxidative Stress, Academic Press, London, pp. 1–8.

Sies H, Stahl W, Sevanian A. (2005) Nutritional, dietary and postprandial oxidative stress, J. Nutr. 135: 969–972.

Sies H. (1997) Oxidative stress: oxidants and antioxidants. Exp Physiol. 82: 291–295.

Sigalov AB and Stern LJ. (1998) Enzymatic repair of oxidative damage to human apolipoprotein A-I.FEBS Lett. 433: 196–200.

Singh NP, McCoy MT, Tice RR. (1988) A simple technique for quantitation of low levels of DNA damage in individual cells. Exp Cell Res. 175: 184–191.

Sinha R, El-Bayoumy K. (2004) Apoptosis is a critical cellular event in cancer chemoprevention and chemotherapy by selenium compounds. Curr. Cancer Drug Targets 4: 13–28.

Sladek NE. (1988) Metabolism of oxazaphosphorines. Pharmacol Ther. 37: 301-55.

Słoczyńska K, Powroźnik B, Pękala E, Waszkielewicz AM. (2014) Antimutagenic compounds and their possible mechanisms of action. J Appl Genet. 55: 273-85.

Snider GW, Ruggles E, Khan N, Hondal RJ. (2013) Selenocysteine confers resistance to inactivation by oxidation in thioredoxin reductase: comparison of selenium and sulfur enzymes. Biochemistry. 52: 5472-81.

Sofo A, Scopa A, Nuzzaci M, Vitti A. (2015) Ascorbate Peroxidase and Catalase Activities and Their Genetic Regulation in Plants Subjected to Drought and Salinity Stresses. Int J Mol Sci. 16: 13561-78.

Soignet SL et al. (1998) Complete remission after treatment of acute promyelocytic leukemia with arsenic trioxide. N. Engl. J. Med. 339, 1341–1348.

Soliman AM, Desouky S, Marzouk M, Sayed AA. (2016) Origanum majorana Attenuates Nephrotoxicity of Cisplatin Anticancer Drug through Ameliorating Oxidative Stress. Nutrients. 8: 5.

Spallholz J E (1994) On the nature of selenium toxicity and carcinostatic activity. Free Radic Biol Med17: 45–64

Spallholz JE, Palace VP, Reid TW. (2004) Methioninase and selenomethionine but not Se-methylselenocysteine generates methylselenol and superoxide in an in vitro chemiluminescent assay: implications for the nutritional carcinostatic activity of selenoamino acids. Biochem Pharmacol. 67: 547–554.

Spallholz JE, Shriver BJ, Reid TW. (2001) Dimethyldiselenide and methylseleninic acid generates superoxide in an in vitro chemiluminesence assay in the presence of glutathione: Implications for the anticarcinogenic activity ofl-selenomethionine andl-Se-methylselenocysteine. Nutr Cancer. 40: 34–41.

Speckmann B, Steinbrenner H. (2014) Selenium and selenoproteins in inflammatory bowel diseases and experimental colitis. Inflamm Bowel Dis. 20: 1110-9.

Sporn MB, Newton DL. (1979) Chemoprevention of cancer with retinoids. Fed. Proc. 38: 2528–2534.

Springer JB, Colvin ME, Colvin OM, Ludeman SM. (1998) Isophosphoramide mustard and its mechanism of bisalkylation. J Org Chem. 63: 7218-22.

Srivastava A and Shivanandappa T. (2010) Hepatoprotective effect of the root extract of Decalepis hamiltonii against carbon tetrachloride-induced oxidative stress in rats. FoodChem. 118: 411–417.

Srivastava A, Shivanandappa T (2010) Hepatoprotective effect of the root extract of *Decalepis hamiltonii* against carbon tetrachloride-induced oxidative stress in rats. Food Chem 118:411–417.

Stadtman ER. (2000) Protein oxidation in aging and age-related diseases. Ann N Y Acad Sci. 928:22–38.

Strebhardt K, Ullrich. (2008) Paul Ehrlich's magic bullet concept: 100 years of progress. Nat Rev Cancer 8: 473-480.

Struck RF, Kirk MC, Witt MH, Laster WR. (1975) Isolation and mass spectral identification of blood metabolites of cyclophosphamide: evidence for phosphoramide mustard as the biologically active metabolite. Biomed Mass Spectrom. 2: 46-52.

Suadicani P, Hein HO, Gyntelberg F. (1992) Serum selenium concentration and risk of ischaemic heart disease in a prospective cohort study of 3000 males. Atherosclerosis. 96: 33-42.

Sugie S, Tanaka T and El-Bayoumy K. (2000) Chemoprevention of carcinogenesis by organoselenium compounds. J Health Sci. 46: 422–425.

Sullivan R & Graham CH. (2008) Chemosensitization of cancer by nitric oxide. Curr. Pharm. Des. 14, 1113–1123.

Sun XM, MacFarlane M, Zhuang J, Wolf BB, Green DR, Cohen GM. (1999) Distinct caspase cascades are initiated in receptor-mediated and chemical-induced apoptosis. J Biol Chem. 274: 5053-60.

Sunde RA. (1997) Selenium. In: O'Dell BL, Sunde RA, eds, Handbook of nutritionally essential mineral elements. New York: Marcel Dekker Inc. pp. 493-556.

Sung MJ, Kim DH, Jung YJ, Kang KP, Lee AS, et al., (2012) Genistein protects the kidney from cisplatin-induced injury. Kidney Int. 74: 1538-47.

Suzuki KT, Kurasaki K, Suzuki N. (2007) Selenocysteine beta-lyase and methylselenol demethylase in the metabolism of Se-methylated selenocompounds into selenide. Biochim Biophys Acta. 1770: 1053–1061.

Suzuki KT, Ogra Y. (2002) Metabolic pathway for selenium in the body: speciation by HPLC-ICP MS with enriched Se. Food Addit Contam. 19: 974-83.

Svensson BG, Schütz A, Nilsson A, Akesson I, Akesson B, Skerfving S. (1992) Fish as a source of exposure to mercury and selenium. Sci Total Environ. 126: 61-74.

Swartz HM & Gutierrez PL. (1977) Free radical increases in cancer: evidence that there is not a real increase. Science 198, 936–938.

Szatrowski TP & Nathan CF. (1991) Production of large amounts of hydrogen peroxide by human tumor cells. Cancer Res. 51, 794–798.

Szatrowski TP, Nathan CF (1991) Production of large amounts of hydrogen peroxide by human tumor cells. Cancer Res 51:794-8

Sznarkowska A, Kostecka A, Meller K, Bielawski KP. (2017) Inhibition of cancer antioxidant defense by natural compounds. Oncotarget. 8: 15996-16016.

Szumilas P, Barcew K, Baskiewicz-Masiuk M, Wiszniewska B, Ratajczak MZ, Machalinski B. (2005) Effect of stem cell mobilization with cyclophosphamide plus granulocyte colony-stimulating factor on morphology of haematopoietic organs in mice. Cell Prolif. 38: 47-61.

Takahashi A. et al. (2006) Mitogenic signalling and the p16INK4a-Rb pathway cooperate to enforce irreversible cellular senescence. Nature Cell Biol. 8, 1291–1297.

Talas ZS, Ozdemir I, Gok Y. (2010) Role of selenium compounds on tyrosine hydroxylase activity, adrenomedullin and total RNA levels in hearts of rats.Regul Pept 159: 137–141.

Tan TW, Pfau B, Jones D, Meyer T. (2014) Stimulation of primary osteoblasts with ATP induces transient vinculin clustering at sites of high intracellular traction force. J Mol Histol. 45: 81-9.

Tanguy S, Boucher F, Besse S, Ducros V, Favier A, de Leiris J. (1998) Trace elements and cardioprotection: increasing endogenous glutathione peroxidase activity by oral selenium supplementation in rats limits reperfusion-induced arrhythmias. J Trace Elem Med Biol. 12:28-38.

Tannock IF, Ahles TA, Ganz PA, Van Dam FS. (2004) Cognitive impairment associated with chemotherapy for cancer: report of a workshop. J Clin Oncol. 22: 2233-9.

Tarze A, Dauplais M, Grigoras I, Lazard M, Ha-Duong NT, Barbier F, Blanquet S, Plateau P. (2007) Extracellular production of hydrogen selenide accounts for thiol-assisted toxicity of selenite against Saccharomyces cerevisiae. J Biol Chem. 282: 8759-67.

Thant AA, Wu Y, Lee J, Mishra DK, Garcia H, Koeffler HP, Vadgama JV. (2008) Role of caspases in 5-FU and seleniuminduced growth inhibition of colorectal cancer cells. Anticancer Res. 28:3579–3592.

The Freedonia Group. Nanotechnology in Health Care; US Industry Study with Forecasts to 2011, 2016, & 2021; Study #2168; The Fredonia Group: Cleveland, OH, USA, 2007.

Thompson HJ, Ip C. (1991) Temporal changes in tissue glutathione in response to chemical form, dose, and duration of selenium treatment. Relevance to cancer chemoprevention by selenium. Biol Trace Elem Res. 30: 163–173.

Thorlacius-Ussing O. (1990) Selenium-induced growth retardation. Histochemical and endocrinological studies on the anterior pituitaries of selenium treated rats. Danish Medical Bulletin 37: 4, 347–358.

Tiwary AK, Stegelmeier BL, Panter KE, James LF, Hall JO. (2006) Comparative toxicosis of sodium selenite and selenomethionine in lambs. J Vet Diagn Invest. 18: 61–70.

Tominaga T, Hachiya M, Shibata T, Sakamoto Y, Taki K, Akashi M. (2012) Exogenously-added copper/zinc superoxide dismutase rescues damage of endothelial cells from lethal irradiation. J Clin Biochem Nutr. 50: 78–83.

Trachootham D, Alexandre J, Huang P. (2009) Targeting cancer cells by ROS-mediated mechanisms: a radical therapeutic approach? Nat Rev Drug Discov. 8: 579–591.

Trachootham D, Lu W, Ogasawara MA, Nilsa RD & Huang P. (2008) Redox regulation of cell survival. Antioxid Redox Signal. 10, 1343–1374.

Tsen CC, Tappel AL. (1958) Catalytic oxidation of glutathione and other sulfhydral compounds by selenite. J Biol Chem. 233: 1230–1232.

Tuomilehto J, Pohjola M, Lindström J, Aro A. (1994) Acarbose and nutrient intake in non-insulin dependent diabetes mellitus. Diabetes Res Clin Pract. 26: 215-22.

Ungva´ri E, Monori I, Megyeri A et al. (2014) Protective effects of meat from lambs on selenium nanoparticle supplemented diet in a mouse model of polycyclic aromatic hydrocarbon-induced immunotoxicity. Food Chem Toxicol 64C:298–306

Ungvári É, Monori I, Megyeri A, Csiki Z, Prokisch J, Sztrik A, Jávor A, Benkő I. (2014) Protective effects of meat from lambs on selenium nanoparticle supplemented diet in a mouse model of polycyclic aromatic hydrocarbon-induced immunotoxicity. Food Chem Toxicol. 64: 298-306.

Ushio-Fukai M & Nakamura Y. (2008) Reactive oxygen species and angiogenesis: NADPH oxidase as target for cancer therapy. Cancer Lett. 266, 37–52.

Ushio-Fukai M, Alexander RW (2004) Reactive oxygen species as mediators of angiogenesis signaling: role of NAD(P)H oxidase. Mol Cell Biochem 264:85-97.

Vadgama JV, Wu Y, Shen D, Hsia S, Block J. (2000) Effect of selenium in combination with Adriamycin or Taxol on several different cancer cells. Anticancer Res. 20: 1391–1414.

Valdiglesias V, Pásaro E, Méndez J, Laffon B. (2010) In vitro evaluation of selenium genotoxic, cytotoxic, and protective effects: a review. Arch Toxicol. 84: 337-51.

Valko M, Izakovic M, Mazur M, Rhodes CJ, Telser J. (2004) Role of oxygen radicals in DNA damage and cancer incidence. Mol Cell Biochem. 266: 37–56.

Valko M, Rhodes CJ, Moncol J, Izakovic M and Mazur M. (2006) Free radicals, metals and antioxidants in oxidative stress-induced cancer. Chem Biol Interact. 160: 1-40.

Van Wart HE, Birkedal-Hansen H. (1990) The cysteine switch: a principle of regulation of metalloproteinase activity with potential applicability to the entire matrix metalloproteinase gene family. Proc Natl Acad Sci U S A. 87: 5578-82.

Vanhaelen N, Francis F, Haubruge E. (2004) Purification and characterization of glutathione-S-transferases from two syrphid flies (Syrphus ribesii and Myathropa florea). Comp Biochem Physiol B Biochem. Mol Biol. 137: 95–100.

Waksman G, Krishna TS, Williams CH Jr, Kuriyan J. (1994) Crystal structure of Escherichia coli thioredoxin reductase refined at 2 A resolution. Implications for a large conformational change during catalysis. J Mol Biol. 236: 800-16.

Wang CH, Huang YF, Yeh CK. (2011a) Aptamer-conjugated nanobubbles for targeted ultrasound molecular imaging. Langmuir. 27: 6971–6976.

Wang X, Zhang J and Xu T. (2007) Cyclophosphamide as a potent inhibitor of tumor thioredoxin reductase in vivo. Toxicol Appl Pharmacol. 218: 88–95.

Wang Y, Chen P, Zhao G, Sun K, Li D, Wan X, Zhang J (2015) Inverse relationship between elemental selenium nanoparticle size and inhibition of cancer cell growth *in vitro* and *in vivo*. Food Chem Toxicol 85:71-7

Wei D, Chen T, Yan M, Zhao W, Li F, Cheng W, Yuan L. (2015b) Synthesis, characterization, antioxidant activity and neuroprotective effects of selenium polysaccharide from Radix hedysari. Carbohydr Polym. 125: 161-8.

Wei J, Zeng C, Gong QY, Yang HB, Li XX, Lei GH, Yang TB. (2015a) The association between dietary selenium intake and diabetes: a cross-sectional study among middle-aged and older adults. Nutr J. 14: 18.

Whanger P, Vendeland S, Park YC, Xia Y (1996) Metabolism of subtoxic levels of selenium in animals and humans. Ann Clin Lab Sci 26:99-113

Whitesides GM. (2003) The "right" size in nanobiotechnology. Nat Biotechnol. 21: 1161 - 5.

Wintrobe MM, Lee DR, Boggs DR, Bithel TC, Athens JW, Foerester J (1961) Clinical Hematology, fifth ed. Philadelphia

World Cancer Report 2014, IARC Nonserial Publication, Stewart, B. W., Wild, C. P. IARC.

Wrobel JK, Power R, Toborek M. (2016) Biological activity of selenium: Revisited. IUBMB Life. 68: 97-105.

Xia Y, Hill KE, Byrne DW, Xu J, Burk RF. (2005) Effectiveness of selenium supplements in a low-selenium area of China. Am J Clin Nutr. 81: 829-34.

Xia Y, Hill KE, Byrne DW, Xu J, Burk RF. (2005) Effectiveness of selenium supplements in a low-selenium area of China. Am J Clin Nutr. 81: 829-34.

Xiang N, Zhao R, Zhong W. (2009) Sodium selenite induces apoptosis by generation of superoxide via the mitochondrial-dependent pathway in human prostate cancer cells. Cancer Chemother Pharmacol. 63: 351–362.

Yan L, Boylan LM, Spallholz JE. (1990) Cytotoxic effect of selenium (Se) on human mammary tumor cells *in vitro*. FASEB J. 4: A1063.

Yan L, Spallholz JE. (1993) Generation of reactive oxygen species from the reaction of selenium compounds with thiols and mammary tumor cells. Biochem Pharmacol. 45: 429–437.

Yan L, Yee JA, Boylan LM, Spallholz JE. (1991) Effect of selenium compounds and thiols on human mammary tumor cells. Biol Trace Elem Res. 30: 145–162.

Yan LJ (2014) Pathogenesis of chronic hyperglycemia: from reductive stress to oxidative stress. J Diabetes Res. 2014-ID 137919.

Yazdi MH, Masoudifar M, Varastehmoradi B, Mohammadi E, Kheradmand E, Homayouni S, Shahverdi AR. (2013) Effect of Oral Supplementation of Biogenic Selenium Nanoparticles on White Blood Cell Profile of BALB/c Mice and Mice Exposed to X-ray Radiation. Avicenna J Med Biotechnol. 5: 158-67.

Yilmaz HR, Iraz M, Sogut S, Ozyurt H, Yildirim Z, Akyol O, Gergerlioglu S (2004) The effects of erdosteine on the activities of some metabolic enzymes during cisplatin-induced nephrotoxicity in rats. Pharmacol Res. 50: 287-90.

Yoon SO, Kim MM, Chung AS (2002) Inhibitory effect of selenite on invasion of HT1080 tumor cells. J Biol Chem 276:20085-20092

Yoshida Y, Itoh N, Saito Y, Hayakawa M, Niki E (2004) Application of water soluble radical initiator, 2,2-azobis[2-(2-imidazolin-2-yl)propane] di-hydrochloride, to a study of oxidative stress. Free Radical Research 38: 375–384

Yousef MI, Saad AA, El-Shennawy LK (2009) Protective effect of grape seed proanthocyanidin extract against oxidative stress induced by cisplatin in rats. Food Chem Toxicol. 47: 1176–1183.

Yousefipour Z, Ranganna K, Newaz MA, Milton SG (2005) Mechanism of acrolein-induced vascular toxicity. J Physiol Pharmacol 56:337–353

Yousefipour Z, Ranganna K, Newaz MA. (2005) Mechanism of acrolein-induced vascular toxicity. J Physiol Pharmacol. 56: 337–353.

Yu MW, Horng IS, Hsu KH, Chiang YC, Liaw YF, Chen CJ. (1999) Plasma selenium levels and risk of hepatocellular carcinoma among men with chronic hepatitis virus infection. Am J Epidemiol.150: 367-74.

Yule SM, Price L, McMahon AD, Pearson AD, Boddy AV. (2004) Cyclophosphamide metabolism in children with non-Hodgkin's lymphoma. Clin Cancer Res. 10: 455-60.

Zanotto-Filho A, Masamsetti VP, Loranc E, Tonapi SS, Gorthi A, Bernard X, Gonçalves RM, Moreira JC, Chen Y, Bishop AJ. (2016) Alkylating Agent-Induced NRF2 Blocks Endoplasmic Reticulum Stress-Mediated Apoptosis via Control of Glutathione Pools and Protein Thiol Homeostasis. Mol Cancer Ther. 15: 3000-3014.

Zemlickis D, Lishner M, Erlich R, Koren G. (1993) Teratogenicity and carcinogenicity in a twin exposed in utero to cyclophosphamide. Teratog Carcinog Mutagen. 13: 139-43.

Zeng H, Combs GF Jr. (2008) Selenium as an anticancer nutrient: roles in cell proliferation and tumor cell invasion. J Nutr Biochem. 19: 1–7.

Zeng HW, Cheng WH, Johnson LK. (2013) Methylselenol, a selenium metabolite, modulates p53 pathway and inhibits the growth of colon cancer xenografts in Balb/c mice. J Nutr Biochem. 24: 776-80.

Zhang J, Wang X and Xu T. (2008) Elemental selenium at nano size (Nano-Se) as a potential chemopreventive agent with reduced risk of selenium toxicity: comparison with semethylselenocysteine in mice. Toxicol Sci. 101: 22–31.

Zhang J, Wang X and Xu T. (2008) Elemental selenium at nanosize (Nano-Se) as a potential chemopreventive agent with reduced risk of selenium toxicity: comparison with semethylselenocysteine in mice.Toxicol Sci. 101: 22–31.

Zhang JS, Gao XY, Zhang LD, Bao YP. (2001) Biological effects of a nano red elemental selenium. Biofactors. 15: 27-38.

Zhang L, Gu FX, Chan JM, Wang AZ, Langer RS, Farokhzad OC. (2008) Nanoparticles in medicine: therapeutic applications and developments. Clin Pharmacol Ther. 83: 761–769.

Zhang Q, Kang X, Zhao W. (2006) Antiangiogenic effect of low-dose cyclophosphamide combined with ginsenoside Rg(3) on Lewis lung carcinoma. Biochem Biophys Res Commun 342: 824–828.

Zhang Q, Yang J, Wang J. (2016) Modulatory effect of luteolin on redox homeostasis and inflammatory cytokines in a mouse model of liver cancer. Oncol Lett. 12: 4767-4772.

Zhang QH, Wu CF, Duan L, Yang JY. (2008) Protective effects of ginsenoside Rg(3) against cyclophosphamide-induced DNA damage and cell apoptosis in mice. Arch Toxicol. 82: 117-23.

Zhang W, Chen Z, Liu H, L. Zhang L, Gao P, Li D. (2011) Biosynthesis and structural characteristics of selenium nanoparticles by *Pseudomonas alcaliphila*. Colloids Surf. B. 88: 196-201.

Zhang XF, Liu ZG, Shen W, Gurunathan S. (2016) Silver Nanoparticles: Synthesis, Characterization, Properties, Applications, and Therapeutic Approaches. Int J Mol Sci. 13: 17.

Zhang ZX, Yang XG, Xia YM, Chen XS. (1998) Progress in the study of mammalian selenoprotein. Sheng Li Ke Xue Jin Zhan. 29: 29-34.

Zhao L, Cox A, Ruzicka JA, Bhat AA, Zhang W, Taylor EW. (2000) Molecular modeling and in vitro activity of an HIV-1-encoded glutathione peroxidase. Proc Natl Acad Sci USA. 97: 6356-6361.

Zhivotovsky B, Samali A, Orrenius S (2001) Determination of apoptosis and necrosis. Curr Protoc Toxicol, Chapter 2:Unit 2.2

Zhou N, Xiao H, Li TK, Nur EK, Liu LF. (2003) DNA damage-mediated apoptosis induced by selenium compounds. J Biol Chem 278: 29532–29537.

Zhou X, Wang Y. (2011) Influence of dietary nano elemental selenium on growth performance, tissue selenium distribution, meat quality, and glutathione peroxidase activity in Guangxi Yellow chicken. Poultry Science. 90: 680-686.

Zhou Y, Hileman EO, Plunkett W, Keating MJ & Huang P. (2003) Free radical stress in chronic lymphocytic leukemia cells and its role in cellular sensitivity to ROSgenerating anticancer agents. Blood 101, 4098–4104.

Zhu Z, Kimura M, Itokawa Y, Nakatsu S, Oda Y, Kikuchi H. (1995) Effect of selenium on malignant tumor cells of brain. Biol Trace Elem Res. 49: 1–7.

Zoidis E, Seremelis I, Kontopoulos N, Danezis GP. (2018) Selenium-Dependent Antioxidant Enzymes: Actions and Properties of Selenoproteins. Antioxidants (Basel).7 (5).

Zorbas H, Keppler BK (2005) Cisplatin damage: are DNA repair proteins saviors or traitors to the cell? Chembiochem. 6: 1157–66.

Zou AP, Li N, Cowley AW Jr (2001) Production and actions of superoxide in the renal medulla. Hypertension 37:547-53

Zurer I. (2004) The roles of p53 in base excision repair following genotoxic stress. Carcinogenesis 25, 11–19

Publications and Presentations

Protective effect of Selenium nanoparticle against cyclophosphamide induced hepatotoxicity and genotoxicity in Swiss albino mice

Arin Bhattacharjee, Abhishek Basu, Prosenjit Ghosh, Jaydip Biswas and Sudin Bhattacharya

J Biomater Appl published online 12 February 2014
DOI: 10.1177/0885328214523323

JOURNAL OF
biomaterials applications

Article

Journal of Biomaterials Applications
0(0) 1–15

DOI: 10.1177/0885328214523323
jba.sagepub.com
SAGE

Protective effect of Selenium nanoparticle against cyclophosphamide induced hepatotoxicity and genotoxicity in Swiss albino mice

Arin Bhattacharjee[1], Abhishek Basu[1], Prosenjit Ghosh[1], Jaydip Biswas[2] and Sudin Bhattacharya[1]

Abstract

Cyclophosphamide (CP) is the most commonly used chemotherapeutic drug for various types of cancer. However, its use causes severe cytotoxicity to normal cells in human. It is well known that the undesirable side effects are caused due to the formation of reactive oxygen species. Selenium is an essential micronutrient for both animals and humans and has antioxidant and membrane stabilizing property, but selenium is also toxic above certain level. Nano selenium has been well proved to be less toxic than inorganic selenium as well as certain organoselenium compounds. The objective of the study is to evaluate the protective role of Nano-Se against CP-induced hepatotoxicity and genotoxicity in Swiss albino mice. CP was administered intraperitoneally (25 mg/kg b.w.) and Nano-Se was given by oral gavages (2 mg Se/kg b.w.) in concomitant and pretreatment scheme. Intraperitoneal administration of CP induced hepatic damage as indicated by the serum marker enzymes aspartate and alanine transaminases and increased the malonaldehyde level, depleted the glutathione content and antioxidant enzyme activity (glutathione peroxidase, glutathione-s-transferase, superoxide dismutase and catalase), and induced DNA damage and chromosomal aberration. Oral administration of Nano-Se caused a significant reduction in malonaldehyde, ROS level and glutathione levels, restoration of antioxidant enzyme activity, reduction in chromosomal aberration in bone marrow, and DNA damage in lymphocytes and also in bone marrow. Moreover, the chemoprotective efficiency of Nano-Se against CP induced toxicity was confirmed by histopathological evaluation. The results support the protective effect of Nano-Se against CP-induced hepatotoxicity and genotoxicity.

Keywords

Nano-Se, cyclophosphamide, oxidative stress, hepatotoxicity, genotoxicity, antioxidant enzyme

Introduction

Cancer chemotherapy has been shown to play an important role in the treatment of most solid tumors, but has also been associated with substantial short- and long-term side effects. These side effects affect the quality of life in cancer patients. A growing body of evidence suggests that a combination treatment of chemotherapy and chemopreventive agents with anticarcinogenic activity may enhance the efficacy of chemotherapeutics and reduce the systemic toxicity induced by chemotherapy.[1] Cyclophosphamide (CP), the alkylating agent is widely used as an anti-tumor and immunosuppressive agent. However, despite the fact that its use causes severe cytotoxicity to normal cells in experimental animals and humans,[2,3] clinicians prescribe it as the first line of treatment for the cancer patients. It shows no activity against cancer cells *in vitro* until it undergoes metabolic activation catalyzed by liver cytochrome P450 enzymes[4] to produce reactive metabolites such as 4-hydroxy-CP, acrolein, and phosphoramide mustard. These metabolites can alkylate nucleophilic sites in DNA, RNA, and protein

[1]Chittaranjan National Cancer Institute, Department of Cancer Chemoprevention, Kolkata, West Bengal, India
[2]Chittaranjan National Cancer Institute, Department of Translational Research, Kolkata, West Bengal, India

Corresponding author:
Sudin Bhattacharya, Chittaranjan National Cancer Institute, Department of Cancer Chemoprevention, 37, S.P. Mukherjee Road, Kolkata 700026, West Bengal, India.
Email: sudinb19572004@yahoo.co.in

such as –SH, –COOH, $–NH_2$, and $–OH^2$ which cause cellular toxicity, genotoxicity, and mutagenic effects.[5]

Selenium (Se) is an essential micronutrient for higher animals and humans.[6,7] The best-known biological roles of selenium are linked to its presence as the functional component in selenoenzymes such as glutathione peroxidase (GPx) and thioredoxin reductase (TrxR). Se incorporates into proteins such as selenocysteine and prevents oxidative damage to body tissues.[8] The cancer-preventive properties of Se have been proved according to epidemiologic, clinical, and experimental studies.[9] A number of experiments have revealed that both organic and inorganic Se compounds possess chemopreventive effects.[10] However, the use of inorganic Se (sodium selenite) as well as naturally occurring Se (such as selenomethionine and selenocystein) is often restricted due to its toxic effects.[11–13] Selenium nano particle is increasingly drawing attention due to its excellent anticancer activities and low toxicity.[14,15] The toxicity reported for elemental selenium (Se^0) at nano size is lower than the toxicity of selenate (Se^{+2}) or selenite (Se^{+4}) ions; therefore, selenium nano particle may be a good candidate to replace other forms of selenium in nutritional supplements or pharmaceutical dosage forms.[14] Many studies showed that Nano-Se exhibited novel *in vitro* and *in vivo* antioxidant activities through the activation of selenoenzymes.[14–18] Thus, the development of nano particles of selenium with higher antioxidative and chemoprotective efficacy is attracting the interest of the researcher.

The aim of this study was to determine whether Nano-Se protects against hepatotoxicity and genotoxicity induced by CP. The extent of the protective effect of Nano-Se against CP-induced hepatotoxicity and its anti-genotoxic effects were determined by studying the antioxidant enzymes status and markers of genotoxicity (comet assay, chromosomal aberration) in Swiss albino mice.

Materials and methods

Experimental animals

Adult (5–6 weeks) Swiss albino female mice (25 ± 2g), bred in the animal colony of Chittaranjan National Cancer Institute (CNCI) (Kolkata, India), were used for this study. The mice were maintained under standard condition of humidity (45–55%), temperature ($23 \pm 2^{\circ}$C), and light (12 h light/12 h dark). Standard food pellets (EPIC rat and mice pellet) from Kalyani Feed Milling Plant, Kalyani, West Bengal, India and drinking water was provided *ad libitum*. The experiments were carried out following strictly the Institute's guideline for the Care and Use of Laboratory Animals (Reg. no. 175/99/CPCSEA).

Chemicals

CP was obtained from Cadila Pharmaceuticals (Bhat, Ahmedabad, India). 1-Chloro-2, 4-dinitrobenzene (CDNB), ethylene diamine tetraacetic acid (EDTA), reduced glutathione (GSH), pyrogallol, 5,5′-dithio-bis (2-nitro benzoic acid) (DTNB), sodium dodecyl sulphate (SDS), bovine serum albumin (BSA), β-nicotinamide adenine dinucleotide phosphate (reduced), glutathione reductase, normal melting agarose, low melting point agarose, ethidium bromide, sodium azide (NaN_3), HEPES, 2′,7′- dichloro fluorescence diacetate (DCFH-DA), dimethyl sulphoxide (DMSO), Triton-X 100, and Giemsa stain were obtained from Sigma-Aldrich Chemicals Private Limited, Bangalore, India. Hydrogen peroxide 30% (H_2O_2), thioberbituric acid (TBA), propylene glycol, sodium carbonate, copper sulfate, sodium hydroxide, potassium-sodium tartrate, sucrose, TRIS, dithiothreitol, calcium chloride, di-sodium hydrogen phosphate, sodium di-hydrogen phosphate, acetic acid, n-butanol, pyridine, hematoxylin, and eosin were obtained from Merck (India) Limited, Mumbai, India. Chloroform and Folin-phenol reagent were purchased from Sisco Research Laboratories Private Limited, Mumbai, India. Magnesium chloride was purchased from Glaxo laboratories (India) Ltd, Bombay. Diethyl ether, dipotassium hydrogen phosphate, and potassium dihydrogen phosphate were obtained from Spectrochem Private Limited, Mumbai, India. Serum alanine transaminas (ALT) and aspartate transaminase (AST) assay kits were obtained from Span Diagnostics Ltd, Udhna, Surat, India.

Preparation of Nano Selenium

The Nano-Se was synthesized following a simplified protocol with slight modifications.[16] Then 5 ml of 25 mM sodium selenite was mixed with 20 ml of 25 mM reduced GSH containing 200 mg BSA. The mixture was adjusted to pH 7.2 with 1.0 M sodium hydroxide, when the red elemental Se and oxidized glutathione (GSSG) formed. The red solution was dialyzed against double distilled water for 96 h with the water changing every 24 h to separate GSSG from Nano-Se under magnetic stirring. The final solution containing Nano-Se and BSA was subjected to centrifugation at 13,000 rpm for 10 min. The pellet thus recovered was subjected to washing by its re-suspension in de-ionized water followed by centrifugation at 13,000 rpm for 10 min, to remove possible organic contamination present in the nano particles. Finally, pellet was freeze-dried using a lyophilizer and stored at room temperature.

Characterization of Nano Selenium

The obtained products were characterized by using various microscopic and spectroscopic methods. Transmission Electron Microscopic (TEM) analysis was carried out with Techni 20 (Philips, Holland) for size determination. For this purpose, a thin film of the sample was prepared on a carbon-coated copper grid by dropping a very small amount of the sample on to the grid. The size and morphology of the synthesized Nano-Se were analyzed using a Scanning Electron Microscope (SEM) (FEI Quanta—200 MK2). The spectrum of the energy dispersive X-ray spectroscopy (EDAX) of the sample was carried out using an XL-30 (Philips, Netherlands) operating at 15–25 kV and employed to examine the elemental composition.

Drug preparation

The synthesized Nano-Se was dissolved in saline (0.9% NaCl) and administered orally. It was prepared on each day just before treatment.

Experimental groups

Animals were distributed into five groups containing six animals in each group.

Vehicle treated group (Group I): Each animal was given oral administration of saline (0.9% NaCl) from day 1 to day 10 and was kept as normal.

Nano Selenium treated group (Group II): Animals were treated orally with Nano-Se only at a dose of 2 mg Se/kg b.w. throughout the experimental period.

CP-treated group (Group III): CP was administered intraperitoneally at a dose of 25 mg/kg b.w. in water for 10 days.

Concomitant treatment group (Group IV): Nano-Se was administered orally at a dose of 2 mg Se/kg b.w. for 10 days and CP was given as in Gr. III.

Pretreatment group (Group V): Nano-Se was administered orally at a dose of 2 mg Se/kg b.w. seven days prior to the CP treatment and then continued along with CP for 10 days.

The mice were sacrificed on day 11, and the parameters described further were studied.

Biochemical estimation

Determination of intracellular ROS production. ROS generation was measured in liver homogenate using DCFH-DA following a simplified protocol with slight modifications.[19,20] DCFH-DA is a non-fluorescent probe that is hydrolyzed by mitochondrial esterase to form 2′, 7′-dichlorodihydrofluorescein (DCFH), which is then oxidized by ROS to form the fluorescent compound 2′, 7′-dichlorofluorescein (DCF). Liver tissues were homogenized in Locke's Buffer (pH 7.4 containing 140 mM NaCl, 5 mM KCl, 10 mM HEPES, 1 mM $CaCl_2$, 1 mM $MgCl_2$, 10 mM glucose) to yield a 10% w/v homogenate. 250 µl of tissue homogenate in whole was taken and then loaded with 30 µl of 10 µM DCFH-DA to make a final volume of 3 ml. The samples were incubated in dark for 45 min to allow the formation of DCF and then analyzed for fluorescence (excitation 485 nm/emission 530 nm) using spectrofluorimeter (Varian Cary Eclipse). Values were expressed as fluorescence intensity normalized per milligram of protein.

Quantitative estimation of lipid peroxidation

The level of lipid peroxides formed was measured using TBA and expressed as nmol of thiobarbituric acid reactive substances (TBARS) formed per milligram of protein using the extinction co-efficient of $1.56 \times 10^5\,M^{-1}\,cm^{-1}$.[21]

Isolation of serum

Blood samples were collected from mice by retro-orbital puncture under anesthesia (Thiopentone Sodium) and centrifuged at 3000 rpm for 5 min for serum separation. Finally, serum samples were stored in aliquots at −20°C for later use. All serum samples were thawed once at the time of the assay.

Measurement of serum biochemical parameters

Alanine aminotransferase (ALT) and aspartate aminotransferase (AST) level were measured spectrophotometrically by standard enzymatic method using commercial kits (Span Diagnostics Ltd.).[22]

Estimation of reduced glutathione level

Glutathione (GSH) level was estimated in liver cytosol spectrophotometrically by determination of DTNB reduced by −SH groups by measuring the absorbance at 412 nm. The level of GSH was expressed as nmol/mg of protein.[23]

Estimation of glutathione-S-transferase activity

Glutathione-S-transferase (GST) activity was measured in the liver cytosol. The enzyme activity was determined from the increase in absorbance at 340 nm with CDNB as the substrate and specific activity of the enzyme was expressed as formation of CDNB-GSH conjugate/min/mg of protein.[24]

Estimation of glutathione peroxidase activity

Glutathione peroxidase (GPx) activity in liver was measured by NADPH oxidation using a coupled reaction system consisting of GSH, glutathione reductase and H_2O_2.[25] Briefly, 100 µl of enzyme sample was incubated for 10 min with 800 µl reaction mixtures (0.25 M potassium phosphate buffer containing 2.5 mM EDTA and 2.5 mM sodium azide, 10 mM GSH, 2.5 mM NADPH, and 2.4 units of glutathione reductase). The reactions started on adding 100 µl H_2O_2 and follow the decrease in NADPH absorbance at 340 nm for 3 min. The enzyme activity was expressed as micromole NADPH utilized/min/mg of protein, using extinction co-efficient of NADPH at 340 nm as 6200 $M^{-1}cm^{-1}$.

Estimation of superoxide dismutase activity

Superoxide dismutase (SOD) activity was determined by quantification of Pyrogallol auto-oxidation inhibition and expressed as unit/mg of protein. One unit of enzyme activity is defined as the amount of enzyme necessary for inhibiting the reaction by 50%. Auto-oxidation of Pyrogallol in Tris–HCl buffer (50 mM, pH 7.5) is measured by increase in absorbance at 420 nm.[26,27]

Estimation of catalase activity

Catalase (CAT) activity in liver cytosol was determined spectrophotometrically at 250 nm and expressed as unit/mg of protein, where the unit is the amount of enzyme that liberates half the peroxide oxygen from H_2O_2 in second at 25°C.[28]

Hemoglobin level

Hemoglobin (Hb) content of blood samples was measured with the Sahli's method.[29]

Estimation of protein

Total protein content in tissue homogenate during biochemical analysis was measured through Lowry method using Folin-Phenol reagent.[30] The absorbance of the color was measured against the colorless blank sample at 660 nm using the Varian Cary 100 UV–Vis Spectrophotometer.

Tissue section preparation and histopathological evaluation

Qualitative changes in liver tissues were determined by histologically. In brief, the tissues were sliced into 5–6 mM thick sections and fixed for 48 h in 10% formaline, dehydrated in an ascending graded series of ethanol, cleared in xylene, and embedded in paraffin. Sections of the tissues were cut by rotary microtome and stained with hematoxylin and eosin. Stained sections were evaluated by observing the arrangement of liver architecture with a light microscope (Leica DM 1000). Photomicrographs were taken with the software Las EZ.

Detection of DNA damage in lymphocyte by Comet assay

Possible DNA damage induced by CP was detected using the alkaline single cell gel electrophoresis (comet assay) following a simplified protocol with slight modification.[31,32] The mice were sacrificed and blood was collected from each mouse of all groups. Lymphocytes were isolated from blood samples by standard centrifugation over a cushion of Histopaque, washed with isotonic solution, and centrifuged. The pellet was re-suspended in isotonic phosphate-buffered saline solution. The cell viability in each group was measured and approximately 10^4 cells/slide were taken for the assay. An aliquot of 10 µl of freshly prepared single cell suspension was mixed with 1% low melting agarose and layered on the half-frosted slides precoated with normal melting agarose. A third layer of 0.5% low melting point agarose was layered on the top of the second layer. The cells were lysed for overnight at 4°C in lysing solution containing 2.5 M NaCl, 100 mM Na_2EDTA, 10 mM Tris buffer, 1% Triton X 100, and 10% DMSO (pH 10.0). After lysis, the slides were subjected to electrophoresis in electrophoresis buffer [1 mM Na_2EDTA and 0.3 M NaOH (pH>13.1)] for 30 min at 300 mA and 20 V. After electrophoresis, the slides were neutralized with neutralizing buffer [0.4 M Tris buffer (pH 7.5)]. The microscopic slides were carefully dried at room temperature and stained with ethidium bromide in water (20 µg/ml; 50 µl/slide). The slides were examined at 400× magnification under a fluorescence microscope (Model: Leica DM 4000B) with imaging system. Komet 5.5 software was used to take the photomicrograph of cells and to determine the length of the comet tail. About 150–200 randomly selected cells (5–7 zones/slide) in each slide were counted (four slides/animals in each group) to determine the number of damaged cells and then the percentage of damaged cells was calculated using the following formula.

$$\%\text{demage cell} = \left(\frac{\text{Number of demaged cell}}{\text{Total number of cells counted}}\right) \times 100 \quad (1)$$

The results were expressed as:

(1) Percentage of cells with tail (tailed cells) in each group was scored and
(2) Average tail length due to DNA migration in each group.

Preparation of bone marrow cells

Bone marrow cells suspension was prepared from femurs of each animal, where the bone was split longitudinally and the marrow was exposed using forceps and the content of the femur was flushed gently using 2 ml syringe containing PBS (pH 7.4) into a centrifuge tube. The cells were collected by centrifugation to perform comet assay, chromosomal aberration, and ROS generation of bone marrow cells.

Detection of DNA Damage in bone marrow (Comet Assay)

The influence of Nano-Se on CP-induced DNA damage in mouse bone marrow cells was studied by alkaline single cell gel electrophoresis (comet assay), according to the *in vivo* comet assay guidelines of Singh et al.[33] The bone marrow cells in PBS were dispersed by gentle pipetting and collected by centrifugation at 1000 rpm for 10 min at 4°C. Cell pellets were re-suspended with PBS and the density of cells was adjusted to 1×10^6/ml and used for further analysis. The methodology was same as described in detection of DNA Damage in lymphocyte by Alkaline Single Cell Gel Electrophoresis (Comet Assay) with modifications.

ROS generation in bone marrow cells

Following animal sacrifice, bone marrow cells from the femur bone were collected in PBS (pH 7.4). Intracellular ROS production was detected by using a fluorescent probe DCFH-DA, according to the method[34] with slight modifications. The cells were then centrifuged and resuspended in PBS in the order of 10^7 cells/ml. Bone marrow cells were then incubated with DCFH-DA (10 μM in DMSO) for 45 min at 37°C in dark to allow the formation of DCF and then analyzed for fluorescence (excitation 485 nm/emission 530 nm) using spectrofluorimeter (Varian Cary Eclipse).

Analysis of chromosomal aberrations

Mice were injected intraperitoneally with 0.03% colchicine at the rate of 1 ml/100 g b.w. 90 min before sacrifice. Marrow of the femur was flushed in 1% sodium citrate solution at 37°C and fixed in acetic acid/ethanol (1:3). Slides were prepared by the conventional flame drying technique[35] followed by Giemsa staining for scoring bone marrow chromosomal aberrations (CA). CA of various natures such as stretching, terminal association, break, fragment, ring formation, etc., were analyzed. A total of 300 bone marrow cells were observed, 60 from each of 5 mice of a set.

Statistical analysis

All data were presented as mean ± SD, $n = 6$ animals per group. One way ANOVA followed by Tukey's Multiple Comparison Test using Graph Pad Prism (Version 5.00) software was performed for comparisons among groups. Significant difference was indicated when the $P < 0.05$.

Result

Characterization of Nano-Se

The properties of Nano-Se were studied by TEM, SEM, and EDAX. The synthesized Nano-Se aqueous solution was clear. Figure 1(a) shows the morphology and microstructure of Nano-Se as examined by TEM and the image revealed the particles to be in the size range of 40–55 nm, with an average size of 45 nm. SEM image (Figure 1b) of the Nano-Se revealed an average size of 35 nm; most of the nano particles being in the size range of 30–40 nm. The purity of the substance was confirmed by EDAX analysis (Figure 1c). EDAX analysis gives qualitative as well as quantitative status of elements that may be involved in formation of nano particles. The EDAX of the nano particle dispersion confirmed the presence of elemental selenium. The analysis revealed the highest proportion of selenium (64.28%) in nano particles followed by carbon (18.03%), oxygen (17.31%), and sulphur (0.38%).

Biological properties and application

Nano selenium did not generate any significant change in the parameters investigated when administered alone as compared to the vehicle control group (Gr. I).

Attenuation of ROS level

Intraperitoneal administration of CP significantly ($P < 0.05$) elevated ROS level in liver and in bone marrow cells by 52.8% and 63.03%, respectively, in Gr. III as compared to the vehicle control group (Gr. I). Concomitant treatment (Gr. IV) and pretreatment (Gr. V) with Nano-Se caused a sharp reduction in ROS level in liver as well as in bone marrow cells. Concomitant treatment (Gr. IV) with Nano-Se significantly reduced ROS level in liver by 13.73% and in bone marrow cells by 37.80% respectively, but on seven days pretreatment (Gr.V) with the same inhibited the ROS level much more significantly by 43.49% in liver and by 52.76% in bone marrow cells in comparison to the CP-treated group (Gr. III) (Figure 2(a) and (b)).

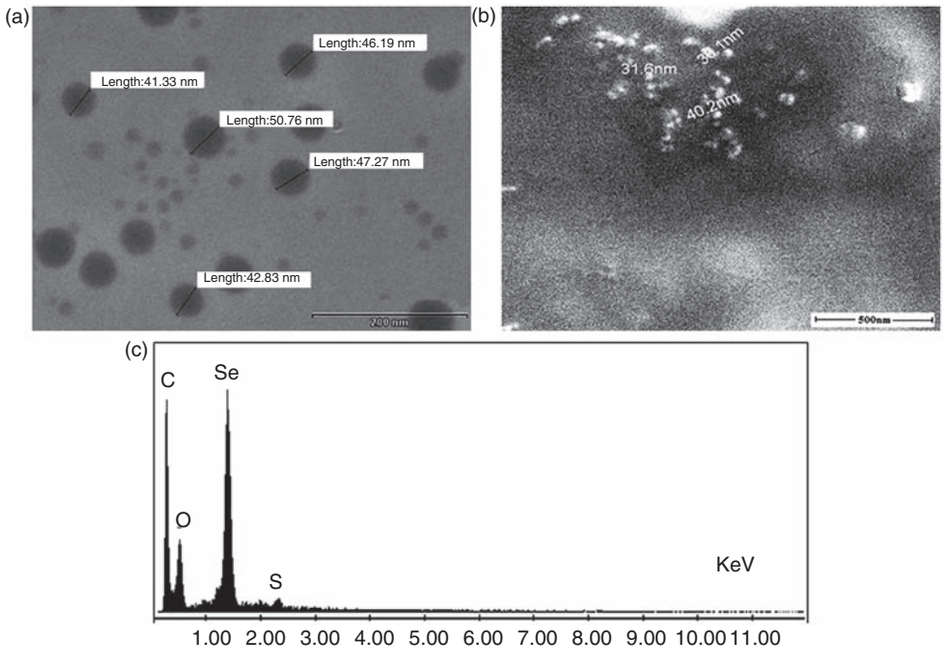

Figure 1. (a) Transmission electron microscope image of Nano-Se; (b) Scanning electron microscope image of Nano-Se; (c) Energy dispersive X-ray spectroscopy analysis of Nano-Se.

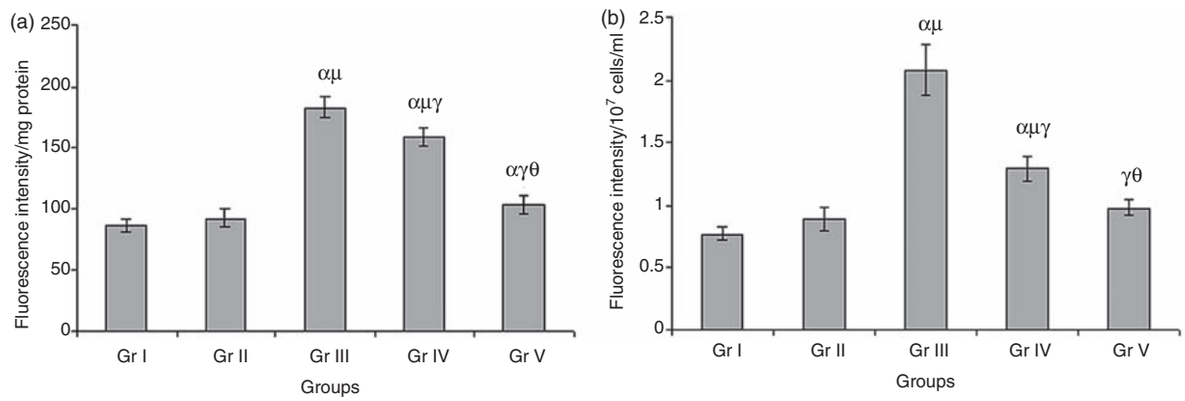

Figure 2. Effect of Nano-Se on hepatic ROS level (a) and bone marrow ROS level (b) after administration of CP. Data were represented as mean ± SD (n=6). α—significant ($P < 0.05$) as compared with Gr. I; μ—significant ($P < 0.05$) as compared with Gr. II; γ—significant ($P < 0.05$) as compared with Gr. III; θ—significant ($P < 0.05$) as compared with Gr. IV.

Inhibition of LPO level

Intraperitoneal administration of CP significantly ($P < 0.05$) elevated LPO level by 47.51% in Gr. III compared to Gr. I (Figure 3(a)). Concomitant treatment (Gr. IV) with Nano-Se inhibited LPO level in liver by 17.73%, but seven days pretreatment (Gr. V) with the same inhibited the elevated LPO level in liver by 26.24% in comparison to Gr. III.

Modulation of serum ALT and AST activity by Nano-Se in CP treated mice

A significant ($P < 0.05$) elevation of 59.47% in ALT activity was observed after 10 days of CP treatment (Gr. III) as compared to vehicle treatment (Gr. I) (Table 1). Concomitant (Gr. IV) and pretreatment (Gr. V) with Nano-Se reduced the enzyme activity significantly by 47.71% and by 58.82% respectively, as

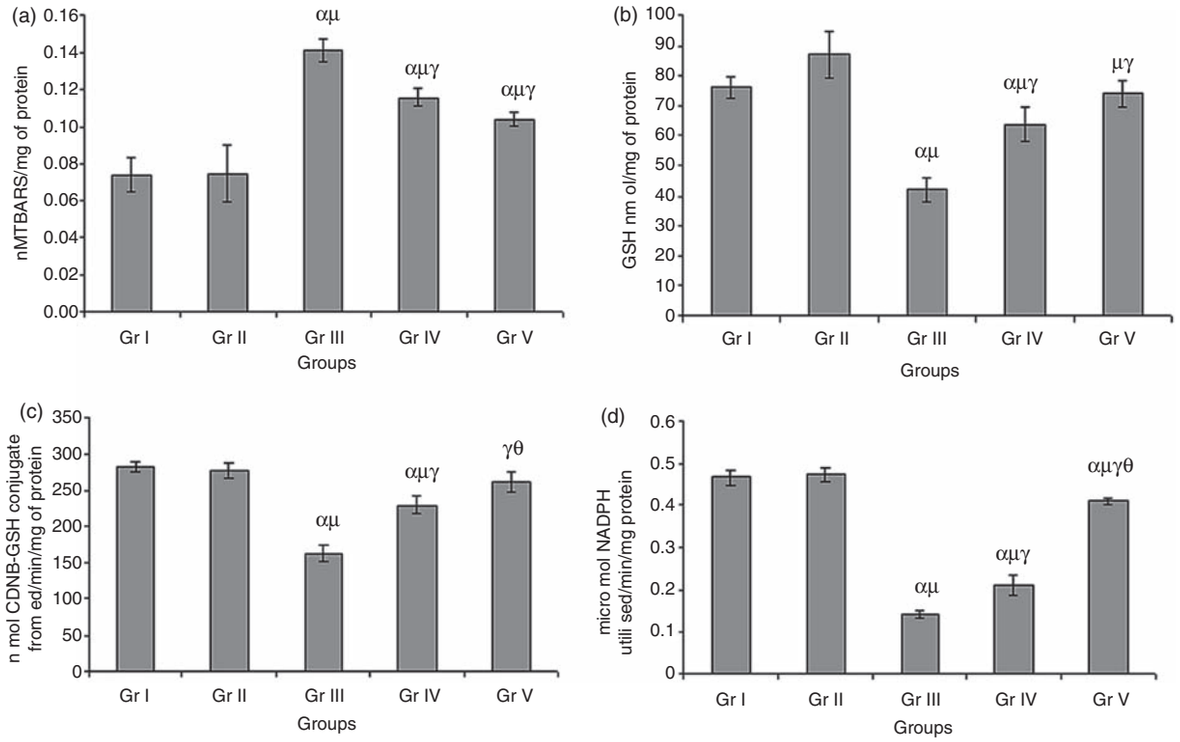

Figure 3. Effect of Nano-Se on hepatic LPO level (a), hepatic GSH level (b), hepatic GST activity (c), and hepatic GPx activity (d) after administration of CP. Data were represented as mean ± SD (n=6). α—significant ($P < 0.05$) as compared with Gr. I; μ—significant ($P < 0.05$) as compared with Gr. II; γ—significant ($P < 0.05$) as compared with Gr. III; θ—significant ($P < 0.05$) as compared with Gr. IV.

compared to CP-treated animals (Gr. III). There was also a significant ($P < 0.05$) elevation in serum AST activity by 44.28% in CP-treated animals as compared to vehicle-treated group (Gr. I). Concomitant (Gr. IV) and pretreatment (Gr. V) with Nano-Se reduced the enzyme activity significantly by 29.14% and by 41.71%, respectively, as compared to CP-treated animals (Gr. III).

Enhancement of GSH level

The liver GSH concentration decreased significantly ($P < 0.05$) by 44.9% in CP-treated animals compared to Gr. I (Figure 3(b)). Nano-Se treatment prevented this depletion of GSH by 34.23% (Gr. IV) in case of concomitant and by 43.18% (Gr. V) in case of pretreatment compared to that observed with CP alone treated mice (Gr. III).

Enhancement of GST activity

The GST activity in liver decreased significantly ($P < 0.05$) by 42.53% in Gr. III in comparison to Gr. I (Figure 3c). Pretreatment with Nano-Se caused the GST activity to rise sharply by 37.85% (Gr. V); however, concomitant treatment with same elevated GST activity by 29.33% (Gr. IV) as compared to CP alone treated group (Gr. III).

Modulation of GPx activity

Administration of CP significantly ($P < 0.05$) reduced the GPx activity by 69.49% in Gr. III compared to Gr. I (Figure 3d). Concomitant treatment (Gr. IV) and pre treatment (Gr. V) with Nano-Se increased the GPx activity significantly by 32.39% and 65.33%, respectively, as compared to the Gr. III.

Amelioration of SOD activity

Intraperitoneal administration of CP substantially ($P < 0.05$) decreased the SOD activity by 63.25% in Gr. III compared to Gr. I (Figure 4(a)). Concomitant administration of Nano-Se increased the enzyme activity by 30.42% (Gr. IV) and seven days pretreatment sharply increased the activity of SOD by 50.47% (Gr. V) as in comparison to the CP-alone treated group (Gr. III).

Increase of CAT activity

CAT activity in the liver decreased significantly ($P < 0.05$) by 50.64% (Gr. III) in the CP-treated

group compared to the Gr. I (Figure 4(b)). Administration of Nano-Se effectively prevented the decline of CAT activity and restored the activity by 41.49% (Gr. IV) in the case of concomitant treatment and by 46.23% (Gr. IV) in the case of pretreatment as compared to CP-alone treated mice (Gr. III).

Modulation of blood Hb level by Nano-Se in CP treated mice

The hemoglobin level in blood decreased significantly by 25.73% in CP-treated group (Gr. III) in comparison to the vehicle control group (Gr. I) (Table 1). Concomitant treatment (Gr. IV) and pretreatment (Gr. V) with Nano-Se increased the hemoglobin level in blood significantly by 19.57% and by 23.27% respectively as compared to the CP treated group (Gr. III).

Histopathological observation

Histopathological analysis of liver tissue sections of mice exposed to CP showed abnormalities as compared to the vehicle control mice (Figure 5(a) to (e)). Liver sections from the vehicle control (Gr. I) and Nano-Se treated mice showed normal hepatic lobules formed of hepatocytes radiating from central vein to the periphery of the lobules. In contrast, the exposure of CP to mice induced degenerative changes in the liver organ. CP caused inflammatory cellular infiltration in between degenerated hepatocytes, formation of pyknotic nuclei, and hepatocellular necrosis. Concomitant treatment (Gr. V) with Nano-Se showed mild cellular infiltration and necrosis, but in pretreatment group (Gr. VI) liver appeared almost normal.

Table 1. Effect of Nano-Se on serum ALT, AST activity and blood Hb levels in mice treated with CP.

Group	ALT (U/ml)	AST (U/ml)	Hb (g/dl)
I	24.8 ± 2.28	156.0 ± 3.16	14.38 ± 0.52
II	24.4 ± 2.96	154.0 ± 5.83	13.44 ± 1.21
III	$61.2 \pm 3.03^{\alpha\mu}$	$280.4 \pm 7.97^{\alpha\mu}$	$10.68 \pm 1.41^{\alpha\mu}$
IV	$32.0 \pm 2.44^{\alpha\mu\gamma}$	$198.4 \pm 8.76^{\alpha\mu\gamma}$	$13.28 \pm 0.46^{\gamma}$
V	$25.2 \pm 2.28^{\gamma\theta}$	$163.2 \pm 3.63^{\gamma\theta}$	$13.92 \pm 0.87^{\gamma}$

Note: Data were represented as mean $\pm$ SD (n=6). α—significant ($P < 0.05$) as compared with Gr. I; μ—significant ($P < 0.05$) as compared with Gr. II; γ—significant ($P < 0.05$) as compared with Gr. III; θ—significant ($P < 0.05$) as compared with Gr. IV.

Comet assay finding in mouse peripheral lymphocyte and bone marrow cells

Evaluation of the level of DNA damage (according to their comet tail length) induced by CP in mouse peripheral lymphocyte (Figure 6(a) to (e)) and in bone marrow cells (Figure 7(a) to (e)) was observed. For this purpose, percentage of damaged cells and the average tail length was measured. Nano-Se did not induce any genotoxicity in mouse peripheral lymphocyte cells and bone marrow cells.

Percentage of damaged cells in each group

The frequency of damaged lymphocytes and of bone marrow cells were 12.65% and 10.02% respectively in Gr. I (Table 2). The CP administration caused a significant ($P < 0.05$) increase in the percentage of damaged lymphocytes and bone marrow cells by 53.69% and 49.51% respectively in Gr. III. In case of concomitant treatment (Gr. IV), the percentages of damaged cells were reduced to 42.41% in lymphocyte and 34.95% in bone marrow cells respectively; however, pretreatment (Gr. V) with Nano-Se sharply decreased the percentage of damaged cells to 32.21% and 26.58% respectively, in lymphocytes and bone marrow cells.

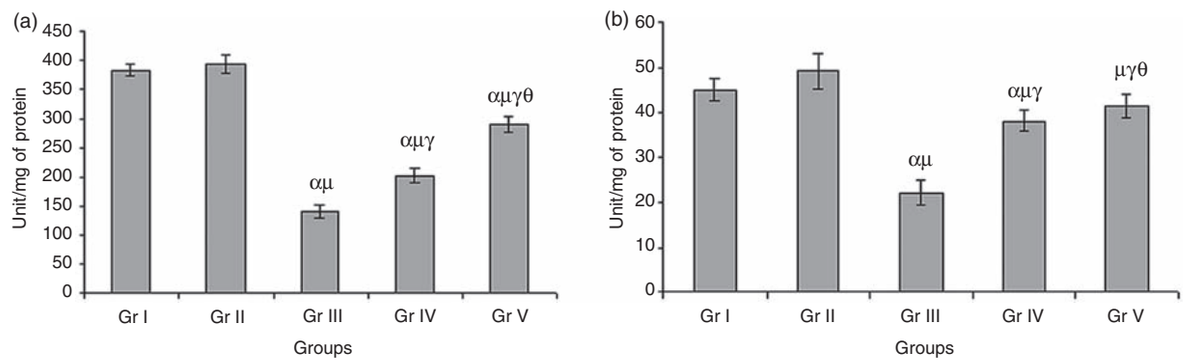

Figure 4. Effect of Nano-Se on hepatic SOD activity (a) and hepatic CAT activity (b) after administration of CP. Data were represented as mean $\pm$ SD (n=6). α—significant ($P < 0.05$) as compared with Gr. I; μ—significant ($P < 0.05$) as compared with Gr. II; γ—significant ($P < 0.05$) as compared with Gr. III; θ—significant ($P < 0.05$) as compared with Gr. IV.

Average Tail Length due to DNA Migration in each group

The magnitudes of average tail length were $15.69 \pm 1.67\,\mu m$ and $7.29 \pm 1.30\,\mu m$, respectively, in lymphocyte and bone marrow cells in Gr. I. CP caused a marked increase in the magnitude of tail length to $66.72 \pm 2.89\,\mu m$ in lymphocyte and to $55.39 \pm 3.83\,\mu m$ in bone marrow cells in Gr. III (Table 2). Oral administration of Nano-Se in concomitant (Gr. IV) and pretreatment (Gr. V) schedule resulted in the reduction of average tail length to $42.13 \pm 1.55\,\mu m$ and $23.07 \pm 1.04\,\mu m$, respectively, in

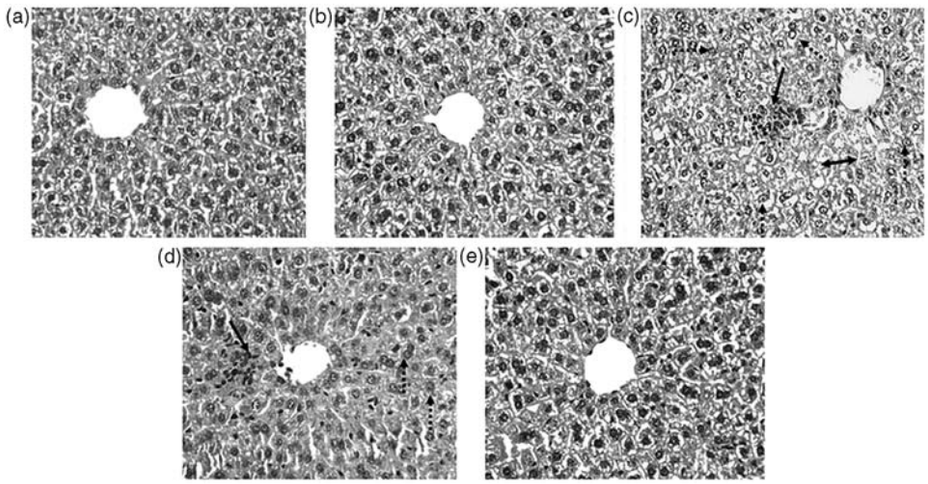

Figure 5. Photograph of liver section of mice stained with hematoxylin and eosin: (a) Liver section from the vehicle control group (Gr. I) showing normal arrangement of hepatocytes with clear nuclei (H&E; 400×); (b) Liver section from only Nano-Se treated group (Gr. II) showing normal liver architecture same as Gr. I (H&E; 400×); (c) Treatment with CP (Gr. III) showing loss of hepatic architecture, inflammatory cellular infiltration (arrow), pyknotic nuclei (dotted arrow) and necrosis (double headed arrow) (H&E; 400×). (d) Concomitant treatment (Gr. IV) with Nano-Se shows minimal cellular infiltration (arrow) and reduced the formation of pyknotic nuclei (dotted arrow) (H&E; 400×); (e) Liver section of pretreated group (Gr. V) with Nano-Se restored the morphology of the liver from the damage induced by CP as marked from the normal histology of vehicle control liver (H&E; 400×). H&E: haematoxylin and eosin.

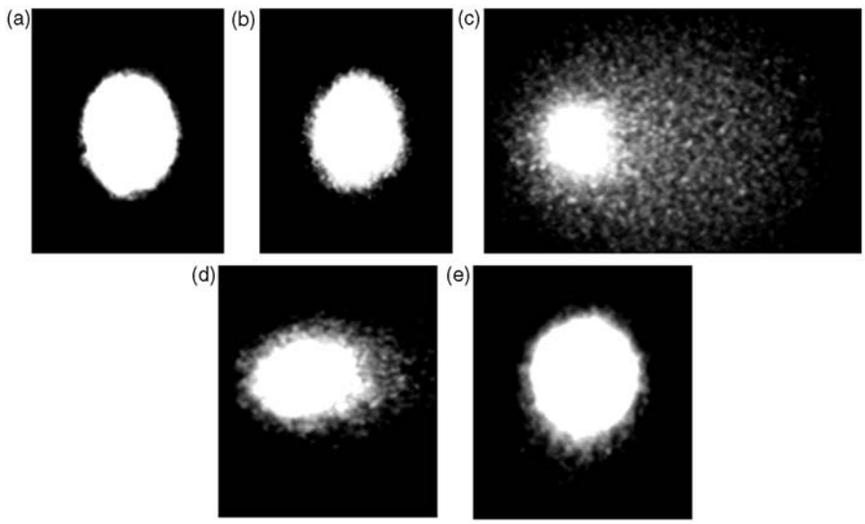

Figure 6. Photomicrographs of lymphocytes showing DNA damage: (a) no significant DNA migration in Gr. I; (b) very fewer DNA migration in Gr. II; (c) highly migrated DNA with distinct scattered comet tail in Gr. III; (d) less migrated DNA and less diffused comet tail in Gr. IV; and (e) no or very less migrated DNA in Gr. V.

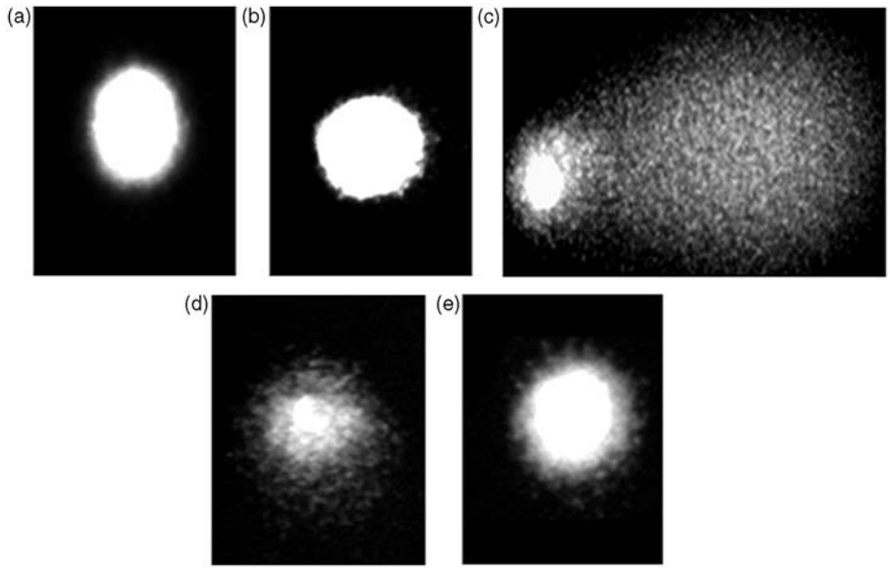

Figure 7. Photomicrographs of bone marrow cells showing DNA damage: (a) no significant DNA migration in Gr. I; (b) very fewer DNA migration in Gr. II; (c) extremely migrated DNA with distinct scattered comet tail in Gr. III; (d) less migrated DNA and less diffused comet tail in Gr. IV; and (e) no or minimal migrated DNA in Gr. V.

Table 2. Effect of Nano-Se against CP induced DNA damage in peripheral lymphocytes and bone marrow of mice.

	Peripheral lymphocyte		Bone marrow	
Group	Damaged cells showing comet (%)	Average tail length (μm)	Damaged cells showing comet (%)	Average tail length (μm)
I	12.65 ± 0.83	15.69 ± 1.67	10.02 ± 1.90	7.29 ± 1.30
II	11.77 ± 1.45	14.03 ± 1.42	9.95 ± 1.08	6.99 ± 0.74
III	$53.69 \pm 1.18^{\alpha\mu}$	$66.72 \pm 2.89^{\alpha\mu}$	$49.51 \pm 3.55^{\alpha\mu}$	$55.39 \pm 3.83^{\alpha\mu}$
IV	$42.41 \pm 2.54^{\alpha\mu\gamma}$	$42.13 \pm 1.55^{\alpha\mu\gamma}$	$34.95 \pm 3.23^{\alpha\mu\gamma}$	$21.45 \pm 2.45^{\alpha\mu\gamma}$
V	$32.21 \pm 1.29^{\alpha\mu\gamma\theta}$	$23.07 \pm 1.04^{\alpha\mu\gamma\theta}$	$26.58 \pm 3.03^{\alpha\mu\gamma\theta}$	$11.8 \pm 1.81^{\alpha\mu\gamma\theta}$

Note: Data were represented as mean ± SD (n=6). α—significant ($P < 0.05$) as compared with Gr. I; μ—significant ($P < 0.05$) as compared with Gr. II; γ—significant ($P < 0.05$) as compared with Gr. III; θ—significant ($P < 0.05$) as compared with Gr. IV.

case of lymphocytes, and 21.45 ± 2.45 μm and 11.8 ± 1.81 μm, respectively, in case of bone marrow cells.

Prevention of chromosomal aberration

Animals treated with CP (Gr. III) showed significantly ($P < 0.05$) high proportion of chromosomal aberration of 41.13% (Figures 8 and 9(a) and (b)) compared to relatively low incidence of chromosomal aberration of 12.67% in vehicle control group (Gr. I). The frequency of chromosomal aberration was 27.85% and 21.24%, respectively, in case of concomitant (Gr. IV) and pre-treatment (Gr. V) groups, which were significantly much lesser compared to the CP-treated group (Gr. III).

Discussion

Chemotherapy has long been a cornerstone of cancer therapy. Extensive research is being done on the development of more effective and less toxic antineoplastic agents, but less attention has been paid to factors that may enhance the therapeutic efficacy of the drugs and at the same time reduce the deleterious side effects imparted by the therapeutic compounds such as CP. The clinical outcome of treatment with these agents is severely limited, mostly due to their toxicity to normal tissues. Therefore, there is a necessity to develop adjuvant therapy to improve the efficacy of the treatment or reduce the associated undesirable side effects. It is well known that the redox balance of a cell is disturbed

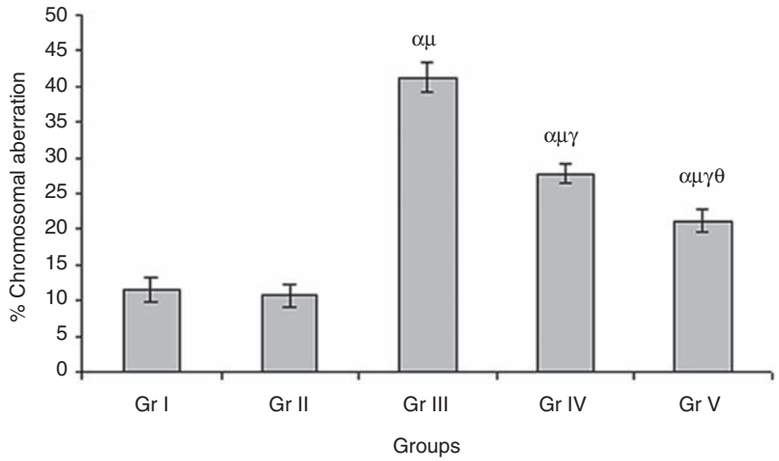

Figure 8. Protective effect of Nano-Se on CP induced chromosomal aberration. Data were represented as mean ± SD. α—significant ($P < 0.05$) as compared with Gr. I; μ—significant ($P < 0.05$) as compared with Gr. II; γ—significant ($P < 0.05$) as compared with Gr. III; θ—significant ($P < 0.05$) as compared with Gr. IV.

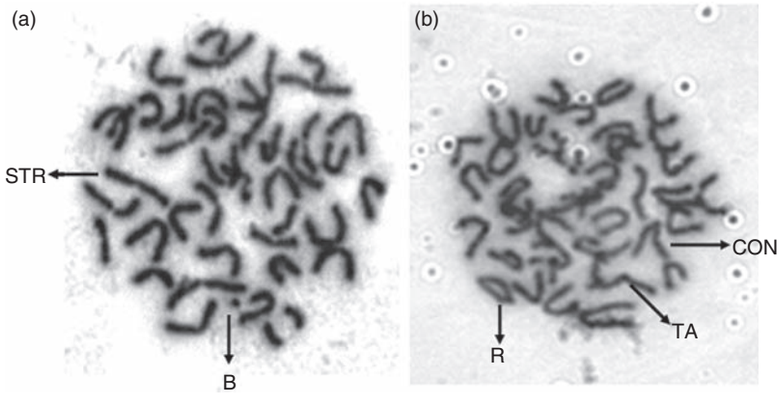

Figure 9. Metaphase complements showing (a) stretching (STR), break (B); (b) terminal association (TA), constriction (CON), and ring (R).

during the excessive production of ROS, causing oxidative stress, cancer, and finally cell death.[36] Several studies described important beneficial properties of selenium as an antioxidant agent.[37,38] Very recently, it has been reported that meat from lamb supplemented with Nano-Se enriched diet has the ability to protect 7,12-dimethyl-benz(a)anthracene (DMBA)-induced oxidative stress injury in mice.[39] Reports obtained from the present study indicated that CP treatment increased ROS level in the liver cytosol as well as in bone marrow cells as measured by the DCFH-DA assay. The oxidation of DCFH to the fluorescent compound DCF is modulated mainly by hydroperoxides including H_2O_2 [40] and peroxynitrite.[41] The endogenous H_2O_2 level may be used as an indirect measure of superoxide anion, which is produced due to the rapid rate of the dismutation of superoxide anions. In the present study, Nano-Se significantly inhibited CP-induced ROS formation in liver cytosol and also in bone marrow cells which may possibly be due to its antioxidant property.

CP has a pro-oxidant character and its administration is associated with induction of oxidative stress by the generation of free radicals.[42] LPO is widely used as a marker of oxidative stress, and cell membrane damage resulting in gradual loss of membrane fluidity, decreased membrane potential, and increased permeability to ions.[43] The present study showed increased lipid peroxidation in the liver of CP-treated mice which was associated with hepatic damage. Treatment with Nano-Se prevented the CP-induced lipid

peroxidation which could be attributed to the free radical quenching activity of Nano-Se and thus protecting against oxidative membrane damage in mice.

ALT and AST are the most sensitive biomarkers directly implicated in the extent of hepatic damage and toxicity.[44] In present study, we demonstrated that CP administration to mice provoked a marked elevation in serum ALT and AST activities which indicated hepatocellular damage. This elevation could potentially be attributed to the release of these enzymes from the hepatic cytoplasm into the blood circulation. However, treatment with Nano-Se restored the activities of ALT and AST toward normal. Pretreatment with Nano-Se exhibited better preventive activity against hepatocellular damage than concomitant treatment group.

GSH plays a vital role in protecting cells against oxidative injury. The depletion of GSH level, due to CP treatment could be attributed to the direct conjugation of metabolites of CP with GSH, which leads to induction of oxidative stress.[45] GSH depletion leads to lowering cellular defense against free radical-induced cellular injury resulting in necrotic cell death.[46] In the present study, the result showed that the mechanism of hepatoprotection by Nano-Se against CP-induced toxicity and hepatic damage involves suppression of oxidative stress by preventing GSH depletion.

GSH metabolizing enzyme GST catalyses the detoxification of endogenous compounds such as lipid peroxide, as well as the metabolites of xenobiotics such as acrolein, a metabolite of CP, through conjugation of GSH via the sulfhydryl group.[47] The hepatic GST activity decreased significantly by CP administration. Concomitant as well as pretreatment with Nano-Se restored the activity near to vehicle-treated group.

The selenium-containing glutathione peroxidase (GPx) contains a single selenocysteine (Sec) residue, which is essential for enzyme activity.[48,49] GPx catalyses the reduction of hydroperoxides utilizing GSH, thereby protecting mammalian cells against oxidative damage. In fact, glutathione metabolism is one of the most essential antioxidative defense mechanisms.[50] The decreased activity of the antioxidant enzyme GPx in this experiment after administration of CP may be either due to the decreased level of GSH as a substrate[51] or inability of liver to produce this enzyme. Treatment with Nano-Se prevented the depletion of GPx activity in liver, thus providing protection of biomembrane from oxidative attack.

Cellular antioxidant defenses involving the enzymes, SOD, and CAT detoxify the free radicals and the consequent oxidative stress. SOD catalyzes dismutation of the superoxide anion to H_2O_2 and O_2. CP-induced hepatotoxicity is associated with oxidative stress caused by the reduction in these antioxidant enzymes activities.[52] In the present observation, the activities of SOD and CAT in the liver were significantly reduced by CP treatment indicating pronounced oxidative stress. In this study, administration of Nano-Se restored SOD and CAT activities, indicating that Nano-Se can modulate these enzyme activities. Pretreating with the Nano-Se restored the antioxidant enzyme activities much more than the concomitant treatment.

The most common problems encountered in cancer chemotherapy are myelosuppression and anemia.[53] This is because chemotherapeutic drugs kill rapidly dividing cells in the body, including cancer cells and normal cells which include red blood cells, at the same time suppress bone marrow ability to produce new ones, resulting in decrease in blood Hb level. In the present study, treatment with CP reduced the blood Hb level which was also attenuated by the treatment with Nano-Se.

The histopathological studies affirm that CP can damage liver tissues. These were manifested by an inflammatory cellular infiltration, formation of pyknotic nuclei and necrosis. These observations indicated marker changes in the overall histoarchitecture of liver in response to CP, which could be due to its toxic effects primarily by the generation of reactive oxygen species causing damage to the various membrane components of the cell. Concomitant treatment with Nano-Se could not prevent hepatotoxicity completely; however, when pretreated with Nano-Se resulted in excellent protection against hepatotoxicity induced by CP and showed predominant normal liver morphology.

The important finding of the present study is that Nano-Se significantly inhibits CP-induced DNA damage in mouse peripheral lymphocyte cells and bone marrow cells. CP can induce DNA–DNA and DNA–protein crosslinks.[54] CP can also generate reactive species, for damaging DNA.[55] In the present study, the percentage of affected cells showing a comet tail significantly increased after CP treatment in blood lymphocytes as well as in bone marrow cells, whereas treatment with Nano-Se significantly decreased DNA damage in peripheral lymphocyte cells and also in bone marrow cells, which clearly indicated the potential role of Nano-Se in protecting DNA damage.

Oxidative stress can induce CA through oxidative base damage and strand breaks in DNA contributing to mutagenesis.[56,57] Genotoxic activity of CP resulted from metabolic activation to the highly reactive metabolite phosphoramide mustard. CP produces chromosome damage and micronuclei formation in the erythropoietic system of rats, mice, and Chinese hamsters via production of highly active carbonium ions.[58,59] In the present study, animals treated with CP presented a significant increase in total number of chromosomal aberration in bone marrow cells when

compared to the vehicle-treated animals. Treatment with Nano-Se produced significant reduction of chromosomal aberration in bone marrow cells.

Conclusion

The present study provided for the first time evidence that Nano-Se attenuates CP-induced oxidative stress and the subsequent DNA damage in both the peripheral blood and the bone marrow cells of mice. The anti-genotoxic effect of Nano-Se might be due to its antioxidant and cytoprotective activity. However, additional studies using other end points with possible mechanistic evidences are required to elucidate the precise mechanism of protection offered by Nano-Se.

Funding

This work was financially supported by Grant from Indian Council of Medical Research, New Delhi, India (no. 45/36/2008/PHA-BMS). Arin Bhattacharjee gratefully acknowledges ICMR for Senior Research Fellowship. Abhishek Basu also gratefully acknowledges ICMR for Senior Research Fellowship (no. 3/2/2/58/2011/NCD-III).

Acknowledgements

The authors wish to thank the Director, CNCI, for supporting this study. The authors are grateful to Mr Sanjay Patel and Mr Vikash Patel, Technical Officer at DST sponsored SICART (Sophisticated Instrumentation Center for Applied Research and Testing) Anand, Gujarat, India, for their help in analysis of sample for TEM and EDAX.

References

1. Sarkar FH and Li Y. Using chemopreventive agents to enhance the efficacy of cancer therapy. *Cancer Res* 2006; 66: 3347–3350.
2. Fraiser LH, Kanekal S and Kehrer JP. Cyclophosphamide toxicity. *Drugs* 1991; 42: 781–795.
3. Gokhale AB, Damre AS and Saraf MN. Investigations into the immunomodulatory activity of Argyreia speciosa. *J Ethnopharmacol* 2003; 84: 109–114.
4. Wang X, Zhang J and Xu T. Cyclophosphamide as a potent inhibitor of tumor thioredoxin reductase in vivo. *Toxicol Appl Pharmacol* 2007; 218: 88–95.
5. Ponticelli C and Passerini P. Alkylating agents and purine analogues in primary glomerulonephritis with nephrotic syndrome. *Nephrol Dial Transplant* 1991; 6: 381–388.
6. Eisler R. *Selenium handbook of chemical risk assessment: health hazards to humans plants and animals*. Vol. 3, Boca Raton, FL: Lewis Publishers, 2000, pp.1649–1705.
7. Klasing KC. *Comparative avian nutrition*. New York: Oxford University Press, 1998.
8. Rotruck JT, Pope AL and Ganther HE. Selenium: biochemical role as a component of glutathione peroxidase. *Science* 1973; 179: 585–590.
9. Whanger PD. Selenium and its relationship to cancer: an update dagger. *Br J Nutr* 2004; 91: 11–28.
10. Sugie S, Tanaka T and El-Bayoumy K. Chemoprevention of carcinogenesis by organoselenium compounds. *J Health Sci* 2000; 46: 422–425.
11. Ip C. Lessons from basic research in selenium and cancer prevention. *J Nutr* 1998; 128: 1845–1854.
12. Narajji C, Karvekar MD and Das AK. Biological importance of organoselenium compounds. *Ind J Pharm Sci* 2007; 69: 344–351.
13. Muller A, Cadenas E, Graf P, et al. A novel biologically active seleno-organic compound-I Glutathione peroxidase-like activity in vitro and antioxidant capacity of PZ 51 (Ebselen). *Biochem Pharmacol* 1984; 33: 3235–3239.
14. Zhang J, Wang X and Xu T. Elemental selenium at nano size (Nano-Se) as a potential chemopreventive agent with reduced risk of selenium toxicity: comparison with se-methylselenocysteine in mice. *Toxicol Sci* 2008; 101: 22–31.
15. Wang H, Zhang J and Yu H. Elemental selenium at nano size possesses lower toxicity without compromising the fundamental effect on selenoenzymes: comparison with selenomethionine in mice. *Free Radic Biol Med* 2007; 42: 1524–1533.
16. Zhang J, Wang H, Bao Y, et al. Nano red elemental selenium has no size effect in the induction of selenoenzymes in both cultured cells and mice. *Life Sci* 2004; 75: 237–244.
17. Peng D, Zhang J, Liu Q, et al. Size effect of elemental selenium nano particles (Nano-Se) at supranutritional levels on selenium accumulation and glutathione S-transferase activity. *J Inorg Biochem* 2007; 101: 1457–1463.
18. Huang B, Zhang J, Hou J, et al. Free radical scavenging efficiency of Nano-Se in vitro. *Free Radic Biol Med* 2003; 35: 805–813.
19. Lu J, Wu DM, Hu B, et al. Chronic administration of troxerutin protects mouse brain against D-galactose induced impairment of cholinergic system. *Neurobiol Learn Mem* 2010; 93: 157–164.
20. Shinomol GK and Muralidhara. Differential induction of oxidative impairments in brain regions of male mice following sub chronic consumption of Khesari dhal (Lathyrus sativus) and detoxified Khesari dhal. *Neurotoxicology* 2007; 28: 798–806.
21. Okhawa H, Ohishi N and Yagi K. Assay for lipid peroxides in animal tissues by thiobarbituric acid reaction. *Annal Biochem* 1979; 95: 351–358.
22. Bergmeyer HU, Scheibe P and Wahlefeld AW. Optimization of methods for aspartate aminotransferase and alanine aminotransferase. *Clin Chem* 1978; 24: 58–61.
23. Sedlack J and Lindsay RN. Estimation of total protein bound and non-protein sulfhydryl groups in tissue with ellman's reagent. *Annal Biochem* 1968; 25: 192–205.
24. Habig WH, Pabst MJ and Jacoby WB. Glutathione S-transferases, the first enzymatic step in marcapturic acid formation. *J Biol Chem* 1974; 249: 7130–7139.
25. Paglia DE and Valentine WN. Studies on the quantitative and qualitative characterization of erythrocyte glutathione peroxidase. *J Lab Clin Med* 1967; 70: 158–169.

26. Marklund S and Marklund G. Involvement of the superoxide anion radical in autooxidation of pyrogallol and a convenient assay for superoxide dismutase. *Eur J Biochem* 1974; 47: 469–474.
27. McCord JM and sand Fridovich I. Superoxide dismutase: an enzymatic function for erythrocuprein (hemoprotein). *J Biol Chem* 1969; 244: 6049–6055.
28. Luck HA. Spectrophotometric method for estimation of catalase. In: Bergmeyer HV (ed.) *Methods of enzymatic analysis*. New York, NY: Academic Press, 1963, pp.886–888.
29. Wintrobe MM. *Clinical hematology*, 7th edn. Philadelphia: Lea & Febiger, 1975, pp.114–115.
30. Lowry OH, Rosenbrough NJ, Farr AL, et al. Protein measurement with the folin phenol reagent. *J Biol Chem* 1951; 193: 265–276.
31. Endoh D, Okui T, Ozawa S, et al. Protective effect of a lignan-containing flaxseed extract against CCl4-induced hepatic injury. *J Vet Med Sci* 2002; 64: 761–765.
32. Singh NP, McCoy MT, Tice RR, et al. A simple technique for quantitation of low levels of DNA damage in individual cells. *Exp Cell Res* 1988; 175: 184–191.
33. Tice RR, Agurell E, Anderson D, et al. Single cell gel/comet assay: guidelines for in vitro and in vivo genetic toxicology testing. *Environ Mol Mutagen* 2000; 35: 206–221.
34. Huang W, Xing W, Li D, et al. Microcystin-RR induced apoptosis in tobacco BY-2 suspension cells is mediated by reactive oxygen species and mitochondrial permeability transition pore status. *Toxicol in Vitro* 2008; 22: 328–337.
35. Biswas SJ, Pathak S and Khuda Bukhsh AR. Assessment of the genotoxic and cytotoxic potential of an antiepileptic drug Phenobarbital, in mice: a time course study. *Mutat Res* 2004; 563: 1–11.
36. Matés JM. Antioxidant enzymes and human diseases. *Clin Biochem* 1999; 32: 595–603.
37. Hassan W, Ibrahim M, Nogueira CW, et al. Effects of acidosis and Fe (II) on lipid peroxidation in phospholipid extract: Comparative effect of diphenyl diselenide and ebselen. *Environ Toxicol Pharmacol* 2009; 28: 152–154.
38. Talas ZS, Ozdemir I, Ates B, et al. Modulating effects of selenium in adrenal medulla of rats exposed to 7,12-dimethylbenz[a]anthracene. *Toxicol Ind Health* 2013; 29: 286–292.
39. Ungvári E, Monori I, Megyeri A, et al. Protective effects of meat from lambs on selenium nanoparticle supplemented diet in a mouse model of polycyclic aromatic hydrocarbon-induced immunotoxicity. *Food Chem Toxicol* 2013; 64C: 298–306.
40. Cathcart R, Schwiers E and Ames BN. Detection of picomole levels of hydroperoxides using a fluorescent dichlorofluorescein assay. *Anal Biochem* 1983; 134: 111–116.
41. Crow JP. Dichlorodihydrofluorescein and dihydrorhodamine 123 are sensitive indicators of peroxynitrite in vitro: implications for intracellular measurement of reactive nitrogen and oxygen species. *Nitric Oxide* 1997; 1: 145–157.
42. Dumontet C, Drai J, Thieblemont C, et al. The superoxide dismutase content in erythrocytes predicts short-term toxicity of high-dose cyclophosphamide. *Br J Haematol* 2001; 112: 405–409.
43. Halliwell B and Gutteridge JM. *Free radicals in biology and medicine*, 2nd edn. Oxford: Clarendon Press, 1989, pp.1–20.
44. El-Demerdash FM. Antioxidant effect of vitamin E and selenium on lipid peroxidation, enzyme activities and biochemical parameters in rats exposed to aluminium. *J Trace Elem Med Biol* 2004; 18: 113–121.
45. Yousefipour Z, Ranganna K, Newaz MA, et al. Mechanism of acrolein-induced vascular toxicity. *J Physiol Pharmacol* 2005; 56: 337–353.
46. Srivastava A and Shivanandappa T. Hepatoprotective effect of the root extract of Decalepis hamiltonii against carbon tetrachloride-induced oxidative stress in rats. *Food Chem* 2010; 118: 411–417.
47. Dirven HA, van Ommen B and van Bladeren PJ. Involvement of human glutathione-S-transferase isoenzymes in the conjugation of cyclophosphamide metabolites with glutathione. *Cancer Res* 1994; 54: 6215–6220.
48. Tappel AL. Glutathione peroxidase and hydroperoxides. *Methods Enzymol* 1978; 52: 506–513.
49. Talas ZS, Ozdemir I, Gok Y, et al. Role of selenium compounds on tyrosine hydroxylase activity, adrenomedullin and total RNA levels in hearts of rats. *Regul Pept* 2010; 159: 137–141.
50. Sigalov AB and Stern LJ. Enzymatic repair of oxidative damage to human apolipoprotein A-I. *FEBS Lett* 1998; 433: 196–200.
51. Vo TK, Druez C, Delzenne N, et al. Analysis of antioxidant defense systems during rat hepatocarcinogenesis. *Carcinogenesis* 1988; 9: 2009–2013.
52. Rajasekaran NS, Devaraj H and Devaraj SN. The effect of glutathione monoester (GME) on glutathione (GSH) depleted rat liver. *J Nutr Biochem* 2002; 13: 302–306.
53. Groopman JE and Itri LM. Chemotherapy-induced anemia in adults: incidence and treatment. *J Natl Cancer Inst* 1999; 91: 1616–1634.
54. Vrzoc M and Petras ML. Comparison of alkaline single cell gel comet and peripheral blood micronucleus assays in detecting DNA damage caused by direct and indirect acting mutagens. *Mutat Res* 1997; 381: 31–40.
55. Matalon ST, Orney A and Lishner M. Review of the potential effects of three commonly used antineoplastic and immunosuppressive drugs (cyclophosphamide, azathioprine, doxorubicinon the embryo and placenta). *Reprod Toxicol* 2004; 18: 219–230.
56. Kussmaul AR, Bogacheva MA, Shkurat TP, et al. Inhibitory effect of apigenin on benzo(a)pyrene-mediated genotoxicity in Swiss albino mice. *J Pharm Pharmacol* 2006; 58: 1655–1660.
57. Vijayalakshmi P, Geetha CS and Mohanan PV. Assessment of oxidative stress and chromosomal aberration inducing potential of three medical grade silicone polymer materials. *J Biomater Appl* 2013; 27: 763–772.

58. Jenderny J, Walk RA, Hackenberg U, et al. Chromosomal abnormalities and sister-chromatid exchange in bone marrow cells of mice and Chinese hamsters after inhalation and intraperitoneal administration. II. Cyclophosphamide. *Mutat Res* 1988; 203: 1–10.

59. Moore FR, Urda GA, Krishna G, et al. An in vivo/in vitro method for assessing micronucleus and chromosome aberration induction in rat bone marrow and spleen. 1. Studies with cyclophosphamide. *Mutat Res* 1995; 335: 191–199.

Nano-Se attenuates cyclophosphamide-induced pulmonary injury through modulation of oxidative stress and DNA damage in Swiss albino mice

Arin Bhattacharjee, Abhishek Basu, Jaydip Biswas & Sudin Bhattacharya

Molecular and Cellular Biochemistry
An International Journal for Chemical Biology in Health and Disease

ISSN 0300-8177

Mol Cell Biochem
DOI 10.1007/s11010-015-2415-1

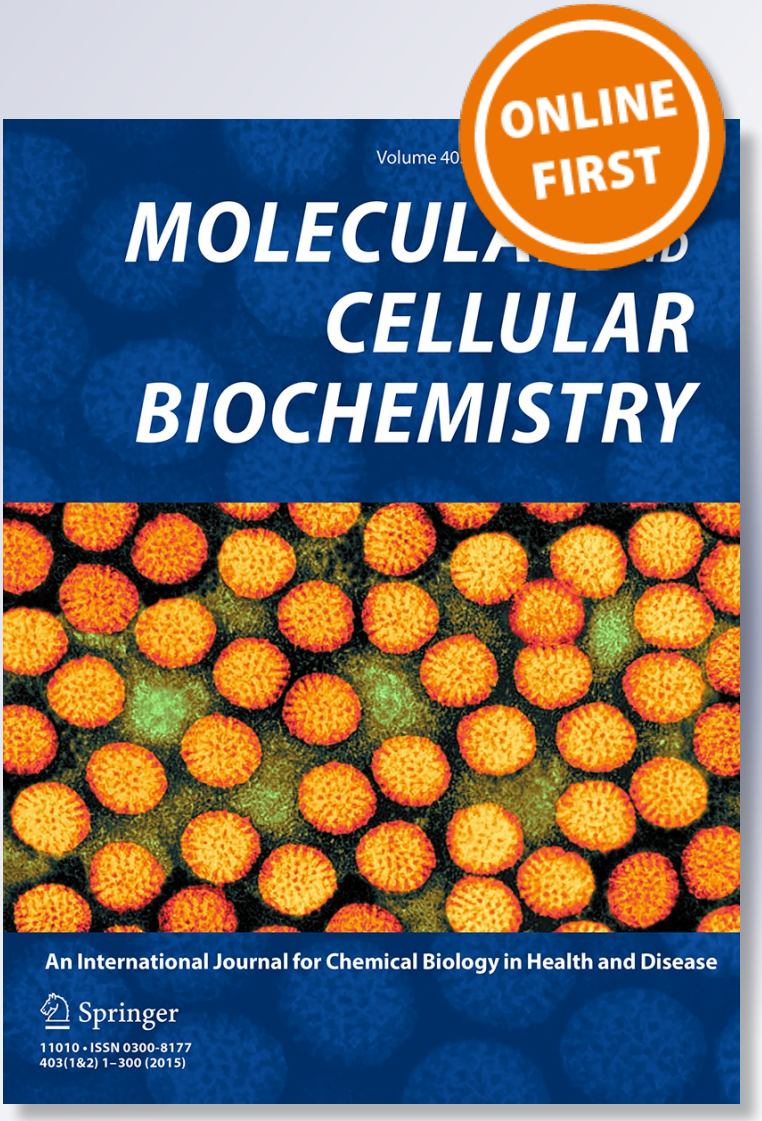

Springer

Mol Cell Biochem
DOI 10.1007/s11010-015-2415-1

Nano-Se attenuates cyclophosphamide-induced pulmonary injury through modulation of oxidative stress and DNA damage in Swiss albino mice

Arin Bhattacharjee[1] · Abhishek Basu[1] · Jaydip Biswas[2] · Sudin Bhattacharya[1]

Received: 28 February 2015 / Accepted: 18 April 2015

Abstract Chemotherapy is an integral part of modern day treatment regimen but anticancer drugs fail to demarcate between cancerous and normal cells thereby causing severe form of systemic toxicity. Among which pulmonary toxicity is a dreadful complication developed in cancer patients upon cyclophosphamide (CP) therapy. Oxidative stress, fibrosis, and apoptosis are the major patho-mechanisms involved in CP-induced pulmonary toxicity. In the present study, we have synthesized Nano-Se, nanotechnology-based new form of elemental selenium which has significantly lower toxicity and acceptable bioavailability. In order to meet the need of effective drugs against CP-induced adverse effects, nano selenium (Nano-Se) was tested for its possible protective efficacy on CP-induced pulmonary toxicity and bone marrow toxicity. CP intoxication resulted in structural and functional lung impairment which was revealed by massive histopathological changes. Lung injury was associated with oxidative stress/lipid peroxidation as evident by increased in reactive oxygen species, nitric oxide level, and malondialdehyde (MDA) formation with decreased in level of antioxidants such as reduced glutathione, glutathione-*S*-transferase, glutathione peroxidase, superoxide dismutase, and catalase. Furthermore, CP at a dose of 25 mg/kg b.w. increased pulmonary DNA damage ('comet tail') and triggered DNA fragmentation and apoptosis in mouse bone marrow cells. On the other hand, Nano-Se at a dose of 2 mg Se/kg b.w., significantly inhibited CP-induced DNA damage in bronchoalveolar lavage cells, and decreased the apoptosis and percentage of DNA fragmentation in bone marrow cells and also antagonized the reduction of the activities of antioxidant enzymes and the increase level of MDA. Thus, our results suggest that Nano-Se in pre- and co-administration may serve as a promising preventive strategy against CP-induced pulmonary toxicity.

Keywords Nano-Se · Cyclophosphamide · Pulmonary toxicity · Oxidative stress · Detoxifying enzymes · DNA damage

Introduction

Cyclophosphamide (CP) is a well-known bi-functional alkylating agent widely used in cancer chemotherapy and in organ transplantation as an immunosuppressant [1]. Despite its wide range of uses in clinical practice, a variety of undesirable effects have been implicated in patients. According to the International Agency for Research on Cancer (IARC), CP is widely used as reference mutagen and has been classified as carcinogenic for both animals and humans [2]. Acrolein, a toxic metabolite of CP, is responsible for chemically alkylate DNA as well as protein, producing cross-links and thereby inducing cytotoxicity [3]. Experimental evidence suggests that the development of oxidative stress after CP administration leads to decrease in the activities of antioxidant enzymes and increase in lipid peroxidation (LPO) level in liver and lungs of mice [4, 5]. In addition, increased ROS production subsequently leads to activation of cells of pulmonary defense system

✉ Sudin Bhattacharya
sudinb19572004@yahoo.co.in

[1] Department of Cancer Chemoprevention, Chittaranjan National Cancer Institute, 37, S.P. Mukherjee Road, Kolkata 700026, West Bengal, India

[2] Department of Translational Research, Chittaranjan National Cancer Institute, 37, S.P. Mukherjee Road, Kolkata 700026, West Bengal, India

Published online: 29 April 2015

like neutrophils, monocytes, and macrophages causing pulmonary fibrosis [6]. Along with these, due to the absence of two key detoxifying enzymes, namely aldehyde oxidase and aldehyde dehydrogenase, which catalyze the conversion of toxic aldehydes to less toxic carboxylic acids, in the lung tissues, CP has been reported to cause selective pulmonary injury [7]. On the other hand, the alveolar epithelial surface under constant exposure to high oxygen pressure makes the lung highly susceptible to free radical generation [8]. Particularly, alveolar epithelial type II cells are much susceptible to the injurious effects of oxidants [9]. Hence, generation of reactive oxygen or nitrogen species and lipid peroxide formation in lung tissues are thought to be a mediator of lung damage in this model. In view of the drawbacks of chemotherapeutic agents, there is a critical need to develop new treatment strategies that minimize or antagonize the toxicity of CP.

Selenium (Se) is an essential micronutrient with well-known antioxidant characteristics. As a component of glutathione peroxidase, Se can scavenge intracellular free radicals directly or indirectly [10]. Pharmacologically, consumption of 200 μg Se per day by cancer patients reduces mortality and decreases the incidence of many diseases including lung, colorectal, and prostate cancers [11, 12]. The antioxidant and pro-oxidant effects of Se as well as its bioavailability and toxicity depend on its chemical form [13]. Toxicity of selenium is now mainly thought to be mediated through its pro-oxidant capability to catalyze the oxidation of thiols and simultaneous generation of superoxide ($O^{\bullet-}$) that can damage cellular components [14]. In this regards, nanotechnology provides the extensive awareness of applied science and technology to organize the matter on the atomic and molecular scale [15]. Se nanoparticles (Nano-Se) are attracting high attention due to their excellent bioavailability, broad range of biological activity, and low toxicity [16]. Nano-Se has a sevenfold lower acute toxicity than sodium selenite in mice (LD_{50} 113 and 15 mg Se/kg body weight, respectively) [17]. Thus, Nano-Se can be used as a cytoprotectant with reduced risk of Se toxicity and kind of chemopreventive agent because the induction of GST by Se is a crucial mechanism for this chemopreventive effect [18].

We had earlier synthesized and characterized Nano-Se and evaluated its chemoprotective activity against CP-induced hepatotoxicity and genotoxicity in normal Swiss albino mice [19]. As per our knowledge, there might not be any reports of potential protective effect of Nano-Se against CP-induced pulmonary toxicity. In the perspective of chemoprotective actions of Nano-Se as well as their genoprotective effect, we anticipated that Nano-Se might be effective in amelioration of CP-induced pulmonary toxicity.

Materials and methods

Chemicals

Cyclophosphamide was obtained from Cadila Pharmaceuticals (Bhat, Ahmedabad, India). 1-chloro-2, 4-dinitrobenzene (CDNB), ethylene diamine tetraacetic acid (EDTA), reduced glutathione (GSH), pyrogallol, 5,5′-dithio-bis (2-nitro benzoic acid) (DTNB), sodium dodecyl sulfate (SDS), bovine serum albumin (BSA), β-nicotinamide adenine dinucleotide phosphate (reduced), glutathione reductase, normal melting agarose, low melting point agarose, ethidium bromide, sodium azide (NaN_3), sodium nitrite, N-(1-naphthyl)ethylenediamine dihydrochloride (NEDD), vanadium chloride (VCl_3), HEPES, 2′,7′- dichloro fluorescence diacetate (DCFH-DA), dihydroethidium (DHE), dimethyl sulphoxide (DMSO), phenylmethanesulfonyl fluoride (PMSF), and Triton X-100 were obtained from Sigma-Aldrich Chemicals Private Limited, Bangalore, India. All the other chemicals used were of analytical grade from Merck (India) Limited, Mumbai, India.

Experimental animals

Adult (5–6 weeks) Swiss albino female mice (23 ± 2 g), bred in the animal colony of Chittaranjan National Cancer Institute (CNCI), Kolkata, were used for this study. Animals were maintained at controlled temperature under alternating light and dark conditions. Standard food pellets and drinking water were provided ad libitum. The experiments were carried out following strictly the Institute's guideline for the Care and Use of Laboratory Animals.

Preparation and characterization of nano selenium

The Nano-Se was synthesized following a simplified protocol with slight modifications [20]. 5 mL of 25 mM sodium selenite was mixed with 20 mL of 25 mM reduced GSH containing 200 mg BSA. The mixture was adjusted to pH 7.2 with 1.0 M sodium hydroxide, instantly forming Nano-Se and oxidized glutathione (GSSG). The red solution was dialyzed against double distilled water for 96 h with the water changing every 24 h to separate GSSG from Nano-Se under magnetic stirring. The final solution containing Nano-Se and BSA was subjected to centrifugation at 13,000 rpm for 10 min. The pellet thus recovered was subjected to washing by its re-suspension in de-ionized water followed by centrifugation at 13,000 rpm for 10 min, to remove possible contamination present in nano particles. Finally, pellet was freeze dried using a lyophilizer and stored at room temperature. The obtained lyophilized

products were characterized by using various microscopic and spectroscopic methods [19].

Experimental design

The animals were distributed into five groups containing six animals in each. Based on our previous study, Nano-Se was dissolved in saline (0.9 % NaCl) and prepared on each day just before treatment (Fig. 1).

Group I (vehicle-treated group): each animal was given oral administration of saline (0.9 % NaCl) day 1 to day 10.
Group II (nano selenium-treated group): animals were treated orally with Nano-Se only at a dose of 2 mg Se/kg b.w. throughout the experimental period.
Group III (CP-treated group): CP was administered intraperitoneally at a dose of 25 mg/kg b.w in water for 10 days.
Group IV (concomitant treatment group): Nano-Se was administered orally at a dose of 2 mg Se/kg b.w. for 10 days and CP was given as in Gr. III.
Group V (pretreatment group): Nano-Se was administered orally at a dose of 2 mg Se/kg b.w. 7 days prior to CP treatment and then continued along with CP for 10 days.

The mice were sacrificed on day 11, and the parameters described below were studied.

Isolation of blood and bronchoalveolar lavage fluid (BALF)

Before sacrifice, all animals were fasted for 4 h and then blood samples were collected from the retro-orbital venous plexus under anesthesia. Lungs were removed and BALF was collected using the method of Henderson et al. [21], with some modifications. Lungs were lavaged five times with 7 mL saline and the lavage fluids were centrifuged at 300 g for 20 min to separate the cells and the supernatants. The cell viability in each group was measured by 0.1 % trypan blue with hemocytometer in phosphate-buffered saline and density of cells was adjusted to 10^5 cells/slide for the comet assay.

Hematopathological studies

Red blood cell (RBC) [22] and white blood cell (WBC) counts were made following a literature procedure [23].

Free radical determination

Determination of pulmonary ROS generation

ROS measurement in lung tissue homogenate was done following two simplified protocol with slight modifications using two probes, DHE [24, 25] and DCFH-DA [26]. DHE is a non-fluorescent dye and freely permeable to the cell.

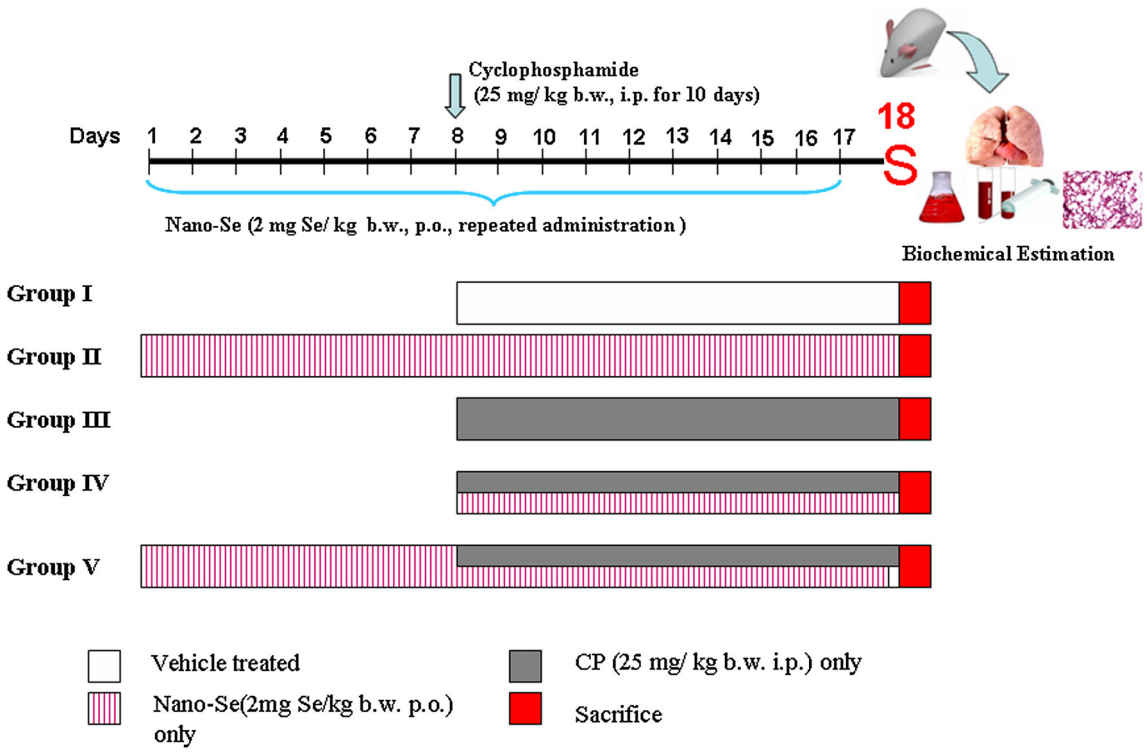

Fig. 1 The basic experimental treatment schedule. CP cyclophosphamide, Nano-Se Selenium nanoparticle. (Color figure online)

Upon oxidation by superoxide anions (O_2^-) forms the red fluorescent product ethidium [27]. Lung tissues were homogenized in HEPES buffer (pH 7.4, containing 25 mM HEPES, 1 mM EDTA and 0.1 mM PMSF) to yield a 4 % w/v homogenate. 150 µL of tissue homogenate in whole was taken and then loaded with 10 µM DHE to make a final volume of 3 mL. The samples were incubated in dark for 30 min to allow the formation of ethidium and then analyzed for fluorescence (excitation 475 nm/emission 610 nm) using spectrofluorimeter (Varian Cary Eclipse). Values were expressed as fluorescence intensity per mg of protein.

DCFH-DA is a non-fluorescent probe that is hydrolyzed by mitochondrial esterase to form 2′,7′-dichlorodihydrofluorescein (DCFH). DCFH upon oxidation by H_2O_2 forms the fluorescent compound 2′,7′-dichlorofluorescein (DCF) [25]. Lung tissues were homogenized in Locke's buffer (pH 7.4, containing 140 mM NaCl, 5 mM KCl, 10 mM HEPES, 1 mM $CaCl_2$, 1 mM $MgCl_2$, and 10 mM dextrose) to yield a 10 % w/v homogenate. 250 µL of tissue homogenate in whole was taken and then loaded with 10 µM DCFH-DA to make a final volume of 3 mL. The samples were incubated in dark for 45 min to allow the formation of DCF and then analyzed for fluorescence (excitation 485 nm/emission 530 nm) using spectrofluorimeter (Varian Cary Eclipse). Values were expressed as fluorescence intensity per mg of protein.

Measurement of nitric oxide (NO) production

Nitric oxide (NO) production in lung homogenate was determined by estimating the level of stable NO metabolites, viz., nitrate (NO_3^-), and nitrite (NO_2^-) ions by reaction with Griess reagent (1 % sulphanilamide, 5 % phosphoric acid, and 0.1 % NEDD), using $NaNO_2$ as standard [28]. The absorbance was taken at 545 nm and expressed as µM nitrite per mg of protein (Infinite® 200 PRO, TECAN).

Genotoxicity studies

Detection of DNA damage in BALF by comet assay

The influence of Nano-Se on cyclophosphamide-induced DNA damage in mouse lung BALF were studied by alkaline single cell gel electrophoresis (comet assay), according to the in vivo comet assay guidelines with slight modification [29]. The BALF in PBS were dispersed by gentle pipetting. The cell viability in each group was measured by trypan blue in phosphate-buffered saline and density of cells was adjusted to 10^5 cells/slide for the assay. An aliquot of 10 µL of freshly prepared single-cell suspension was mixed with 1 % low melting agarose and layered on the half-frosted slides precoated with normal melting agarose. A third layer of 0.5 % low melting point agarose was layered on the top of the second layer. The cells were lysed for overnight at 4 °C in lysing solution containing 2.5 M NaCl, 100 mM Na_2EDTA, 10 mM Tris buffer, 1 % Triton X-100, and 10 % DMSO (pH 10.0). After lysis, the slides were subjected to electrophoresis in electrophoresis buffer [1 mM Na_2EDTA and 0.3 M NaOH (pH > 13.1)] for 30 min at 300 mA and 20 V. After electrophoresis, the slides were neutralized with neutralizing buffer [0.4 M Tris buffer (pH 7.5)]. The microscopic slides were carefully dried at room temperature and stained with ethidium bromide in water (20 µg/mL; 80 µL/slide). The slides were examined at ×400 magnification under a fluorescence microscope (Model: Leica DM 4000B) with imaging system. Komet 5.5 software was used to take the photomicrograph of cells and to determine the length of the comet tail. 50–100 randomly selected cells in each slide were analyzed (two slides/animals in each group). The damage is represented by an increase of DNA fragments that have migrated out of the cell nucleus during electrophoresis and formed an image of a 'comet' tail [30]. The damaged cell (%) was calculated using the following formula:

$$\text{Damaged cell}\,(\%) = \frac{\text{Number of damaged cells}}{\text{Total number of cells counted}} \times 100$$

The parameters analyzed for detection of DNA damage were damaged cell (%) in each group, tail DNA (%), tail length [migration of the DNA from the nucleus (µm)], and Olive tail moment [product of tail length and the fraction of total DNA in the tail (arbitrary units)].

Preparation of bone marrow cells and splenocytes

Femurs were aseptically removed from the normal and experimental groups of mice, where the bone was split longitudinally and the marrow was exposed using forceps and the content of the femur was flushed gently using 22 gauze needles containing cold PBS (pH 7.4, Ca^{++} and Mg^{++} free) into a centrifuge tube. The marrow plug was dissociated into single-cell suspension by repeatedly passing this suspension through 22 gauze needles and the total volume was measured. The total number of nucleated cells was counted in hemocytometer after treatment with 2 % glacial acetic acid. In case of splenocyte, whole spleen was minced in ice cold PBS (pH 7.4, Ca^{++} and Mg^{++} free) and the resultant mixture was passed repeatedly through 22 gauze needles to make a single-cell suspension. The total number of nucleated cells in spleen was counted in hemocytometer after treatment with 2 % glacial acetic acid.

DNA fragmentation by diphenylamine (DPA assay)

DNA fragmentation in bone marrow cells were carried out according to [31]. Briefly, about 2×10^6 bone marrow cells were lysed in lysis buffer (pH 8.0 containing 5 mM Tris-HCl, 20 mM EDTA, and 0.5 % Triton X-100) for 30 min at 4 °C. The cell lysate were centrifuged at $15{,}000 \times g$ for 15 min at 4 °C. Then, the supernatant containing small DNA fragments was separated from the pellet containing large pieces of DNA. The supernatant and pellet were re-suspended in 10 and 5 % of trichloroacetic acid (TCA), respectively, and kept overnight. Then both samples were heated at 95 °C for 15 min and centrifuged at $2500 \times g$ for 5 min to remove proteins. Supernatant fractions were reacted with DPA for 4 h at 37 °C and the developing blue color was measured at 600 nm and expressed as

$$\text{Fragmented DNA}\,(\%) = \frac{\text{Absorbance of the supernatant}}{\text{Absorbance of supernatant} + \text{pellet}} \times 100$$

Apoptosis study using fluorescence microscopy

Fluorescence-based in vivo apoptosis was determined by using acridine orange (AO)/ethidium bromide (EtBr) staining method as described by Shylesh et al. [32]. Bone marrow cells were collected and washed with PBS and treated with AO/EtBr. In details, 100 µL of the cell suspension was mixed with 4 µL of dye mixture containing AO (1 mg/mL) and EB (1 mg/mL) in PBS. The cells were visualized immediately under a fluorescence microscope (Model: Leica DM 4000B) using a blue and green filter and photomicrographs (Leica FW 4000) were taken at ×400 magnification. Viable cell's nucleus is stained green due to permeability of only AO, whereas apoptotic cells appear yellow-red due to co-staining of both stains.

Biochemical estimation

Quantitative estimation of lipid peroxidation (LPO) level

LPO level was estimated in lung microsomal fraction. The level of lipid peroxides formed was measured using TBA and expressed as nmol of thiobarbituric acid reactive substances (TBARS) formed per mg of protein using the extinction co-efficient of $1.56 \times 10^5\ M^{-1}\ cm^{-1}$ [33].

Estimation of reduced glutathione (GSH) level

GSH level was estimated in lung cytosol spectrophotometrically by determination of DTNB reduced by –SH groups by measuring the absorbance at 412 nm. The level of GSH was expressed as nmol/mg of protein [34].

Estimation of glutathione-S-transferase (GST) activity

GST activity was measured in the lung cytosol. The enzyme activity was determined from the increase in absorbance at 340 nm with CDNB as the substrate and specific activity of the enzyme was expressed as formation of CDNB-GSH conjugate/min/mg of protein [35].

Estimation of superoxide dismutase (SOD) activity

SOD activity in lung was determined by quantification of pyrogallol auto-oxidation inhibition and expressed as unit/mg of protein. One unit of enzyme activity is defined as the amount of enzyme necessary for inhibiting the reaction by 50 %. Auto-oxidation of pyrogallol in Tris-HCL buffer (50 mM, pH 7.5) is measured by increase in absorbance at 420 nm [36, 37].

Estimation of catalase (CAT) activity

CAT activity in lung cytosol was determined spectrophotometrically at 250 nm and expressed as unit/mg of protein, where the unit is the amount of enzyme that liberates half the peroxide oxygen from H_2O_2 in second at 25 °C [38].

Estimation of glutathione peroxidase (GPx) activity

GP*x* activity in lung was measured by NADPH oxidation using a coupled reaction system consisting of GSH, glutathione reductase, and H_2O_2 [39]. Briefly, 100 µL of enzyme sample was incubated for 10 min with 800 µL reaction mixtures (0.25 M potassium phosphate buffer containing 2.5 mM EDTA and 2.5 mM NaN_3, 10 mM GSH, 2.5 mM NADPH, and 2.4 units of glutathione reductase). The reactions started on adding 100 µL H_2O_2 and follow the decrease in NADPH absorbance at 340 nm for 3 min. The enzyme activity was expressed as micro-mol NADPH utilized/min/mg of protein, using extinction co-efficient of NADPH at 340 nm as $6200\ M^{-1}\ cm^{-1}$.

Estimation of protein

Total protein content in tissue homogenate during biochemical analysis was measured through Lowry method using Folin-phenol reagent [40]. The absorbance of the color was measured against the color less blank sample at 660 nm using the TECAN Infinite® 200 PRO Multimode Reader.

Tissue section preparation and histopathological evaluation

Immediately after dissection, lungs tissues were excised and immersed in 10 % neutral buffered formalin solution. The samples were dehydrated in ascending concentrations of ethanol, cleared in xylene, and embedded in paraffin to prepare the block. Lung tissues were sectioned, mounted on slides, and stained. The 5-μm serial sections were used for staining with hematoxylin-eosin. Stained sections were evaluated by observing the arrangement of lung architecture with a light microscope (Leica DM 1000). Photomicrographs were taken with the software Las EZ at ×400 magnification.

Statistical analysis

All data were presented as mean ± SD, $n = 6$ animals per group. One-way ANOVA followed by Tukey's Multiple Comparison Test using Graph Pad Prism (Version 5.00) software was performed for comparisons among groups. Significant difference was indicated when the P value was <0.05.

Results

Nano-Se did not produce any significant change in the parameters investigated when administered alone as compared with the vehicle control group.

Enhancement of depressed cellular system

Table 1 depicts the haematopoietic cell, bone marrow, and spleen cellularity in normal and experimental animals. The exposure of CP resulted in a significant ($P > 0.05$) decline in RBC and WBC counts. In addition to this, bone marrow as well as splenic cell counts also decreased significantly ($P < 0.05$) after CP treatment. This decreased cell counts in both the primary and secondary immune organs were significantly ($P < 0.05$) prevented on oral administration of Nano-Se in concomitant and pretreatment schedule.

Inhibition of pulmonary ROS level

ROS level in lung tissue homogenate was estimated by using DHE and DCFH-DA to quantify the level of super oxide and H_2O_2, respectively. The super oxide and H_2O_2 level in lung was found to increase significantly ($P < 0.05$) by 122.38 and 237.71 %, respectively, after the administration of CP (Gr. III), compared to the vehicle control group (Gr. I). Concomitant treatment (Gr. IV) with Nano-Se reduced the pulmonary super oxide and H_2O_2 level by 29.95 and 27.22 %, respectively, in comparison to CP-treated group, whereas in 7 days pretreatment (Gr. V), the reduction in super oxide and H_2O_2 levels was found to be 45.16 and 58.31 %, respectively, in comparison to CP-treated group (Gr. III) (Fig. 2a, b).

Modulation of pulmonary NO level

Intraperitoneal administration of CP significantly ($P < 0.05$) elevated NO level in lungs by 67.69 % in Gr. III as compared to the vehicle control group (Gr. I) (Fig. 2c). Concomitant treatment (Gr. IV) with Nano-Se inhibited NO level in lungs by 16.36 %, but 7 days pretreatment (Gr. V) with the same inhibited the elevated pulmonary NO level by 25.84 % in comparison to Gr. III.

Protection from CP-induced DNA damage in BALF

Bronchoalveolar lavage cells were isolated from the lungs and assessed for DNA damage using the comet assay (Fig. 3a–e). Large round head and no tail was observed in the bronchoalveolar lavage (BAL) cells of Gr. I mice. But CP at a dose of 25 mg/kg b.w./day treatment resulted in

Table 1 Effect of Nano-Se on RBC, WBC, Bone marrow, and Splenic cell counts in mice treated with CP

Group	RBC (10^6/mm^3)	WBC (10^3/mm^3)	Bone marrow cell count ($\times 10^6$)	Splenic cell count ($\times 10^6$)
I	6.27 ± 0.33	6.61 ± 0.32	28.6 ± 1.76	89.44 ± 1.6
II	6.37 ± 0.26	6.53 ± 0.49	29.45 ± 0.7	96.01 ± 1.09
III	$4.05 \pm 0.49^{\alpha\mu}$	$3.22 \pm 0.11^{\alpha\mu}$	$5.87 \pm 0.87^{\alpha\mu}$	$15.47 \pm 1.52^{\alpha\mu}$
IV	$4.67 \pm 0.37^{\alpha\mu\gamma}$	$4.55 \pm 0.21^{\alpha\mu\gamma}$	$10.07 \pm 0.55^{\alpha\mu\gamma}$	$36.73 \pm 1.04^{\alpha\mu\gamma}$
V	$5.75 \pm 0.26^{\gamma\theta}$	$5.47 \pm 0.19^{\alpha\mu\gamma\theta}$	$20.37 \pm 1.73^{\alpha\mu\gamma\theta}$	$47.0 \pm 1.12^{\alpha\mu\gamma\theta}$

Data were represented as Mean ± SD ($n = 6$)

$^{\alpha}$ Significant ($P < 0.05$) as compared with Gr. I

$^{\mu}$ Significant ($P < 0.05$) as compared with Gr. II

$^{\gamma}$ Significant ($P < 0.05$) as compared with Gr. III

$^{\theta}$ Significant ($P < 0.05$) as compared with Gr. IV

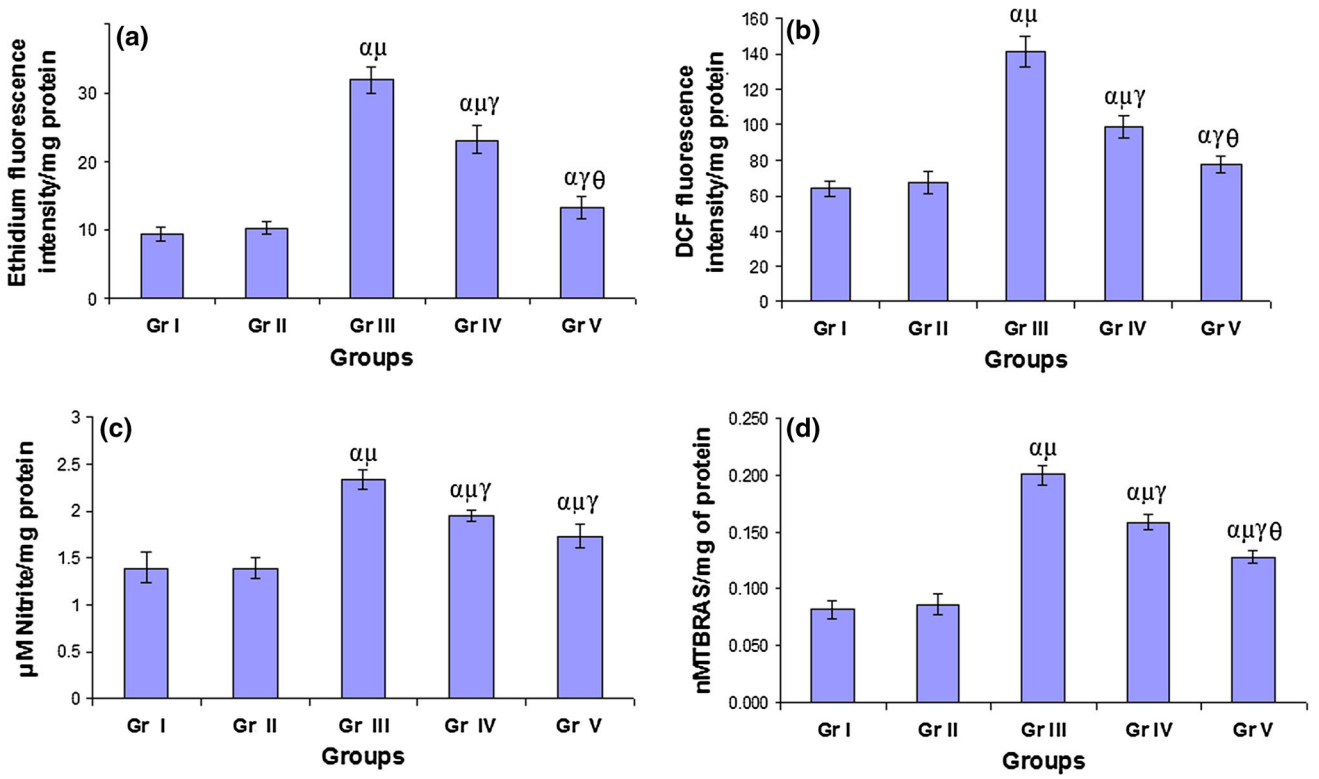

Fig. 2 Effect of Nano-Se on pulmonary H_2O_2 level (**a**), pulmonary superoxide level (**b**), pulmonary NO level, (**c**) and pulmonary LPO level (**d**) after administration of CP. *Data* were represented as mean ± SD ($n = 6$). α significant ($P < 0.05$) as compared with Gr. I; μ significant ($P < 0.05$) as compared with Gr. II; γ significant ($P < 0.05$) as compared with Gr. III; θ significant ($P < 0.05$) as compared with Gr. IV

long comet tail formation due to DNA damage in large number of cell population. Concomitant and pretreatment with Nano-Se significantly reduced % of damaged cells, comet tail length, and Olive tail moment (Fig. 4a–d).

Attenuation of CP-induced DNA fragmentation

Genomic DNA fragmentation in bone marrow cells was found 6.71 % in Gr. I. CP administration caused a significantly ($P < 0.05$) greater rate (52.55 %) of DNA fragmentation in Gr. III mice. In case of concomitant and pretreatment, the percentages of DNA fragmentation were reduced to 39.08 and 24.56 %, respectively (Fig. 5).

Acridine orange (AO)–ethidium bromide (EB) double staining cell morphological analysis

The results obtained from the acridine orange–ethidium bromide double staining are shown in (Fig. 6a, b). Acridine orange is a vital dye that stains both live and dead cells, whereas ethidium bromide will stain only those cells that have lost their membrane integrity [32]. Cells stained green represents viable cells, whereas yellowish-red staining represents apoptotic cells. The cells in CP group, due to the increase in cell membrane permeability, showed green and red fluorescence. The cells pre-treated with Nano-Se before CP administration, showed green and slight red fluorescence with few apoptotic cells and nucleus fragmented or apoptotic bodies. In contrast, the cells in vehicle control and Nano-Se groups all showed green fluorescence and normal structures.

Attenuation of pulmonary LPO level

Intraperitoneal administration of CP (Gr. III) resulted in a significant ($P < 0.05$) enhancement in pulmonary LPO level by 145.12 % in comparison to vehicle control group (Gr. I) (Fig. 2d). Oral administration of Nano-Se caused a significant depletion of CP-induced elevated pulmonary LPO level by 20.89 % in case of concomitant treatment schedule (Gr. IV) and by 36.31 % in case of pretreatment schedule (Gr. V) in comparison to CP-treated group (Gr. III).

Enhancement of pulmonary GSH level

The GSH content in lung was found to decline significantly ($P < 0.05$) by 56.64 % after CP administration (Gr. III) as

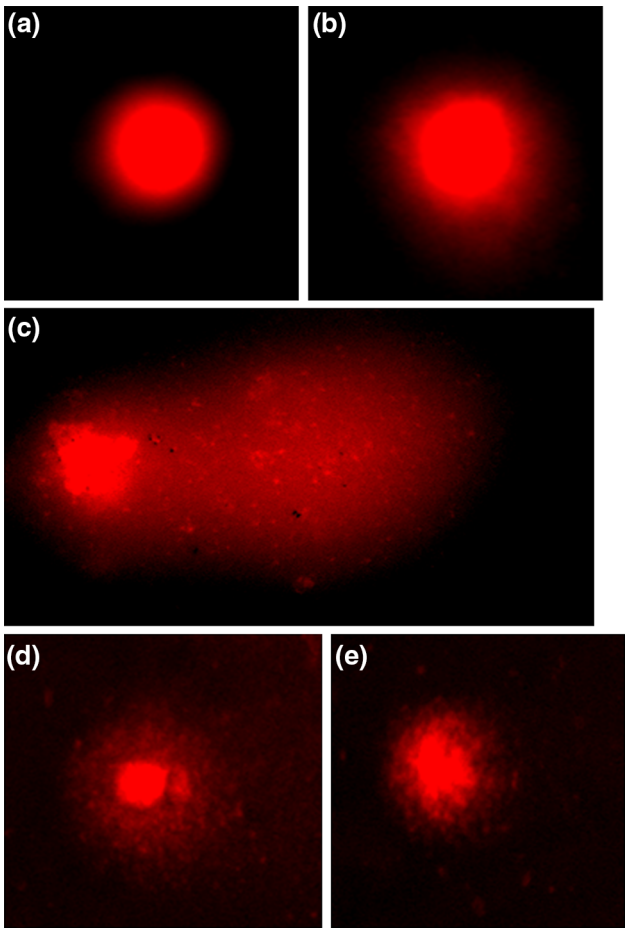

Fig. 3 Photomicrographs of bronchoalveolar lavage fluid (BALF) showing DNA damage, magnification ×400, **a** significant DNA migration in Gr. I; **b** very fewer DNA migration in Gr. II; **c** highly migrated DNA with distinct scattered comet tail in Gr. III; **d** less migrated DNA and less diffused comet tail in Gr. IV; **e** no or very less migrated DNA in Gr. V

compared to vehicle control group (Gr. I) (Fig. 7a). Nano-Se treatment prevented this depletion of GSH by 38.16 % in case of concomitant (Gr. IV) and by 76.29 % in pre-treatment (Gr. V) compared to that observed with CP alone treated mice (Gr. III).

Restoration of pulmonary GST activity

Intraperitoneal administration of CP substantially ($P < 0.05$) decreased the GST activity by 36.2 % in Gr. III compared to Gr. I. Concomitant administration of Nano-Se increased the enzyme activity by 31.46 % (Gr. IV) and 7 days pretreatment sharply increased the activity of GST by 52.18 % (Gr. V) as in comparison to CP alone treated group (Gr. III) (Fig. 7b).

Enhancement of pulmonary SOD, CAT, and GP*x* activity

Intraperitoneal administration of CP significantly ($P < 0.05$) reduced the pulmonary SOD, CAT, and GP*x* activity by 75.09, 54.03, and 74.71 %, respectively, in CP-treated group (Gr. III) in comparison to vehicle control group (Gr. I). Concomitant administration of Nano-Se (Gr. IV) resulted in a significant enhancement in pulmonary SOD, CAT, and GPx activity by 73.95, 51.4, and 69.46 %, respectively, in comparison to CP-treated group (Gr. III). However, in case of 7 days pretreatment with Nano-Se (Gr. V) increased the pulmonary SOD, CAT, and GP*x* activity by 171.1, 77.75, and 241.22%, respectively, as compared to CP-treated group (Gr. III) (Fig. 8a–c).

Histopathology of lung tissue

Lung histology of vehicle control animals (Gr. I) showed normal structure, whereas lung tissues of CP-treated animals showed distinct cellular and architectural changes including pulmonary congestion, pulmonary inflammation, thickened alveolar septa, and distortion of alveoli. Nano-Se treatment alone induced no remarkable alteration in lung histology. However, Nano-Se when administered combination with CP either in concomitant or pretreatment schedule, a protective effect of Nano-Se was revealed, where the most effective protection was exerted by the administration of test compound in the pretreatment schedule (Fig. 9a–f).

Discussion

Despite the ever increasing population of chemotherapeutic agents, including several anticancer drugs like cyclophosphamide, the clinical outcome of treatments with these agents is severely limited, mostly due to their toxicity to normal tissues. Therefore, there is a necessity to develop potential therapeutic strategy to encounter the problem through concomitant use of potent adjuvant agents which can decrease toxicity of chemotherapeutic drugs without compromising their efficacy. In the present study, we demonstrated for the first time that systemic administration of Nano-Se significantly attenuated the CP-induced pulmonary toxicity in mice by mitigating pulmonary oxidative stress and DNA damage.

Chemotherapy inevitably leads to the decrease in bone marrow function that reflects by a substantial decrease in the mature blood elements [41]. In the present investigation, significant decrease of RBC and WBC numbers was evident following CP treatment. Treatment with Nano-Se brought back the RBC and WBC counts more or less to

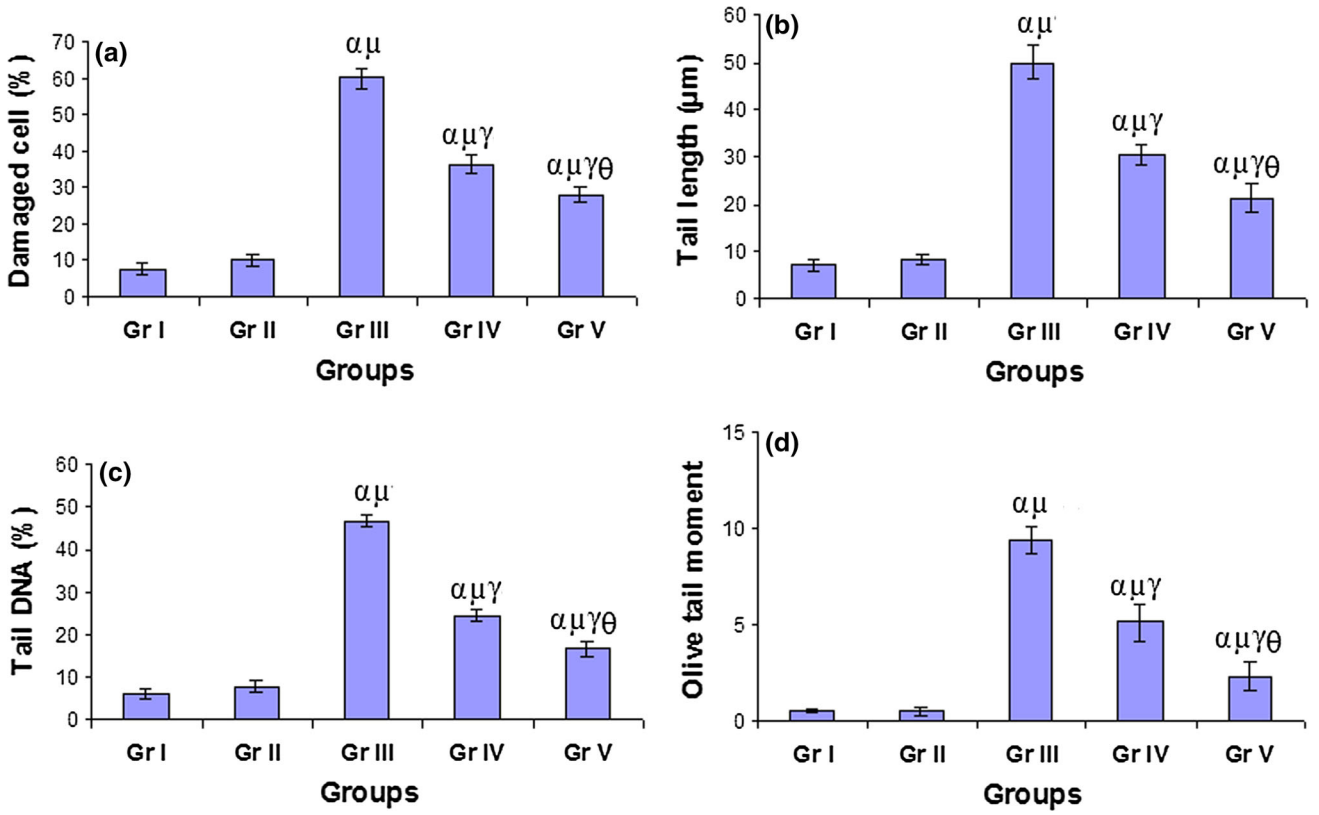

Fig. 4 Nano-Se prevented CP-induced DNA damage as evident from **a** damage cell %, **b** comet tail length, **c** tail DNA %, and **d** Olive tail moment. *Data* were represented as mean ± SD ($n = 6$). α significant ($P < 0.05$) as compared with Gr. I; μ significant ($P < 0.05$) as compared with Gr. II; γ significant ($P < 0.05$) as compared with Gr. III; θ significant ($P < 0.05$) as compared with Gr. IV

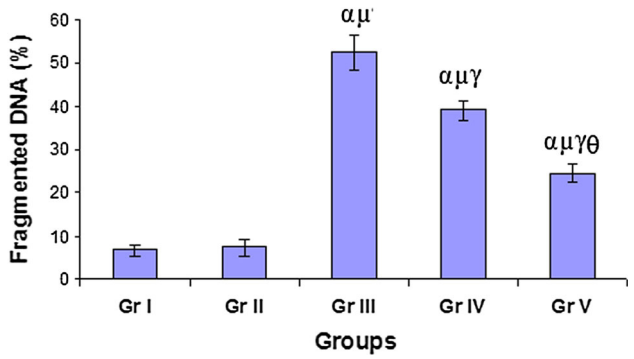

Fig. 5 Effect of Nano-Se on DNA fragmentation in bone marrow cells. *Data* were represented as mean ± SD ($n = 6$). α significant ($P < 0.05$) as compared with Gr. I; μ significant ($P < 0.05$) as compared with Gr. II; γ significant ($P < 0.05$) as compared with Gr. III; θ significant ($P < 0.05$) as compared with Gr. IV

near normal levels. CP treatment also, significantly decreased bone marrow and spleen cell counts. Interestingly, the results of the present investigation revealed that concomitant and pretreatment with Nano-Se abrogated the CP-induced depression of bone marrow and spleen cell numbers. This indicates the protective effect of Nano-Se on the haematopoietic system.

Several mechanisms have been proposed to explain the adverse health effects of particulate of chemotherapeutic drug. ROS production and the generation of oxidative stress have received the most attention. ROS, such as superoxide, hydrogen peroxide, hydroxyl, and other oxygen radicals, are capable of directly oxidizing the DNA, proteins, and lipids [42]. Reports obtained from the present study indicated that CP treatment increased ROS level in the lungs tissues measured spectrofluorometrically by the use of DHE and DCFH-DA. The oxidation of DHE to fluorescent compound ethidium is mainly modulated by superoxide anion [27], whereas DCFH-DA as a cell permeable specific dye probe fluoresces to 2′,7′-dichlorofluorescein (DCF) which is mainly regulated by H_2O_2 [43]. In this study, CP treatment substantially elevated superoxide and H_2O_2 levels in lung tissue of mice as measured by DHE and DCFH-DA, respectively. Nano-Se prevented CP-induced ROS generation which could be attributed to free radical scavenging activity of the test compound.

Recently, it has been suggested that reactive nitrogen species (RNS), including nitric oxide (NO), peroxynitrite ($ONOO^-$), and nitrogen dioxide, which are released from

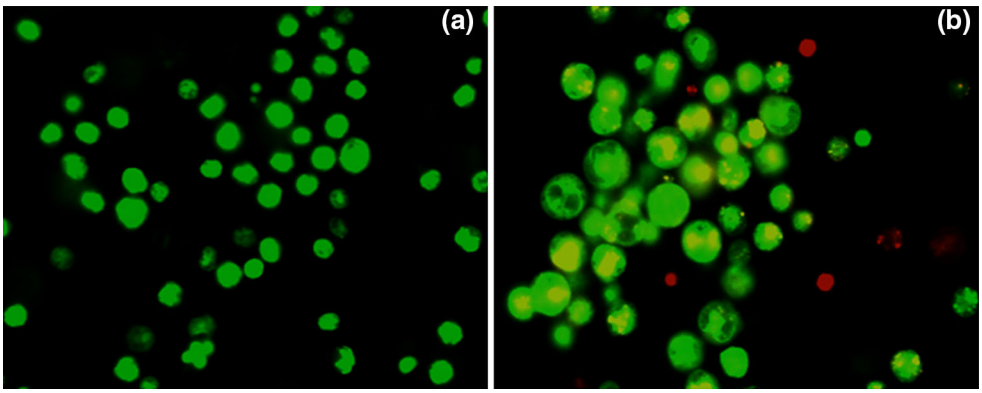

Fig. 6 Effect of Nano-Se against CP-induced cell morphological changes with fluorescence microscope in mouse bone marrow cells, magnification ×400. **a** Cells were stained *green* and showed normal structure, **b** Cell structure was damaged, the cells are not only stained with AO and EB, but the fragmented or apoptotic bodies could be seen clearly. (Color figure online)

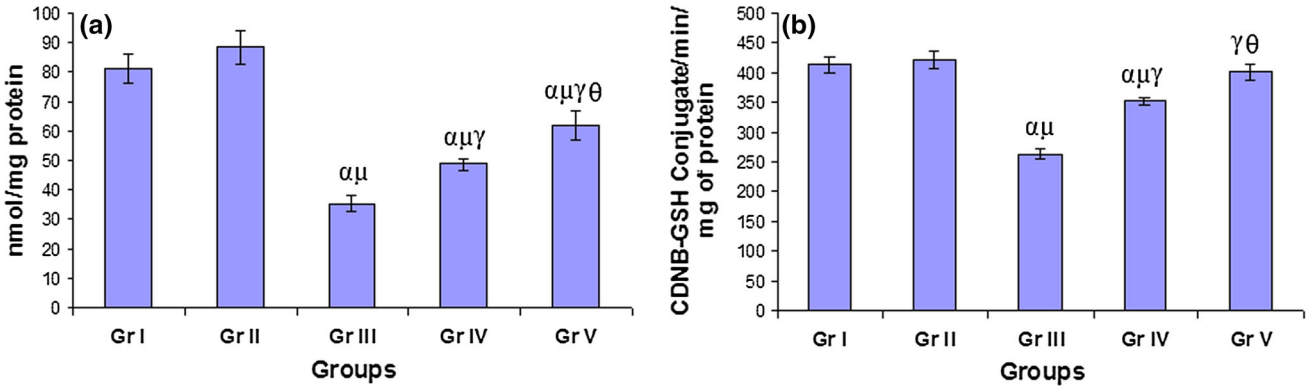

Fig. 7 Effect of Nano-Se on pulmonary GSH level (**a**) and pulmonary GST activity (**b**) after administration of CP. *Data* were represented as mean ± SD ($n = 6$). α significant ($P < 0.05$) as compared with Gr. I; μ significant ($P < 0.05$) as compared with Gr. II; γ significant ($P < 0.05$) as compared with Gr. III; θ significant ($P < 0.05$) as compared with Gr. IV

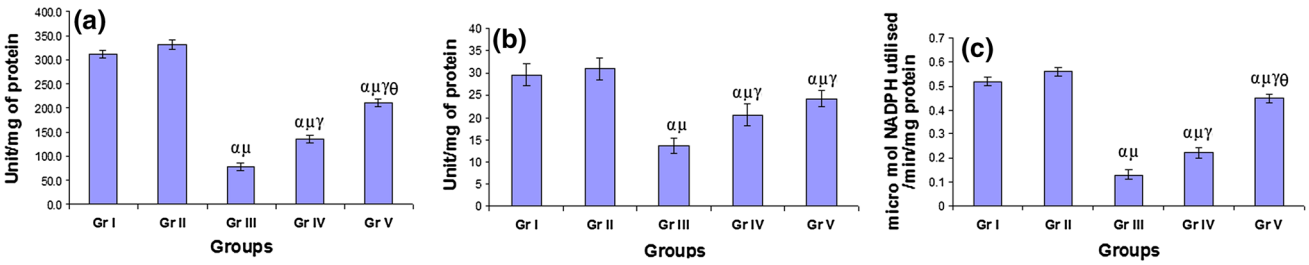

Fig. 8 Effect of Nano-Se on pulmonary SOD activity (**a**), pulmonary CAT activity (**b**), and pulmonary GP*x* activity after administration of CP. *Data* were represented as mean ± SD ($n = 6$). α significant ($P < 0.05$) as compared with Gr. I; μ significant ($P < 0.05$) as compared with Gr. II; γ significant ($P < 0.05$) as compared with Gr. III; θ significant ($P < 0.05$) as compared with Gr. IV

neutrophils and macrophages, play an important role in the pathogenesis of lung diseases [44]. NO is also produced in high concentrations during infection, acute lung injury, and adult respiratory distress syndrome [45]. Therefore, suppression of NO production may be beneficial against disorders caused due to its increased production. Our study highlights that NO production is induced by CP in lung tissues and Nano-Se suppressed it. This observation is supported by the findings that Nano-Se inhibits NO production and scavenges peroxynitrite and peroxynitrate.

CP, an indirect-acting mutagen, damages chromosomes through generation of free radicals and alkylating DNA thereby producing mutation [46]. To explore the extent of CP-induced DNA damage, we further measured DNA

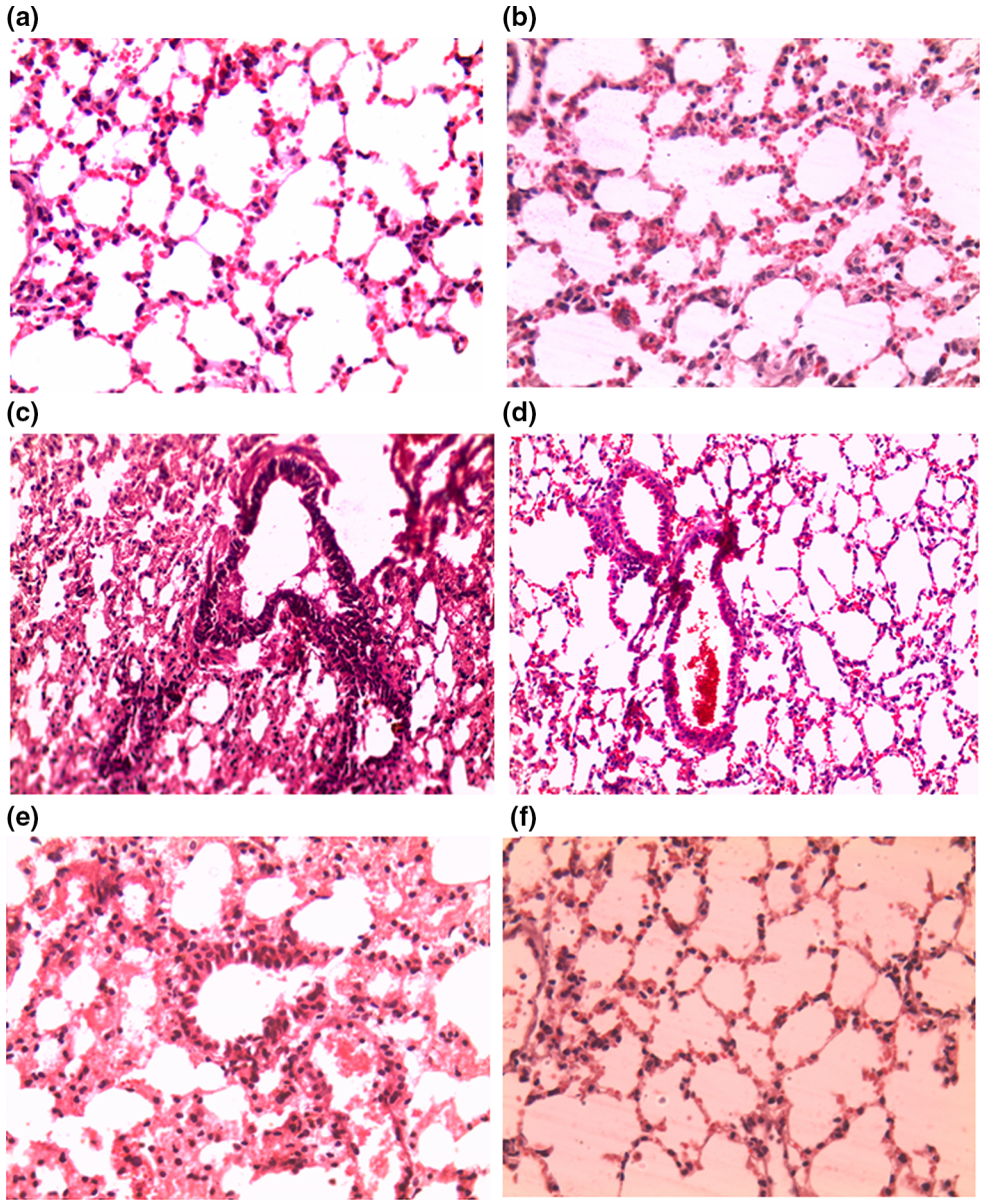

Fig. 9 Photograph of lung section of mice stained with hematoxylin and eosin, (H & E): **a** Normal histology of lung with normal alveolar architecture without any epithelial damage in Gr. I; **b** lung section from only Nano-Se-treated group (Gr. II) showing normal lung architecture same as Gr. I; **c** treatment with CP (Gr. III) showing loss of pulmonary architecture, thickening of alveolar septa, alveolar damage, and fibrous tissue proliferation; **d** CP-treated group also showing pulmonary congestion and pulmonary inflammation also; **e** concomitant treatment (Gr. IV) with Nano-Se shows mild to moderate thickening of alveoli and moderate reduction in alveolar distortion; **f** lung section of pre-treated group (Gr. V) with Nano-Se showing with no or very slight thickening of alveolar septa and no indication of inflammation; magnification ×400

migration in bronchoalveolar lavage (BAL) cells of mice after pre- and co-treatment with Nano-Se in the comet assay. The important finding of the present studies is that Nano-Se could significantly inhibit CP-induced DNA damage in bronchoalveolar lavage (BAL) cells of mice. These results suggest a protective effect of Nano-Se against pulmonary DNA damage induced by CP. Therefore, it can be considered that Nano-Se plays an important part in the protection against DNA damages in bronchoalveolar lavage cells exposed to CP, which emphasizes the involvement of oxidative stress as a mediator in the induction of DNA lesions in CP-treated bronchoalveolar lavage cells.

Some studies suggest that CP induced apoptosis, as indicated by the derivatives of CP to stimulate outer membrane blebbing and DNA fragmentation [47]. In this study, percentage of DNA fragmentation assay and apoptosis were performed in murine bone marrow cells. CP administration, at a dose of 25 mg/kg b.w triggered the

percentage of DNA fragmentation in bone marrow cells. The AO/EB staining assay further demonstrated that CP increased the number of apoptotic cells in bone marrow. Taken together, it is clear that CP can cause DNA damage and apoptosis in non-tumor cells, which can potentially lead to the secondary mutagenesis and carcinogenesis when it is used for chemotherapy [48]. Pre- and co-treatment with Nano-Se reduced the percentage of DNA fragmentation and number of apoptotic cells in bone marrow cells. It had already been proved in our previous study that Nano-Se has the capability to reduce the percentage of chromosomal aberration and the subsequent DNA damage in both the peripheral blood lymphocyte and the bone marrow cells of mice due to its genoprotective and cytoprotective activity [19].

It was reported that an increase in MDA level in the lungs reflected the enhanced oxidative damage to biological membrane [49]. Lung injury and its pathogenesis involve peroxidative breakdown of polyunsaturated fatty acids, which affects the membrane function, inactivates membrane bound receptors, and increases tissue permeability. Aldehydes which are generated during the process of LPO have been associated with oxidative stress in tissues [50]. It has been reported that Nano-Se is a good antioxidant [19, 51]. In our study, the result clearly showed that acute intoxication with CP caused a significant increase in pulmonary LPO level. Concomitant and pretreatment with Nano-Se effectively inhibited the CP-induced pulmonary LPO level. This may be in part, due to scavenging of ROS and consequent inhibition of oxidative stress, produced by CP, by Nano-Se. This proves the protective role of the Nano-se in preventing lipid peroxidation and in maintaining the integrity and normal function of the lungs.

Non-enzymatic antioxidants like glutathione is considered as second line of defense and protect the cells against oxidative stress mediated cellular injury either by scavenging free radicals or by converting the toxic radicals to non-toxic end products. Administration of CP in the current study significantly reduced the pulmonary content of GSH. CP metabolism produces highly reactive electrophiles that lead to electrophilic burden on the cells and also due to the formation of acrolein, which deplete GSH contents [52]. This is in line with other reports that demonstrated GSH reduction or depletion following CP injection in animals [53, 54]. Further, treatment with Nano-Se both pre- and concomitant schedule significantly increased the reduced glutathione level which can be attributed to the free radicals scavenging ability of Nano-Se.

The GSTs catalyze the GSH-dependent detoxification of reactive electrophiles such as genotoxic chemical carcinogens and cytotoxic chemotherapeutic agents [55, 56]. In the present study, CP administration resulted in a decreased activity of this GSH metabolizing enzyme in lung tissue. The oxidative modification in the native protein structure of GST and its increased utilization in the detoxification processes that involve GSH may be the most probable explanation of the reduced GST activity in the CP-treated mice. In the present investigation, pre- and concomitant treatment with Nano-Se restored the activity near to vehicle-treated group.

Cellular antioxidant defenses involving the enzymes, SOD, CAT, and GP*x* play an important role against ROS generation during oxidative stress and protect tissues including lung from oxidative damage [57–60]. SOD catalyzes dismutation of the superoxide anion to H_2O_2 and O_2. The harmful H_2O_2 is further detoxified to water by CAT and GP*x*. Therefore, the activity of theses antioxidant enzymes is a vital protection against oxidative stress. CP-induced pulmonary toxicity is associated with oxidative stress caused by the reduction in the antioxidant enzymes [61]. In our present study, the activities of the antioxidant enzymes SOD, CAT, and GP*x* in the lung were significantly reduced by CP treatment indicating pronounced oxidative stress. Nano-Se administration produced a significant protection against CP-induced changes in antioxidant enzyme activity by restoring them to normal by preventing the induction of oxidative stress and enhancing the pulmonary antioxidant defenses involving SOD- and GSH-dependent enzymes.

Finally, histopathological studies also provided evidence for the protective effect of Nano-Se on CP-induced pulmonary toxicity in mice. Findings similar to present study such as pulmonary fibrosis, thickened alveolar septa, pulmonary congestion, and pulmonary inflammation have been reported in CP-treated animals [54]. Nano-Se treatment effectively reverts histological changes demonstrating a protective role of Nano-Se against anticancer drug-induced lung injury, and the best result is obtained in the pretreatment group.

Conclusion

This study demonstrates for the first time that Nano-Se has a protective role in the abatement of CP-induced pulmonary toxicity and apoptosis in bone marrow cells in mice. In conclusion, the present studies further demonstrated that CP may induce oxidative stress, genotoxicity, and trigger apoptosis in lungs and in bone marrow cells also. Nano-Se, a pharmacologically active and less toxic new form of selenium reduced CP-induced functional and histological damage in lung as well as genotoxicity. Furthermore, Nano-Se suppressed the generation of ROS, lipid peroxidation, and oxidative stress. This protective effect resides, at least in part, in its radical scavenger activity. The

improvement of anti-genotoxic activity on bone marrow cells of animal pre-treated with Nano-Se in CP toxicity may focus attention on the beneficial effect of Nano-Se to overcome one of the serious problems in cancer chemotherapy, which is the bone marrow suppression and related immunosuppression. Therefore, Nano-Se can be a promising chemoprotective agent and may be useful to avert secondary malignancy and to reduce the risk for abnormal reproductive outcomes in cancer patients and medical personnel exposed to CP.

Acknowledgements This work was financially supported by Grant from Indian Council of Medical Research, New Delhi, India (no. 45/36/2008/PHA-BMS). Arin Bhattacharjee gratefully acknowledges ICMR for Senior Research Fellowship. Abhishek Basu also gratefully acknowledges ICMR for Senior Research Fellowship (no. 3/2/2/58/2011/NCD-III). The authors wish to thank the Director, CNCI, for supporting this study.

Compliance with Ethical Standards The entire experiments were carried out strictly following compliance with the ethical standards and guidelines of Institutional Animal Ethics Committee [Committee for the Purpose of Control and Supervision of Experiment on Animals, India].

Conflict of interest We declare that we have no conflict of interest.

References

1. Rehman MU, Tahir M, Ali F, Qamar W, Lateef A, Khan R, Quaiyoom A, Oday-O-Hamiza, Sultana S (2012) Cyclophosphamide-induced nephrotoxicity, genotoxicity, and damage in kidney genomic DNA of Swiss albino mice: the protective effect of ellagic acid. Mol Cell Biochem 365:119–127
2. IARC (2012) IARC Working Group on the evaluation of carcinigenic risks to human, pharmaceuticals, volume 100 A, a review of human carcinogenesis. IACR Monogr Eval Carcinog Risks Hum 100:1–401
3. Nafees S, Ahmad ST, Arjumand W, Rashid S, Ali N, Sultana S (2012) Modulatory effects of gentisic acid against genotoxicity and hepatotoxicity induced by cyclophosphamide in Swiss albino mice. J Pharm Pharmacol 64:259–267
4. Basu A, Bhattacharjee A, Roy SS et al (2014) Vanadium as a chemoprotectant: effect of vanadium(III)-L-cysteine complex against cyclophosphamide-induced hepatotoxicity and genotoxicity in Swiss albino mice. J Biol Inorg Chem 19:981–996
5. Ghosh P, Bhattacharjee A, Basu A, Roy SS, Bhattacharya S (2014) Attenuation of cyclophosphamide-induced pulmonary toxicity in Swiss albino mice by naphthalimide-based organoselenium compound 2-(5-selenocyanatopentyl)-benzo[de]isoquinoline 1,3- dione. Pharm Biol 4:1–9
6. Chaudhary NI, Schnapp A, Park JE (2006) Pharmacologic differentiation of inflammation and fibrosis in the rat bleomycin model. Am J Respir Crit Care Med 173:769–776
7. Sulkowska M, Skrzydlewska E, Sobaniec-Lotowska M (2002) Effect of cyclophosphamide-induced generation of oxygen forms on ultrastructure of liver and lung. Bull Vet Inst Pulawy 46:239–246
8. Pacht ER, Davis WB (1988) Role of transferin and ceruloplasmin in antioxidant activity of lung epithelial lining fluid. J Appl Physiol 64:2092–2099
9. Suntres ZE, Shek PN (1996) Alleviation of paraquat-induced lung injury by pretreatment with bifunctional liposomes containing α-tocopherol and glutathione. Biochem Pharmacol 52:1515–1520
10. Drake EN (2006) Cancer chemoprevention: selenium as a prooxidant not an antioxidant. Med Hypotheses 67:318–322
11. Zhang JS, Gao XY, Zhang LD, Bao YP (2001) Biological effects of a nano red elemental selenium. Biofactor 15:27–38
12. Pagmantidis V, Meplan C, van Schothorst EM, Keijer J, Hesketh JE (2008) Supplementation of healthy volunteers with nutritionally relevant amounts of selenium increases the expression of lymphocyte protein biosynthesis genes. Am J Clin Nutr 87:181–9
13. El-Bayoumy K, Sinha R (2004) Mechanisms of mammary cancer chemoprevention by organoselenium compounds. Mutat Res 551:181–197
14. Spallholz JE (1994) On the nature of selenium toxicity and carcinostatic activity. Free Radic Biol Med 17:45–64
15. Prathna TC, Chandrasekaran N, Raichur AM, Mukherjee A (2011) Biomimetic synthesis of silver nanoparticles by Citrus limon (lemon) aqueous extract and theoretical prediction of particle size. Colloids Surf B Biointerfaces 82:152–9
16. Tanaka T, Kohno H, Murakami M, Kagami S, El-Bayoumy K (2000) Suppressing effects of dietary supplementation of the organoselenium 1,4-phenylene bis(methylene)selenocyanate and the Citrus antioxidant auraptene on lung metastasis of melanoma cells in mice. Cancer Res 60:3713–3716
17. Clark LC, Combs GF Jr, Turnbull BW et al (1996) Effects of selenium supplementation for cancer prevention in patients with carcinoma of the skin. A randomized controlled trial. Nutritional Prevention of Cancer Study Group. JAMA 276:1957–63
18. Wang H, Zhang J, Yu H (2007) Elemental selenium at nano size possesses lower toxicity without compromising the fundamental effect on selenoenzymes: comparison with selenomethionine in mice. Free Radic Biol Med 42:1524–1533
19. Bhattacharjee A, Basu A, Ghosh P, Biswas J, Bhattacharya S (2014) Protective effect of selenium nanoparticle against cyclophosphamide induced hepatotoxicity and genotoxicity in Swiss albino mice. J Biomater Appl 29:303–317
20. Zhang J, Wang H, Bao Y, Zhang L (2004) Nano red elemental selenium has no size effect in the induction of seleno-enzymes in both cultured cells and mice. Life Sci 75:237–244
21. Henderson RF, Benson JM, Hahn FF, Hobbs CH et al (1985) New approaches for the evaluation of pulmonary toxicity: bronchoalveolar lavage fluid analysis. Fundam Appl Toxicol 5:451–458
22. D'Armour FE, Blood FR, Belden DA (1965) The manual for laboratory work in mammalian physiology, 3rd edn. The University of Chicago Press, Chicago
23. Wintrobe MM, Lee DR, Boggs DR, Bithel TC, Athens JW, Foerester J (1961) Clinical hematology, 5th edn. Lea and Febiger, Philadelphia
24. Zou AP, Li N, Cowley AW Jr (2001) Production and actions of superoxide in the renal medulla. Hypertension 37:547–53
25. Robinson JP (2001) Oxidative metabolism. Curr Protoc Cytom 9:9.7. doi:10.1002/0471142956.cy0907s02
26. Driver AS, Kodavanti PR, Mundy WR (2000) Age-related changes in reactive oxygen species production in rat brain homogenates. Neurotoxicol Teratol 22:175–81
27. Carter WO, Narayanan PK, Robinson JP (1994) Intracellular hydrogen peroxide and superoxide anion detection in endothelial cells. J Leukoc Biol 55:253–8
28. Coşkun S, Gönül B, Ozer C, Erdoğan D, Elmas C (2007) The effects of dexfenfluramine administration on brain serotonin immunoreactivity and lipid peroxidation in mice. Cell Biol Toxicol 23:75–82
29. Dhawan A, Mathur N, Seth PK (2001) The effect of smoking and eating habits on DNA damage in Indian population as measured in the Comet assay. Mutat Res 474:121–8

30. Abid-Essefi S, Zaied C, Bouaziz C, Salem IB, Kaderi R, Bacha H (2012) Protective effect of aqueous extract of Allium sativum against zearalenone toxicity mediated by oxidative stress. Exp Toxicol Pathol 64:689–95
31. Zhivotovsky B, Samali A, Orrenius S (2001) Determination of apoptosis and necrosis. Curr Protoc Toxicol, Chapter 2: Unit 2.2. doi:10.1002/0471140856.tx0202s00
32. Shylesh BS, Nair SA, Subramoniam A (2005) Induction of cell specific apoptosis and protection from Dalton's lymphoma challenge in mice by an active fraction from Emilia Sonchifolia. Indian J Pharmacol 37:232–7
33. Okhawa H, Ohishi N, Yagi K (1979) Assay for lipid peroxides in animal tissues by thiobarbituric acid reaction. Anal Biochem 95:351–358
34. Sedlack J, Lindsay RN (1968) Estimation of total protein bound and non-protein sulfhydryl groups in tissue with ellman's reagent. Anal Biochem 25:192–205
35. Habig WH, Pabst MJ, Jacoby WB (1974) Glutathione S-transferases, the first enzymatic step in marcapturic acid formation. J Biol Chem 249:7130–7139
36. Marklund S, Marklund G (1974) Involvement of the superoxide anion radical in autooxidation of pyrogallol and a convenient assay for superoxide dismutase. Eur J Biochem 47:469–474
37. McCord JM, Fridovich I (1969) Superoxide dismutase: an enzymatic function for erythrocuprein (hemoprotein). J Biol Chem 244:6049–6055
38. Luck HA (1963) Spectrophotometric method for estimation of catalase. In: Bergmeyer HV (ed) Methods of enzymatic analysis. Academic Press, New York, pp 886–888
39. Paglia DE, Valentine WN (1967) Studies on the quantitative and qualitative characterization of erythrocyte glutathione peroxidase. J Lab Clin Med 70:158–169
40. Lowry OH, Rosenbrough NJ, Farr AL, Randall RJ (1951) Protein measurement with the folin phenol reagent. J Biol Chem 193:265–276
41. Blackwell S, Crawford J (1994) Filgrastim (r-metHuG-CSF) in the chemotherapy setting. In: Morstyn G, Dexter TM, Foote M (eds) Filgrastim (r-metHuGCSF) in clinical practice. Marcel Dekker, New York, pp 103–106
42. Yoshida Y, Itoh N, Saito Y, Hayakawa M, Niki E (2004) Application of water soluble radical initiator, 2,2-azobis[2-(2-imidazolin-2-yl)propane] di-hydrochloride, to a study of oxidative stress. Free Radical Res 38:375–384
43. Halliwell B, Whiteman M (2004) Measuring reactive species and oxidative damage in vivo and in cell culture: how should you do it and what do the results mean? Br J Pharmacol 142:231–255
44. Boyaci H, Maral H, Turan G, Başyiğit I, Dillioğlugil MO, Yildiz F, Tugay M, Pala A, Erçin C (2006) Effects of erdosteine on bleomycin-induced lung fibrosis in rats. Mol Cell Biochem 281:129–37
45. Ricciardolo FL, Sterk PJ, Gaston B, Folkerts G (2004) Nitric oxide in health and disease of the respiratory system. Physiol Rev 84:731–765
46. Povirk LF, Shuker DE (1994) DNA damage and mutagenesis induced by nitrogen mustards. Mutat Res 318:205–26
47. Bullock G, Tang C, Tourkina E, Ibrado AM, Lutzky J, Huang Y, Mahoney ME, Bhalla K (1993) Effect of combined treatment with interleukin-3 and interleukin-6 on 4- hydroperoxycyclophosphamide-induced programmed cell death or apoptosis in human myeloid leukemia cells. Exp Hematol 21:1640–1647
48. Ferguson LR, Pearson AE (1996) The clinical use of mutagenic anticancer drugs. Mutat Res 355:1–12
49. Husain K, Somani SM (1997) Interaction of exercise training and chronic ethanol ingestion on hepatic and plasma antioxidant system in rat. J Appl Toxicol 17:189–194
50. Uchida K, Shiraishi M, Naito Y, Torii N, Nakamura Y, Osawa T (1999) Activation of stress signaling pathways by the end product of lipid peroxidation. J Biol Chem 274:2234–2242
51. Hassanin KM, Abd El-Kawi SH, Hashem KS (2013) The prospective protective effect of selenium nanoparticles against chromium-induced oxidative and cellular damage in rat thyroid. Int J Nanomed 8:1713–20
52. McDiarmid MA, Iype PT, Kolodner K et al (1991) Evidence for acrolein-modified DNA in peripheral blood leucocytes of cancer patients treated with cyclophosphamide. Mutat Res 248:93–9
53. Manda K, Bhatia AL (2003) Prophylactic action of melatonin against cyclophosphamide-induced oxidative stress in mice. Cell Biol Toxicol 19:367–72
54. Ashry NA, Gameil NM, Suddek GM (2013) Modulation of cyclophosphamide-induced early lung injury by allicin. Pharm Biol 51:806–11
55. Coles BF, Kadlubar FF (2003) Detoxification of electrophilic compounds by glutathione S-transferase catalysis: determinants of individual response to chemical carcinogens and chemotherapeutic drugs? BioFactors 17:115–30
56. Jagetia GC, Reddy TK (2011) Alleviation of iron induced oxidative stress by the grape fruit flavanone naringin in vitro. Chem Biol Interact 190:121–8
57. Day BJ (2008) Antioxidants as potential therapeutics for lung fibrosis. Antioxid Redox Signal 10:355–370
58. Selvakumar E, Prahalathan C, Mythili Y, Varalakshmi P (2005) Mitigation of oxidative stress in cyclophosphamide-challenged hepatic tissue by DL-α-lipoic acid. Mol Cell Biochem 272:179–85
59. Das JK, Sarkar S, Hossain SU, Bhattacharya S (2013) Diphenylmethyl selenocyanate attenuates malachite green induced oxidative injury through antioxidation and inhibition of DNA damage in mice. Indian J Med Res 137:1163–1173
60. Talas ZS, Ozdemir I, Yilmaz I, Gok Y (2009) Antioxidative effects of novel synthetic organoselenium compound in rat lung and kidney. Ecotoxicol Environ Saf 72:916–921
61. Saba Khan S, Parvez S, Chaudhari B, Ahmad F, Anjum S, Raisuddin S (2013) Ellagic acid attenuates bleomycin and cyclophosphamide-induced pulmonary toxicity in Wistar rats. Food Chem Toxicol 58:210–9

Chemoprotective and chemosensitizing properties of selenium nanoparticle (Nano-Se) during adjuvant therapy with cyclophosphamide in tumor-bearing mice

Arin Bhattacharjee, Abhishek Basu, Jaydip Biswas, Tuhinadri Sen & Sudin Bhattacharya

Molecular and Cellular Biochemistry
An International Journal for Chemical Biology in Health and Disease

ISSN 0300-8177

Mol Cell Biochem
DOI 10.1007/s11010-016-2839-2

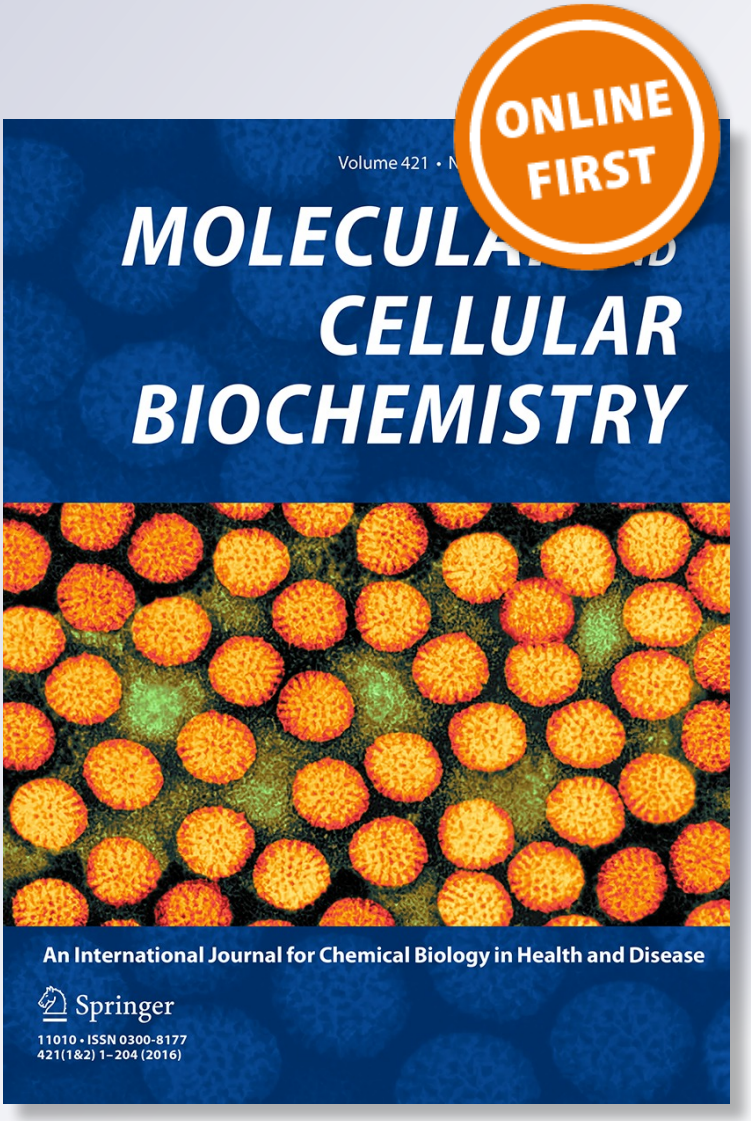

Springer

Mol Cell Biochem
DOI 10.1007/s11010-016-2839-2

Chemoprotective and chemosensitizing properties of selenium nanoparticle (Nano-Se) during adjuvant therapy with cyclophosphamide in tumor-bearing mice

Arin Bhattacharjee[1] · Abhishek Basu[1] · Jaydip Biswas[2] · Tuhinadri Sen[3] · Sudin Bhattacharya[1]

Received: 14 July 2016 / Accepted: 24 September 2016

Abstract Cyclophosphamide (CP) is one of the widely used anticancer agents; however, it has serious deleterious effects on normal host cells due to its nonspecific action. The essential trace element Selenium (Se) is suggested to have chemopreventive and chemotherapeutic efficacy and currently used in pharmaceutical formulations. Previous report had shown Nano-Se could protect CP-induced hepatotoxicity and genotoxicity in normal Swiss albino mice; however, its role in cancer management is still not clear. The aim of present study is to investigate the chemoprotective efficacy of Nano-Se against CP-induced toxicity as well as its chemoenhancing capability when used along with CP in Swiss albino mice against Ehrlich's ascites carcinoma (EAC) cells. CP was administered (25 mg/kg b.w., i.p.) and Nano-Se was given (2 mg Se/kg b.w., p.o.) in concomitant and pretreatment schedule. Increase levels of serum hepatic marker, hepatic lipid peroxidation, DNA damage, and chromosomal aberration in CP-treated mice were significantly ($P < 0.05$) reversed by Nano-Se. The lowered status of various antioxidant enzymes in tumor-bearing mice after CP treatment was also effectively increased by Nano-Se. Administration of Nano-Se along with CP caused a significant reduction in tumor volume, packed cell volume, viable tumor cell count, and increased the survivability of the tumor-bearing hosts. The results suggest that Nano-Se exhibits significant antitumor and antioxidant effects in EAC-bearing mice. The potential for Nano-Se to ameliorate the CP-evoked toxicity as well as to improve the chemotherapeutic effect could have beneficial implications for patients undergoing chemotherapy with CP.

Keywords Nano-Se · Cyclophosphamide · Chemoprotection · Chemopotentiation · Angiogenesis · Apoptosis

Introduction

Nanotechnology and nanoengineering stand to produce significant scientific and technological advances in diverse fields including pathology and medicine. The combination of cancer biology and nanotechnology has led to the development of an interdisciplinary area, cancer nanotechnology, which shows broad applications in molecular imaging, molecular diagnosis, and targeted therapy [1]. The excellent performance of bionanomaterials opens novel horizons for diagnosis and therapy of diseases such as malignant neoplasms that have traditionally been recognized as incurable via basic therapies or surgical methods [2].

Cancer chemotherapy is one of the major therapeutic modalities used for the treatment of a large number of cancer patients. However, in many cases, chemotherapy alone cannot achieve a satisfactory therapeutic outcome, namely the complete remission of tumors, and induction of severe form of toxicity at therapeutically effective doses. Most of the commonly used anticancer drugs currently

✉ Sudin Bhattacharya
sudinb19572004@yahoo.co.in

[1] Department of Cancer Chemoprevention, Chittaranjan National Cancer Institute, 37, S. P. Mukherjee Road, Kolkata, West Bengal 700026, India

[2] Department of Translational Research, Chittaranjan National Cancer Institute, 37, S. P. Mukherjee Road, Kolkata, West Bengal 700026, India

[3] Division of Pharmacology, Department of Pharmaceutical Technology, Jadavpur University, 188, Raja S. C. Mullick Road, Kolkata, West Bengal 700032, India

Published online: 01 October 2016

used in chemotherapy are nonspecific in action; hence cytotoxic to normal cells, leading to unwanted adverse effects. Chemotherapy-associated adverse effects in cancer patients have been linked to generation of oxidative stress in normal organs and tissues [3]. CP is a bifunctional alkylating agent and has been in the clinic since the late-1950s, indicated for various forms of malignancies in combination with other chemotherapeutic drugs [4]. Although there is broad-spectrum clinical applications of cyclophosphamide for tumor treatment, as a double-edged sword it imparts severe toxic side effects, hematopoietic suppression, hepatotoxicity, immunotoxicity, mutagenicity, urotoxicity, cardiotoxicity, teratogenicity, and carcinogenicity [5–7]. In view of the drawbacks of chemotherapeutic agents, there is an urgent need for a sensitizing agent which can selectively exert its cytotoxic effect toward cancer cells when used alone or in combination with other chemotherapeutic agents, at the same time protecting the normal cells.

Selenium (Se) is one of the essential trace elements present in the body and has great importance in maintaining physiological homeostasis [8, 9]. High levels of selenium in blood plasma have been correlated with prevention of several types of cancers, several cardiovascular diseases, muscle disorders, and, to a certain extent, diabetes mellitus [10]. The role of selenocompounds as chemopreventive and chemotherapeutic agents has been supported by a large number of epidemiological, preclinical, and clinical studies [11]. Results from epidemiologic, ecological, and clinical studies have shown that Se has the potential to reduce the incidence of some cancers, such as prostate, lung, and colon cancers [12]. Accumulative evidences have suggested that the dose and the chemical form (structure) are determinants for anticancer activities of selenocompounds [13]. Several different kinds of Se compounds, such as selenomethionine (SeMet), sodium selenite, monomethylated Se etc., had been tested for their chemotherapeutic activity [14]. They are more effective at high dosage, however high dosage of these compounds incurs some side effects [15]. Se occurs in a variety of oxidation states like selenate (SeO_4^{2-})/selenite (SeO_3^{2-}) oxyanions, wherein the oxidation states are +6 and +4; elemental selenium (Se^0), and selenide (Se^{2-}) [16]. The toxicity of these states is related to their degrees of solubility in water and hence their bioavailability. In recent times, there has been increasing interest in medicinal importance of nanoparticles using biological systems leading to the development of various biomimetic approaches. Nano-sized particles exhibit unique properties that arise from their larger surface/volume ratio and higher surface energy [17]. Recently, the introduction of nanosize selenium (Nano-Se) produces a highly effective molecular compound in medical diagnostics and therapy. It showed similar efficacy in increasing antioxidant GP*x* activity while displaying lower toxicity when compared to SeMet [18, 19]. These nanoparticles also show better biological activity due to good adsorptive ability as a result of interaction between the nanoparticles and NH, C=O, COO^-, and C–N groups of proteins present in the cell membrane [20]. In addition, nanoparticles of selenium are able to cause apoptosis in drug-resistance hepatocarcinoma cells by destabilizing their mitochondrial membrane [21]. Nano-Se has also been reported to possess antibacterial as well as antiviral activities [22].

We had earlier synthesized and characterized Nano-Se and evaluated its chemoprotective activity against CP-induced hepatotoxicity, pulmonary, and genotoxicity in normal Swiss albino mice [23, 24]. The present study was designed to examine the antitumor efficacy of synthesized Nano-Se in the tumor-bearing Swiss albino mice. In this study design, Nano-Se was also administered along with a widely used broad-spectrum chemotherapeutic agent CP to investigate the 'chemoprotective' (protection against chemotherapeutic drug-induced toxicity) and 'chemosensitization' (potentiation of cytotoxicity of chemotherapeutic drugs toward tumor cells) efficacy of Nano-Se.

Materials and methods

Animals enrolled in the study

Adult (5–6 weeks) Swiss albino female mice (25 ± 2 g), bred in the animal colony of Chittaranjan National Cancer Institute (CNCI) (Kolkata, India), were used for this study. The mice were maintained under standard condition of humidity (45–55 %), temperature (23 ± 2 °C), and light (12 h light/12 h dark). Standard food pellets (EPIC rat and mice pellet) from Kalyani Feed Milling Plant, Kalyani, West Bengal, India and drinking water were provided ad libitum. The experiments were carried out following strictly the Institute's Guideline for the Care and Use of Laboratory Animals (CPCSEA Reg. No. 175/99/CPCSEA).

Tumor cells

EAC cells were maintained in Swiss mice by weekly intraperitoneal (i.p.) transplantation of 1×10^6 viable tumor cells suspended in phosphate buffer saline (PBS).

Chemicals

Cyclophosphamide was obtained from Cadila Pharmaceuticals (Bhat, Ahmedabad, India). 1-Chloro-2, 4-dinitrobenzene (CDNB), ethylene diamine tetraacetic acid (EDTA), reduced glutathione (GSH), pyrogallol, 5,5′-

dithio-bis (2-nitro benzoic acid) (DTNB), sodium dodecyl sulfate (SDS), bovine serum albumin (BSA), β-nicotinamide adenine dinucleotide phosphate (reduced), glutathione reductase, normal melting agarose, low melting point agarose, ethidium bromide, sodium azide (NaN_3), HEPES, 2′,7′-dichlorofluorescein diacetate (DCFH-DA), dimethyl sulphoxide (DMSO), Triton X-100, and Giemsa stain were obtained from Sigma-Aldrich Chemicals Private Limited, Bangalore, India. Hydrogen peroxide 30 % (H_2O_2) and thiobarbituric acid (TBA), propylene glycol, sodium carbonate, copper sulfate, sodium hydroxide, potassium sodium tartrate, sucrose, TRIS, dithiothreitol, calcium chloride, di-sodium hydrogen phosphate, sodium dihydrogen phosphate, acetic acid, *n*-butanol, pyridine, hematoxylin, and eosin were obtained from Merck (India) Limited, Mumbai, India. Chloroform and Folin-phenol reagent were purchased from Sisco Research Laboratories Private Limited, Mumbai, India. Magnesium chloride was purchased from Glaxo laboratories (India) Ltd, Bombay. Diethyl ether, dipotassium hydrogen phosphate, and potassium dihydrogen phosphate were obtained from Spectrochem Private Limited, Mumbai, India. Serum alanine transaminase (ALT) and aspartate transaminase (AST) assay kits were obtained from Span Diagnostics Ltd, Udhna, Surat, India. In situ cell detection kit and Mouse Total MMP-9 ELISA Kit were purchased from Roche Molecular and R&D System USA, respectively.

Preparation of nano selenium

The Nano-Se was synthesized following a simplified protocol with slight modifications [25]. 5 ml of 25 mM sodium selenite was mixed with 20 ml of 25 mM reduced GSH containing 200 mg BSA. The mixture was adjusted to pH 7.2 with 1.0 M sodium hydroxide. Upon pH adjustment, the red elemental Se and oxidized glutathione (GSSG) were formed. The red solution was dialyzed against double-distilled water for 96 h with the water changing every 24 h to separate GSSG from Nano-Se under magnetic stirring. The final solution containing Nano-Se and BSA was subjected to centrifugation at 13,000 rpm for 10 min The pellet thus recovered was subjected to washing by its re-suspension in de-ionized water followed by centrifugation at 13,000 rpm for 10 min, to remove possible organic contamination present in nano particles. Finally, pellet was freeze dried using a lyophilizer and stored at room temperature.

Characterization of nano selenium

The obtained lyophilized products were characterized using various microscopic and spectroscopic methods. Transmission electron microscopic (TEM) analysis was performed with Techni 20 (Philips, The Netherlands) for size determination. For this purpose, a thin film of the sample was prepared on a carbon-coated copper grid by dropping a very small amount of the sample on to the grid. The size and morphology of the synthesized Nano-Se were analyzed using a scanning electron microscope (SEM) (FEI Quanta—200 MK2). The spectrum of the energy dispersive X-ray spectroscopy (EDAX) of the sample was carried out using an XL-30 (Philips, The Netherlands) operating at 15–25 kV and employed to examine the elemental composition. The mean size and size distribution were measured at 25 °C by dynamic light scattering (DLS) technique (Zen 3690 Zetasizer Nano ZS 90, Version 7.03).

Drug preparation

Based on our previous study, the synthesized Nano-Se was dissolved in saline (0.9 % NaCl) and administered orally. It was prepared on each day just before treatment.

Experimental design

Mice were acclimatized for 3 days. Mice were divided into seven groups; six mice were kept in the vehicle control group (VC), and 12 mice were kept each in the rest of the six groups (E-PECD). Six animals from these groups were taken to check the survivability of each group; while rest of the animals were kept for the study of hematological and biochemical parameters and antitumor activity. Animals of Group (E-PECD) were injected with EAC cells (1×10^6 cells/mouse) intraperitoneally. The day of EAC cell inoculation was counted as day zero. No treatment was given on the day of EAC cell inoculation. The groups were treated as follows:

Vehicle control (VC): Each animal was given oral administration of saline (0.9 % NaCl) from day 1 to day 10 and was kept as normal.

EAC control (E): Animals were given saline (0.9 % NaCl) by oral gavages from day 1 to day 10.

Only CP-treated group (EC): Animals were received CP at a dose of 25 mg/kg b.w. in water by intraperitoneal administration from day 1 to day 10.

Only Nano-Se concomitant-treated group (ED): Animals were treated only with Nano-Se at a dose of 2 mg Se/kg b.w. 24 h after tumor inoculation from day 1 to day 10.

Only Nano-Se-pretreated group (PED): Animals were pretreated with the Nano-Se at a dose of 2 mg Se/kg b.w. 7 days prior to tumor inoculation, and the treatment was continued 24 h after tumor inoculation from day 1 to day 10. (The day of EAC cell inoculation was count as day zero.)

Concomitant treatment with CP and Nano-Se (ECD): Nano-Se was administered orally at a dose of 2 mg Se/kg b.w. along with CP (25 mg/kg b.w.) from day 1 to day 10.

Pretreatment with CP and Nano-Se (PECD): Animals were given Nano-Se orally at a dose of 2 mg Se/kg b.w. 7 days prior to tumor inoculation and the treatment was continued from day 1 to day 10 starting from 24 h after tumor inoculation along with CP (25 mg/kg b.w.).

Biochemical estimation

Determination of hepatic ROS production

ROS generation was measured in liver homogenate using DCFH-DA following a simplified protocol with slight modifications [5, 26]. DCFH-DA is a non-fluorescent probe that is hydrolyzed by mitochondrial esterase to form 2′,7′-dichlorodihydrofluorescein (DCFH), which is then oxidized by ROS to form the fluorescent compound 2′,7′-dichlorofluorescein (DCF). Liver tissues were homogenized in Locke's buffer (pH 7.4), and tissue homogenate was loaded with 10 μM DCFH-DA. The samples were incubated in dark for 45 min to allow the formation of DCF and then analyzed for fluorescence (excitation 485 nm/emission 530 nm) using spectrofluorimeter (Varian Cary Eclipse). Values were expressed as fluorescence intensity normalized per mg of protein.

Quantitative estimation of lipid peroxidation

The level of lipid peroxides formed was measured using TBA and expressed as nmol of thiobarbituric acid reactive substances (TBARS) formed per mg of protein using the extinction co-efficient of 1.56×10^5 m/cm [27].

Isolation of serum

Blood samples were collected from mice by retro-orbital venous plexus under anesthesia and centrifuged at $2000 \times g$ for 10 min for serum separation. Finally, serum samples were stored in aliquots at −20 °C for later use. All serum samples were thawed once at the time of the assay.

Measurement of serum biochemical parameters

Alanine aminotransferase (ALT) and aspartate aminotransferase (AST) levels were measured spectrophotometrically by the standard enzymatic method using commercial kits (Span Diagnostics Ltd.) [28].

Estimation of reduced glutathione (GSH) level

GSH level was estimated in liver cytosol spectrophotometrically by determination of DTNB reduced by –SH groups by measuring the absorbance at 412 nm. The level of GSH was expressed as nmol/mg of protein [29].

Estimation of glutathione-s-transferase (GST) activity

GST activity was measured in the liver cytosol. The enzyme activity was determined from the increase in absorbance at 340 nm with CDNB as the substrate and specific activity of the enzyme was expressed as formation of CDNB-GSH conjugate/min/mg of protein [30].

Estimation of glutathione peroxidase (GPx) activity

GP*x* activity in liver was measured by NADPH oxidation using a coupled reaction system consisting of GSH, glutathione reductase, and H_2O_2 [31]. Briefly, 100 μl of enzyme sample was incubated for 10 min with 800 μl reaction mixtures (0.25 M potassium phosphate buffer containing 2.5 mM EDTA and 2.5 mM sodium azide, 10 mM GSH, 2.5 mM NADPH, and 2.4 units of glutathione reductase). The reactions started on adding 100 μl H_2O_2 and follow the decrease in NADPH absorbance at 340 nm for 3 min. The enzyme activity was expressed as micromole NADPH utilized/min/mg of protein, using extinction co-efficient of NADPH at 340 nm as 6200 m/cm.

Estimation of superoxide dismutase (SOD) activity

SOD activity was determined by quantification of Pyrogallol auto-oxidation inhibition and expressed as unit/mg of protein. One unit of enzyme activity is defined as the amount of enzyme necessary for inhibiting the reaction by 50 %. Auto-oxidation of Pyrogallol in Tris–HCl buffer (50 mM, pH 7.5) is measured by increase in absorbance at 420 nm [32, 33].

Estimation of catalase (CAT) activity

CAT activity in liver cytosol was determined spectrophotometrically at 240 nm and expressed as unit/mg of protein, where the unit is the amount of enzyme that liberates half the peroxide oxygen from H_2O_2 in second at 25 °C [34].

Hematopathological studies

Hemoglobin (Hb) content of blood sample was measured following Sahli's method [35]. RBC [36] and WBC counts were made following a literature procedure [37].

Estimation of protein

Total protein content in tissue homogenate during biochemical analysis was measured through Lowry method using Folin-Phenol reagent [38]. The absorbance of the

color was measured against the colorless blank sample at 660 nm using the Varian Cary 100 UV–Vis Spectrophotometer.

Histopathological studies

Qualitative changes in liver tissues were determined histologically. In brief, the tissues were sliced into 5–6 mm thick sections and fixed for 48 h in 10 % formaline, dehydrated in an ascending graded series of ethanol, cleared in xylene, and embedded in paraffin. Sections of the tissues were cut by rotary microtome and stained with hematoxylin and eosin. Stained sections were evaluated by observing the arrangement of liver architecture with a light microscope (Leica DM 1000). Photomicrographs were taken with the software Las EZ at ×400 magnification.

Detection of DNA damage in peripheral blood lymphocyte by comet assay

Possible DNA damage induced by cyclophosphamide was detected using the alkaline single cell gel electrophoresis (comet assay) following a simplified protocol with slight modification [39, 40]. The mice were sacrificed and blood was collected from each mouse of all groups. Lymphocytes were isolated from blood samples by standard centrifugation over a cushion of Histopaque, washed with isotonic solution, and centrifuged. The pellet was re-suspended in isotonic phosphate-buffered saline solution. The cell viability in each group was measured, and approximately 10^4 cells/slide were taken for the assay. An aliquot of 10 µl of freshly prepared single cell suspension was mixed with 1 % low melting agarose and layered on the half frosted slides precoated with normal melting agarose. A third layer of 0.5 % low melting point agarose was layered on the top of the second layer. The cells were lysed for overnight at 4 °C in lysing solution containing 2.5 M NaCl, 100 mM Na_2EDTA, 10 mM Tris buffer, 1 % Triton X-100, and 10 % DMSO (pH 10.0). After lysis, the slides were subjected to electrophoresis in electrophoresis buffer [1 mM Na_2EDTA and 0.3 M NaOH (pH > 13.1)] for 30 min at 300 mA and 20 V. After electrophoresis, the slides were neutralized with neutralizing buffer [0.4 M Tris buffer (pH 7.5)]. The microscopic slides were carefully dried at room temperature and stained with ethidium bromide in water (20 µg/ml; 50 µl/slide). The slides were examined at ×400 magnification under a fluorescence microscope (Model: Leica DM 4000B) with imaging system. Komet 5.5 software was used to take the photomicrograph of cells and to determine the length of the comet tail. A total of 150–200 randomly selected cells (5–7 zones/slide) in each slide were counted (4 slides/animals in each group) to determine the number of damaged cells, and then the percentage of damaged cells were calculated using the following formula:

$$\text{Damaged cell } (\%) = \frac{\text{Number of damaged cells}}{\text{Total number of cells counted}} \times 100.$$

The results were expressed as:

1. Percentage of cells with tail (tailed cells) in each group was scored and
2. Average tail length due to DNA migration in each group.

Preparation of bone marrow cells

Bone marrow cell suspension was prepared from femurs of each animal, where the bone was split longitudinally and the marrow was exposed using forceps, and the content of the femur was flushed gently using 2 ml syringe containing PBS (pH 7.4) into a centrifuge tube. The cells were collected by centrifugation to perform chromosomal aberration and ROS generation in bone marrow cells.

Chromosomal aberration from bone marrow cells

Mice were injected intraperitoneally with 0.03 % colchicine at the rate of 1 ml/100 g b.w. 90 min before sacrifice. Marrow of the femur was flushed in 1 % sodium citrate solution at 37 °C and fixed in acetic acid/ethanol (1:3). Slides were prepared by the conventional flame drying technique [41] followed by Giemsa staining for scoring bone marrow chromosomal aberrations (CA). CA of various natures like stretching, terminal association, break, fragment, ring formation etc. were analyzed. A total of 300 bone marrow cells were observed, 60 from each of 5 mice of a set.

ROS generation in bone marrow cells

Following animal sacrifice, bone marrow cells from the femur bone were collected in PBS (pH 7.4). Intracellular ROS production was detected using a fluorescent probe DCFH-DA, according to the method by Huang [42] with slight modifications. The cells were then centrifuged and re-suspended in PBS in the order of 10^7 cells/ml. Bone marrow cells were then incubated with DCFH-DA (10 µM in DMSO) for 45 min at 37 °C in dark to allow the formation of DCF and then analyzed for fluorescence (excitation 485 nm/emission 530 nm) using spectrofluorimeter (Varian Cary Eclipse).

Tumor growth response

The antitumor effect of Nano-Se on therapeutic efficacy of CP was assessed by measuring the changes in ascites tumor

volume, packed cell volume, and viable tumor cell count. Mean survival time (MST) of each group containing six mice was monitored, and percentage increase in life span (% ILS) was calculated using following equation. MST = (Day of first death + Day of last death)/2. ILS (%) = [(Mean survival time of treated group/Mean survival time of control group) − 1] × 100 [43, 44].

Measurement of intracellular reactive oxygen species (ROS) generation

Intracellular reactive oxygen species were analyzed by spectrofluorimeter using 2′,7′-dichlorodihydrofluorescein diacetate (DCFH-DA) as a specific dye probe which fluoresces on oxidation by ROS to 2′,7′-dichlorofluorescein (DCF). Tumor cells were harvested by centrifugation at 1000 rpm (4 °C, 10 min), washed twice with PBS, and suspended in PBS (1×10^7 cells/ml). Cell suspension was incubated with DCFH-DA (10 μM in DMSO) for 30 min at 37 °C. ROS levels were measured using spectrofluorimeter (Varian Cary Eclipse, with an excitation set at 485 nm and emission at 530 nm) as a change in fluorescence intensity because of the conversion of non-fluorescent DCFH-DA to the highly fluorescent compound 2′,7′-dichlorofluorescein [8].

Detection of DNA damage in tumor cells (comet assay)

Tumor cells in PBS were dispersed by gentle pipetting and collected by centrifugation at 1000 rpm for 10 min at 4 °C. Cell pellets were re-suspended with PBS and the density of cells was adjusted to 1×10^6/ml and used for further analysis. The methodology was same as described in detection of DNA damage in lymphocyte by alkaline single cell gel electrophoresis (comet assay) with modifications.

Immunocytochemical detection of apoptosis by terminal deoxynucleotidyl transferase dUTP nick end labeling (TUNEL) technique

Apoptosis of EAC cells was determined using the terminal deoxynucleotidyl transferase (TdT)-mediated dUTP nick end labeling (TUNEL) method with the help of in situ cell death detection kit. The slides were analyzed under a fluorescence microscope (Leica DM 4000B), and photomicrographs (Leica FW 4000) were taken at ×200 magnification. The cells with apoptosis were identified by green fluorescence. Randomly selected 80–100 cells from 5–6 zones/slide were counted to determine the number of apoptotic cells [45]. The apoptotic index (AI) was calculated using the following equation AI = (Number of labeled cells/Total number of cell counted) × 100.

Peritoneal angiogenesis

To determine the angiogenic response, the tumor-bearing mice were sacrificed and the peritoneum was opened after dissection. The inner lining of the peritoneal cavity was examined for angiogenesis in both tumor control and treated groups and photographed.

Measurement of metallo matrix protein-9 (MMP-9 total) in serum and in ascites fluid of tumor-bearing mice

Total MMP-9 in serum and ascites fluid of EAC-bearing mice was measured by the help of Quantikine Mouse MMP-9 (total) Immunoassay solid-phase kit from R&D systems using quantitative sandwich enzyme immunoassay technique.

Statistical analysis

All data were presented as mean ± standard deviation (SD), $n = 6$ animals per group. One-way ANOVA followed by Tukey's Multiple Comparison Test using Graph Pad Prism (Version 5.00) software was performed for comparisons among groups. Significant difference was indicated when the P value was < 0.05.

Results

Characterization of Nano-Se

For characterizations and biological experiments, lyophilized Nano-Se was characterized by TEM and DLS. TEM images (Fig. 1b) show that the synthesized Nano-Se presents monodisperse and homogeneous spherical structures with an average diameter of about 23.3 nm. The synthesized Nano-Se aqueous solution was stable and clear and Nano-Se is well dispersed in solution, the average size of Nano-Se in aqueous solution measured by DLS is 33.09 nm (Fig. 1c). In our previous study, the purity of the substance was confirmed by EDAX analysis. The EDAX of the nanoparticle dispersion confirmed the presence of elemental selenium [24].

Attenuation of hepatic and bone marrow ROS production by Nano-Se treatment

As shown in Fig. 2a, b, the ROS level in hepatic tissue and bone marrow cell was significantly ($P < 0.05$) higher in EAC-bearing mice (E) compared to the vehicle control group (VC). Intraperitoneal administration of CP significantly ($P < 0.05$) elevated ROS level in liver and in bone

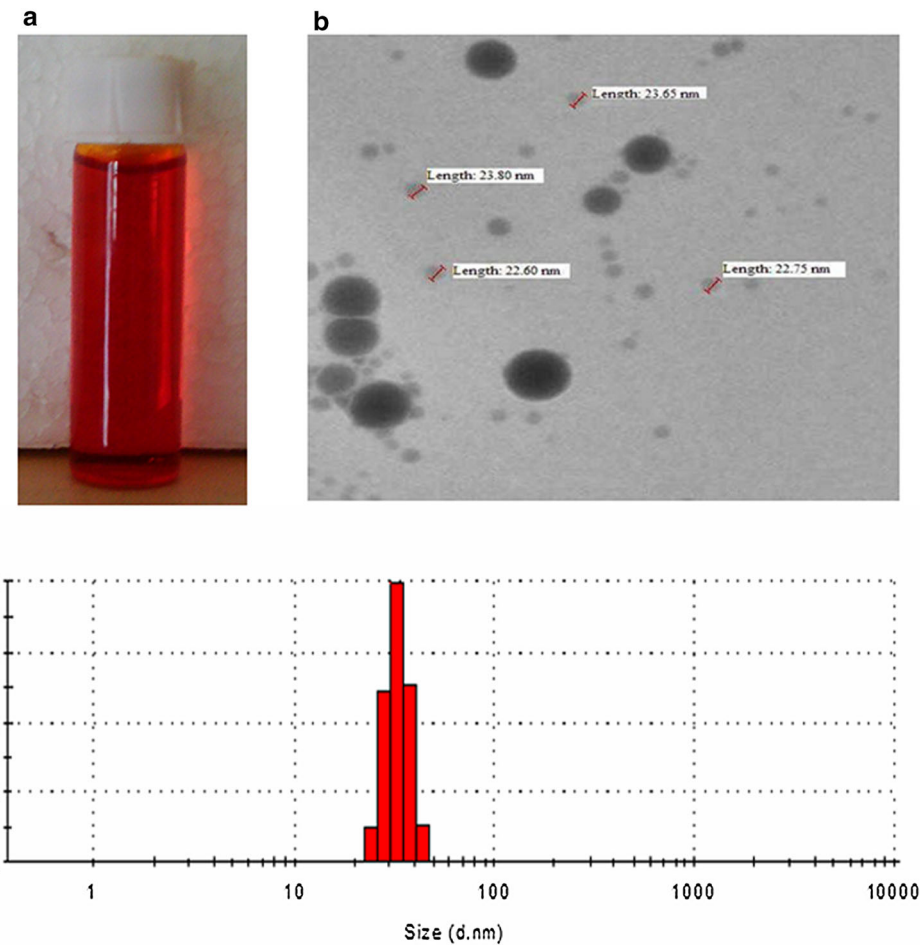

Fig. 1 Characterization of selenium nanoparticles (Nano-Se). **a** Light image of Nano-Se solution. **b** TEM image of Nano-Se. **c** Size distribution of Nano-Se by dynamic light scattering (DLS)

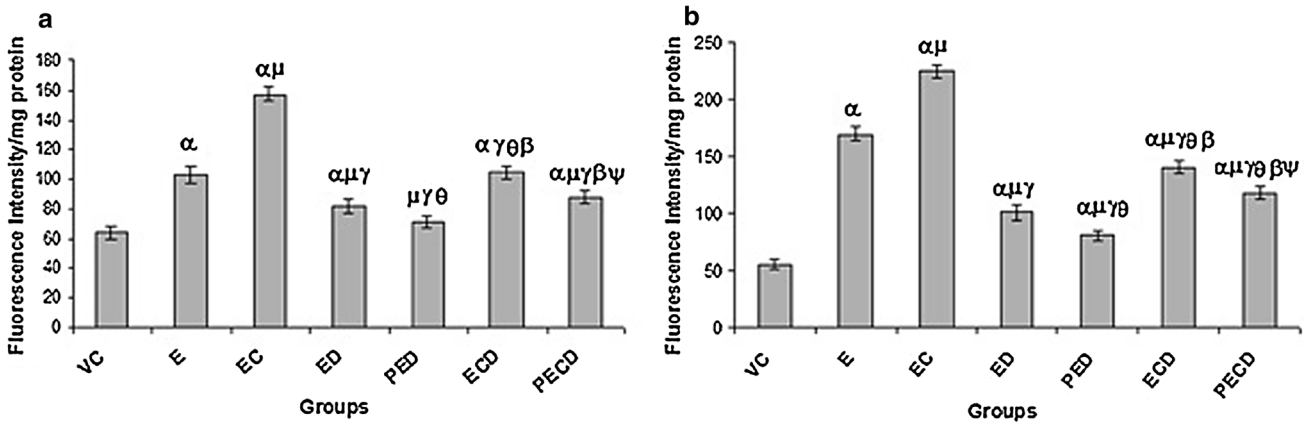

Fig. 2 Effect of monotherapy and combination treatment on **a** hepatic ROS level and **b** bone marrow ROS level of different groups of mice. Data were represented as mean ± standard deviation (SD) ($n = 6$). α—Significant ($P < 0.05$) as compared with VC, μ—significant ($P < 0.05$) as compared with E, γ—significant ($P < 0.05$) as compared with EC, θ—significant ($P < 0.05$) as compared with ED, β—significant ($P < 0.05$) as compared with PED, ψ—significant ($P < 0.05$) as compared with ECD

marrow cells by 53.23 and 32.01 %, respectively, in EC group as compared to the EAC control group (E). Treatment with the Nano-Se itself decreased ROS level by 20.61 % (ED) and 31.12 % (PED) in liver and by 40.47 % (ED) and 52.28 % (PED) in bone marrow as compared to the EAC control group (E). Concomitant treatment (ECD) and pretreatment (PECD) with Nano-Se caused a sharp reduction in ROS level in liver as well as in bone marrow cells. Concomitant treatment (ECD) with Nano-Se significantly reduced ROS level in liver by 33.75 % and in bone

marrow cells by 37.28 %, but on 7 days pretreatment (PECD) with the same inhibited, the ROS level much more significantly by 44.53 % in liver and by 47.1 % in bone marrow cells in comparison to the CP only treated group (EC).

Inhibition of LPO level in liver tissue by Nano-Se treatment

As shown in Fig. 3a, lipid peroxidation level was increased significantly ($P < 0.05$) by 105.69 % in EAC-bearing group (E) compared to the vehicle control group (VC). CP treatment of tumor-bearing mice for 10 days showed a further significant increase of LPO level in liver by 90.17 % in comparison to the EAC control group (E). These enhancements were inhibited during the treatment with Nano-Se in concomitant and pretreatment schedules. Nano-Se itself reduced LPO level by 43.57 % (ED) and 45.84 % (PED) as compared with EAC control group (E). Concomitant treatment (ECD) with Nano-Se inhibited LPO level in liver by 61.19 %, but 7 days pretreatment (PECD) with the same inhibited the elevated LPO level by 68.34 % in comparison to CP-treated group (EC).

Alteration of ALT and AST levels after treatment with Nano-Se

Tumor growth was associated with alteration in liver function as revealed by sharp rise in serum ALT and AST activities (Table 1). The activity of ALT in serum of EAC-bearing mice increased significantly ($P < 0.05$) by 28.16 % (E) compared with vehicle control (VC). After CP treatment (EC), ALT activity in serum again increased by 31.57 % in comparison to the EAC control group. Nano-Se itself reduced the ALT activity by 14.47 % (ED) and 26.71 % (PED) in comparison to EAC control group (E). Nano-Se during CP treatment also significantly reduced the ALT activity by 20 % in case of concomitant treatment (ECD) and by 28 % in case of 7 days pretreatment (PECD) in comparison with EC. There was also a significant rise in AST activity by 45.17 % in the EAC control group (E) as compared to vehicle control (VC) (Table 1). CP treatment again increased the AST activity by 57.97 % in comparison to EAC control group (E). Nano-Se itself decreased AST activity by 25 % (ED) and 29.89 % (PED) as compared to EAC control group (Gr. II). Nano-Se during CP treatment also significantly reduced the AST activity by 30.97 % in

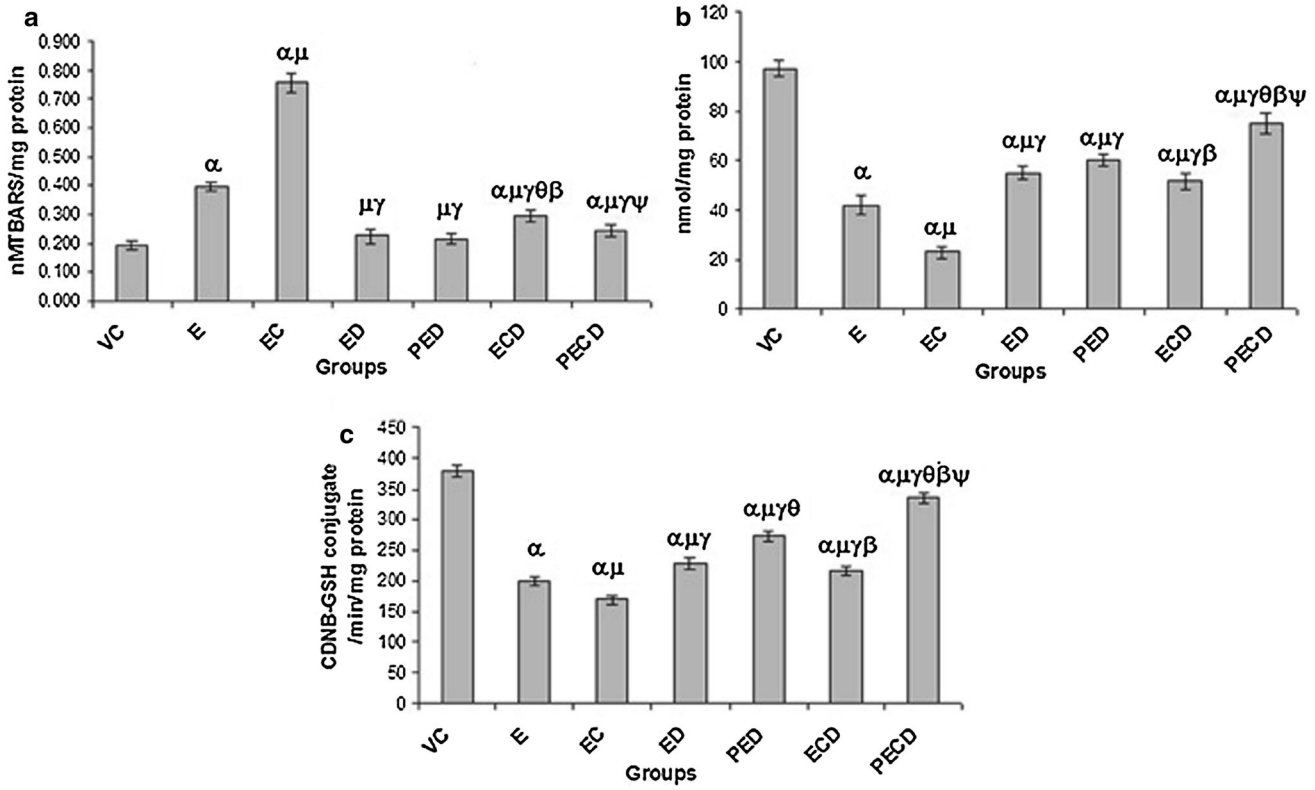

Fig. 3 Effect of monotherapy and combination treatment on **a** LPO level, **b** GSH level and **c** GST activity of different groups of mice. Data were represented as mean ± standard deviation (SD) ($n = 6$). α—Significant ($P < 0.05$) as compared with VC, μ—significant ($P < 0.05$) as compared with E, γ—significant ($P < 0.05$) as compared with EC, θ—significant ($P < 0.05$) as compared with ED, β—significant ($P < 0.05$) as compared with PED, ψ—significant ($P < 0.05$) as compared with ECD

Table 1 Effect of combination treatment of Nano-Se and CP on hematological parameters in tumor-bearing mice

Groups	Hemoglobin (g/dl)	RBC ($\times 10^6$)	WBC ($\times 10^3$)	Alanine transaminase (IU/ml)	Aspartate transaminase (IU/ml)
VC	14.38 ± 0.52	10.08 ± 0.54	6.52 ± 0.46	23.72 ± 0.99	51.8 ± 3.34
E	9.96 ± 0.57$^{\alpha}$	7.08 ± 0.27$^{\alpha}$	14.32 ± 0.69$^{\alpha}$	30.4 ± 1.67$^{\alpha}$	75.2 ± 3.63$^{\alpha}$
EC	6.92 ± 0.67$^{\alpha\mu}$	5.1 ± 0.23$^{\alpha\mu}$	4.18 ± 0.5$^{\alpha\mu}$	40 ± 1.41$^{\alpha\mu}$	118.8 ± 5.93$^{\alpha\mu}$
ED	11.4 ± 1.06$^{\alpha\mu\gamma}$	8.18 ± 0.48$^{\alpha\mu\gamma}$	9.62 ± 0.42$^{\alpha\mu\gamma}$	26 ± 1.4$^{\mu\gamma}$	56.4 ± 3.84$^{\mu\gamma}$
PED	12.28 ± 0.48$^{\alpha\mu\gamma}$	9.88 ± 0.52$^{\mu\gamma\theta}$	8.46 ± 0.46$^{\alpha\mu\gamma\theta}$	22.28 ± 1.63$^{\mu\gamma\theta}$	52.72 ± 3.37$^{\mu\gamma}$
ECD	11.72 ± 0.46$^{\alpha\mu\gamma}$	7.92 ± 0.52$^{\alpha\mu\gamma\beta}$	5.6 ± 0.61$^{\mu\gamma\theta\beta}$	32 ± 2.44$^{\alpha\gamma\theta\beta}$	82 ± 2.44$^{\alpha\gamma\theta\beta}$
PECD	13.6 ± 0.4$^{\mu\gamma\theta\beta\psi}$	9.04 ± 0.47$^{\alpha\mu\gamma\theta\beta\psi}$	7.28 ± 0.42$^{\mu\gamma\theta\beta\psi}$	28.8 ± 2.28$^{\alpha\gamma\beta\psi}$	59.6 ± 3.57$^{\alpha\mu\gamma\psi}$

Data were represented as Mean ± SD ($n = 6$)

$^{\alpha}$ Significant ($P < 0.05$) as compared with VC

$^{\mu}$ Significant ($P < 0.05$) as compared with E

$^{\gamma}$ Significant ($P < 0.05$) as compared with EC

$^{\theta}$ Significant ($P < 0.05$) as compared with ED

$^{\beta}$ Significant ($P < 0.05$) as compared with PED

$^{\psi}$ Significant ($P < 0.05$) as compared with ECD

case of concomitant treatment (ECD) and by 49.83 % in case of 7 days pretreatment (PECD) as in comparison with EC.

Augmentation of GSH level in liver tissue after Nano-Se treatment

Inoculation of EAC drastically decreases the GSH content in liver by 56.92 % in the EAC control (E) when compared with the vehicle control (VC). Anticancer drugs administered independently in EAC bearing caused a significant ($P < 0.05$) reduction in the levels of GSH in liver tissues when compared to EAC control group (E). Nano-Se alone and in the Nano-Se plus CP combination groups showed protective effects on GSH, as there was a significant ($P < 0.05$) increase in GSH level in those groups when compared to the respective groups (Fig. 3b).

Effect of Nano-Se on different antioxidant/ detoxifying enzyme system in tumor-bearing mice

The activity of GST, SOD, CAT, and GP*x* in the liver of EAC-bearing mice decreased significantly ($P < 0.05$) as in comparison with the vehicle control (VC), and these downregulations were even more accelerated by independent administration of anticancer drug. Nano-Se alone in concomitant (ED) and pretreatment (PED) showed a significant protective effect on enzyme activity in comparison to the EAC control (E). Nano-Se during CP treatment (ECD and PECD) also significantly ($P < 0.05$) elevated the activity of enzyme system in tumor-bearing mice (Figs. 3c, 4a, b, c).

Effect of Nano-Se along with CP on hematological parameters

As shown in Table 1, EAC-inoculated mice showed significant ($P < 0.05$) lowering of Hb level and RBC count compared to the vehicle control group. Treatment for consecutive 10 days of CP further declined the Hb level and RBC count significantly ($P < 0.05$) by 30.52 and 28 %, respectively, compared to EAC control group. Treatment with Nano-Se along with CP in concomitant (ECD) and in pretreatment (PECD) scheme increased the Hb level by 69.36 % (ECD), 52.6 % (PECD), and RBC count by 55 % (ECD), 77.25 % (PECD), respectively. Besides EAC inoculation radically increased the WBC count compared to the vehicle control group (VC). Administration of CP led to a huge fall in WBC count. Treatment with Nano-Se in CP-treated mice in ECD and PECD schedule, rose the WBC count significantly ($P < 0.05$) compared to the EC control group. However, monotherapy with Nano-Se in concomitant (ED) and pretreatment (PED) scheme declined the WBC count significantly ($P < 0.05$) compared to the EAC control group.

Histopathological observation

The liver sections of the EAC-inoculated animals showed several changes in hepatic tissue; hepatocytes showed vacuolar degeneration (hydropic changes) with deeply stained pyknotic nuclei and necrosis. These pathological changes became more severe when EAC-inoculated mice treated with chemotherapeutic drug CP and revealed the loss of normal appearance which includes congestion of

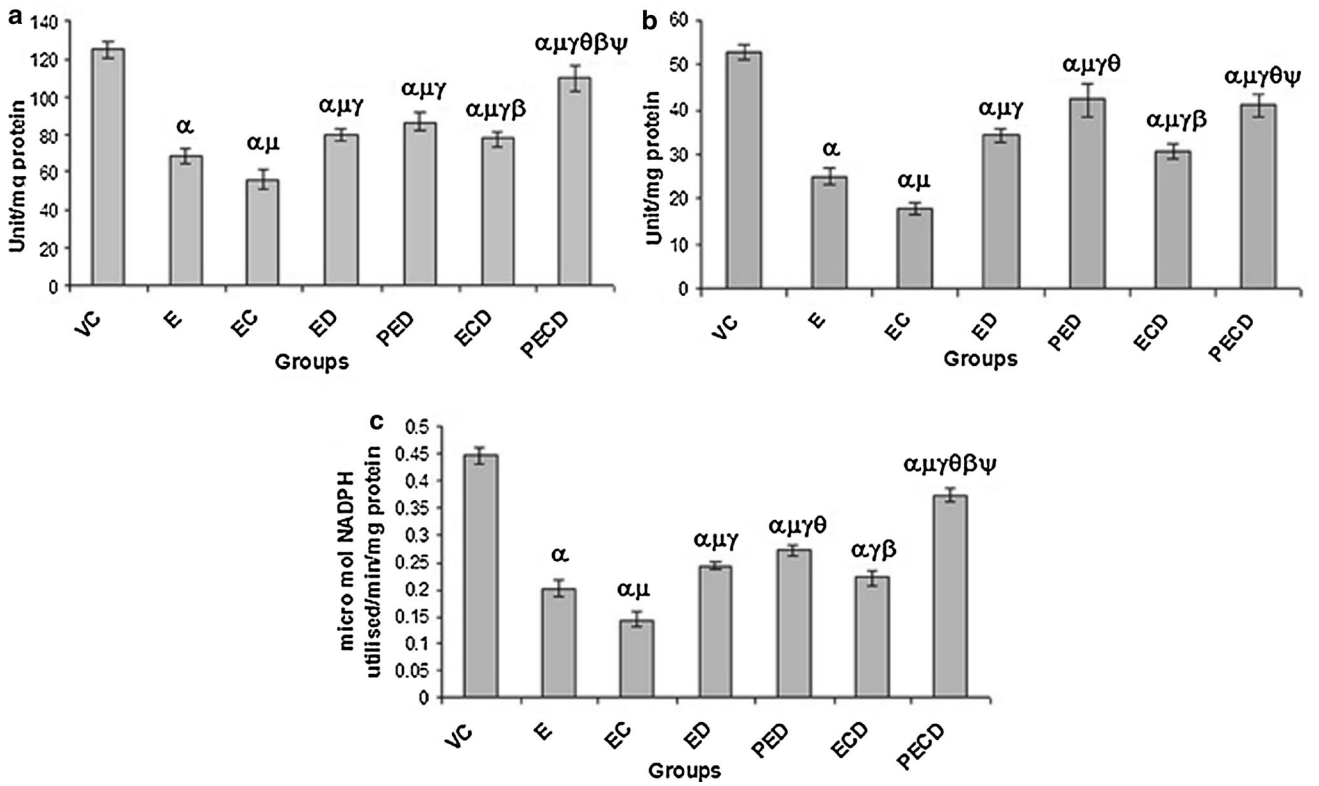

Fig. 4 Effect of monotherapy and combination treatment on **a** SOD activity, **b** CAT activity, and **c** GPx activity of different groups of mice. Data were represented as mean ± standard deviation (SD) ($n = 6$). α—significant ($P < 0.05$) as compared with VC, μ—significant ($P < 0.05$) as compared with E, γ—significant ($P < 0.05$) as compared with EC, θ—significant ($P < 0.05$) as compared with ED, β—significant ($P < 0.05$) as compared with PED, ψ—significant ($P < 0.05$) as compared with ECD

central vein, mononuclear cellular infiltration, dilatation of blood sinusoids and formation of pyknotic nuclei and hepatocellular necrosis. Nano-Se itself in concomitant (ED) and pretreatment (PED) schedule in EAC-bearing mice produced almost normal histoarchitecture with fewer numbers of pyknotic nuclei. In combination treatment with Nano-Se and CP, liver sections from concomitant treatment group (ECD) showed mild cellular infiltration and blood sinusoids more or less normal, where as in pretreatment group (PECD) showed almost normal (Fig. 5a–h).

Protective effect of Nano-Se on CP-induced DNA damage in mouse peripheral lymphocyte cells

Comet assay was carried out to examine the CP-induced DNA damage in lymphocytes (Fig. 6a–g), and for this purpose percentage of damaged cells and the average tail length was measured. In the present study, this technique was adopted to show the anti-genotoxic property of bio-functionalized selenium nanoparticles. The frequency of damaged lymphocytes was 9.14 % in (VC), whereas EAC-inoculated and CP-treated mice caused a significant increase in the percentage of damaged lymphocytes to 44.46 and 76.04 %, respectively; whereas treatment with the Nano-Se inhibited the percentage of damage of lymphocytes in respective groups. According to Table 2, EAC infected and CP-treated mice led to significant increase the magnitude of average tail length compared to the EAC control group (E). Oral administration of single and combination therapy of Nano-se along with CP in PED and PECD group reduces the magnitude of tail length as in compared to EAC control group and CP-treated group, respectively.

Prevention of chromosomal aberration

Bone marrow of the EAC-inoculated animals showed several types of chromosomal aberration. EAC inoculation (E) showed significantly ($P < 0.05$) high proportion of chromosomal aberration of 54.2 % compared to the vehicle control group (Fig. 7). In addition to that when CP treatment was given to EAC-inoculated animals, it showed further more rise in chromosomal aberration of about 67.36 %. Treatment with Nano-Se in pretreatment and concomitant treatment schedules was able to lessen these chromosomal aberrations. Pretreatment with Nano-Se caused inhibition of chromosomal aberration to 38.02 % in PECD group and 25.86 % in PED group compared to their respective control groups.

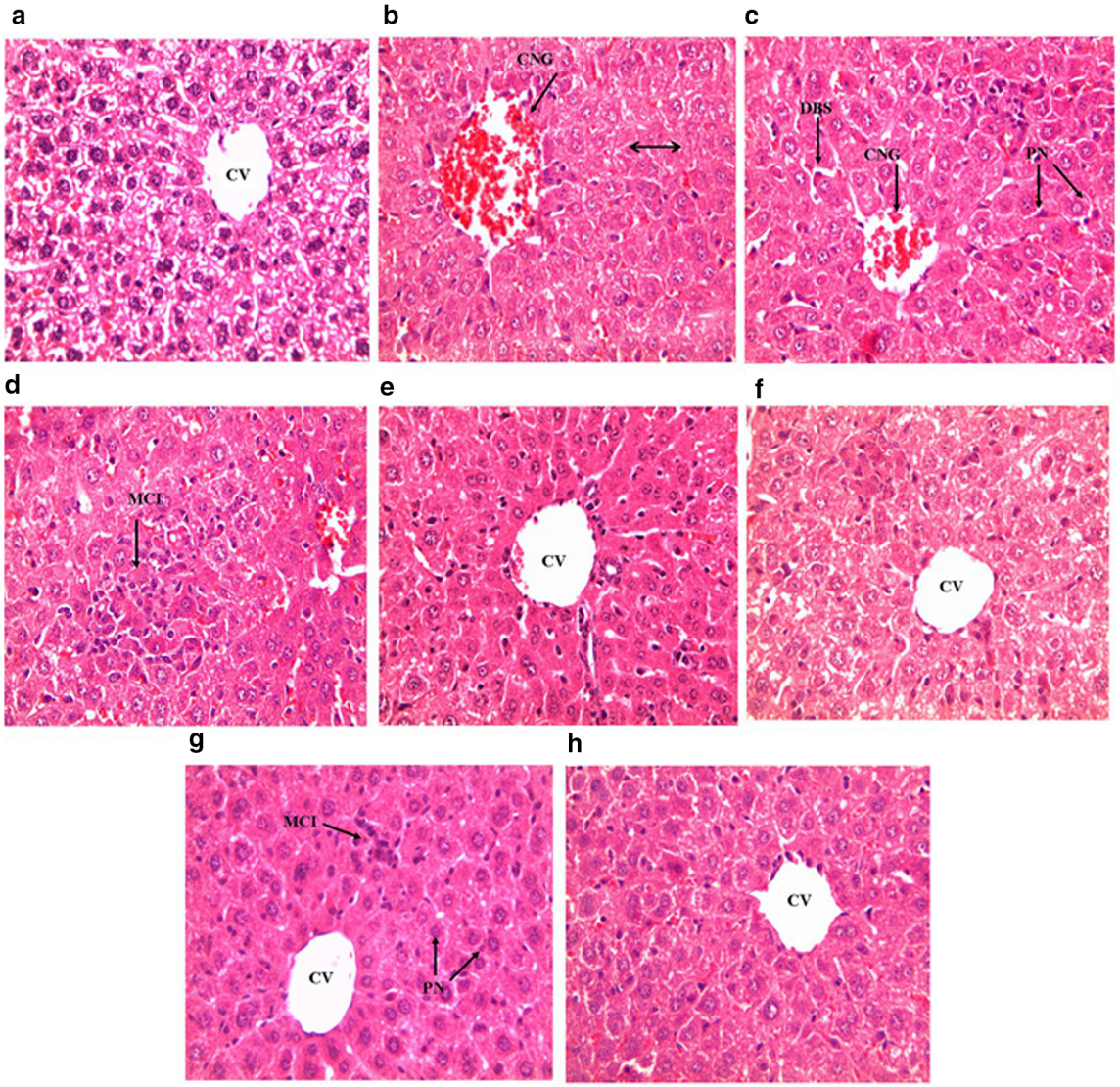

Fig. 5 Photomicrographs of liver section of mice stained with hematoxylin and eosin. **a** Liver section from the vehicle control group (VC) showing normal arrangement of hepatocytes radiating from the central vein (CV) with clear nuclei (H&E; ×400). **b** EAC control, EAC cells inoculation displaying congestion of blood vessels (CNG) and necrosis (*double headed arrow*) (H&E; ×400). **c** Treatment with CP (EC) showing loss of hepatic architecture, dilatation of blood sinusoids (DBS), pyknotic nuclei (PN) and also congestion of blood vessels (CNG) (H&E; ×400). **d** Treatment with CP (EC) showing also mononuclear cellular infiltration (MCI) (H&E; ×400). **e** Concomitant treatment and **f** pretreatment with only Nano-Se showing normal liver architecture same as in vehicle control group with no marked hepatotoxicity. **g** Concomitant treatment with CP and Nano-Se, ECD. Very little portion of mononuclear cellular infiltration (MCI) and pyknotic nuclei (PN) were observed (H&E; ×400). **h** Liver section of pretreatment with Nano-Se in CP-treated EAC-bearing mice, PECD. Treatment with Nano-Se together with CP markedly reduced the severity of the CP- and EAC-induced hepatic damage (H&E; ×400)

Effect of Nano-Se along with CP on tumor growth, mean survival time, % ILS, and apoptosis

Antitumor activity of CP along with Nano-Se against EAC-bearing mice was assessed by evaluating such parameters such as tumor volume, packed cell volume, viable cell count, mean survival time, and % ILS (Table 3). Treatment with Nano-Se alone in EAC-bearing mice was capable of minimizing the tumor volume, packed cell volume, and tumor cell count compared to the untreated EAC control group (E). Nano-Se treatment significantly ($P < 0.05$) decreased the tumor volume by 39 and 52 %, packed cell volume by 21 and 45 %, and tumor cell count by 37 and 52 % in concomitant and pretreatment schedule, respectively, compared to the EAC control group. On another side, monotherapy of CP caused a drastic reduction in these parameters compared to the EAC control group. In addition, in combination management with CP and Nano-Se in

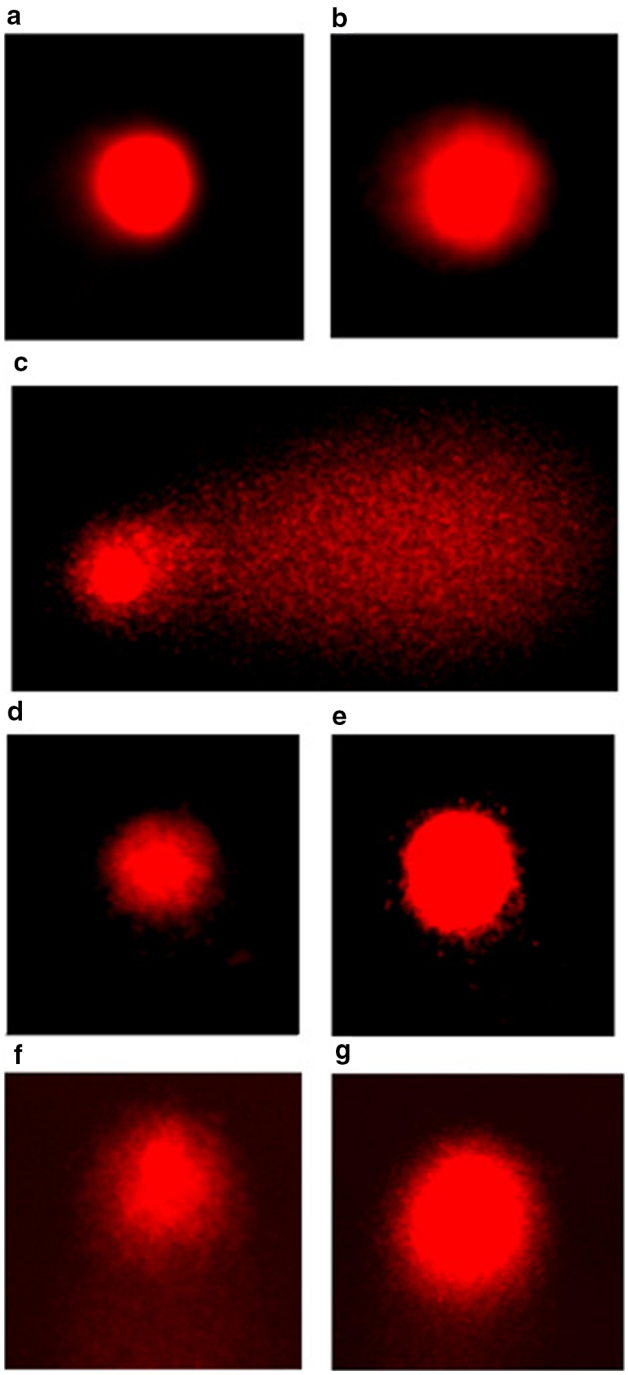

Fig. 6 Photomicrographs showing comet of lymphocytes from different groups of mice. **a** Vehicle control group showed intact DNA with no migration, EAC inoculation (**b**) and CP treatment (**c**) showed highly migrated DNA with distinct scattered comet tail, Concomitant treatment (**d**) and pretreatment (**e**) with Nano-Se capable to reduce the migration of DNA and less diffused comet tail, Combined treatment with Nano-Se and CP (**f, g**) showed no or very less migrated DNA (magnification ×400)

ECD and PECD group significantly ($P < 0.05$) decreased the tumor volume by 41 and 56 %, packed cell volume by 55 and 68 % and tumor cell count by 34 and 54 %, respectively, compared to the CP-treated control group (EC).

The effect of Nano-Se on the survival of tumor-bearing mice is shown in Table 3. The MST of the EAC control group was 22.1 ± 1.83 days, whereas CP monotherapy for ten consecutive days it was 41.9 ± 2.26 days. Nano-Se itself was also capable to fairly enhance the mean survivability of the tumor-bearing host. In case of concomitant group (ED) and pretreatment group (PED), the survival time significantly ($P < 0.05$) increased to 27.55 ± 2.61 days and 33.05 ± 2.19 days. In the groups treated with Nano-Se and CP in combination a further significant ($P < 0.05$) increase in survival up to 52.45 ± 2.47 days (ECD) and 62.85 ± 3.46 days (PECD) was observed. The increase in the lifespan of tumor-bearing mice treated with CP and Nano-Se itself was 89.5 % (EC), 24 % (ED), and 49.5 % (PED), respectively. Combination of CP and Nano-Se increases lifespan much more significantly by 153.16 % (ECD) and 184.38 % (PECD), respectively.

Apoptosis enhancement effect of Nano-Se along with CP on EAC cell was confirmed by TUNEL assay (Fig. 8c). Apoptotic index (AI) in the EAC control group was 8.01 ± 2.02 (E), which was increased significantly after treatment with CP and Nano-Se and the values are 42.73 ± 3.43 (EC), 15.73 ± 2.66 (ED), and 28.92 ± 2.53 (PED), respectively, but much more pronounced enhancement of apoptotic induction was observed in combined treatment with Nano-Se and CP and AI was found to be 52.17 ± 2.56 (ECD) and 67.96 ± 4.95 (PECD), respectively.

Effect of Nano-Se along with CP on intracellular ROS generation

To evaluate the mechanism of cell death on the basis of ROS production, we have carried out DCFH-DA assay in tumor cells. As shown in Fig. 9, treatment with Nano-Se alone was able to enhance ROS level in tumor cell significantly ($P < 0.05$) by 60.48 % (ED) and 123.19 % (PED) compared to the EAC control group (E). In addition, when Nano-Se was used along with chemotherapeutic drug CP in combination regimen, ROS in the tumor cells was boosted up by 21.12 % in case of concomitant treatment (ECD) and by 64.48 % in case of pretreatment (PECD) compared to the CP control group (EC).

Influence of Nano-Se along with CP on DNA damage in tumor cell (comet assay)

The most widely used method for assessment of DNA damage is the alkaline comet assay. In the present study, comet assay in tumor cell was performed to observe the extent of DNA damage (Fig. 10a–e).

Table 2 Effect of Nano-Se alone or in combination with CP on DNA damage in peripheral lymphocytes and tumor cells

Groups	Peripheral lymphocyte		Tumor cells	
	Damaged cells showing comet (%)	Average tail length (μm)	Damaged cells showing comet (%)	Average tail length (μm)
VC	9.14 ± 0.47	7.88 ± 0.75	–	–
E	44.46 ± 3.08$^{\alpha}$	64.1 ± 1.42$^{\alpha}$	13.64 ± 2.44	8.19 ± 2.07
EC	76.04 ± 2.39$^{\alpha\mu}$	96.71 ± 1.25$^{\alpha\mu}$	56.29 ± 2.14$^{\mu}$	32.15 ± 2.63$^{\mu}$
ED	19.37 ± 2.15$^{\alpha\mu\gamma}$	29.42 ± 1.26$^{\alpha\mu\gamma}$	21.6 ± 1.89$^{\mu\gamma}$	16.57 ± 2.98$^{\mu\gamma}$
PED	15.74 ± 1.04$^{\alpha\mu\gamma\theta}$	22.3 ± 2.24$^{\alpha\mu\gamma\theta}$	35.99 ± 3.16$^{\mu\gamma\theta}$	26.78 ± 2.67$^{\mu\theta}$
ECD	33.41 ± 0.9$^{\alpha\mu\gamma\theta\beta\psi}$	58.19 ± 1.21$^{\alpha\mu\gamma\theta\beta}$	66.29 ± 2.65$^{\mu\gamma\theta\beta}$	41.89 ± 2.08$^{\mu\gamma\theta\beta t}$
PECD	23.75 ± 2.39$^{\alpha\mu\gamma\theta\beta\psi}$	37.91 ± 1.99$^{\alpha\mu\gamma\theta\beta\psi}$	72.35 ± 4.35$^{\mu\gamma\theta\beta}$	56.41 ± 6.1$^{\mu\gamma\theta\beta\psi}$

Data were represented as Mean ± SD ($n = 6$)

$^{\alpha}$ Significant ($P < 0.05$) as compared with VC

$^{\mu}$ Significant ($P < 0.05$) as compared with E

$^{\gamma}$ Significant ($P < 0.05$) as compared with EC

$^{\theta}$ Significant ($P < 0.05$) as compared with ED

$^{\beta}$ Significant ($P < 0.05$) as compared with PED

$^{\psi}$ Significant ($P < 0.05$) as compared with ECD

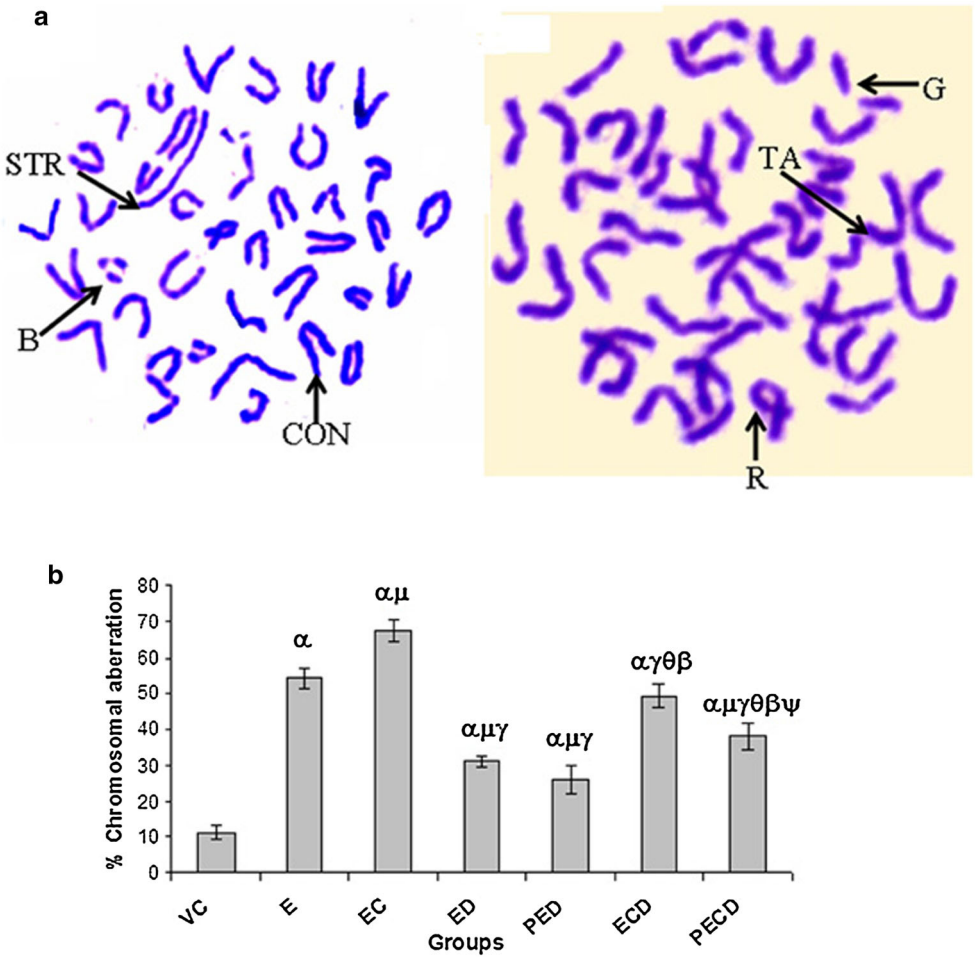

Fig. 7 Photographs of metaphase chromosomes of bone marrow cells from treated and untreated EAC-bearing mice. **a** *Arrows* indicate stretching (STR), break (B), constriction (CON), ring (R), terminal association (TA), and gap (G). **b** Effect of monotherapy and combination treatment on percentage chromosomal aberration of bone marrow cells. Data were represented as mean ± standard deviation (SD) ($n = 6$). α—significant ($P < 0.05$) as compared with VC, μ—significant ($P < 0.05$) as compared with E, γ—significant ($P < 0.05$) as compared with EC, θ—significant ($P < 0.05$) as compared with ED, β—significant ($P < 0.05$) as compared with PED, ψ—significant ($P < 0.05$) as compared with ECD

Table 3 Effect of Nano-Se alone or in combination with CP on tumor growth, mean survival time, and % ILS in tumor-bearing mice

Groups	Tumor volume (ml)	Packed cell volume (ml)	Tumor cell count ($\times 10^6$)	Mean survivability (days)	Increase in life span (%)
E	4.84 ± 0.47	2.32 ± 0.22	55.12 ± 3.42	22.1 ± 1.83	–
EC	1.36 ± 0.16$^{\mu}$	0.8 ± 0.24$^{\mu}$	18.66 ± 2.24$^{\mu}$	41.9 ± 2.26$^{\mu}$	89.5
ED	2.96 ± 0.32$^{\mu\gamma}$	1.84 ± 0.35$^{\mu\gamma}$	34.88 ± 3.88$^{\mu\gamma}$	27.55 ± 2.61$^{\mu\gamma}$	24
PED	2.32 ± 0.3$^{\mu\gamma\theta}$	1.28 ± 0.22$^{\mu\gamma\theta}$	26.12 ± 1.67$^{\mu\gamma\theta}$	33.05 ± 2.19$^{\mu\gamma\theta}$	49.5
ECD	0.8 ± 0.14$^{\mu\gamma\theta\beta}$	0.36 ± 0.15$^{\mu\gamma\theta\beta}$	12.2 ± 1.14$^{\mu\gamma\theta\beta}$	52.45 ± 2.47$^{\mu\gamma\theta\beta}$	153.16
PECD	0.6 ± 0.15$^{\mu\gamma\theta\beta}$	0.26 ± 0.08$^{\mu\gamma\theta\beta}$	8.64 ± 1.55$^{\mu\gamma\theta\beta}$	62.85 ± 3.46$^{\mu\gamma\theta\beta\psi}$	184.38

Data were represented as Mean ± SD ($n = 6$)

$^{\mu}$ Significant ($P < 0.05$) as compared with E

$^{\gamma}$ Significant ($P < 0.05$) as compared with EC

$^{\theta}$ Significant ($P < 0.05$) as compared with ED

$^{\beta}$ Significant ($P < 0.05$) as compared with PED

$^{\psi}$ Significant ($P < 0.05$) as compared with ECD

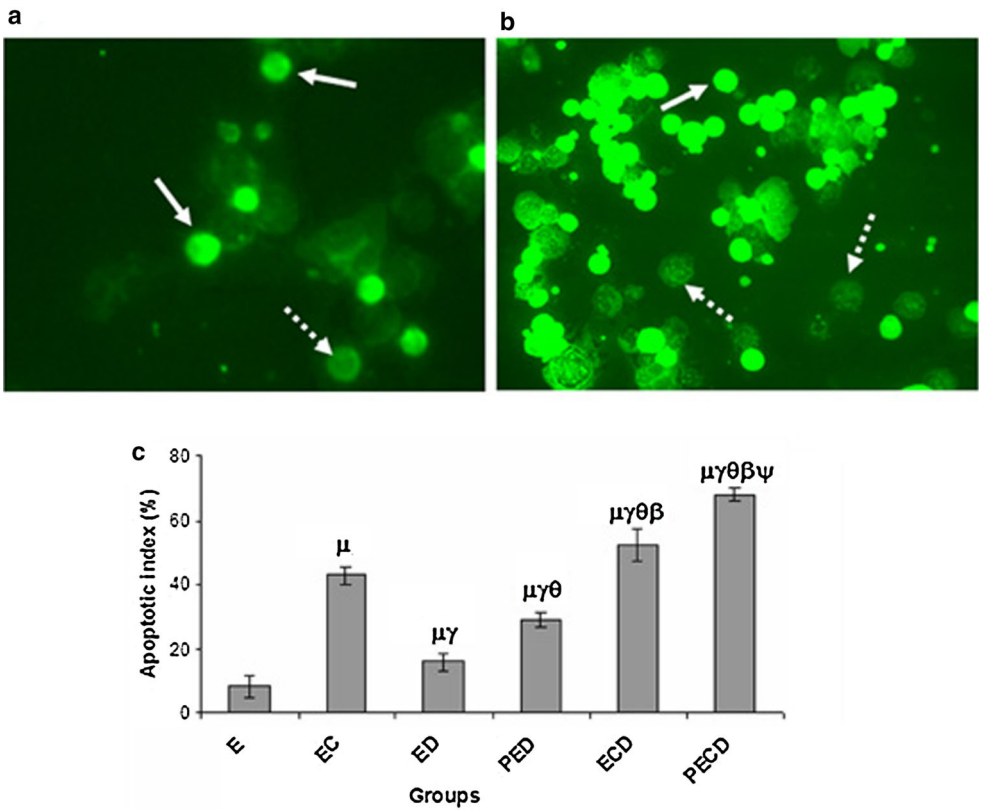

Fig. 8 Representative photomicrographs of TUNEL assay performed in tumor cells. Apoptotic cells (TUNEL label cells) are indicated by *white arrows* whereas non-apoptotic cells are indicated by *white broken arrows* (**a**) and (**b**), (Magnification ×200). **c** Effect of Nano-Se alone or in combination with CP on Apoptotic index of tumor cells. Data were represented as mean ± standard deviation (SD) ($n = 6$). μ—significant ($P < 0.05$) as compared with E, γ–significant ($P < 0.05$) as compared with EC, θ—significant ($P < 0.05$) as compared with ED, β—significant ($P < 0.05$) as compared with PED, ψ—significant ($P < 0.05$) as compared with ECD

Percentage of damaged cells in each group

CP administration in EAC-bearing mice caused a significant ($P < 0.05$) increase in the percentage of damaged tumor cell (56.29 %). In addition, stunning observation was found in the combination regimen when Nano-Se was used along with CP. In case of concomitant treatment (ECD) and in pretreatment (PECD) scheme the percentage of damaged tumor cells increased to 66.29 and 72.35 %, respectively. Furthermore, oral administration of only Nano-Se enhances the percentage of damaged tumor cells which was 21.6 % in (ED) and 36 % in (PED), respectively, compared to EAC control group (Table 2).

Average tail length due to DNA migration in each group

The magnitude of average tail length was 8.19 ± 2.07 μm in EAC control group. CP administration caused a marked increase in the magnitude of tail length to 32.15 ± 2.63 μm

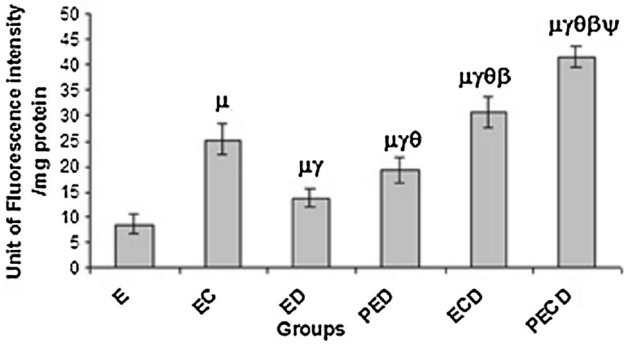

Fig. 9 Effect of monotherapy and combination treatment on the ROS of tumor cells. Data were represented as mean ± standard deviation (SD) ($n = 6$). μ—significant ($P < 0.05$) as compared with E, γ—significant ($P < 0.05$) as compared with EC, θ—significant ($P < 0.05$) as compared with ED, β—significant ($P < 0.05$) as compared with PED, ψ—significant ($P < 0.05$) as compared with ECD

(Table 2). Oral administration of Nano-Se itself in concomitant (ED) and pretreatment (PED) schedule, resulted in the enhancement of average tail length to 16.57 ± 2.98 and 26.78 ± 2.67 μm, respectively. However, the combination management caused enormous enhancement of average tail length to 41.89 ± 2.08 μm in concomitant (ECD) and 56.41 ± 6.10 μm in pretreatment (PECD) group, respectively.

Nano-Se inhibits tumor-induced neo-vascularization and lowered the MMP-9 level

Evident angiogenesis in the inner peritoneal lining of EAC-bearing mice has been adopted as a reliable model of in vivo angiogenesis assay [46]. The peritoneum of EAC-bearing mice was rich in blood vessels (Fig. 11a) when compared to that of normal mice due to angiogenesis. This enables the delivery of oxygen and nutrients essential for growth and metastasis of tumor. However, reduction in sprouting due to inhibition of the neo-vasculature in peritoneal angiogenesis was observed in mice that were treated with Nano-Se during concomitant and pretreatment schedule.

Untreated EAC-bearing mice elicited significant increase in MMP-9 level of serum (546 ng/ml), which was reduced and normalize in mice treated with Nano-Se at a dose of 2 mg Se/kg b.w. (476 ng/ml for ED and 457 ng/ml

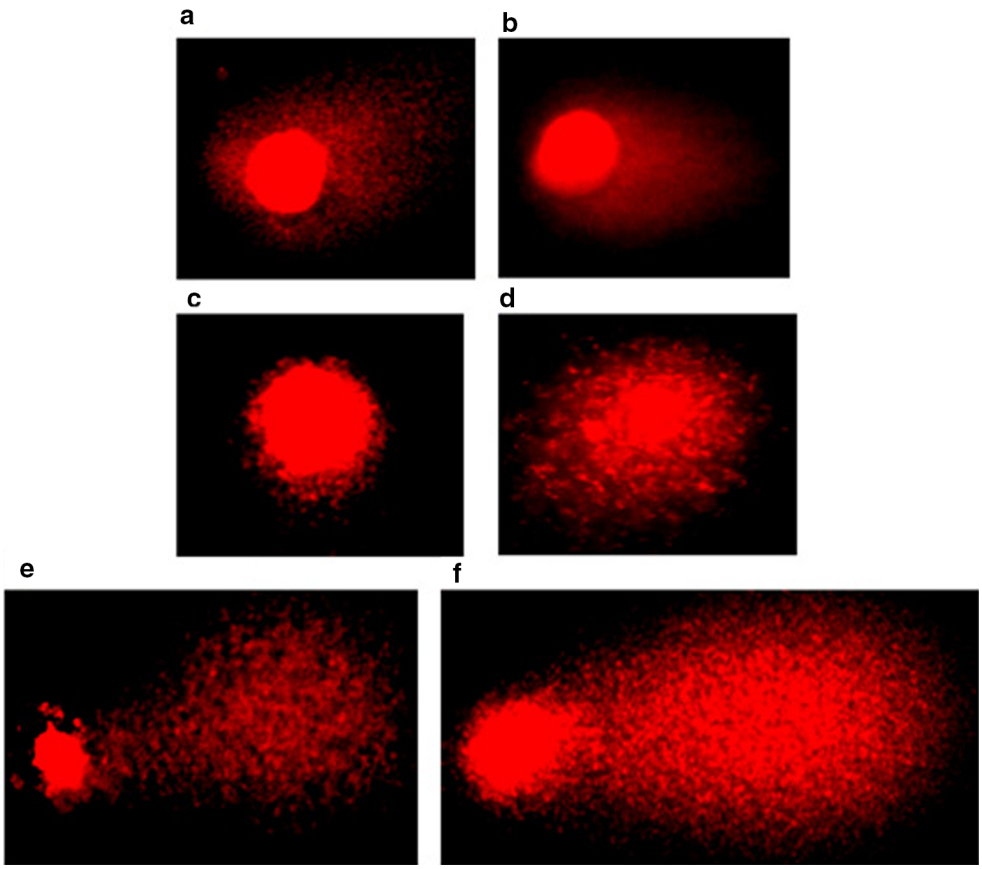

Fig. 10 Photomicrographs showing comet of tumor cells from different groups of mice. EAC inoculation (**a**) showed less migrated DNA with less diffused comet tail. Treatment with CP (**b**) showed highly migrated DNA with distinct scattered comet tail. Monotherapy with the Nano-Se able to induce the DNA damage (**c**, **d**). Combined treatment with Nano-Se with CP showed extremely migrated DNA with distinct scattered comet tail (**e, f**). (magnification ×400)

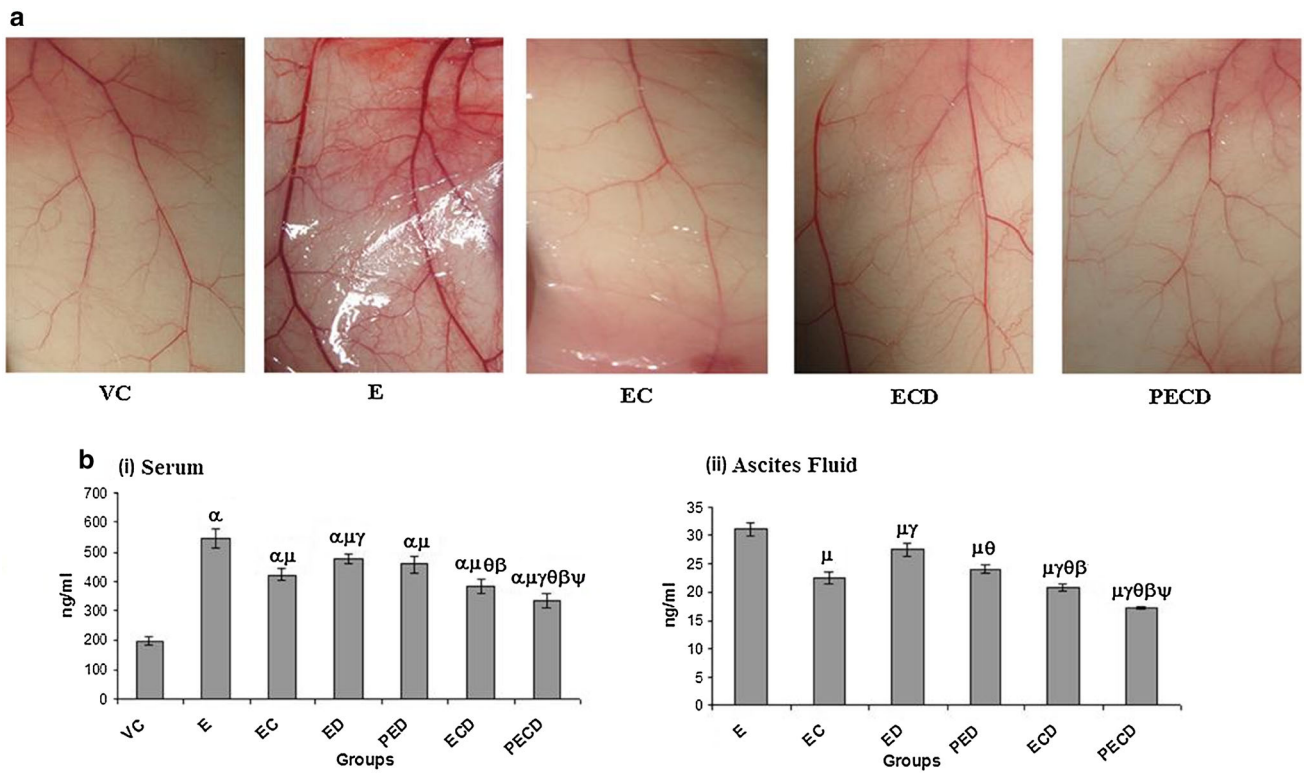

Fig. 11 Photograph of peritoneal lining of tumor-bearing animals. **a** (*VC*) shows normal architecture of peritoneal lining of vehicle control group. (*E*) Shows sprouting of new capillaries and leaky blood vessels of the peritoneal membrane in EAC control groups. Treatment with CP (*EC*) showed reduction in the peritoneal vasculature and treatment with Nano-Se along with CP in concomitant (*ECD*) and pretreatment (*PECD*) scheme showed markedly reduced peritoneal vasculature and normalization of blood vessels. **b** Effect of monotherapy and combination treatment on MMP-9 level in (i) serum and (ii) ascites fluids. Data were represented as mean ± standard deviation (SD) ($n = 6$). α—significant ($P < 0.05$) as compared with VC, μ—significant ($P < 0.05$) as compared with E, γ—significant ($P < 0.05$) as compared with EC, θ—significant ($P < 0.05$) as compared with ED, β—significant ($P < 0.05$) as compared with PED, ψ—significant ($P < 0.05$) as compared with ECD

for PED). In addition, when Nano-Se used along with chemotherapeutic drug CP in combination regimen could also significantly ($P < 0.05$) decrease the MMP-9 level of serum (383 ng/ml for ECD and 335 ng/ml for PECD, respectively). Furthermore, treatment with Nano-Se could also significantly ($P < 0.05$) decrease the MMP-9 level in ascites fluid of the treated group compared to the EAC control groups (Fig. 11b).

Discussion

The use of antioxidant supplements by patients with cancer is estimated between 13 and 87 %. This wide range of percentages might be attributed to the variability of definitions of complementary and alternative medicine used in the different studies, and to differences in the cancer types, age, education, economic status, and ethnicity of the groups assessed [47]. Patients may take different types of supplements while undergoing chemotherapy to help alleviate side effects from toxic chemotherapies and to increase the efficacy of chemotherapy [48], as it enable patients to tolerate chemotherapy during the full course of treatment and possibly at higher doses. As a result, patients may have better tumor response rates and improved quality of life.

Antineoplastic agents have been shown to produce multi-organ toxicity due to drug-induced oxidative stress in patients [3]. Chemotherapeutic drugs mostly kill rapidly dividing cells in the body, targeting cancer cells as well as normal cells originating from bone marrow [49]. In the present study, a noticeable decrease of Hb level, WBC count, and RBC count was observed in the CP-treated tumor-bearing mice compared to untreated tumor-bearing mice. Treatment with Nano-Se brought back the Hb level, RBC, and WBC count to near normal levels, indicating the protective effects of Nano-Se on the hemopoietic system.

Cancer cells can generate large amounts of hydrogen peroxide which may contribute to their ability to mutate and damage normal tissues, and moreover, facilitate tumor growth and invasion [50]. Many chemopreventive and chemotherapeutic agents have been found to induce cancer cell apoptosis through upregulation of intracellular ROS

generation [51]. Growing evidences suggest that ROS generation acts as an important cellular event induced by Se compounds and resulted in cell apoptosis [8]. Results obtained from the present study indicated that CP treatment increased ROS production in the liver cytosol as well as in bone marrow cells as measured by the DCFH-DA assay. In the present study, Nano-Se significantly inhibited CP-induced ROS formation in liver cytosol and also in bone marrow cells and at the same time significantly enhanced the intracellular ROS level in EAC cells, suggesting the involvement of ROS as a critical mediator in Nano-Se-induced apoptosis in tumor cells and protection in normal cells.

Thiobarbituric acid reactive substance such as malondialdehyde (MDA), a degradation product of lipid hydroperoxides, is considered as an index of lipid peroxidation, which was reported to be higher in cancer tissues than in non-diseased organ [52]. Metabolism of CP results in production of acrolein which is a toxic metabolite responsible for production of ROS and enhancement of LPO [53]. The present study showed increased lipid peroxidation in the liver of CP-treated mice which was associated with hepatic damage. Concomitant and pretreatment with Nano-Se effectively inhibited the CP-induced hepatic LPO level. It means that Nano-Se evoked an antioxidant action and eliminated peroxides such as hydrogen peroxide and lipid peroxide. This proves the protective role of the Nano-Se in preventing lipid peroxidation and in maintaining the integrity and normal function of the liver cells.

In the current study, liver function was significantly impaired after EAC inoculation which was further appended by CP treatment. ALT and AST are marker enzymes for assessment of liver functions. Elevated levels of transaminase enzymes are indicative of cellular damages and loss of functional integrity of cell membrane in liver [54]. Damage to liver cells causes release of these enzymes into serum. Hepatic activation of CP leads to the formation of toxic metabolites which further cause damage to the liver tissues as shown by increased AST and ALT levels. Treatment with Nano-Se resulted in significant reduction in the level of these transaminase activities in both EAC control and also in CP-treated EAC-bearing mice indicating hepatocellular protection.

GSH acts as a multifunctional intracellular non-enzymatic antioxidant and protects cells against several toxic oxygen-derived chemical species. It is considered to be an important scavenger of free radicals and a cofactor of several detoxifying enzymes against oxidative stress, e.g., glutathione-*S*-transferase, glutathione peroxidase and others [55]. Several studies demonstrated that EAC inoculation induced a decrease in hepatic glutathione (GSH) content associated with inhibition of hepatic glutathione peroxidase (GP*x*) and superoxide dismutase (SOD) activity [56]. In the present study, we found that EAC inoculation significantly reduced the GSH level, this level which was further suppressed by CP treatment. The depletion of GSH level caused due to CP treatment could be attributed to the direct conjugation metabolites of CP with GSH, thereby reducing its cellular level which leads to induction of oxidative stress [57]. GSH depletion leads to lowered cellular defense against free radicals-induced cellular injury resulting in necrotic cell death [58]. Our study shows that the mechanism of hepatoprotection by Nano-Se against CP toxicity and hepatic damage involves suppression of oxidative stress by preventing GSH depletion. Very recently, it has been reported that meat from lamb supplemented with Nano-Se enriched diet has the ability to protect 7, 12-dimethylbenz(a)anthracene (DMBA)-induced oxidative stress injury in mice [59].

Antioxidant enzyme GST catalyzes the detoxification of endogenous compounds such as lipid peroxide, as well as the metabolites of xenobiotics like acrolein from CP through conjugation of GSH via the sulfhydryl group with these toxic compounds. Several reports suggest that increased ROS generation after CP treatment reduced the GSH level and GST activity in several organs including liver [60]. The hepatic GST activity was decreased significantly by EAC inoculation which was further diminished by CP treatment. Treatment with Nano-Se invariably increased the GST activity and reduced the CP-mediated oxidative stress in liver cells.

SOD, CAT, and GP*x* are involved in the clearance of superoxide and hydrogen peroxide (H_2O_2). SOD catalyses the diminution of superoxide into H_2O_2, which has to be eliminated by CAT and/or GP*x*. The balance between the dismutation of superoxide anion (by SOD) and its conversion to molecular oxygen and water (by CAT or GP*x*) may be critical to maintain cellular antioxidant defense [5, 61]. CP-induced hepatotoxicity is associated with oxidative stress caused by the reduction in these antioxidant enzymes activities [24]. Further, it has been reported that a decrease in SOD activity in EAC-bearing mice may be due to loss of Mn^{2+} containing SOD activity in EAC cells and loss of mitochondria, leading to a decrease in total SOD activity in the liver [62]. Similar findings were observed in our present study in EAC-bearing and also in CP-treated mice. Treatment with Nano-Se invariably increased the SOD, CAT, and GP*x* activity and reduced the CP-mediated stress in liver cells. It may be possible that treatment with Nano-Se increased the activity of antioxidant selenoenzyme GP*x* which, in turn, upregulated the other antioxidant enzyme systems.

Histopathological studies also provided clear evidence for the protective effect of Nano-Se on CP-induced hepatotoxicity in EAC-bearing mice. In the liver sections of the EAC-inoculated animals, hepatocytes showed vacuolar

degeneration (hydropic changes), pyknotic nuclei, and necrosis. This may be due to the accumulation of hemorrhagic ascetic fluid within the peritoneal cavity in which the cells proliferate and move to invade the internal organs; these activities were further suppressed by CP treatment. Nano-Se effectively diminished EAC- and CP-induced hepatopathological alterations.

DNA is probably the most biologically significant target of oxidative attack, and it is widely thought that continuous oxidative damage to DNA is a significant contributor for the development of major cancers. Excessive production of ROS might be the prime cause of severe DNA damage as observed from the comet assay of lymphocytes [63]. Phosphoramide and acrolein are the major metabolites of CP, induces DNA strand breaks, cessation of DNA synthesis, DNA–protein cross-links, and DNA adducts formation. This DNA damage ultimately leads to the secondary tumors in humans. In the present study, it was observed that percentage of damaged cells of lymphocytes showed a significant increase of the comet tail after treatment with CP in tumor-bearing mice. Administration of Nano-Se before and during CP treatment ameliorated the DNA damages induced by EAC inoculation and CP treatment. This anti-genotoxic effect of Nano-Se might be due to its antioxidant and chemoprotective activity. On the other hand, striking observation was found. The comet tail length of tumor cells was significantly enhanced after administration of Nano-Se along with CP in pre and concomitant treatment, respectively, in the same mice.

Oxidative stress can induce chromosomal aberrations through oxidative base damage and strand breaks in DNA contributing to mutagenesis [64]. Such genetic damage caused by CP is not cancer cell specific, as it may also occur in the normal tissues leading to gene mutations. It has been reported that mutations may lead to the formation of secondary tumors if they occur in somatic cells [65]. In the present investigation, mice treated with CP presented a marked increase in percentage of chromosomal aberrations in bone marrow cells in tumor-bearing mice. Restoration of these levels toward normal after Nano-Se treatment in tumor-bearing CP-treated mice suggests an anti-genotoxic efficacy of Nano-Se. This might be in part due to the direct scavenging activity of Nano-Se against the ROS, which is one of the major causes of DNA damage and chromosomal aberration.

Ascitic fluid is the essential nutritional source for proliferation of tumor cells and a rapid increase in ascitic fluid with tumor growth which would provide the essential nutritional requirement of tumor cells [43]. In this study, the antitumor effect of Nano-Se on Ehrlich ascites carcinoma was demonstrated. The Nano-Se, when used alone to treat tumor-bearing mice, showed moderate antitumor efficacy without any toxicity on normal tissue compared to the CP monotherapy. The advantage of combination therapy significantly reduced the tumor volume, packed cell volume, and the viable number of tumor cells, as well as it also increased the mean survival time and life span of tumor-bearing host. Prolongation of life span of animals and enhancing the quality of health are a reliable standard for evaluating the outcome of chemotherapy. Thus, it may be conceivable that Nano-Se exerts its antitumor effect by decreasing viable tumor cells counts and consequently decreased ascitic volume and increased the life span of EAC-bearing mice.

It has been reported that chemotherapy-induced ROS generation diminishes the efficacy of the cancer treatment by interfering with anticancer drug-induced apoptosis, which is important for chemotherapeutic agents to exert their optimal effect on cancer cells [3]. In this study, we demonstrate that Nano-Se is capable of inducing apoptosis in EAC cells. The morphological hallmarks of apoptosis such as nuclear fragmentation, membrane blebbing, and inter nucleosomal fragmentation of DNA. So an agent which can selectively modulate the ability of antineoplastic drugs to induce apoptosis may enhance treatment efficacy, and prevent tissue damaging inflammatory response. In the present study, it was observed that the percentage of apoptotic cells increased after the treatment with Nano-Se alone or in combination with CP. However, the exact mechanism of cell death has not been determined fully. However, from the above discussion, it can be inferred that the Nano-Se can generate ROS in tumor cell which sensitized them to apoptosis.

Tumor growth and metastasis are dependent on angiogenesis [66]. Increased neo-vasculature may allow not only an increase in tumor growth but also enhance hematogenous tumor embolization. It is well known that ascites tumor growth including EAC cell are angiogenesis-dependent [67]. Thus, inhibiting tumor angiogenesis may halt the tumor growth and decrease metastatic potential of tumors. Inhibition of angiogenesis by Nano-Se is thought to be another major effecter in enhancing the therapeutic efficacy of cyclophosphamide. It has been reported that selenium metabolite, CH_3SH, is the key inhibitor of angiogenic switching in early lesions and in tumor [68]. Here the angiostatic property of Nano-Se was established by substantial reduction of the neo-vascularization in the peritoneum lining of tumor-bearing mice. Furthermore, to strongly claim the angiostatic property of Nano-Se, we have measured the MMP-9 level in serum as well as in ascites fluid of tumor-bearing mice. MMP-9 is a mediator of angiogenesis which in turn causes tumor growth and metastasis [69]. In the present investigation, we have found that with the combined treatment of Nano-Se and CP, there is a highly significant reduction of MMP-9 level in serum and ascites fluid. Various report suggested that

antiangiogenic compound regularizes the blood flow in dilated, chaotic, hemorrhagic, and leaky tumor vasculatures, ensuring proper homogenous delivery of anticancer drugs to the tumor bed. In combination with anticancer drugs, antiangiogenic compounds enhance their antitumor efficacy by diffusing the chemotherapeutic drugs to the distant tumor cells [70]. The results clearly demonstrated that Nano-Se does not interfere with the antitumor efficacy of CP and on the other hand administration of Nano-Se in CP-treated animals synergistically enhanced the therapeutic efficacy of CP.

In conclusion, the mechanism of such selective protection of normal cells over the tumor cells by the Nano-Se against CP-induced toxicity is exactly not known. Schwartz [71] suggested that dietary antioxidants may act as an antioxidant to normal cells and as a prooxidant to cancer cells. The prooxidant activity of an antioxidant may be the reason for the antitumor activity of many antioxidants [45]. Nevertheless, the mechanisms of action of Nano-Se, either via a prooxidant pathway, as seen in cytotoxicity and apoptosis, or via an antioxidant pathway, as proposed in cancer chemoprevention, are still unclear but intriguing. Further investigations are required to fully explore the exact molecular mode of action of Nano-Se on CP-induced toxicity and antitumour efficacy.

Acknowledgments This work was supported by the Grant from Indian Council of Medical Research (ICMR) (No. 45/36/2008/PHA-BMS), New Delhi, India. Arin Bhattacharjee gratefully acknowledges ICMR for Senior Research Fellowship. Abhishek Basu also gratefully acknowledges ICMR for Senior Research Fellowship (No. 3/2/2/58/2011/NCD-III). The authors wish to thank the Director, CNCI for the support in this study.

Compliance with ethical standards

Conflict of interest The authors declare that there are no conflicts of interest.

Ethical approval The entire experiments were carried out strictly following compliance with the ethical standards and guidelines of the Institutional Animal Ethics Committee [Committee for the Purpose of Control and Supervision of Experiment on Animals, India].

References

1. Nie S, Xing Y, Kim GJ, Simons JW (2007) Nanotechnology applications in cancer. Annu Rev Biomed Eng 9:257–288
2. Rozhkova EA, Ulasov I, Lai B, Dimitrijevic NM, Lesniak MS, Rajh T (2009) A high performance nanobio photocatalyst for targeted brain cancer therapy. Nano Lett 9:3337–3342
3. Conklin KA (2004) Chemotherapy-associated oxidative stress: impact on chemotherapeutic effectiveness. Integr Cancer Ther 3:294–300
4. Kim SH, Lee IC, Baek HS, Shin IS, Moon C, Bae CS, Kim SH, Kim JC, Kim HC (2014) Mechanism for the protective effect of diallyl disulfide against cyclophosphamide acute urotoxicity in rats. Food Chem Toxicol 64:110–118
5. Basu A, Bhattacharjee A, Samanta A, Bhattacharya S (2015) Prevention of cyclophosphamide-induced hepatotoxicity and genotoxicity: effect of an L-cysteine based oxovanadium(IV) complex on oxidative stress and DNA damage. Environ Toxicol Pharmacol 40:747–757
6. Rehman MU, Tahir M, Ali F, Qamar W, Lateef A, Khan R, Quaiyoom A, Oday-O-Hamiza, Sultana S (2012) Cyclophosphamide-induced nephrotoxicity, genotoxicity, and damage in kidney genomic DNA of Swiss albino mice: the protective effect of Ellagic acid. Mol Cell Biochem 365:119–127
7. Vijayalakshmi P, Geetha CS, Mohanan PV (2013) Assessment of oxidative stress and chromosomal aberration inducing potential of three medical grade silicone polymer materials. J Biomater Appl 27:763–772
8. Ghosh P, Singha SR, Basu A, Bhattacharjee A, Bhattacharya S (2015) Sensitization of cisplatin therapy by a naphthalimide based organoselenium compound through modulation of antioxidant enzymes and p53 mediated apoptosis. Free Radic Res 49:453–471
9. Misra S, Boylan M, Selvam A, Spallholz JE, Bjornstedt M (2015) Redox-active selenium compounds-from toxicity and cell death to cancer treatment. Nutrients 7:3536–3556
10. Navarro-Alarcón M, López-Martínez MC (2000) Essentiality of selenium in the human body: relationship with different diseases. Sci Total Environ 249:347–371
11. Gao F, Yuan Q, Gao L, Cai P, Zhu H, Liu R, Wang Y, Wei Y, Huang G, Liang J, Gao X (2014) Cytotoxicity and therapeutic effect of irinotecan combined with selenium nanoparticles. Biomaterials 35:8854–8866
12. Kong L, Yuan Q, Zhu H, Li Y, Guo Q, Wang Q, Bi X, Gao X (2011) The suppression of prostate LNCaP cancer cells growth by Selenium nanoparticles through Akt/Mdm2/AR controlled apoptosis. Biomaterials 32:6515–6522
13. El-Bayoumy K, Sinha R (2004) Mechanisms of mammary cancer chemoprevention by organoselenium compounds. Mutat Res 551:181–197
14. Fernandes AP, Gandin V (2015) Selenium compounds as therapeutic agents in cancer. Biochim Biophys Acta 1850:1642–1660
15. Whanger P, Vendeland S, Park YC, Xia Y (1996) Metabolism of subtoxic levels of selenium in animals and humans. Ann Clin Lab Sci 26:99–113
16. Dhanjal S, Cameotra SS (2010) Aerobic biogenesis of selenium nanospheres by *Bacillus cereus* isolated from coalmine soil. Microb Cell Fact 9:52
17. Prasad KS, Patel H, Patel T, Patel K, Selvaraj K (2013) Biosynthesis of Se nanoparticles and its effect on UV-induced DNA damage. Colloids Surf B 103:261–266
18. Wang Y, Chen P, Zhao G, Sun K, Li D, Wan X, Zhang J (2015) Inverse relationship between elemental selenium nanoparticle size and inhibition of cancer cell growth in vitro and in vivo. Food Chem Toxicol 85:71–77
19. Benko I, Nagy G, Tanczos B, Ungvari E, Sztrik A, Eszenyi P, Prokisch J, Banfalvi G (2012) Subacute toxicity of nano-selenium compared to other selenium species in mice. Environ Toxicol Chem 31:2812–2820
20. Hassanin KM, Abd El-Kawi SH, Hashem KS (2013) The prospective protective effect of selenium nanoparticles against chromium-induced oxidative and cellular damage in rat thyroid. Int J Nanomedicine 8:1713–1720
21. Hassan CE, Webster TJ (2016) The effect of red-allotrope selenium nanoparticles on head and neck squamous cell viability and growth. Int J Nanomedicine 11:3641–3654
22. Stevanović M, Filipović N, Djurdjević J, Lukić M, Milenković M, Boccaccini A (2015) 45S5Bioglass®-based scaffolds coated with selenium nanoparticles or with poly(lactide-co-glycolide)/

selenium particles: processing, evaluation and antibacterial activity. Colloids Surf B 132:208–215
23. Bhattacharjee A, Basu A, Biswas J, Bhattacharya S (2015) Nano-Se attenuates cyclophosphamide-induced pulmonary injury through modulation of oxidative stress and DNA damage in Swiss albino mice. Mol Cell Biochem 405:243–256
24. Bhattacharjee A, Basu A, Biswas J, Bhattacharya S (2014) Protective effect of Selenium nanoparticle against cyclophosphamide induced hepatotoxicity and genotoxicity in Swiss albino mice. J Biomater Appl 29:303–317
25. Zhang J, Wang H, Bao Y, Zhang L (2004) Nano red elemental selenium has no size effect in the induction of selenoenzymes in both cultured cells and mice. Life Sci 75:237–244
26. Dwivedi N, Flora G, Kushwaha P, Flora SJ (2014) Alpha-lipoic acid protects oxidative stress, changes in cholinergic system and tissue histopathology during co-exposure to arsenic-dichlorvos in rats. Environ Toxicol Pharmacol 37:7–23
27. Okhawa H, Ohishi N, Yagi K (1979) Assay for lipid peroxides in animal tissues by thiobarbituric acid reaction. Anal Biochem 95:351–358
28. Bergmeyer HU, Scheibe P, Wahlefeld AW (1978) Optimization of methods for aspartate aminotransferase and alanine aminotransferase. Clin Chem 24:58–61
29. Sedlack J, Lindsay RN (1968) Estimation of total protein bound and non-protein sulfhydryl groups in tissue with ellman's reagent. Anal Biochem 25:192–205
30. Habig WH, Pabst MJ, Jacoby WB (1974) Glutathione S-transferases, the first enzymatic step in marcapturic acid formation. J Biol Chem 249:7130–7139
31. Paglia DE, Valentine WN (1967) Studies on the quantitative and qualitative characterization of erythrocyte glutathione peroxidase. J Lab Clin Med 70:158–169
32. Marklund S, Marklund G (1974) Involvement of the superoxide anion radical in autooxidation of pyrogallol and a convenient assay for superoxide dismutase. Eur J Biochem 47:469–474
33. McCord JM, Fridovich I (1969) Superoxide dismutase: an enzymatic function for erythrocuprein (hemoprotein). J Biol Chem 244:6049–6055
34. Luck HA (1963) Spectrophotometric method for estimation of catalase. In: Bergmeyer HV (ed) Methods of enzymatic analysis. Academic Press, New York, pp 886–888
35. Sahli H (1909) Klinische Untersuchungs methoden, 5th edn. Leipsic and Vienna
36. D'Armour FE, Blood ER, Belden DA (1965) The manual for laboratory work in mammalian physiology, 3rd edn. The University of Chicago Press, Chicago
37. Wintrobe MM, Lee GR, Boggs DR (1961) Clinical hematology, 5th edn. Lea & Febiger, Philadelphia
38. Lowry OH, Rosenbrough NJ, Farr AL et al (1951) Protein measurement with the Folin phenol reagent. J Biol Chem 193:265–276
39. Endoh D, Okui T, Ozawa S, Yamato O, Kon Y, Arikawa J, Hayashi M (2002) Protective effect of a lignan-containing flaxseed extract against CCl_4-induced hepatic injury. J Vet Med Sci 64:761–765
40. Singh NP, McCoy MT, Tice RR, Schneider EL (1988) A simple technique for quantitation of low levels of DNA damage in individual cells. Exp Cell Res 175:184–191
41. Das JK, Sarkar S, Hossain SU, Bhattacharya S (2013) Diphenylmethyl selenocyanate attenuates malachite green induced oxidative injury through antioxidation and inhibition of DNA damage in mice. Indian J Med Res 137:1163–1173
42. Huang W, Xing W, Li D, Liu Y (2008) Microcystin-RR induced apoptosis in tobacco BY-2 suspension cells is mediated by reactive oxygen species and mitochondrial permeability transition pore status. Toxicol In Vitro 22:328–337
43. Gupta M, Mazumder UK, Rath N, Mukhopadhyay DK (2000) Antitumor activity of methanolic extract of *Cassia fistula* L. seed against Ehrlich ascites carcinoma. J Ethnopharmacol 72:151–156
44. Mazumdar UK, Gupta M, Maiti S, Mukherjee D (1997) Antitumor activity of *Hygrophila spinosa* on Ehrlich ascites carcinoma and sarcoma-180 induced mice. Indian J Exp Biol 35:473–477
45. Caderni G, De Filippo C, Luceri C, Salvadori M, Giannini A, Biggeri A, Remy S, Cheynier V, Dolara P (2000) Effects of black tea, green tea and wine extracts on intestinal carcinogenesis induced by azoxymethane in F344 rats. Carcinogenesis 21:1965–1969
46. Salimath BP, Tabassum A, Anupama EG, Bindumalini GB, Preethi PV et al (1999) Molecular mechanism of action of butyric acid in Ehrlich ascites tumor cells. Nutr Res 19:589–600
47. Block KI, Koch AC, Mead MN, Tothy PK, Newman RA, Gyllenhaal C (2007) Impact of antioxidant supplementation on chemotherapeutic efficacy: a systematic review of the evidence from randomized controlled trials. Cancer Treat Rev 33:407–418
48. Ladas EJ, Jacobson JS, Kennedy DD, Teel K, Fleischauer A, Kelly KM (2004) Antioxidants and cancer therapy: a systematic review. J Clin Oncol 22:517–528
49. Szatrowski TP, Nathan CF (1991) Production of large amounts of hydrogen peroxide by human tumor cells. Cancer Res 51:794–798
50. Pelicano H, Carney D, Huang P (2004) ROS stress in cancer cells and therapeutic implications. Drug Resist Updates 7:97–110
51. Nilsonne G, Sun X, Nyström C, Rundlöf AK, Potamitou FA, Björnstedt M, Dobra K (2006) Selenite induces apoptosis in sarcomatoid malignant mesothelioma cells through oxidative stress. Free Radic Biol Med 41:874–885
52. Liu F, Li XL, Lin T, He DW, Wei GH, Liu JH, Li LS (2012) The cyclophosphamide metabolite, acrolein, induces cytoskeletal changes and oxidative stress in Sertoli cells. Mol Biol Rep 39:493–500
53. Matés JM (2000) Effects of antioxidant enzymes in the molecular control of reactive oxygen species toxicology. Toxicology 153:83–104
54. Gong P, Chen FX, Wang L, Wang J, Jin S, Ma YM (2014) Protective effects of blueberries (*Vaccinium corymbosum* L.) extract against cadmium-induced hepatotoxicity in mice. Environ Toxicol Pharmacol 37:1015–1027
55. Bhattacharyya A, Mandal D, Lahiry L, Bhattacharyya S, Chattopadhyay S, Ghosh UK et al (2007) Black tea-induced amelioration of hepatic oxidative stress through antioxidative activity in EAC-bearing mice. J Environ Pathol Toxicol Oncol 26:245–254
56. Yousefipour Z, Ranganna K, Newaz MA, Milton SG (2005) Mechanism of acrolein-induced vascular toxicity. J Physiol Pharmacol 56:337–353
57. Srivastava A, Shivanandappa T (2010) Hepatoprotective effect of the root extract of *Decalepis hamiltonii* against carbon tetrachloride-induced oxidative stress in rats. Food Chem 118:411–417
58. Kaya H, Oral B, Ozgüner F, Tahan V et al (1999) The effect of melatonin application on lipid peroxidation during cyclophosphamide therapy in female rats. Zentralbl Gynakol 121:499–502
59. Ungvári E, Monori I, Megyeri A et al (2014) Protective effects of meat from lambs on selenium nanoparticle supplemented diet in a mouse model of polycyclic aromatic hydrocarbon-induced immunotoxicity. Food Chem Toxicol 64C:298–306
60. Ghosh P, Bhattacharjee A, Basu A, Roy SS, Bhattacharya S (2014) Attenuation of cyclophosphamide-induced pulmonary toxicity in Swiss albino mice by naphthalimide-based organoselenium compound 2-(5-selenocyanatopentyl)-benzo[de]isoquinoline 1,3-dione. Pharm Biol 4:1–9
61. Selvakumar E, Prahalathan C, Mythili Y, Varalakshmi P (2005) Mitigation of oxidative stress in cyclophosphamide-challenged

hepatic tissue by DL-α-lipoic acid. Mol Cell Biochem 272:179–185
62. Di Bucchianico S, Fabbrizi MR, Cirillo S (2014) Aneuploidogenic effects and DNA oxidation induced in vitro by differently sized gold nanoparticles. Int J Nanomedicine 9:2191–2204
63. Ghosh M, Manivannan J, Sinha S, Chakraborty A, Mallick SK, Bandyopadhyay M, Mukherjee A (2012) In vitro and in vivo genotoxicity of silver nanoparticles. Mutat Res 749:60–69
64. Sanderson BJ, Shield AJ (1996) Mutagenic damage to mammalian cells by therapeutic alkylating agents. Mutat Res 355:41–57
65. Selvakumar E, Prahalathan C, Varalakshmi P et al (2006) Modification of cyclophosphamide-induced clastogenesis and apoptosis in rats by alpha-lipoic acid. Mutat Res 606:85–91
66. Ushio-Fukai M, Alexander RW (2004) Reactive oxygen species as mediators of angiogenesis signaling: role of NAD(P)H oxidase. Mol Cell Biochem 264:85–97
67. Saraswati S, Agrawal SS, Alhaider AA (2013) Ursolic acid inhibits tumor angiogenesis and induces apoptosis through mitochondrial-dependent pathway in Ehrlich ascites carcinoma tumor. Chem Biol Interact 206:153–165
68. Nagy JA, Morgan ES, Herzberg KT, Manseau EJ, Dvorak AM, Dvorak HF (1995) Pathogenesis of ascites tumor growth: angiogenesis, vascular remodeling, and stroma formation in the peritoneal lining. Cancer Res 55:376–385
69. Yoon SO, Kim MM, Chung AS (2002) Inhibitory effect of selenite on invasion of HT1080 tumor cells. J Biol Chem 276:20085–20092
70. Lu J, Jiang C (2001) Antiangiogenic activity of selenium in cancer chemoprevention: metabolite-specific effects. Nutr Cancer 40:64–73
71. Gupta M, Mazumder UK, Kumar RS, Kumar TS (2004) Antitumor activity and antioxidant role of *Bauhinia racemosa* against Ehrlich ascites carcinoma in Swiss albino mice [corrected]. Acta Pharmacol Sin 25:1070–1076

Nano-Se as a novel candidate in the management of oxidative stress related disorders and cancer

Arin Bhattacharjee, Abhishek Basu, Tuhinadri Sen, Jaydip Biswas & Sudin Bhattacharya

The Nucleus
An International Journal of Cytology and Allied Topics

ISSN 0029-568X
Volume 60
Number 2

Nucleus (2017) 60:137-145
DOI 10.1007/s13237-016-0183-2

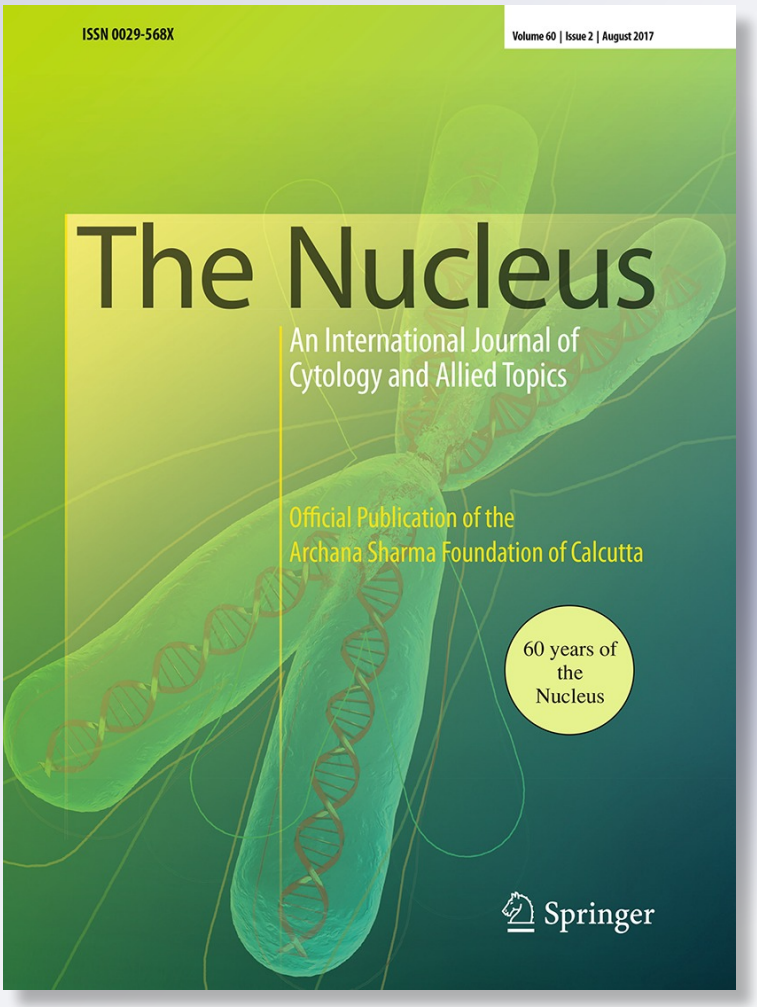

Springer

Nucleus (2017) 60:137–145
DOI 10.1007/s13237-016-0183-2

REVIEW ARTICLE

Nano-Se as a novel candidate in the management of oxidative stress related disorders and cancer

Arin Bhattacharjee[1] · Abhishek Basu[1] · Tuhinadri Sen[2] · Jaydip Biswas[3] · Sudin Bhattacharya[1]

Received: 12 May 2016 / Accepted: 29 August 2016 / Published online: 9 September 2016

Abstract Oxidative stress occurs when the antioxidant defense of the cellular system is unable to counteract the formation of reactive oxygen species and/or oxidants, as a result, reactive oxygen species prevails in the system. Oxidative stress leads to damages at macromolecular level and hence is involved in various forms of diseases and disorders. Nanotechnology is a booming field with tremendous potential in biology, biotechnology, medicines and medical technology. Novel nanomaterials and nanodevices are designed and controlled by nanotechnological tools and systems, which inspect and tune the properties, and functions of both living- and non-living materials, at sizes below 100 nm. Selenium (Se) is of fundamental importance to human health. As a potential chemoprotectant, its administration necessitates consumption for a long term, thus the toxicity of selenium is always a crucial concern. Recently, nanotechnology based new form of selenium, i.e., selenium nanoparticle (Nano-Se) has attracted attention of researchers owing to its low toxicity and high bioavailability, because at nano range selenium particles exhibit excellent characteristics, for example great surface area, effective surface activity, lots of surface active centers, high catalytic efficiency, strong adsorbing ability and minor toxicity. This review presents an overview on the novel use of Nano-Se in the management and therapy of oxidative stress related disorders.

Keywords Selenium nanoparticles · Oxidative stress · Toxicity · DNA damage · Apoptosis · Angiogenesis

Introduction

In recent years there is an increasing awareness amongst people on prevention of oxidative stress related disease. The term oxidative stress was first introduced 30 years ago. Oxidants are being formed during the normal physiological process in the body, by some cytosolic enzyme systems as well as by some exogenous source. Our body possesses two categories of protective systems, enzymatic and non enzymatic, which makes a balance between the formation and removal of these oxidants in normal cells. However this stability gets shifted towards the prooxidant state when excessive formation of free radicals occurred and/or when the levels of antioxidants are diminished by various pathological and external factors. This condition is generally known as 'oxidative stress'. The oxidative stress can lead to severe cell damage if the amount of stress is prolonged or massive. It plays a pivotal role in the development of various degenerative as well as chronic disorders like cancer, diabetes, arthritis, cardiovascular and neurodegenerative disorders [16, 17, 25] (Fig. 1).

This article is based on the presentation made during the 17th All India Congress of Cytology and Genetics and International Symposium on "Exploring Genomes: The New Frontier" held at CSIR-Indian Institute of Chemical biology, Kolkata in collaboration with Archana Sharma Foundation of Calcutta during December 22-24, 2015.

✉ Sudin Bhattacharya
sudinb19572004@yahoo.co.in

[1] Department of Cancer Chemoprevention, Chittaranjan National Cancer Institute, 37, S.P. Mukherjee Road, Kolkata, West Bengal 700026, India

[2] Division of Pharmacology, Department of Pharmaceutical Technology, Jadavpur University, 188, Raja S.C. Mullick Road, Kolkata, West Bengal 700032, India

[3] Department of Translational Research, Chittaranjan National Cancer Institute, 37, S.P. Mukherjee Road, Kolkata, West Bengal 700026, India

Fig. 1 The relations between oxidative stress and consequent cell death or dysfunctions

Normal oxygen metabolism leads to the formation of certain reactive oxygen species (ROS) like superoxide anion ($O_2^{\bullet -}$), hydrogen peroxide (H_2O_2) and hydroxyl radical ($OH^{\bullet}$). On the other hand these free radicals have abeyant quality that leads to induction of oxidative damage via interaction with the biomolecules. It is quite obvious that ROS is also sometimes useful for the normal physiological homeostasis of the cells. In normal cells during mitochondrial activity lower amounts of ROS are produced to act as the signaling molecules. The point is that to keep physiological homeostasis the levels of oxidants and antioxidants must be in a balance [50] (Fig. 2).

There are growing interests in using nanotechnology based elements or biomaterials as potential cancer therapeutics and chemoprotective agents for human cancer. Lots of preclinical and clinical data illustrate that the currently used antineoplastic agents have been shown to produce oxidative stress-mediated toxicities in patients who receive these drugs during cancer chemotherapy [15]. Due to the inefficiency of current cancer chemotherapy, there is an urgent need of 'chemoprotective' (protection against chemotherapeutic drug induced toxicity) and 'chemoenhancing' (enhancement of therapeutic efficacy of chemotherapeutic drugs) drug with low toxicity. In this regard fighting cancer with novel selenium species, nanoparticles of selenium (Nano-Se), specially synthesized with the help of combination of nanotechnology and biotechnology seems to be a fascinating strategy. Furthermore, in vivo and in vitro studies show that various nanoparticles have anticancer and different therapeutic properties [4, 21]. Nanotechnology based Nano-Se belongs to such kind of therapeutics.

Nanotechnology and Nano-Se

The word 'Nanotechnology' is a single word but has a broad spectrum of applications. It includes an assortment of sub

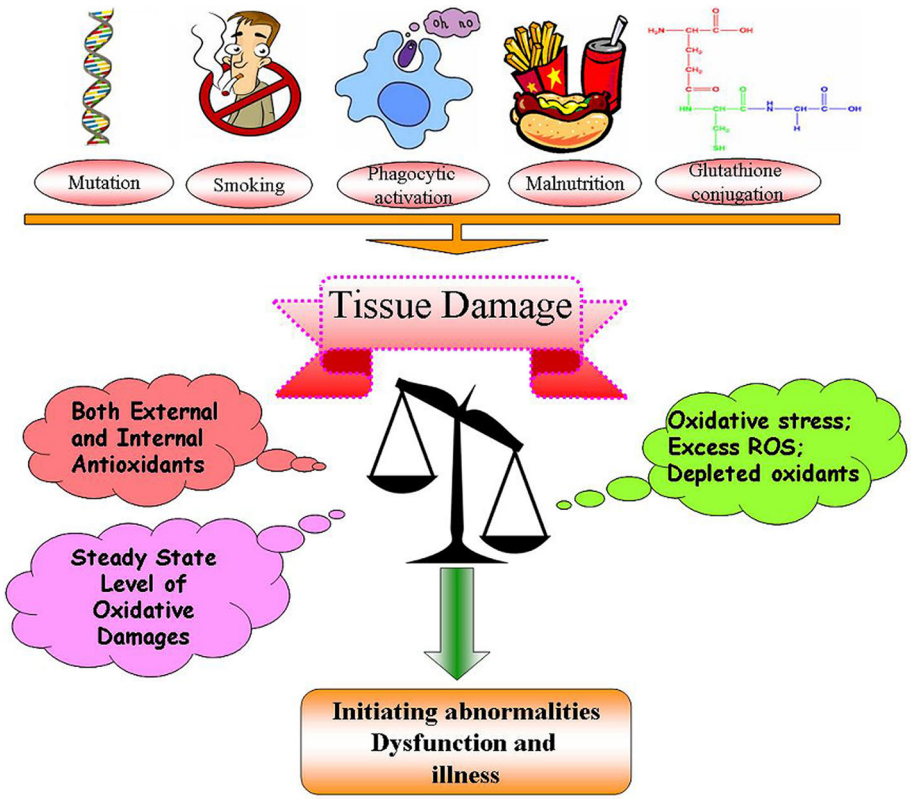

Fig. 2 Induction of oxidative stress and consequent damages leading to oxidative stress related disorder (OSRD); *ROS* reactive oxygen species

disciplines such as biology, biotechnology, engineering, chemistry, and physics. Basically, it is that branch of technology which deals with dimension and tolerances of less than 100 nm [38]. Nanoparticles are subcellular and submicron in size. They have huge advantages such as greater surface area and reactivity, adequate gastric residence time and high permeability, and increased solubility in both hydrophilic and lipophilic phases [27]. By exploiting these unique properties, scientists are developing nanodrugs that have an enhanced efficiency over the conventional system in terms of drug delivery, diagnostic, and as imaging agents.

In the year 2001, nanoparticle of selenium (Nano-Se) was first synthesized by a group of Scientist from Chinese Academy of Science, Hefei, China [69]. The red elemental selenium in the size range of 5–100 nm is synthesized by reducing selenite in presence of bovine serum albumin (BSA) by dialysis process, which make selenium atoms to adhere and control their size. Thus the size of Nano-Se is dependent on BSA concentration in the preparation. BSA at higher concentration produces smaller Nano-Se particles, hence a series of Nano-Se particles of different sizes were prepared by varying the concentration of BSA. We have also prepared Nano-Se following the same method with slight modification (Fig. 3) [6]. In this new era of nanobiotechnology, bacteria, fungi and plants are also able to produce nano-particles. Nano-Se is also produced microbiologically by using *Pseudomonas alcaliphila* strain with or without addition of poly (vinyl pyrrolidone) (PVP) [70]. In the work of Thirunavukkarasu and his colleagues, it is evident that Nano-Se can also be prepared through green synthesis by using the reducing power of the extract fenugreek seed under ambient conditions. By this method Nano-Se can be prepared in the size range of 50–150 nm [44]. It has been observed in many works that monosaccharide or polysaccharide has been used as a stabilizer in order to produce Nano-Se [12, 72].

Advantages of Nano-Se over inorganic and organic selenium compounds

On the basis of toxicity profile

Nanomedicine offers the utilization of nanomaterial based technology for the benefit and treatment of human health. All the conventional medicines have one major limitation, i.e., adverse effects, which occur due to non-specificity of drug action and/or ineffective dosage formulation. Thus designing of medicinal agents with greater degree specificity improves efficacy and as well as minimizes adverse reactions [7].

Selenium (Se) is an essential micronutrient with well-known antioxidant characteristics. The antioxidant and prooxidant effects of selenium as well as its bioavailability and toxicity depend upon its chemical form, dose and duration of intake [46]. The major chemical forms of selenium are organic, as selenomethionine (SeMet), selenocysteine (SeCys), and methylselenocysteine (MeSeCys), and inorganic as selenite and selenate [32]. Selenium naturally exists in a various oxidation states, like selenate (SeO_4^{2-}), selenite (SeO_3^{2-}), selenide (Se^{2-}), and elemental selenium (Se°), where the oxidation states are +6, +4, +2 and 0, respectively [45]. The toxicity of the different states of selenium is associated with their degree of aqueous solubility and their bioavailability [18]. The US National Research Council in 1976 had published a statement that to evaluate the toxic effects of selenium, growth inhibition is one of the best indicators [42]. On the basis of this, a comparative study of toxicity has been made between Nano-Se and inorganic as well as organic selenium compound. Zhang [67] found large difference in toxicity between Nano-Se and sodium selenite. In this study, they compared the short-term toxicity of the two selenium forms in mice. Both Nano-Se and sodium selenite

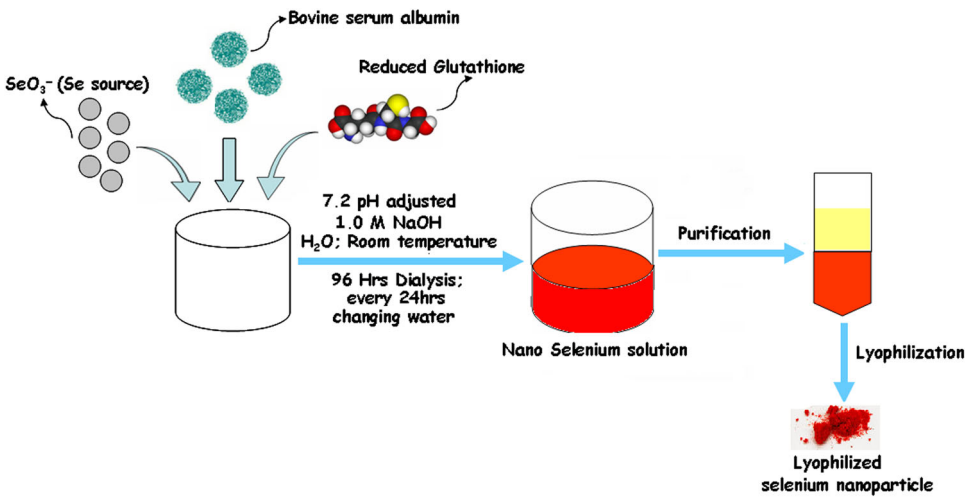

Fig. 3 Schematic presentation of preparation and reaction condition of nano particle of selenium (Nano-Se)

were fed orally at the doses of 2, 4, 6 mg Se/kg b.w. The results showed that Nano-Se was much less toxic than sodium selenite in the same dose range, in terms of growth inhibition, hepatotoxicity, and antioxidant status. This study also indicated that among the three doses, Nano-Se at the dose of 2 mg Se/kg b.w. was non-toxic and showed optimum antioxidant efficacy. Similarly in our study, we found Nano-Se (at 2 mg Se/kg b.w. oral dose) to be less toxic than inorganic as well as organic form of selenium compounds on the basis of lipid peroxidation level and histopathological study in liver, kidneys and lungs, bone marrow toxicity and hematological parameters. We also found that Nano-Se at 4 mg Se/kg b.w. is toxic (unpublished data). In another study, Liu et al. [34] has reported, acute toxicity of newly synthesized folate (FA)-conjugated selenium nanoparticles (Nano-Se) is much lower compared to selenomethionine and selenite. Nano-Se also has a sevenfold lower acute toxicity than sodium selenite in mice (LD_{50} 113 and 15 mg Se/kg body weight, respectively) [14].

On the basis of pharmacokinetic profile

Animal studies have demonstrated that the liver is not only the organ of metabolism but also the main target organ of selenium toxicity [19] due to the consequence of hyper-accumulation of the absorbed selenium in liver and the fact that selenium-generated reactive oxygen species (ROS) formation are the major mechanisms for selenium toxicity [57]. The route of absorption of inorganic selenium, such as selenite, is mainly through passive diffusion from the intestine, and then 50–75 % of total ingested selenium is excreted in the urine [3]. This may be the reason of high selenium accumulation in the kidneys [54]. In contrary to inorganic forms, organic selenium, such as seleno-methionine, is utilized in the intestinal wall by active transportation (e.g. by amino acid transport systems) and non-specifically incorporated into body proteins in place of methionine during protein synthesis, providing a means of reversible selenium storage in organs and tissues [51]. Nanoparticles, such as Nano-Se, are absorbed in the duodenum also by active transportation [69].

In pharmacology, one of the major pharmacokinetic properties of drug is bioavailability which defined as is the fraction of the administered dose of drug that enters into the systemic circulation [10]. In the view of bioavailability, Nano-Se has higher plasma bioavailability as compared to the other forms of selenium compounds [62]. This was evident in broiler chicken and goat as compared to selenite [54, 74].

Pre-clinical application and therapeutic efficacy of Nano-Se

Chemopreventive agent

Chemoprevention is defined as the use of chemical compounds and/or specific nutrients to inhibit, reverse, or delay tumorigenesis. It is an economic and beneficial approach to decline the morbidity and mortality related to cancer through inhibition of pre-cancerous events [11, 58]. In this regard, modulation of phase I and phase II enzymes by selenium based compounds at supranutritional dietary levels has been considered as a probable chemopreventive mechanism [68]. In the work of Zhang [68], it was stated that Nano-Se can serve as a potential chemopreventive agent with reduced risk of selenium toxicity. It can also be noted in their study that Nano-Se possesses enhancement of phase II enzymes activities, such as glutathione peroxidase, thioredoxin reductase, and glutathione-*S*-transferase.

Chemoprotective agent

The broad-spectrum clinical applications of chemotherapeutic drugs for tumor treatment, as a single-edged sword, possess severe toxic side effects, such as myelosuppression, severe damage to digestive tract, liver, kidneys and other vital organs, which restrict their therapeutic efficacy and even directly or indirectly may lead to death by reducing body's natural anti-tumor immunity [33]. Pharmacologically speaking, to overcome the toxic effects of chemotherapy, a variety of drugs, such as white blood cell growth factor, painkillers, antiemetics and so on are employed for clinical use to improve patients' quality of life. One potential therapeutic strategy to solve the problem is concomitant use of adjuvant agents which can decrease toxicity of chemotherapy drugs without compromising their efficacy. In our study [5, 6], we have used Nano-Se in combination with chemotherapeutic drug like cyclophosphamide to check whether, Nano-Se is able to combat the toxic effects of cyclophosphamide. Result showed that, Nano-Se can efficiently attenuate cyclophosphamide-induced hepatotoxicity, pulmonary toxicity and genotoxicity by modulating the oxidative stress. Similar findings have also been noted by Rezvanfar et al. [47]. They had demonstrated that Nano-Se may be useful to prevent cisplatin-induced gonadotoxicity through its antioxidant potential. In 2014, Gao and his colleague reported that, Nano-Se as preventive agent to protect against toxicities of anticancer drug irinotecan and synergistically enhance the therapeutic efficacy in vitro and in vivo [20]. Recently, there was a report that Nano-Se could protect chromium-induced oxidative and cellular damage in rat thyroid [23].

Nano-Se also showed protective effect against As(III)-induced cell death and DNA damage on human lymphocyte [43].

Chemotherapeutic agent

Several mechanisms associated with the antineoplastic activity of selenium have been postulated, which include induction of apoptosis [24, 71], anti-inflammatory [37], alteration in DNA methylation status of tumor suppressor genes [66], antioxidation [8], cell cycle arrest [34], stimulation of the immune system [49] and inhibition of angiogenesis [63]. In a panel of human cancer cell lines, including HeLa (human cervical carcinoma), MDA-MB-231 (human breast carcinoma), A375 (human melanoma cells) and LNCaP (human prostate adeno-carcinoma cell line), Nano-Se was able to effectively decrease the cell viability [12, 29, 36]. In another study, the growth of human ileocecal adenocarcinoma (HCT-8) cells and IEC-6 (rat gut epithelial) cells were significantly inhibited after treated by Nano-Se [20]. The Nano-Se-induced growth inhibition was concentration dependent [29, 36]. Nano-Se also showed the direct cytotoxicity to various cancer cells. It was reported that Nano-Se could kill nasopharyngeal carcinoma (CNE-2), human hepatocellular liver carcinoma (HepG2) and human breast adenocarcinoma (MCF-7) cell lines in a dose-dependent manner with IC_{50} values ranging from 3.0 to 14.1 μM [12]. Further studies showed that induction of mitochondrial membrane potential depolarization, release of cytochrome *c* to cytosol from mitochondria, and activation of caspases-9 and -3 was associated with Nano-Se-induced apoptosis [12, 29]. In addition, molecular studies demonstrated that the mechanism of Nano-Se-induced apoptosis was related to the Akt/Mdm2/AR pathway [29]. Recently, there was a report that Nano-Se could modulate Prx1, Trx1 and p-Nrf2 expression in liver and tumor tissue [20]. Matrix metalloproteinase-9 (MMP-9) is a mediator of angiogenesis which in turn, causes tumor growth and metastasis [65]. Nano-Se also showed significant inhibition of MMP-2 production [52]. Even in our study, it has been proved that Nano-Se is able to reduce the MMP-9 level in serum and ascitic fluid of tumor bearing mice (unpublished data). In a mouse model of breast cancer cell 4T1, the tumor growth was also slightly inhibited by Nano-Se [64]. In cancer chemotherapy, overcoming the multidrug resistance (MDR) and reduction of adverse effects are two of the greatest challenges for every scientist. Importantly, a serious obstacle for the successful treatment of liver cancer is the development of drug resistance. Very recently, Liu and his group synthesized folate (FA)-conjugated selenium nanoparticles (Nano-Se) as cancer-targeted nano-drug delivery system and they also reported the folate (FA)-conjugated selenium nanoparticles (FA-Nano-Se) triggered ROS overproduction and induced apoptosis by activating p53 and MAPKs pathways [34]. In another study, the molecular mechanism of Nano-Se on hepatocellular carcinoma (HCC) induced by *N*-nitrosodiethylamine was established. In this model, Nano-Se up-regulated the expression of Aldo–keto reductase 1B10 (*AKR1B10*) and a tumor suppressor protein *ING3* gene in HCC rat [1]. Zheng and his colleagues, developed amine-terminated generation of 5-polyamidoamine (PAMAM) dendrimers ($G5{\cdot}NH_2$) modified selenium nanoparticle (Nano-Se) for the systemic dual-delivery of MDR1 small interfering RNA (siRNA) and cisplatin. PAMAM dendrimer-modified selenium nanoparticles (Nano-Se) that simultaneously delivered cisplatin and siRNA to adenocarcinomic human alveolar basal epithelial cells (A549/CDDP) to downregulate the expression of P-glycoprotein (P-gp) and induce cell apoptosis [73]. Recently, Hassan and his colleague [22] successfully applied red-allotrope selenium nanoparticle (Nano-Se) to treat head and neck squamous cell carcinoma (HNSCC). Based on the findings, they claimed that red-allotrope Nano-Se induced apoptosis in HNSCC and has the potential for treating HNSCC without any negative effect on healthy normal cells.

Reproductive agent

Several studies have claimed that selenium plays a pivotal role for maintenance of fertility of male [53, 61]. One of the major causes of sperm dysfunction is stated to be oxidative stress as because sperm cells contain a high amount of polyunsaturated fatty acids. It is observed in small ruminant sperm membrane that the ratio of unsaturated to saturated fatty acids is higher as compared to other species; thus the membrane becomes quite vulnerable to ROS attacks leading to the loss of membrane integrity in the acrosomal region, dysregulated cell function and reduced motility of sperm [2]. A study with male goats showed that Nano-Se (60–80 nm) supplementation with 0.3 mg/kg of diet from weaning to sexual maturity has beneficial effects on testicular and spermatozoa microstructure, testicular antioxidative enzyme activity and semen quality in male goats compared to sodium selenite fed control [55].

Antidiabetic agent

One of the main causes of diabetic nephropathy (DN) is found to be oxidative stress, which is the common cause for the genesis of end stage renal disease (ESRD) in type 1 diabetic pateints [39]. In the hyperglycemic condition the production of ROS is influenced by accumulation of advanced glycation end products, elevated polyol pathway

and induction of protein kinase C (PKC) [28]. GP*x* is a selenoprotein which plays pivotal role to protect the host organs from oxidative damage in hyperglycemic condition [40]. A study with male Sprague–Dawley (SD) rats showed that Nano-Se (40–90 nm) supplementation with 0.5 mg/kg/day could protect the development of streptozotocin-induced diabetic nephropathy by modulating the expression of cytoprotective protein HSP70 and longevity protein SIRT-1 [30].

Role of Nano-Se on ROS mediated apoptosis in cancer cells

An increase in intracellular ROS in cancer cell above threshold level can induce cell cycle arrest, senescence and apoptosis. This is generally achieved by chemotherapeutic drugs due to depletion of antioxidants and/or production of ROS. Apoptosis is associated with an increment in mitochondrial oxidative stress that further causes release of cytochrome *c*, which is an irrevocable event leading to activation of caspases and apoptosis [9, 56]. Recent findings indicate that generation of ROS by Se compounds acts as a major cellular event that proceeded to cell cycle arrest and/or apoptosis [41]. In 2008, Chen and his group measured the generation of intracellular ROS by using dichlorofluorescein (DCF) spectrofluorometric assay in A375 cells (human melanoma cells) and the results indicated that treatment with Nano-Se induced a dose-dependent elevation of intracellular levels of ROS, suggesting the influence of ROS in Nano-Se-mediated apoptosis [12].

Various evidences has demonstrated that ROS-induced DNA damage cause cancer cell death via induction of apoptosis through several signaling pathways, such as p53, ATM/ATR, AKT and MAPKs pathways [13]. Moreover, phosphorylation of tumor suppressor p53 at Serine 15 resulted into apoptosis mediated by antineoplastic drugs and chemopreventive agents like selenocompounds [26]. In connection with this, newly synthesized tansferrin (Tf)-conjugated selenium nanoparticle (Nano-Se) did not interfere with the expression profile of total p53 in MCF-7 cells but significantly induced the phosphorylation of p53 at serine 15 and thus caused apoptosis. In addition, Tf-Nano-Se significantly stimulated the phosphorylation of histone at Serine 139 and induced apoptosis via DNA damage-mediated p53 activation in cancer cells. Tf-Nano-Se also showed dissimilar effects on the phosphorylation of ERK, JNK, p38 and AKT. In this regard, the phosphorylation of proapoptotic kinase p38 showed a trend of dose-dependent up-regulation. On the other hand, Tf-Nano-Se effectively suppressed the phosphorylation of antiapoptotic kinase ERK, whereas, the phosphorylation of JNK and AKT was unaltered. Thus, these findings suggested that modulation of p38 and ERK pathway by Tf-Nano-Se contributed to apoptosis induction [24]. In this connection, Liu et al. [34] also reported that the folate (FA)-conjugated selenium nanoparticles (FA-Nano-Se) induced apoptosis by ROS-mediated p53 phosphorylation in cancer cells.

In another study, Tikoo and his group [60] demonstrated a role of Nano-Se on ROS mediated apoptosis. They performed western blot analysis to analyze the expression and role of ERα, Bax, Cyt *c*, and phospho-p38 in MDA-MB-231 and MCF7 cells treated with Nano-Se. After the treatment with Nano-Se in MCF-7 cells, the level of estrogen receptor-α (ERα) showed a trend of down-regulation in a dose-dependent manner, whereas, the levels of ERα remained unalterd in MDA-MB-231 cells. Bax is a pro-apoptotic madiator of the Bcl-2 family of proteins and is located primarily in the cytosol and during apoptosis relocalizes to the mitochondrial. Thus the elevated expression of Bax is an indication of activation of mitochondrial apoptotic pathway within the cell. A considerable increment in the expression of Bax and cytochrome *c* in ERα-positive MCF-7 cells implies that Nano-Se-induced apoptosis in MCF-7 cells is regulated mitochondrial pathway of apoptosis.

Conclusions

It is evident through many examples given by several authors that oxidative stress play a major role in the host tissue and organ damage that may occur in response to both toxicants and in the etiopathogenesis of numerous human diseases [48]. Selenium is a quintessential trace element for both human and animals as because it is a component of many selenoprotein with essential biological function leading to many cellular processes [31]. Selenium also possess some toxic properties leading to selenosis, dysregulation of endocrine function, biosynthesis of growth hormones and thyroid hormones, and an insulin-like growth factor metabolism in human and animals [59]. Nanotechnology in modern medicine is still in infancy, holds the ability to dramatically change the medical research in the twenty-first century. It is expected that several nanoparticle and nanodevices would be used and that will lead to an enormous positive effect on human health. In addition, the benefit also extends to early diagnosis, improved implantation, cancer therapy and minimum invasive approaches for cardiovascular disease, metabolic disorders and other diseases [35]. For drug research and design, Nano-Se opens a new perspective to selectively develop the health beneficial properties of those other forms of selenium for the prevention and treatment of various human diseases. There are more and more scientific data to support the use of Nano-Se for human disease prevention or lifespan extension. Nano-Se targets a wide

range of molecules that influence cell proliferation, apoptosis, and metastasis.

Summing up everything, the above discussed studies suggest that further understandings of the multiple aspects of Nano-Se at the molecular level in responses to toxicants by using in vivo and in vitro model systems mimicking pathophysiological conditions may serve as an interesting and fruitful mode of future investigation which may lead to the abrogation of the oxidative stress-mediated toxic effects.

Acknowledgments Arin Bhattacharjee gratefully acknowledges Indian Council of Medical Research (ICMR), New Delhi, for Senior Research Fellowship (No. 45/36/2008/PHA-BMS). Abhishek Basu also gratefully acknowledges Council of Scientific and Industrial Research (CSIR), New Delhi, for Research Associateship [No. 09/030(0075)/2015 EMR-I]. The authors wish to thank the Director, CNCI, for supporting this study.

References

1. Ahmed HH, Khalil WK, Hamza AH. Molecular mechanisms of Nano-Selenium in mitigating hepatocellular carcinoma induced by *N*-nitrosodiethylamine (NDEA) in rats. Toxicol Mech Methods. 2014;24:593–602.
2. Aitken RJ. Baker MA oxidative stress and male reproductive biology. Reprod Fertil Dev. 2004;16:581–8.
3. Alaejos MS, Romero CD. Urinary selenium concentrations. Clin Chem. 1993;39:2040–52.
4. Baharara J, Namvar F, Ramezani T, Mousavi M, Mohamad R. Silver nanoparticles biosynthesized using *Achillea biebersteinii* flower extract: apoptosis induction in MCF-7 cells via caspase activation and regulation of Bax and Bcl-2 gene expression. Molecules. 2015;20:2693–706.
5. Bhattacharjee A, Basu A, Biswas J, Bhattacharya S. Nano-Se attenuates cyclophosphamide-induced pulmonary injury through modulation of oxidative stress and DNA damage in Swiss albino mice. Mol Cell Biol. 2015;405:243–56.
6. Bhattacharjee A, Basu A, Ghosh P, Biswas J, Bhattacharya S. Protective effect of Selenium nanoparticle against cyclophosphamide induced hepatotoxicity and genotoxicity in Swiss albino mice. J Biomater Appl. 2014;29:303–17.
7. Boulaiz H, Alvarez PJ, Ramirez A, Marchal JA, Prados J, Rodríguez-Serrano F, Perán M, Melguizo C, Aranega A. Nanomedicine: application areas and development prospects. Int J Mol Sci. 2011;12:3303–21.
8. Brozmanova J, Manikova D, Vlckova V, Chovanec M. Selenium: a doubleedged sword for defense and offence in cancer. Arch Toxicol. 2010;84:919–38.
9. Cadenas E. Mitochondrial free radical production and cell signaling. Mol Aspects Med. 2004;25:17–26.
10. Chabner BA, Ryan DP, Paz-Ares L, Garcia-Carbonero R, Calabresi P. In: Goodman LS, Hardman JG, Limbird LE, Gilman AG, editors. Goodman and Gilman's the pharmacological basis of therapeutics. New York: McGraw Hill; 2001. p. 1389–459.
11. Chen C, Kong AN. Dietary cancer-chemopreventive compounds: from signaling and gene expression to pharmacological effects. Trends Pharmacol Sci. 2005;26:318–26.
12. Chen T, Wong YS, Zheng W, Bai Y, Huang L. Selenium nanoparticles fabricated in *Undaria pinnatifida* polysaccharide solutions induce mitochondria-mediated apoptosis in A375 human melanoma cells. Coll Surf B Biointerfaces. 2012;67:26–31.
13. Chen T, Wong YS. Selenocystine induces apoptosis of A375 human melanoma cells by activating ROS-mediated mitochondrial pathway and p53 phosphorylation. Cell Mol Life Sci. 2008;65:2763–75.
14. Clark LC, Combs GF Jr, Turnbull BW, et al. Effects of selenium supplementation for cancer prevention in patients with carcinoma of the skin. A randomized controlled trial. Nutritional Prevention of Cancer Study Group. JAMA. 1996;276:1957–63.
15. Conklin KA. Chemotherapy-associated oxidative stress: impact on chemotherapeutic effectiveness. Integr Cancer Ther. 2004;3:294–300.
16. Dalle-Donne I, Rossi R, Colombo R, Giustarini D, Milzani A. Biomarkers of oxidative damage in human disease. Clin Chem. 2006;52:601–23.
17. Dhalla NS, Temsah RM, Netticadan T. Role of oxidative stress in cardiovascular diseases. J Hypertens. 2000;18:655–73.
18. Dhanjal S, Cameotra SS. Aerobic biogenesis of selenium nanospheres by *Bacillus cereus* isolated from coalmine soil. Microb Cell Fact. 2010;9:52.
19. Diskin CJ, Tomasso CL, Alper JC, Glaser ML, Fliegel SE. Long-term selenium exposure. Arch Intern Med. 1979;139:824–6.
20. Gao F, Yuan Q, Gao L, Cai P, Zhu H, Liu R, Wang Y, Wei Y, Huang G, Liang J, Gao X. Cytotoxicity and therapeutic effect of irinotecan combined with selenium nanoparticles. Biomaterials. 2014;35:8854–66.
21. Guo L, Yan DD, Yang D, Li Y, Wang X, Zalewski O, Yan B, Lu W. Combinatorial photothermal and immuno cancer therapy using chitosan-coated hollow copper sulfide nanoparticles. ACS Nano. 2014;8:5670–81.
22. Hassan CE, Webster TJ. The effect of red-allotrope selenium nanoparticles on head and neck squamous cell viability and growth. Int J Nanomed. 2016;11:3641–54.
23. Hassanin KM, El-Kawi SHA, Hashem KS. The prospective protective effect of selenium nanoparticles against chromium-induced oxidative and cellular damage in rat thyroid. Int J Nanomed. 2013;8:1713–20.
24. Huang Y, He L, Liu W, Fan C, Zheng W, Wong YS, Chen T. Selective cellular uptake and induction of apoptosis of cancer-targeted selenium nanoparticles. Biomaterials. 2013;34:7106–16.
25. Jenner P. Oxidative stress in Parkinson's disease. Ann Neurol. 2003;53:26–36.
26. Jiang C, Hu H, Malewicz B, Wang Z, Lü J. Selenite-induced p53 Ser-15 phosphorylation and caspase-mediated apoptosis in LNCaP human prostate cancer cells. Mol Cancer Ther. 2004;3:877–84.
27. Jun JY, Nguyen HH, Paik SYR, Chun HS, Kang BC, Ko S. Preparation of size-controlled bovine serum albumin (BSA) nanoparticles by a modified desolvation method. Food Chem. 2011;127:1892–8.
28. Kanwar YS, Wada J, Sun L, Xie P, Wallner EI, Chen S, Chugh S, Danesh FR. Diabetic nephropathy: mechanisms of renal disease progression. Exp Biol Med. 2008;233:4–11.
29. Kong L, Yuan Q, Zhu H, Li Y, Guo Q, Wang Q, Bi X, Gao X. The suppression of prostate LNCaP cancer cells growth by Selenium nanoparticles through Akt/Mdm2/AR controlled apoptosis. Biomaterials. 2011;32:6515–22.
30. Kumar GS, Kulkarni A, Khurana A, Kaur J, Tikoo K. Selenium nanoparticles involve HSP-70 and SIRT1 in preventing the progression of type 1 diabetic nephropathy. Chem Biol Interact. 2014;223C:125–33.
31. Letavayová L, Vlasakova D, Spallholz JE, Brozmanova J, Chovanec M. Toxicity and mutagenicity of selenium compounds in *Saccharomyces cerevisiae*. Mutat Res. 2008;638:1–10.

32. Letavayová L, Vlcková V, Brozmanová J. Selenium: from cancer prevention to DNA damage. Toxicology. 2006;227:1–14.
33. Lheureux S, Clarisse B, Launay-Vacher B, Gunzer K, Delcambre-Lair C, BouhierLeporrier K, et al. Evaluation of current practice: management of chemotherapy-related toxicities. Anticancer Drugs. 2011;22:919–25.
34. Liu T, Zeng L, Jiang W, Fu Y, Zheng W, Chen T. Rational design of cancer-targeted selenium nanoparticles to antagonize multidrug resistance in cancer cells. Nanomedicine. 2015;11:947–58.
35. Logothetidis S. Nanotechnology in medicine: the medicine of tomorrow and nanomedicine. Hippokratia. 2006;1:7–21.
36. Luo H, Wang F, Bai Y, Chen T, Zheng W. Selenium nanoparticles inhibit the growth of HeLa and MDA-MB-231 cells through induction of S phase arrest. Coll Surf B Biointerfaces. 2012;94:304–8.
37. Miroliaee AE, Esmaily H, Vaziri-Bami A, Baeeri M, Shahverdi AR, Abdollahi M. Amelioration of experimental colitis by a novel nanoselenium–silymarin mixture. Toxicol Mech Methods. 2011;21:200–8.
38. Mousa SA, Bharali DJ. Nanotechnology-based detection and targeted therapy in cancer: nano-bio paradigms and applications. Cancers (Basel). 2011;3:2888–903.
39. Najafian B, Mauer M. Progression of diabetic nephropathy in type 1 diabetic patients. Diabetes Res Clin Pract. 2008;83:1–8.
40. Naziroğlu MI, Cay C. Protective role of intraperitoneally administered vitamin E and selenium on the antioxidative defense mechanisms in rats with diabetes induced by streptozotocin. Biol Trace Elem Res. 2001;79:149–59.
41. Nilsonne G, Sun X, Nystrom C, Rundlof AK, Fernandes AP, Bjornstedt M, Dobra K. Selenite induces apoptosis in sarcomatoid malignant mesothelioma cells through oxidative stress. Free Radic Biol Med. 2006;41:874–85.
42. Øarskov H, Flyvbjerg A. Selenium and human health. Lancet. 2000;356:942–3.
43. Prasad KS, Selvaraj K. Biogenic synthesis of selenium nanoparticles and their effect on As(III)-induced toxicity on human lymphocytes. Biol Trace Elem Res. 2014;157:275–83.
44. Ramamurthy Ch, Sampath KS, Arunkumar P, Kumar MS, Sujatha V, Premkumar K, Thirunavukkarasu C. Green synthesis and characterization of selenium nanoparticles and its augmented cytotoxicity with doxorubicin on cancer cells. Bioprocess Biosyst Eng. 2013;36:1131–9.
45. Rathgeber C, Yurkova N, Stackebrandt E, Beatty JT, Yurkov V. Isolation of tellurite- and selenite-resistant bacteria from hydrothermal vents of the Juan de Fuca Ridge in the Pacific Ocean. Appl Environ Microbiol. 2002;68:4613–22.
46. Rayman MP. Selenium in cancer prevention: a review of the evidence and mechanism of action. Proc Nutr Soc. 2005;64:527–42.
47. Rezvanfar MA, Rezvanfar MA, Shahverdi AR, Ahmadi A, Baeeri M, Mohammadirad A, Abdollahi M. Protection of cisplatin-induced spermatotoxicity, DNA damage and chromatin abnormality by selenium nano-particles. Toxicol Appl Pharmacol. 2013;266:356–65.
48. Roberts RA, Smith RA, Safe S, Szabo C, Tjalkens RB, Robertson FM. Toxicological and pathophysiological roles of reactive oxygen and nitrogen species. Toxicology. 2010;276:85–94.
49. Ryan-Harshman M, Aldoori W. The relevance of selenium to immunity, cancer, and infectious/inflammatory diseases. Can J Diet Pract Res. 2005;66:98–102.
50. Saeidnia S, Abdollahi M. Antioxidants: friends or foe in prevention or treatment of cancer: the debate of the century. Toxicol Appl Pharmacol. 2013;271:49–63.
51. Schrauzer GN. Selenomethionine: a review of its nutritional significance, metabolism and toxicity. J Nutr. 2000;130:1653–6.
52. Shakibaie M, Khorramizadeh MR, Faramarzi MA, Sabzevari O, Shahverdi AR. Biosynthesis and recovery of selenium nanoparticles and the effects on matrix metalloproteinase-2 expression. Biotechnol Appl Biochem. 2010;56:7–15.
53. Shalini S, Bansal MP. Dietary selenium deficiency as well as excess supplementation induces multiple defects in mouse epididymal spermatozoa: understanding the role of selenium in male fertility. Int J Androl. 2008;31:438–49.
54. Shi L, Xun W, Yue W, Zhang C, Ren Y, Shi L, Wang Q, Yang R, Lei F. Effect of sodium selenite, Se-yeast and nano-elemental selenium on growth performance, Se concentration and antioxidant status in growing male goats. Small Rumin Res. 2001;96:49–52.
55. Shi LG, Yang RJ, Yue WB, Xun WJ, Zhang XC, Ren YS, Shi L, Lei FL. Effect of elemental Nano-Selenium on semen quality, glutathione peroxidase activity, and testis ultrastructure in male Boer goats. Anim Reprod Sci. 2010;118:248–54.
56. Simon HU, Haj-Yehia A, Levi-Schaffer F. Role of reactive oxygen species (ROS) in apoptosis induction. Apoptosis. 2000;5:415–8.
57. Spallholz JE, Palace VP, Reid TW. Methioninase and selenomethionine but not Se-methylselenocysteine generates methylselenol and superoxide in an in vitro chemiluminescent assay: implications for the nutritional carcinostatic activity of selenoamino acids. Biochem Pharmacol. 2004;67:547–54.
58. Surh YJ. Cancer chemoprevention with dietary phytochemicals. Nat Rev Cancer. 2003;3:768–80.
59. Valdiglesias V, Pásaro E, Méndez J, Laffon B. In vitro evaluation of selenium genotoxic, cytotoxic, and protective effects: a review. Arch Toxicol. 2010;84:337–51.
60. Vekariya KK, Kaur J, Tikoo K. ERα signaling imparts chemotherapeutic selectivity to selenium nanoparticles in breast cancer. Nanomedicine. 2012;8:1125–32.
61. Wallace E, Cooper GW, Calvin HI. Effects of selenium deficiency on the shape and arrangement of rodent sperm mitochondria. Gamete Res. 1983;4:389–99.
62. Wang H, Zhang J, Yu H. Elemental selenium at nano size possesses lower toxicity without compromising the fundamental effect on selenoenzymes: comparison with selenomethionine in mice. Free Radic Biol Med. 2007;42:1524–33.
63. Wang Z, Hu H, Li G, Lee HJ, Jiang C, Kim SH, et al. Methylseleninic acid inhibits microvascular endothelial G1 cell cycle progression and decreases tumor microvessel density. Int J Cancer. 2008;122:15–24.
64. Yazdi MH, Mahdavi M, Varastehmoradi B, Faramarzi MA, Shahverdi AR. The immunostimulatory effect of biogenic selenium nanoparticles on the 4T1 breast cancer model: an in vivo study. Biol Trace Elem Res. 2012;149:22–8.
65. Yoon SO, Kim MM, Chung AS. Inhibitory effect of selenite on invasion of HT1080 tumor cells. J Biol Chem. 2002;276:20085–92.
66. Yu YP, Yu GY, Tseng G, Cieply K, Nelson J, Defrances M, et al. Glutathione peroxidase 3, deleted or methylated in prostate cancer, suppresses prostate cancer growth and metastasis. Cancer Res. 2007;67:8043–50.
67. Zhang J, Wang H, Yan X, Zhang L. Comparison of short-term toxicity between Nano-Se and selenite in mice. Life Sci. 2004;76:1099–109.
68. Zhang J, Wang X, Xu T. Elemental selenium at nano size (Nano-Se) as a potential chemopreventive agent with reduced risk of selenium toxicity: comparison with se-methylselenocysteine in mice. Toxicol Sci. 2008;101:22–31.
69. Zhang JS, Gao XY, Zhang LD, Bao YP. Biological effects of a nano red elemental selenium. BioFactors. 2001;15:27–38.
70. Zhang W, Chen Z, Liu H, Zhang L, Gao P, Li D. Biosynthesis and structural characteristics of selenium nanoparticles by

Pseudomonas alcaliphila. Coll Surf B Biointerfaces. 2011;88: 196–201.

71. Zhang Y, Li X, Huang Z, Zheng W, Fan C, Chen T. Enhancement of cell permeabilization apoptosis-inducing activity of selenium nanoparticles by ATP surface decoration. Nanomed Nanotechnol Biol Med. 2013;9:74–84.
72. Zheng JS, Zheng SY, Zhang YB, Yu B, Zheng W, Yang F, Chen T. Sialic acid surface decoration enhances cellular uptake and apoptosis-inducing activity of selenium nanoparticles. Coll Surf B Biointerfaces. 2011;83:183–7.
73. Zheng W, Cao C, Liu Y, Yu Q, Zheng C, Sun D, Ren X, Liu J. Multifunctional polyamidoamine-modified selenium nanoparticles dual-delivering siRNA and cisplatin to A549/DDP cells for reversal multidrug resistance. Acta Biomater. 2015;11:368–80.
74. Zhou X, Wang Y. Influence of dietary nano elemental selenium on growth performance, tissue selenium distribution, meat quality, and glutathione peroxidase activity in Guangxi Yellow chicken. Poult Sci. 2011;90:680–6.

30TH ANNUAL CONVENTION OF INDIAN ASSOCIATION FOR CANCER RESEARCH AND INTERNATIONAL SYMPOSIUM ON "SIGNALING NETWORK AND CANCER"

CSIR-IICB CELEBRATING 75TH YEAR

Certificate of Participation

This is to certify that Dr./Mr./Ms. Arin Bhattacharjee

presented a research ~~paper~~/poster/~~participated~~ at the Symposium

held at Indian Institute of Chemical Biology, Kolkata, India,

during February 6 - 9, 2011.

Dr. Susanta Roy Choudhury
Jt. Organizing Secretary
IACR 2011

Dr. Chitra Mandal
Jt. Organizing Secretary
IACR 2011

Dr. Rita Mulherkar
President, IACR

Prof. Siddhartha Roy
Chairman, Organizing Committee
IACR 2011

Certificate

This is to certify that

Arin Bhattacharjee

participated in the

31st Annual Convention of Indian Association for Cancer Research
&
International Symposium on
"Cancer Genomics and its Impact in the Clinics"

held at
Advanced Centre for Treatment, Research and Education in Cancer,
Kharghar, Navi Mumbai
26th - 29th January 2012

Dr. R. Mulherkar
Chairperson

Dr. T. Teni
Organizing Secretary